

Glycosylation and Sialylation during Wound Healing

BY

VERONICA A. HAYWOOD

B.S., Marquette University, Milwaukee 2008

D.P.T., Marquette University, Milwaukee 2010

THESIS

Submitted as partial fulfillment of the requirements
for the degree of Doctor of Philosophy in Oral Sciences
in the Graduate College of the
University of Illinois at Chicago (UIC), 2019
Chicago, Illinois

Thesis Defense Committee

Dr. Luisa A. DiPietro, Chair and Advisor, Center for Wound Healing and Tissue Regeneration, UIC

Dr. Karen Colley, Biochemistry and Molecular Genetics, UIC

Dr. Praveen Gajendrareddy, Periodontics, UIC

Dr. Timothy Koh, Kinesiology and Nutrition, UIC

Dr. Dr. Luan Xianghong, Biomedical Sciences, Baylor College

Dr. Yi-Ting Tzen, School of Health Professions, University of Texas, Southwestern Medical Center

This thesis is dedicated to Warren, Mom and Dad for all your love, support, faith and presence; my nieces and nephews for giving me a reason to push harder; Yolanda Webb and Luther Kloth for always knowing I was capable even when I didn't and providing the foundation for my interests in wound healing, and Dr. DiPietro for all the encouragement, guidance, and persistence throughout this difficult journey.

ACKNOWLEDGEMENTS

I would like to thank my thesis committee, Drs. DiPietro, Colley, Gajendrareddy, Koh, Luan and Tzen for their support and assistance. Thank you to my extended lab family: Drs. Colley, Bhide, Nairns, Archer and Lehoux for your guidance and patience during my glycobiology and statistical modeling journey. Thank you to my wound care team and patients at Advocate Christ Medical Center and UIC for inspiring me to pursue this journey and your encouragement and support during my limited availability. Thank you to my students Vidhath and Maitri for your help and allowing me to mentor you. Lastly a special thank you to my lab family: Dr. DiPietro, Lin, Yan, Wendy, Trevor, Anna, May, Liz, Uzoagu, and Junhe for always being there for me.

VAH

TABLE OF CONTENTS

<u>CHAPTER</u>		<u>PAGE</u>
1.	INTRODUCTION	
1.1	Background.....	1
1.1.1	Overview of Wound Healing.....	1
1.1.1.1	Hemostasis during Wound Healing.....	1
1.1.1.2	Inflammation During Wound Healing.....	2
1.1.1.3	Proliferation During Wound Healing.....	4
1.1.1.4	Remodeling During Wound Healing.....	5
1.1.2	Defining Wound Healing and Differential Responses to Wound Healing.....	5
1.1.2.1	Clinical Assessment of Wound Healing.....	5
1.1.2.2	Differential Wound Healing in Mouse Skin and Oral Mucosa.....	6
1.1.2.3	Differential Healing in Diabetic and Non- Diabetic Wounds...	10
1.1.2.4	AGE's Impaired Wound Healing and Altered Enzymatic Glycosylation.....	11
1.1.3	Glycosylation.....	11
1.1.3.1	Defining Glycosylation.....	11
1.1.3.2	Substrates Involved in Glycosylation.....	12
1.1.3.2.1	N- Linked Glycosylation.....	17
1.1.3.2.2	O- Linked Glycosylation.....	21
1.1.3.3	Terminal Glycans and Nomenclature.....	22
1.1.3.4	Function and Roles of Glycosylation.....	26
1.1.3.4.1	Role of Glycosylation in Inflammation.....	27
1.1.3.4.2	Contribution of Glycosylation to Wound- Related Processes	30
1.1.3.4.3	Glycosylation in Disease Processes.....	32
1.1.4	Disease, Glycosylation, and AGEs are Intertwined.....	32
1.2	Significance and Motivation of Thesis.....	34
1.3	Specific Aims.....	35
2.	ORGAN SPECIFIC REGULATION OF GLYCOSYLATION- RELATED GENES DURING SKIN AND TONGUE WOUND HEALING	
2.1	Introduction.....	37
2.2	Materials and Methods.....	39
2.2.1	Microarray Normalization and Pathway Analysis.....	39
2.2.2	Animal Wound Models.....	40
2.2.3	Sample Preparation and Protein Extraction.....	41
2.2.4	Recovery of Polysialylated Proteins.....	42

TABLE OF CONTENTS (continued)

<u>CHAPTER</u>		<u>PAGE</u>
2.2.5	Protein Electrophoresis and Transfer	42
2.2.6	Lectin Blotting Analysis of α 2,3- and α 2,6- Linked Sialic Acid, and α 2-8, Polysialic Acid Expression during Wound Healing.....	43
2.2.7	Microscopy.....	44
2.2.8	In-gel Digestion and Mass Spectroscopy Analysis.....	45
2.2.9	Statistical Analysis.....	47
2.3	Experimental Results.....	49
2.3.1	Microarray Analysis of Skin versus Tongue Wound Healing..	49
2.3.2	Microarray Analysis of Glycosylation- related Genes Reveals Opposing Gene Clusters in Skin versus Tongue Wound Healing.....	53
2.3.3	Genes related to Amino and Nucleotide Sugars are Differentially Regulated in Skin versus Tongue Wound Healing.....	57
2.3.4	Genes Related to Sialic Acid Glycan Capping (Sialylation) are Differentially Regulated in Skin versus Tongue Wound Healing.....	63
2.3.4.1	Genes Related to Sialyltransferases and the Sialylation of Glycans, are Differentially Regulated in Skin versus Tongue Wound Healing.....	63
2.3.5	α 2,3-, α 2,6-, and α 2,8- Polysialylation are Differentially Regulated in Skin versus Tongue Wound Healing.....	78
2.4	Discussion.....	97
3.	DISEASE SPECIFIC REGULATION OF GLYCOSYLATION DURING DIABETIC AND NON-DIABETIC WOUND HEALING	
3.1	Introduction.....	105
3.2	Materials and Methods.....	106
3.2.1	Animal Wound Models.....	106
3.2.2	Protein Sample Preparation.....	107
3.2.3	Gene Expression with HT-qRT PCR.....	108
3.2.4	Statistical Analysis.....	122
3.3	Results	123

TABLE OF CONTENTS (continued)

<u>CHAPTER</u>		<u>PAGE</u>
3.3.1	Screening Reveals Differential Glycosylation- related Gene Expression in Uninjured Skin Models of Pre-Diabetes and Diabetes.....	123
3.3.2	Diabetic and Non- Diabetic Skin and Wounds Exhibit Differential Glycosylation- related Gene Expression.....	126
3.3.3	Non- Diabetic Skin and Wounds Demonstrate Differential Glycosylation- related Gene Expression Over the Course of Wound Healing.....	126
3.3.4	Differential Glycosylation- related Gene Expression Occurs between the Diabetic and Non- Diabetic Conditions.....	131
3.3.5	Regulation and Roles of Genes Expressed during Normal, Non- Diabetic Wound Healing that are Differentially Expressed between the Diabetic and Non- Diabetic Condition.....	145
3.3.6	Differential Expression of Genes between the Diabetic and Non- Diabetic Condition that are Primarily Regulated during Diabetic Wound Healing.....	150
3.3.7	The Expression of Glycosylation- Related Genes is Altered in Intact and Wounded Human DM Skin.....	150
3.3.8	Skin Characteristics during Wound Healing in db/db Mice Mimic those Observed in Diabetic Humans.....	155
3.4	Discussion.....	158
4.	DISEASE SPECIFIC GLYCOSYLATION DURING DIABETIC AND NON-DIABETIC WOUND HEALING- GLYCOMICS ANALYSIS	
4.1	Introduction.....	168
4.2	Materials and Methods.....	171
4.2.1	Animal Wound Models.....	171
4.2.2	Description of Glycomics Analysis Performed by the Glycomics Core.....	172
4.2.2.1	Protein Sample Preparation.....	172
4.2.2.2	Trypsin and PNGase Digestion.....	173
4.2.2.3	β Elimination of O- Linked Glycans.....	173
4.2.2.4	Permethylation of N- and O- Linked Glycans.....	174
4.2.2.5	MALDI-TOF MS Analysis of Permethylated N- and O- Glycans.....	174

TABLE OF CONTENTS (continued)

<u>CHAPTER</u>	<u>PAGE</u>
4.2.3 Statistical Analysis.....	175
4.3 Results.....	175
4.3.1 Diabetic and Non- Diabetic Skin and Wounds Demonstrate Differential N- Linked Glycosylation.....	175
4.3.2 Diabetic and Non- Diabetic Skin and Wounds Demonstrate Differential Expression of High Mannose Structures.....	198
4.3.3 Diabetic and Non- Diabetic Skin and Wounds Demonstrate Differential O- linked Glycosylation.....	200
4.4 Discussion.....	209
 5. THESIS CONCLUSIONS & FUTURE DIRECTIONS	
5.1 AGL, PYGM, and the Importance of Glycogen Accumulation and GSK3 β	217
5.2 Reduced AGL Expression is Observed in Cancer and may be Correlated with Differential Glycosaminoglycan Expression.....	219
5.3 Differential Sulfation may Contribute to Impaired Healing Phenotypes.....	220
5.4 Differential Expression of O- linked Glycans in Impaired Healing phenotypes.....	221
5.5 Differential Expression of O- linked Glycans in Impaired Healing phenotypes.....	222
5.6 Novel Statistical Assessment Focuses Our Assessment of Glycosylation- related Gene Expression in Wounds.....	224
5.7 Limitations	224
 APPENDICES	
Appendix A.....	226
Appendix B.....	254
Appendix C.....	262
Appendix D.....	269
Appendix E.....	297
 CITED LITERATURE	 309
 VITA.....	 345

LIST OF TABLES

<u>TABLE</u>	<u>PAGE</u>
I. CONSENSUS MOTIFS AND ENZYMES RESPONSIBLE FOR VARIOUS GLYCOSYLATION REACTIONS.....	13
II. TABLE OF COMMON GLYCAN STRUCTURES & FEATURES.....	24-25
III. TABLE OF RESULTS OF MICROARRAY EXPRESSION SET- BY STATISTICAL CONTRAST.....	51
IV. TABLE OF TOP 10 PANTHER BIOLOGICAL PROCESS PATHWAYS AMONG GENES DOWNREGULATED IN THE SKIN.....	52
V. TABLE OF TOP 10 PANTHER BIOLOGICAL PROCESS PATHWAYS AMONG GENES UPREGULATED IN THE SKIN.....	53
VI. ACTIVITY AND FUNCTION OF SIALYLTRANSFERASES.....	66-69
VII. TABLE OF GLYCOSYLATION RELATED GENES SCREENED DURING HT- QRT PCR.....	110 -121
VIII. TABLE OF TOP 10 PANTHER BIOLOGICAL PROCESS PATHWAYS AMONG GENES DIFFERENTIALLY REGULATED IN NON-DIABETIC SKIN.....	130
IX. TABLE OF GENES AND THEIR FUNCTIONS AMONG THE DIFFERENTIALLY EXPRESSED GENES OBSERVED IN HUMAN DIABETIC FOOT ULCERS.....	153
X. TABLE OF GENES REGULATED IN HUMAN DIABETIC VERSUS NON-DIABETIC FOOT SKIN AND DIABETIC VERSUS UNINJURED FOOT SKIN DATASETS THAT ARE RELATED TO THOSE EXPRESSED IN THE DB/DB MOUSE MODEL.....	154

LIST OF TABLES (continued)

<u>TABLE</u>	<u>PAGE</u>
XI. TABLE OF GENES ENCODING LYSOSOMAL ENZYMES.....	162
XII. TABLE OF CRITERIA FOR EACH DEFINED N- GLYCAN CORE STRUCTURE.....	179
XIII. TABLE OF N- LINKED GLYCAN DESCRIPTORS FOR EACH STRUCTURE AS INDICATED BY THE MASS- TO -CHARGE RATIO.....	180 -184
XIV. TABLE OF O- LINKED GLYCAN DESCRIPTORS FOR EACH STRUCTURE AS INDICATED BY THE MASS- TO -CHARGE RATIO.....	201
XV. TABLE OF GENES DIFFERENTIALLY REGULATED BETWEEN TISSUES WITH AND WITHOUT IMPAIRED HEALING PHENOTYPES AND THEIR ASSOCIATED ENZYME FAMILY.....	216
XVI. TABLE OF PEPTIDES IDENTIFIED FROM UNINJURED SKIN FOLLOWING ENDONT IP.....	236
XVII. TABLE OF EXPECTED POLYSIALIC ACID ACCEPTOR PROTEINS, MW, ENZYMES INVOLVED, AND THE LOCATION OF POLYSIALIC ACID.....	239
XVIII. GENES UPREGULATED IN SKIN VERSUS TONGUE WOUND HEALING.....	240 -248
XIX. GENES DOWNREGULATED IN SKIN VERSUS TONGUE WOUND HEALING.....	249 253

LIST OF FIGURES

<u>FIGURE</u>	<u>PAGE</u>
1. Depiction of wound healing patterns during skin and tongue wound healing.....	9
2. Major classes of vertebrate glycan structures.....	15
3. N-glycan lipid-linked oligosaccharide processing reactions.....	18
4. Protein N glycosylation and quality control of protein folding....	19
5. GalNAc (mucin-type) core synthesis and branching reactions	22
6. Depiction of wound healing patterns during skin and tongue wound healing.....	39
7. Principal components of glycogenes expressed between skin and tongue wound healing.....	55
8. Hierarchical clustering reveals genes sets are more highly upregulated in skin wound healing when compared to tongue wound healing.....	56
9. Regulation of gene expression in amino sugar and sugar nucleotide metabolism during skin and tongue wound healing.	60
10. Expression of genes related to sugar and sugar nucleotide metabolism during skin and tongue wound healing.....	61
11. Expression of α 2,3- sialyltransferase related genes demonstrate significant differences in expression during skin and tongue wound healing.....	73
12. Expression of α 2,6- sialyltransferase related genes demonstrate significant differences in expression during skin and tongue wound healing.....	74

LIST OF FIGURES (continued)

<u>FIGURE</u>	<u>PAGE</u>
13. Expression of α 2,8- sialyltransferase related genes demonstrate significant differences in expression during skin and tongue wound healing.....	75
14. Expression of neuraminidase related genes demonstrate significant differences in expression during skin and tongue wound healing.....	77
15. Expression of α 2,3- linked sialic acids is differentially regulated in specific proteins during skin and tongue wound healing.....	81
16. Tongue and skin wound healing.....	82
17. Localization of α 2-3 sialic acids in uninjured skin and tongue...	83
18. Localization of α 2-3 sialic acids in skin and tongue wound Healing.....	84
19. Localization of α 2-3 and α 2-6 sialic acids in uninjured skin and tongue.....	87
20. Expression of α 2, 6- linked sialic acids is differentially regulated during skin and tongue wound healing.....	88
21. Expression of α 2, 8- linked polysialic acids is differentially regulated during skin and tongue wound healing.....	92
22. Localization of α 2-8 polysialic acids in skin and tongue wound healing.....	93
23. Expression of 12F8, 735, and NCAM-1 in skin and tongue wound healing.....	95
24. Differential expression of glycosylation related genes in uninjured skin.....	125

LIST OF FIGURES (continued)

<u>FIGURE</u>		<u>PAGE</u>
25.	Regulation of glycosylation related genes in normal, non-diabetic skin wound healing.....	129
27.	Graphical representation of glycosylation related genes from Cluster 1 that are downregulated in diabetic skin and wounds relative to non- diabetic skin and wounds and are related to sialidase activity and terminal glycan capping.....	134
28.	Graphical representation of glycosylation related genes from Clusters 1 & 3 that are downregulated in diabetic skin and wounds relative to non- diabetic skin and wounds and are related to mucin related O-linked glycan biosynthesis.....	135
29.	Graphical representation of glycosylation related genes from Custer 1 that are downregulated in diabetic skin and wounds relative to non- diabetic skin and wounds and are related to local glycogenolysis, while those from Cluster 2 are upregulated and involved in liver glycogenolysis.....	136
30.	Graphical representation of glycosylation related genes from Cluster 3 that are downregulated in diabetic wounds relative to non- diabetic wounds and involved in α -dystroglycan synthesis and function and β - galactosidase activity.....	137
31.	Graphical representation of glycosylation related genes from Cluster 4 that are upregulated in the diabetic condition when compared to the non- diabetic condition and are involved in sulfate precursor formation and tyrosine sulfotransferase activity.....	138
32.	Graphical representation of glycosylation related genes from Cluster 4 & 5 that are upregulated in the diabetic wounds relative to non- diabetic wounds and have sulfatase activity targeting the removal of sulfates at C6 in hexoses associated with glycosaminoglycans.....	139

LIST OF FIGURES (continued)

<u>FIGURE</u>		<u>PAGE</u>
33.	Graphical representation of glycosylation related genes from Cluster 4 & 5 that are upregulated in the diabetic wounds relative to non- diabetic wounds and are related to glycosaminoglycan metabolism.....	140
34.	Graphical representation of glycosylation related genes from Cluster 4 & 5 that are upregulated in the diabetic wounds relative to non- diabetic wounds and have lysosomal hydrolase activity targeting glycosaminoglycans and fucose and sialic acids on glycolipids and glycoproteins.....	141
35.	Graphical representation of glycosylation related genes from Cluster 4 & 5 that are upregulated in the diabetic wounds relative to non- diabetic wounds and are related to O- mucin elongation and glycolipid biosynthesis of isoglobosides and gangliosides.....	142
36.	Graphical representation of glycosylation related genes from Cluster 4 & 5 that are upregulated in the diabetic skin relative to non- diabetic skin and are related to N- glycan biosynthesis and trimming and GPI anchor biosynthesis.....	143
37.	Graphical representation of glycosylation related genes from Cluster 4 & 5 that are upregulated in the diabetic skin and wounds relative to non- diabetic skin and wounds and are related to inactive O- glycosyl hydrolases that act as lectins and the production of polysialic acid.....	144
38.	Glycosylation related genes are differentially regulated in diabetic and non- diabetic wound healing.....	149
39.	Diabetic mice exhibit increased blood glucose, obesity, and delayed wound closure.....	156
40.	Histologic comparison of uninjured skin and wounds 1- and 10-days post- wounding in non- diabetic and diabetic skin.....	157

LIST OF FIGURES (continued)

<u>FIGURE</u>	<u>PAGE</u>
41. Core glycolipid and GM3 ganglioside biosynthesis reactions...	159
42. N-glycosylation profile of high abundance structures in uninjured skin and wounds obtained from diabetic and non-diabetic mice.....	177
43. N-glycosylation profile of low abundance structures in uninjured skin and wounds obtained from diabetic and non-diabetic mice.....	178
44. Expression of glycan m/z2734.6 is downregulated during diabetic more than non-diabetic wound healing.....	185
45. Expression of H ₇ NHex-1F ₄ S1 structures is downregulated in wound healing and upregulated in the diabetic versus non-diabetic condition.....	187
46. Comparison of N- glycan profiles in uninjured skin and wounds from diabetic and non- diabetic mice.....	191
47. Comparison of N- glycan profiles in uninjured skin and wounds from diabetic and non- diabetic mice (continued).....	194
48. Comparison of N- glycan fucosylation in uninjured skin and wounds from diabetic and non- diabetic mice (continued).....	196
49. The relative expression of high/ oligo- mannose structures by mannose # is different in diabetic and non- diabetic skin and wounds.....	199
50. Neutral core 2 O- linked glycans are upregulated in uninjured skin and wounds when compared to non-diabetic samples.....	202
51. Increased fucosylation and decreased sialylation of core 1 & core 2 O-linked glycans in diabetic skin and wounds.....	203

LIST OF FIGURES (continued)

<u>FIGURE</u>		<u>PAGE</u>
52.	Comparison of O- glycan profiles in uninjured skin and wounds from diabetic and non- diabetic mice.....	207
53.	The expression of genes related to polysialyltransferase activity and its correlation with the expression of polysialic acid carrying proteins in skin and tongue wound healing.....	227
54.	The combinatorial expression of all significantly expressed transcript probes related to polysialyltransferase activity a in skin and tongue wound healing.....	233
55.	Expression of polysialic acid, NCAM, and CCR7 in EndoNt proteins during skin and tongue wounds healing.....	234
56.	CCR7 is more highly expressed in skin wounds than uninjured skin and tongue wounds.....	235
57.	735 reactivity to polysialylic acid is observed in uninjured skin, but not wounds and neither express NCAM-140.....	237
58.	Expression of polysialic acid in EndoNT proteins during skin and tongue wounds healing.....	254
59.	Expression of NCAM1 in EndoNT proteins during skin and tongue wounds healing.....	256
60.	Expression of CCR7 in EndoNT proteins during skin and tongue wounds healing.....	258
61.	Housekeeping proteins are not consistently expressed in uninjured tongue, skin, and their respective wounds.....	260
62.	Immunohistochemical staining of polysialic acid and NCAM1 in diabetic (db/db) and non- diabetic (C57) skin and wounds...	266

LIST OF FIGURES (continued)

<u>FIGURE</u>		<u>PAGE</u>
63.	Increased expression of polysialic acid, NCAM1, and NRP2 overlap occurs in the inflammatory phase of non- diabetic wound healing, yet is delayed through the proliferative phase in diabetic wounds.....	268
64.	Glycosylation related gene expression in diabetic and non-diabetic skin and wounds.....	269
65.	Glycosylation related gene expression in diabetic and non-diabetic skin and wounds. (continued).....	270
66.	Glycosylation related gene expression in diabetic and non-diabetic skin and wounds. (continued).....	271
67.	Glycosylation related gene expression in diabetic and non-diabetic skin and wounds. (continued).....	272
68.	Glycosylation related gene expression in diabetic and non-diabetic skin and wounds. (continued).....	273
69.	Glycosylation related gene expression in diabetic and non-diabetic skin and wounds. (continued).....	274
70.	Glycosylation related gene expression in diabetic and non-diabetic skin and wounds. (continued).....	275
71.	Glycosylation related gene expression in diabetic and non-diabetic skin and wounds. (continued).....	276
72.	Glycosylation related gene expression in diabetic and non-diabetic skin and wounds. (continued).....	277
73.	Glycosylation related gene expression in diabetic and non-diabetic skin and wounds. (continued).....	278

LIST OF FIGURES (continued)

<u>FIGURE</u>	<u>PAGE</u>
74. Glycosylation related gene expression in diabetic and non-diabetic skin and wounds. (continued).....	279
75. Glycosylation related gene expression in diabetic and non-diabetic skin and wounds. (continued).....	280
76. Glycosylation related gene expression in diabetic and non-diabetic skin and wounds. (continued).....	281
77. Glycosylation related gene expression in diabetic and non-diabetic skin and wounds. (continued).....	282
78. Glycosylation related gene expression in diabetic and non-diabetic skin and wounds. (continued).....	283
79. Glycosylation related gene expression in diabetic and non-diabetic skin and wounds. (continued).....	284
80. Glycosylation related gene expression in diabetic and non-diabetic skin and wounds. (continued).....	285
81. Glycosylation related gene expression in diabetic and non-diabetic skin and wounds. (continued).....	286
82. Glycosylation related gene expression in diabetic and non-diabetic skin and wounds. (continued).....	287
83. Glycosylation related gene expression in diabetic and non-diabetic skin and wounds. (continued).....	288
84. Glycosylation related gene expression in diabetic and non-diabetic skin and wounds. (continued).....	289
85. Glycosylation related gene expression in diabetic and non-diabetic skin and wounds. (continued).....	290

LIST OF FIGURES (continued)

<u>FIGURE</u>		<u>PAGE</u>
86.	Glycosylation related gene expression in diabetic and non-diabetic skin and wounds. (continued).....	291
87.	Glycosylation related gene expression in diabetic and non-diabetic skin and wounds. (continued).....	292
88.	Glycosylation related gene expression in diabetic and non-diabetic skin and wounds. (continued).....	293
89.	Glycosylation related gene expression in diabetic and non-diabetic skin and wounds. (continued).....	294
90.	Glycosylation related gene expression in diabetic and non-diabetic skin and wounds. (continued).....	295
91.	Glycosylation related gene expression in diabetic and non-diabetic skin and wounds. (continued).....	296

LIST OF ABBREVIATIONS

AGEs	advance glycation end-products
ANOVA	analysis of variance
APS	adenosine 5'-phosphosulfate
Ara	L-arabinose
ATP	adenosine triphosphate
CS	chondroitin sulfate
CSPG	chondroitin sulfate proteoglycan
DM	diabetes mellitus; also references Lepr ^{db/db} mice
DS	dermatan sulfate
EC	endothelial cell
ECM	extracellular matrix
EDTA	ethylenediaminetetraacetic acid
EGF	epidermal growth factor
endo	endoglycosidase
EndoN	catalytically active endo-N-acetylneuraminidase
EndoNt	glutathione sepharose tagged PKIE (inactive) endo-N-acetylneuraminidase trap
exo	exoglycosidase
FGF	fibroblast growth factor
Fru	D- fructose
Fuc	fucose
GAG	glycosaminylglycan
Gal	galactose
GalNAc	N-acetylgalactosamine
GAPDH	glyceraldehyde 3-phosphate dehydrogenase
GH	glycosylhydrolase/ glycosidase
Glc	glucose
GlcNAc	N-acetylglucosamine
GlcUA/ GlcA	glucuronic acid

LIST OF ABBREVIATIONS (continued)

GP	glycoprotein
GT	glycosyltransferase
HA	hyaluronic acid/ hyaluronan
Hex	hexose
HexNAc	N-acetylhexosamine
HS	heparan sulfate
HSPG	heparan sulfate proteoglycans
IdoN	L-idosamine
IdoUA/ IdoA	iduronic acid
IGF	insulin growth factor
IL	interleukin
Kdn	Deaminoneuraminic Acid
KEGG	Kyoto encyclopedia of genes and genomes
KS	keratan sulfate
LLO	lipid linked oligosaccharide
Man	mannose
ManNAc	N-acetylmannosamine
MAPK	mitogen-activated protein kinase
<i>mz</i>	mass-to-charge ratio
Neu	neuraminic acid
Neu5Ac	N-acetylneuraminic acid
Neu5Gc	N-glycolylneuraminic acid
NS	normal (uninjured) skin
PANTHER	protein annotation through evolutionary relationship
PBS	phosphate buffered saline
PDGF	platelet-derived growth factor
PEDF	pigment epithelium-derived factor
PG	proteoglycan

LIST OF ABBREVIATIONS (continued)

PolySia	polysialic acid
Rha	L-rhamnose
Rib	D- ribose
ROUT	robust regression and outlier removal
RT-PCR	reverse transcription polymerase chain reaction
S	skin
SA	sialic acid
SDS	sodium dodecyl sulfate
SEM	standard error of the mean
T	tongue
TGF- β	transforming growth factor β
UV	ultraviolet
VEGF	vascular endothelial growth factor
WT	wild- type, in reference to C57BL/6 line
Xyl	xylose
α	alpha
β	beta

SUMMARY

Wounds develop as a consequence of impaired tissue homeostasis or acute tissue injury. Differential wound healing is studied among tissue and disease specific models to better understand the mechanisms that contribute to each phase of healing and overall wound resolution. Prior studies have identified specific differences in the regulation of cellular, genomic, and proteomic events that occur during each phase of wound healing including hemostasis, inflammation, proliferation, and wound resolution and remodeling. Despite the significant advancements in research, few clinical tools have been established for clinical diagnostics related to wound progression and the clinical treatment of wounds.

As technology and scientific discovery continues to advance, post- transcriptional and post- translational modifications have been identified as a possible important contributor to the regulation of biological processes involved in wound healing. However, little is understood about the how the various subtypes of modifications are regulated over the course of wound healing. Glycosylation is one post- translational modification that has recently been identified as having significant importance in the pathology and clinical diagnostics of cancer development and invasiveness and a host of inflammatory diseases including rheumatoid arthritis.

Glycosylation is an enzymatic process where carbohydrates are added to proteins and lipids to facilitate protein folding, binding, and signaling. Interestingly, most secreted molecules and nearly all membrane proteins/ lipids and extracellular matrix proteins are glycosylated. This process is very different from, yet commonly confused with, the process of glycation, which is sometimes referred to as glucosylation.

SUMMARY (continued)

Glycation is a non-enzymatic process involving the accumulation of advanced glycation end products (AGEs) that is associated with aging, ultraviolet light (UV) exposure, and metabolic disease processes like diabetes associated retinopathy, neuropathy, and wound development. Additionally, dietary AGEs have been found to promote glycation of tissues including the skin and mucosa. While glycation and glycosylation are not related to one another, previous studies have found that increased glycation of retinal microvascular cells leads to alterations in overall glycosylation.

When considering the vast number of proteins and lipid that are glycosylated, changes in overall protein and lipid glycosylation have the potential to significantly impair the function and regulation of growth factors, transmembrane proteins, ECM proteins and signaling molecules that are required for tissue homeostasis and wound healing. To examine the regulation of glycosylation during wound healing, two model systems were used for comparisons. The first model systems examined were that of the skin, which is non- mucosal, and the tongue, which is a mucosal tissue, using BALB/c mice as the animal model. Mucosal tissues are known to heal faster than skin, with a blunted inflammatory response and reduced scar tissue formation. Additionally, healthy mucosal tissues are protected from sun induced glycation. The second model system comparison used was diabetic (C57 Bl/Ks-Lepr^{db/db}) and non- diabetic (C57BL/6) mouse skin. It has been well established that diabetic skin undergoes more tissue breakdown and impaired healing when compared to non-diabetic skin. Additionally, diabetic wounds are associated with an impaired inflammatory response and prolonged time to achieve closure. Since impaired glycosylation has the potential to impair wound healing, it was

SUMMARY (continued)

hypothesized that enzymatic glycosylation would be differentially regulated in uninjured tissue and over the course of wound healing.

The objective of this research was to evaluate the organ specific and disease specific expression of glycosylation- related genes and glycans during wound healing using the skin and tongue as model organs, and diabetes as a model of disease. Furthermore, the aim was to identify whether differential glycosylation trended consistently with the trend of impaired wound healing to suggest a role for alterations in specific types of glycosylation. Mouse excisional skin and tongue wounds were used to provide a reproducible model for wound healing. Differential expression of genes related to glycosylation were measured by re-analysis of GSE23006 microarray data in skin and tongue wound healing, while high-throughput qualitative real- time polymerase chain reaction (HT-qRT-PCR) was utilized to evaluate differential expression in diabetic and non-diabetic wounds. Our results indicate that glycosylation- related gene expression is differentially regulated in skin versus tongue wound healing and diabetic versus non-diabetic wound healing. More specifically, tissues with the impaired healing phenotype, skin compared to tongue and diabetic skin compared to non- diabetic skin respectively, demonstrated considerably higher expression of genes related to: 1) glycosaminoglycan hydrolase and sulfatase activity; 2) polysialylation; and the metabolism and transfer of 3) galactose; 4) fucose; and 5) sialic acid.

To identify whether differences in glycosylation- related gene expression lead to changes in downstream glycosylation, lectin blots were used to probe sialic acids in skin and tongue wounds and glycomics analysis was performed in the diabetic and non-

SUMMARY (continued)

diabetic skin samples. Lectin blotting for the expression of sialic acids in uninjured and wounded skin and tongue identified: 1) decreased α 2,3- linked sialic acids; 2) increased α 2,6- linked sialic acids; and 3) increased α 2,8- linked polysialic acids during the late inflammatory phase of wound healing. Interestingly, the magnitude and pattern of polysialylation, a conserved type of glycosylation occurring on few proteins, could not be directly matched with the expression pattern of any singular protein in the skin, tongue, and wounds. In the diabetic disease model system, uninjured BALBc skin and diabetic skin both displayed enhanced expression of polysialic acid and/or polysialyltransferase related genes at baseline and during wound healing. Additionally, the data provides clues to suggest that baseline expression and time to peak expression of polysialyltransferases and polysialic acid may be important factors in regulating wound healing.

Glycomics analysis of diabetic and non-diabetic skin wounds revealed mass spectroscopy peaks associated with enhanced tri- and tetra- sialylated N- glycans in addition to complex N-glycans containing sialo-fucosylated carbohydrate determinants ($\text{Hex}_{\geq 7}\text{HexNAc}_{\text{Hex}-1}\text{Fuc}_{\geq 4}\text{Neu}_1$) that most likely correspond to fucosylated polylactosamines. Furthermore, the sialo-fucose carbohydrate determinants were found to be more abundant in diabetic skin at baseline and during the inflammatory phase of healing. These findings suggest a role for sialo-fucose carbohydrate determinants in wound healing and further support the gene expression analysis.

Overall this research suggests that polysialylation and sialo-fucose carbohydrate determinants may play an important role in wounding healing. Interestingly these two

SUMMARY (continued)

glycosylation types are associated with E- selectin, an important cellular adhesion molecule. E-selectin ligand (GSLG1/ GLG-1/ ESL-1) is one of few proteins that are known to be polysialylated. Additionally, E- selectin itself binds sialo- fucose carbohydrate determinants on Sialyl Lewis^x structures. While E-selectin itself is promiscuous, other selectins don't bind E- selectin ligands unless they are sulfated. Interestingly, many genes related to sulfatase activity were also upregulated in both models of wound healing. While the relationship of ESL-1 expression was minimally explored, preliminary screenings suggest that it is upregulated in uninjured skin, but not during wound healing. This may suggest that the regulation of carbohydrate determinants plays a more important role during wound healing than the protein expression itself. The relationship between E- selectin, E-selectin ligand and the enhanced regulation of polysialic acid and sialo-fucose carbohydrate determinants will need to be further investigated to elucidate their role in wound healing.

1 INTRODUCTION

1.1 BACKGROUND

1.1.1 Overview of Wound Healing

Wound healing is a complex process composed of 4 stages: 1) Hemostasis; 2) Inflammation; 3) Proliferation; and 4) Remodeling/ Resolution. The four stages overlap in time-sequence and each stage influences the other. The stages are frequently described independently to provide an understandable description of the elements that contribute to successful repair. The overview here particularly focuses on proteins and elements that might be affected by glycosylation.

1.1.1.1 Hemostasis during Wound Healing

Within the first few moments following wounding, pathways mediating hemostasis are activated to minimize blood loss. During primary hemostasis the blood vessels undergo reflexive vasoconstriction to cease blood flow. Expression of von Willebrand factor (vWF) by the sub-endothelium binds Glycoprotein Ib-IX (Gp Ib-IX) expressed on platelets to promote the adhesion of platelets to the site of injury. Exposed collagen fibrils and other extracellular matrix proteins release adenosine triphosphate, alter their surface charge, bind two platelet receptors - platelet glycoprotein VI precursor (GPVI) and $\alpha_2\beta_1$ integrins - and activate the release of inflammatory mediators²⁷⁻²⁸. Following adhesion, platelets accumulate intracellular calcium and express receptors to proteins like thrombin and GpVI which activate phospholipase C β (PLC β) and phospholipase C γ (PLC γ), respectively, to further mediate the intracellular accumulation of free calcium. This calcium accumulation alters platelet morphology and

stimulates the liberation of arachidonic acid and its conversion to thromboxane A₂ (TXA₂) which facilitates vasoconstriction and activates platelets. Activated platelets promote further aggregation to one another via GPIIb/IIIa complex interactions with vWF, fibrin, integrins and P-selectin and undergo degranulation releasing adenosine diphosphate, serotonin, additional platelet activating factors, procoagulant vesicles and stimulate the formation of thrombin ^{28, 30}. This complex set of events help to generate a platelet plug.

In secondary hemostasis, intrinsic and extrinsic pathways mediate the blood coagulation cascade and stabilization of the platelet plug by the deposition and stabilization of fibrin. This phase heavily relies on a complex set of chemical reactions to convert prothrombin into thrombin via the extrinsic pathways. Activation of coagulation factors then facilitates thrombin expansion and activation during the intrinsic pathways where the plasma glycoprotein Fib is converted into fibrin and fibrin crosslinks with Factor XIIIa to produce a stable clot. Once the fibrin clot is stabilized, activated platelets bound to the fibrin matrix contract to reduce the volume of the fibrin clot during tertiary hemostasis ²⁸. These activated platelets concurrently contribute to the initiation of the inflammatory phase of wound healing.

1.1.1.2 Inflammation During Wound Healing

The primary role of the inflammatory phase of healing is to prevent infection and remove non-viable cells and debris. The inflammatory phase is initiated almost instantaneously when injured epithelium release IL-1 α ³⁴ in response to the barrier disruption and platelets release thrombin. IL-1 and thrombin activate injured endothelium to express P-

selectin and E-selectin^{28, 35}. The P-selectins of activated endothelium adhere and “tether” to constitutively expressed ligands (PSLG-1) on neutrophil microvilli and other circulating leukocytes. As a result, circulating leukocytes begin to roll, bringing them in closer proximity to the endothelium. As mentioned above, P-selectins bind PSGL-1, while E-selectin bind PSGL-1, CD44, E-selectin ligand (GSGL1/GLG1/ESL-1).

Leukocytes roll across the endothelium via these interactions. During this time, the binding between selectins and their respective ligands promote leukocytes to exhibit and activate surface integrins including lymphocyte function-associated antigen 1 (LFA-1) and macrophage-1 antigen (Mac-1). LFA-1 ($\alpha_L\beta_2$, CD11a/CD18) and Mac-1 ($\alpha_M\beta_2$, CD11b/CD18) then interact with ICAM-1 and ICAM-2 on endothelial cells to promote firm adhesion of the leukocytes to the endothelial wall³⁵⁻³⁸. Following the integrin dependent adhesion, neutrophils extravasate between adjacent endothelial cells and migrate to sites of injury. Chemoattractants released by platelets and other cells, including CXCL8, CXCL1, and CXCL2, stimulate this extravasation. Once in the wound, neutrophils clear debris and microbes, and release chemoattractants such as CCL2, CCL3, and CCL5 to promote monocyte infiltration to the wound bed³⁹. Once in the wound, monocytes differentiate into macrophages, thereby increasing the population of resident macrophages. In wounds, macrophages phagocytose non-viable cells, foreign bodies, and invading microbial organisms. Platelets, epithelial cells, macrophages and other cell types release growth factors such as platelet derived growth factor (PDGF) to support the deposition of a provisional matrix containing collagen III, fibrin, fibronectin, and hyaluronan. This matrix allows newly proliferating and migrating cells to migrate through the wound bed.

1.1.1.3 Proliferation During Wound Healing

During the proliferative phase of healing epithelial cells, endothelial cells and macrophages release abundant growth factors to promote cell and extracellular matrix (ECM) expansion to granulate and revascularize the tissue. During this time epithelial cells and macrophages release transforming growth factor β (TGF β). TGF β stimulates fibroblast proliferation and the secretion of mature collagen ⁴⁰. Concurrently fibroblasts secrete proteases to degrade the provisional matrix, allowing fibroblasts and newly proliferating endothelial and epidermal cells to migrate across the wound. Each of these cells secretes other vital extracellular matrix proteins including laminin (α , β , and γ chains), integrins ($\alpha 1\beta 1$, and $\alpha 2\beta 1$), fibronectin, collagen (I, III, V, XII, XIV, XVI, and VI), elastin, heparin and heparin sulphate, hyaluronan, and proteoglycans (decorin and versican) ⁴¹. Proliferating epidermal cells migrate across the wound bed to create a barrier from the outside environment. This process has been described to include a large number of factors such as EGF, HB-EGF, TGF- α , HGF, FGF receptor 2 IIIb (FGFR2-IIIb), FGF-7 and -10. Endothelial cells, stimulated by growth factors including HGF, IL-6, and VEGF, proliferate and organize to re-establish blood flow ³⁹.

Among the proangiogenic growth factors in wounds, vascular endothelial growth factor (VEGF), a homodimer glycoprotein secreted by macrophages, endothelial cells, smooth and skeletal muscle cells ⁴², accounts for the majority of the proangiogenic stimulus. VEGF also promotes vasodilation and increased cell membrane permeability to allow the influx of leukocytes and proteins from the blood vessels ⁴³⁻⁴⁵.

1.1.1.4 Remodeling During Wound Healing

The remodeling phase of healing is the final phase of wound healing and involves the maturation and stabilization of the newly formed extracellular matrix, microvasculature, and epithelium. Though this is the last phase of healing, it requires the most time for completion. Furthermore, while remodeling attempts to return the tissue to its original functional state, most adult tissues never fully remodel, and demonstrate residual scarring, decreased functional capacity, elasticity and tensile strength, and increased risk of reinjury. During the remodeling process, chemokines suppress cell proliferation and migration, fibroblasts become contractile, newly formed vessels are pruned, and smooth muscle cells or pericytes structurally reinforce the vessel tubes to form functioning blood vessels ⁴⁶. The epidermal basement membrane is reinforced while the collagen within the ECM undergoes cross-linking. The end result is the restoration of a functional epidermal barrier.

1.1.2 Defining Wound Healing and Differential Responses to Wound Healing

1.1.2.1 Clinical Assessment of Wound Healing

Wounds develop as a consequence of impaired tissue homeostasis and/or acute tissue injury. In order to better understand the factors that contribute to impairments in tissue homeostasis and repair, differential comparisons are made between tissues that exhibit optimal versus suboptimal phenotypes. The broadest means of tracking these changes is via macroscopic records and measuring wound closure. Clinically, a wound whose area is not reduced by 25% within a 4- week period, is suspected to have an impaired healing phenotype⁴⁷. Additional characteristics to impaired healing include

poor hemostasis, increased inflammation, reduced blood flow, and increased scar tissue formation. However, the clinically utilized subjective descriptive terms used to describe these characteristics including erythema, pallor, and fibrotic respectively, don't provide much information regarding the molecular or biochemical cause that is contributing to each impaired healing phenotype.

Though not always clinically feasible, microscopic wound assessments have been able to identify suboptimal healing characteristics including: 1) increased inflammatory cell infiltration; 2) impaired vasculature which may include reduced or excessive vasculature size and/or number, and incompetent/dilated vessels; 3) epithelial hyperproliferation; 4) increased collagen and decreased collagen maturity; 5) increased myofibroblast and smooth muscle actin presence; and 5) specific disease related markers. These markers have been beneficial in helping to assess the pathology and etiology associated with impaired healing. However, it's not feasible or ethical to perform multiple biopsies to track the progression of healing in patients.

1.1.2.2 Differential Wound Healing in Mouse Skin and Oral Mucosa

In order to better understand the pathology of wounds and the progression of wounds throughout the course of healing, animal models are utilized to assess differential wound healing. This may include tissue and disease specific models. One interesting comparison for wound healing is the differential response between cutaneous skin and mucosal tissues. Importantly, previous studies demonstrate that nearly all oral mucosa wounds heal significantly faster than the skin ⁴⁸⁻⁴⁹. In mice, this model comparison allows is readily performed and highly reproducible.

Detailed studies of paired mucosal and skin wound have provided a good picture of how such wounds differ in the healing response. As compared to skin, 1mm tongue wounds achieved histologic re-epithelialization within 0.5 days post- wounding, while skin wounds required an average of 2.5 days to re-epithelialize ¹. Additionally, the oral mucosal has been found to heal with significantly less inflammation than skin. Mucosal wounds exhibit less neutrophil, T-cell, and macrophage infiltration ⁵⁰, and less inflammatory cytokine and chemokine production, including interleukins (IL-1a, IL-1b, IL-6), tumor necrosis factor (TNF-a) ¹ and keratinocyte chemoattractant (KC) ⁵¹. Furthermore, the oral mucosa produces less inflammatory cytokines and monocyte chemoattractants ⁵² than the skin over the time course of healing ¹. The general pattern of differences in mucosal versus skin wounds is depicted in Figure 1. As is shown, the oral mucosa initiates a lower acute inflammatory response to injury and exhibits a blunted inflammatory response. In vitro studies suggest that this is due to a decreased responsiveness to downstream inflammatory signals ^{51, 53}. However, the mechanisms that cause differential expression in response to injury, and those that mediate the oral mucosa's differential response to stimuli are not well understood.

In addition to a differential inflammatory response, the skin and oral mucosa also exhibit differences during the proliferative and remodeling phases of healing. One key difference that is observed during the proliferative phase includes hyperplasia and increased cornification of cutaneous epithelia, which is not observed in most mucosal epithelia ⁵⁴. Another key difference that occurs during the proliferative phase of healing is differential angiogenesis of skin and oral mucosal wounds ⁵⁵. When compared to skin, the oral mucosal demonstrates a well-orchestrated angiogenic response during wound

healing. This is highlighted by reduced vascularity⁵⁵ and expression of angiogenic genes including vascular endothelial growth factor (VEGF)¹, despite having less hypoxia and HIF1 α expression⁵⁶. Lastly the oral mucosa also has an advantage over cutaneous skin during the remodeling phase of healing. During remodeling the oral mucosa demonstrates more efficient resolution and the ability to heal with minimum to no scarring⁵⁷. This is of high importance as scarring limits the functional capacity of a tissue. While heightened inflammatory responses are suggested to propagate enhanced fibrotic phenotypes⁴⁹, it remains inconclusive as to whether the differential scarring in the skin and oral mucosa are exclusively related to the differential inflammatory response.

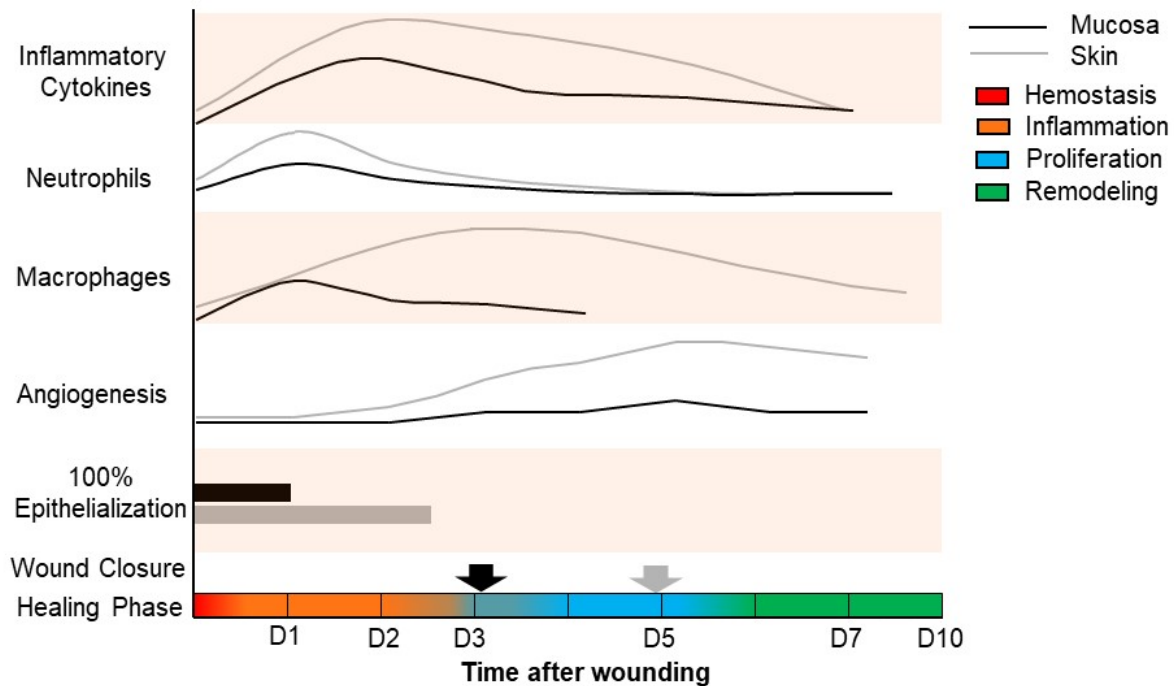


Figure 1. Depiction of wound healing patterns during skin and tongue wound healing. Modified from Chen et al. ¹ the tongue (black) healing faster with less inflammatory cytokines and macrophages when compared to the skin (grey). Each phase of wound healing is mapped by time after wounding. As noted by the gradient change, each phase of wound healing demonstrates some overlap with other phases. Reprinted with permission of the publisher ¹.

Some of the differences between skin and oral mucosal healing have been attributed to the different microenvironments of cutaneous and mucosal epithelia. While oral mucosa epithelia reside in an ultraviolet (UV) light deprived, warm, moist environment apically coated with mucins, apical cutaneous epithelia remain exposed to UV light and air and require very tight junctions between epithelial cells to maintain barrier function and prevent trans-epidermal water loss (TEWL)⁵⁸. Interestingly, both environmental triggers experienced by skin have themselves been linked to impaired healing. UV light exposure has been associated with the accumulation of advanced glycation end products (AGE's) which are known to disrupt tissue homeostasis and

repair by increasing inflammation, decreasing angiogenesis and promoting tissue fibrosis⁵⁹⁻⁶¹. In addition to this, air exposure as opposed to a moist healing environment, has been found to delay tissue repair up to 3-fold and increase scarring⁶²⁻⁶⁴.

While comparisons of the skin and oral mucosa are not directly related to a specific disease process, identifying factors that contribute to their differential inflammatory response, keratinocyte proliferation, angiogenesis, and scarring/ fibrosis can provide insight in establishing the characteristics of regenerative healing versus scar formation.

1.1.2.3 Differential Healing in Diabetic and Non- Diabetic Wounds

Diabetes (DM) is a metabolic disorder characterized by impaired insulin secretion and/ or insulin resistance leading to increased circulating blood glucose (Glc). Diabetes has been associated with the development of multiple comorbidities including cardiovascular disease, nephropathy, neuropathy, and the development of diabetic lower extremity ulcers (DLEU). Common impairments in DM skin and repair include epithelial hyperplasia⁶⁵, decreased epithelial barrier function⁶⁶, increased susceptibility to multi-drug resistant organism coinfections⁶⁷, increased neurogenic inflammation, impaired neutrophil chemotaxis, phagocytosis, adhesion, impaired VEGF regulation⁶⁸, increased arteriole wall/basement membrane thickening, increased collagenase and protease activity, extracellular matrix (ECM) resistance to proteolytic degradation⁶⁹⁻⁷¹, and tissue scarring⁷²⁻⁷³.

Chronic hyperglycemia has been recognized as an initiating factor in the pathology of multiple DM related comorbidities including wound development and oral

mucosal inflammatory conditions ^{65, 67, 69-70, 74-76}. While normalizing blood glucose levels have been found to improve healing outcomes, persons with controlled DM and pre-DM are at continued risk for chronic cutaneous wound development and epithelial infections ⁷⁶⁻⁸⁰.

1.1.2.4 AGE's Impaired Wound Healing and Altered Enzymatic Glycosylation

An important consequence of hyperglycemia is the spontaneous, non-enzymatic glycation of proteins and lipids ⁸¹ leading to the accumulation of advanced glycation end products (AGE). AGE accumulation is also believed to contribute to the diabetes related impairments in healing, as AGEs are known to increase collagen crosslinking ⁸²⁻⁸⁴ and impair normal cell migration, proliferation, adhesion, growth factor expression, and cell signaling ⁸⁵⁻⁸⁸.

While advanced glycation end products (AGE's) have been found to impact multiple biological processes related to tissue homeostasis and repair, no single pathway has been identified as the primary mediator of the downstream changes that occur apart from differences in physical interactions between proteins. One suggested intermediate pathway that has been implicated is that of protein glycosylation.

1.1.3 Glycosylation

1.1.3.1 Defining Glycosylation

In contrast to glycation and AGE accumulation, glycosylation is a normal enzymatic protein and lipid modification that is required for proper protein folding and cellular function³⁶. There are six types of normal enzymatic glycosylation, which includes N-

linked, O- linked, glypiation, C- mannosylation (C-type), phosphoglycosylation, and sulfo-glycosylation. The most commonly examined forms of glycosylation are N- linked and O-linked glycosylation. Examples of mammalian glycosylation reactions published in a review by Moremen et al. ²¹ are shown in Table I and Figure 2.

1.1.3.2 Substrates Involved in Glycosylation

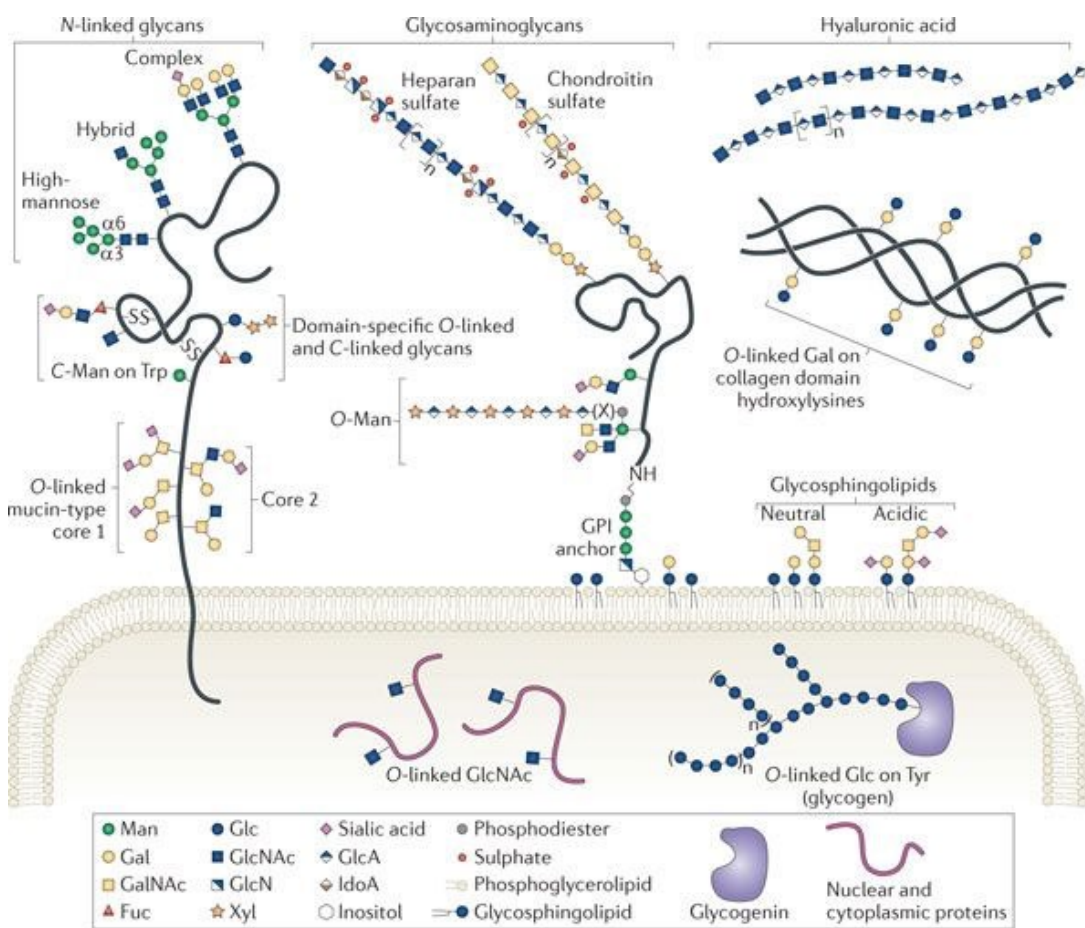
The process of glycosylation first requires monosaccharide biosynthesis or processing via metabolic pathways. These monosaccharides contribute to the formation of nucleotide sugars containing the following sugar-nucleotide pairings: 1) Uridine diphosphate (UDP) attached to glucose (Glc), galactose (Gal), N- acetylglucosamine (GlcNAc), N-Acetylgalactosamine (GalNAc), glucuronic acid (GlcA), or xylose (Xyl); 2) Guanosine diphosphate (GDP) attached to mannose (Man) or fucose (Fuc); or 3) Cytidine-5'-monophosphate (CMP) attached to sialic acid (Sia) which is most commonly in the form of N-acetylneuraminic acid (Neu5Ac) or N-glycolylneuraminic acid (Neu5Gc). These nucleotide sugars become donors that are transported by solute carriers into the Golgi apparatus (Golgi) or endoplasmic reticulum (ER), along with adenosine triphosphate (ATP), and 3'-phosphoadenosine-5'-phosphosulfate (PAPS), which are used for carbohydrate and protein sulfation. Interestingly, this process is competitively inhibited by nucleoside accumulation in the cytosol and overall nucleotide availability, but not the actual carbohydrate itself. Upon transport into the Golgi and ER, monosaccharides are transferred from the nucleotide sugars either co- or post-translationally to proteins and lipids by glycosyltransferases.

TABLE I.
CONSENSUS MOTIFS AND ENZYMES RESPONSIBLE FOR VARIOUS
GLYCOSYLATION REACTIONS^b

Type	Linkage	Enzyme	Consensus sequence	Domain	Examples
N-glycosylation	GlcNAc- β -Asn	OST	N-X-(S/T) ^b (standard sequons)		Nascent polypeptides
			N-X-C ^{b,c} , N-G ^c , N-X-V ^{b,c} (non-standard sequons)		
O-glycosylation	GalNAc- α -Ser/Thr	ppGALNTs	Isoform specific ^d		Mucins
	GlcNAc- β -Ser/Thr	OGT	No set consensus ^e		Cytosolic, nuclear proteins
	GlcNAc- β -Ser/Thr	EOGT	Unknown	EGF	Notch, Dumpy
	Xyl- β -Ser	XYLT1, XYLT2	a-a-a-a-G-S-G-a-(a/G)-a ('a' represents Asp or Glu) ^f		Heparin, proteoglycan core proteins
	Fuc- α -Ser/Thr	POFUT2	C-X-X-(S/T)-C-X-X-G	TSR	Thrombospondin, ADAMTS family
		POFUT1	C2-X-X-X-X-(S/T)-C3	EGF	Notch, clotting factors
	Glc- β -Ser	POGLUT1	C1-X-S-X-(A/P)-C2	EGF	Notch, clotting factors
	Man- α -Ser/Thr	POMT1, POMT2	I-X-P-T-(P/X)-T-X-P-X-X-X-X-P-T-X-(T/X)-X-X ^g		α -dystroglycan
	Gal- β -Hyl	GLT25D1, GLT25D2	X-Hyl-Gly (collagen repeats) ^h		Collagen, adiponectin
	Glc- α -Tyr	GYG	Tyr194 of GYG ⁱ		GYG (autoglycosylation during glycogen formation)
C-mannosylation	Man- α -Trp	Unknown	W-X-X-W ^j	TSR	Thrombospondin, ADAMTS family
Glypiation	Pr-C(O)EthN-6-P-Man	Transamidase	No set consensus ^k		THY1, NCAM1

TABLE I.**CONSENSUS MOTIFS AND ENZYMES RESPONSIBLE FOR VARIOUS GLYCOSYLATION REACTIONS CONTINUED^a**

^aReferences provided in the text except where noted. ^bX cannot be Pro. ^cDetermined by high-throughput proteomic analysis of lectin-enriched glycopeptides ⁷. Other non-standard sequons have been observed for recombinant immunoglobulin G2 antibodies expressed in Chinese hamster ovary cells ⁸ or mouse laminin¹¹, but these structures have not been confirmed more widely in animal systems. ^dVariation in ppGALNT specificities was determined empirically ¹³. ^ePrediction software available from the [YinOYang WWW server](#) ¹⁶. ^fThe specificity for the initiation of proteoglycan core synthesis is defined empirically ¹⁷. ^gProposed consensus ¹⁸ with variable support from mass spectrometry analysis ¹⁹. ^hCollagen domains are modified at Lys residues to form hydroxylysine (Hyl) and galactosylated, then they are extended with an α 1,2-Glc residue prior to triple helix formation ²⁰. ⁱAutoglucosylation and extension of the initial glycogen polymer on the glycogenin backbone occurs on the Tyr194 hydroxyl group ²⁵. ^jMannose linked to the C2 of the indole ring of the tryptophan residue based on the corresponding consensus sequence ²⁹. ^kPrediction of consensus sequence has been defined based on hidden Markov model and prediction software ³². ADAMTS, a disintegrin and metalloproteinase with thrombospondin motifs; EOGT, EGF domain-specific O-linked GlcNAc transferase; GLT25D1/2, glycosyltransferase 25 family member 1/2; GYG, glycogenin; NCAM1, neural cell adhesion molecule 1; OGT, O-linked GlcNAc transferase; OST, oligosaccharyltransferase; POFUT, protein O-fucosyltransferase; POGLUT, protein O-glucosyltransferase; POMT, protein O-mannosyltransferase; ppGALNTs, polypeptide GalNAc transferases; TSR, thrombospondin type 1 repeat; XYLT, xylosyltransferase. Reprinted with permission of the publisher ²¹.



Nature Reviews | Molecular Cell Biology

Figure 2. Major classes of vertebrate glycan structures

Figure 2. Major classes of vertebrate glycan structures. Most glycans on membrane and secreted proteins are found in N-linkage to Asn or in O-linkage to Ser/Thr. N-linked glycans that have undergone minimal mannosidase processing are called 'high-mannose' glycans. Addition of N-acetylglucosamine (GlcNAc) to the $\alpha 3$ arm of an acceptor containing five Man residues produces a hybrid glycan³⁻⁴. Hybrid glycans can be extended on the $\alpha 3$ arm with galactose (Gal), N-acetylgalactosamine (GalNAc), fucose (Fuc) and sialic acid (SA). Further processing of hybrid glycans produces complex glycans, which can also be decorated with Gal, GalNAc, Fuc and SA. Glycosaminoglycans (GAGs) are O-linked glycans initiated by a conserved tetrasaccharide (GlcA- $\beta 1,3$ -Gal- $\beta 1,3$ -Gal- $\beta 1,4$ Xyl- β) and classified by the composition of their disaccharide repeat. GAG chains can be post-synthetically modified by sulphation and epimerization (GlcA conversion to IdoA), producing substantial heterogeneity¹⁰. Glycoproteins carrying one or more GAG chains are called proteoglycans, and can be secreted or transmembrane or glycosylphosphatidylinositol (GPI)-anchored. Hyaluronic acid, a GAG-like polymer of the extracellular matrix, is the only glycan that is not linked to a protein or lipid¹⁵. Other O-linked glycans are classified by their initiating monosaccharide. Addition of GalNAc to Ser/Thr initiates mucin-type O-linked glycans. Extension with Gal, GlcNAc or GalNAc produces eight different core structures²². For example, addition of a branching GlcNAc to a core 1 disaccharide (Gal- $\beta 1,3$ -GalNAc) produces core 2. Man initiates another class of O-linked glycan (O-Man glycans). A subset of O-Man glycans are extended with a repeating disaccharide — (-3-Xyl- $\alpha 1,3$ -GlcA- β -)_n — in phosphodiester linkage to an incompletely defined bridging moiety (X)²³⁻²⁴. Two types of O-linked Fuc glycan and one type of O-linked Glc glycan can be added to specific Cys-rich domains, as well as C-Man residues on Trp side chains²⁶. O-linked GlcNAc is found on the extracellular domains of some proteins and on numerous cytosolic and nuclear proteins, but different enzymes mediate extracellular and nucleocytoplasmic O-GlcNAcylation³¹. O-linked glycan structures attached to other amino acids include Gal on hydroxylysine of collagen domains that is extended by the addition of an $\alpha 1,2$ -Glc residue and the addition of a Glc on Tyr of glycogenin that is extended and branched with additional Glc residues to form glycogen^{20, 25}. In addition to proteins, sphingolipids can be modified by glycosylation. Eukaryotic cell surfaces are enriched in glycosphingolipids, which are ceramide-linked glycans that can be capped and branched with Fuc and SA³³. Reprinted with permission of the publisher²¹.

1.1.3.2.1 N- Linked Glycosylation

For N- linked glycosylation, a lipid linked oligosaccharide (LLO) is first synthesized by the addition of 2 GlcNAc, 9 mannose, and 3 glucose residues to dolichol embedded in the ER membrane. The LLO serves as a donor for the oligosaccharyltransferase (OST), a complex of proteins that transfers the $\text{Glc}_3\text{GlcNAc}_2\text{Man}_9$ oligosaccharide from the LLO to the side chain of an asparagine (Asn) in the Asn-X-Ser/Thr consensus sequence of a translating or newly synthesized protein (Figure 3). Glycosylhydrolases, which catalyze the removal of carbohydrates and glycan moieties, then remove the 3 glucoses and 2 mannoses. If the protein is properly folded, then it is transported to the Golgi where its oligosaccharides undergo further trimming and maturation/capping. However, if it is not folded properly, a specialized enzyme re-glucosylates the oligosaccharide allowing recognition and binding by the lectin chaperones, calreticulin and calnexin. If the protein remains unfolded even after 2 mannoses are removed from the new oligosaccharide, other chaperones direct the protein across the ER membrane for destruction by the proteasome (Figure 4) ^{21, 36}.

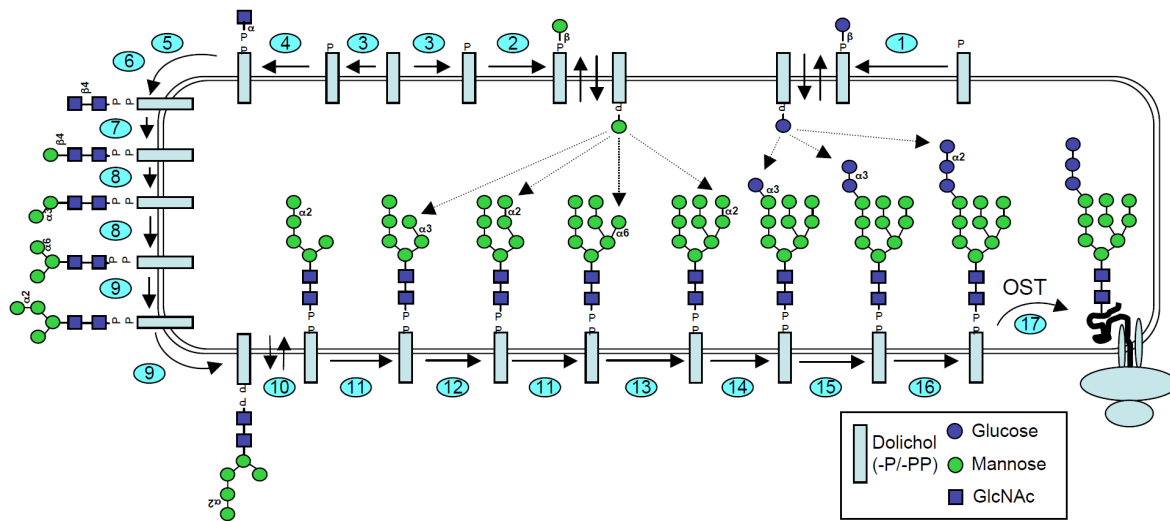


Figure 3. N-glycan lipid-linked oligosaccharide processing reactions.

Synthesis and transfer of LLO and glycan transfer during N-linked glycosylation. Additionally, the OST complex in step 17 is comprised of STT3A, STT3B, DDOST, TUSC3, and MAGT1. Reprinted with permission of the publisher ².

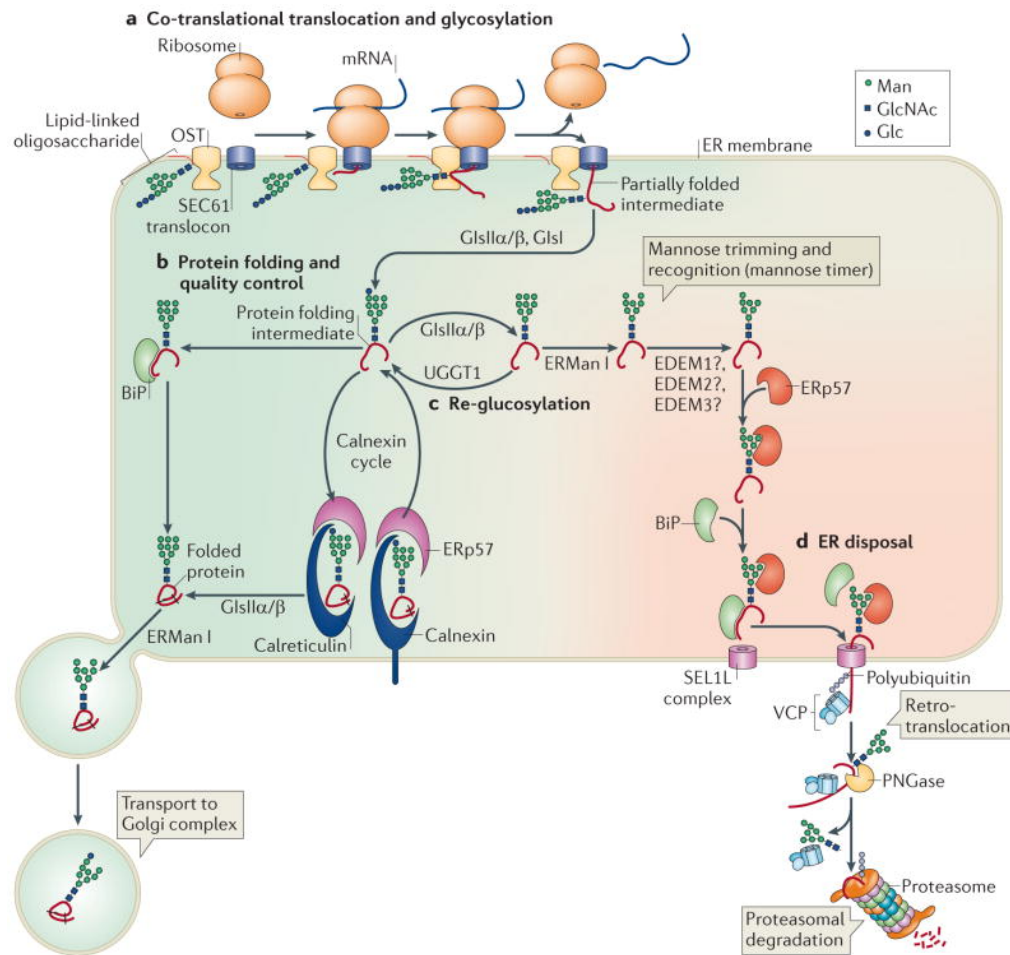


Figure 4. Protein N glycosylation and quality control of protein folding.

Figure 4. Protein N glycosylation and quality control of protein folding.

a | During glycoprotein biosynthesis, the translation of nascent polypeptides is followed by their translocation through the SEC61 pore and the simultaneous transfer of a glycan from a lipid-linked intermediate to peptide acceptor sequons by the oligosaccharyltransferase (OST). One cleft in the STT3 subunit of OST scans for Asn-X-Ser/Thr acceptor sequons, while an adjacent cleft binds the glycan donor. **b** | Glycan trimming through Glc removal occurs immediately after transfer by α -glucosidase I (GlsI) and the α -glucosidase II α - β heterodimer (GlsII α / β). Folding intermediates containing Glc1Man9GlcNAc2 structures are ligands for the lectins calnexin or calreticulin, which function in complex with ERp57. Dissociation from the lectins is followed by further Glc cleavage. Additional chaperone assistance is provided by the ATP-driven chaperone BiP (also known as GRP78). Correctly folded glycoproteins are packaged for transport to the Golgi. **c** | Incompletely folded glycoproteins are recognized by the folding sensor UDP-Glc:glycoprotein glucosyltransferase (UGGT1). They are then re-glucosylated through the addition of a Glc residue back to the glycan structure and are reintegrated into the calnexin cycle. **d** | Terminally misfolded glycoproteins are subjected to endoplasmic reticulum (ER) disposal by Man trimming (through the activity of ER α -mannosidase I (ERManI) or GolgiManIA, GolgiManIB and GolgiManIC (not shown), followed by the activity of ER degradation-enhancing α -mannosidase-like 1 (EDEM1), EDEM2 and EDEM3 (which are homologues of Htm1 (also known as Mnl1) in yeast)). The trimmed glycans bind the ER lectins OS9 or XTP3B (not shown) and are translocated into the cytosol via a complex of derlin 1 (DER1), DER2 and DER3 (the SEL1L complex; Hrd3 in yeast) using the driving force of the cytosolic ubiquitin binding protein and ATPase functions of valocin-containing protein (VCP; also known as TER ATPase; known as Cdc48, Ufd1 or Npl4 in yeast). The peptide is deglycosylated by a cytosolic PNGase and degraded by the proteasome ¹². Reprinted with permission of the publisher ²¹.

1.1.3.2.2 O- Linked Glycosylation

The most common forms of O-linked glycosylation occur via the addition of a single GalNAc or GlcNAc monosaccharide to a serine or threonine residue in a secretory pathway protein. Other forms of O-glycosylation include the addition of a single GlcNAc, Fuc, Man or Glc to a serine or threonine or a single Gal to a hydroxyproline residue in a protein. These glycans are often referred to as either having a GalNAc core, non-GalNAc core, or a GlcNAc core. Upon maturation and capping these structures are referenced by their core presentation and/or the presence of charged and uncharged terminal monosaccharides as described below ⁸⁹. O-GalNAc structures are made by the addition of N-acetylgalactosamine from UDP-GalNAc to serine or threonine residues by a family of enzymes, the UDP-GalNAc:polypeptide N-acetylgalactosaminyltransferases or ppGALNTs ⁹⁰. From the base GalNAc, there are 7 additional core structures synthesized that are identified based on their capping and are commonly observed on mucins (Figure 5). GalNAc's helps to mediate the innate and adaptive immune response by binding to selectins and galectins, contribute to protein conformation and peptide epitope exposure, and synthesizes mucins to help provide a barrier to microbial organisms ⁹⁰.

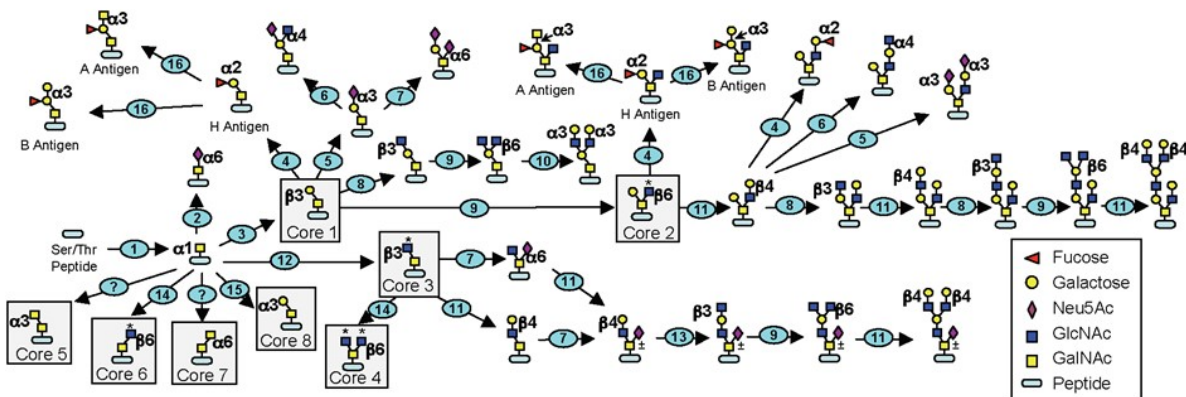


Figure 5. GalNAc (mucin-type) core synthesis and branching reactions. Synthesis of O- GalNAc and the formation of core1-7 structures during O- linked glycosylation. Reprinted with permission of the publisher ².

1.1.3.3 Terminal Glycans and Nomenclature

Upon maturation, the N- and O- linked glycans are capped by a terminal monosacchrides and can be categorized based on the: 1) complexity of their core structure (oligomannose, hybrid or complex bi-, tri-, tetra- antennary, bisecting for N-linked glycans); 2) the presence of a fucose on the core structure (core fucosylated); 3) presence of uncharged terminal monosaccharides including galactose, glucose, GalNAc, or GlcNAc (neutral or galactosylated, glucosylated, GalNAcylation, or GlcNAcylation respectively); or 4) the presence of charged terminal monosaccharides including sialic acids or fucose (sialylated, fucosylated) ^{36, 89}. Furthermore, when these charged terminal monosaccharides are clustered, they are considered di-, oligo- or polysialylated/ fucosylated. In standard nomenclature di- refers to 2 monosachrides, oligo- refers to 3-8, and poly- refers to >8, however, polyfucosylated structures are typically referenced when there are >2 fucose residues. Polysialylation involves the addition of long chains of α 2,8-linked sialic acid (>8; PolySia) to terminal positions of N-linked and

O-linked glycans ¹⁴. Polysialylation is a unique type of glycosylation found on a small number of proteins including neural cell adhesion molecule (NCAM-1), neuropilin 2 (NRP2), synaptic cell adhesion molecule 1 (SynCAM-1, CADM1), E-selectin ligand-1 (ESL-1, GSLG, GLG1), and others ⁹¹. PolySia is highly expressed during development and during times when cell migration is essential, such as during tissue regeneration and cancer metastasis ^{14, 92-94}.

Some N- and O- linked glycans have additional nomenclature that is referenced by their function, location, composition or source that they were first identified. Some commonly utilize structures and nomenclature include: 1) repeats of galactose and GlcNAc with a β 1-3 linkage (Gal β 1-3GlcNAc) referred to as type 1, N-acetylactosamine (LacNAc); 2) repeats of galactose and GlcNAc with a β 1-4 linkage (Gal β 1-4GlcNAc) referred to as type 2, LacNAc; 3) repeats of GalNAc and GlcNAc with a β 1-4 linkage (GalNAc β 1-4GlcNAc) referred to as N-acetyl, N-acetylactosamine (LacdiNAc). Additional features and nomenclature categorized as blood groupings can be found in Table II along with some associated glycoproteins and glycolipids. Interestingly, for a long time it was assumed that these blood groupings had no distinguishable impact on physiology, however, colonizing bacteria and fungi carry antigens identical to A and B blood groups, and recent evidence suggests that infection and cancer susceptibility are associated with blood group status. Additionally, the Lewis blood groups play a critical role in signaling of C- type lectins such as E-, P-, and L- selectins³⁶.

TABLE II.
TABLE OF COMMON GLYCAN STRUCTURES & FEATURES

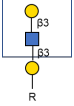
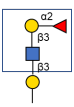
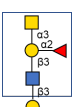
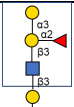
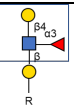
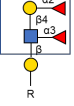
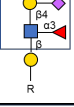
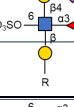
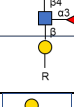
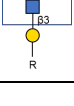
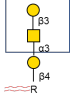
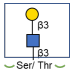
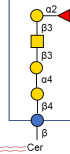
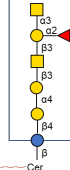
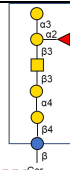
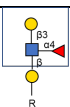
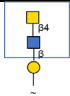
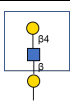
Name	Structure	Composition	Identified cell/ molecular location	Common glycan type/ pathways	Common Features
LacNAc, type 1		Gal β 1-3GlcNAc	Mucosal epithelia (GI, reproductive)	O- > N- glycoproteins/ glycolipids;	Sialylated, fucosylated, or sulfated; Blood group determinants
H antigen		(Fuc α 1-2)Gal β 1- 3GlcNAc	Mucosal epithelia (GI, reproductive, respiratory, exocrine and salivary glands); Milk	O- > N- glycoproteins/ glycolipids;	H antigens form ABO blood groups
A antigen		GalNAc α 1-3(Fuc α 1- 2)Gal β 1-3GlcNAc	Erythrocytes, mucosal epithelial, endothelial cells	N- > O- glycoproteins/ glycolipids; Membrane and secreted glycoproteins and glycolipids, free glycans	A blood group
B antigen		Gal α 1-3(Fuc α 1-2)Gal β 1- 3GlcNAc	mucosal epithelial	“ “	B blood group
Lewis x (Le ^x)		Gal β 1-4(Fuc α 1- 3)GlcNAc			
Lewis y (Le ^y)		(Fuc α 1-2)Gal β 1- 4(Fuc α 1-3)GlcNAc			
Sialyl Lewis x (SLe ^x)		NeuAc/NeuGc α 2- 3Gal β 1-4(Fuc α 1- 3)GlcNAc			
6-Sulfo Lewis x (6-Sulfo-Le ^x)		NeuAc2-3Gal β 1-4 (Fuc α 1-3)(SO4- 6)GlcNAc			
6'-Sulfo Sialyl Lewis x (6'-Sulfo-SLe ^x)		NeuAc2-3(SO4-6)Gal β 1- 4 (Fuc α 1-3)GlcNAc			
LacNAc, type 2		Gal β 1-4GlcNAc	Erythrocytes, Epidermis		Sialylated, fucosylated, or sulfated. Blood group determinants
H antigen		(Fuc α 1-2)Gal β 1- 4GlcNAc	epidermis	N- > O- glycoproteins/ glycolipids;	
A antigen		GalNAc α 1-3(Fuc α 1- 2)Gal β 1-4GlcNAc	Epidermis, erythrocytes, endothelial cells	N- > O- glycoproteins/ glycolipids; free glycans	Membrane and secreted glycoproteins and glycolipids
B antigen		Gal α 1-3(Fuc α 1-2)Gal β 1- 4GlcNAc	Epidermis		

TABLE II. (continued)
TABLE OF COMMON GLYCAN STRUCTURES & FEATURES

Name	Structure	Composition	Identified cell/ molecular location	Common glycan type/ pathways	Common Features
LacNAc, type 3			Mucin specific	Glycolipid associated	
				Mucin Associated	
H antigen		(Fuc α 1-2)Gal β 1-3GalNAc	mucins	O-glycan and glycolipids	H antigens- form ABO blood groups.
A/B antigen		GalNAc/Gal α 1-3 (Fuc α 1-2)Gal β 1-3GalNAc	Mucins (GI)	O-glycan and glycolipids	
LacNAc, type 4			Glycolipid/ ceramide		
H antigen		(Fuc α 1-2)Gal β 1-3GalNAc β 1-3Gal α 1-4Gal β 1-4Glc β -Cer	erythrocyte glycolipids	Mucin associated ceramide glycolipids	
A antigen Globoseries Glycolipid		GalNAc α 1-3(Fuc α 1-2)Gal β 1-3GalNAc β 1-3Gal α 1-4Gal β 1-4Glc β -Cer		Mucin associated ceramide glycolipids	
B antigen		Gal α 1-3(Fuc α 1-2)Gal β 1-3GalNAc β 1-3Gal α 1-4Gal β 1-4Glc β -Cer	erythrocyte glycolipids	Mucin associated ceramide glycolipids	
Lewis a (Le ^a)		Gal β 1-3(Fuc α 1-4)GlcNAc			
LacdiNAc		GalNAc β 1-4GlcNAc	Kidney epithelial cells		α 2-6-sialylated
poly-LacNAc		[β 1-4Gal β 1-4GlcNAc β 1-] _n	Mucin glycoproteins	Multi-antennary N-glycans > core 2 O-glycans	On β 1-6GlcNAc; sialylated, fucosylated, or sulfated; Binds galectins with high affinity at internal and terminal Gal.
			Keratan sulfate	6-O-sulfated;	Not recognized by galectins.
I and i antigens (branched and unbranched poly-LacNAc)		[β 1-4Gal β 1-4GlcNAc β 1-] ₃ ; up to [β 1-4Gal β 1-4GlcNAc β 1-] ₂ on each of the first 2 LacNAc	Embryonic erythrocytes, erythrocytes during erythropoiesis	N- and O-glycans or glycolipids	
A/B/H				Poly-glycosyl-ceramides or macro-glycolipids	
Sialyl Tn antigen		NeuAc/NeuGc α 2-6GalNAc α -	Mucins	O- linked	

1.1.3.4 Function and Roles of Glycosylation

Glycosylation is a critical process that is necessary to expand the diversity of proteins and regulatory processes necessary for survival. Some of the molecular roles and functions that are regulated by glycosylation include protein transit, chaperoning and selective protein targeting, surveillance of the innate and adaptive immune systems, hormone actions, and cytosolic and nuclear protein functions. While many of these regulatory effects of glycosylation are directly related to the interactions between carbohydrate determinants and their respective carbohydrate binding moieties and lectins, some effects are mediated by competing with other post-translational modifications. This is observed in the interplay between O-GlcNAcylation and phosphorylation. O-GlcNAcylation plays roles in cell division, metabolism, and cell signaling. The glycosyltransferase OGT has been found to add O-GlcNAc residues on all serines and threonines with a consensus sequence of (S/T)P(V/A/T)(gS/gT)(X-P) (lacking proline) that would otherwise be phosphorylated by serine/threonine kinases as long as P-3 is not phosphorylated. With both PTM's being dynamically regulated, the interplay between O-GlcNAcylation and phosphorylation has the potential to robustly impact cell signaling. Indeed, it has been established that one modification competitively inhibits the other and that there are several situations where cell signaling is regulated via cross talk between phosphorylation and O-GlcNAcylation at these consensus sites

95-96

Since glycosylation impacts the structure and function of proteins and lipids, affecting basic molecular functions and biological processes vital for host survival, it has the potential to significantly impact homeostasis, disease processes, and regeneration if

mis-regulated. Though the promiscuity of many enzymes involved in glycosylation help to curtail some of the changes that can occur when a single enzyme is impaired, mis-regulation at multiple levels or across multiple enzymes, which occurs during disease processes, can significantly impact critical processes including the regulation of inflammation.

1.1.3.4.1 Role of Glycosylation in Inflammation

Glycosylation has been observed to have a substantial role in regulating inflammatory mediators and their responses. When examining overall glycosylation-related changes during the inflammatory process, reduced fucosylation and increased sialylation have been reported to occur in the first 24 hours after an induced acute inflammatory peritonitis ⁹⁷. While it is probable that this altered glycan abundance is the result of global changes in glycosylation, it may be the result of changes in protein abundance and/ or changes that are necessary for cells to transition between peripheral and local circulation.

One highly abundant protein involved in humoral immunity that is important for pathogen elimination is immunoglobulin G (IgG). Under normal conditions IgG is heavily glycosylated, with the constant, or Fc, region containing primarily neutral oligosaccharides and the Fab, or antigen binding, regions being more sialylated (~15-20% in human IgG)⁹⁸⁻¹⁰⁰. Previous studies suggest that galactosylation of serum IgG enhances complement dependent cytotoxicity that is mediated by antibody, while the absence of fucose- containing carbohydrate determinants on the CH2 domain of IgG

enhances antibody dependent cytotoxicity ¹⁰¹. Furthermore, α 2,6- sialylation of the Fc region has been suggested to protect against enhanced inflammation ¹⁰².

When examining selectin- and interleukin dependent inflammatory responses, the binding affinity and availability of targeted carbohydrate determinants has demonstrated importance in mediating downstream protein expression and signaling. Most interleukins have lectin-like activity, and have been observed to have R-type carbohydrate binding domains³⁶. Additionally, IL-1 α / β , IL-1, IL-4, IL-6, and IL-7 have differing carbohydrate determinants which likely regulates their differential signaling¹⁰³. The carbohydrate determinants for each interleukin is listed follows: 1) IL-1 α binds to biantennary α 2,3-di-sialylated type- II LacNAc's of N-glycans; 2) IL-1 β binds the ganglioside GM4 (Neu5Ac α 2–3Gal β 1-Cer) containing long-chain bases; 3) IL-4 binds to the 1,7 intramolecular lactone of Neu5Ac on sialo-fucosylated structures (Hex₅HexNAc₄Fuc3S_x); 4) IL-6 binds HNK-1-like epitopes of N- and O-linked glycans ((OSO₃) α 1-3GlcA β 1-3Gal β 1-4GlcNAc); and 5) IL-7 binds the sialyl-Tn antigen¹⁰³. In some cases, the presence of glycans on carbohydrate binding proteins, and the availability of their carbohydrate determinants, can impact the inflammatory response. This has been observed in IL-1, as previous studies demonstrate that N- linked glycosylation is required for IL-1 to stimulate the upregulation of E-selectin ¹⁰⁴.

Selectins are C-type lectins that generally recognize sialo-fucose determinants on sialyl Lewis^x (sLe^x) ^{36, 103, 105} carbohydrate structures and are involved in inflammation and leukocyte homing ^{37, 106}. P-selectin and E-selectin are expressed by endothelial cells stimulated during the inflammatory process, and recognize carbohydrate ligands on proteins expressed by circulating leukocytes. This allows the

initial slow rolling of leukocytes along the endothelium and supports their extravasation into injured tissue. L-selectin is expressed on leukocytes and binds its carbohydrate ligands on proteins expressed by endothelial cells lining the blood vessels, facilitating their entry into tissues. An example of L-selectin function is mediating the transit of naïve lymphocytes from the bloodstream into secondary lymphoid organs, like the lymph node ¹⁰⁷.

While all three selectins bind the sialo-fucose determinant of the sLe^x structure, there are subtle differences in their specificity. P-selectin binds P-selectin glycoprotein ligand-1 (PSGL-1), a protein that is not only modified by sLe^x carbohydrate structures, but also contains three sulfated tyrosine residues that are essential for P-selectin binding. L-selectin binds preferentially to 6-sulfo-sLe^x carbohydrate structures as well as a variety of other ligands. E-selectin binds to the sLe^x structures on PSGL-1, L-selectin ligands, on E-selectin ligand 1 (GSLG1/GLG1/ESL-1), and to sLe^x or sialyl Lewis^a (sLe^a) on lactosylceramides and leukosialin ³⁵. Unlike the promiscuous E-selectin, P-selectin and L-selectin do not bind with the carbohydrate determinants that are bound by E-selectin as they require proper sulfation of either protein or carbohydrate for proper binding ³⁷. Both P-selectin and L-selectin also bind HNK-1 epitopes of O- glycans ^{36, 103, 105}.

A unique characteristic specific to E-selectin ligand (GSLG1/GLG1/ESL1) is its ability to be polysialylated. ESL-1 is a substrate for the polysialyltransferase, ST8Sia-IV (*ST8SIA4*) ⁹¹⁻⁹². In microglia and THP-1 macrophages cells, polysialylated ESL-1 is retained in the Golgi under normal condition, however it is translocated to the cell surface and undergoes ectodomain shedding upon proinflammatory LPS stimulation ¹⁰⁸.

This LPS induced shedding has been similarly observed for polysialylated NRP-2 in these cells ¹⁰⁸⁻¹⁰⁹. This process has been determined to be restricted to proinflammatory stimuli as it does not occur with anti-inflammatory, IL-4 activation. Furthermore, in this study the shedded/soluble polySia-modified proteins were found to reduce LPS induced production of nitric oxide (NO) and reduce TNF α and IL-1 β mRNA levels ¹⁰⁸.

1.1.3.4.2 Contribution of Glycosylation to Wound- Related Processes

Glycosylation is critical for appropriate protein and cellular function, and impaired glycosylation is linked to several disease states. Not surprisingly, a few studies show that appropriate enzymatic glycosylation is critical to tissue homeostasis and wound healing. For example, ceramide glycosyltransferases, including B4galnt ¹¹⁰, St8Sia1/B4galnt1, Ugcg ¹¹¹, and some GPI anchor proteins including PigA ¹¹² are important in maintaining normal epidermal homeostasis, with perturbations leading to significant impairments in skin barrier function and wound healing ¹¹²⁻¹¹⁵. Additionally, an *in vivo* study of corneal wounds revealed changes in the expression of the glycosyltransferases responsible for sialylation, galactosylation, and N-acetylglycosaminyl glycan branching during healing ¹¹⁶⁻¹²⁴. Changes in glycan branching during glycosylation can influence the signaling of carbohydrate binding receptors including Galectin- 3/AGE-R3 ¹²⁵, which mediates wound re-epithelialization ^{117, 119-122} and immune modulation ^{121, 124, 126}. When Galectin-3 (Gal-3) binds B- galactoside (Galbeta1-4GlcNAc)(n) ¹²⁷ carbohydrate determinants, including the internal N-acetyllactosamine (LacNAc) of poly-N-acetyllactosamine (poly(LacNAc)) ¹²⁷, it induces increased caspase-3-ERK mediated T- cell apoptosis¹²⁸. However, Gal-3 also reduces ERK mediated apoptosis in injured

keratinocytes¹²⁹ and binds polylactosamines¹³⁰ on CD-147 to promote MMP9 mediated destabilization of the adherens and junction to promote enhanced migration¹³¹. When bound to its carbohydrate determinant, Galectin-7 decreases cell junction protein expression, impairs epithelial adherence and migration¹³², and induces caspase-3 mediated cell apoptosis¹³²⁻¹³⁴.

As previously discussed, glycosylation plays an important role in the inflammatory response, but it also plays an important role in the regulation and function of growth factors involved in wound healing including VEGF, PDGF, and IGF. Furthermore, growth factor receptors bind and/ or require specific carbohydrate determinants to modulate growth factor signaling. This was previously reviewed by Ferreira & Dall'Olio et. al¹³⁵.

Mounting evidence also exists for the role of polysialic acid in neuronal/ axonal regeneration, cancer development and metastasis, T-cell regulation, FGF-2 mediated cell growth, and inflammation.^{91-92, 108-109, 136-144}. Though the evidence is limited, polysialic acid has been demonstrated to play a role in mediating the transition between circulating and peripheral monocytes and may play a role in fibrosis^{108, 144}

Lastly, protein glycosylation is required for the synthesis of several cutaneous extracellular matrix (ECM) proteins that are important for wound healing including collagen IV, whose glycans mediate its macrophage induced endocytosis via mannose receptor-mediated pathways¹⁴⁵⁻¹⁴⁸.

1.1.3.4.3 Glycosylation in Disease Processes

Impaired glycosylation is linked to several disease states including cancer metastasis, inflammatory lung conditions¹⁴⁴, rheumatoid arthritis, and diabetes. In rheumatoid arthritis, under-galactosylation of serum IgG has been associated with the disease. Pulmonary¹⁴⁹, thyroid¹⁴¹, pituitary¹⁵⁰, and neuroendocrine cancers¹⁵¹ have been found to express high levels of polysialylated NCAM-1, and is correlated with increased migration and invasion of tumor cells¹³⁶ especially under hypoxic conditions¹⁵².

Evidence that diabetes mellitus (DM) alters enzymatic glycosylation is growing^{81, 153-161}. For example, endothelial cells from DM rats demonstrated significantly increased fucosidase and neuraminidase activity¹⁵³. Additionally, altered glycosylation-related gene expression in humans with DM has been shown to have important downstream effects. In women with gestational DM, impaired sialylation has been shown to lead to increased IL-2 secretion and an altered immune response that may impact fetal mortality¹⁵⁹. More related to wound healing, two previous studies by Paller et al.^{160, 162} demonstrate that the expression of the ceramide sialyltransferase, GM3 synthase, is increased in human DM foot skin¹⁶⁰. This increased GM3 synthase was found to suppress insulin/IGF-1 axis signaling, decrease keratinocyte migration and proliferation, and delay wound healing^{160, 162}.

1.1.4 Disease, Glycosylation, and AGEs are Intertwined

Though the relationship has not been fully elucidated, growing evidence suggests that the altered enzymatic glycosylation in DM is likely associated with the

presence of non- enzymatic advanced glycation end products (AGE). AGEs play a role in diabetic-related comorbidities and are also observed in aging and inflammatory conditions. Studies by Wiernsperger et al ¹⁵³, demonstrated that glycated bovine serum albumin (BSA) decreased $\beta(1,3)$ galactosylated and $\alpha2,3$ sialylated glycoproteins by 40%, and additionally reported reduced $\alpha1,6$ fucose recognition with no change in $\alpha2,6$ sialylation or β -D-galactosylation in bovine retinal endothelial cells (BREC). Furthermore, they later reported increased β -D galactosidase, α -L fucosidase, and neuraminidase activity with accompanying decreases in galactosyltransferase, fucosyltransferase, and sialyltransferase activity, respectively, in retinal endothelial cells ¹⁵⁴. This suggests that AGEs have the potential to decrease fucosylation and sialylation by modulating the enzymes responsible for adding and removing fucose and sialic acid moieties.

Additional studies have identified a role for AGEs and glucosamine production in pathologic proliferation and growth associated with microvascular complications that are mediated by the dysregulation of sphingosine and ganglioside enzyme activity, leading to the accumulation of sphingosine and GM3 and decreased GD2. ¹⁶³⁻¹⁶⁸. These studies by Wiernsperger ¹⁵³ and others demonstrated similar results in diabetic rodents and suggests that AGEs are likely associated with the GM3 associated impairments in keratinocyte activity that was described in diabetic foot skin by Paller and colleagues ¹⁶⁰⁻¹⁶¹.

Furthermore, previous studies report that AGE's bind and modify important regulators of glycosylation including DDOST, also known as AGE receptor 1 (AGER1), which is one of the stabilizing proteins within the OST complex responsible for attaching

oligomannose glycans to proteins during N-linked glycosylation. Another important AGE receptor that is related to glycosylation mediated signaling is AGE receptor 3 (AGER3), also known as Galectin-3, a galactose binding protein that has been shown to play an important role in a variety of key biological processes including wound healing ^{117, 120, 124, 131, 169}.

1.2 Significance and Motivation of Thesis

While previous studies have examined the role of lectins (galectins) and gangliosides in skin wound healing, very few studies have focused on the overall changes in enzymatic glycosylation. Furthermore, while there are many lectin specific interactions with carbohydrate determinants that positively and negatively regulate pathways involved in wound healing, some carbohydrates demonstrate generalizable actions on cell behavior. Previous studies suggest that AGEs accumulate in UV exposed tissues, like the skin, and in pathological conditions, like diabetes, and that AGEs bind important regulators of glycosylation mediated pathways. Protein linked AGEs have been found to independently decrease the abundance of protein sialylation and fucosylation. Furthermore, increases in protein sialylation and decreased fucosylation have been observed when the acute inflammatory response is induced by noxious stimuli in models of peritonitis ⁹⁷. Cutaneous homeostasis and wound healing require the synthesis of specific glycans, both for the synthesis of functional ECM glycoproteins ¹⁷⁰⁻¹⁷³ and for immune function ^{35, 37, 174}. Altered patterns of glycosylation-related gene expression in DM clearly have the potential to significantly impair skin integrity and repair.

1.3 Specific Aims

Aim 1. Identify changes in protein glycosylation in the oral mucosa and cutaneous skin during wound healing.

The tongue and skin are both sensory organs that are prone to mechanical and thermal injury. The tongue, an oral mucosal tissue, has been found to demonstrate enhanced recovery from injury when compared to the skin. While there are many structural and functional differences between the two tissues, the environment in which the skin and tongue reside plays a role in some of these differences. Saliva and carbohydrate-rich mucins coat epidermal cells of the tongue to keep it moist while the skin remains dry and exposed to air. Previous studies demonstrate that this environmental difference contributes to the differential epithelial cornification. Additionally, mucins coating the oral mucosa are heavily glycosylated and are required to maintain mucosal epithelial homeostasis, however, no study has examined whether there was differential glycosylation in oral mucosal (tongue) and cutaneous wound healing. In this aim we examine whether differential glycosylation occurs in oral mucosal and cutaneous sensory organs during homeostasis (uninjured) and during wound healing. The objective of this study is to demonstrate a role for enzymatic glycosylation in the differential healing responses observed between the tongue and skin. The central hypothesis is that altered glycosylation contributes to differential healing in normal skin and oral mucosa, and more specifically that altered sialylation likely contributes to these differences. In this aim I will characterize the patterns of glycosylation in uninjured and wounded skin and tongue of BALB/c mice and determine whether the two sites exhibit altered expression of glycosylation- related genes during wound healing. The alignment

of gene expression changes and the changes in glycosylation itself will also be examined.

Aim 2. Identify changes in protein glycosylation in non-diabetic and diabetic/ (AGE) accumulated skin during wound healing.

Previous studies suggest that AGEs induce altered enzymatic glycosylation in diabetes. However, the AGE-induced changes in enzymatic glycosylation in uninjured and wounded skin have yet to be elucidated. In this aim, we examine whether differential glycosylation occurs in diabetic and non-diabetic skin and wounds. The objective of this study is to demonstrate a role for AGE induced changes in enzymatic glycosylation in the diabetic wound healing process. The central hypothesis is that the known chronic accumulation of skin AGEs in DM and pre-DM induces impairments in wound healing by altering normal skin glycosylation during the inflammatory phase of wound healing.

In this aim I will characterize the patterns of glycosylation during normal wound healing and determine whether diabetes alters the expression of glycosylation- related enzyme gene families and pathways during wound healing. I will also determine if such changes align with downstream changes in glycosylation during the inflammatory phase of wound healing.

2 ORGAN SPECIFIC REGULATION OF GLYCOSYLATION- RELATED GENES

DURING SKIN AND TONGUE WOUND HEALING

2.1 Introduction

The regenerative capacity of the oral mucosa exceeds that of the skin and is characterized by a well-orchestrated immune and angiogenic response along with less scar tissue formation. While previous evidence demonstrates that increased inflammation can scar tissue formation, the mechanisms by which this occurs are not completely understood. The advantageous healing of the oral mucosa suggests an altered series of events occurs in response to injury.

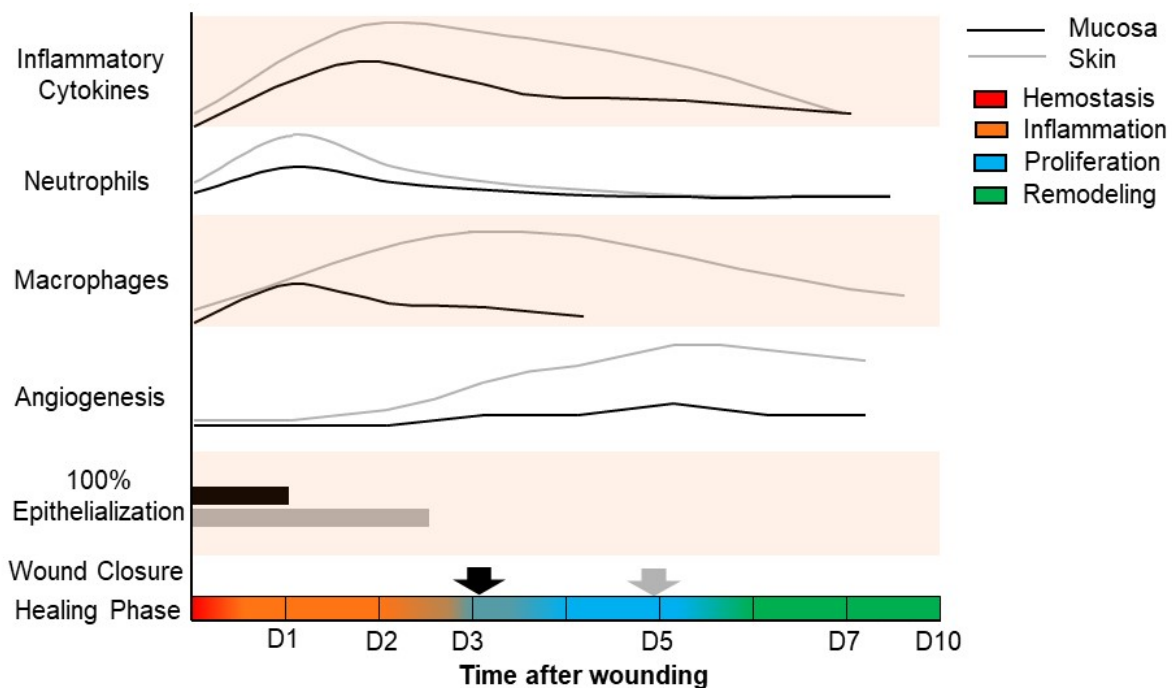


Figure 5.1 Depiction of wound healing patterns during skin and tongue wound healing. Modified from Chen et al. the tongue (black) healing faster with less inflammatory cytokines and macrophages when compared to the skin (grey). Each phase of wound healing is mapped by time after wounding. As noted by the gradient change, each phase of wound healing demonstrates some overlap with other phases.

The skin and tongue are sensory organs belonging to the integumentary system and gastrointestinal systems respectively. The tongue is a part of the oral mucosa and exhibits advantageous healing over cutaneous skin. Although the differential inflammatory response between skin and tongue wound healing is not well understood, a process called enzymatic glycosylation plays an important role in regulating inflammatory mediators and may help to explain some of these changes. Glycosylation is a post-translational modification by which carbohydrates are enzymatically attached to proteins and lipids. Immune cells display and bind to respective carbohydrate binding proteins, known as lectins, and their respective carbohydrate moieties, known as glycans, to trigger intercellular signaling, inflammatory cytokine and inflammatory chemokine expression. While previous studies have examined the role of these galectins in skin wound healing, very few studies have focused on the carbohydrate determinants that trigger lectin mediated signaling. Furthermore, while there are many lectin specific interactions with carbohydrate determinants that positively and negatively regulate pathways involved in wound healing, some carbohydrates demonstrate generalizable actions on cell behavior. Examples of this includes terminally localized sialic acids and/or neuraminic acids (Neu5Gc and Neu5Ac) which regulate ion transport, protein stabilization, inflammatory cell binding, cell adhesion, and act to alter recognition sites for cell binding^{91, 175}. Sialic acids are also critical to ganglioside biosynthesis and alter the affinity of integrin-galectin binding¹⁷⁵, both of which modify wound epithelialization^{122, 161}. In order to better understand the regulation of glycosylation and carbohydrate determinants in cutaneous and oral mucosal wound healing, we aimed to identify whether differential glycosylation- related gene expression occurs throughout

skin and tongue wound healing and more specifically, whether these glycosylation-related proteins trigger downstream changes to protein and lipid glycosylation.

2.2 Materials and Methods

2.2.1 Microarray Normalization and Pathway Analysis

Gene expression was analyzed from microarray data (GEO-GSE23006) examining the tongue and skin at baseline and in 1mm excisional wounds (harvested at 0.25, 0.5, 1, 3, 5, 7, and 10 days post-wounding, n=3 per time point). Affymetrix GeneChip CEL files for GEO-GSE23006¹ were read into the R programming environment¹⁷⁶ using the *affy* Bioconductor package¹⁷⁷. Quality assessment of each GeneChip was performed by assessing the percent present calls using the MAS5 Detection Call algorithm and the 3':5' ratios for glyceraldehyde-3-phosphate dehydrogenase (GAPDH)¹⁷⁸⁻¹⁷⁹. The robust multiarray average method was used to obtain probe-set expression summaries¹⁸⁰. Prior to performing statistical analyses, probe sets called Absent in all samples and control probe sets were removed.

Genes demonstrating statistical significance between skin and tongue wound healing (FDR≤0.05) underwent PANTHER Overrepresentation Testing to identify PANTHER Protein Classes, Molecular Functions (MF), and Biological Processes (BP) that the genes clustered into based on the log2 fold change in gene expression. Groups were identified as having log2 fold change ≤-1 or log2 fold change ≥1. Additionally, significantly regulated probe sets (FDR<0.05) were filtered for genes related to glycosylation by their Entrez ID and GO ontology and cross referenced with the gene

lists and biosynthetic pathways provided by the Complex Carbohydrate Research Center (Moreman Lab, University of Georgia).

Using the online tool ClustVis (<http://biit.cs.ut.ee/clustvis/>), principal component and hierarchical cluster analysis were performed to visually assess the dataset homogeneity and to identify gene clusters with similar expression patterns, respectively. Genes were clustered as being: 1) Relatively Upregulated in Skin Wound Healing; or 2) Relatively Downregulated in Skin Wound Healing as Compared to the Tongue. PANTHER Overrepresentation Testing using Reactome was performed to identify the reactions that the up- and down-regulated glycogenes carried out. KEGG Pathway Mapper was then used to map the genes that were differentially upregulated (red) or downregulated (blue) in skin wound healing when compared to the tongue (FDR<0.05).

2.2.2 Animal Wound Models

All animal work was approved by the Institutional Animal Care and Use Committee (IACUC) at the University of Illinois at Chicago and conducted according to the recommendations of the Guide for the Care and the Use of Laboratory Animals. Six-week-old female Balb/C mice were purchased from The Jackson Laboratory (Bar Harbor, ME) and allowed to habituate for a minimum of 1 week. All mice were housed in groups of five at 22 to 24°C on a 12-h:12-h light/dark cycle and fed a standard chow *ad libitum*.

Following the habituation period, mice were subjected to wounding as previously described¹. Briefly, each mouse was anesthetized with ketamine (100mg/kg) and xylazine (5 mg/kg). One-millimeter excisional skin and tongue wounds were induced via

punch biopsy (Acu-Punch, Acuderm Inc., Ft. Lauderdale, FL). Following euthanasia, samples of the wound bed and 1-2mm of the surrounding periwound area (n=3-5) were harvested 3 days and/or 10 days post-wounding. Baseline, uninjured skin and tongue samples were harvested using 3-5mm punch biopsies and were harvested from tissue opposite the wound site. Samples were flash frozen and stored at -80° C.

2.2.3 Sample Preparation and Protein Extraction

To ensure adequate quantities for protein extraction, skin and tongue samples were pooled by time point in duplicate or triplicate (n=3-4). Whole brain homogenates were also processed to serve as a positive control. All samples were ground into a fine powder via CryoMill (Retsch GmbH, Haan, Germany) with liquid nitrogen cooling system and resuspended in Tris tissue lysis buffer (50mM Tris HCl pH8, 150mM NaCl, 5mM EDTA, 1% Triton-X100, and 0.5% Sodium Deoxycholate) or PBS tissue lysis buffer (1X PBS, pH 7.4 (Fisher BioReagents, Pittsburgh, PA), 1% Triton-X100, and 0.5% Sodium Deoxycholate, and 0.1% SDS) containing 1x Protease Inhibitor (PI) (Thermo-Fischer or Sigma Aldrich). Samples were then vortexed for 30-60 minutes at room temperature and the soluble protein lysate was stored at -80°C until ready for subsequent use.

Following centrifugation at 500xg for 5 minutes, the remaining fraction of insoluble proteins were subjected to further extraction using 1-5% SDS in 1 X PBS (pH 7.4) and PI and/or 4M guanidine hydrochloride in 1X PBS (ThermoFisher, pH 7.4) plus PI. Samples were then precipitated via ethanol and stored at -80°C until ready for subsequent use. To determine the protein concentration of each sample,

MicroBCA/BCA assays (ThermoScientific, Pierce Biotechnology, Rockford, IL) were used per the manufacturer's instructions.

2.2.4 Recovery of Polysialylated Proteins

To determine whether polysialylated proteins were present in tissue samples, inactive PKIE endo-N-neuraminidase was used to trap polysialylated proteins. Each sample (500 μ L of 0.5-2mg/mL sample resuspended in TBS) was incubated on an end-over-end rocker with 50 microliters of a 50% slurry of GST.PKIE endo-N-acetylneuraminidase Trap (EndoNt) bound to glutathione-Sepharose beads in RIPA lysis buffer (50mM Tris HCl pH7.5, 150mM NaCl, 5mM EDTA, 0.5% for 6h at 4° C. After 3-4 washes with PBS samples were prepared for gel electrophoresis. The specificity of the EndoNt and the presence of polySia on the protein was confirmed by treating half of the precipitated proteins for each condition/time point with 5 μ L of 20mM Tris (pH 7.8) or 5 μ L of catalytically active endo-N-acetylneuraminidase (endoN) in 60 μ L buffer (10:10:50 ratio of NP-40, 1x Glycobuffer 2 (New England BioLabs, Ipswich, MA), and 20mM Tris, pH 8.0) overnight at 37° C.

2.2.5 Protein Electrophoresis and Transfer

Equal amounts of each sample protein homogenate (25 ug) or 50 μ L of the protein bound EndoNt beads from above were resuspended in 2X sample buffer (a 1:1 dilution of 4X Lamelli sample buffer (Biorad, Hercules, CA, USA) in Tris/ Glycine/ SDS buffer/ 10% β -mercaptoethanol (BME) and heated to 65°C for 10 minutes. SDS PAGE was performed at 110V for 1.5 hours at 25° C (n=3). Following SDS PAGE, proteins

were transferred onto a PVDF membrane at 100V for 1 hour at 4° C to minimize over-heating and sample loss.

2.2.6 Lectin Blotting Analysis of α 2,3- and α 2,6-linked Sialic Acid, and α 2-8, Polysialic Acid Expression during Wound Healing

Following SDS PAGE and membrane transfer as above, membranes were blocked using 1X Carbo-Free Blocking solution (Vector Laboratories, Burlingame, CA) or 2% non-fat dry milk in TBS supplemented with 0.1% Tween 20 overnight at 4° C.

Each membrane (n=3) was incubated with 20ug/mL biotinylated MAL-II (Vector Laboratories, Burlingame, CA) and 5ug/mL biotinylated SNA lectin (Vector Laboratories, Burlingame, CA) in TBS at room temperature for 30 min to detect α 2,3- and α 2,6-sialylated proteins, respectively. After the blots were thoroughly washed, bound lectins were detected using Vectastain® *Elite* Avidin-Biotin Complex Kit (Vector Laboratories, Burlingame, CA) for 30 minutes at room temperature.

To identify polysialylated proteins, membranes with EndoN trap isolated proteins were incubated with 1: 1000 CD56 12F8 anti-polySia antibody (BDBiosciences, Franklin Lakes, NJ, USA) or 1:500 735 anti-polySia (Absolute Antibody, Oxford, England, UK) in TBS (or 0.1% TBS-T) overnight at 4° C. After washing, bound antibodies were detected by incubating the membranes with 1:1000 HRP conjugated goat anti-rat IgM (for 12F8) or goat anti-mouse IgG2a (for 735) overnight at 4° C.

Each immunoblot was developed using Clarity Western ECL Substrate (Bio-Rad). Following chemiluminescent detection (ChemiDoc™, Bio-Rad) of the respective immunoblots, total protein sialylation and protein sialylation at designated molecular

weights were quantified (Quantity One® 1-D analysis software, Bio-Rad) using the mean adjusted volume of each sample's lane and band, respectively. Each sample on the SNA and MAL-II immunoblots were normalized to the positive control (brain).

2.2.7 Microscopy

Following euthanasia, samples were embedded in OCT (Fisher Healthcare, Houston, TX) and either 1) embedded in OCR and stored at -80° C or 2) fixed in 10% formalin for 44 hours, dehydrated with ethanol, and stored in paraffin until further processing. Eight to ten micrometer thick frozen sections were obtained from OCT embedded samples using the Leica Cryostat (Leica Biosystems, Wetzlar, Germany). Ten-micrometer thick paraffinized sections were obtained using a microtome (Leica Biosystems, Wetzlar, Germany).

To analyze the expression and localization of α 2-3, α 2-6, and α 2-8 poly-sialylated proteins, 8 μ m frozen section were fixed in pre-cooled (-20° C) acetone or 4% paraformaldehyde. Following permeabilization, and thorough washing, carbohydrate binding specificity was confirmed by incubating the sections in Glycobuffer 3/2 with or without the catalytically active α 2-3, -6, -8, -9 neuraminidase (New England BioLabs, Ipswich, MA) or endoneuraminidase at 37° C for 2-4 h or 24 h, respectively. Slides were then blocked with blocking buffer (5% BSA, 1% GSA, 0.1% Triton X-100, 0.05% Tween-20) and streptavidin/biotin as indicated by manufacturer instructions (Vector Labs). Additionally, to reduce non-specific binding to the Fc region of the rat IgM, mouse IgG, and rabbit IgG secondary antibodies, slides stained for 12F8/ 735/NCAM-1, were additionally blocked using 100 μ g/mL of unconjugated AffiniPure monovalent Fab

Fragment (H+L) antibodies (Jackson ImmunoResearch) relative to each respective secondary antibody. Following a brief washing, slides were incubated overnight at 4° C with the respective primary antibodies diluted in antibody dilution buffer (1% BSA/ 0.1% Triton X-100/ 0.05% Tween-20). After washing, slides were incubated with the respective biotinylated MAL-II or SNA lectin in PBS/ TBS at room temperature for 45 minutes or overnight at 4° C with CD29. 12F8/735 ± NCAM immuno-stained slides were incubated overnight at 4° C. After washing, the slides were incubated at room temperature for 45 min in the respective secondary antibodies; 1:500 Alexa Fluor 594 conjugated goat anti-rabbit IgG (for CD29), 1:1000 Alexa Fluor 488 conjugated goat anti-rat IgM (for 12F8), 1:200 Alexa Fluor 594 conjugated goat anti-mouse IgG2a (for 735), 1:1000 biotin conjugated goat anti- rabbit (NCAM), and/or 10ug/mL Streptavidin Fluorescein/ Aminomethylcoumarin (AMCA)/ Texas Red in antibody dilution buffer or TBS. Each slide contained a negative control for the respective lectin and/or a negative control for the respective protein target.

2.2.8 In-gel Digestion and Mass Spectroscopy Analysis

Five-hundred micrograms of uninjured skin underwent EndoNt digestion, and . 50uL of the immunoprecipitated proteins were subjected to SDS PAGE. Gels were rinsed three times in MilliQ water and the gel lanes containing uninjured skin samples were excised from ~ 40-300kDa using a sterile scalpel. The gel pieces were placed in sterile 5mL centrifuge tubes with MilliQ water and stored at -20°C until they were delivered to the UIC Mass Spectroscopy Core directed by Dr. Hui Chen.

Gel samples were further cut into individual bands, washed with MilliQ water, and then incubated on vortex for 10m in a 25mM ammonium bicarbonate/ 50% acetonitrile solution. Supernatants were extracted stepwise following 2-3 repetitions. Samples then underwent reduction and alkylation followed by in-gel digestion with trypsin (ThermoScientific, Pierce Biotechnology, Rockford, IL) overnight at 37°C. After digestion, the resulting peptides were purified on a C18 column and analyzed by LC-MS/MS mass spectroscopy.

Per the UIC Proteomics Core, samples were run on Thermo Fisher Orbitrap Velos Pro coupled with Agilent NanoLC system (Agilent, Santa Clara, CA) over a 60 min gradient. Samples were analyzed with a 60 minutes linear gradient (0–35% acetonitrile with 0.1% formic acid) and data were acquired whereby MS/MS fragmentation was performed on the top 12 intense peaks of every full MS scan. RAW files were converted into .mgf files using MSConvert (ProteoWizard 3.0.3768). “Database search was carried out using Mascot server (Matrix Science, London, UK; version 2.6.2). Mascot was set up to search the Uniprot_mouse_20181106 database (version, 86119 entries). Mascot was searched with a fragment ion mass tolerance of 0.30 Da and a parent ion tolerance of 20 PPM. Carbamidomethyl of cysteine was specified in Mascot as a fixed modification. Deamidation of asparagine and glutamine and oxidation of methionine were specified in Mascot as variable modifications”¹⁸¹.

To identify the proteins "Scaffold (version Scaffold_4.8.8, Proteome Software Inc., Portland, OR) was used to validate MS/MS based peptide and protein identifications. Peptide identifications were accepted if they could be established at greater than 95.0% probability by the Peptide Prophet algorithm¹⁸² with Scaffold delta-

mass correction. Protein identifications were accepted if they could be established at greater than 99.0% probability and contained at least 1 identified peptide. Protein probabilities were assigned by the Protein Prophet algorithm ¹⁸³. Proteins that contained similar peptides and could not be differentiated based on MS/MS analysis alone were grouped to satisfy the principles of parsimony. Proteins sharing significant peptide evidence were grouped into clusters” ¹⁸¹.

2.2.9 Statistical Analysis

The normalized microarray probe set expression was used to identify whether there were statistically significant differences between skin and tongue gene expression during homeostasis and wound healing. In R, the *limma* package ¹⁸⁴ was used for fitting the probe set level models whereby the probe-set expression was modeled using a linear regression of the condition and the interaction between each condition and the time post-wounding. Pairwise contrasts were made between skin and tongue wound healing, where S represents skin, T represents tongue, and *t* represents each time in days post- wounding as follows:

At baseline

$$a. S_{t=0} - T_{t=0}$$

2) Between baseline and each respective timepoint

$$a. (S_t - S_{t=0}) - (T_t - T_{t=0}); \text{ and}$$

3) Between baseline and all timepoints to assess differences in the skin and tongue across all time points during wound healing,

$$a. [(S_{t=0.25} + S_{t=0.5} + S_{t=1} + S_{t=3} + S_{t=5} + S_{t=7} + S_{t=10}) - S_{t=0}] -$$

$$[(T_{t=0.25} + T_{t=0.5} + T_{t=1} + T_{t=3} + T_{t=5} + T_{t=7} + T_{t=10}) - T_{t=0}].$$

The resulting p-values were adjusted using Benjamini and Hochberg's false discovery rate method¹⁸⁵. The probe sets were then filtered for genes demonstrating significant regulation ($FDR \leq 0.05$) in all the following conditions: 1) During wound healing in the skin; 2) During wound healing in the tongue; 3) During wound healing in the skin and tongue; and 4) Between the skin and tongue during wound healing across all timepoints after adjusting for baseline differences.

Following statistical analysis, significantly expressed glycogene probe sets were scaled via unit variance scaling and row-wise hierarchical clustering was applied to the probe sets using the Euclidean distance and Ward linkage with the ClustVis webtool¹⁸⁶. The number of clusters applied was identified with the NbClust package¹⁸⁷ using the silhouette index method¹⁸⁸. Additionally, PANTHER Overexpression Tests (Released 20181113; <http://www.pantherdb.org>) were performed using binomial test type and Bonferroni correction for multiple testing¹⁸⁹⁻¹⁹⁴.

For western blot analysis, each blot was assessed for outliers using the ROUT method ($Q=1\%$). Additionally, for lectin blot analysis, blot- to blot variance was assessed across the respective lectin stained blots using control skin samples via One-Way Analysis of Variance with a Bonferroni adjustment for multiple comparisons between the blots. (GraphPad Prism version 7.00 for Windows, GraphPad Software, La Jolla California USA, www.graphpad.com). The expression levels/values of $\alpha 2,3$ -, $\alpha 2,6$ - and $\alpha 2,8$ - polysialylated proteins were analyzed by molecular weight via Two-Way ANOVA modeled over the polynomial of time with a Benjamini Hochberg correction for

false discoveries between condition, time, and condition: time. Least-squares means for factor combinations of the two fitted models were performed to estimate the time and significance of each interaction.

2.3 Experimental Results

2.3.1 Microarray Analysis of Skin versus Tongue Wound Healing

Microarray data sets on skin and oral mucosal wound healing generated by our lab established that the pattern of peak gene expression is relatively consistent between oral mucosal and skin wounds of the same size; however, the magnitude of inflammatory gene expression is dampened in the oral mucosa relative to the skin ¹. While this previous study contrasted the temporal wound healing profiles of the skin and tongue, differential gene expression was not assessed. In order to identify transcript differences in tongue and skin, we first performed an overall analysis of the existing microarray dataset GSE23006 to determine: 1) which genes were differentially expressed during skin or tongue wound healing; and 2) among the genes that are differentially expressed during wound healing, which genes are also differentially expressed between the skin and tongue. There were 17403 genes significantly regulated in skin or tongue wound healing. When examining the inherent differences between skin and tongue across all timepoints, 12705 genes were differentially expressed between the skin and tongue (Table III). Cross referencing the genes that were differentially regulated between skin and tongue and also significantly regulated during wound healing in either or both models lead to the identification of 11909 genes.

The genes demonstrating significant differential expression between the skin and tongue and during wound healing in the skin and/or tongue, with a log₂ fold change <-1 were considered downregulated in skin relative to tongue), while genes with a log₂ fold change >1 were considered to be upregulated in skin relative to tongue. Gene ontology using PANTHER Overrepresentation Testing (Released 20181113) revealed genes with a log₂ fold change <-1 (i.e., downregulated in skin relative to tongue) had biological processes associated with myofibril assembly, ATP synthesis coupled proton transport, mitochondrion organization, cellular respiration, muscle contraction, cellular amino acid metabolic process, and cellular protein-containing complex assembly (adjusted $p \leq 0.05$, Fold Enrichment ≥ 1.5) (Table IV). Conversely, genes with a log₂ fold change >1 i.e. upregulated in skin relative to tongue) were associated with regulation of mitotic cell cycle phase transition, DNA biosynthetic process, cell cycle phase transition, protein glycosylation, rRNA processing, regulation of kinase activity, mRNA splicing via spliceosome, regulation of cellular component organization, and cellular lipid metabolic process (adjusted $p \leq 0.05$, Fold Enrichment ≥ 1.5) (Table V).

TABLE III.
TABLE OF RESULTS OF MICROARRAY EXPRESSION SET- BY STATISTICAL CONTRAST

Condition	Model	Contrast Variables	Total Genes/ Probes	Total Glycogenes/ Probes
All Probes/ Probe Subsets	Dataset post normalization		17693 genes	763 genes corresponding with mouse Entrez ID
Tongue or Skin Wound Healing ²	y= Condition: Time + Condition	$T_t - T_{t=0}$ OR $S_t - S_{t=0}$	17403 genes	743 genes
Interaction of Time and Condition ¹	y= Condition: Time	None Specified	14225 genes	644 genes
Difference between Tongue & Skin Wound Healing ³	y=Condition: Time	$(\sum S_t - S_{t=0}) - (\sum T_t - T_{t=0})$	12705 genes	567 genes
Full Model	Full	All above	11909 genes (67%)	529 genes (69%)

Represented in the statistical contrasts described in the methodology: 1) comparison 1; 2) comparison 2; 3) comparison 3.

TABLE IV.

TABLE OF TOP 10 PANTHER BIOLOGICAL PROCESS PATHWAYS AMONG GENES DOWNREGULATED IN THE SKIN.

PANTHER GO-Slim Biological Process	# in Reference List	Number of Genes Mapped	Expected Number of Genes	Over (+) Under (-) Enriched	Fold Enriched	Adjusted P-value
Total Genes Examined	22296	5023	-	-	-	-
myofibril assembly (GO:0030239)	19	19	4.28	+	4.44	2.06E-04
ATP synthesis coupled proton transport (GO:0015986)	33	28	7.43	+	3.77	9.03E-06
actomyosin structure organization (GO:0031032)	36	29	8.11	+	3.58	1.49E-05
mitochondrion organization (GO:0007005)	33	24	7.43	+	3.23	1.56E-03
cellular respiration (GO:0045333)	28	19	6.31	+	3.01	4.92E-02
ATP biosynthetic process (GO:0006754)	54	35	12.17	+	2.88	1.00E-04
actin cytoskeleton organization (GO:0030036)	86	47	19.37	+	2.43	1.06E-04
actin filament-based process (GO:0030029)	95	50	21.4	+	2.34	1.28E-04
purine ribonucleotide biosynthetic process (GO:0009152)	84	44	18.92	+	2.33	8.23E-04
purine ribonucleotide metabolic process (GO:0009150)	97	50	21.85	+	2.29	2.35E-04

Adjusted $p \leq 0.05$, Fold Enrichment ≥ 1.5

TABLE V.

TABLE OF TOP 10 PANTHER BIOLOGICAL PROCESS PATHWAYS AMONG GENES UPREGULATED IN THE SKIN.

PANTHER GO-Slim Biological Process	# in Reference List	Number of Genes Mapped	Expected Number of Genes	Over (+) Under (-) Enriched	Fold Enriched	Adjusted P-value
Total Genes Examined	22296	5844/ 5924	-	-	-	-
regulation of mitotic cell cycle phase transition (GO:1901990)	32	23	8.5	+	2.71	4.1E-02
DNA biosynthetic process (GO:0071897)	55	38	14.61	+	2.6	3.5E-04
cell cycle phase transition (GO:0044770)	42	29	11.16	+	2.6	8.7E-03
mitotic cell cycle process (GO:1903047)	66	39	17.54	+	2.22	9.6E-03
mitotic nuclear division (GO:0140014)	145	83	38.53	+	2.15	4.4E-07
regulation of cell cycle (GO:0051726)	161	87	42.78	+	2.03	2.5E-06
protein glycosylation (GO:0006486)	86	46	22.85	+	2.01	1.9E-02
cell cycle process (GO:0022402)	198	104	52.61	+	1.98	3.1E-07
mRNA processing (GO:0006397)	207	106	55	+	1.93	8.1E-07
RNA processing (GO:0006396)	256	131	68.02	+	1.93	8.6E-09

Adjusted $p \leq 0.05$, Fold Enrichment ≥ 1.5

2.3.2 Microarray Analysis of Glycosylation- related Genes Reveals Opposing Gene Clusters in Skin versus Tongue Wound Healing

Protein glycosylation was listed as a significantly overrepresented biological process in the PANTHER analysis in Table V. Protein glycosylation and the respective glycans of glycoproteins have been found to regulate wound epithelialization, inflammatory cell binding, cell adhesion and migration and may occur independent of protein abundance^{98, 195}. Since these processes are all required for successful wound healing, the differential regulation of all genes related to glycosylation were chosen for further examination. Among the 11, 909 genes that were differentially regulated in our

final statistical model, 529 genes were identified as related to protein glycosylation (Table III).

Principal component analysis of the normalized glycosylation- related gene dataset revealed 16 principal components that accounted for 92% of the variance observed through the dataset. A clear distinction between the global expression data from the three replicates of skin and tongue wounds at all time points was observed with 2 major clusters and 5 distinct minor clusters (Figure 7A) in the first principal component (PC1). The second most significant principal component (PC2) identified accounted for 41.3% of the variance and most likely represents the inherent differences between the skin and tongue. This implies that tissue type explains many of the observed variances (Figure 7A). The next principal component accounted for 15.5% of the variance and most likely represents differences between the skin's inflammatory phase of healing (0.5 days to 1-day post-wounding) compared to all other timepoints/ tissue types (Figure 7A, 7B) and/or differences in hemostasis through the early inflammatory phase of wound healing (0.25 days to 1-day post-wounding) compared to all other timepoints (Figure 7B). Additionally, the 3rd principal component, which accounts for 9.5% of the variance further distinguishes the hemostasis phase from the inflammatory phase and the proliferation phase from uninjured skin and tongue and resolved wounds (10-days post-wounding). The remaining variance is likely explained by the additional distinct phase and/or timepoint specific differences across each tissue type.

Hierarchical cluster analysis revealed 2 major gene clusters: 1) relatively downregulated in the skin; or 2) relatively upregulated in the skin as compared to the tongue (Figure 8). The up- (red) and down- (blue) regulation of each genes expression

in the skin relative to the tongue was assessed independently from their contribution to the wound healing process (independent of time), however, only genes that were differentially expressed between uninjured skin or tongue and at least 1 timepoint post-wounding were included in the cluster analysis.

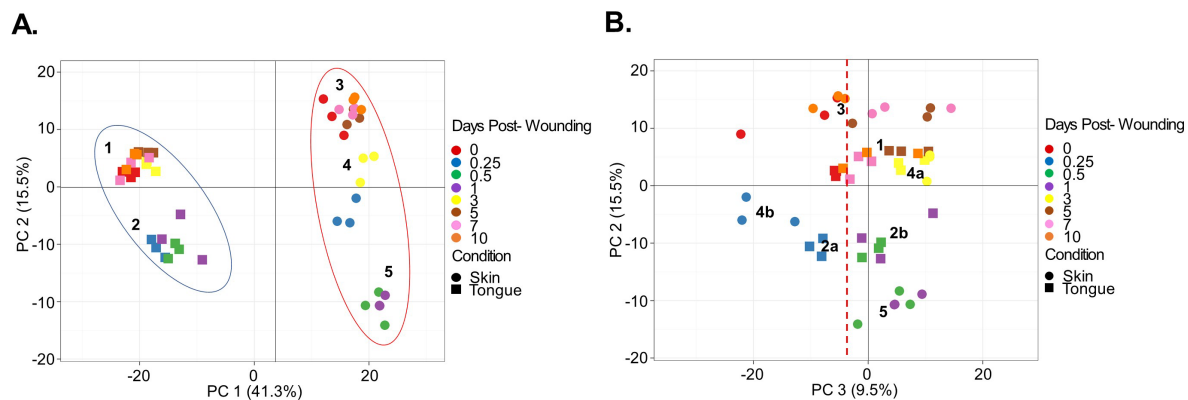


Figure 7. Principal components of glycogenes expressed between skin and tongue wound healing. Principal components 1 and 2 (A) along with components 3 and 2(B) reveal a cluster of all timepoints in the tongue (square, blue oval) and skin (circle, red oval). Minor clusters are numbered based on condition/ phase of healing: 1) Tongue at baseline and the proliferative and remodeling phases of healing; 2) Tongue at hemostasis (a) and the inflammatory phase of healing (b); 3) Skin at baseline and the late proliferative and remodeling phases of healing; 4) Skin at hemostasis (b) and the late inflammatory/ proliferative phase of healing (a); 5) Skin during the inflammatory phase of healing.

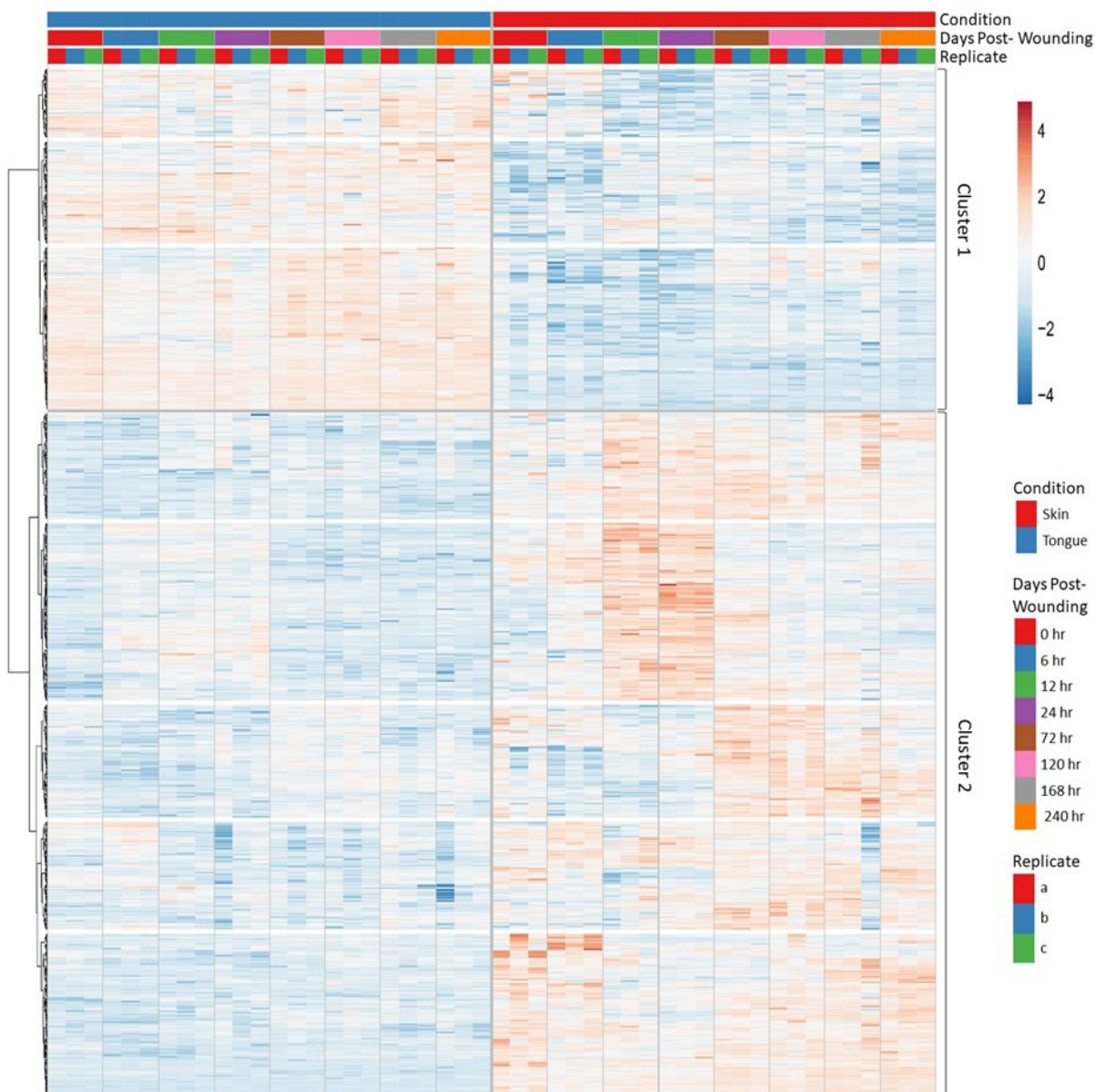


Figure 8. Hierarchical clustering reveals genes sets are more highly upregulated in skin wound healing when compared to tongue wound healing
Cluster 1 demonstrates gene clusters that are downregulated in the skin relative to the tongue. Cluster 2 demonstrates gene clusters that are upregulated in the skin relative to the tongue.

2.3.3 Genes related to Amino and Nucleotide Sugars are Differentially Regulated in Skin versus Tongue Wound Healing

Gene ontology and pathway analysis provides little information regarding the location, activity, and specificity of glycosylation- related genes and their respective pathways due to the limited current understanding of these genes and pathways. In order to better visualize the directional differential regulation of skin and tongue glycogenes that are involved in wound healing across all timepoints, KEGG pathway mapper was used to map genes according to the gene expression clusters across known pathways involved with glycosylation including: 1) mmu00520- Amino Sugar and Nucleotide Sugar Metabolism; 2) mmu00600- Sphingolipid Metabolism; 3) mmu00601- Glycosphingolipid Biosynthesis; and 4) mmu00531- Glycosaminoglycan Degradation. Gene expression clusters were mapped to represent genes that were relatively upregulated (red) or downregulated (blue) in the skin when compared to the tongue.

Examination of the mmu00520 (amino sugar and nucleotide sugar metabolism) pathway (Figure 9) identified 27 genes involved in 35 enzyme reactions that were differentially expressed during wound healing and between the skin and tongue. Figure 9 displays the portions of the KEGG pathway mmu00520 that demonstrate that the highest concentration of differentially expressed genes were involved in the synthesis of sialic acid (SA) and N- acetyl mannosamine (ManNAc) which is a SA precursor. These sugars are synthesized as uridine diphosphate- N- acetyl glucosamine (UDP- GlcNAc) and N- acetyl glucosamine (GlcNAc), and are converted to N- acetyl mannosamine (ManNAc) by glucosamine (UDP-N-acetyl)-2-epimerase/N-acetylmannosamine kinase (*GNE*) and renin binding protein (*RENBP*), respectively ¹⁹⁶. Both *GNE* and *RENBP* were

upregulated in the skin as compared to the tongue (Figure 9 and Figures 10A-B, FDR<0.005). N-acetylneuraminase synthase (*NANS*) and N-acetylneuraminic acid phosphatase (*NANP*) convert ManNAc to N-acetylneuraminic acid (Neu5Ac). While these genes demonstrated no significant difference between the skin and tongue or during wound healing (Figure 9), (*NPL*), cytidine monophosphate-N-acetylneuraminic acid hydroxylase (*CMAH*) were both upregulated in the skin as compared to the tongue (Figure 9 and Figures 10C-D, FDR<0.005). N-acetylneuraminic acid lyase (*NPL*) and *CMAH* are responsible for converting Neu5Ac to ManNAc and N-glycolylneuraminic acid (Neu5Gc), respectively, suggesting the lack of differential expression in *NANS* and *NANP* didn't impact the upregulation of NeuAc. The sialic acid sugar nucleotides are then synthesized in the nucleus by cytidine monophosphate N-acetylneuraminic acid synthetase (*CMAS*), which was downregulated in the skin as compared to the tongue (Figures 9 and 10E, FDR<0.005).

Nucleotide sugar donors, cytidine monophosphate- N-acetylneuraminic acid (CMP-Neu5Ac) and cytidine monophosphate- N-glycolylneuraminic acid (CMP-Neu5Gc), are sialic acid sugar donors that are required for all sialylation reactions^{91, 175} and act as a feedback inhibitor to *GNE*¹⁹⁷⁻¹⁹⁸. Decreased expression of *CMAS* would be expected to decrease the production of CMP-Neu5Ac and CMP-Neu5Gc required for inhibition of *GNE*. Reduced *GNE* feedback inhibition may explain the increased expression of *NPL* and *CMAH* as the system attempts to reduce the cytosolic accumulation of Neu5Ac by converting it into ManNAc and Neu5Gc. Interestingly, previous studies identified that both loss of *GNE* feedback inhibition and exogenous increases in ManNAc independently doubled the production of total sialic acid and

increased the expression of polysialylated neural cell adhesion molecule (NCAM) in epithelial (CHO) cell lines ¹⁹⁹.

Overall this data demonstrated consistent upregulation of multiple genes regulating the synthesis of ManNAc in the skin when compared to the tongue, including *GNE*, *RENBP*, and *NPL*. ManNAc is required for synthesis of sialic acid and sialic acid sugar donors and has been observed to independently promote protein sialylation. Sialic acid sugar donors (CMP- sialic acids) provide feedback inhibition to *GNE* and are synthesized by *CMAS* which was downregulated in the skin as compared to the tongue. This could be expected to reduce the availability of CMP- sialic acids and overall protein and lipid sialylation in the skin as compared to the tongue. However, decreased *CMAS* along with increased *GNE*, *RENBP*, and *CMAH* may also suggest decreased *CMAS* induced upregulation of *GNE* which increases the intracellular sialic acid accumulation and protein polysialylation. Therefore, it is also conceivable that there would be increased sialic acid in the skin as compared to the tongue. Since *GNE* has been considered the “master regulator of sialic acid” and *CMAS* is not depleted in the skin, it is expected that the skin contains increased levels of sialic acid.

Black bracket= pathways regulating the metabolism of neuraminic/ sialic acid donor sugars.

White box= enzymes within this pathway that were not differentially regulated between the skin and tongue.

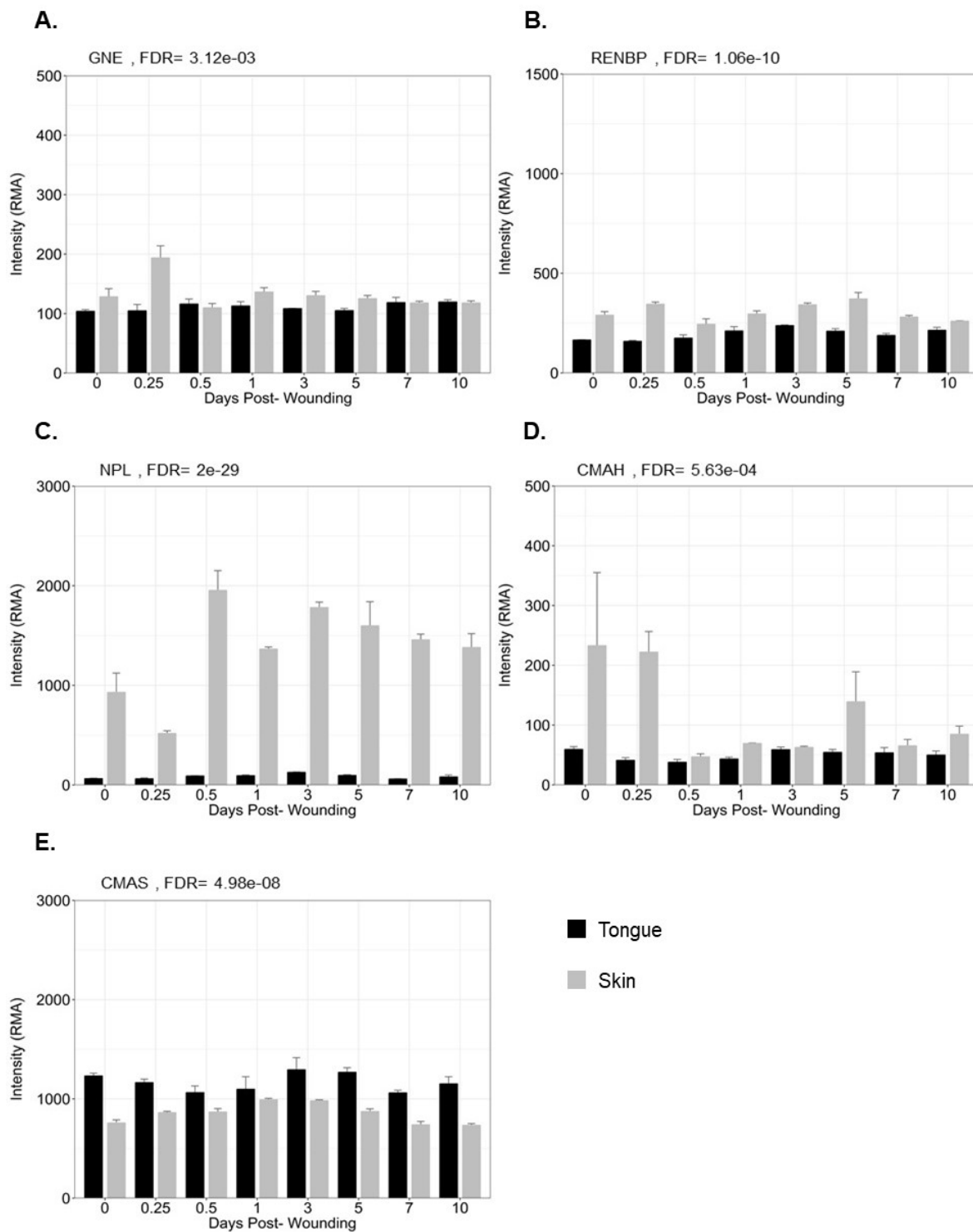


Figure 10. Expression of genes related to sugar and sugar nucleotide metabolism during skin and tongue wound healing.

Figure 10. Expression of genes related to sugar and sugar nucleotide metabolism during skin and tongue wound healing. Expression of genes within the sugar nucleotide metabolism pathway *GNE* (A), *RENBP* (B), *NPL* (C), and *CMAH* (D) were all upregulated, while *CMAS* (B) was downregulated in the skin (grey) compared to the tongue (black) during wound healing ($FDR \leq 0.05$, $\log_2 FC > 2$). Scale base on overall intensity across gene samples.

2.3.4 Genes Related to Sialic Acid Glycan Capping (Sialylation) are Differentially Regulated in Skin versus Tongue Wound Healing

Sialic acids terminally cap N- and O-glycans of glycoproteins and the glycans of glycosphingolipids. They can be easily removed by both endogenous neuraminidases and exogenous microbial neuraminidases. The complexity of sialic acids also allows for a number of modifications to occur including sulfation, methylation, phosphorylation, and polysialylation^{36, 91}. Since genes of sialic acid metabolism and nucleotide sugar donor biosynthesis appear to be differentially regulated in skin and tongue wound healing, and the literature suggests sialic acid bioavailability regulates the expression of sialyltransferases²⁰⁰, we chose to further examine the gene expression profiles for genes involved in catalyzing the transfer of sialic acid sugar donors (sialyltransferases) and those involved in sialic acid hydrolysis/removal (neuraminidases).

2.3.4.1 Genes Related to Sialyltransferases and the Sialylation of Glycans, are Differentially Regulated in Skin versus Tongue Wound Healing

The expression levels of all statistically significant genes ($FDR \leq 0.05$, $\log_2FC > 2$) related to transferring and hydrolyzing $\alpha 2,3$ -, $\alpha 2,6$ -, and $\alpha 2,8$ -linked sialic acids on N- and O-glycosylated glycoproteins and glycolipids were extracted from the microarray gene analysis. Genes encoding $\alpha 2,3$ -, 6-, 8- sialyltransferases involved in sialylation were observed between skin and tongue and throughout wound healing. The function of all $\alpha 2,3$ -, 6-, 8- sialyltransferases are located in Table VI. When examining the genes that encode $\alpha 2,3$ - sialyltransferases, ST3 beta-galactoside alpha-2,3-sialyltransferase 1 (*ST3GAL1*) which transfers $\alpha 2,3$ - linked sialic acids to core 1 and 2 O- glycans and

glycosphingolipids (Figure 11A, FDR<0.005), and ST3 beta-galactoside alpha-2,3-sialyltransferase 4 (*ST3GAL4*) which transfers α 2,3- linked sialic acids to glycosphingolipids in addition to Type II extended N- and O- linked glycans (Figure 11B, FDR<0.005), were upregulated in the skin relative to the tongue. Both ST3GAL1 (Figure 11A, FDR<0.005) and ST3GAL4 (Figure 11B, FDR<0.005) were upregulated within 0.25 day (6 hours) during the hemostasis phase of healing in the tongue, however, the skin demonstrated delayed upregulation of ST3GAL1 which occurred 0.5- 1 day post wounding during the inflammatory phase. Previous studies suggest ST3GAL1 reduces CD8+ T cell susceptibility to apoptosis while ST3GAL4 sialylates Lewis x structures on selectin ligands in human myeloid leukocytes to allow them to interact with selectins on endothelium, both of which are important for mediating inflammatory responses. This data along with previous studies suggest ST3GAL1 and ST3GAL4 play an important role in modulating the inflammatory response in wounds. Two additional genes encoding α 2,3- sialyltransferases were also downregulated in the skin when compared to the tongue. These include ST3 beta-galactoside alpha-2,3-sialyltransferase 3 (ST3GAL3) which has specificity for N- and O- linked glycans with Type II extensions and lactoseries glycosphingolipids (Figure 11C, FDR<0.005) and ST3 beta-galactoside alpha-2,3-sialyltransferase 6 (ST3GAL6) which has specificity for Type II extensions on N- and O- linked glycans and neolactoseries glycosphingolipids (Figure 11D, FDR<0.005). Less is known about the functional role of these enzymes, however, ST3GAL6 may play a role in the formation of sialyl Lewis x structure in selectins. Interestingly ST3GAL6 expression was reciprocal to the expression of ST3GAL4 and

ST3GAL3 expression was reciprocal to the expression of ST3GAL1 at all timepoints and in both the skin and tongue.

TABLE VI (continued)
ACTIVITY AND FUNCTION OF SIALYLTRANSFERASES - CONTINUED

Gene Symbol	Protein- ID	Protein Name	Location	Product Catalyzed	Family	Subtype	Functions/ literature
<i>ST3GAL5</i>	ST3Gal- V	ST3 beta-galactoside alpha-2,3-sialyl-transferase 5	Type II membrane protein. May be localized to the Golgi apparatus	NeuAc(α3)Gal	Glyco-sphingo-lipid	Glucosyl-ceramide base	Forms GM3 that participates in integrin mediated cell adhesion, cell signaling, proliferation, and differentiation, as well as the maintenance of fibroblast shape.
<i>ST3GAL6</i>	ST3Gal- VI	ST3 beta-galactoside alpha-2,3-sialyl-transferase 6	Type II membrane protein. May be localized to the Golgi apparatus	NeuAc(α3)Gal	Glyco-sphingo-lipid	Neo-Lactoseries (NL) [Type 2]	
						Neo-Lactoseries (NL) [Type 2]	
						Isogloboside	
					Extension	Type 2	May participate in sialyl Lewis x formation. Active against asialofetuin.
<i>ST6GAL1</i>	ST6Gal- I	ST6 beta-galactoside alpha-2,6-sialyl-transferase 1	Golgi, but also proteolytically processed to a soluble form.	NeuAc(α6)Gal	Glyco-sphingo-lipid	Neo-Lactoseries (NL) [Type 2]	Upregulated during hypoxia and in many cancers.
					Extension	Type 2	
				NeuAc(α6)Gal NAc		LacDiNAc	
<i>ST6GAL2</i>	ST6Gal- II	ST6 beta-galactoside alpha-2,6-sialyl-transferase 2	Type II transmembran e protein.	NeuAc(α6)Gal NAc	Extension	LacDiNAc	Limited mammalian expression. May have a preference for free glycans.
				NeuAc(α6)Gal		Type 2	
					Glyco-sphingo-lipid	Neo-Lactoseries (NL) [Type 2] Globoside Ganglioside	

TABLE VI (continued)
ACTIVITY AND FUNCTION OF SIALYLTRANSFERASES - CONTINUED

Gene Symbol	Protein- ID	Protein Name	Location	Product Catalyzed	Family	Subtype	Functions/ literature
<i>ST6GALNAC1</i>	ST6GalNAc- I	ST6 N-acetylgalactosaminide alpha-2,6-sialyl-transferase 1	Type II membrane protein. May be localized to the Golgi apparatus	NeuAc(α6)GalNAc	O-Linked	Core 1/ Core 2	Involved in the synthesis of sialylTn antigens on mucins (cancer-associate). Affects cell to cell, and cell to matrix interactions, and the function of intracellular molecules.
<i>ST6GALNAC2</i>	ST6GalNAc- II	ST6 N-acetylgalactosaminide alpha-2,6-sialyl-transferase 2	Golgi	NeuAc(α6)GalNAc	O-Linked	Core 1/ Core 2	Participates in cell-cell and cell-substrate interactions, protein targeting, and bacterial adhesion. Mediates cancer invasion via PI3K/Akt/NF-κB signaling pathways. Expressed in skin.
<i>ST6GALNAC3</i>	ST6GalNAc- III	ST6 N-acetylgalactosaminide alpha-2,6-sialyl-transferase 3		NeuAc(α6)GalNAc	Glycosphingolipid	Globoside Ganglioside	
<i>ST6GALNAC4</i>	ST6GalNAc- IV	ST6 N-acetylgalactosaminide alpha-2,6-sialyl-transferase 4		NeuAc(α6)GalNAc	Glycosphingolipid O-Linked	Ganglioside Globoside Core 1/ Core 2	
<i>ST6GALNAC5</i>	ST6GalNAc- V	ST6 N-acetylgalactosaminide alpha-2,6-sialyl-transferase 5	Golgi type II transmembrane glycosyl-transferase	NeuAc(α6)GalNAc	Glycosphingolipid	Ganglioside Globoside	Synthesizes GD1α. Linked to metastasis of breast cancer cells to the brain.

TABLE VI (continued)
ACTIVITY AND FUNCTION OF SIALYLTRANSFERASES - CONTINUED

Gene Symbol	Protein- ID	Protein Name	Location	Product Catalyzed	Family	Subtype	Functions/ literature
<i>ST6GALNAC6</i>	ST6GalNAc-VI	ST6 N-acetylgalactosaminide alpha-2,6-sialyl-transferase 6		NeuAc(α6) GlcNAc	Extension	Type 1	Synthesizes disialyl Lewis a structures.
						Type 2	
				NeuAc(α6) GalNAc	Glyco-sphingo-lipid	Globoside	
						Lactoseries (L)	
						Ganglioside	
<i>ST8SIA1</i>	ST8Sia- I	ST8 Alpha-N-Acetyl-Neuraminid e Alpha-2,8-Sialyl-transferase 1	Type II membrane protein. May be localized to the Golgi apparatus	NeuAc(α8) NeuAc	Glyco-sphingo-lipid	Glucosyl-ceramide base	Involved in the production of gangliosides GD2/3. Upregulated by melanocytes in response to TNF-alpha and IL-6 secretion. Activates cMet.
<i>ST8SIA2</i>	ST8Sia- II	ST8 Alpha-N-Acetyl-Neuraminid e Alpha-2,8-Sialyl-transferase 2	Type II membrane protein. May be localized to the Golgi apparatus	NeuAc(α8) NeuAc	Glyco-sphingo-lipid	Neo-Lactoseries (NL) [Type 2]	Responsible for polysialylation of NCAM and CADM1.
					Extension	Type 2	
<i>ST8SIA3</i>	ST8Sia- III	ST8 Alpha-N-Acetyl-Neuraminid e Alpha-2,8-Sialyl-transferase 3		NeuAc(α8) NeuAc	Glyco-sphingo-lipid	Lactoseries (L)	
						Neo-Lactoseries (NL) [Type 2]	
<i>ST8SIA4</i>	ST8Sia- IV	ST8 Alpha-N-Acetyl-Neuraminid e Alpha-2,8-Sialyl-transferase 4		NeuAc(α8) NeuAc	Extension	Type 2	Responsible for polysialylation of NCAM, NRP2, ESL-1.
					Glyco-sphingo-lipid	Neo-Lactoseries (NL) [Type 2]	
<i>ST8SIA5</i>	ST8Sia- V	ST8 Alpha-N-Acetyl-Neuraminid e Alpha-2,8-Sialyl-transferase 5	Type II membrane protein that may be present in the Golgi apparatus	NeuAc(α8) NeuAc	Glyco-sphingo-lipid	Glucosyl-ceramide base	Highly expressed by NK cells.
						Globoside	
						Ganglioside	
<i>ST8SIA6</i>	ST8Sia- VI	ST8 Alpha-N-Acetyl-Neuraminid e Alpha-2,8-Sialyl-transferase 6		NeuAc(α8) NeuAc	O-Linked	Core 1/ Core 2	May mediate NK cell interactions with Siglec-7. Contributes to multidrug resistance in cancer cells.

Among the genes that encoded α 2,6- sialyltransferases, ST6 N-acetylgalactosaminide alpha-2,6-sialyltransferase 5 (*ST6GALNAC5*), which has specificity for gangliosides and globosides, was upregulated in the skin relative to the tongue. Interestingly *ST6GALNAC5* (Figure 12A, FDR<0.005) was upregulated in tongue wounds 0.25 days post wounding, however, it was not upregulated in the skin until day 1. *ST6GALNAC5* synthesizes GD1 α gangliosides and has been associated with promoting cancer metastasis to the brain by enhancing cancer cell adhesion to brain endothelial cells and promoting their passage through the blood-brain barrier. While the time of peak upregulation of *ST6GALNAC5* in skin and tongue wound healing suggests a role for *ST6GALNAC5* in the inflammatory phase of healing, *ST6GALNAC5* hasn't been previously associated with inflammatory processes. Additionally, 3 genes encoding α 2,6- sialyltransferases were downregulated in the skin relative to the tongue. The downregulated genes included ST6 N-acetylgalactosaminide alpha-2,6-sialyltransferase 2-, 3-, and 6- (*ST6GALNAC2*, *ST6GALNAC3*, and *ST6GALNAC6*, respectively). *ST6GALNAC2* demonstrates substrate specificity towards core 1 and 2 glycans and participates in a number of cell functions including cell-cell and cell-substrate interactions, bacterial adhesion, and protein targeting glycosphingolipids (Figure 12B, FDR<0.005). *ST6GALNAC3* and *ST6GALNAC6* have substrate specificity towards glycolipids including globosides and gangliosides (Figures 12C and 12D, respectively, FDR<0.005).

Among the genes that encoded α 2,8- sialyltransferases, ST8 Alpha-N-Acetyl-Neuraminide Alpha-2,8-Sialyltransferase 1-, 2-, 4-, and 6- (*ST8SIA1*, *ST8SIA2*, *ST8SIA4*, and *ST8SIA6*, respectively) were upregulated in the skin as compared to the

tongue. ST8SIA1, which sialylates glucosylceramides and synthesizes GD2/3 (Figure 13A, FDR<0.005) and ST8SIA6, which has preference for core 1 and 2 O- glycans (Figure 13B, FDR<0.05), both demonstrated significantly reduced expression 0.25 days post wounding and remained downregulated throughout the course of in skin wound healing. Interestingly both ST8SIA1 and ST8SIA6 are implicated in enhancing cancer cell proliferation, and ST8SIA6 has been suggested to play a role in NK cell mediated inhibition by producing di-sialic acid bearing counterreceptors that ligate Siglec-7 via cis interactions²⁰¹⁻²⁰², however, its role in masking Siglec-7 mediated proinflammatory signaling in monocytes is not well understood²⁰³. Among the 4 genes encoding α 2,8-sialyltransferases that were differentially regulated, 2 are responsible for a conserved type of glycosylation known as polysialylation. Polysialylation involves the synthesis of multiple sialic acids at least 8 monosaccharides in length. Polysialic acid acts as an anti-adhesion molecule and has been implicated in fibroblast growth factor signaling and resolution of the inflammatory phase of healing. Polysialylation is mediated by *ST8SIA2* which has a preference for neural cell adhesion molecule (NCAM1) and cell adhesion molecule (CADM1/ SynCam) (Figure 13C, FDR<0.05). Polysialylation is also mediated by *ST8SIA4* which has a preference for NCAM1, neuropilin 2 (NRP2), and E-selectin ligand (also known as Golgi apparatus protein 1) (ESL1/ GLG1/ GSLG1) (Figure 13D, FDR<0.05). Both ST8SIA2 and ST8SIA4 were upregulated in the skin relative to the tongue, however, their expression was time dependent. In the tongue, both genes achieved peak upregulation 1-3 days post wounding. *ST8SIA4* (Figure 13D, FDR<0.05) demonstrated similar expression patterns between the skin and tongue but was significantly upregulated in the skin compared to the tongue 1-day post-wounding.

Additionally, ST8SIA2 achieved peak up regulation in the skin 7 days post wounding which was 4 days later than in the tongue. This delay occurs during the remodeling phase of healing and could be implicated in scar development. Lastly, ST8 Alpha-N-Acetyl-Neuraminide Alpha-2,8-Sialyltransferase 5 (*ST8SIA5*) (Figure 13E, FDR<0.005) was considered downregulated in the skin relative to the tongue and demonstrated significantly increased expression during the remodeling phase of tongue wound healing. However, ST8SIA5 did not appear to be regulated in the skin. Interestingly ST8SIA5 is highly expressed in NK cells and has substrate specificity towards gangliosides. This combined data identifies a number of sialyltransferases that are differentially regulated between the skin and tongue and during wound healing. Many of the genes demonstrate variable substrate specificity and have been previously associated with cancer mediated proliferation and/ or inflammatory processes which are necessary for wound healing.

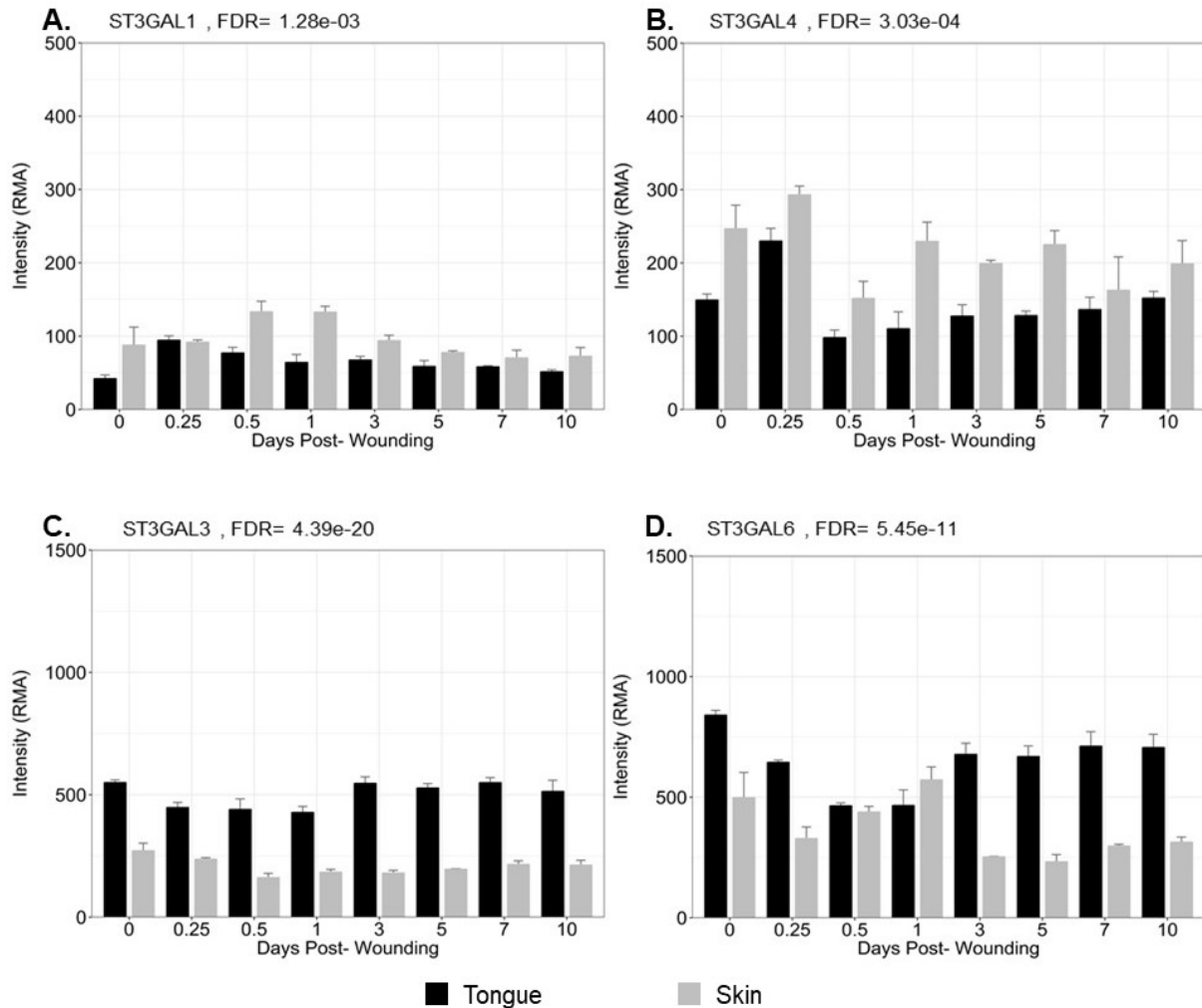


Figure 11. Expression of α 2,3- sialyltransferase related genes demonstrate significant differences in expression during skin and tongue wound healing.

Expression of *ST3GAL1* (A) was upregulated, *ST3GAL4* (B) was upregulated, *ST3GAL3* (C) was downregulated, and *ST3GAL6* (D) was downregulated in the skin (grey) compared to the tongue (black) during wound healing (FDR \leq 0.05, log₂ FC > 2).

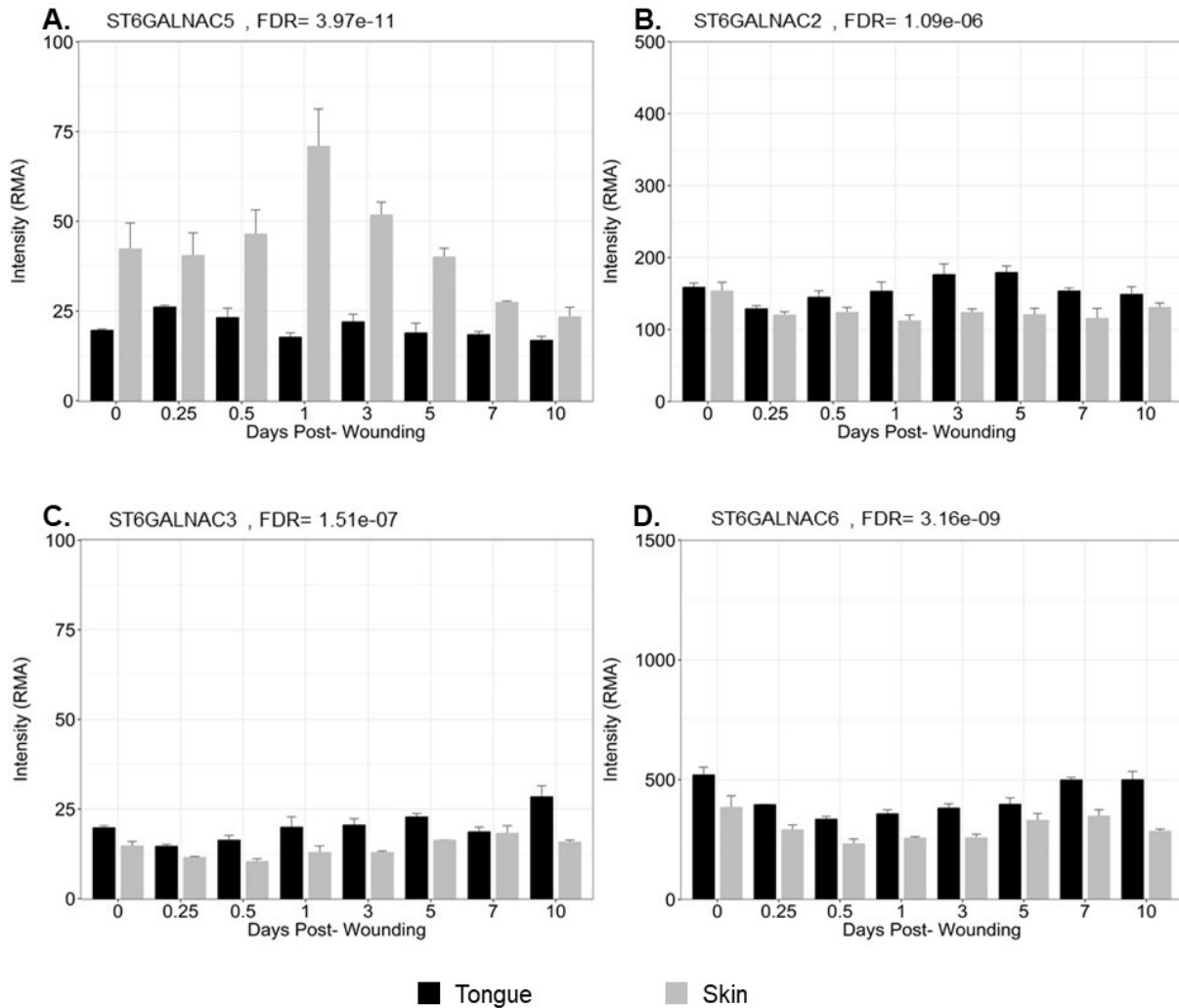


Figure 12. Expression of α 2,6- sialyltransferase related genes demonstrate significant differences in expression during skin and tongue wound healing. Expression of *ST6GALNAC5* (A) was upregulated while *ST6GALNAC2* (B), *ST6GALNAC3* (C) and *ST6GALNAC6* (D) were downregulated in the skin (grey) compared to the tongue (black) during wound healing (FDR \leq 0.05, log₂ FC > 2).

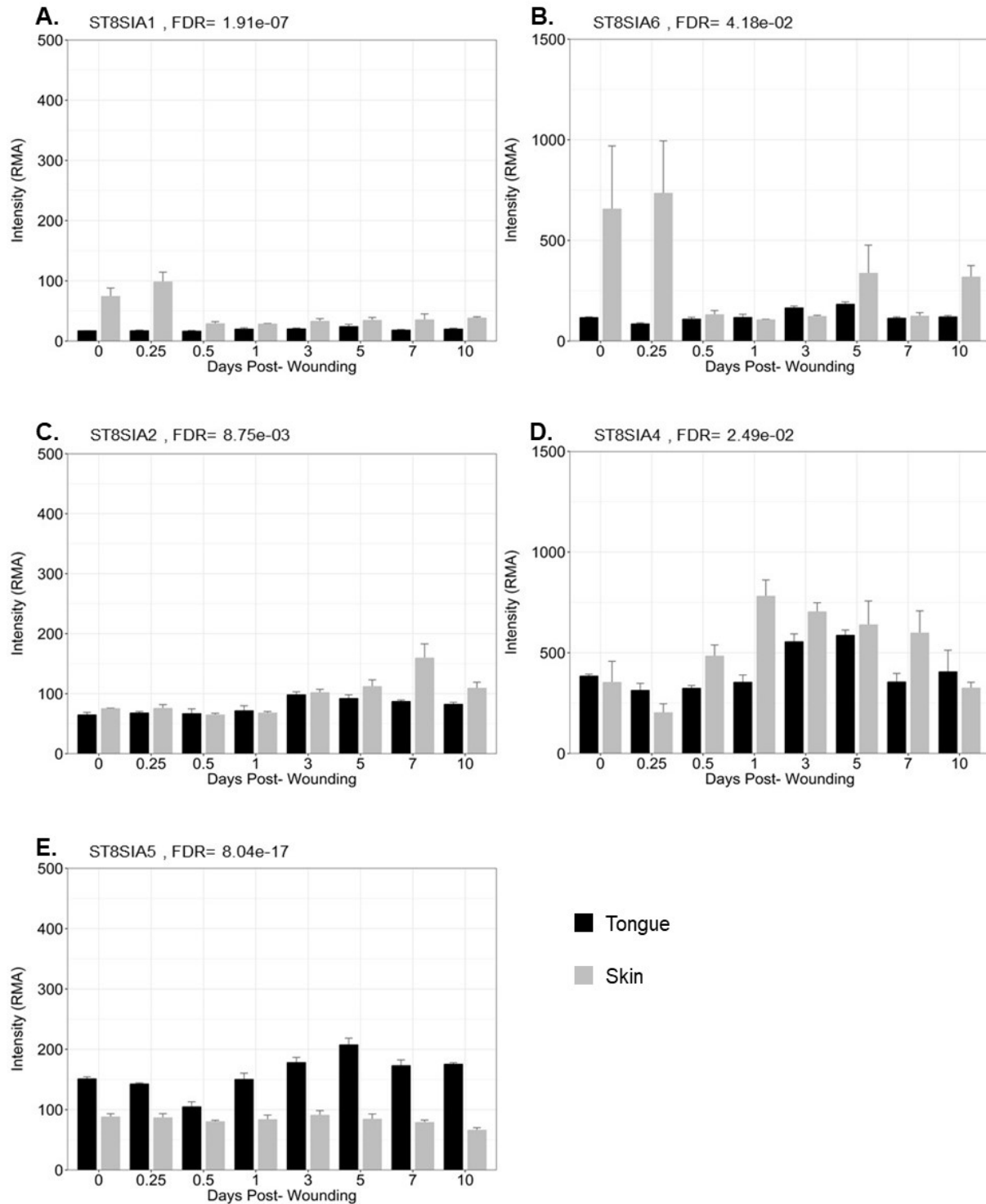


Figure 13. Expression of α 2,8- sialyltransferase related genes demonstrate significant differences in expression during skin and tongue wound healing.

Figure 13. Expression of α 2,8- sialyltransferase related genes demonstrate significant differences in expression during skin and tongue wound healing.

Expression of *ST8SIA1* (A), *ST8SIA6* (B), *ST8SIA2* (C), and *ST8SIA4* (D) were upregulated while *ST8SIA5* (E), was downregulated in the skin (grey) compared to the tongue (black) during wound healing (FDR \leq 0.05, log2 FC>2).

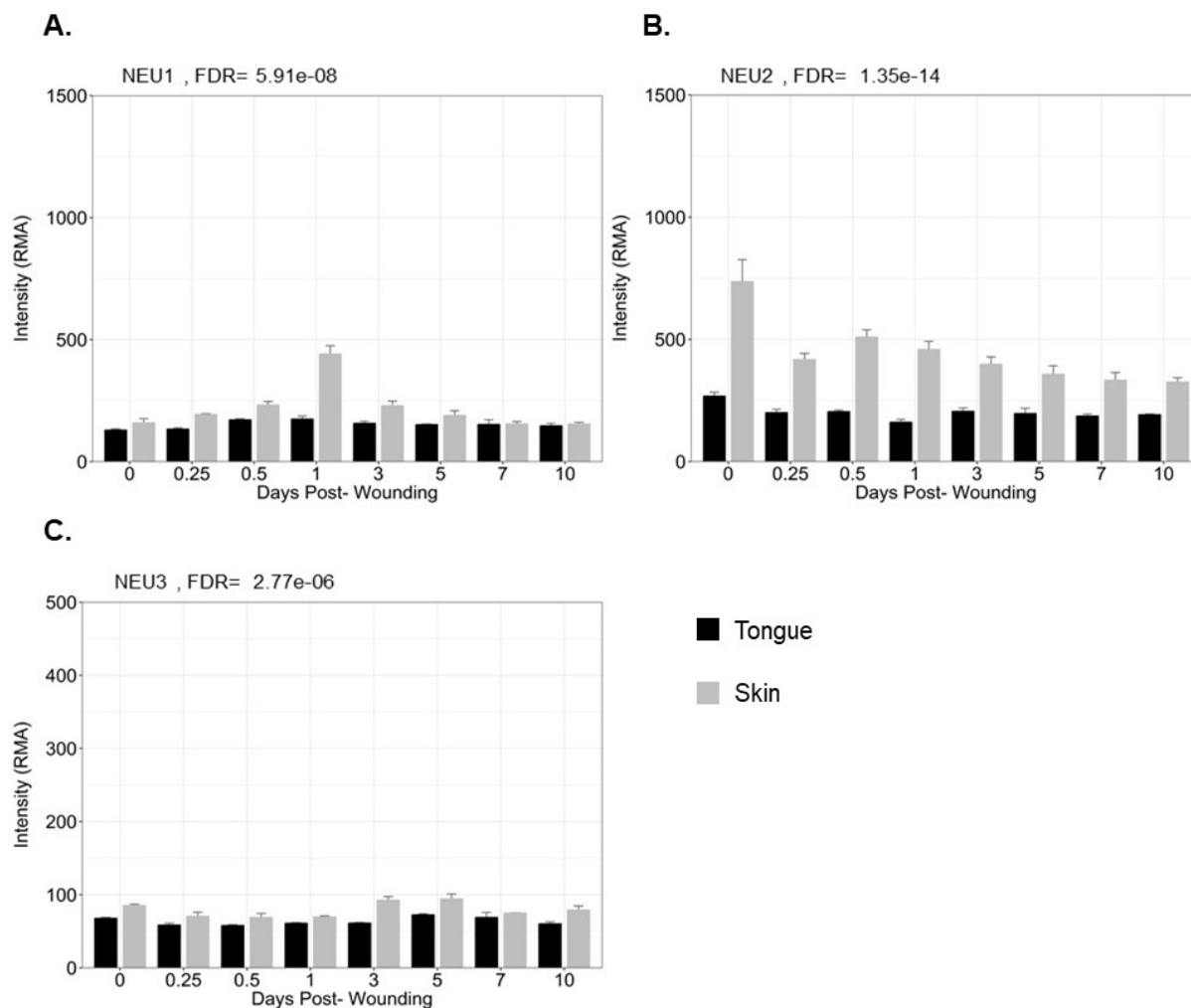


Figure 14. Expression of neuraminidase related genes demonstrate significant differences in expression during skin and tongue wound healing. Expression of lysosomal neuraminidase, NEU1 (A), cytosolic neuraminidase, NEU2 (B), and plasma membrane neuraminidase, NEU3 (C) were all upregulated in the skin (grey) compared to the tongue (black) during wound healing (FDR ≤ 0.05 , log2 FC > 2).

2.3.5 α 2,3-, α 2,6-, and α 2,8- Polysialylation are Differentially Regulated in Skin versus Tongue Wound Healing

Since glycosylation-related gene expression may not correlate with downstream changes in glycosylation, tissues were probed for changes in sialylation and polysialylation. Sialylation and polysialylation were chosen as targets based on the observed changes in sialyltransferase and polysialyltransferase transcripts, the terminal availability of these carbohydrates, their known impact on cell behavior, and their ability to be released by endogenous or exogenous neuraminidases^{36, 91}. Total free and bound sialic acids were measured, however, their expression was below the detectable range of the assay (data not shown). To assess overall sialylation the lectins Maackia amurensis and Sambucus nigra were used to probe for α 2,3- and α 2,6- linked sialic acids respectively, and antibodies 12F8 and 735 were used to identify α 2-8 polysialylated proteins. No significant outliers or blot to blot variance were identified via ROUT and ANOVA analysis. When examining total α 2,3- and α 2,6-linked sialic acid expression it was found that their regulation was inversely correlated. A downregulation of α 2,3-linked sialylation (Figure 15) and a significant upregulation of α 2,6-linked sialylation (Figure 20) (adjusted $p \leq 0.05$) was observed 3-days post wounding during the late inflammatory/proliferative phase of skin and tongue wound healing.

More specifically, time dependent differences in the α 2,3-sialylation of proteins in molecular weight range of 69-90kDa was observed, with significant downregulation occurring 3 days post-wounding during the late inflammatory/proliferative phase of wound healing when compared to uninjured tissue. Proteins with molecular weights between 69-90kDa and 125kDa demonstrated condition dependent differences in α 2,3-

sialylation with significant downregulation occurring over the course of wound healing in the skin, but not the tongue (adjusted $p \leq 0.05$). Additionally, uninjured skin demonstrated 15.6% and 46.7% more $\alpha 2,3$ -linked sialylation of 69-90kDa and 125kDa proteins, respectively, when compared to the uninjured tongue. Lastly, $\alpha 2,3$ -linked sialylation of 330kDa proteins did not demonstrate statistically significant differences despite having a 18.3% and 33.5% decrease in expression at baseline and 3 days post-wounding when comparing the skin to the tongue (Figure 15).

Fluorescence microscopy produced complex data regarding protein specific and location specific variations in $\alpha 2,3$ -sialylation. Figure 16 is an H&E stain of uninjured and wounded skin and tongue. In uninjured tongue expression of $\alpha 2,3$ -linked sialic acids, detected using MAL-II staining, was observed throughout the basal epithelial cells, papillary (above the white line) and reticular layers (below the white line) of the lamina propria (outlined in grey), and throughout the submucosa (Figure 17A), while the skin demonstrated diffused staining throughout the epidermal and dermal layers (Figure 17B). In order to better localize the $\alpha 2,3$ - sialic acids and identify cells in the dermis that express $\alpha 2,3$ - sialic acids, skin and tongue wounds were subjected to co- staining with MAL-II and $\beta 1$ -integrin (CD29) which is localized to the plasma membrane, endoplasmic reticulum (ER) and focal adhesion sites on T cells, B cells, monocytes, platelets, fibroblasts, endothelial cells, mast cells, adipocytes, hepatocytes, smooth muscle cells²⁰⁴, epithelial, myoepithelial, and mesenchymal stromal cells²⁰⁵. When simultaneously examining the expression of MAL-II (green) and $\beta 1$ -integrin (CD29, red), co-expression (orange/yellow) was identified throughout the submucosa and skeletal muscle of uninjured tongue (Figures 18A and 19A), epithelial cells, dermal extracellular matrix

(ECM) proteins, and CD29(-) more than CD29(+) cells in the dermis of intact skin (Figures 18B and 19B). More specifically, decreased epithelial distribution of MAL-II with CD29 was noted in the intact epithelium of the tongue (Figure 19A) when compared to that of the skin (Figure 19B). In uninjured skin, MAL-II was distributed throughout the basement membrane and most cells in the intact dermis with minimal co-localizing CD29 expression among dermal fibroblast and capillaries (yellow arrows). After wounding, the skin demonstrated reduced MAL-II localization to the epithelium (Figure 18D). However, increased expression occurred among platelets and other inflammatory cells localized to the scab/wound bed interface (yellow outline). During wound healing in the tongue, MAL-II expression was downregulated within the developing papillary region (Figure 18C). However, a mild increase in MAL-II expression occurred within the proliferating epithelium and inflammatory cells of the submucosa.

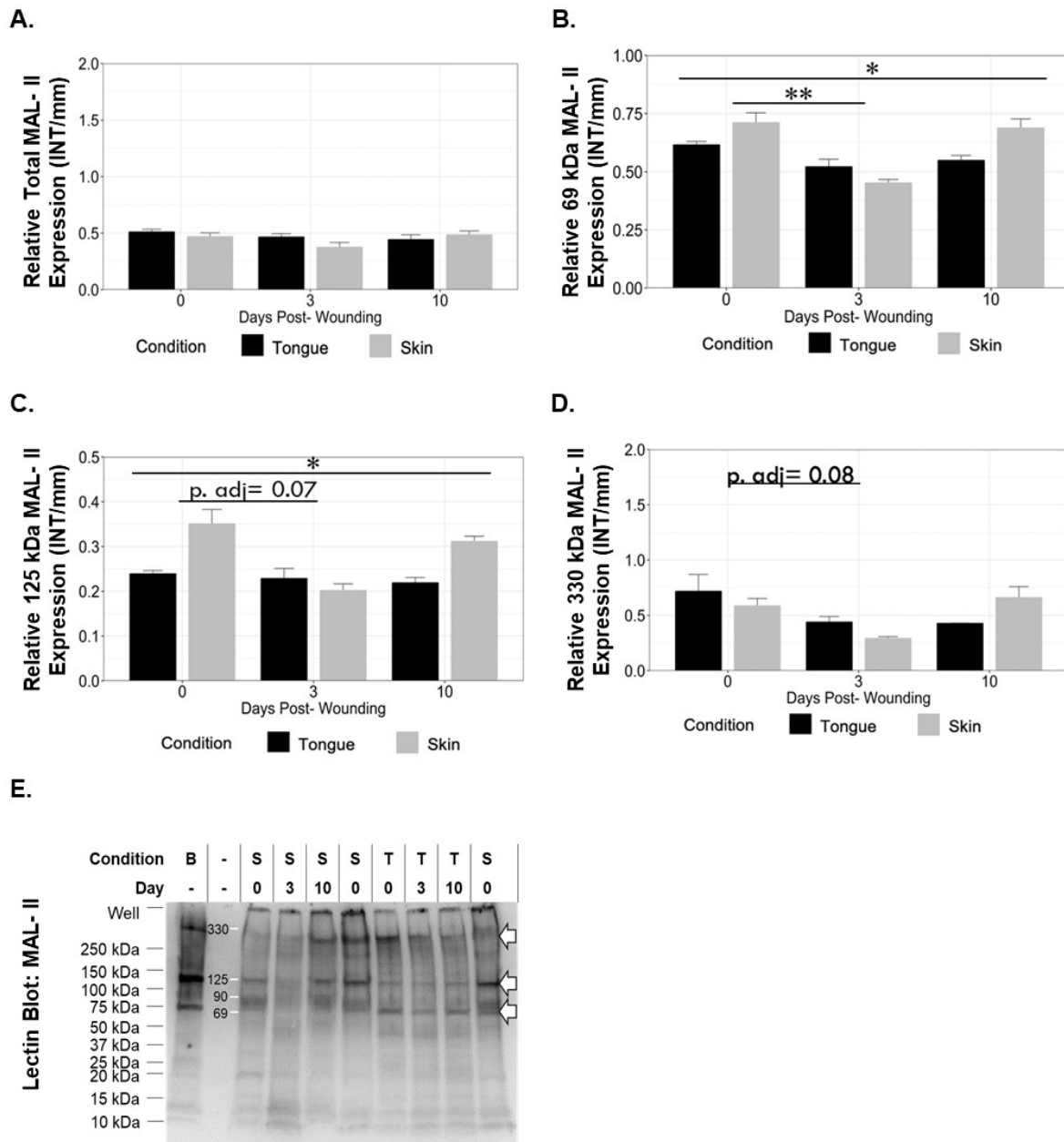


Figure 15. Expression of α 2,3- linked sialic acids is differentially regulated in specific proteins during skin and tongue wound healing. Expression of total α 2,3- linked sialic acids is not significantly regulated in skin (grey) or tongue (black) wound healing (A), however, 69kDa (B) and 125kDa (C) proteins are significantly upregulated in the skin relative to the tongue (adjusted $p \leq 0.05$) while 330kDa proteins were downregulated 3 days post- wounding (adjusted $p = 0.08$) in both skin and tongue in wound healing. Lectin blot of α 2,3- linked sialic acids (E). Brain (B) lysates were used as a positive control.

* $p < 0.05$; ** $p < 0.01$

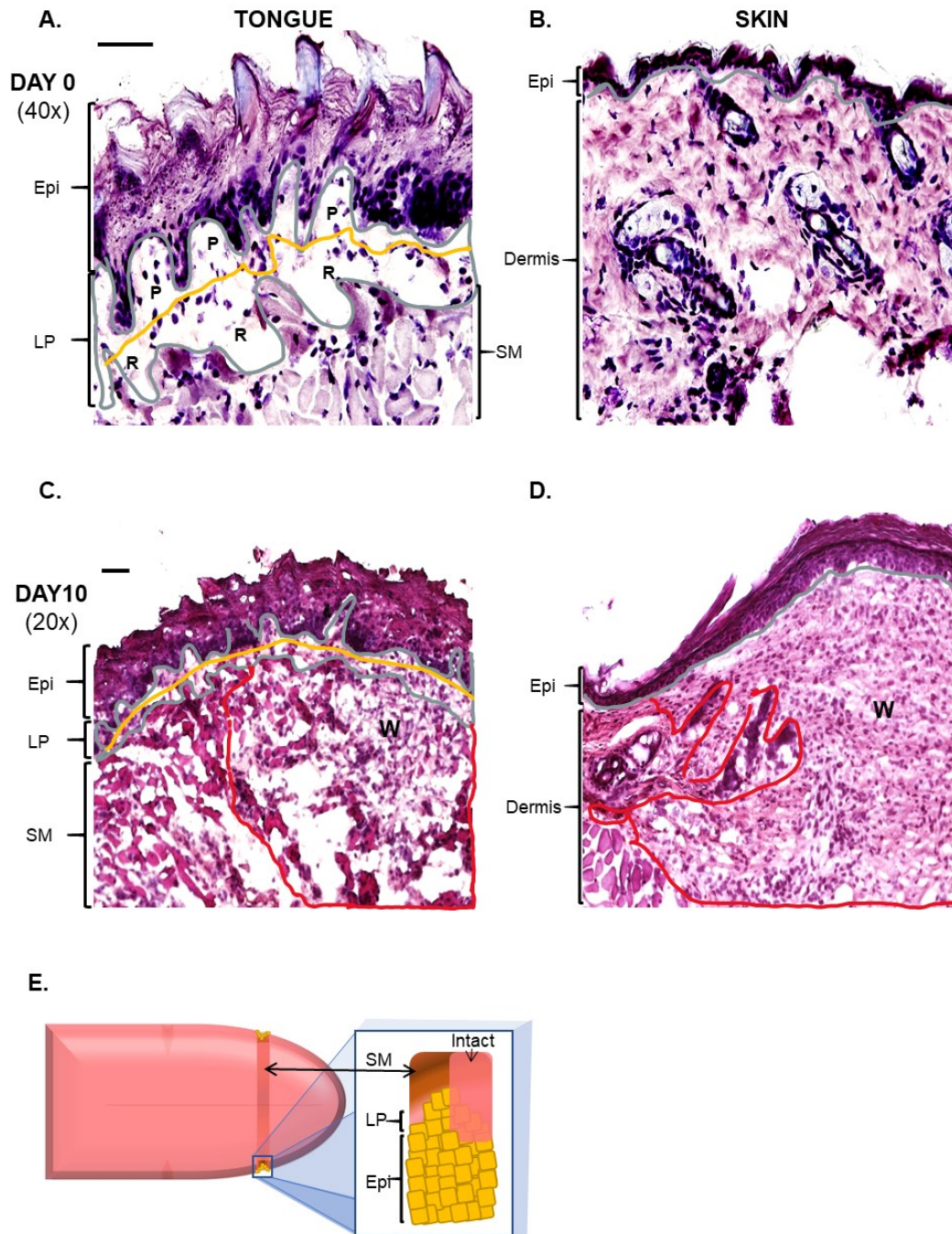


Figure 16. Tongue and skin wound healing. H&E staining of uninjured tongue (A) and skin (B) and wounds 10 days post- wounding (C & D respectively). The grey line in skin separates the epidermis (Epi) and dermis. The grey line in tongue outlines the lamina propria (LP). The white line separates papillary (P) and reticular/ fibrous (R) layers. The red border represents the wound bed (W). Black scale bar 50 μ m. Animation of 1mm transverse lateral tongue wounds represented (E). Note the caudal and cephalic portions of the tongue remain intact as not to interfere with feeding. Also note that these wounds completely epithelialize with 24hr and epithelial cells tend to migrate inward towards the wound base.

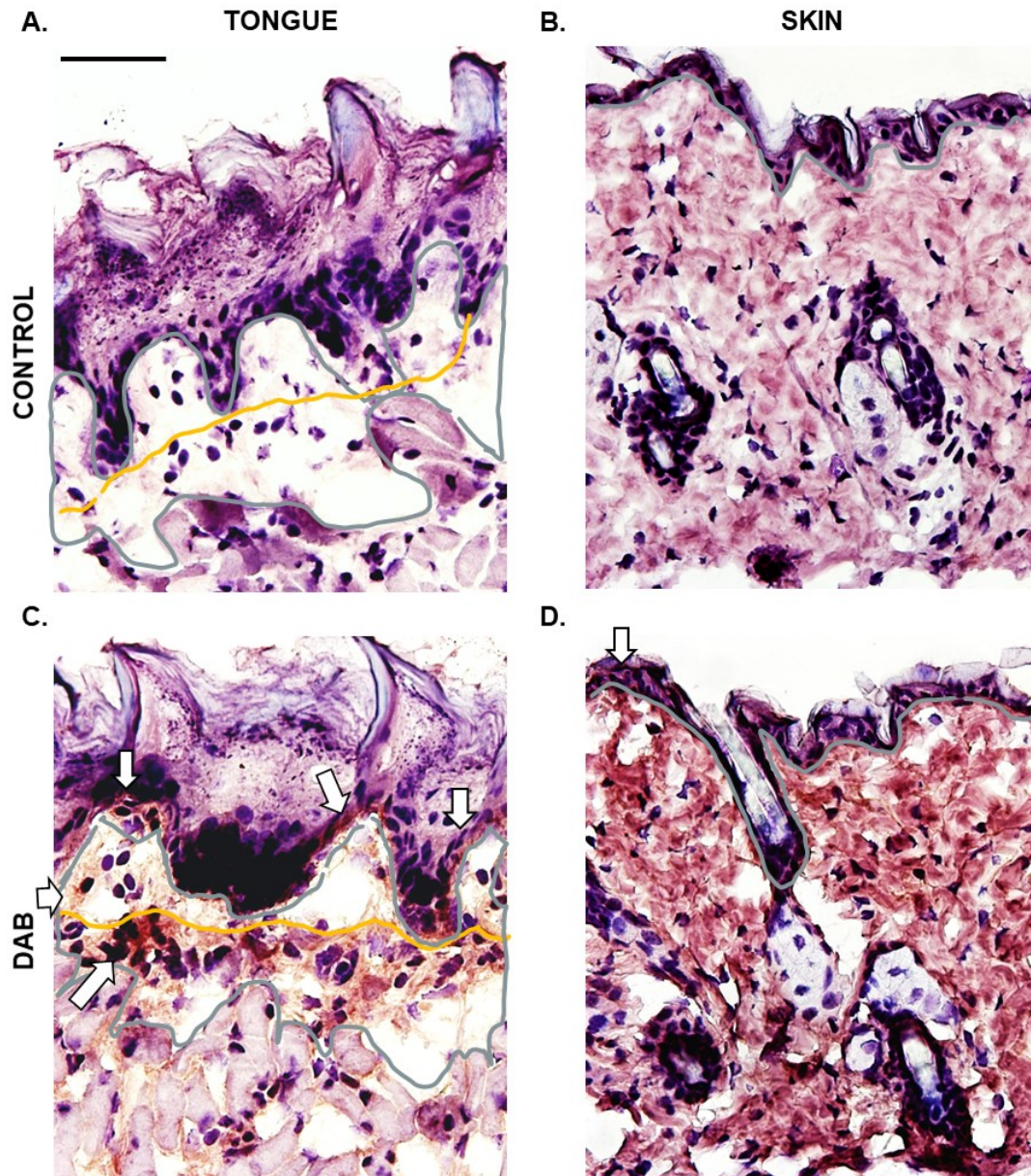


Figure 17. Localization of $\alpha 2$ -3 sialic acids in uninjured skin and tongue. MAL-II staining of $\alpha 2$ -3 linked sialic acids (DAB) with H&E staining in uninjured tongue (A, C) and skin (B, D). Controls are found in top panel (A, B). Positive staining via DAB (brown) in lower panel (C, D). The grey line in skin separates the epidermis and dermis. The grey line in tongue outlines the lamina propria. The yellow line separates papillary and reticular/ fibrous layers. Black scale bar 50 μ m.

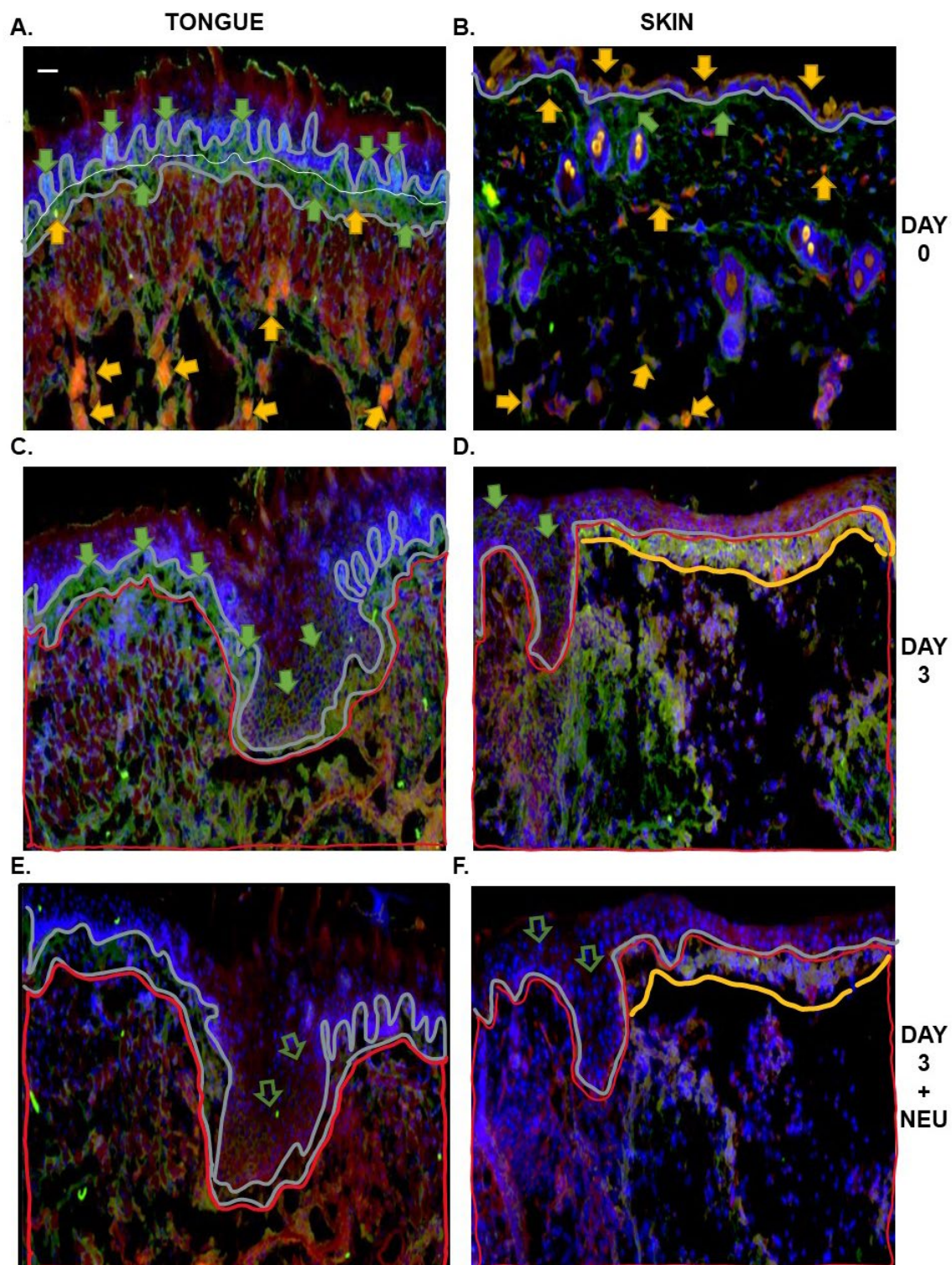


Figure 18. Localization of α 2-3 sialic acids in skin and tongue wound healing.

Figure 18. Localization of α 2-3 sialic acids in skin and tongue wound healing.

MAL-II staining of α 2-3 linked sialic acids (green) and β 1-integrins/ CD29 (red) in uninjured tongue (A) and skin (B) and wounds 3 days- post-wounding (C & D respectively). Coincidence staining (orange/yellow) noted in the submucosa and dermis. Treatment with α 2 -3, -6, -8, -9 neuraminidase confirms the MAL-II Ab bound sialic acids in wounded tongue (E) and skin (F). The grey line in skin separates the epidermis and dermis. The grey line in tongue outlines the lamina propria. The white line separates papillary and reticular/ fibrous layers. The red border represents the wound bed. White scale bar 50 μ m.

SNA lectin was then used to probe blots of wound extracts. This analysis revealed time dependent differences in total $\alpha 2,6$ -sialylation of all proteins (Figure 20A) and those with molecular weights of 50kDa (Figure 20B) and 75kDa (Figure 20C), including significant upregulation 3 days post-wounding during the late inflammatory/proliferative phase of wound healing. When compared to tongue wounds 3-days post-wounding, the skin demonstrated a 32%, 49%, and 49.5% increase in $\alpha 2,6$ -sialylation respectively among total proteins and those with molecular weights of 50kDa and 75kDa (adjusted $p \leq 0.05$). Localization of $\alpha 2,6$ -sialic acids demonstrated higher expression on CD29(+) cells along the reticular layer when compared to the papillary region of the lamina propria in the uninjured tongue and on CD29(+) cells relative to CD29(-) cells in the dermis of uninjured skin (Figure 19, right). Interestingly, the distribution and pattern of $\alpha 2,6$ -sialic acids (SNA) and CD29 opposed the co-expression of $\alpha 2,3$ -sialic acids (MAL-II) and CD29 in uninjured skin and was much higher in the reticular layer of the lamina propria in the tongue (Figure 19).

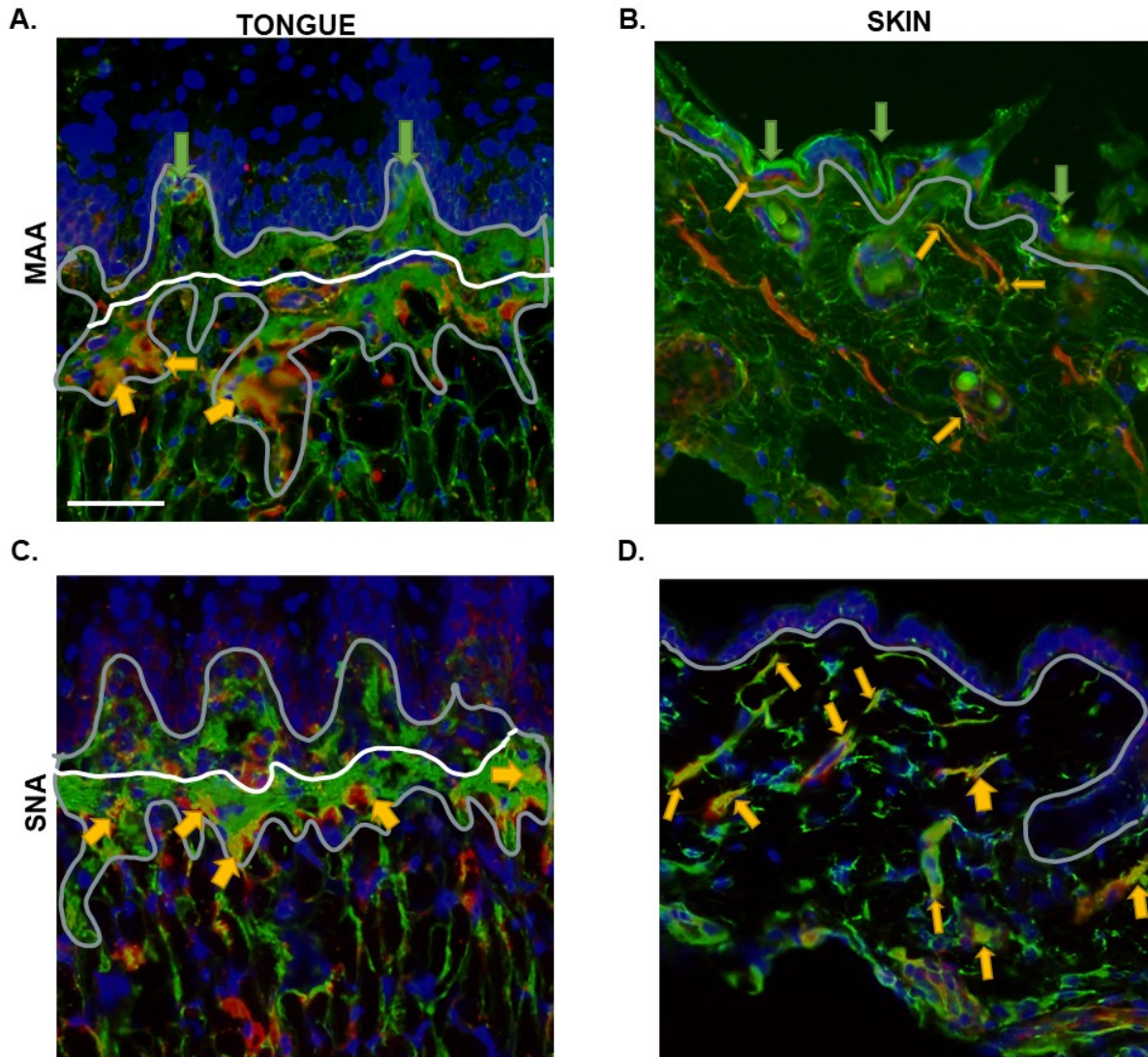


Figure 19. Localization of α 2-3 and α 2-6 sialic acids in uninjured skin and tongue. MAL-II staining of α 2-3 linked sialic acids (green) in uninjured tongue (A) and skin (B) and SNA staining α 2-6 linked sialic acids (green) (C, D respectively) with CD29/ β 1-integrin (red). Coincidence staining (yellow/orange) with CD29 is higher in α 2-6 sialylated proteins of uninjured tongue (C) and skin (D) when compared to α 2-3 sialylated proteins within the submucosa (A) and dermis (B) respectively. The grey line in skin separates the epidermis and dermis. The grey line in tongue outlines the lamina propria. The white line separates papillary and reticular/ fibrous layers. The red border represents the wound bed. White scale bar 50 μ m.

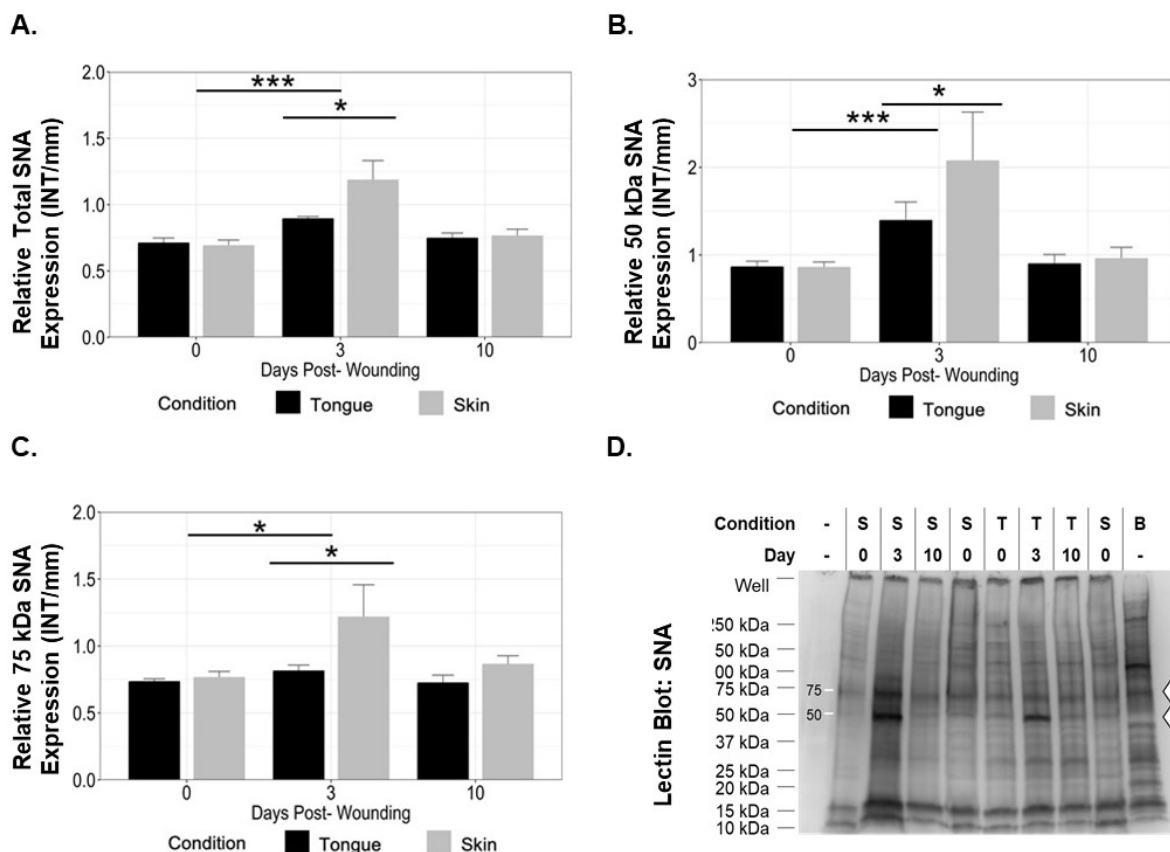


Figure 20. Expression of α 2, 6- linked sialic acids is differentially regulated during skin and tongue wound healing. Expression of total α 2, 6 - linked sialic acids (A) and α 2, 6 - linked sialic acids on proteins with molecular weights of 50kDa (B) and 75kDa (C) are significantly upregulated during wound healing (adjusted $p \leq 0.05$). Additionally, proteins with α 2, 6 - linked sialic acids demonstrate differential expression between the skin (grey) and tongue (black) at 3 days post- wound healing (adjusted $p \leq 0.05$). Lectin blot of α 2, 6- linked sialic acids (D) where brain (B) lysates were used as a positive control.

* = $p < 0.05$; ***= $p < 0.005$

Polysialic acid (polySia), which is composed of long chains of α 2,8-linked sialic acid of 8-100 units in length, caps N-linked and O-linked glycoproteins and is highly expressed during nervous system development ¹³⁹. More recent evidence suggests that polySia may also be important in mediating the adaptive response to injury during liver and neuronal regeneration ¹³⁹. To examine the expression of total α 2,8-linked polySia expression, polysialylated proteins were trapped using EndoNt, an inactive endoneuraminidase, and then were identified following SDS PAGE by blotting with the anti-polySia antibody, 12F8. Three primary bands were identified, however, only the 12F8 staining of those with molecular weights of 150-250kDa was eliminated following treatment with catalytically active endoneuraminidase (Figure 21B). Time dependent changes in expression were again noted at 3 days post-wounding (adjusted $p \leq 0.05$) for polysialylated proteins with a molecular weight of 250kDa. Furthermore, the skin demonstrated a 2.0-fold increase in polySia expression between 0 and 3- days post-wounding, and this change in expression was significantly less than the 4.2-fold increase observed in the tongue (adjusted $p \leq 0.05$). The inability of endoneuraminidase to eliminate 12F8 binding at 75kDa and 50kDa suggests that both EndoNt and 12F8 may bind non-specifically to other proteins.

Localization of polySia among paraffin embedded sections demonstrated punctate expression in the epithelial and submucosa layers of uninjured tongue (Figure 22A), however, this was poorly visualized in the skin. Tongue and skin wounds demonstrated increased punctate expression of polySia in the apical epithelium, lamina propria and submucosa/dermis (Figure 22C and 22G respectively). However, polySia expression was higher and primarily restricted to the apical epithelium in skin wounds

by day 10 (Figure 22H), along with the periwound (area just outside of the wound bed) on day 3. Furthermore, periwound epithelium 3 days post wounding and the remodeling epithelium 10 days post wounding demonstrated the greatest amount of 12F8 staining in the cytosol of epithelial cells in the stratum granulosum.

Immunoblots revealed that polysialic acid was upregulated 3 days post-wounding during the proliferative phase of healing, however, inflammatory cells including macrophages remain present in these wounds up through day 5 in the skin and day 3 in the tongue. Since e-selectin ligand is known to be polysialylated and involved in inflammation, coincidence staining between polysialic acid (12F8) and e-selectin ligands were probed. Increased magnification of tongue wounds revealed restricted coincidence of polySia (12F8) and ESL-1 (GSGL1, GLG-1), a protein frequently found sequestered in the Golgi and previously shown to be polysialylated (Figure 22 E, yellow arrows). Treatment with endoneuraminidase obliterated the 12F8 staining of polysialic acids in uninjured tongue (Figure 22B), tongue wounds (Figure 22D), and skin wounds (Figure 22I). The enhanced presence of 12F8 binding and punctate polySia expression with and without coincidence staining with anti-ESL-1 antibody suggests that intracellular polySia expression is modifying proteins other than ESL-1.

Since 12F8 staining appeared without GLG-1/ ESL-1 staining, coincidence staining was observed between NCAM1, 12F8 which labels polysialic acid, 735 which labels polysialic acid, polysialylated NCAM1, and non-specifically to non-polysialylated NCAM. Yellow coincidence staining was determined to be true polysialic acid staining between the 12F8 and 735 antibodies, while white coincidence staining was determined

to represent polysialylated NCAM1. Punctate yellow coincidence staining was consistent with the previous 12F8 staining in the lamina propria and submucosa of uninjured tongue and wounds 3 days post- wounding, however, increased intracellular staining of larger cells dispersed within the tongue's periwound epithelium was also identified (Figure 23A). Additionally, increased NCAM1 Ab binding in the epithelium may have obscured the punctate epithelial polysialic acid that was observed previously in the uninjured and wounded tongue. Furthermore, intracellular coincidence staining of all three antibodies was observed sparingly in the epithelium and submucosa of tongue wounds, indicating that NCAM1 may be one of the polysialylated proteins, however, it is likely not the only protein displaying polysialic acid (Figures 23A-D).

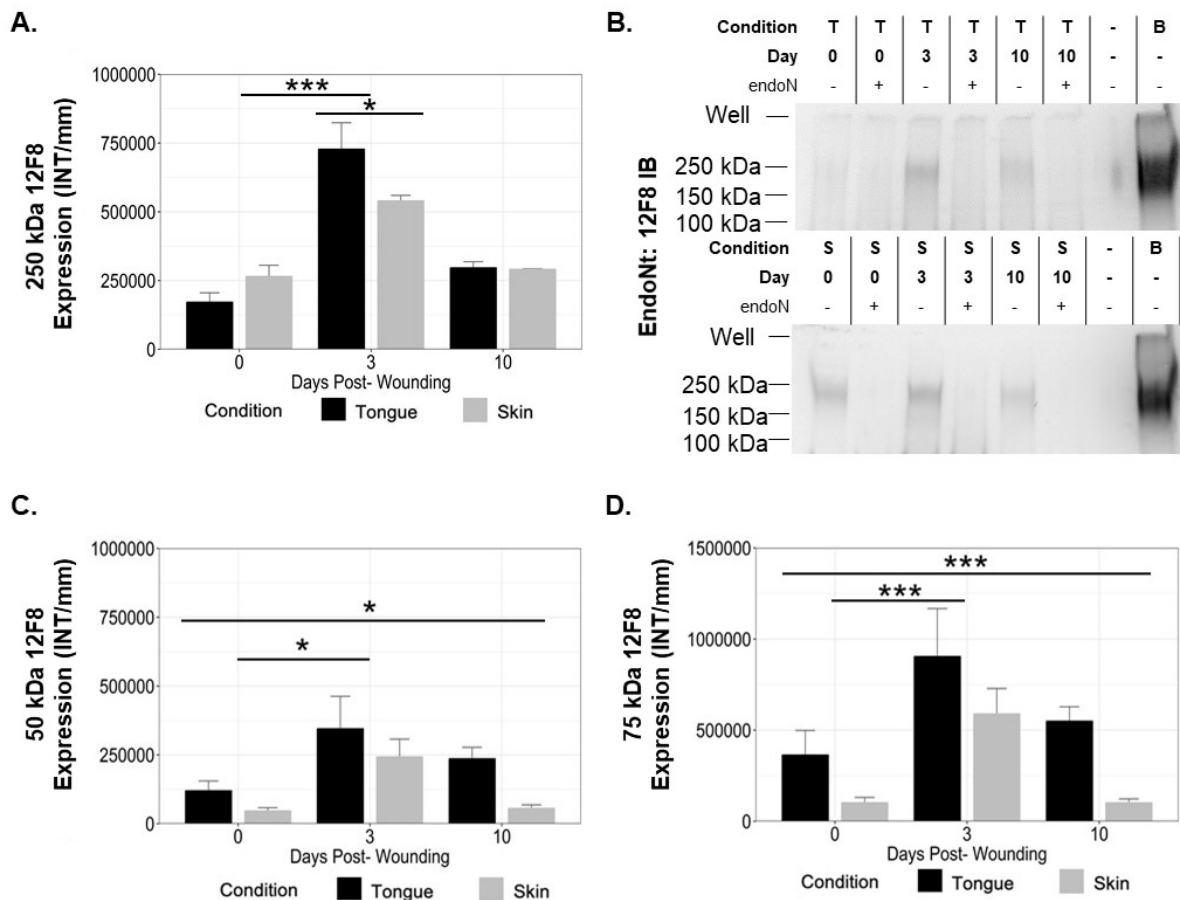


Figure 21. Expression of α 2, 8- linked polysialic acids is differentially regulated during skin and tongue wound healing. Expression α 2, 8 - linked polysialic acid on proteins with a molecular weight of 250kDa (A) are significantly upregulated during wound healing (adjusted $p \leq 0.05$) and demonstrate differential expression between the skin (grey) and tongue (black) at 3 days post- wounding (adjusted $p \leq 0.05$). EndoNt recovered proteins immunoblotted with 12F8 identified the presence of α 2, 8-linked polysialic acid (B) in tongue wound healing (top) and skin wound healing (bottom). Brain lysates (B) were used as a positive control. Treatment with endoN confirms the specificity for polysialic acid and.

* = $p < 0.05$; ***= $p < 0.005$

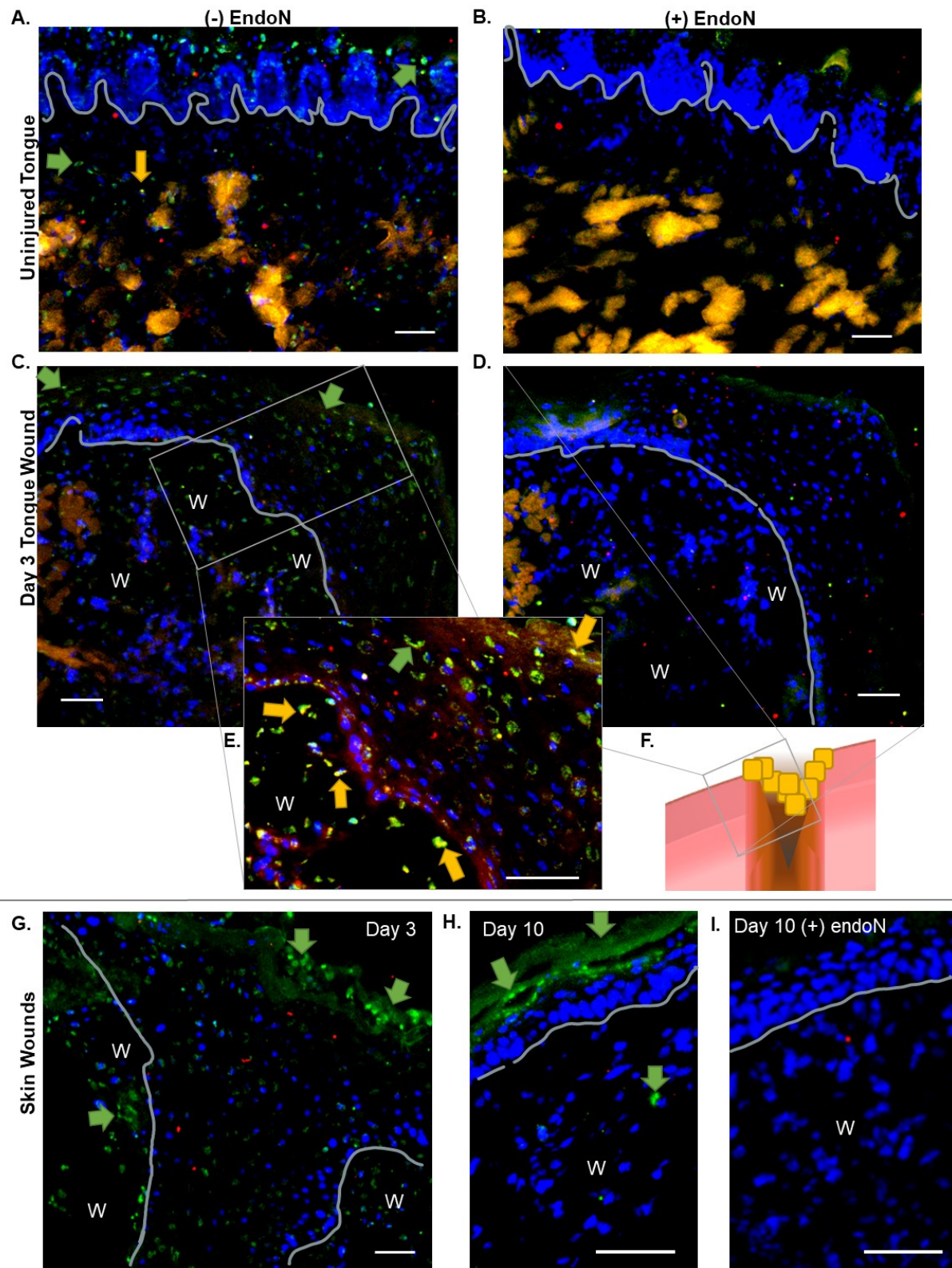


Figure 22. Localization of $\alpha 2-8$ polysialic acids in skin and tongue wound healing.

Figure 22. Localization of α 2-8 polysialic acids in skin and tongue wound healing. 12F8 staining of α 2-8 polysialic acids (green) and Golgi glycoprotein/ GSGL1/GLG-1/ESL-1 (red) in uninjured (A, B) and wounded tongue (C, D) and skin (G) 3 days- post-wounding, and skin wounds 10 days post wounding (H,I). Coincidence staining (orange/yellow) rarely noted except at 40x magnification (E). The animation of tongue wounds (F) depicts the location where the 20x and 40x magnifications were obtained. Treatment with catalytically active endoneuraminidase confirms the 12F8 Ab bound polysialic acids in uninjured (B) and wounded tongue (D) and skin (I). The grey line in skin separates the epidermis and dermis. The grey line in tongue outlines the lamina propria. The white line separates papillary and reticular/ fibrous layers. The red border represents the wound bed. White scale bar 50 μ m.

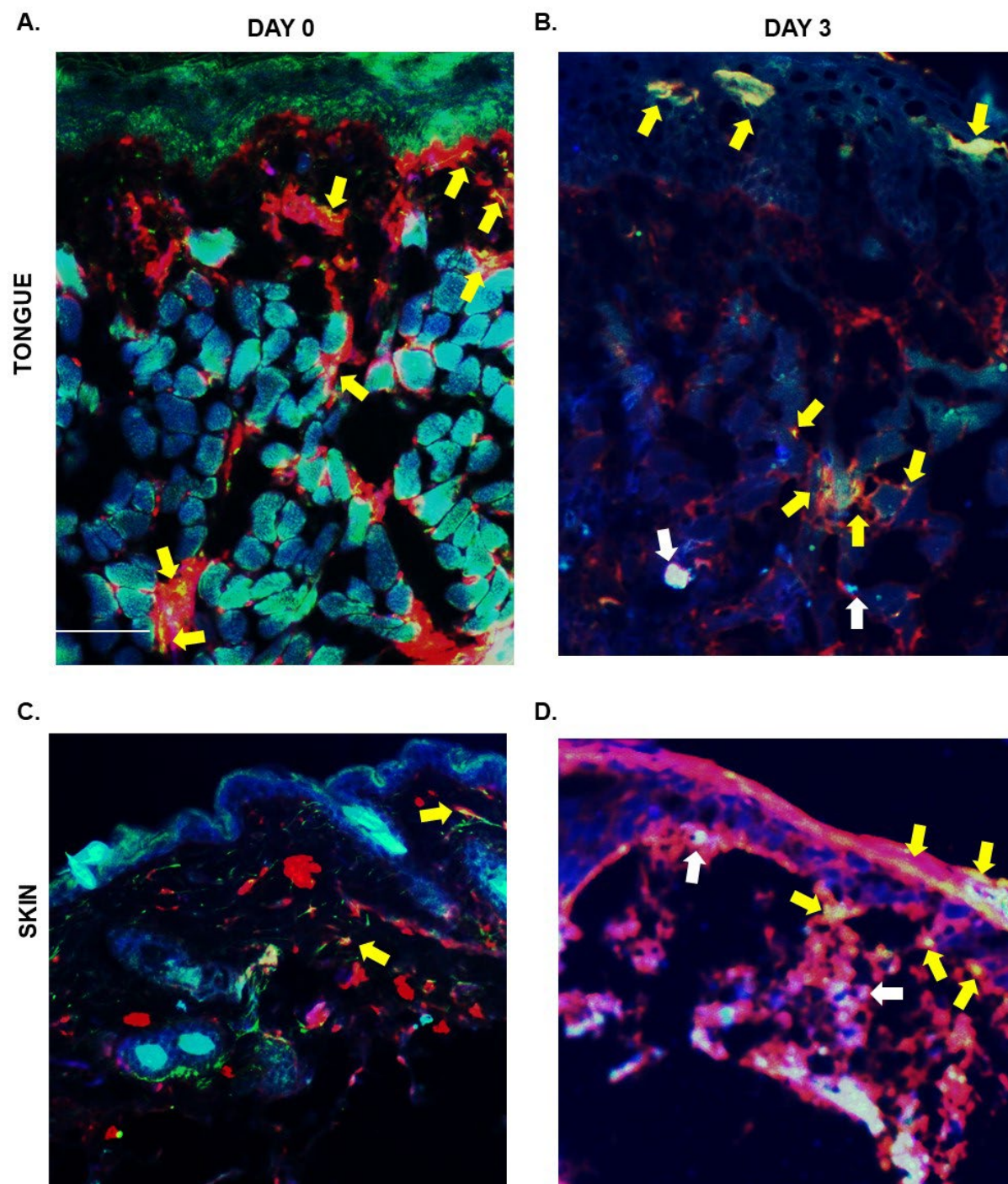


Figure 23. Expression of 12F8, 735, and NCAM-1 in skin and tongue wound healing.

Figure 23. Expression of 12F8, 735, and NCAM-1 in skin and tongue wound healing. Staining of α 2-8 polysialic acids via 12F8 (green) and 735 (red) antibodies in addition to neural cell adhesion molecule (NCAM) (blue) in uninjured (A) and wounded tongue (B) and uninjured (C) and wound skin (D) 3 days- post-wounding. Coincidence staining by 12F8 and 735 (yellow; yellow arrows) confirm the presence of polysialic acid. Coincidence staining by 12F8, 735, and NCAM1 (white; white arrows) confirm the presence of polysialylated NCAM1. The grey line in skin separates the epidermis and dermis. The grey line in tongue outlines the lamina propria. The white line separates papillary and reticular/ fibrous layers. The red border represents the wound bed. White scale bar 50 μ m

2.4 Discussion

In this study we demonstrate that there are differences in the regulation of genes related to glycosylation and more specifically in the regulation of protein and lipid sialic acids in tongue and skin wounds. Additionally, the differential gene expression of sialyltransferase genes correlate with downstream changes in protein sialylation. While using glycomics analysis may have provided each glycans structure and more insight to the overall glycan modifications, we chose to focus on a targeted type of glycosylation, (poly)sialylation, based on the results of our gene and pathway analysis. Additionally, the established role of sialic acid in modulating and mediating cell adhesion and cell signaling made these related modifications interesting targets for further investigation.

Previous studies have identified that *GNE* upregulation and the sialic acid precursor ManAc both stimulate increased sialic acid accumulation and polysialylation¹⁹⁹. *GNE* and presumably ManAc were increased in the skin relative to the tongue, especially in the first 6 hours post-wounding. However, *GNE* expression is rate limited by its feedback inhibitor CMP- sialic acid. The conversion of sialic acid (NeuAc and NeuGc) to CMP-NeuAc and CMP- NeuGc is regulated by *CMAS* which was downregulated in the skin as compared to the tongue throughout the course of wound healing. When CMP-sialic acid is unable to bind the abundantly expressed *GNE*, or if ManAc is upregulated, free sialic acid accumulates in the cytosol^{197, 199, 206-207}. This increases sialic acid bioavailability to microbial organisms which promotes their resistance and nutrient support²⁰⁸, increases neural cell adhesion molecule polysialylation, and impacts other metabolic pathways. In this investigation, total sialic acid content was assessed using total and free sialic acid assays; however, the

magnitude of skin and tongue sialic acid expression were below the detectable range set forth by the assay and were therefore unable to be determined.

Though we were unable to glean any additional information regarding the sialic acid donor sugars and free sialic acid accumulation, we were able to probe for sialic acids in uninjured skin and tongue and their wounds using lectins for α 2,3- and α 2,6-linked sialic acids and the 12F8 antibody for polysialic acid. When examining the overall α 2,3- and α 2,6-linked sialylation of proteins in the lectin blot analysis, the magnitude of expression between days 0, 3 and 10 post- wounding were minimal in the tongue and much larger in the skin. This aligned with the overall glycogene clustering of variance within the 1st and 2nd principle components in which days 0, 3, and 10 clustered into the same group in the tongue. In contrast, glycogene clustering of skin wounds revealed different groups with day 3 being one group, and days 0 and 10 another (Figure 7A). Additionally, the expression of sialic acids during the wound healing process were linkage specific and an inverse relationship in the expression of α 2,3- and α 2,6- linked protein sialylation was observed 3- days post- wounding during skin and tongue wound healing. Skin and tongue wounds demonstrated decreased expression of α 2,3- linked sialic acids and increased expression of α 2,6- linked sialic acids 3 days post wounding, however, these changes were heavily blunted in the tongue when compared to the skin. With regards to the distribution of sialic acids, α 2,3- and α 2,6- linked protein sialylation both demonstrate increased expression within the lamina propria. However, α 2,3- linked sialic acids are more highly abundant in the papillary and reticular layers of the tongue and epidermis of the skin, while α 2,6-linked sialic acids are more highly abundant in the reticular/fibrous layer of the lamina propria of the tongue and demonstrate little to no

epidermal distribution in the skin. While no previous literature exists regarding the overall impact of changes in sialic acid linkage, previous studies indicate that α 2-6 sialylation of Fc regions of IgG may play an important role in enhancing the tissues protection against excessive inflammation ¹⁰². Interestingly, Siglecs which help to mediate a number of inflammatory responses, preferentially bind α 2,6- linked sialic acids in B cells (Siglec-2 and Siglec-6) and monocytes (Siglec-3), while α 2,3- linked sialic acids are preferentially bound by macrophages (Siglec-1), eosinophils, basophils, and mast cells (Siglec-8). Additionally, α 2-6 sialylation of 130kDa β 1-integrin proteins interferes with galectin 3 binding by blocking the β 1-integrin binding site, subsequently reducing galectin 3-induced apoptosis ¹⁶⁹. This aligns with the high degree of coincidence staining observed among α 2,6-linked sialic acids and CD29 (β 1-integrin) in uninjured skin and tongue where gross apoptosis would be undesirable during tissue homeostasis. Though the skin and tongue demonstrate a large increase in α 2,6-sialylation of 50kDa proteins, which could potentially represent the heavy chain of IgG, the skin additionally demonstrated significantly more global α 2,6-sialylation and α 2,6-sialylation of 75kDa proteins during wound healing. It has been previously established that the tongue heals with less inflammation when compared to the skin, however, the expression of α 2,6-sialic acids and thus their protection against inflammation was lower in tongue wounds. This discrepancy suggests that either: 1) the tongue achieves peak upregulation of α 2-6 sialic acids prior to day 3; 2) excessive and prolonged α 2-6 sialylation of injured and potentially nonviable cells interferes with galectin-3 mediated apoptosis which in turn delays inflammatory cell infiltration and the clearance of nonviable cells during skin wound healing; or 3) α 2-6 sialic acids are promiscuous and

the role that they play during inflammation are mediated by the actions of other unidentified proteins involved in wound healing.

When examining the expression of total α 2,8- linked polysialic acids, using an EndoNt trap and the 12F8 anti-polySia antibody, three primary bands were identified. However, the 12F8 recognition of only those of molecular weights between 150-250kDa was abrogated when treated with catalytically active endoneuraminidase. The inability of endoneuraminidase to eliminate 12F8 recognition of the protein bands at 75kDa and 50kDa suggests that EndoNt and 12F8 also bind other proteins non-specifically. For example, the 50 kDa band could represent the Ig heavy chain. When examining 12F8 immunoblots of proteins with an approximate molecular weight of 250kDa there was a larger increase in polySia between day 0 and day 3 in the tongue than in the skin. While this did not match the increased polysialyltransferase gene expression observed in skin wound healing relative to the tongue, this discrepancy may be attributed to the time of peak gene expression, changes in protein substrate expression, or differences in donor nucleotide sugar availability.

Differential polysialylation in skin and tongue wound healing is also likely attributed to differences in combinatorial polysialyltransferase gene expression. In the tongue *ST8SIA2* and *ST8SIA4* reached peak expression 3-5 days post-wounding during the late inflammatory/ proliferative phase of healing. However, the skin achieved peak *ST8SIA4* expression 1-day post-wounding during the inflammatory phase, while *ST8SIA2* achieved peak expression 7 days post-wounding during the remodeling phase of healing. When the expression of all significantly regulated polysialyltransferase transcript probes were combined (Figure 54, Appendix A), the uninjured tongue

demonstrated lower total expression than the uninjured skin. Additionally, tongue wounds demonstrated a larger increase in polysialyltransferase gene expression between day 0 and day 3 compared to the skin, which was consistent with the 12F8 immunoblot data.

Here our data confirms that polySia is enhanced during the late inflammatory/proliferative phase of healing and that polysialyltransferase gene expression may act as a predictor for downstream polysialylation. PolySia has also been observed in other models of regeneration and during processes that are critical to wound healing. These studies identified that polySia increases neuronal progenitor cell migration and axonal regeneration ¹³⁹, weakens hepatic progenitor cell-matrix interactions to facilitate progenitor cell migration, decreases cell aggregation, and increases growth factor induced migration ²⁰⁹⁻²¹¹ which is important during wound healing. PolySia has also been suggested to play an important role in mediating the transition between circulating and peripheral monocytes ¹⁰⁹. This is a key component of wound healing as wounds transition from hemostasis and exhibit active clearance of nonviable cells and debris during the inflammatory phase of healing. This previously published study found that polySia is downregulated as bone marrow derived monocytes enter the circulation and again when they leave the circulation and initiate phagocytosis in peripheral tissues¹⁰⁹. Additional studies indicate that polysialylated NRP-2 and ESL-1 sequestered in the Golgi in THP macrophage cells are released to the cell surface and shed into the extracellular space in response to injury and LPS stimulation to attenuate LPS induced nitric oxide (NO), interleukin-1 (IL-1), and tumor necrosis factor- alpha (TNF α) production ¹⁰⁸. Furthermore, in both studies, polysialylation was catalyzed by the

polysialyltransferase, ST8SIA4. While these studies only focused on cells of myeloid lineages, polySia has demonstrated increased expression in migrating dendritic cells, hepatic progenitor cells, and axons, suggesting that its effects may be broad across cell types. We observed increased polySia in both epithelial cells and cells throughout the dermis and submucosa, which likely represent migrating myeloid cells in wounds during the late inflammatory/proliferative phase of healing. The polySia expressed in uninjured skin and tongue may potentially represent cells of neural lineage or myeloid cells beginning to shed their polySia, as previous reports indicate that the polySia shedding may be nearly instantaneous following injury ¹⁰⁸.

Evidence that polySia may contribute to enhanced inflammation and scarring in disease processes such as chronic obstructive pulmonary disease and in the bleomycin induced pulmonary fibrosis model exists ¹⁴⁴. In our study the skin demonstrated peak expression of *ST8SIA4* during early inflammation and a late peak expression of *ST8SIA2* during remodeling. This diverges from the dual peak expression of both polysialyltransferase genes observed in the tongue during the late inflammatory/proliferative phase of healing. Roles for *ST8SIA4* mediated polysialylation in prolonged inflammation and *ST8SIA2* mediated polysialylation in fibrosis and scar formation may be suggested by several observations including 1) that the tongue heals with less inflammation and scarring; 2) there are time specific differences in the peak regulation of polysialyltransferase genes, *ST8SIA2* & *ST8SIA4*, in tongue and skin wound healing; 3) *ST8SIA4* has been found to mediate phenotypic changes in myeloid lineage cells; along with 4) evidence that polySia contributes to inflammation and scarring in other models.

Another potential contribution to the differences observed in skin and tongue may lie in other pathways that were identified in the microarray analysis. PANTHER biological process over-representation testing identified numerous processes related to cell cycle, mRNA splicing, mRNA and rRNA processing, and DNA, RNA and rRNA metabolism that were upregulated in the skin, while processes related to the generation of precursor metabolites, ATP synthesis, purine nucleotide and ribonucleotide metabolism were downregulated. Since protein and lipid glycosylation are heavily dependent upon congruent metabolic processes, a disruption in these processes might be expected to interrupt glycosylation. This may suggest that the metabolism of the tongue allows more efficient transcription, translation, and post-translational modifications including glycosylation, than the skin. Both the pathway analysis and differential sialylation patterns between skin and tongue wound healing suggests a role for metabolic differences being a contributing factor in mediating the differences in skin and tongue wound healing and warrants further investigation.

One limitation in this study included the limited time points that were examined for downstream differential glycosylation analysis. The largest percentage of glycogenes were differentially regulated during the early inflammatory phase of wound healing (days 0.25, 0.5, and 1 post-wounding). Day 3 was chosen as a subsequent timepoint to investigate as the translation of enzymes and glycosylation of subsequent proteins would be expected to be slightly delayed relative to the timepoints of gene transcription. We also wanted to capture timepoints that could traverse the inflammatory, proliferative and remodeling phases of wound healing. The largest variance in gene expression occurred as a result of innate differences between the skin and tongue. While significant

differences in glycosylation were observed between the skin and tongue over days 0, 3, and 10, more differences would likely be observed at earlier timepoints as the clusters representing hemostasis and the inflammatory phase of healing were far more divergent in the skin (Figure 7A, cluster 4b and 5) than in the tongue (Figure 7A, cluster 2a and 2b). Future studies should assess the regulation of glycosylation during earlier timepoints and use glycomic and metabolomic analysis to further elucidate the role of glycosylation as a driving force for the differential inflammatory responses and scarring that are observed between skin and tongue wound healing.

3 DISEASE SPECIFIC REGULATION OF GLYCOSYLATION DURING DIABETIC AND NON-DIABETIC WOUND HEALING- GENOMICS ANALYSIS

3.1 Introduction

Diabetes (DM) is a growing epidemic that impacts 9.3% of the US population, with approximately 29.1 million persons affected in the US as of 2012. Additionally, an alarming ~89 million adults were found to be pre-diabetic (pre-DM) in the 2012 estimates ²¹². Some of the largest healthcare related economic burdens are those associated with DM, costing \$277 and \$44 billion annually for DM and pre-DM related medical treatment, respectively ²¹³. Of this amount, 38 billion dollars of annual healthcare cost can be attributed to complications associated with Diabetic Lower Extremity Ulcerations (DLEUs) ²¹⁴. With DM reaching epidemic proportions, and diabetics having a 10-20 times greater amputation risk ²¹², a thorough understanding of the pathogenesis involved in wound development and impaired healing is required for the treatment of DLEU and limb salvage.

Chronic hyperglycemia is recognized as an initiating factor in the pathology of multiple DM related comorbidities. An important consequence of hyperglycemia is the spontaneous, non-enzymatic glycation of proteins and lipids ⁸¹ leading to the accumulation of advanced glycation end products (AGE). AGE accumulation is believed to impair healing, as AGEs are known to increase collagen crosslinking ⁸²⁻⁸⁴ and impair normal cell migration, proliferation, adhesion, growth factor expression, and cell signaling ⁸⁵⁻⁸⁸.

Although AGEs and glycosylation have generally been considered as independent variables that can influence healing wounds, previous evidence clearly demonstrates that AGEs can alter the expression and activity of genes and enzymes involved in enzymatic glycosylation. For example, endothelial cells (EC) from DM rats demonstrate significantly increased fucosidase and neuraminidase activity¹⁵³⁻¹⁵⁴. Glycated serum albumin, containing soluble AGEs, has also been shown to independently alter protein fucosylation and sialylation along with the activity of the respective glycosyltransferase and glycosylhydrolase enzymes *in vitro*¹⁵⁴. Since AGEs influence enzymatic glycosylation, and AGE accumulation is a known phenomenon associated with DM, we hypothesized that DM may alter the normal patterns of enzymatic protein glycosylation both during skin turnover and maintenance and over the course of wound healing. This study compared glycosylation- related gene expression in uninjured skin and wounds of diabetic and non-diabetic mice. Our results show that differential glycosylation- related gene expression occurs in diabetic versus non-diabetic skin and wounds, yielding downstream changes in overall protein glycosylation.

3.2 Methods and Materials

3.2.1 Animals Wound Models

All animal work was approved by the Institutional Animal Care and Use Committee (IACUC) at the University of Illinois at Chicago and conducted according to the recommendations of the Guide for the Care and the Use of Laboratory Animals. Seven-week-old female Lepr^{db/db} and C57BL/6J mice, were purchased from Jackson Laboratories (Bar Harbor, ME), housed in groups of five at 22 to 24°C on a 12-h:12-h

light/dark cycle, and allowed to habituate for a minimum of 1 week. All mice were fed a standard chow *ad libitum*.

Following the habituation period mice were subjected to wounding as previously described. Briefly, each mouse was anesthetized with ketamine (100mg/kg) and xylazine (5 mg/kg). Four, five-millimeter excisional skin wounds were produced via punch biopsy (Acu-Punch, Acuderm Inc., Ft. Lauderdale, FL) on the dorsal surface of each mouse. The tissue removed by the injury procedure was used as baseline, uninjured skin control.

Following euthanasia, wound samples (n=4) were obtained at days 3 and 10 post wounding. One sample was embedded in optimal cutting temperature media (OCT), 1 frozen and stored at -80 °C for protein analysis, and 2 samples were snap frozen in liquid nitrogen and shipped on dry ice for glycotranscriptomic analysis to the Moreman Lab at University of Georgia Complex Carbohydrate Research Center.

3.2.2 Protein Sample Preparation

Samples were ground into a fine powder using a CryoMill (Retsch GmbH, Haan, Germany) with liquid nitrogen cooling system and resuspended in Tris tissue lysis buffer (50mM Tris HCl pH8, 150mM NaCl, 5mM EDTA, 1% Triton-X100, and 0.5% Sodium Deoxycholate) with protease inhibitor (Sigma). Samples were vortexed then centrifuged at 14,000xg for 1 minute. The supernatant was stored at -20°C. The pellet was resuspended in 2 times volume of 4M Guanidine Hydrochloride (in 0.1M PBS pH 6.4), vortexed x6m at RT, centrifuged, and the pellet was then treated as previously described.

3.2.3 Gene Expression with HT-qRT PCR

Total RNA was isolated using TRIzol reagent (Invitrogen) and digested with RNase-free DNase I. The digested samples were then re-extracted with TRIzol, precipitated with isopropyl alcohol, and resuspended in diethyl pyrocarbonate-treated water. Following quantification samples were stored at -80 °C or subjected to Poly(A⁺) mRNA isolation from total RNA using Dynabeads mRNA direct kit (Dyna, Invitrogen). Total mRNA was then quantified and stored at -80 °C. Five-hundred nanograms of Poly(A⁺) mRNA was used to synthesize cDNA using the SuperScript III First Strand synthesis kit (Invitrogen) with both oligo(dT) and random primers (1:1) included in the cDNA synthesis reactions. As a control, one reaction lacking reverse transcriptase was utilized to detect the presence of genomic DNA contamination.

The expression of 112 glycosylation- related genes (Table VII) was selected for analysis using high-throughput qualitative real-time polymerase chain reaction (HT-qRT PCR) ²¹⁵. Each qRT- PCR reaction took place in 96 well plates with 29 gene targets/ plate, and 3 housekeeping genes including *RPL4*, *GAPDH*, and *ACTB*. Three technical replicates were run per plate and each tissue sample/replicate was run on a separate group of 96-well plates. To maintain consistency between runs, a common threshold was set for each primer pair. A standard deviation of 0.5 cycle threshold (Ct) was chosen as the cutoff. Technical replicates with a standard deviation greater than 0.5 Ct were re-assayed. Amplification efficiency of each reaction was analyzed using LinRegPCR ²¹⁶ with the acceptable variability set to <5%. The averaged Ct data was converted to linear amplicon abundance (2^{-Ct}) and normalized to the housekeeping gene demonstrating the most stable expression over the range of samples (*RPL4*). The

average expression of the technical replicates was used to identify the relative transcript abundance (*expression*) for each sample replicate using the $\Delta\Delta\text{Ct}$ method²¹⁷⁻²¹⁹. The relative transcript abundance (RTA) levels were read into the R programming environment¹⁷⁶ and quality assessment of each gene's expression was performed. Genes with RTA levels less than 1×10^{-6} in more than 75% of the sample replicates were removed from statistical analysis.

TABLE VII.

TABLE OF GLYCOSYLATION RELATED GENES SCREENED DURING HT- QRT PCR.

Gene List #	Gene Symbol	Gene Name	Group	Function	RefSeq
GH13_M06	AGL	amylase-1,6-glucosidase, 4-alpha-glucanotransferase	Glycosyl-hydrolase	Enzyme with amylase-1,6-glucosidase activity involved in glycogenolysis.	NM_001081326
GT57_M01	ALG6	asparagine-linked glycosylation 6 (alpha-1,3-glucosyltransferase)	Glycosyl-transferase	Enzyme that transfers the first glucose residue from dolichyl phosphate glucose (Dol-P-Glc) onto the lipid-linked oligosaccharide Man(9)GlcNac(2)-PP-Dol during N-linked glycosylation.	NM_001081264
GT57_M02	ALG8	asparagine-linked glycosylation 8 (alpha-1,3-glucosyltransferase)	Glycosyl-transferase	Enzyme that adds the second of three glucoses to the Glc3Man9GlcNac2-lipid linked precursor for all N-linked glycosylation.	NM_199035
GT04_M02	ALG11	asparagine-linked glycosylation 11 (alpha-1,2-mannosyltransferase)	Glycosyl-transferase	Enzyme that adds the terminal α 1,2-Man to the Man5GlcNac2-lipid linked precursor for all N-linked glycosylation. Occurs on the cytosolic side of the ER.	NM_183142, NM_001243161
GT01_M22	ALG13	asparagine-linked glycosylation 13	Glycosyl-transferase	Enzyme that adds the second of two GlcNAc sugars to the Glc3Man9GlcNac2-lipid linked precursor for all N-linked glycosylation.	NM_026247
GH13_M01	AMY1	amylase 1, salivary	Glycosyl-hydrolase	Enzymes with amylase activity that degrades 1, 4-alpha-glucoside and is involved in the degradation of glycogen and starch.	NM_007446, NM_001110505,
GH13_M02	AMY2	Amylase 2	Glycosyl-hydrolase		NM_001042711 NM_001190404 NM_001160150
SAS_M02	ARSB	arylsulfatase B	Sulfate Related/ Arylsulfatase	Enzyme (lysosomal) that removes sulfate groups from chondroitin-4-sulfate (C4S) and degrades CS and dermatan sulfate. Regulates cell adhesion, epithelial migration & invasion and neural outgrowth/ plasticity.	NM_009712
SAS_M09	ARSI	arylsulfatase I	Sulfate Related/ Arylsulfatase	Secreted enzyme with arylsulfatase activity at neutral pH, when co-expressed with Sumf1.	NM_001038499

TABLE VII. (continued)

TABLE OF GLYCOSYLATION RELATED GENES SCREENED DURING HT- QRT PCR.

Gene List #	Gene Symbol	Gene Name	Group	Function	RefSeq
SAS_M10	<i>ARSJ</i>	arylsulfatase J	Sulfate Related/ Arylsulfatase	Secreted enzyme with arylsulfatase activity towards carbohydrates, proteoglycans and glycolipids.	NM_173451
GT31_M07	<i>B3GALT2</i>	UDP-Gal:betaGlcNAc beta 1,3-galactosyl-transferase, polypeptide 2	Glycosyl-transferase	Enzyme with multiple enzymatic functions. Transfers Gal onto Gal>>>beta-GlcNAc. Functions in N-linked glycoprotein glycosylation. Suggested in lacto- and neolacto- glycolipid glycosylation.	NM_020025
GT43_M01	<i>B3GAT3</i>	beta-1,3-glucuronyltransferase 3 (glucuronosyl-transferase I)	Glycosyl-transferase	Enzyme that transfers GlcUA to Gal-beta-1,3-Gal-beta-1,4-Xyl-Ser during biosynthesis of I2/HNK-1 epitope on glycoproteins. Forms the linkage tetrasaccharide present in heparan sulfate and chondroitin sulfate.	NM_024256
GT31_M08	<i>B3GALNT1/</i> <i>B3GALT3</i>	UDP-GalNAc:betaGlcNAc beta 1,3-galactos-aminyl-transferase, polypeptide 1	Glycosyl-transferase	Enzyme with diverse enzymatic functions that transfers Gal or GlcNAc onto the Gal or GalNAc found on globotriaosyl-ceramides.	NM_020026
GT31_M16	<i>B3GNT2</i>	UDP-GlcNAc:betaGal beta-1,3-N-acetyl-glucosaminyl-transferase 2	Glycosyl-transferase	Enzyme that transfers GlcNAc onto Gal to form poly-N-lactosamine chains that terminate N- and O-glycans.	NM_016888, NM_001169114,
GT31_M02	<i>B3GNT3</i>	UDP-GlcNAc:betaGal beta-1,3-N-acetyl-glucosaminyl-transferase 3	Glycosyl-transferase	Enzyme that transfers GlcNAc onto Gal to form poly-N-lactosamine chains that terminate N- and O-glycans. Specific activity for type 2 oligosaccharides and extended core 1 O-glycans. Involved in L-selectin ligand biosynthesis, lymphocyte homing and trafficking.	NM_028189
GT31_M14	<i>B3GNT5</i>	UDP-GlcNAc:betaGal beta-1,3-N-acetyl-glucosaminyl-transferase 5	Glycosyl-transferase	Enzyme that transfers GlcNAc onto Gal to form lactotriaosyl-ceramide chains that terminate glycolipid substrates. Involved in the synthesis of Lewis X epitopes on glycolipids.	NM_054052, NM_001159407, NM_001159408,

TABLE VII. (continued)

TABLE OF GLYCOSYLATION RELATED GENES SCREENED DURING HT- QRT PCR.

Gene List #	Gene Symbol	Gene Name	Group	Function	RefSeq
GT31_M17	<i>B3GN77</i>	UDP-GlcNAc:betaGal beta-1,3-N-acetyl-glucosaminyl-transferase 7	Glycosyl-transferase	Enzyme that transfers GlcNAc onto Gal to form poly-N-lactosamine chains on O-glycans and KS. May play a role in preventing cell migration and invasion.	NM_145222
GT31_M01	<i>B3GN79/C76566</i>	UDP-GlcNAc:betaGal beta-1,3-N-acetyl-glucosaminyl-transferase 9	Glycosyl-transferase	Enzyme that transfers GlcNAc onto Gal to form poly-N-lactosamine chains.	NM_146184, NM_001036740,
GT12_M02	<i>B4GALNT1</i>	beta-1,4-N-acetyl-galactosaminyl-transferase 1	Glycosyl-transferase	Enzyme that transfers GalNAc and is involved in the biosynthesis of gangliosides GM2, GD2 and GA2.	NM_008080, NM_001244617, NM_001244618, NM_027739
GT12_M01	<i>B4GALNT2</i>	beta-1,4-N-acetyl-galactosaminyl-transferase 2	Glycosyl-transferase	Enzyme that adds to the low MW 3'-sialyl-n- acetyllactosamine. Forms tetrasaccharide structure. Involved in synthesis of t-lymphocyte Sd(a) & Cad antigen.	NM_008081
GT07_M10	<i>B4GALNT3</i>	beta-1,4-N-acetyl-galactosaminyl transferase 3	Glycosyl-transferase	Enzyme that transfers beta-1, 4-GalNAc to N-acetylglucosamine-beta-benzyl to form LacdiNAc.	NM_173593
GT07_M04	<i>B4GALT3</i>	UDP-Gal:betaGlcNAc beta 1,4-galactosyl-transferase, polypeptide 3	Glycosyl-transferase	Enzyme that transfers Gal via beta 1,4 linkage to GlcNAc, Glc, and Xyl. Type II membrane protein.	NM_020579
GT07_M06	<i>B4GALT5</i>	UDP-Gal:betaGlcNAc beta 1,4-galactosyl-transferase, polypeptide 5	Glycosyl-transferase	Enzyme that transfers Gal via beta 1,4 linkage to GlcNAc, Glc, and Xyl. Type II membrane protein.	NM_019835
GT07_M07	<i>B4GALT6</i>	UDP-Gal:betaGlcNAc beta 1,4-galactosyl-transferase, polypeptide 6	Glycosyl-transferase	Enzyme that transfers Gal via beta 1,4 linkage to GlcNAc, Glc, and Xyl. Type II membrane protein.	NM_019737
GH18_M04	<i>CHI3L1/CHIL1</i>	chitinase-like 1	Lectin/ Misc. Glycan-binding/ Chitinase-like	Enzyme specificity not well defined. No hydrolase activity. Secreted by neutrophils and activated macrophages.	NM_007695

TABLE VII. (continued)

TABLE OF GLYCOSYLATION RELATED GENES SCREENED DURING HT- QRT PCR.

Gene List #	Gene Symbol	Gene Name	Group	Function	RefSeq
GH18_M06	<i>CHI3L3/YM1/CHIL3</i>	chitinase-like 3	Glycosyl-hydrolase	Enzyme (secreted) specificity not well defined. Weak GlcNAc hydrolase activity. Involved in inflammation and hematopoiesis.	NM_009892
STR_M04	<i>CHST11</i>	carbohydrate sulfo-transferase 11	Sulfate Related/ Sulfotransferase	Enzyme required for the synthesis of chondroitin sulfate proteoglycan 4 (CSPG4)- ligand for P- selectin.	NM_021439
GT07_M11	<i>CHSY1</i>	chondroitin sulfate synthase 1	Glycosyl-transferase	Enzyme that functions as glucuronyltransferase and galactosaminyltransferase.	NM_001081163
GH47_M03	<i>EDEM1</i>	endo-beta-N-acetyl-glucosaminidase	Glycosyl-hydrolase	Enzyme involved in ERAD and trims mannose from Man8GlcNAc2 to Man7GlcNAc2	NM_172573
GH85_M01	<i>ENGASE</i>	ER degradation enhancer, mannosidase alpha-like 1	Glycosyl-hydrolase	Enzyme which hydrolyzes mannose and processes free glycans in the cytosol.	NM_138677
GT64_M01	<i>EXTL2</i>	exostoses (multiple)-like 2	Glycosyl-transferase	Enzyme involved in the synthesis of heparan sulfate.	NM_021388, NM_001163514, NM_001163515,
MISC_UGT_M01	<i>FKTN/FCMD</i>	fukutin	Miscellaneous	Enzyme that transfers CDP-Rbo to β -GalNAc-3 Rbo5P of dystroglycan.	NM_139309
GH29_M02	<i>FUCA1</i>	fucosidase, alpha-L- 1, tissue	Glycosyl-hydrolase	Enzyme (lysosomal) that hydrolyzes the bond between alpha-1,6-linked fucose and N-acetylglucosamine.	NM_024243
GT11_M01	<i>FUT1</i>	fucosidase, alpha-L- 1, tissue	Glycosyl-hydrolase	Enzyme (lysosomal) that transfers α 1,2 linked Fuc to beta-Gal to synthesize a soluble precursor oligosaccharide called the H antigen. Observed on glycolipids> O- linked glycans.	NM_000148, NM_001329877
GT11_M02	<i>FUT2</i>	fucosyl-transferase 1	Glycosyl-transferase	Plays a role in cell-cell interaction, including host-microbe mediated interactions ⁵⁻⁶ .	NM_008051, NM_00127198
GT23_M01	<i>FUT8</i>	fucosyl-transferase 8	Glycosyl-transferase	Enzyme (lysosomal) that transfers α 1,6 linked Fuc to GlcNAc.	NM_016893, NM_001252614, NM_001252615, NM_001252616,
STR_M07	<i>GAL3ST1</i>	galactose-3-O-sulfo-transferase 1	Sulfate Related/ Sulfotransferase	Enzyme that transfers sulfates to form galactosylceramide sulfate (sulfatide).	NM_016922, NM_001177691, NM_001177703,
STR_M09	<i>GAL3ST4</i>	galactose-3-O-sulfo-transferase 4	Sulfate Related/ Sulfotransferase	Enzyme that transfers sulfate to Gal with high specificity for core 1 O- linked glycan structures.	NM_001033416

TABLE VII. (continued)

TABLE OF GLYCOSYLATION RELATED GENES SCREENED DURING HT- QRT PCR.

Gene List #	Gene Symbol	Gene Name	Group	Function	RefSeq
ST_M01	<i>GALNS</i>	galactosamine (N-acetyl)-6-sulfate sulfatase	Sulfate Related/ Sulfatase	Enzyme (lysosomal) required for breakdown of keratan sulfate and chondroitin 6-sulfate.	NM_016722, NM_001193645
GT27_M05	<i>GALNT3</i>	UDP-N-acetyl-alpha-D-galactosamine: polypeptide N-acetyl-galactosaminyl-transferase 3	Glycosyl-transferase	Enzyme that transfers GalNAc to serine or threonine for O- glycan biosynthesis.	NM_015736
GT27_M07	<i>GALNT6</i>	UDP-N-acetyl-alpha-D-galactosamine: polypeptide N-acetyl-galactosaminyl-transferase 6	Glycosyl-transferase	Enzyme that transfers GalNAc to serine or threonine for O- glycan biosynthesis.	NM_172451, NM_001161767, NM_001161768
GT27_M02	<i>GALNT7</i>	UDP-N-acetyl-alpha-D-galactosamine: polypeptide N-acetyl-galactosaminyl-transferase 7	Glycosyl-transferase	Enzyme that transfers GalNAc to serine or threonine for O- glycan biosynthesis.	NM_144731, NM_001167981
GT27_M12	<i>GALNT12</i>	UDP-N-acetyl-alpha-D-galactosamine: polypeptide N-acetyl-galactosaminyl-transferase 12	Glycosyl-transferase	Enzyme that transfers GalNAc to serine or threonine for O- glycan biosynthesis.	NM_172693
GT27_M14	<i>GALNT15</i>	UDP-N-acetyl-alpha-D-galactosamine: polypeptide N-acetyl-galactosaminyl-transferase 15	Glycosyl-transferase	Enzyme that transfers GalNAc to serine or threonine for O- glycan biosynthesis.	NM_030166
GT27_M15	<i>GALNT16</i>	UDP-N-acetyl-alpha-D-galactosamine: polypeptide N-acetyl-galactosaminyl-transferase 16	Glycosyl-transferase	Enzyme that transfers GalNAc to serine or threonine for O- glycan biosynthesis.	XM_283069, NM_001081421

TABLE VII. (continued)

TABLE OF GLYCOSYLATION RELATED GENES SCREENED DURING HT- QRT PCR.

Gene List #	Gene Symbol	Gene Name	Group	Function	RefSeq
GH31_M02	<i>GANAB</i>	alpha glucosidase 2 alpha neutral subunit	Glycosyl-hydrolase	Enzyme that hydrolyzes alpha-1,3-linked glucose residues from the Glc(2)Man(9)GlcNAc(2) N-glycan precursor.	NM_008060, NM_001293621
GH31_M05	<i>GANC</i>	glucosidase, alpha; neutral C	Glycosyl-hydrolase	Enzyme that hydrolyzes 1,4-linked alpha-D-glucose residues.	NM_172672
GH30_M01	<i>GBA</i>	glucosidase, beta, acid	Glycosyl-hydrolase	Enzyme (lysosomal) that hydrolyzes glucose from glucosylceramide.	NM_008094, NM_001077411
GT14_M02	<i>GCNT1</i>	glucosaminyl (N-acetyl) - transferase 1, core 2	Glycosyl-transferase	Enzyme that transfers GlcNAc to core 1 O-glycan to form the core 2 O-glycans.	NM_173442, NM_001136484, NM_010265
GT14_M01	<i>GCNT2</i>	glucosaminyl (N-acetyl) - transferase 2, I-branching enzyme	Glycosyl-transferase	Enzyme that transfers a branching beta-1,6-GlcNAc onto linear poly-N-acetyl-lactosaminoglycans.	NM_008105, NM_023887, NM_133219
GH27_M01	<i>GLA</i>	galactosidase, alpha	Glycosyl-hydrolase	Enzyme that hydrolyzes α -Gal from glyco- lipids and proteins.	NM_013463
GH35_M03	<i>GLB1</i>	galactosidase, beta 1	Glycosyl-hydrolase	Enzyme (lysosomal) that cleaves β -Gal from gangliosides.	NM_009752
GH35_M01	<i>GLB1L</i>	galactosidase, beta 1-like	Glycosyl-hydrolase	Enzyme that may hydrolyze beta- galactose in KS & DS.	AK014667, NM_029010
GT01_M21	<i>GLT28D2</i>	glycosyl-transferase 28 domain containing 2	Glycosyl-transferase	Enzyme that transfers the 2 nd GlcNAc in LLO pathway.	NM_177130
GT08_M05	<i>GLT8D2</i>	glycosyl-transferase 8 domain containing 2	Glycosyl-transferase	Enzyme specificity not well defined, but transfers GlcNAc. Involved in ApoB100 regulation associated with fatty liver.	NM_029102
GL_M47	<i>GM2A</i>	GM2 Ganglioside Activator	Glycolipid	Glycolipid transport protein.	NM_000405
MISC_M1	<i>GNPTAB</i>	N-acetyl-glucosamine-1-phosphate - transferase, alpha and beta subunits	Miscellaneous	Enzyme (lysosomal) responsible for creating the mannose-6-phosphate recognition marker. Targets degradative enzymes to the lysosome.	NM_001004164
ST_M05	<i>GNS</i>	glucosamine (N-acetyl)-6-sulfatase	Sulfate Related/ Sulfatase	Enzyme (lysosomal) that degrades heparin, heparan sulphate, and keratan sulphate.	NM_029364
GH02_M01	<i>GUSB</i>	glucuronidase, beta	Glycosyl-hydrolase	Enzyme (lysosomal) that degrades heparan/ dermatan/ 4,6 chondroitin sulphate.	NM_010368

TABLE VII. (continued)

TABLE OF GLYCOSYLATION RELATED GENES SCREENED DURING HT- QRT PCR.

Gene List #	Gene Symbol	Gene Name	Group	Function	RefSeq
GT08_M07	<i>GXYLT2/GLT8D4</i>	glucoside xylosyl-transferase 2	Glycosyl-transferase	Enzyme that transfers xylose to O- linked glucose associated with EGF repeats on Notch.	NM_198612
GT02_M04	<i>HAS 1</i>	hyaluronan synthase1	Glycosyl-transferase	Enzyme that transfers GlcNAc or GlcUA to synthesize low MW HA.	NM_008215
GT02_M05	<i>HAS 2</i>	hyaluronan synthase 2	Glycosyl-transferase	Enzyme that transfers GlcNAc or GlcUA to synthesize high MW hyaluronic acid. Actively produced during wound healing.	NM_008216
GT02_M06	<i>HAS 3</i>	hyaluronan synthase 3	Glycosyl-transferase	Enzyme that transfers GlcNAc/ GlcUA to synthesize low MW HA.	NM_008217
GH79_M01	<i>HPSE</i>	heparanase	Glycosyl-hydrolase	Enzyme that hydrolyzes N-sulfo glucosamines carrying 2-O-/ 3-O-/6-O-sulfo group from GlcUA.	NM_152803
STR_M14	<i>HS2ST1</i>	heparan sulfate 2-O-sulfo-transferase 1	Sulfate Related/ Sulfotransferase	Enzyme that transfers 2-O- sulfo group onto L-iduronyl and D-glucuronyl of HS.	NM_011828
STR_M15	<i>HS3ST1</i>	heparan sulfate (glucosamine) 3-O-sulfo-transferase 1	Sulfate Related/ Sulfotransferase	Enzyme that transfers 3-O- sulfo group onto glucosamine of HS. Rate limiting step for HS biosynthesis.	NM_010474
STR_M25	<i>HS3ST2</i>	heparan sulfate (glucosamine) 3-O-sulfo-transferase 2	Sulfate Related/ Sulfotransferase	Enzyme that transfers 3-O- sulfo group to an N-unsubstituted glucosamine linked to 2-O-sulfo IdoUA on HS.	NM_001081327
STR_M16	<i>HS3ST3B1</i>	heparan sulfate (glucosamine) 3-O-sulfo-transferase 3B1	Sulfate Related/ Sulfotransferase	Enzyme that transfers 3-O- sulfo group to an N-unsubstituted glucosamine linked to 2-O-sulfo IdoUA (IdoUA2S-GlcNS and IdoUA2S-GlcNH2) of HS.	NM_018805
STR_M18	<i>HS6ST2</i>	heparan sulfate 6-O-sulfo-transferase 2	Sulfate Related/ Sulfotransferase	Enzyme that transfers 6-O- sulfo group to N-sulfoglucosamine residue (GlcNS) of HS.	NM_015819, NM_001077202, NM_001290467, NM_001290468
GH56_M04	<i>HYAL2</i>	hyaluronoglucosaminidase 2	Glycosyl-hydrolase	Enzymes that hydrolyzes high MW hyaluronic acid (HA) to an intermediate MW HA.	NM_010489
GT54_M07	<i>ITGA3</i>	integrin alpha 3/beta-1	Glycosyl-transferase	Receptor for chondroitin sulfate proteoglycan 4 and other ECM proteins including FN & collagen.	NM_013565, NM_001306071, NM_001306162,
GH01_M01	<i>KLB</i>	klotho beta	Glycosyl-hydrolase	Enzyme with undefined specificity. Likely inactive hydrolase activity. Involved in FGF21 binding to other fibroblast growth factors.	NM_031180

TABLE VII. (continued)

TABLE OF GLYCOSYLATION RELATED GENES SCREENED DURING HT- QRT PCR.

Gene List #	Gene Symbol	Gene Name	Group	Function	RefSeq
GT08_M06	<i>LARGE1</i>	glycosyl-transferase-like 1B	Glycosyl-transferase	Enzyme that transfers α 1,3-xylose to β -GlcA and α -Xyl- and beta-1,3-glucuronic acid to GlcA on α -dystroglycan. LARGE is required for laminin binding.	NM_172670, NM_001166633, NM_001290773, NM_001290774, NM_001290775
GT08_M06	<i>GYLTL1B / LARGE2</i>	glycosyl-transferase-like 1B	Glycosyl-transferase	Activity towards α -dystroglycan LARGE2 >LARGE1.	
GT31_M10	<i>LFNG</i>	LFNG O-fucosylpeptide 3-beta-N-acetylglucosaminyl-transferase	Glycosyl-transferase	Enzyme that transfers beta-1, 3 GlcNAc to elongate O- linked fucose. Decreases JAG1 and increases DLL1 mediated NOTCH1 activation.	NM_008494
GH47_M07	<i>MAN1B1</i>	mannosidase, alpha, class 1B, member 1	Glycosyl-hydrolase	Enzyme that removes α 1,2-Man from Man(9)GlcNAc(2) to produce Man(8)GlcNAc(2).	NM_001029983
GH47_M05	<i>MAN1C1</i>	mannosidase, alpha, class 1C, member 1	Glycosyl-hydrolase	Enzyme that removes α 1,2-Man from Man(8)GlcNAc(2) to produce Man(7)GlcNAc(2), Man(6)GlcNAc, and Man(5)GlcNAc respectively.	NM_207237
GH02_M02	<i>MANBA</i>	mannosidase, beta A, lysosomal	Glycosyl-hydrolase	Enzyme (lysosomal) that cleaves beta-Man from N- linked glycans.	NM_027288
GH99_M01	<i>MANEA</i>	mannosidase, endo-alpha	Glycosyl-hydrolase	Enzyme that removes α 1,2-Man residues from Glc-Man(9)GlcNAc(2) to produce Man(8)GlcNAc(2).	NM_172865
GH99_M02	<i>MANEAL / GM50</i>	mannosidase, endo-alpha-like	Glycosyl-hydrolase	Enzyme paralog to MANEA that cleaves endo- α 1,2-Man.	NM_001007573
GH31_M07	<i>MGAM</i>	maltase-glucoamylase	Glycosyl-hydrolase	Enzyme involved in the hydrolysis of starch.	XM_001481277, NM_001171003
GT54_M04	<i>MGAT4B</i>	mannoside acetyl-glucosaminyl-transferase 4, isoenzyme B	Glycosyl-transferase	Enzyme that transfers beta-1,4-GlcNAc to core mannose N-linked glycans to build complex N- glycan structures.	NM_145926
GH33_M04	<i>NEU1</i>	neuraminidase 1	Glycosyl-hydrolase	Enzyme localized in the lysosome that hydrolyzes sialic acid (aka N-acetylneuraminic acid) from oligosaccharides, glycoproteins, and glycolipids including gangliosides.	NM_010893

TABLE VII. (continued)

TABLE OF GLYCOSYLATION RELATED GENES SCREENED DURING HT- QRT PCR.

Gene List #	Gene Symbol	Gene Name	Group	Function	RefSeq
GH33_M01	<i>NEU2</i>	neuraminidase 2	Glycosyl-hydrolase	Enzyme localized in the cytoplasm (intracellular) that hydrolyzes sialic acid (aka N-acetylneuraminic acid) from oligosaccharides, glycoproteins, and glycolipids including gangliosides.	NM_015750, NM_001160163, NM_001160164, NM_001160165
GH33_M03	<i>NEU3</i>	neuraminidase 3	Glycosyl-hydrolase	“ ” Localized in the plasma membrane	NM_016720
STR_M21	<i>NDST1</i>	N-deacetylase/ N-sulfo-transferase (heparan glucosaminyl) 1	Sulfate Related/ Sulfotransferase	Enzyme that induces N-deacetylation and N-sulfation of GlcNAc-GlcA on HS. Prerequisite to HS synthesis.	NM_008306
GT41_M01	<i>OGT</i>	O-linked N-acetyl-glucosamine (GlcNAc) - transferase (UDP-N-acetyl-glucosamine: polypeptide-N-acetyl-glucosaminyl - transferase)	Glycosyl-transferase	Enzyme that adds GlcNAc to serine/ threonine to produce O-GlcNAcylation of O- linked glycans. Cytoplasmic and nuclear modification that may interfere with serine/ threonine phosphorylation.	NM_139144, NM_001290535
GH18_M10	<i>OVGP1/ MUC9</i>	oviductal glycoprotein 1	Glycosyl-hydrolase	Protein mucin or enzyme with undefined specificity that is rich in O- glycosylation sites.	NM_007696,
NSN_M20	<i>PAPSS2</i>	3'-phospho-adenosine 5'-phosphosulfate synthase 2	Carbohydrate Synthesis and Metabolism/ Nucleotide Synthesis	Enzyme that transfers sulfate to ATP and phosphate to adenosine 5'-phosphosulfate (PAPS). Generates activated sulfate precursor for all sulfation.	NM_011864, NM_001201470
STR_M03	<i>PHACTR 1</i>	phosphatase and actin regulator 1	Sulfate Related/ Sulfotransferase	Enzyme that hydrolyzed phosphate and regulated actin reorganization.	NM_198419, NM_001005740, NM_001005748, NM_001302635, NM_001302636
GT04_M03	<i>PIGA</i>	phosphatidyl-inositol glycan anchor biosynthesis, class A	Glycosyl-transferase	Enzyme that transfers GlcNAc to phosphatidyl-1D-myo-inositol during the first step of GPI anchor biosynthesis.	NM_011081
GPI_M14	<i>PIGG</i>	phosphatidyl-inositol glycan anchor biosynthesis, class G	GPI anchor biosynthesis Related	Enzyme that transfers the 3 rd phosphoethanolamine to the 2 nd mannose of GPI during the 10 th step of GPI anchor biosynthesis.	NM_001081234, NM_001310689

TABLE VII. (continued)

TABLE OF GLYCOSYLATION RELATED GENES SCREENED DURING HT- QRT PCR.

Gene List #	Gene Symbol	Gene Name	Group	Function	RefSeq
GPI_M05	<i>PIGK</i>	phosphatidyl-inositol glycan anchor biosynthesis, class K	GPI anchor biosynthesis Related	Enzyme involved in transamidation reaction that attaches the GPI with the substrate protein during the 11 th step of GPI anchor biosynthesis.	NM_025662, NM_178016
GPI_M18	<i>PIGP</i>	phosphatidyl-inositol glycan anchor biosynthesis, class P	GPI anchor biosynthesis Related	Enzyme that transfers GlcNAc to phosphatidyl-1D-myo-inositol during the first step of GPI anchor biosynthesis.	NM_019543, NM_001159616, NM_001159617, NM_001159618, NM_001159619
GT35_M01	<i>PYGL</i>	liver glycogen phosphorylase	Glycosyl-transferase	Enzymes that hydrolyzes phosphate from glycogen (liver) during glycogenolysis.	NM_133198
GT35_M02	<i>PYGM</i>	muscle glycogen phosphorylase	Glycosyl-transferase	Enzymes that hydrolyzes phosphate from glycogen (muscle) during glycogenolysis.	NM_011224
GT29_M01	<i>ST3GAL1</i>	ST3 beta-galactoside alpha-2,3-sialyl-transferase 1	Glycosyl-transferase	Enzyme that transfers alpha-2,3 sialic acid to Gal and may contribute to reduced CD8+ T-cell susceptibility to apoptosis.	NM_009177
GT29_M02	<i>ST3GAL2</i>	ST3 beta-galactoside alpha-2,3-sialyl-transferase 2	Glycosyl-transferase	Enzyme that transfers alpha- 2,3 sialic acid to Gal and synthesizes GD1a. Upregulated in multiple cancer types.	NM_178048, NM_009179
GT29_M19	<i>ST3GAL5</i>	ST3 beta-galactoside alpha-2,3-sialyl-transferase 5	Glycosyl-transferase	Enzyme that transfers alpha- 2,3 sialic acid to Gal and forms GM3.	NM_011375, NM_001035228
GT29_M07	<i>ST6GAL1</i>	beta galactoside alpha 2,6 sialyl-transferase 1	Glycosyl-transferase	Enzyme that transfers alpha- 2,6 sialic acid to Gal.	NM_145933, NM_001252505, NM_001252506
GT29_M11	<i>ST6GALNAC4</i>	ST6 (alpha-N-acetyl-neuraminy-2,3-beta-galactosyl-1,3)-N-acetyl-galactosaminide alpha-2,6-sialyl-transferase 4	Glycosyl-transferase	Enzyme that transfers alpha-2,6 sialic acid to GalNAc on O-linked glycans.	NM_011373, NM_001276425
GT29_M18	<i>ST6GALNAC5</i>	ST6 (alpha-N-acetyl-neuraminy-2,3-beta-galactosyl-1,3)-N-acetyl-galactosaminide alpha-2,6-sialyl-transferase 5	Glycosyl-transferase	Enzyme that transfers alpha-2,6 sialic acid to GalNAc on O-linked glycans.	NM_012028

TABLE VII. (continued)

TABLE OF GLYCOSYLATION RELATED GENES SCREENED DURING HT- QRT PCR.

Gene List #	Gene Symbol	Gene Name	Group	Function	RefSeq
GT29_M20	<i>ST6GALNAC6</i>	ST6 (alpha-N-acetyl-neuraminy-2,3-beta-galactosyl-1,3)-N-acetyl-galactosaminide alpha-2,6-sialyl-transferase 6	Glycosyl-transferase	Enzyme that transfers alpha-2,6 sialic acid to GalNAc on O-linked glycans.	NM_016973, NM_001025310, NM_001025311, NM_001289547, NM_001289548, NM_001289549
GT29_M12	<i>ST8SIA1</i>	ST8 alpha-N-acetyl-neuraminide alpha-2,8-sialyl-transferase 1	Glycosyl-transferase	Enzyme that transfers alpha- 2,8 sialic acid to sialic acid and is involved in the production of gangliosides GD2/3.	NM_011374
GT29_M14	<i>ST8SIA2, STX</i>	ST8 alpha-N-acetyl-neuraminide alpha-2,8-sialyl-transferase 2	Glycosyl-transferase	Enzyme that transfers alpha- 2,8 sialic acid to sialic acid to form polysialic acid.	NM_009181
GT29_M15	<i>ST8SIA4, PST</i>	ST8 alpha-N-acetyl-neuraminide alpha-2,8-sialyl-transferase 4	Glycosyl-transferase	Enzyme that transfers alpha- 2,8 sialic acid to sialic acid to form polysialic acid.	NM_009183, NM_001159745
GT29_M13	<i>ST8SIA6</i>	ST8 alpha-N-acetyl-neuraminide alpha-2,8-sialyl-transferase 6	Glycosyl-transferase	Enzyme that transfers alpha- 2,8 sialic acid to sialic acid.	NM_145838
SAS_M03	<i>STS</i>	steroid sulfatase	Sulfate Related/ Arylsulfatase	Enzyme that hydrolyzes 3-beta-hydroxysteroid sulfates.	NM_009293
ST_M03	<i>SULF1</i>	sulfatase 1	Sulfate Related/ Sulfatase	Enzyme that hydrolyzes 6-O-sulfate groups from intact heparin. SULF1 inhibits heparin dependent growth factor signaling.	NM_172294, NM_001198565, NM_001198566
ST_M04	<i>SULF2</i>	sulfatase 2	Sulfate Related/ Sulfatase		NM_028072, NM_001252578, NM_001252579
STR_M02	<i>TPST2</i>	protein-tyrosine sulfo-transferase 2	Sulfate Related/ Sulfotransferase	Enzyme that transfers O- sulfate to tyrosine using PAPS.	NM_009419
GT21_M01	<i>UGCG</i>	UDP-glucose ceramide glucosyl-transferase	Glycosyl-transferase	Enzyme that transfers Glc to ceramides during the first step in glycosphingolipid biosynthesis.	NM_011673

TABLE VII. (continued)

TABLE OF GLYCOSYLATION RELATED GENES SCREENED DURING HT- QRT
PCR.

Gene List #	Gene Symbol	Gene Name	Group	Function	RefSeq
GT24_M01	<i>UGGT1</i>	UDP-glucose glycoprotein glucosyl-transferase 1	Glycosyl-transferase	Enzyme that transfers Glc to unfolded proteins. Sensor that recognizes improperly folded proteins during ER quality control in the ERAD pathway.	NM_198899
STR_M28	<i>UST</i>	uronyl-2-sulfo-transferase	Sulfate Related/ Sulfotransferase	Enzyme that transfers sulfate onto IdoUA of dermatan sulfate with weaker activity toward GlcUA of chondroitin sulfate.	NM_177387
NA	<i>ACTB</i>	Beta Actin	Control gene	Serves as housekeeping gene.	NM_001101.5
NA	<i>GAPDH</i>	Glyceraldehyde 3-phosphate dehydrogenase	Control gene	Serves as housekeeping gene.	NM_001256799 NM_001289745 NM_001289746
NA	<i>RPL4</i>	Ribosomal Protein L4	Control gene	Serves as housekeeping gene.	NM_000968.4

3.2.4 Statistical analysis

To identify whether there were statistically significant differences in relative transcript abundance during diabetic and non-diabetic wound healing, a 1-way ANOVA was used to compare the *condition* versus the polynomial representation of the *time post-wounding* and p-values were adjusted for false discoveries using the Benjamini Hochberg method ¹⁸⁵. To identify whether there were statistically significant differences in gene expression within non-diabetic (WT) wound healing, diabetic (DM) wound healing, and between the diabetic and non-diabetic mice at days 0, 3, and 10, genes with a FDR <0.1 were further analyzed via pairwise contrasts and adjusted for multiple comparisons using the Tukey Honest Significance Difference adjustment method ²²⁰⁻²²¹. Following statistical analysis, significantly regulated genes (FDR<0.1) underwent pathway analysis.

To perform pathway analysis, significantly expressed glycogene probe sets were scaled via unit variance scaling and row-wise hierarchical clustering was applied to the probe sets using the Euclidean distance and Ward linkage with the ClustVis webtool ¹⁸⁶. DAVID pathway enrichment analysis for functional annotation clustering was performed across the genes demonstrating statistical significance (FDR <0.1). Clustering across KEGG pathways was used to identify specific glycosylation- related pathway that were differentially regulated in diabetic and non- diabetic wound healing. PANTHER Overexpression Tests (Released 20181113; <http://www.pantherdb.org>) were performed using binomial test type and Bonferroni correction for multiple testing¹⁸⁹⁻¹⁹⁴.

3.3 **Results**

3.3.1 **Screening Reveals Differential Glycosylation- related Gene Expression in Uninjured Skin Models of Pre-Diabetes and Diabetes**

To determine the likelihood that glycosylation- related gene expression was differentially regulated in diabetic and non-diabetic skin, GEO datasets were screened for microarray data related to diabetes and diabetes related conditions. The microarray dataset GSE22196²²²⁻²²³ comparing high-fat diet (HFD) fed mice (n=3) to controls (n=3) was identified. In the HFD model, mice are fed chow containing either 60% (high fat) or 20% (control/normal) saturated fat. Mice placed on a high fat diet composed of 60% fat have been found to mimic pre-diabetes and some diabetes related comorbidities, however, the phenotype observed in this model is typically less severe than what is observed clinically. This dataset, while limited, provided data on the expression of over 300 glycosylation- related genes in HFD and control mouse epidermis. Genes with a present probe response call in at least 67% of the samples were analyzed by multiple T-test with BH adjustment. It was observed that genes related to sphingolipid, proteoglycan, and glycolipid metabolism including sphingomyelin phosphodiesterase (*SMPD1*), hyaluronan synthase (*HAS1*) and Phosphatidylinositol N-acetylglucosaminyltransferase subunit A (*PIGA*) were significantly decreased, while Beta-1,4-Galactosyltransferase 1 (*B4GALT1*) was significantly increased in the HFD fed mice versus the control mice ($FC \geq 1.2$, $FDR \leq 0.005$) (Figure 24A). Genes responsible for N- and O- linked glycosylation, Mannosidase Alpha Class 2A Member 1 (*MAN2A1*) and Beta-1,3-N-acetylgalactosaminyltransferase (*B3GALNT2*), demonstrated a trend for increased expression in HFD skin, however it was not statistically significant.

Glycosylation- related gene expression was also examined in uninjured diabetic and non-diabetic skin using db/db (DM) and C57 (WT) mice. Four glycosylation- related genes were initially screened based on their placement within pathways related to N-linked glycosylation, O-linked glycosylation, and glycosaminoglycan biosynthesis that were associated with the differential expression of related genes in the BALB/c skin and tongue data, and the HFD data. When screened via qRT-PCR, it was found that uninjured diabetic skin (n=3) demonstrated a 2-fold increase in the expression of Asparagine-Linked Glycosylation 12 Homolog, Alpha-1,6-Mannosyltransferase (*ALG12*) and Polypeptide N-acetylgalactosaminyltransferase 18 (*GALNT18*) (adjusted p-value \leq 0.05) as compared to non-diabetic skin (n=4). These genes are involved in N- and O- linked glycosylation respectively. Additionally, Alpha-1,3-Mannosyl-Glycoprotein 4-Beta-N-Acetylglucosaminyltransferase A (*MGAT4a*) and Extotosin/ Glucuronosyl-N-Acetylglucosaminyl-Proteoglycan/N-Acetylglucosaminyl-Proteoglycan 4-Alpha-N-Acetylglucosaminyltransferase (*EXT1*) demonstrated a trend for increased expression in diabetic skin, however, this difference was not statistically significant (Figure 24B).

When examining the HFD model and the db/db mouse models, genes involved in glycosaminoglycan metabolism were significantly decreased in the HFD model (*HAS1*, $p\leq$ 0.05), yet demonstrated a trend for increased expression in the diabetic db/db model (*EXT1*, $p\geq$ 0.05). While this could suggest a reversal in overall glycosaminoglycan metabolism, it's more likely that the shift in expression is attributed to differences in the glycosaminoglycans that they synthesize; hyaluronan and heparan sulfate, respectively. Interestingly, genes involved in N- and O-linked glycosylation only demonstrated a trend for increased expression in the HFD model (*MAN2A1* and *B3GALNT2*, $p\geq$ 0.05) while

the db/db diabetic model demonstrated significantly increased expression (*ALG12*, *GALNT18*, $p \leq 0.05$). Though these genes impact different paths within each glycosylation- related pathway, this may suggest a role for increased N- and O-linked glycosylation- related gene expression in the disease progression from prediabetes to diabetes.

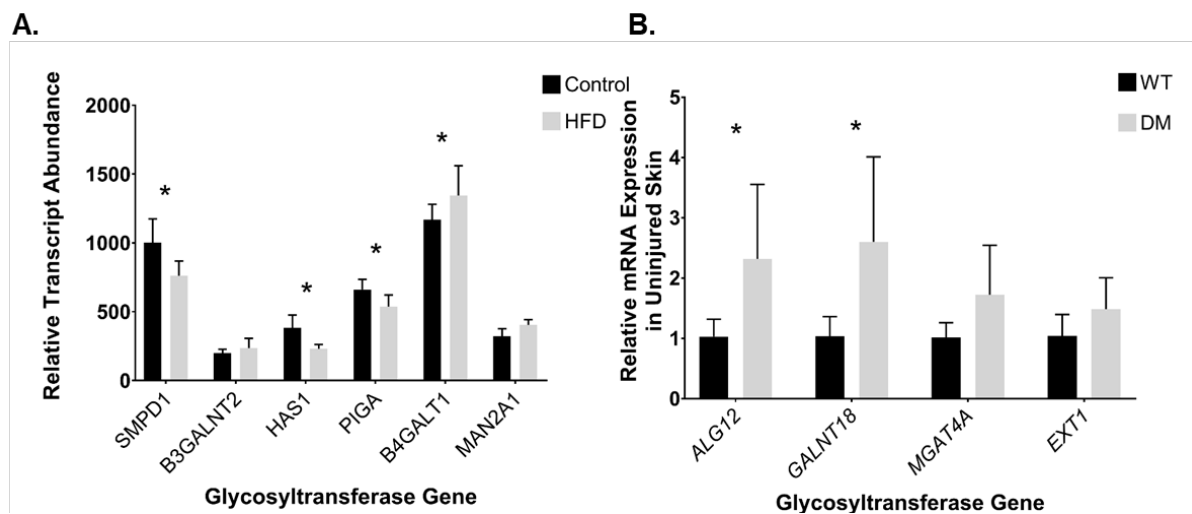


Figure 24. Differential expression of glycosylation related genes in uninjured skin. A) Differential glycosyltransferase expression observed in available microarray data from HFD fed and control mice (asterick * = $FC \geq 1.2$, $FDR \leq 0.005$); B) Differential glycosyltransferase expression from qRT-PCR of diabetic and non-diabetic skin. asterick * = $\text{adj.}p\text{-value} \leq 0.05$.

3.3.2 Diabetic and Non- Diabetic Skin and Wounds Exhibit Differential

Glycosylation- related Gene Expression

To determine whether glycosylation- related gene expression is differentially regulated in diabetic and non-diabetic wound healing, a HT-qRT PCR screening platform was employed. A 114 gene set (Table VII) was chosen based on the genes that were differentially regulated in BALB/c skin and tongue wounds and/or those that were in pathways likely to significantly impact wound healing. After an initial screening of uninjured diabetic and non-diabetic skin and wounds 3- and 10-days post-wounding, *H3ST2* and *GLB1L* were poorly detected and were thus removed from subsequent analysis. Of the remaining 112 glycosylation- related genes that were analyzed, 111 genes met the threshold criterion. Overall, of the 111 genes analyzed, 77 genes were differentially regulated by day over the course of wound healing, 35 genes were differentially expressed during non-diabetic wound healing, and 38 genes demonstrated differential expression (Figure 26; FDR<0.1) between the diabetic and non-diabetic conditions.

3.3.3 Non- Diabetic Skin and Wounds Demonstrate Differential Glycosylation- related Gene Expression Over the Course of Wound Healing

In order to first identify the genes that are expressed during normal, non-diabetic wound healing, we performed a multiple comparisons analysis to identify the genes that were differentially expressed between uninjured non-diabetic skin (Day 0) and wounds during the inflammatory phase (Day 3) and proliferative phase (Day 10) of healing using a Two-Way ANOVA with Tukey Honest Significance Difference adjustment. When

compared to the expression of uninjured non- diabetic skin, non-diabetic wounds demonstrated differential expression (adjusted p-value <0.1) in 35 genes during the inflammatory and/ or proliferative phases of wound healing when compared to uninjured non- diabetic skin. Genes that were upregulated in non- diabetic wounds compared to uninjured, non-diabetic skin included those that encode asparagine-linked glycosylation 8 (*ALG8*), arylsulfatase B (*ARSB*), arylsulfatase I (*ARSI*), UDP-GlcNAc:betaGal beta-1,3-N-acetylglucosaminyltransferase -2, -3, and -5 (*B3GNT2*, *B3GNT3*, *B3GNT5*), beta-1,4-N-acetyl-galactosaminyltransferase 1 (*B4GALNT1*), UDP-Gal:betaGlcNAc beta 1,4-galactosyltransferase, polypeptide 5 (*B4GALT5*), carbohydrate sulfotransferase 11 (*CHST11*), ER degradation enhancer, mannosidase alpha-like 1 (*EDEM1*), endo-beta-N-acetylglucosaminidase (*ENGASE*), galactosamine (N-acetyl)-6-sulfate sulfatase (*GALNS*), UDP-N-acetyl-alpha-D-galactosamine:polypeptide N-acetylgalactosaminyltransferase 6 (*GALNT6*), glucosaminyl (N-acetyl) transferase 1, core 2 (*GCNT1*), hyaluronan synthase 3 (*HAS3*), heparan sulfate 6-O-sulfotransferase 2 (*HS6ST2*), phosphatase and actin regulator 1 (*PHACTR1*), beta galactoside alpha 2,6 sialyltransferase 1 (*ST6GAL1*), ST8 alpha-N-acetyl-neuraminide alpha-2,8-sialyltransferase 2 (*ST8SIA2*), sulfatase 2 (*SULF1*), and UDP-glucose ceramide glucosyltransferase (*UGCG*). Genes that were downregulated in non- diabetic wounds compared to uninjured, non-diabetic skin included amylo-1,6-glucosidase, 4-alpha-glucanotransferase (*AGL*), beta-1,4-N-acetyl-galactosaminyl transferase 2 (*B4GALNT2*), fukutin (*FCMD/ FKTN*), fucosyltransferase 1 (*FUT1*), fucosyltransferase 2 (*FUT2*), galactose-3-O-sulfotransferase 1 (*GAL3ST1*), galactose-3-O-sulfotransferase 4 (*GAL3ST4*), UDP-N-acetyl-alpha-D-galactosamine:polypeptide N-

acetylgalactosaminyltransferase 15 (*ppGALNT15*), glucosidase, alpha; neutral C (*GANC*), heparan sulfate (glucosamine) 3-O-sulfotransferase 3B1 (*HS3ST3B1*), mannosidase, endo-alpha-like (*MANEAL/ GM50*), neuraminidase 2 (*NEU2*), muscle glycogen phosphorylase (*PYGM*), and ST8 alpha-N-acetyl-neuraminide alpha-2,8-sialyltransferase 1 (*ST8SIA1*) (Figure 25). The function of each gene is provided in Table VII and the relative transcript abundance of each gene is provided alphabetically in Appendix D. PANTHER biological process overrepresentation testing (Table VIII) identified that these genes were related to poly-N-acetyllactosamine biosynthetic process (type of glycan elongation/ capping), ganglioside biosynthetic process (glycolipid subtype), and aminoglycan biosynthetic process (related to glycosaminoglycans, GAG).

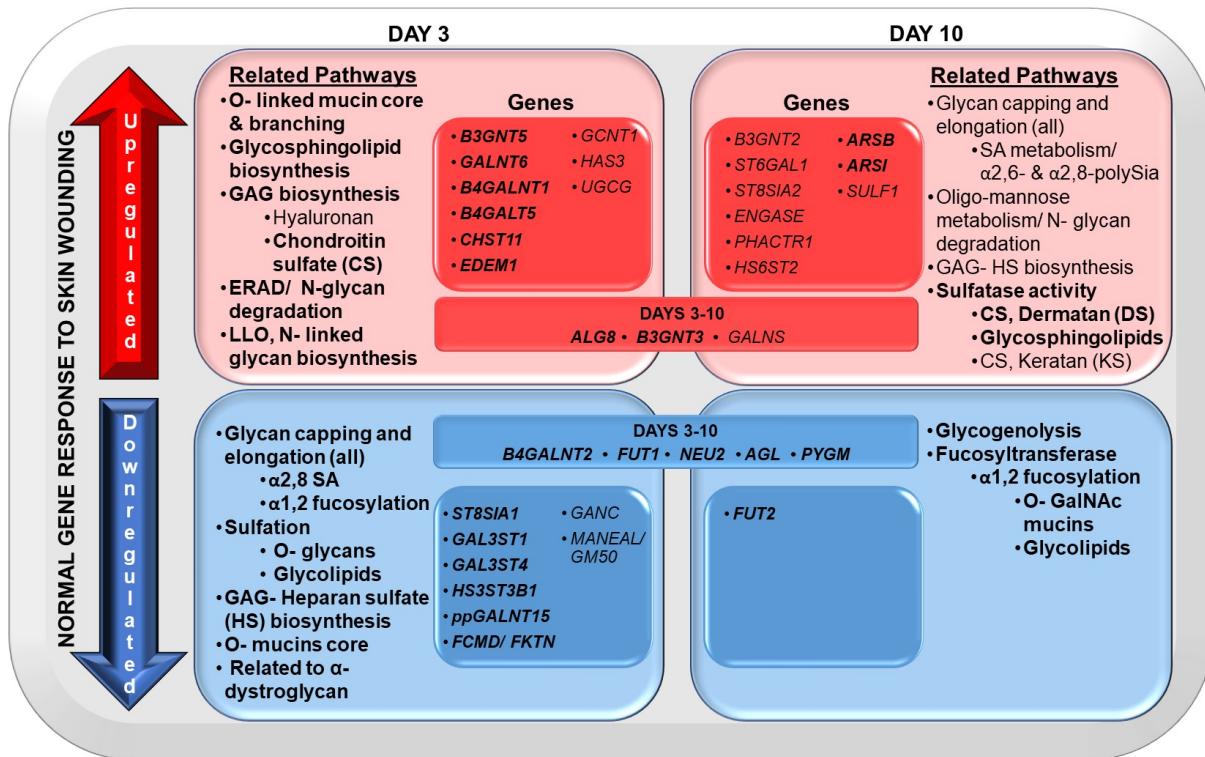


Figure 25. Regulation of glycosylation related genes in normal, non-diabetic skin wound healing. The direction of gene expression is indicated as either upregulated (top, red) or downregulated (bottom, blue) in non-diabetic wounds 3 (left) and 10 days (right) post-wounding. The pathways associated with each cluster of genes (inner most box) is labeled in the outermost box. Bolded genes and pathways represent those whose gene expression was significant with an adjusted p-value ≤ 0.05 , otherwise the adjusted p-value was greater than 0.05, but less than 0.1.

TABLE VIII.

TABLE OF TOP 10 PANTHER BIOLOGICAL PROCESS PATHWAYS AMONG GENES DIFFERENTIALLY REGULATED IN NON-DIABETIC SKIN.

PANTHER GO-Slim Biological Process	# in Reference List	Number of Genes Mapped	Expected Number of Genes	Over (+) Under (-) Enriched	Fold Enriched	Adjusted P-value
Total Genes Examined	22296	35	-	-	-	-
poly-N-acetyllactosamine biosynthetic process (GO:0030311)	10	4	0.02	+	> 100	2.28E-05
poly-N-acetyllactosamine metabolic process (GO:0030309)	10	4	0.02	+	> 100	2.28E-05
ganglioside biosynthetic process (GO:0001574)	11	3	0.02	+	> 100	7.95E-03
glycosphingolipid biosynthetic process (GO:0006688)	20	5	0.03	+	> 100	2.13E-06
ganglioside metabolic process (GO:0001573)	20	4	0.03	+	> 100	3.61E-04
glycosphingolipid metabolic process (GO:0006687)	41	6	0.07	+	88.18	7.39E-07
aminoglycan biosynthetic process (GO:0006023)	42	6	0.07	+	86.08	8.53E-07
cellular polysaccharide biosynthetic process (GO:0033692)	37	5	0.06	+	81.43	4.53E-05
polysaccharide biosynthetic process (GO:0000271)	37	5	0.06	+	81.43	4.53E-05
ceramide biosynthetic process (GO:0046513)	44	5	0.07	+	68.48	1.07E-04

Adjusted $p \leq 0.05$, Fold Enrichment ≥ 1.5

3.3.4 Differential Glycosylation- related Gene Expression Occurs between the Diabetic and Non- Diabetic Conditions

Cluster analysis of the 38 genes differentially expressed between the diabetic and non-diabetic conditions was performed via the Ward method with Euclidean distance. Five main clusters were identified that differentiated between diabetic and non-diabetic wound healing. As shown in Figure 26, the significantly regulated genes clustered as follows: 1) downregulated in uninjured, diabetic skin; 2) upregulated in uninjured, diabetic skin; 3) downregulated in diabetic wounds during early proliferation (10 days post- wounding); 4) upregulated in diabetic wounds during early proliferation (10 days post- wounding); and 5) upregulated in diabetic wounds during the early inflammatory phase through the early proliferative phase of healing. DAVID pathway enrichment analysis for functional annotation clustering revealed that the 38 genes significantly clustered in the following KEGG pathways: 1) sphingolipid metabolism; 2) glycosaminylglycan degradation; 3) lysosomal degradation; 4) and other glycan degradation. Further manual annotation identified genes that were downregulated in the diabetic condition were responsible for intracellular/ cytosolic sialidase activity (*NEU2*; Figure 27A), terminal glycan capping with fucose and sulfate in globoside/ isogloboside glycolipids and O- linked glycans (*FUT1*, *FUT2*, *GAL3ST1*; Figures 27B-D), mucin related O-linked glycan core biosynthesis and elongation (*GALNT15*, *B4GALNT2*, *B3GNT3*; Figures 28A-C), local/ skeletal muscle glycogenolysis (*AGL*, *PYGM* Figures 29 A-B), α -dystroglycan glycosylation (*GYLTL1B*/ *LARGE2*, *FCMD*/ *FKTN*; Figures 30A-B), and function, and β - galactosidase activity (*GLB1*; Figure 30C). Furthermore genes that were upregulated in the diabetic condition were responsible for

sulfate precursor formation and tyrosine sulfotransferase activity (*PAPSS2*, *TPST2*; Figures 31A-B), sulfatase activity targeting the removal of sulfates at C6 in hexose and N-acetyl-hexosamine associated with heparin, heparan sulfate (HS), and keratan sulfate (KS), and chondroitin-6-sulfate (CS) (*SULF2*, *GNS*, *GALNS*; Figures 32A-C), HS extension and sulfation at C2, chondroitin sulfation at position 4 on GalNAc, and degradation of high molecular weight (MW) hyaluronan into intermediate molecular weight (MW) (*HS2ST1*, *EXTL2*, *CHST11*, *HYAL2*; Figures 33A- D); lysosomal degradation of HS, dermatan sulfate (DS), KS, and chondroitin-4,6-sulfate, and α 1,6 fucose and sialic acids (SA) from glycolipids and glycoproteins (*GUSB*, *GLA*, *FUCA*, *NEU1*; Figures 34A-D, and *GLB1* in Figure 76D , Appendix D); O- mucin elongation and glycolipid biosynthesis of isoglobosides and gangliosides (*B3GNT9*, *B3GNT2*, *B3GALT3*/ *B3GALNT1*, *B4GALNT1*; Figures 35A-D); N- glycan biosynthesis/ trimming (*ALG6*, *MANEA*; Figures 36A-B) and GPI anchor biosynthesis (*PIGK*; Figure 36C); inactive chitinase like lectins (*CHI3L1*, *CHI3L3*; Figures 37A-B) and polysialic acid biosynthesis (*ST8SIA4*; Figure 37D).

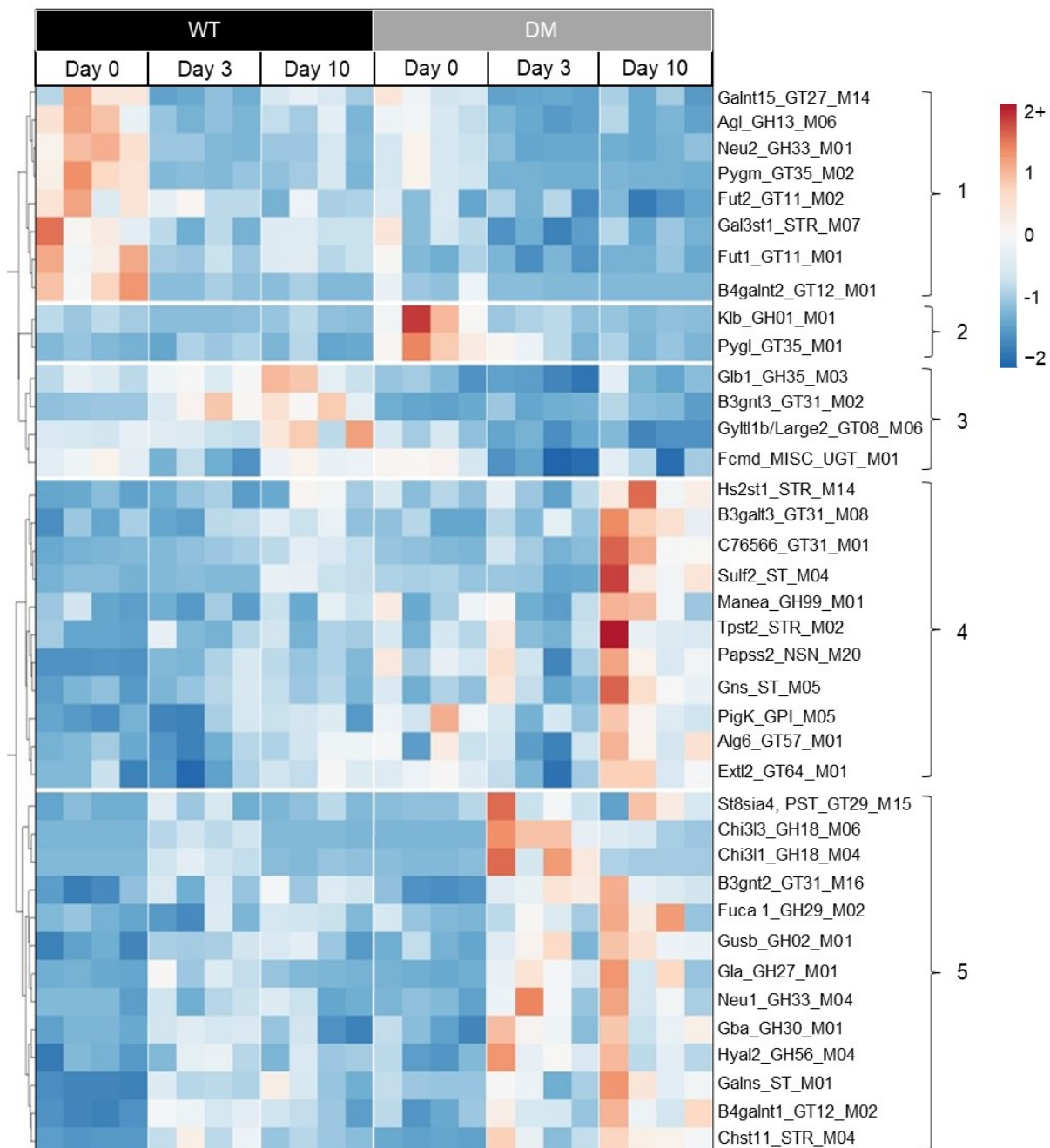


Figure 26. Hierarchical cluster analysis of glycosylation related genes in diabetic and non- diabetic skin and wounds. Uninjured skin and wounds 3- and 10-days post wounding was analyzed in non- diabetic (WT; black) and diabetic mice (DM; grey). FDR \leq 0.1.

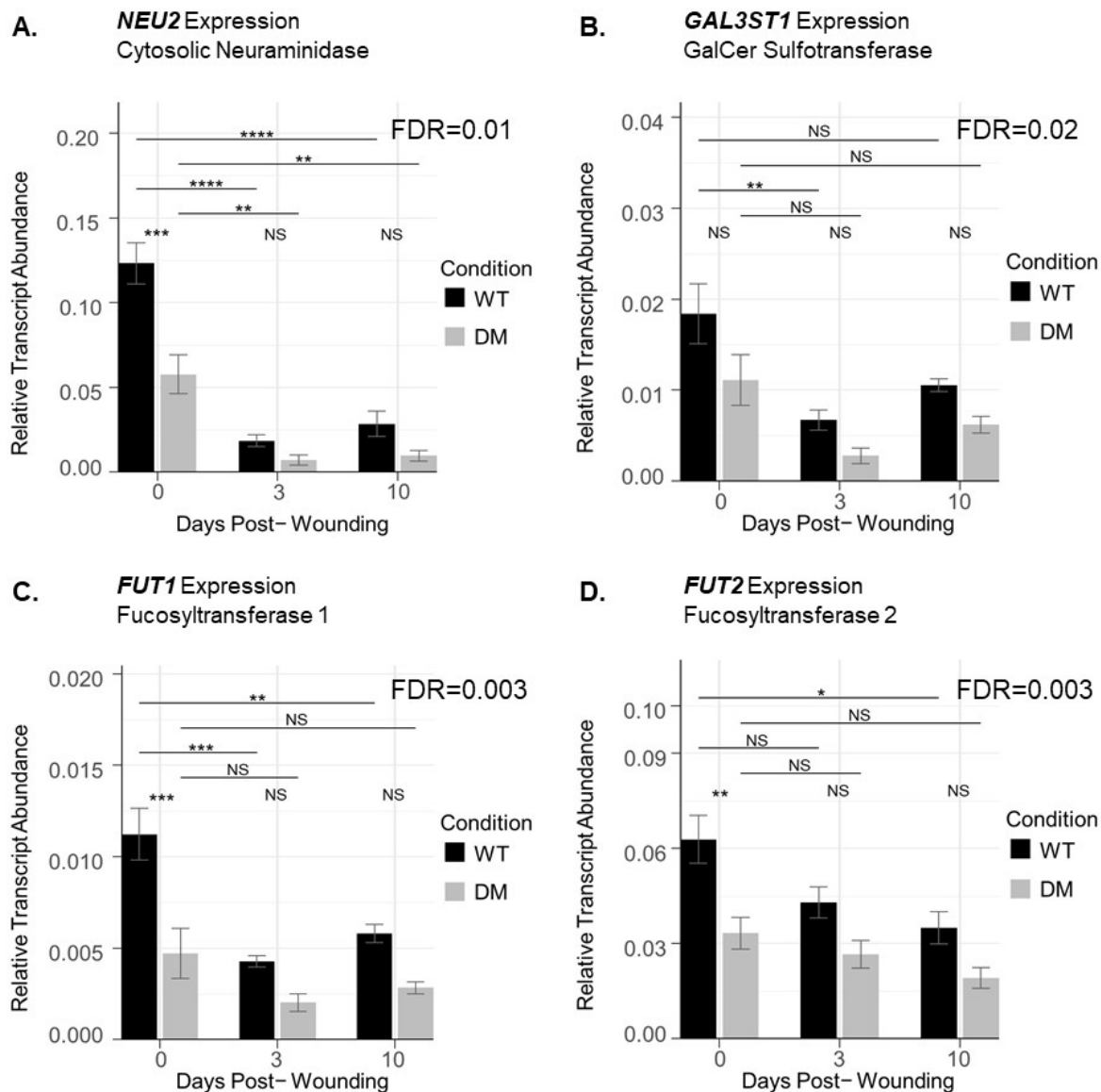


Figure 27. Graphical representation of glycosylation related genes from Cluster 1 that are downregulated in diabetic skin and wounds relative to non- diabetic skin and wounds and are related to sialidase activity and terminal glycan capping. Genes downregulated in uninjured, diabetic skin including cytosolic sialidase (A), galactose- ceramide sulfotransferase (B), and fucosyltransferases (C and D). adj. p- value * ≤ 0.05 ; ** ≤ 0.01 , *** ≤ 0.005 , **** ≤ 0.001 .

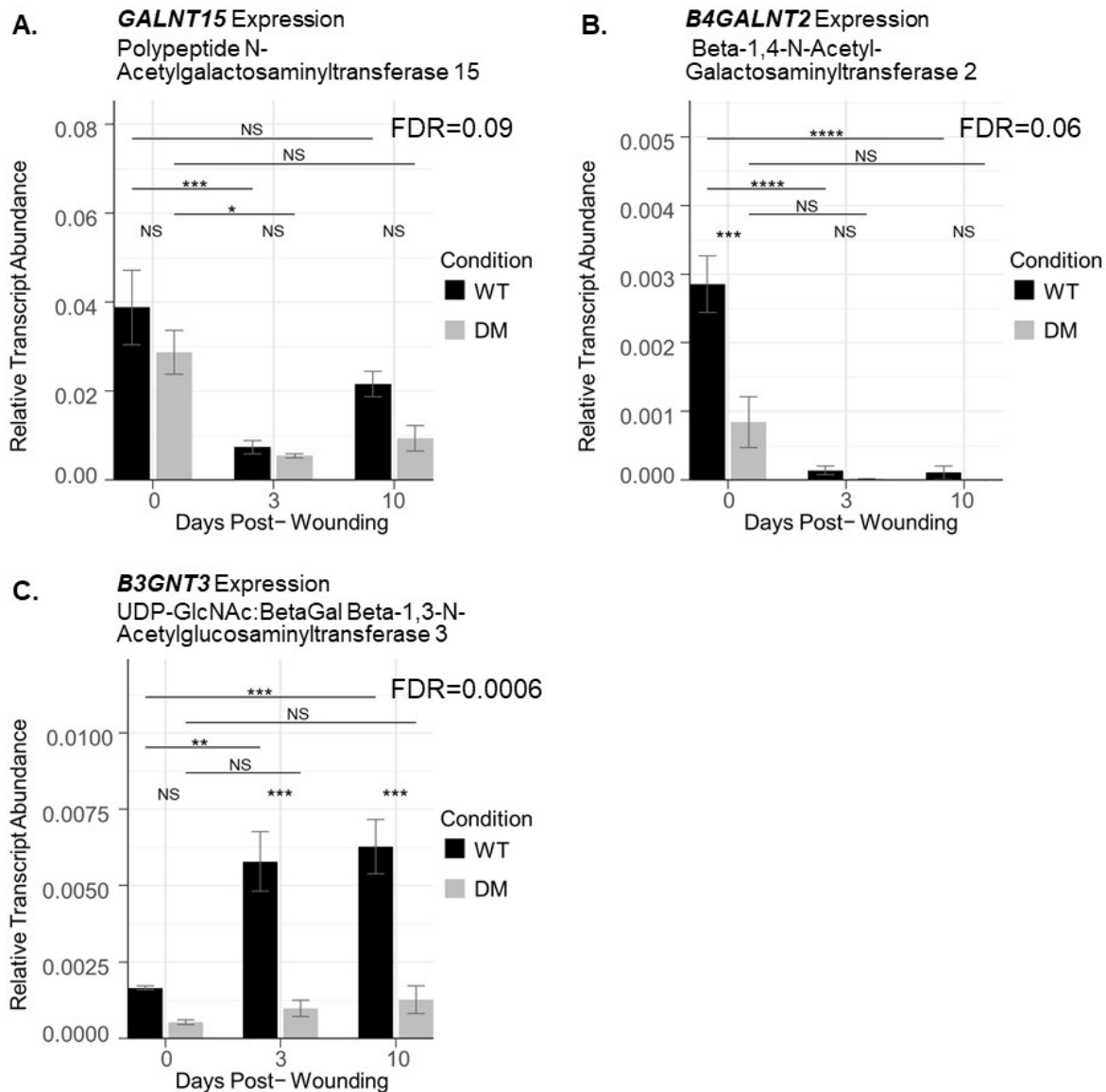


Figure 28. Graphical representation of glycosylation related genes from Clusters 1 & 3 that are downregulated in diabetic skin and wounds relative to non-diabetic skin and wounds and are related to mucin related O-linked glycan biosynthesis. Genes downregulated in uninjured, diabetic skin including polypeptide N-Acetylgalactosaminyltransferase (A) that takes part in the first step of O-linked glycosylation, β -1,4-N-Acetyl-Galactosaminyltransferase (B) that takes part in O-glycan branching, and UDP-GlcNAc:BetaGal Beta-1,3-N-Acetylglucosaminyltransferase 3 (C) which participates in the elongation of core 1 glycans into core 2 glycans. adj. p-value * ≤ 0.05 ; ** ≤ 0.01 , *** ≤ 0.005 , **** ≤ 0.001 .

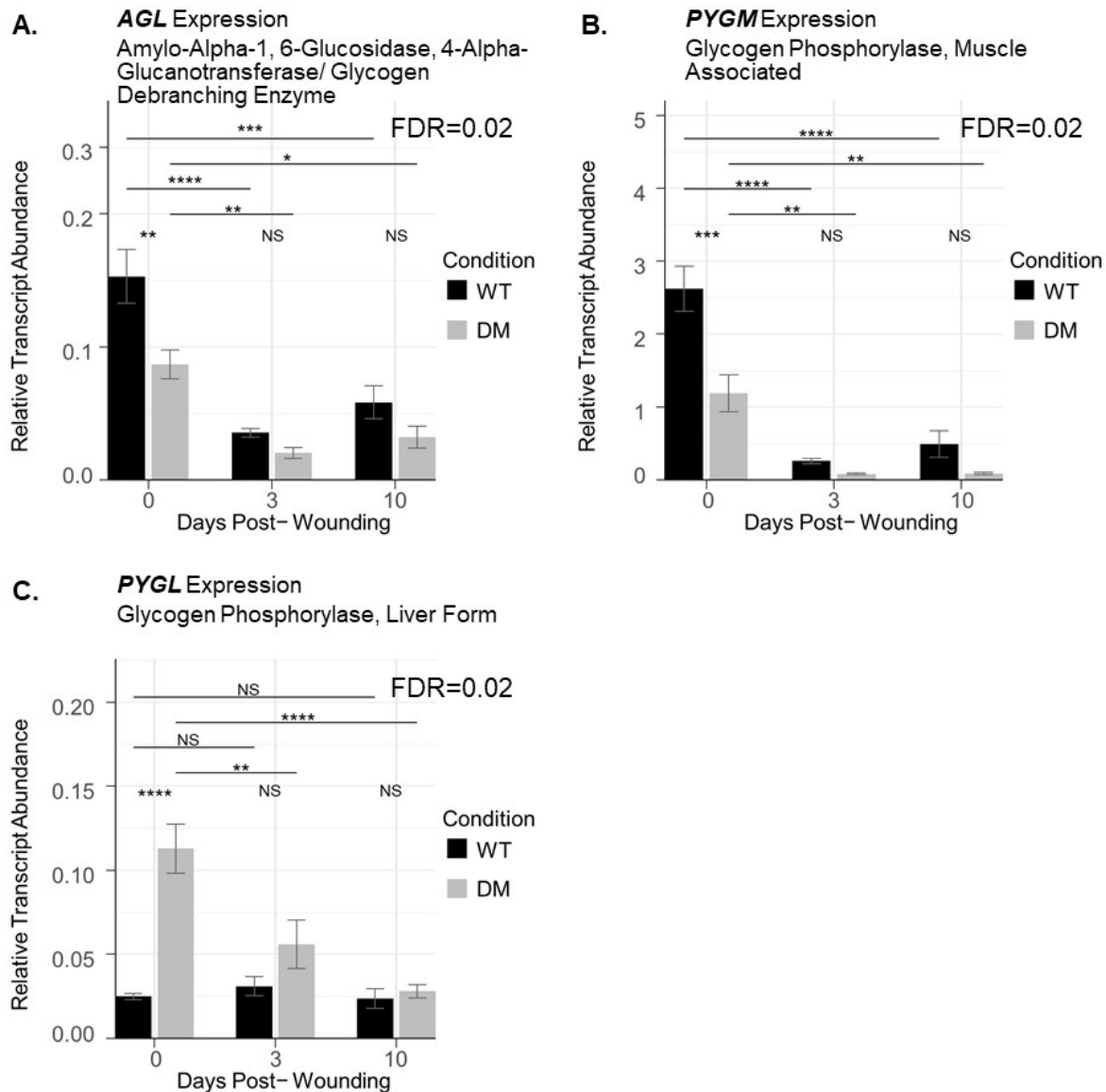


Figure 29. Graphical representation of glycosylation related genes from Cluster 1 that are downregulated in diabetic skin and wounds relative to non- diabetic skin and wounds and are related to local glycogenolysis, while those from Cluster 2 are upregulated and involved in liver glycogenolysis. Genes associated with cluster 1 and downregulated in uninjured, diabetic skin includes the glycogen debranching enzyme (A) and muscle glycogen phosphorylase (B) which catalyzes local glycogen degradation; Genes associated with cluster 2 were upregulated in uninjured, diabetic skin and included liver glycogen phosphorylase (C) which degrades liver stored glycogen when local stores are low. adj. p- value * ≤ 0.05 ; ** ≤ 0.01 , *** ≤ 0.005 , **** ≤ 0.001 .

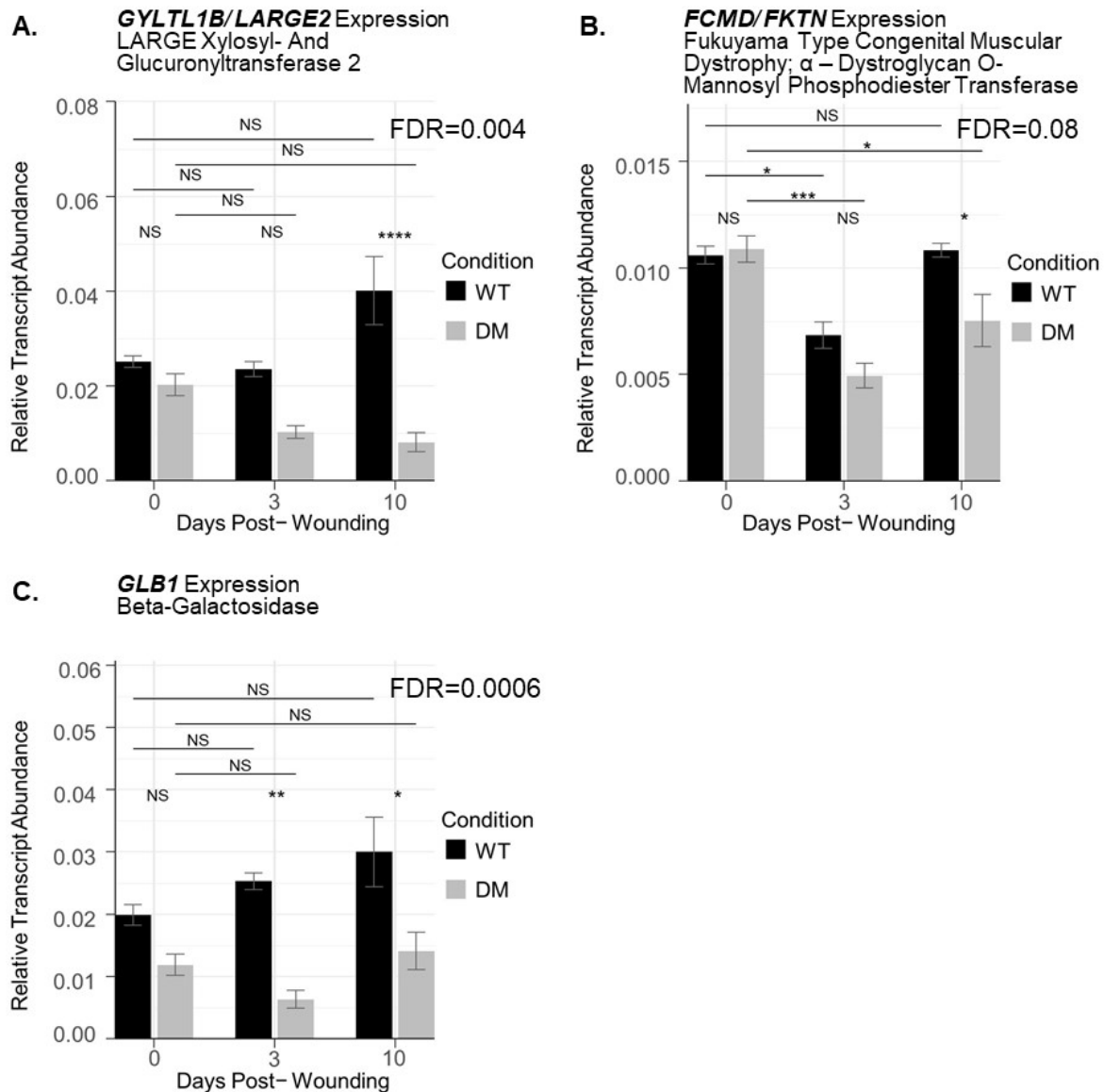
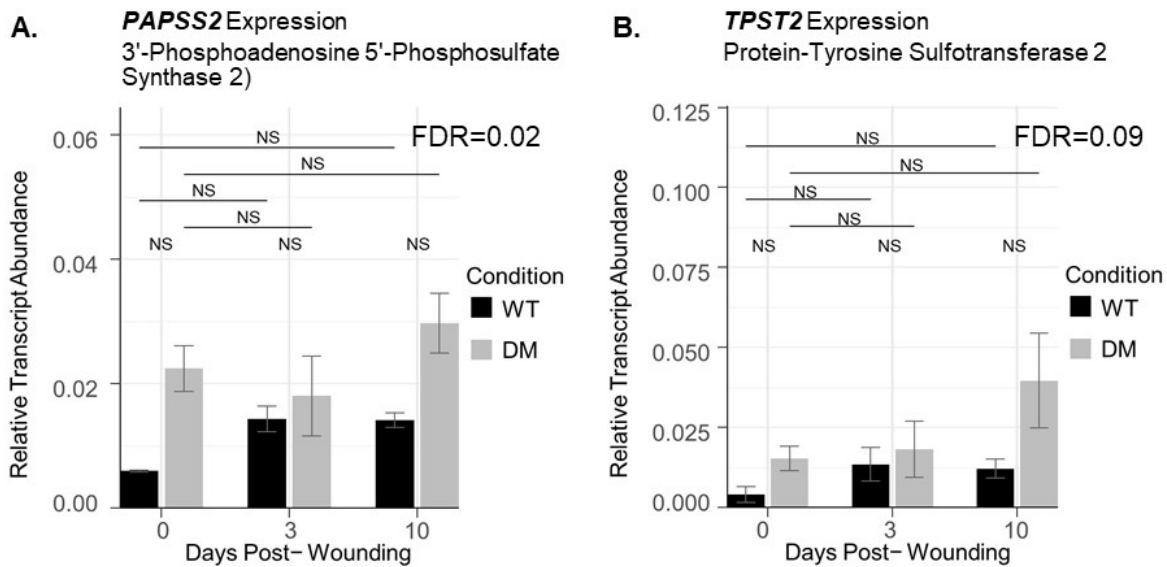


Figure 30. Graphical representation of glycosylation related genes from Cluster 3 that are downregulated in diabetic wounds relative to non-diabetic wounds and involved in α -dystroglycan synthesis and function and β -galactosidase activity. Genes associated with cluster 3 and are downregulated in diabetic wounds during early proliferation (10 Days post-wounding) includes Large xylosyl glucuronyltransferase 2 (A) and α -dystroglycan O-mannosyl phosphodiester transferase (B) which are involved in α -dystroglycan synthesis and binding to laminin. The downregulation of the lysosomal enzyme, β -galactosidase, was also demonstrated (C). adj. p-value * ≤ 0.05 ; ** ≤ 0.01 , *** ≤ 0.005 , **** ≤ 0.001 .



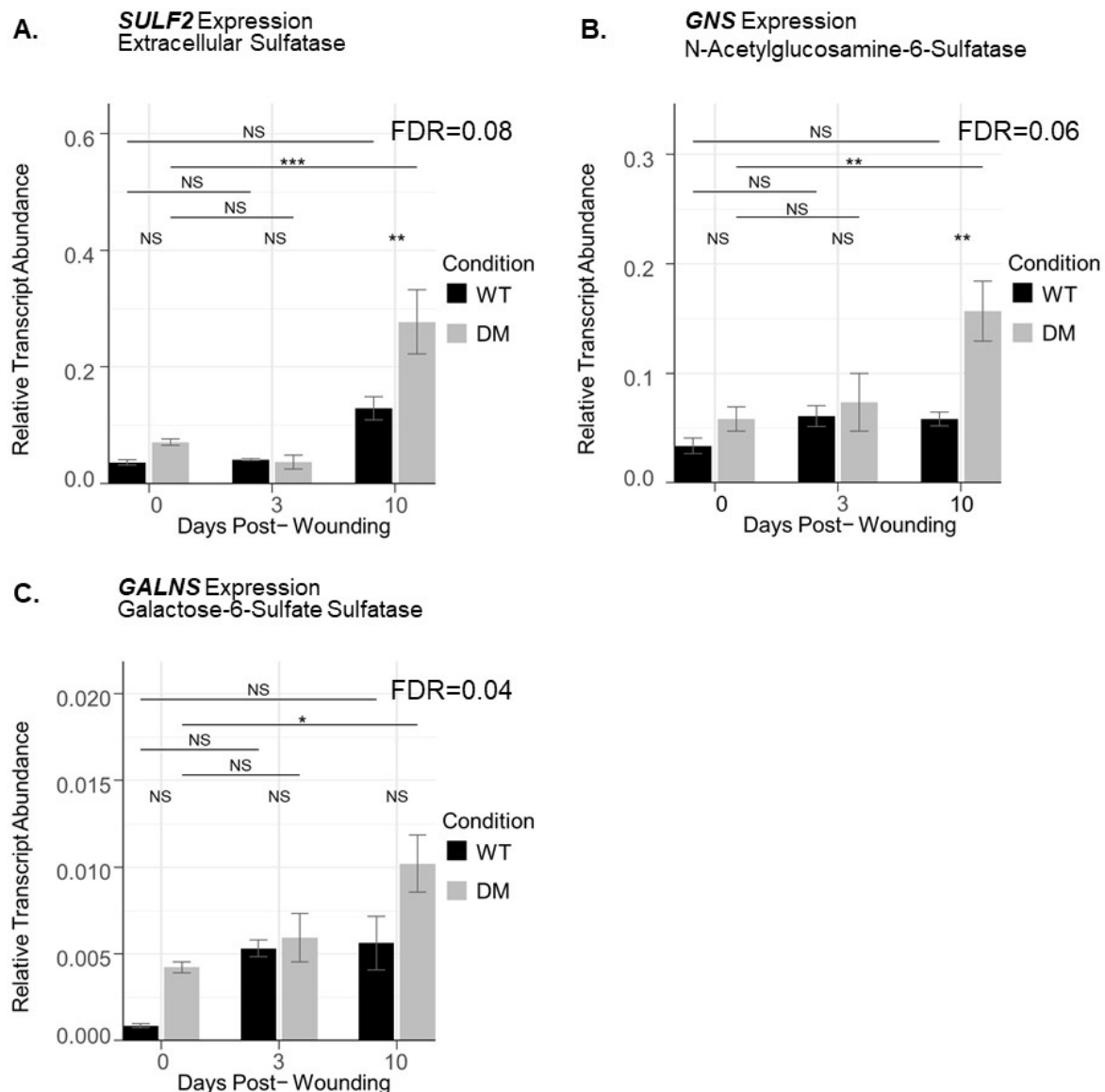


Figure 32. Graphical representation of glycosylation related genes from Cluster 4 & 5 that are upregulated in the diabetic wounds relative to non-diabetic wounds and have sulfatase activity targeting the removal of sulfates at C6 in hexoses associated with glycosaminoglycans. Genes associated with cluster 4 & 5 and are upregulated in the diabetic condition when compared to the non-diabetic condition includes Extracellular Sulfatase (A) an ECM and lysosomal enzyme that removes 6-O-sulfate groups from heparan sulfate; N-Acetylglucosamine-6-Sulfatase (B) a lysosomal enzyme that catabolizes heparin, heparan sulphate, and keratan sulphate; and Galactose-6-Sulfate Sulfatase (C) a lysosomal enzyme that catabolizes keratan sulfate, and chondroitin 6-sulfate. adj. p- value * ≤ 0.05 ; ** ≤ 0.01 , *** ≤ 0.005 , **** ≤ 0.001 .

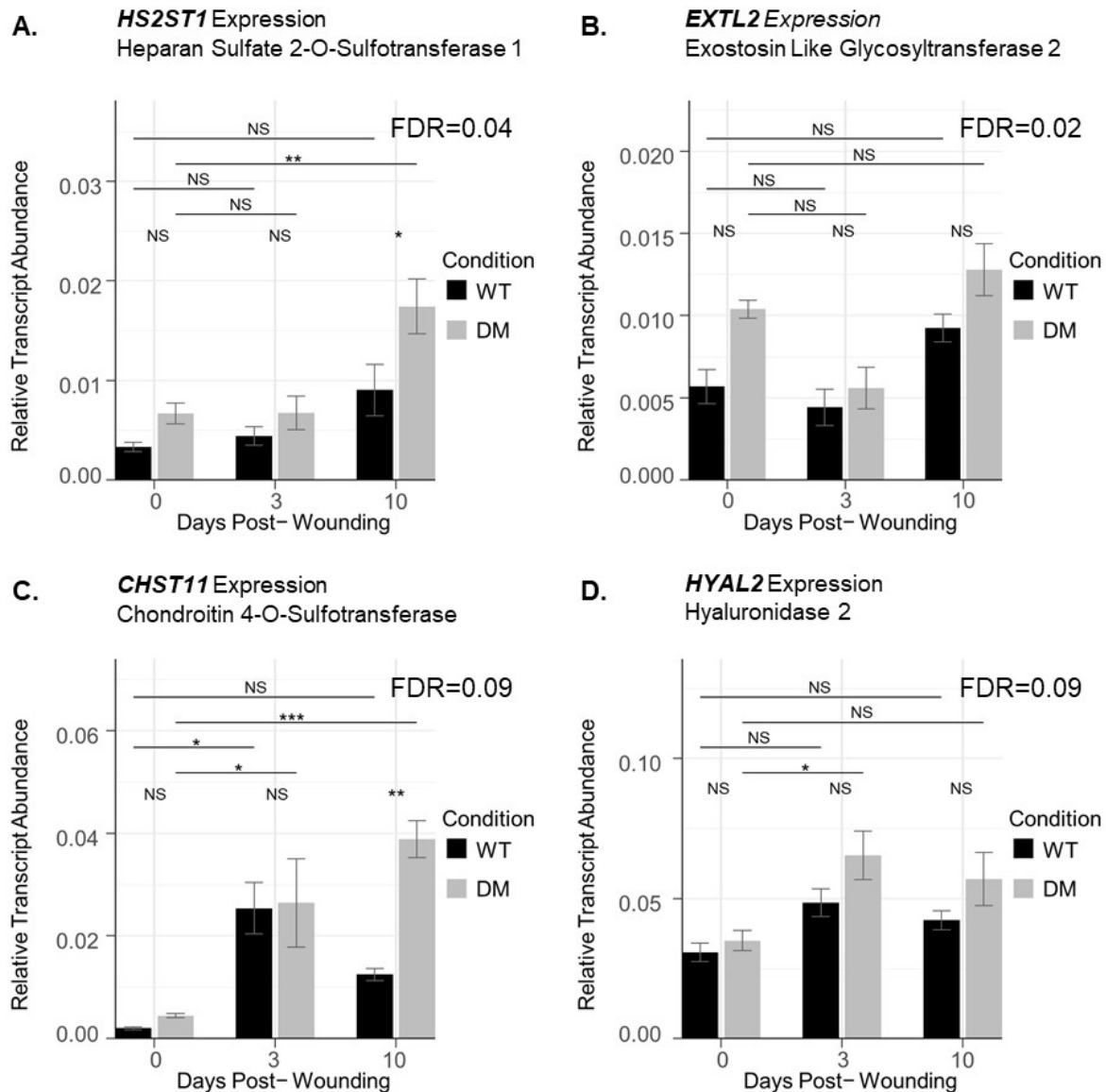


Figure 33. Graphical representation of glycosylation related genes from Cluster 4 & 5 that are upregulated in the diabetic wounds relative to non-diabetic wounds and are related to glycosaminoglycan metabolism. Genes associated with cluster 4 & 5 and are upregulated in the diabetic condition when compared to the non-diabetic condition includes Heparan Sulfate 2-O-Sulfotransferase 1 (A) and Exostosin Like Glycosyltransferase 2 (B) which participate in heparan sulphate biosynthesis and are responsible for sulfation at C2 and HS extension respectively; Chondroitin 4-O-Sulfotransferase (C) which participates in chondroitin sulfation at position 4 on GalNAc; and Hyaluronidase 2 (D) an enzymes that hydrolyzes high MW hyaluronan into intermediate MW hyaluronan. adj. p-value * ≤ 0.05 ; ** ≤ 0.01 , *** ≤ 0.005 , **** ≤ 0.001 .

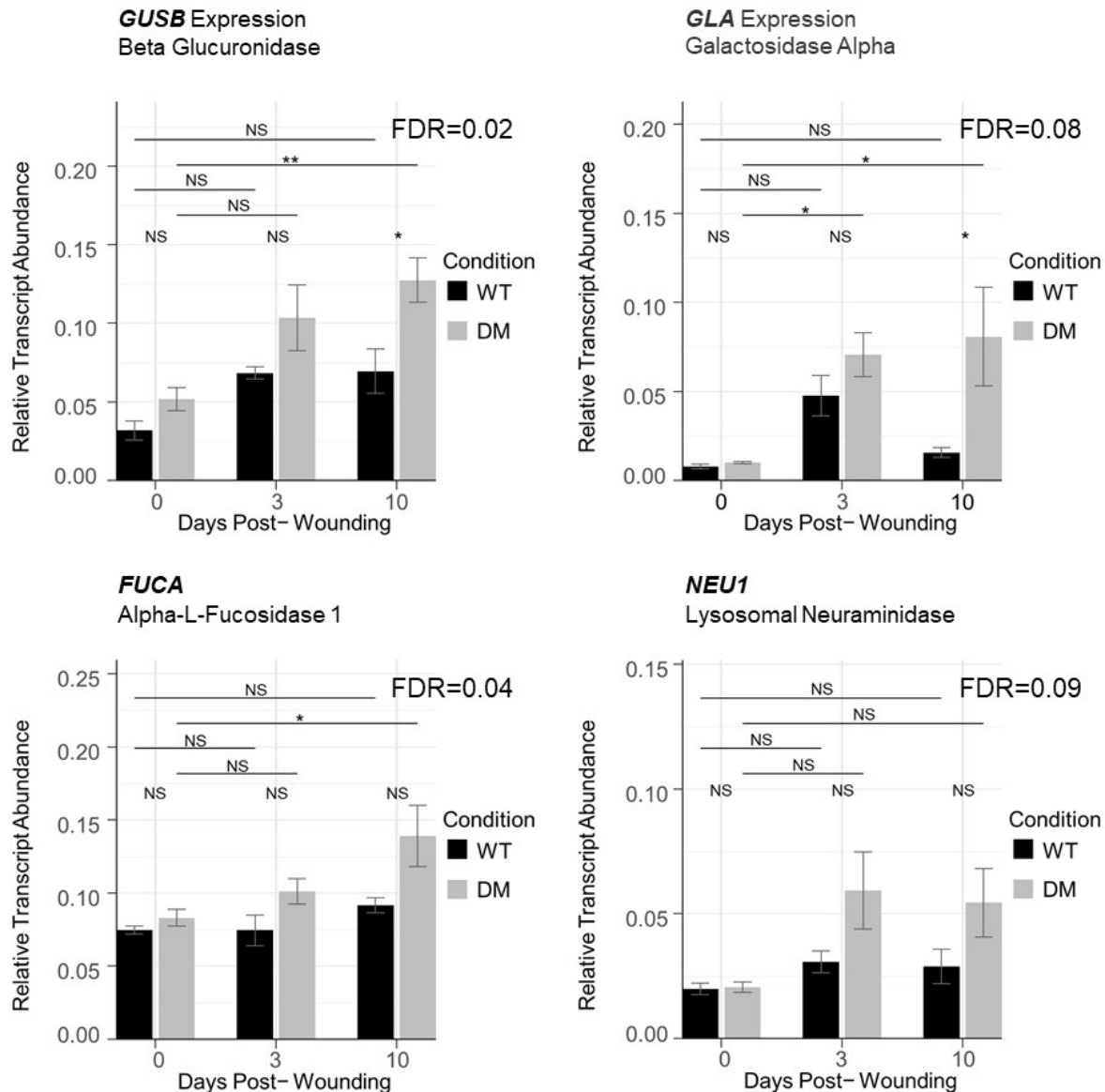


Figure 34. Graphical representation of glycosylation related genes from Cluster 4 & 5 that are upregulated in the diabetic wounds relative to non- diabetic wounds and have lysosomal hydrolase activity targeting glycosaminoglycans and fucose and sialic acids on glycolipids and glycoproteins. Genes associated with cluster 4 & 5 and are upregulated in the diabetic condition when compared to the non- diabetic condition includes β - glucouronidase (A) which hydrolyzes O- glycosyl compounds on heparan, dermatan and keratan sulfate, and chondroitin-4,6- sulfate; Galactosidase alpha (B) which hydrolyze ceramide trihexoside and melibiose into galactose and glucose in glycolipids (globosides) > glycoproteins; α -L- fucosidase 1 (C) which cleave α 1, 6 fucose from the reducing end of GlcNAc; and Lysosomal Neuraminidase (D) which cleave sialic acids from glycolipids and glycoproteins. adj. p- value * ≤ 0.05 ; ** ≤ 0.01 , *** ≤ 0.005 , **** ≤ 0.001 .

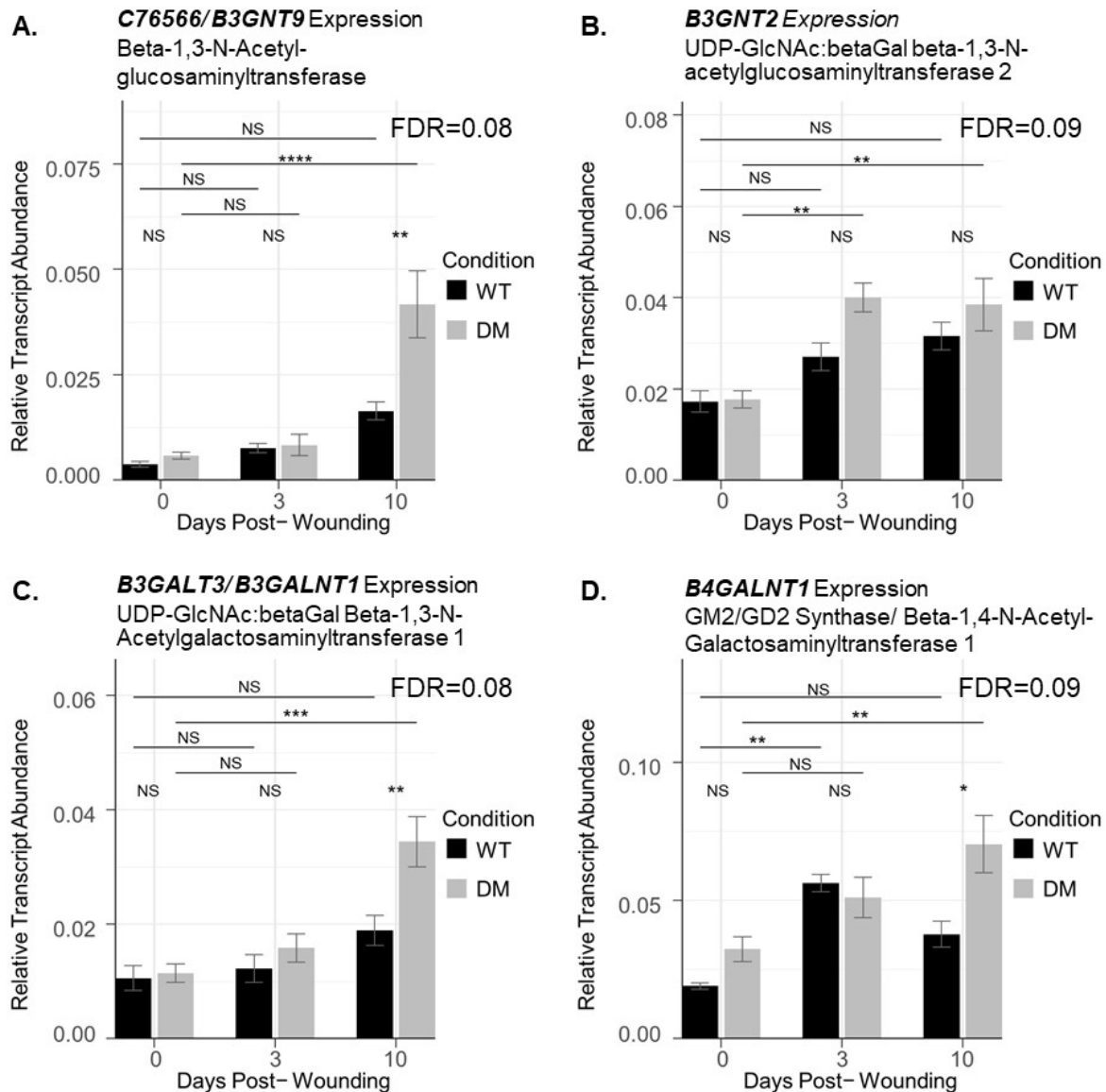


Figure 35. Graphical representation of glycosylation related genes from Cluster 4 & 5 that are upregulated in the diabetic wounds relative to non- diabetic wounds and are related to O- mucin elongation and glycolipid biosynthesis of isoglobosides and gangliosides. Genes associated with cluster 4 & 5 and are upregulated in the diabetic condition when compared to the non- diabetic condition includes β -1,3-N-Acetyl- Glucosaminyltransferase (A) and UDP-GlcNAc:betaGal beta-1,3-N-acetylglucosaminyltransferase 2 (B) which synthesize and elongate O-mucins and glycolipids; UDP-GlcNAc:betaGal Beta-1,3-N-Acetylgalactosaminyltransferase 1 (C) which aids in the biosynthesis of glycolipids (isogloboside iGb₅); and GM2/GD2 Synthase/ Beta-1,4-N-Acetyl-Galactosaminyltransferase 1 (D) which synthesizes gangliosides (GM2, GD2, GT2), isoglobosides (iGb₄), and contributes to N- and O- glycan elongation. adj. p- value * ≤ 0.05 ; ** ≤ 0.01 , *** ≤ 0.005 , **** ≤ 0.001

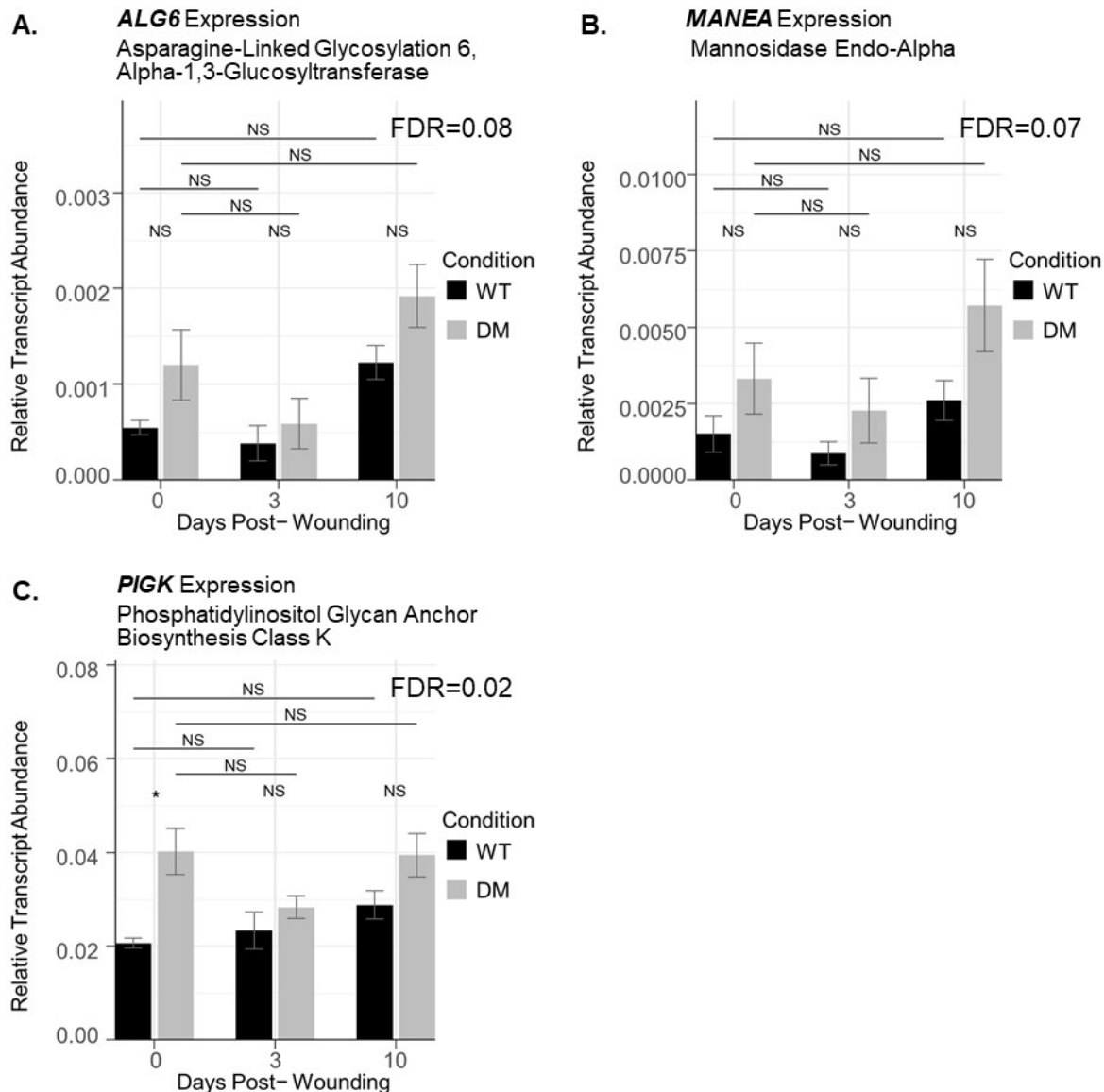


Figure 36. Graphical representation of glycosylation related genes from Cluster 4 & 5 that are upregulated in the diabetic skin relative to non-diabetic skin and are related to N-glycan biosynthesis and trimming and GPI anchor biosynthesis. Genes associated with cluster 4 & 5 and are upregulated in the diabetic condition when compared to the non-diabetic condition includes Asparagine-Linked Glycosylation 6, Alpha-1,3-Glucosyltransferase (A) which is related to the glycan formation during LLO precursor formation in N-glycan biosynthesis; Mannosidase Endo-Alpha (B) which trims N-glycan oligomannose structures; and Phosphatidylinositol Glycan Anchor Biosynthesis Class K (C) which adds phosphatidylinositol glycans to proteins. adj. p-value * ≤ 0.05 ; ** ≤ 0.01 , *** ≤ 0.005 , **** ≤ 0.001 .

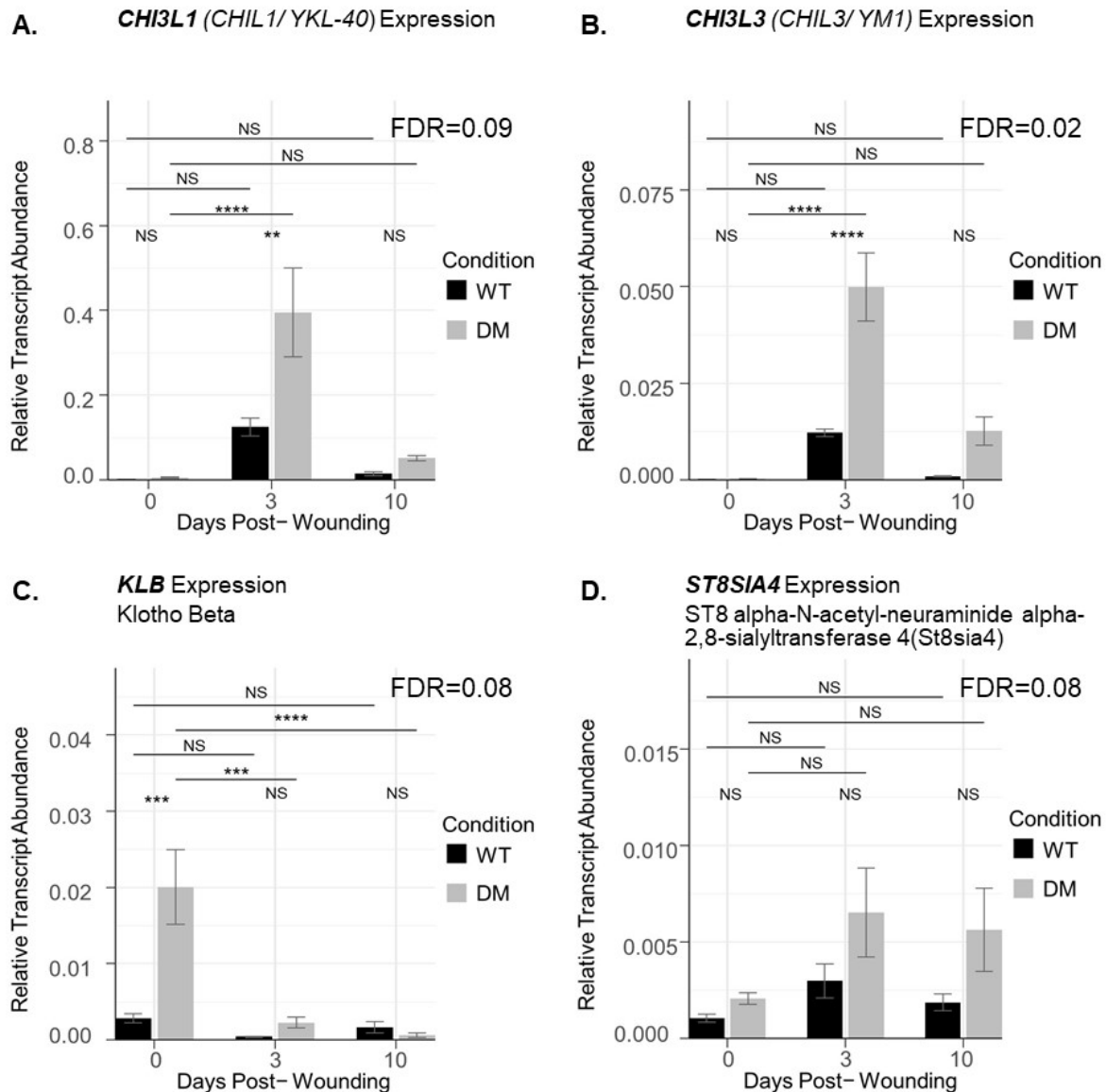


Figure 37. Graphical representation of glycosylation related genes from Cluster 4 & 5 that are upregulated in the diabetic skin and wounds relative to non-diabetic skin and wounds and are related to inactive O- glycosyl hydrolases that act as lectins and the production of polysialic acid. Genes associated with cluster 4 & 5 that are upregulated in the diabetic condition when compared to the non- diabetic condition include Chitinase 3-Like 1(A) and Chitinase 3-Like 3 (B) which lacks chitinase activity and acts as a chitin binding lectin that plays a role in inflammatory cell apoptosis, dendritic cell accrual and M2 macrophage differentiation.; Klotho Beta (C) which is a glycosylhydrolase likely to be inactive, yet regulates FGF21 signaling and is abundant in adipose tissue; ST8 alpha-N-acetyl-neuraminide alpha-2,8-sialyltransferase 4 (D) which adds polysialic acid to ST8Sia-IV, NCAM1, NRP2, and ESL-1. adj. p- value * ≤ 0.05 ; ** ≤ 0.01 , *** ≤ 0.005 , **** ≤ 0.001 .

3.3.5 Regulation and Roles of Genes Expressed during Normal, Non- Diabetic Wound Healing that are Differentially Expressed between the Diabetic and Non- Diabetic Condition

Among the 38 genes that were differentially expressed between the diabetic and non- diabetic conditions, 12 genes were expressed during normal, non-diabetic wound healing during the inflammatory and/or proliferative phases of wound healing. During the inflammatory phase (Day 3) of wound healing, diabetic and non- diabetic wounds demonstrated significantly increased expression of *CHST11* (Figure 33C) and *B4GALNT1* (Figure 35D) which was decreased by day 10 in non-diabetic wounds yet remained upregulated in diabetic wounds. According to the GlycoGene Database these genes encode enzymes that are responsible for transferring GalNAc to GM3 and LacCer via UDP sugar nucleotides during ganglioside glycolipid synthesis (*B4GALNT1*) and transferring sulfate to chondroitin and dermatan via the PAPS donor (*CHST11*). *GAL3ST1* (Figure 27B), *ppGALNT15* (Figure 28A) and *FCMD* (Figure 30B) were all downregulated 3-days post-wounding in diabetic and non-diabetic wounds, however, diabetic wounds demonstrated a trend for decreased expression at one or more timepoints including day 10 when compared to the non- diabetic condition. According to the GlycoGene Database these genes encode enzymes that are responsible for 1) synthesizing the Tn antigen on mucins via UDP sugar nucleotides (*ppGALNT15*), 2) transferring sulfate groups to glycolipids including LacCer and GalCer and chondroitin/ dermatan via the PAPS donor (*GAL3ST1*); and 5) and transferring ribitol 5-phosphate to α -dystroglycan via CDP sugar nucleotides (*FCMD/FKTN*).

Throughout the inflammatory and proliferative phases of healing diabetic and non-diabetic wounds demonstrated significantly decreased expression of *NEU2*, *FUT1* (Figures 27A and 27C), *B4GALNT2*, *B3GNT3* (Figures 28B-C), *AGL* and *PYGM* (Figures 29A-B), however, uninjured skin and wounds from diabetic samples demonstrated a trend for decreased expression of these genes at all timepoints when compared to the non-diabetic condition. The regulation of these genes in non-diabetic wound healing is detailed in Figure 25. According to the GlycoGene Database these genes encode enzymes that are responsible for 1) transferring GalNAc to synthesize blood group Sda/Cad antigens via UDP sugar nucleotides (*B4GALNT2*); 2) removing sialic acids from cytosolic proteins (*NEU2*); 3) transferring fucose to lacto-, neo-lacto-, and globo- series glycolipids via GDP to synthesize H blood group antigens (*FUT1*); 4) promoting local muscle glycogenolysis (*AGL*, *PYGM*); and 5) transferring GlcNAc to core 1 O- linked glycans of glycolipids to synthesize elongated core 1 O-glycans, poly-N- acetyllactosamine, and polylactosamine via UDP sugar nucleotides (*B3GNT3*). Lastly, during the proliferative phase (Day 10) of wound healing non- diabetic wounds demonstrate significantly decreased *FUT2* expression (Figure 27D and Cluster 1 genes of Figure 26), which encodes an enzyme that is responsible for H antigen synthesis on glycolipids and has been observed in intestinal epithelium.

After identifying genes that exhibit significant regulation over the course of non-diabetic wound healing, we evaluated the gene set for those that were differentially expressed between the diabetic and non-diabetic conditions at each timepoint (Figure 38). Among the genes that demonstrated differential expression during non-diabetic wound healing, uninjured diabetic skin demonstrated significantly decreased expression

of Cluster 1 genes (adjusted p-value <0.05) including *NEU2*, *FUT1*, *FUT2* (Figure 27A, 27C, and 27D; adjusted p-value <0.05), *B4GALNT2* (Figure 28B; adjusted p-value <0.05), *AGL* and *PYGM* (Figures 29A-B; adjusted p-value <0.05) when compared to uninjured non-diabetic skin. Additionally, diabetic wounds demonstrated: 1) prolonged upregulation of *B4GALNT1* (Figure 35D; adjusted p-value <0.05) and *CHST11* (Figure 33C; adjusted p-value <0.05); 2) prolonged downregulation of *FCMD* (Figure 30B; adjusted p-value <0.05) and *B3GNT3* (Figure 28C; adjusted p-value <0.05); 3) a trend for downregulation of *ppGALNT15* (Figure 28A; adjusted p-value <0.05) at days 0 and 10; and 4) a trend for sustained downregulation of *GAL3ST1* (Figure 27B; adjusted p-value <0.05) at all timepoints when compared to non-diabetic skin. Overall, these genes are related to pathways involving the metabolism of glycolipids/gangliosides, glycosaminoglycans, O-linked glycans, and blood group antigens and polylactosamines that are likely involved in mediating the inflammatory response to healing. Furthermore, the differential regulation of these genes in non-diabetic wound healing indicates that these genes likely play an important role in normal wound healing, while the additional differential expression in diabetes likely contributes to the impaired healing phenotype observed during diabetic wound healing. Interestingly, many of these genes encode proteins that are suggested to play a role in inflammation. Our data demonstrated that there was downregulation of *B4GALNT2* and upregulation of *B3GNT3* and *CHST11* during the inflammatory phase of wound healing (3 days post wounding when compared to uninjured skin). Previous studies have demonstrated that upregulation of CHST is required for P-selectin ligand mediated binding to P-selectin during leukocyte rolling. Additionally, increased *B3GNT3* expression is involved in L-selectin mediated

leukocyte homing and decreased *B4GALNT2* has been correlated with increased sialyl Lewis x antigen expression in colon cancer ²²⁴. Increased sialyl Lewis x antigen expression and selectin ligand binding are required for selectin mediated leukocyte trafficking during the inflammatory phase of wound healing. Overall the expression patterns of *B4GALNT2*, *B3GNT3*, and *CHST11* during the inflammatory phase of non-diabetic wound healing were consistent with the need for selectin mediated leukocyte trafficking. However, increased leukocyte trafficking and rolling would not be desirable in uninjured skin or when wounds are transitioning out of the inflammatory phase as may be expected by the decreased levels of *B4GALNT2* at day 0 and increased *CHST11* at day 10, respectively, when comparing the diabetic and non- diabetic conditions. Furthermore, AGL and PYGM are downregulated in the inflammatory phase of wound healing (day 3) which would permit increased glycogen storage at this time. Enhanced glycogen storage has been associated with an exaggerated inflammatory response highlighted by increased neutrophil motility, functional capacity, and survival ²²⁵ which is important during the inflammatory phase of wound healing. However, the diabetic condition demonstrated lower levels of AGL and PYGM expression throughout all timepoints and demonstrated delayed upregulation of PYGM. This would be expected to produce an exaggerated neutrophilic response in uninjured diabetic skin and during the proliferative phase of wound healing when compared to the non- diabetic skin.

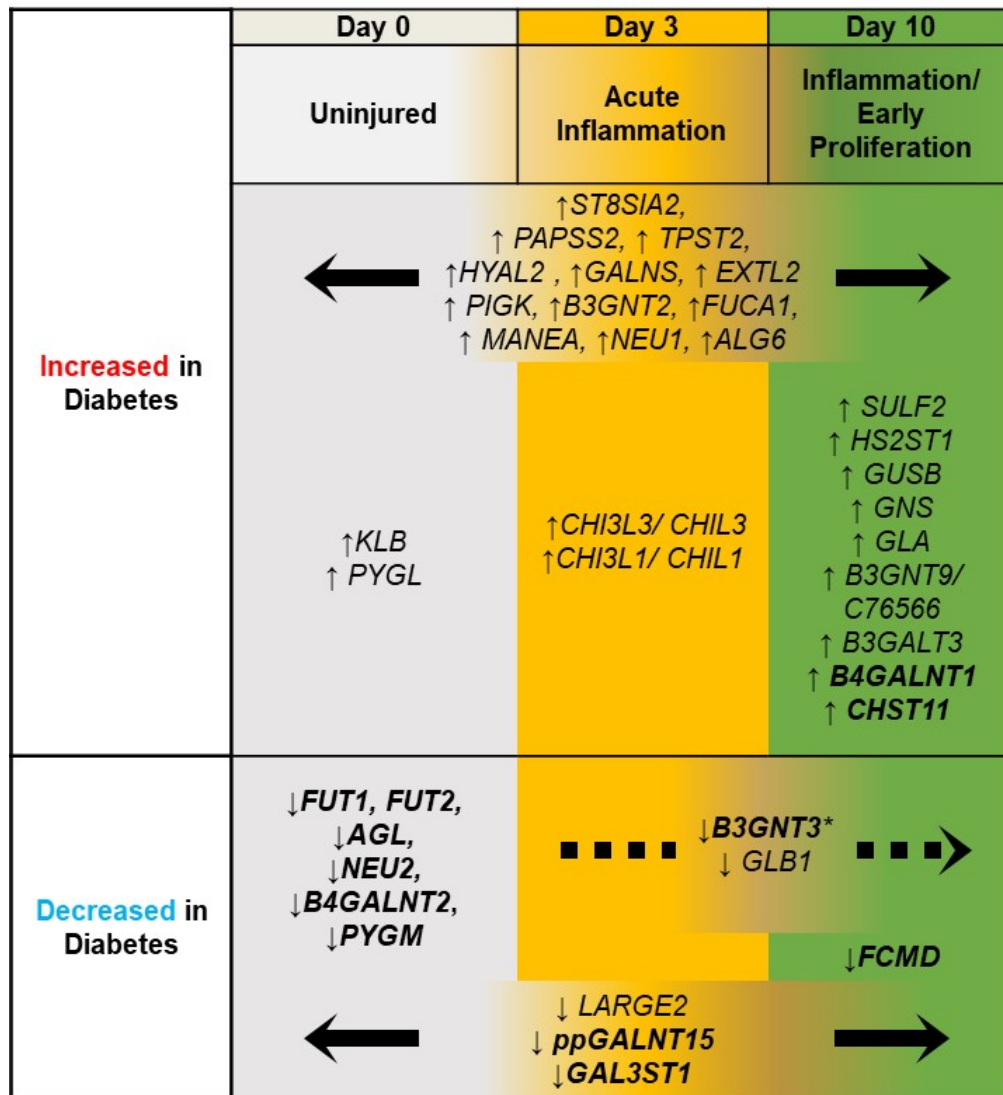


Figure 38. Glycosylation related genes are differentially regulated in diabetic and non- diabetic wound healing. Genes with significance in pairwise comparisons at 1 timepoint are identified under each timepoint. Genes identified with significance between days 0 and 10 are place between the 2 timepoints with a dashed unidirectional arrow. Genes with overall significance due to differences between the 2 conditions span the entire length of time and are indicated with a solid bidirectional arrow. Bolded genes indicate those which are significantly regulated in non- diabetic wound healing (FDR<0.1 for overall comparison of skin and tongue, $p \leq 0.05$ for multiple timepoint comparisons). The gene with the most drastic differential expression between diabetic and nondiabetic wounds is represented by the asterisk.

3.3.6 Differential Expression of Genes between the Diabetic and Non- Diabetic Condition that are Primarily Regulated during Diabetic Wound Healing

When examining diabetic wound healing, multiple comparisons analysis identified 16 genes that demonstrated statistically significant differences during diabetic wound healing that were not significantly regulated during non-diabetic wound healing. These genes included *HYAL2*, *GUSB*, *GALNS*, *GLA*, *GBA*, *B3GNT2* and *FUCA1* (Cluster 5, adjusted p-value <0.05), *B3GNT9/ C76566*, *B3GALT3/ B3GALNT1*, *SULF2*, *GNS* and *HS2ST1*, *CHI3L1*, *CHI3L3* (Cluster 4, adjusted p-value <0.05), and *KLB*, and *PYGL* (Cluster 2, adjusted p-value <0.05). DAVID pathway analysis and manual annotation of these differentially expressed genes revealed enriched gene ontologies related to the lysosome, sulfuric ester hydrolase activity, and aminoglycan catabolic processes during diabetic wound healing. Increased hydrolase activity would be expected to cause increased degradation of the respective glycoconjugates, most notably those related to glycosaminoglycans. Increased glycosaminoglycan degradation has been previously reported in diabetes and has the potential to impair extracellular matrix interactions and reduce tissue integrity ²²⁶⁻²²⁸.

3.3.7 The Expression of Glycosylation- Related Genes is Altered in Intact and Wounded Human DM Skin

To determine if glycosylation- related gene expression differs in human diabetic skin and wounds as compared to non-diabetic human skin, we compared available microarray data of uninjured human skin. Uninjured skin obtained from subjects with diabetes (DFS) and those without a history of diabetes (NFS) was examined in the GEO

dataset GSE68183^{223, 229-230}. Diabetic foot ulcers (DFU) were then compared to uninjured skin obtained from subjects with and without diabetes (FS) in the GEO dataset GSE80178^{223, 231}. In this study we screened the 2 microarray datasets for glycosylation- related genes that were differentially expressed. Since the entire uninjured skin dataset (GSE68183) demonstrated minimal statistical significance, genes with an $FDR > 0.05$ were examined if the genes were statistically significant in the diabetic foot ulcer (DFU) dataset ($FDR \leq 0.05$ in GSE80178). This comparison identified 15 glycosylation- related genes that were differentially expressed in diabetic foot ulcers (DFU/ FS) and were present in the uninjured skin dataset (DFS/ NFS). Genes that demonstrated increased significance and/or a higher absolute linear fold change between the uninjured skin dataset and the diabetic foot ulcer dataset were also identified. The genes encoding fucosyltransferase 8 (*FUT8*), heparanase (*HPSE*), glycosyltransferase 8 domain containing 2 (*GLT8D2*), mannosidase, alpha, class 1C, member 1 (*MAN1C1*), uronyl-2-sulfotransferase (*UST*), exostoses (multiple)-like 2 (*EXTL2*), mannosidase, endo-alpha (*MANEA*), hyaluronan synthase 3 (*HAS3*), and UDP-N-acetyl-alpha-D-galactosamine:polypeptide N-acetylgalactosaminyltransferase 6 (*GALNT6*) demonstrated $\geq 25\%$ difference in the linear fold change between uninjured DFS and NFS (Table IX and Table X). Among these genes the average linear fold change between diabetic foot ulcers and uninjured foot skin from non-diabetic and diabetic subjects was 1.89 (range 1.33-2.46) times higher than the linear fold change between uninjured foot skin from diabetic subjects and non- diabetic subjects alone. Differentially expressed genes underwent pathway analysis via Reactome and were further manually annotated using KEGG, The Functional Glycomics Gateway, and

CAZy^{215, 232-238}. These differentially expressed genes were associated with pathways including glycosaminoglycan metabolism and N- and O-linked protein modifications including O- glycan biosynthesis, trimming of high mannose N- glycans, and N- linked precursor core fucosylation. Furthermore, genes encoding asparagine-linked glycosylation 8 (*ALG8*), asparagine-linked glycosylation 13 (*ALG13*), N-acetylglucosamine-1-phosphate transferase, alpha and beta subunits (*GNPTAB*), meningioma expressed antigen 5 (*MGEA5*), beta-1,4-N-acetyl-galactosaminyltransferase (*B4GALNT3*) and UDP-GlcNAc:betaGal beta-1,3-N-acetylglucosaminyltransferase 2 (*B3GNT2*) were also found to be differentially expressed in the DFU dataset. The linear fold change of these genes was <25% and demonstrated no differential expression between uninjured DFS and NFS, however, they were differentially regulated between diabetic foot ulcers and uninjured foot skin. These genes were related to pathways including lysosomal enzyme targeted glycan degradation, cytosolic/nuclear protein O-GlcNAc removal, and the biosynthesis of lactosamine and LacdiNAc structures. A description (Table IX) and comparison of the genes observed in both datasets is provided in Table X. The enhanced significance and increased linear fold change observed between these two datasets data suggests the presence in baseline differences between uninjured, diabetic and non-diabetic skin may precipitate enhanced differential glycosylation- related gene expression during wound healing. Furthermore, the differentially expressed genes in the human dataset are involved in O-linked protein modifications and glycosaminoglycan metabolism, coincide with what was observed in the *db/db* mouse data analysis.

TABLE IX.

TABLE OF GENES AND THEIR FUNCTIONS AMONG THE DIFFERENTIALLY EXPRESSED GENES OBSERVED IN HUMAN DIABETIC FOOT ULCERS.

Enzyme/ GENE	Function
Asparagine-linked glycosylation 8 Glc ₁ Man ₉ GlcNAc ₂ α 1, 3-glucosyltransferase (<i>ALG8</i>)	Enzyme that adds the second of three glucoses to the Glc ₃ Man ₉ GlcNAc ₂ -lipid linked precursor for all N-linked glycosylation.
Asparagine-linked glycosylation 13 UDP-GlcNAc glycosyltransferase subunit (<i>ALG13</i>)	Enzyme that adds the second of two GlcNAc sugars to the Glc ₃ Man ₉ GlcNAc ₂ -lipid linked precursor for all N-linked glycosylation.
N-acetylglucosamine-1-phosphotransferase (<i>GNPTAB</i>)	Enzyme responsible for creating the mannose-6-phosphate recognition marker essential for the targeting of degradative enzymes to the lysosome.
Meningioma expressed antigen 5 O-GlcNAcase (<i>MGEA5</i>)	Enzyme responsible for removing O-GlcNAc from cytoplasmic and nuclear proteins to regulate their signaling and function.
β 1,4-N-acetylgalactosaminyltransferase 3 (<i>B4GALNT3</i>)	Enzyme that transfers GalNAc onto a GlcNAc residue to form the GalNAc β 1-4GlcNAc (LacdiNAc) structure on N- and O-glycans; notably found as part of the unique glycan essential for α -dystroglycan function.
β 1,3-N-acetylglucosaminyltransferase 2 (<i>B3GNT2</i>)	Enzyme that transfers GlcNAc onto Gal to form poly-N-lactosamine chains that terminate N- and O-glycans.
Fucosyl- transferase 8 (<i>FUT8</i>)	Enzyme that transfers α 1-6 linkage to the first GlcNAc residue next to the peptide chains in precursor N-glycans during N-glycan biosynthesis.
Heparanase (<i>HPSE</i>)	Enzyme that removes the linkage between glucuronic acid and N-sulfo glucosamines carrying either a 2-O-sulfo, 3-O-sulfo, or a 6-O-sulfo group.
Glycosyltransferase 8 domain containing 2 (<i>GLT8D2</i>)	Enzyme specificity not well defined, but involved in transferring glycosyl groups and involved in the regulation of ApoB100.
Mannosidase, alpha, class 1C, member 1 (<i>MAN1C1</i>)	Enzyme that removes α 1,2-Man residues from Man(8)GlcNAc(2) to produce Man(7)GlcNAc(2), Man(6)GlcNAc, and Man(5)GlcNAc respectively.
Mannosidase, endo-alpha (<i>MANEA</i>)	Enzyme that removes α 1,2-Man residues from Man(9)GlcNAc(2) to produce first Man(8)GlcNAc(2).
Uronyl-2-sulfotransferase (<i>UST</i>)	Enzyme that transfers sulfate to the 2-position of IdoA dermatan sulfate and GlcA on chondroitin sulfate.
Exostoses (multiple)-like 2 (<i>EXTL2</i>)	Enzyme that transfers β -1-4-GlcA and α -1-4GlcNAc units to nascent heparan sulfate chains.
Hyaluronan Synthase (<i>HAS3</i>)	Enzyme that transfers GlcNAc or GlcUA to the low MW hyaluronan polymers.
UDP-N-acetyl-alpha-D-galactosamine: polypeptide N-acetylgalactosaminyltransferase 6 (<i>GALNT6</i>)	Enzyme that transfers GalNAc to serine and threonine residues on target proteins including Muc1a, Muc2, EA2 and fibronectin.

TABLE X.

TABLE OF GENES REGULATED IN HUMAN DIABETIC VERSUS NON-DIABETIC FOOT SKIN AND DIABETIC VERSUS UNINJURED FOOT SKIN DATASETS THAT ARE RELATED TO THOSE EXPRESSED IN THE DB/DB MOUSE MODEL.

Gene Symbol	Linear FC DFU vs. FS	ANOVA p-value DFU vs FS	FDR p-value DFU vs. FS	Linear FC DFS vs. NFS	ANOVA p-value DFS vs NFS	FDR p-value DFS vs. NFS	FC between DFU vs. FS and DFS vs. NFS
<u>FUT8</u>	-2.63	0.000009	0.000357	-1.32	0.010239	0.839945	1.99
HPSE	2.68	0.011289	0.031041	1.87	0.017703	0.857428	1.43
<u>GLT8D2</u>	-3.07	0.013399	0.035145	-1.77	0.022093	0.857428	1.73
MAN1C1	-2.22	0.000062	0.001027	-1.67	0.039747	0.874426	1.33
UST	-2.25	0.000139	0.001659	-1.46	0.051492	0.888491	1.54
EXTL2	-2.59	0.000083	0.001217	-1.31	0.057768	0.88946	1.98
B4GALNT3	2.4	0.0063	0.02042	1.07	0.227996	0.904852	2.24
MGEA5	-2.15	0.014364	0.03687	1.11	0.249053	0.909045	
MANEA	-3.32	0.000632	0.004241	-1.35	0.250975	0.909045	2.46
<u>HAS3</u>	3.26	0.000849	0.005143	1.42	0.318623	0.917346	2.3
<u>GALNT6</u>	3.08	0.012297	0.033	1.38	0.328835	0.919464	2.23
ALG13	-3.45	0.00003	0.000675	1	0.420996	0.930246	
GNPTAB	-3.16	0.000539	0.00383	-1.09	0.501604	0.94068	2.9
B3GNT2	2.36	0.016799	0.041319	-1.02	0.513692	0.944635	
<u>ALG8</u>	-2.77	0.000932	0.005472	1.08	0.588872	0.955219	

Comparison of data set GSE80178 (diabetic foot ulcers [DFU] compared to foot skin of diabetic and nondiabetic patients [FS] with the data set GSE68183 (diabetic foot skin [DFS] and non-diabetic foot skin [NFS]).

Bolded genes represent those that were observed to be significant in human diabetic ulcers and demonstrated a similar trend in the glycotranscriptomics analysis of db/db (diabetic) and C57 (non-diabetic) mouse skin.

Underlined genes represent those that were observed to be significant in human diabetic ulcers and demonstrated a similar trend in the microarray analysis of BALB/c skin and tongue wounds.

3.3.8 Skin Characteristics during Wound Healing in *db/db* Mice Mimic those Observed in Diabetic Humans

Previous studies suggest that the *db/db* mouse model provides an informative model with features that parallel human wound healing. To confirm that the mouse model aligned with the clinical phenotype of human diabetic and non-diabetic wound healing, diabetic, *db/db* (DM) and non-diabetic C57 mice (WT) blood glucose, bodyweight, and wound closure were measured. As indicated by Figure 39, diabetic *db/db* mice demonstrated significantly increased blood glucose (Figure 39A) and body weight (Figure 39B) which was approximately double that of the non-diabetic mice. Diabetic mice also demonstrated delayed wound closure which was most prominent 3 days post-wounding (Figures 39C-D). Nearly all of the diabetic mice demonstrated a slight increase in the wound area at this time. Histologic evidence of a delayed wound healing response was observed as early as 1-day post-wounding (Figure 40C and 40D, left) when diabetic mice demonstrated reduced epithelial proliferation (Figure 40D, left) and decreased platelet and inflammatory cell migration to the wound bed with increased inflammatory cell infiltration throughout the intact tissue when compared to the non-diabetic mice (Figure 40C, left). Furthermore, all non-diabetic mice demonstrated macroscopic wound closure by day 10 during the proliferative phase of healing (Figures 40C-D), while diabetic mice only achieved 80% closure by this time. Wounds of diabetic mice demonstrated a heightened proliferative response at day 10 as noted by the increased epithelial thickness. Overall this data confirmed the diabetic mouse model replicated the clinical phenotype that is observed in humans with diabetes and lower extremity ulcers.

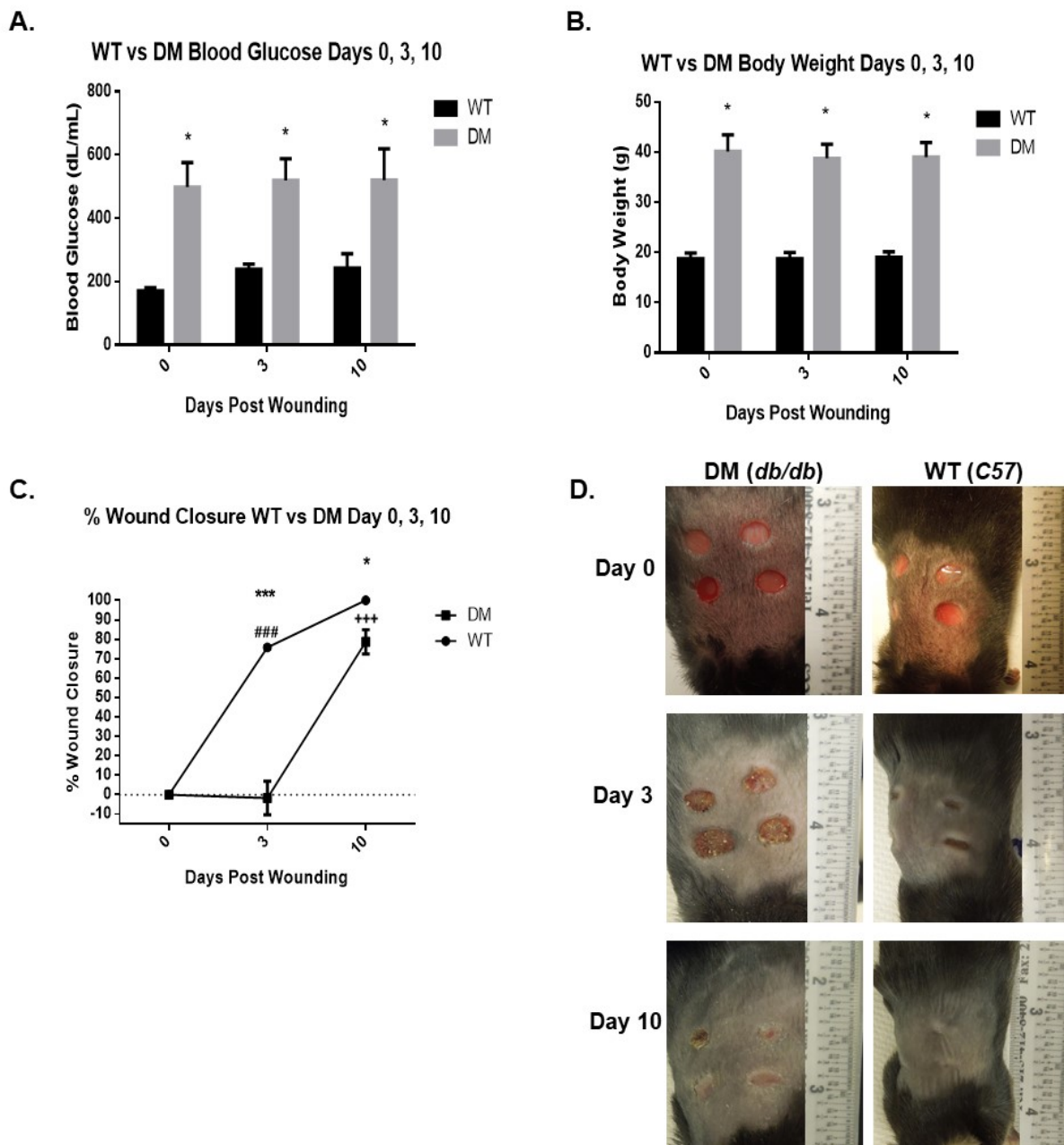


Figure 39. Diabetic mice exhibit increased blood glucose, obesity, and delayed wound closure.

Blood glucose (A), body weight (B), and quantification of wound closure (C) were measured in diabetic (DM, *db/db*) and non-diabetic mice (WT, C57). D) Photograph of wounds in *db/db* mice (DM). * = WT vs DM; # = Day 3 and 0 in WT; + = Day 10 and 0 in DM. * ≤ 0.05 ; *** ≤ 0.005 .

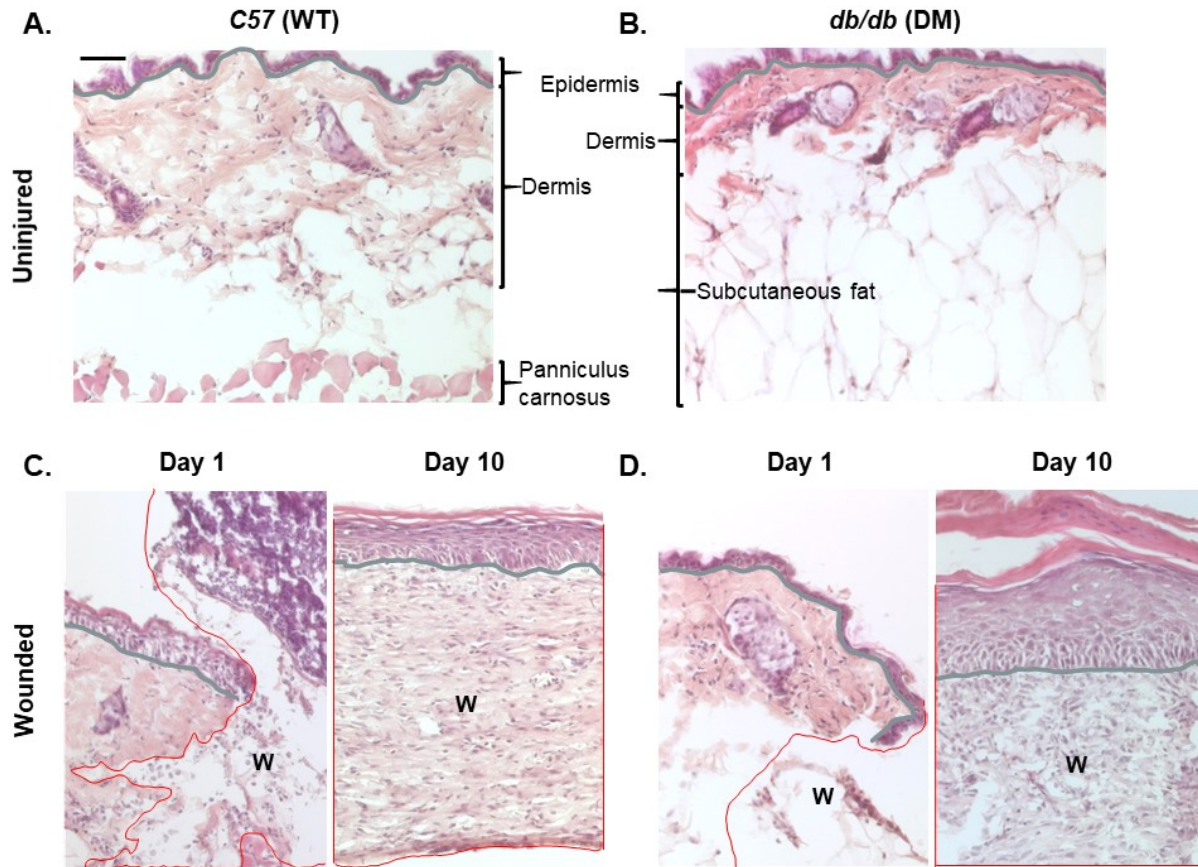


Figure 40. Histologic comparison of uninjured skin and wounds 1- and 10-days post- wounding in non- diabetic and diabetic skin. H&E staining of uninjured non-diabetic/ WT skin (A) and diabetic/ DM skin (B), non- diabetic wounds (C), and diabetic wounds (D) 1 day (left) and 10- days post- wounding (right). The grey line separates the epidermis and dermis. The red border represents the wound bed (W). Black scale bar 50µm.

3.4 Discussion

This study identified 38 glycosylation- related genes that were differentially expressed between the diabetic and non-diabetic conditions and were significantly regulated during non-diabetic wound healing. Pathway analysis and manual annotation of genes that were differentially expressed between the diabetic and non-diabetic conditions and those modulated during wound healing were related to ceramide/glycolipid/ganglioside biosynthesis, metabolism, glycosaminoglycan metabolism, and poly-N-acetyllactosamine metabolism. Previous studies have confirmed that gangliosides play an important role in mediating the impaired phenotype observed in diabetic wound healing. These previous studies attribute increased GM3 gangliosides and sphingolipids to impairments in epithelial migration and angiogenesis in diabetic subjects ^{110, 160-161, 239}. Our study identified the presence of decreased *GM2/GD2* synthase downregulation in diabetic wounds 10 days post wounding. The increased expression of *GM2/GD2* synthase and its inability to return to baseline would be expected when there is increased GM3, as GM3 is the precursor of GM2 (Figure 41). Additionally, when examining the genes that encode enzyme that precede GM3 synthesis, a trend of increased expression of *UGCG*, *B4GALT6*, and *ST3GAL5* was observed in diabetic mice between 3- and 10-days post wounding (Figures 91B; 69D; and 87D, Appendix D) when compared to non-diabetic mice. Since sphingolipid/ganglioside metabolism has been thoroughly investigated for its role in epithelial ¹⁶⁰⁻¹⁶¹ and microvascular dysfunction in diabetes ^{167-168, 240-241}, further investigation is not of interest. However, this study provides evidence that additional

glycosylation- related pathways of interest modulate the differential healing observed between diabetic and non-diabetic skin and wounds.

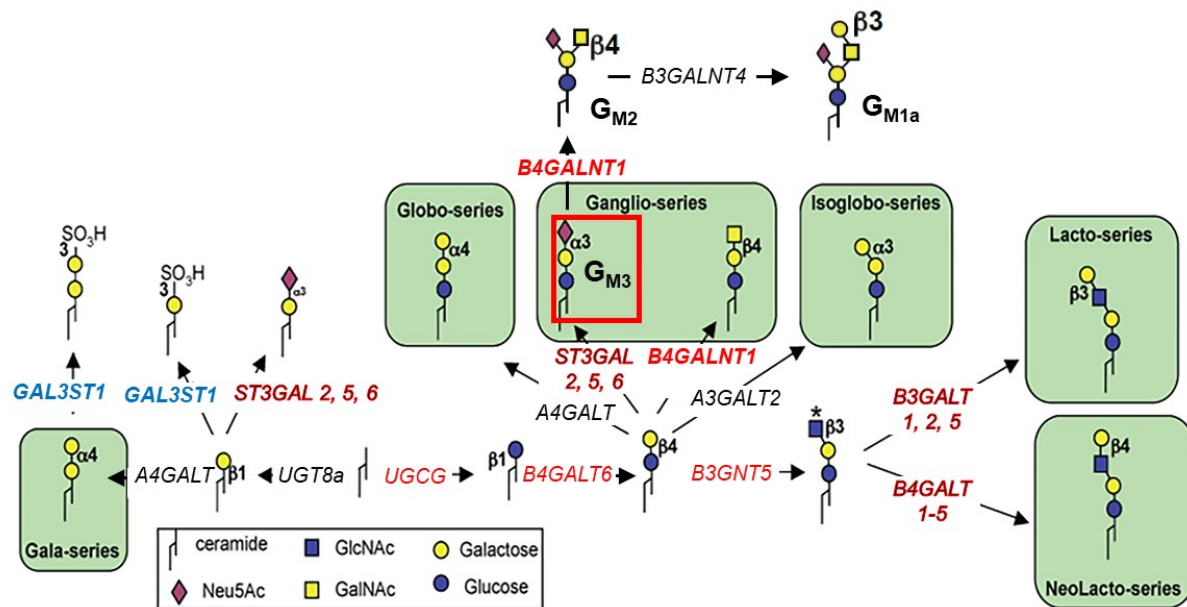


Figure 41. Core glycolipid and GM3 ganglioside biosynthesis reactions.

Genes encoding enzyme reaction involved in core glycolipid biosynthesis leading up to the production of GM3, GM2, and GM1a are indicated as text between the reactions. Genes demonstrating **upregulation** and **downregulation** in diabetic skin when compared to non- diabetic skin are colored red and blue respectively. Bolded genes represent those that demonstrated statistically significant differences between the diabetic and non- diabetic conditions. Red, unbolded genes exhibited a trend for increased expression in the diabetic condition when compared to the non- diabetic condition. Genes indicated in black were not assessed.

The glycosylation- related pathways that were of interest include those related to glycogenolysis, glycosaminoglycan metabolism, and N- and O- linked glycosylation. Our study demonstrated genes involved in local carbohydrate metabolism and glycogenolysis (*AGL* and *PYGM*) were downregulated in uninjured diabetic skin when compared to non-diabetic skin and during the inflammatory phase of wound healing when compared to uninjured skin. *AGL* encodes the glycogen debranching enzyme and *PYGL* encodes glycogen phosphorylase, both of which are involved in glycogenolysis. Decreased glycogenolysis leads to the accumulation of glycogen and decreased availability of glucose-1-phosphate (G-1-P) ²⁴². G-1-P is the precursor of the UDP-Glc sugar nucleotide ²⁴³ and has been found to increase intracellular calcium influx in microorganisms ²⁴⁴ and mammals ²⁴⁵. Decreased availability of G-1-P, in response to decreased glycogenolysis, would be expected to reduce the influx of intracellular calcium. Calcium regulation is vital to most cellular functions including wound repair. A recent study observed that extracellular calcium release upon wounding stimulates intracellular calcium accumulation via calcium sensing receptors (CaSR). CaSR mediated intracellular calcium accumulation triggers E-cadherin/ epidermal growth factor receptor/ mitogen-activated protein kinase signaling to promoting keratinocyte migration, proliferation, and differentiation during wound repair ²⁴⁶. Together, this data suggests a role for *AGL* and *PYGM* downregulation in mediating impaired keratinocyte migration, proliferation, and differentiation by decreasing glucose-1-phosphate availability and intracellular calcium accumulation.

Enhanced glycogen storage has also been associated with an exaggerated inflammatory response highlighted by increased neutrophil motility, functional capacity,

and survival ²²⁵. While neutrophils play an important role in wound surveillance during the inflammatory phase of healing and are ultimately required for wound resolution, an exaggerated neutrophilic response in uninjured skin and during the later stages of wound healing would be undesirable. Despite the potential, yet unclear role that these genes play in wound healing, *AGL* downregulation has been observed in bladder cancer growth and invasiveness ²⁴⁷. These changes have been associated with excessive protease activity and excessive hyaluronan induced proliferation ²⁴⁸. This data additionally coincides with the increased regulation of genes related to glycosaminoglycan metabolism observed in our db/db model of diabetic wound healing. Further research examining the link between reduced *AGL/PYGM* expression and glycogenolysis, glycosaminoglycan regulation, and their impact on wound healing would be of interest considering its association with cancer and its success with aiding in cancer prognosis.

Interestingly, many of the genes involved in glycosaminoglycan metabolism and others that were only differentially regulated in diabetic wound healing have biological processes related to neutrophil degranulation including *FUCA1*, *GALNS*, *GLA*, *GLB1*, *GNS*, *GUSB*, *NEU1*, *AGL*, *PYGL*, *CHI3L1*. The genes *FUCA1*, *GALNS*, *GLA*, *GLB1*, *GNS*, *GUSB*, and *NEU1* encode lysosomal enzymes, while *CHI3L1* encodes a secreted glycoprotein that has been shown to induce pro-inflammatory and pro-tumorigenic factors ²⁴⁹. Lastly, according the Reactome pathway annotations ^{189, 235}, *CHI3L3*, along with *GBA* ²⁵⁰ and *HYAL2* ²⁵¹ are activated in response to IL-1 and/or TNF α . Considering the importance that neutrophils play in promoting wound repair and the development of chronic wounds, it would be of interest to identify whether changes in these neutrophil

degranulating enzymes are controlled by upstream alterations in *AGL* and *PYGM* expression.

TABLE XI.
TABLE OF GENES ENCODING LYSOSOMAL ENZYMES.

Lysosomal enzyme/GENE	Function
Tissue alpha-L-fucosidases (<i>FUCA1</i>)	Enzyme responsible for the breakdown of fucose in the lysosome.
N-acetylgalactosamine-6-sulfatase (<i>GALNS</i>)	Sulfatase required for breakdown of keratan sulfate and chondroitin 6-sulfate glycosaminoglycans.
α -galactosidase A (<i>GLA</i>)	Removes terminal α -galactose residues from glycolipids and glycoproteins.
β -1-galactosidase (<i>GLB1</i>)	Enzyme that cleaves terminal beta-galactose from glycolipids, glycosaminoglycans and other glycoconjugates.
N-acetylglucosamine-6-sulfatase (<i>GNS</i>)	Enzyme involved in breakdown of glycosaminoglycans.
β -glucuronidase (<i>GUSB</i>)	Enzyme involved in breakdown of glycosaminoglycans.
Sialidase (neuraminidase) 1 (<i>NEU1</i>)	Enzyme that removes terminal sialic acid residues from glycoproteins and glycolipids.

Interestingly, genes FCMD/ FKTN and LARGE2 were found to be downregulated in the diabetic condition when compared to the non-diabetic condition and are involved in α -dystroglycan glycosylation and activity. We were unable to find many studies associating these enzymes and wound healing. However, dystroglycan is located in the basement membrane of the skin ²⁵², contains several glycosaminoglycan attachment sites ²⁵³, and remains stable in fibroblast extracellular matrix fibrils when bound to perlecan ²⁵². Alpha-dystroglycan is also modified by a unique O-mannose glycan that is synthesized by many enzymes including LARGE and LARGE2, two enzymes with dual xylosyltransferase and glucuronyltransferase activity ²⁵⁴ and FCMD/ FKTN ²⁵⁵. FCMD/ FKTN is involved in the transfer of ribitol 5-phosphate to α -dystroglycan via CDP sugar nucleotides and initiates elongation of the mannose 3 core (M3). This O-mannose glycan is essential for α -dystroglycan's mediated interaction with extracellular matrix ²⁵⁵. Previous studies observed S91 cancer cells with altered α -dystroglycan glycosylation demonstrate decreased laminin binding and cell migration ²⁵⁶. Furthermore, α -dystroglycan mediated reductions in laminin binding and cell migration would be expected to impair skin integrity and cutaneous wound healing. Interestingly, B4GALNT3 which transfers GalNAc onto a GlcNAc residue to form the GalNAc β 1-4GlcNAc (LacdiNAc) structure on N- and O-glycans, is also important for α -dystroglycan function and demonstrated increased expression in human diabetic foot ulcers when compared to intact skin (REF). Differential regulation of genes related to α -dystroglycan glycosylation were observed in the mouse and human data which warrants further investigation regarding the role that α -dystroglycan glycosylation plays in diabetic skin homeostasis and wound healing.

The expression of polysialyltransferase, ST8SialV, encoded by the *ST8SIA4* gene, stood alone outside of any clustered gene pathway in the study described in this chapter. However, the study described in Chapter 5 showed that tissues demonstrating an impaired healing phenotype (the skin when compared to the tongue) demonstrated increased expression of genes encoding polysialyltransferase activity, *ST8SIA2* and *ST8SIA4*, and increased protein polysialylation during the proliferative/ late inflammatory phase of wound healing. While comparisons of skin and tongue did not identify any statistically significant differences in the expression of polySia, examining additional timepoints would likely implicate the day of peak *ST8SIA2* and *ST8SIA4* expression as important regulators for protein polysialylation. Because of this, a short screen of polySia expression was observed in diabetic and non- diabetic skin and wounds 1, 3, and 10 days post- wounding (Figure 63, Appendix C, n=1). PolySia was upregulated in the non- diabetic skin 1- day post wounding and diminished by day 3. Diabetic skin demonstrated delayed upregulation of polySia with no visible 12F8 staining observed until 3 days post wounding. Additionally, diabetic skin demonstrated continued polySia expression through day 10 despite the signal being decreased. While replicate experiments were not able to be completed, it was observed that *ST8SIA4* gene expression is likely associated with protein polysialylation. Overall this data combined demonstrates an association between highly impaired healing phenotypes (diabetes and skin when compared to tongue) and increased *ST8SIA2/4* gene expression. Considering the role that polySia plays in mediating the transition of bone marrow derived monocytes to peripheral monocytes and in increasing cell migration, it would be interesting to assess the role that polysialic acid plays in wound repair.

Differential expression of glycosylation- related genes were also observe in human diabetic foot ulcers when compared to uninjured skin obtained from non-diabetic and diabetic subjects. When comparing these differentially expressed genes to another human dataset of uninjured non- diabetic and diabetic skin, it was found that the fold-change and statistical significance was lower when examining foot skin alone. This suggests that the differentially expressed glycogenes were implicated in wound healing. Though the FC and significance were lower in the uninjured non-diabetic and diabetic foot skin data, it doesn't rule out the potential that inherent differences in glycosylation-related gene expression may exist between diabetic and non- diabetic skin. In fact, the human dataset supported some of our prior findings related to the differential expression of genes that encoded N- and O- glycans. Some of these genes included those that encode asparagine-linked glycosylation 13 (*ALG13*), asparagine-linked glycosylation 8 (*ALG8*), and asparagine-linked glycosylation 6 (*ALG6*) which are required for the synthesis of N- linked glycans processed in the dolichol-linked oligosaccharide pathway. Interestingly, *ALG13* which adds the second of two GlcNAcs during the second step of the dolichol-linked oligosaccharide pathway and *ALG8* which adds the second of 3 glucoses during the fifteenth step of the dolichol-linked oligosaccharide pathway demonstrated minimal to slightly increased expression in uninjured, diabetic skin compared to non- diabetic skin. However, *ALG13* and *ALG8* were significantly downregulated between uninjured skin and diabetic wounds. This finding was consistent with the expression pattern of *ALG6* in the mouse data. The Alg6 enzyme adds the first of 3 glucoses during the fifteenth step of the dolichol-linked oligosaccharide pathway. In our db/db mouse model *ALG6* demonstrated increased

expression in the diabetic condition when compared to the non- diabetic condition and decreased expression in wounds during the inflammatory phase of healing when compared to uninjured skin. This data together suggests enzymes within the dolichol-linked oligosaccharide pathway are differentially expressed between the diabetic and non- diabetic condition, in *in-vivo* models of wound healing, and clinically in human diabetic foot wounds. Furthermore, the in- vivo model of diabetic and non- diabetic wound healing identified that *ALG6* was downregulated during the inflammatory phase of wound healing. This would be expected to decrease the synthesis of N- linked glycans during the inflammatory phase of wound healing. Loss of N- glycosylation induces endoplasmic reticulum (ER) stress, glycogen synthase kinase 3 beta (GSK3 β) activation, increases apoptosis, and inhibits Akt signaling to VEGFR2 which has the potential to prevent new capillary formation ²⁵⁷ all of which are critical, yet time dependent, changes that are necessary for wound healing.

One gene observed in the human diabetic foot ulcer data set involved in O- glycan biosynthesis included *MGEA5* which encodes O-GlcNAcase. The O-GlcNAcase enzyme removes GlcNAc from serine and threonine residues from key structural and signaling proteins in the cytoplasm and nucleus ²⁵⁸. Though interesting, it would be of more interest to identify other types of O-glycans that are differentially regulated, as previous studies related to diabetes and O-glycans have mainly focused on this reversible nuclear/cytoplasmic O-GlcNAcylation process ¹⁵⁷.

Genes encoding proteins involved in the synthesis of O- glycan biosynthesis, blood antigen glycans, and poly-N-acetyllactosamines were also differentially expressed in diabetes and/ or during wound healing. These genes included *GALNT15*, *B3GNT2*,

B3GNT3, *B3GNT9*, *B4GALNT2*, and *B3GALT3/B3GALNT1*. While the role of these molecules in wound healing is not yet known, blood antigen and poly-N-acetyllactosamine structures are part of selectin glycan ligands- molecules which are important for mediating the marginalization of leukocytes during the inflammatory phase of healing. Interestingly, neutrophil and leukocyte homing have been suggested to contribute to the delayed yet prolonged inflammatory phase of wound healing that occurs in diabetic wounds ²⁵⁹, and has been heavily implicated throughout this analysis. Together, our data provides evidence that glycosylation- related gene expression may be likely to be an important biomarker in human wounds. These markers appear to be largely related to the regulation of leukocytes during the inflammatory phase of healing. Like the advances in biomarker identification that have occurred in the field of cancer, future studies in humans might successfully identify glycosylation- related genes that can act as prognostic markers for wound healing and wound associated mortality.

4 DISEASE SPECIFIC GLYCOSYLATION DURING DIABETIC AND NON-DIABETIC WOUND HEALING- GLYCOMICS ANALYSIS

4.1 Introduction

Diabetic wounds demonstrated deficits in wound healing and dysregulation of glycosylation- related genes was observed in the glycotranscriptomics analysis. While many of these changes were associated with glycosaminoglycan metabolism, a number of genes related to N- and O- linked glycosylation were also differentially regulated in diabetic mouse wound healing and in the human microarray analysis of diabetic foot ulcers. These genes included those which encode asparagine-linked glycosylation glycosyltransferases (*ALG6*, *ALG8*, *ALG13*), mannosidases (*MANEA*, *MAN1C1*), UDP-N-acetyl-alpha-D-galactosamine:polypeptide N-acetylgalactosaminyltransferase (*GALNT6*), and UDP-GlcNAc:betaGal beta-1,3-N-acetylglucosaminyltransferase (*B3GNT2*). The following findings were observed:

1. Genes encoding enzymes involved in lipid linked oligosaccharide (LLO) N-glycan biosynthesis (*ALG6*, *ALG8*, *ALG13*) were:
 - a. Upregulated in *db/db* mouse diabetic skin (*ALG6*) and un-changed in human diabetic skin (*ALG8*, *ALG13*) when compared to non- diabetic skin.
 - b. Downregulated in wounds when compared to uninjured skin in both datasets.
2. Genes encoding enzymes involved in trimming of high mannose N- glycan structures from Man9 to Man8 (*MANEA*) were:

- a. Upregulated in *db/db* mouse diabetic skin but demonstrated a trend for downregulation in human diabetic skin when compared non- diabetic skin.
 - b. Downregulated in wounds when compared to uninjured skin in both datasets.
- 3. Genes encoding enzymes involved in trimming of high mannose N- glycan structures from Man8 to Man5 (*MAN1C1*) demonstrated:
 - a. A trend for downregulation in diabetic skin when compared to non-diabetic skin in both data sets
 - b. A trend for upregulation in mouse wounds and significant downregulation in human diabetic foot wounds when compared to uninjured skin.
- 4. Genes which encode enzymes involved in O- glycan biosynthesis (*GALNT6*) and elongation (*B3GNT2*) demonstrated:
 - a. Upregulation in *db/db* mouse diabetic skin and a trend for upregulation in human diabetic foot skin when compared to the non- diabetic skin
 - b. Significant upregulation in wounds when compared to uninjured skin in both datasets.

Impaired fucosylation and sialylation were also implied in our previous analysis.

The following findings were observed:

- 1. Genes encoding enzymes responsible for the biosynthesis of terminal α 1,2- fucosylation demonstrated:

- a. Significantly decreased expression in diabetic mice (FUT1, FUT2) when compared to non- diabetic mice.
 - b. Significantly decreased expression in diabetic and non- diabetic wounds when compared to uninjured skin
- 2. Genes encoding enzymes responsible for the biosynthesis of core α 1,6- fucosylation (FUT8) demonstrated:
 - a. A trend for decreased expression in diabetic mice and human diabetic foot skin when compared to non-diabetic skin.
 - b. A trend for decreased expression in diabetic mouse wounds with significantly decreased expression noted in diabetic foot ulcers when compared to uninjured skin.

Furthermore, genes encoding enzymes that remove α 1,6-fucose (FUCA) from glycans were upregulated in diabetic mice and during wound healing. Together this data suggests diabetes and wounds exhibit decreased α 1,2- and α 1,6- fucosylation.

Interestingly this is similar to what has been reported in models of acutely enhanced inflammation ⁹⁷, but opposite of that which has been previously observed in diabetes ¹⁵⁴.

When examining genes that encode the transfer of sialic acids onto glycan moieties, only those involved in α 2,6-, and α 2,8- sialylation were differentially regulated and these changes were only observed in the mouse model. The following findings were observed:

- 1. Genes encoding α 2,8- polysialyltransferases were:
 - a. Upregulated in the diabetic mice when compared to the non- diabetic mice (ST8SIA4).

- b. Upregulated in mouse wounds when compared to uninjured skin (ST8SIA2).
- 2. Genes leading to the expression of α 2,8 sialic acids via ST8SIA1 were:
 - a. Downregulated in non-diabetic and diabetic wounds when compared to uninjured skin, but remained downregulated in diabetic wounds 10 days post- wounding.
- 3. Genes encoding enzymes responsible for the addition of α 2,6- sialic acids were:
 - a. Upregulated in non- diabetic wounds 10- days post- wounding, but not diabetic wounds, when compared to uninjured skin.

Together this suggests there may be some linkage specific differences in the regulation of sialic acids during wound healing. This is similar to what was observed in Chapter 2 and aligns with what has been previously observed in diabetic rat endothelial cells ¹⁵⁴.

To identify whether differential glycosylation- related gene expression correlated with downstream changes in glycoprotein glycosylation, N- and O- linked glycans were identified using mass spectroscopy. This glycomics profiling was performed on diabetic and non-diabetic skin and wounds during the hemostasis/early inflammatory, inflammatory, and proliferative phases of wound healing.

4.2 Materials and Methods

4.2.1 Animal Wound Models

All animal work was approved by the Institutional Animal Care and Use Committee (IACUC) at the University of Illinois at Chicago and conducted according to the recommendations of the Guide for the Care and the Use of Laboratory Animals.

Seven-week-old female Lepr^{db/db} and C57BL/6J mice, were purchased from Jackson Laboratories (Bar Harbor, ME), housed in groups of five at 22 to 24°C on a 12-h:12-h light/dark cycle, and allowed to habituate for a minimum of 1 week. All mice were fed a standard chow *ad libitum*.

Following the habituation period mice were subjected to wounding as previously described. Briefly, each mouse was anesthetized with ketamine (100mg/kg) and xylazine (5 mg/kg). Four, five-millimeter excisional skin wounds were produced via punch biopsy (Acu-Punch, Acuderm Inc., Ft. Lauderdale, FL) on the dorsal surface of each mouse. The tissue removed by the injury procedure was used as baseline, uninjured skin control.

Following euthanasia, wound samples (n=3) were obtained as previously described at baseline and Days 1, 3, 10, and Day 21 post wounding. One sample was frozen and stored at -80 °C for protein analysis and 3 samples were snap frozen in liquid nitrogen and shipped on dry ice to the Beth Israel Deaconess Medical Center-National Center of Functional Glycomics, Glycomics Core directed by Dr. Sylvain Lehoux for the mass spectroscopy glycomics assessment.

4.2.2 Description of Glycomics Analysis Performed by the Glycomics Core

4.2.2.1 Protein Sample Preparation

Tissues were lysed via ice-cold lysis buffer: 25 mM TRIS, 150 mM NaCl, 5 mM EDTA and 0.5% (w/v) CHAPS, pH 7.4 and sonication. Samples were then dialyzed (1 and 5 kDa) against 50 mM ammonium bicarbonate at 4°C for 16h-24h and were subject to lyophilization.

4.2.2.2 Trypsin and PNGase Digestion

Lyophilized samples were resuspended in 2 mg/ml solution of 1,4-dithiothreitol (DTT) in 0.6 M TRIS buffer pH 8.5 and incubated at 50°C for 1.5 hours. One- milliliter of 12 mg/ml iodoacetamide (IAA) solution was added and incubated at RT in the dark for 1.5 hours. The samples were dialyzed against 50 mM ammonium bicarbonate and then incubated in 1 ml of a 500 µg/ml solution of TPCK-treated trypsin in 50 mM ammonium bicarbonate and incubated overnight (12-16h) at 37°C. Two drops of 5% acetic acid were added to stop the reaction.

Trypsin-digested samples were loaded onto a C18 column to capture peptides. The column was washed in 5% acetic acid and peptides were eluted sequentially with 20% 1-propanol, 40% 1-propanol, and 100% 1-propanol. Eluted fractions were then pooled and subject to lyophilization.

Lyophilized samples were resuspended in 50 mM ammonium bicarbonate and 3µl of PNGaseF (New England Biolabs, #P0704) and incubated at 37°C for 4h. An additional 5µl of PNGaseF was then added and incubated overnight (12-16h) at 37°C. Two drops of 5% acetic acid were added to stop the reaction and the PNGaseF-digested samples were again loaded onto a C18 column to separate the tissue N-glycans from the respective peptides. The flow through and wash fractions were then pooled and subject to lyophilization.

4.2.2.3 β Elimination of O- Linked Glycans

N- glycan free glycopeptides were incubated in 400µL borohydride solution at 45°C overnight (14-16 hours). The reaction was terminated with 4-6 drops of 100%

acetic acid. Samples were then loaded onto a desalting column containing Dowex resin. The column was washed with 5% acetic acid and the flow through and wash were collected and lyophilized. The lyophilized samples were then co-evaporated in a 1:9 solution of acetic acid: methanol under a stream of nitrogen and resuspend in 200µL of 50% methanol. Following resuspension, samples were loaded onto a C18 column and washed with 5% acetic acid. The flow through and wash fractions were then pooled and subject to lyophilization.

4.2.2.4 Permethylation of N- and O- Linked Glycans

Samples were then permethylated as previously described²⁶⁰⁻²⁶². Briefly, samples were incubated at RT while shaking in NaOH/DMSO solution and Iodomethane for 30 minutes. Chloroform and MilliQ water were added and the sample was vortexed and centrifuged at 5000rpm for 20s. The aqueous phase was then discarded. After 2 additional washes in MilliQ water, the chloroform fraction was dried via SpeedVac for 20-30 minute. The sample was then resuspended in 15% acetonitrile and loaded onto a C18 column. Samples were then eluted with 50% acetonitrile and the eluted fraction was subject to lyophilization.

4.2.2.5 MALDI-TOF MS Analysis of Permethylated N- and O- Glycans

The eluted, permethylated, and lyophilized glycan fractions were resuspended in a matrix containing 10 µL of 75% methanol containing 1 µL of 10 mg/mL 2,5-dihydrobenzoic acid (DHB). The UltraFlex II MALDI-TOF mass spectrometer (Bruker) was used for spectral analysis in reflectron positive ion mode with at least 20000 laser

shots acquired and accumulated per sample over a mass range of 500–6000 Da for N-glycans and 500–2000 Da for O-glycans. Spectra were processed using mMass ²⁶³.

Glycan structures were assigned both manually and with the help of GlycoWorkbench

264-265.

4.2.3 Statistical Analysis

To identify whether there were statistically significant differences in the relative percent abundance of N- and O- linked glycans during diabetic and non-diabetic wound healing, a 2-way ANOVA was used to compare the *condition* versus the polynomial representation of the *time post-wounding*. p-values were adjusted for false discovery using the Benjamini Hochberg method ¹⁸⁵.

4.3 Results

4.3.1 Diabetic and Non- Diabetic Skin and Wounds Demonstrate Differential N-Linked Glycosylation

MALDI MS glycan profiling was used to determine whether N- and O- linked glycosylation was different in diabetic (DM) versus non- diabetic uninjured skin and wounds 1, 3, and 10 days post wounding. MALDI MS glycan profiling is commonly referred to as a semi-quantitative method. While the patterns are very reproducible for identical samples, it is common to observe a 20-30% variation in glycan intensities between biological replicates, as it is the case for many biological variables. As such, the N- and O- linked glycans were assessed via both quantitative and semi- quantitative methods.

N-glycan profiling was used to characterize the N-glycosylation of diabetic and non-diabetic skin and wounds. The N-glycan profile spectra of each uninjured diabetic and non-diabetic skin sample in Figure 42 highlights the variability of N- glycan coverage between replicates, however, magnification of this spectra (Figure 43) also demonstrates that semi-quantitative differences can be identified when the level of expression between different conditions is consistent across each respective group. In Figures 42 and 43, the glycans highlighted by the red vertical bar demonstrate changes in glycan abundance over the course of diabetic and/or non-diabetic wound healing, whereas the yellow vertical bar highlights glycans whose abundance is differentially expressed between the diabetic and non- diabetic condition. Each individual glycan, represented by its mass- to-charge ratio (m/z), was analyzed for statistical significance. Comparisons were also made by examining the global glycan changes by feature including glycan core type, core modifications, and capping monosaccharides (sialic acid, fucose). Core N- linked glycan structures were classified as: 1) High Mannose; 2) Precursor; 3) Complex; 4) Bisected; or 5) Hybrid. The criteria used to specify each core N- glycan structure is described in Table XII.

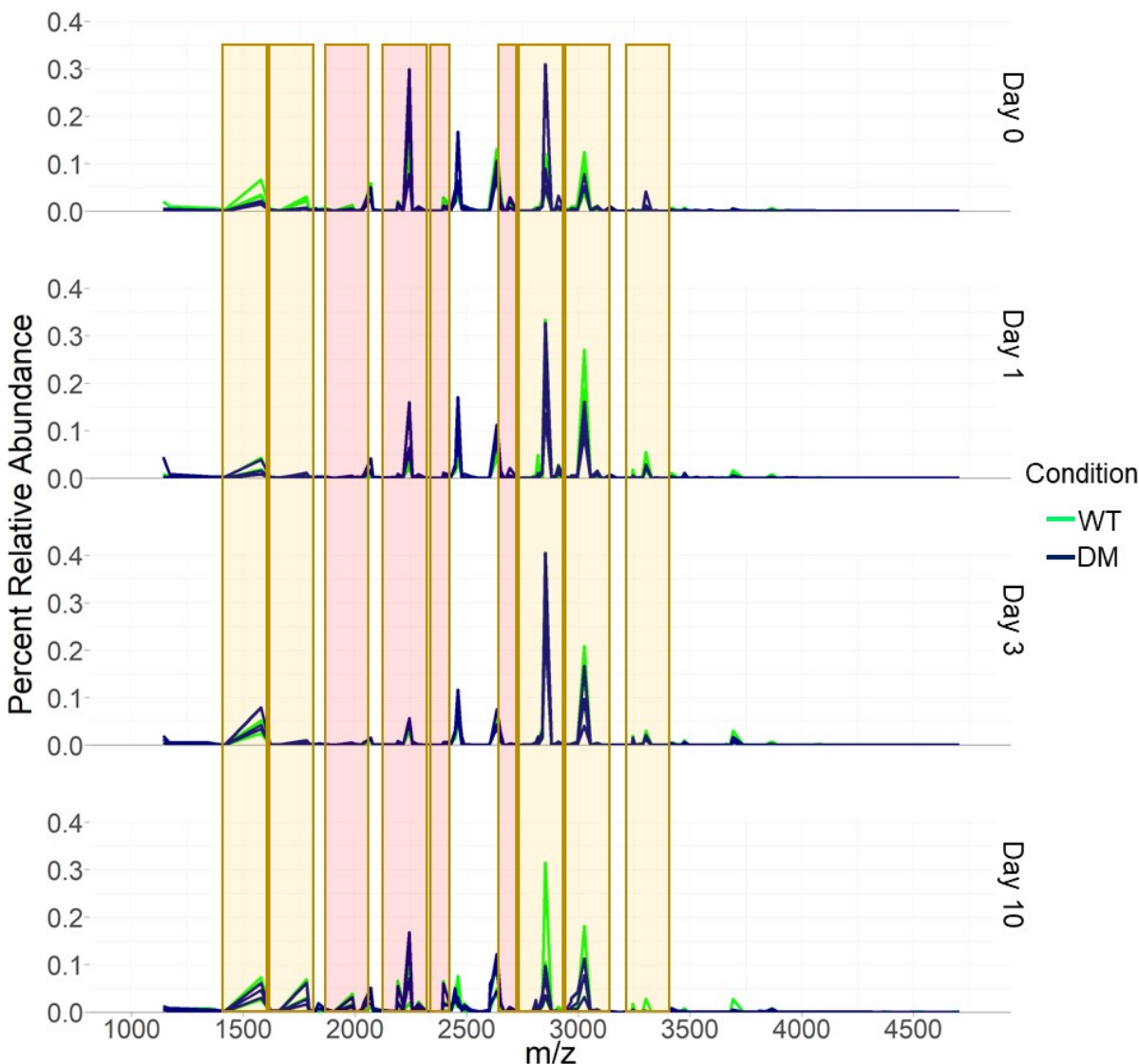


Figure 42. N-glycosylation profile of high abundance structures in uninjured skin and wounds obtained from diabetic and non- diabetic mice. Each glycan structure is represented by individual peaks and those with a relative percent abundance ≥ 0.025 represent high abundance glycans in non-diabetic (green) and diabetic (blue) skin and wounds. The percent relative abundance of each (peak) glycan structure changes between uninjured skin (Day 0, top panel) and each respective wound timepoint (panels 2-4). Additionally, an increased number of structures appear 10- days post- wounding (bottom panel) when compared to uninjured skin (Day 0, top panel).

red= m/z peaks changing over- time. Yellow= m/z peaks changing between diabetic (DM, green) and non- diabetic (WT, navy) conditions.

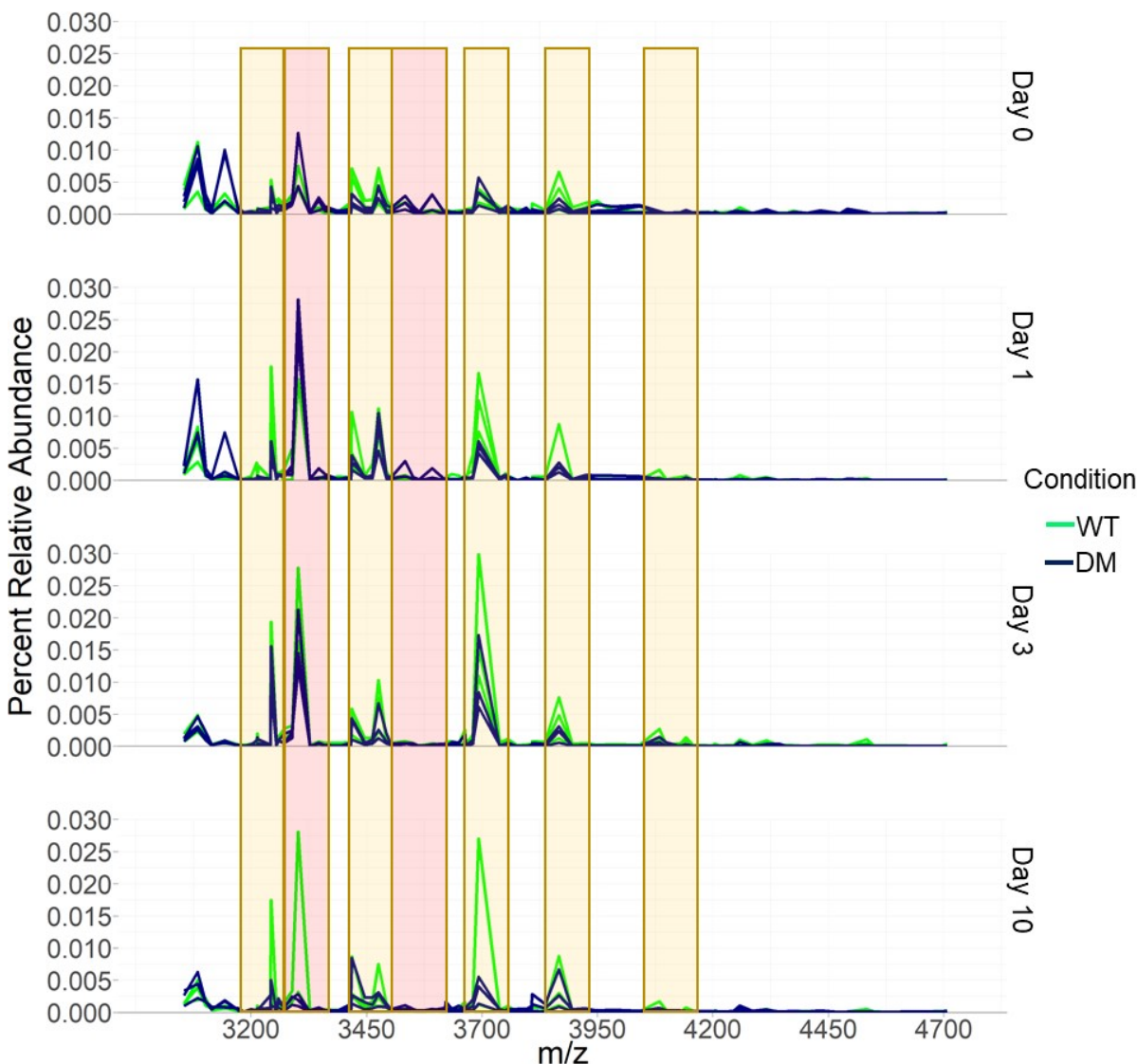


Figure 43. N-glycosylation profile of low abundance structures in uninjured skin and wounds obtained from diabetic and non- diabetic mice. Each glycan structure is represented by individual peaks and those with a relative percent abundance <0.025 represent low abundance glycans in non-diabetic (green) and diabetic (blue) skin and wounds. The percent relative abundance of each (peak) glycan structure changes between uninjured skin (Day 0, top panel) and each respective wound timepoint (panels 2-4). Additionally, an decreased number of N-glycan structures 10- days post- wounding (bottom panel) when compared to uninjured skin (Day 0, top panel).

red= m/z peaks changing over- time. Yellow= m/z peaks changing between diabetic (DM, green) and non- diabetic (WT, navy) conditions.

TABLE XII.
TABLE OF CRITERIA FOR EACH DEFINED N- GLYCAN CORE STRUCTURE.

N- Glycan Core Classification	Structural Composition
Precursor	Hex1-4HexNAc2, Hex10HexNAc2, Hex3HexNAc3
High Mannose	Hex4-10HexNAc2
Hybrid	$\Sigma(\text{Hex-HexNAc}) > 2$
Complex	$\Sigma(\text{Hex-HexNAc}) \leq 2$
Bisecting	HexNAc >5 , $\Sigma(\text{Hex-HexNAc}) \leq 2$
Mono- antennary	$\Sigma(\text{HexNAc}) \leq 3$
Di- antennary	$\Sigma(\text{Hex} = 5)$ and $(\text{HexNAc} = 4)$
Di/tri- antennary	$\Sigma(\text{Hex} \leq 5)$ and $(\text{HexNAc} = 5)$
Tri- antennary	$\Sigma(\text{Hex} = 6)$ and $(\text{HexNAc} = 5)$
Tri/tetra- antennary	$\Sigma(\text{Hex} \leq 6)$ and $(\text{HexNAc} = 6)$
Tetra- antennary	$\Sigma(\text{Hex} = 7)$ and $(\text{HexNAc} = 6)$
Tetra/poly- antennary	$\Sigma(\text{Hex} \leq 7)$ and $(\text{HexNAc} = 7)$
Poly- antennary	$\Sigma(\text{Hex} > 7)$ and $(\text{HexNAc} > 6)$

Core modifications and capping were determined based on the number of fucose and sialic acid residues. The absence of (0) fucose or sialic acid residues were termed non- fucosylated (0- Fuc) and non- sialylated (0- SA) respectively. Core fucose modifications were assumed in the presence of 1 fucose monosaccharide (1- Fuc). A single (1) sialic acid monosaccharide (NeuAc or NeuGc) was termed mono- sialylated (1- SA). Two fucose or sialic acids were termed di- fucosylated (2-Fuc) and di- sialylated (2- SA) respectively. Lastly, more than 2 fucose or sialic acids were termed tri-/ poly- fucosylated (3-Fuc, 4-Fuc) and tri-/ oligo-/ poly- sialylated (3-SA, ≥ 4 -SA), respectively. A table of each glycans composition and the respective core type can be found in Table XIII).

TABLE XIII.

TABLE OF N- LINKED GLYCAN DESCRIPTORS FOR EACH STRUCTURE AS INDICATED BY THE MASS- TO -CHARGE RATIO.

m/z	Composition	Core	# Fucose	# Sialic Acid	Charge
1141.6	Hex2HexNAc2Fuc1	Precursor	1	0	Neutral
1171.6	Hex3HexNAc2	Precursor	0	0	Neutral
1345.7	Hex3HexNAc2Fuc1	Precursor	1	0	Neutral
1375.7	Hex4HexNAc2	Precursor	0	0	Neutral
1416.8	Hex3HexNAc3	Precursor	0	0	Neutral
1579.9	Hex5HexNAc2	High Mannose	0	0	Neutral
1620.9	Hex4HexNAc3	Complex	0	0	Neutral
1661.9	Hex3HexNAc4	Complex	0	0	Neutral
1784.0	Hex6HexNAc2	High Mannose	0	0	Neutral
1795.0	Hex4HexNAc3Fuc1	Complex	1	0	Neutral
1825.0	Hex5HexNAc3	Complex	0	0	Neutral
1836.1	Hex3HexNAc4Fuc1	Complex	1	0	Neutral
1866.1	Hex4HexNAc4	Complex	0	0	Neutral
1907.1	Hex3HexNAc5	Bisected	0	0	Neutral
1988.1	Hex7HexNAc2	High Mannose	0	0	Neutral
1999.1	Hex5HexNAc3Fuc1	Hybrid	1	0	Neutral
2012.2	Hex4HexNAc3NeuGc1	Complex	0	1	Neutral
2029.2	Hex6HexNAc3	Hybrid	0	0	Neutral
2040.2	Hex4HexNAc4Fuc1	Complex	1	0	Neutral
2070.2	Hex5HexNAc4	Complex	0	0	Neutral
2081.2	Hex3HexNAc5Fuc1	Bisected	1	0	Neutral
2111.2	Hex4HexNAc5	Bisected	0	0	Neutral
2186.2	Hex5HexNAc3NeuAc1	Hybrid	0	1	Neutral
2192.2	Hex8HexNAc2	High Mannose	0	0	Neutral
2216.3	Hex5HexNAc3NeuGc1	Hybrid	0	1	Neutral
2244.3	Hex5HexNAc4Fuc1	Complex	1	0	Neutral
2257.3	Hex4HexNAc4NeuGc1	Complex	0	1	Neutral
2274.3	Hex6HexNAc4	Complex	0	0	Neutral
2285.3	Hex4HexNAc5Fuc1	Bisected	1	0	Neutral
2315.3	Hex5HexNAc5	Bisected	0	0	Neutral
2326.3	Hex3HexNAc6Fuc1	Complex	1	0	Neutral
2360.4	Hex5HexNAc3Fuc1NeuAc1	Complex	1	1	Neutral
2390.4	Hex6HexNAc3NeuAc1	Hybrid	0	1	Neutral
2396.4	Hex9HexNAc2	High Mannose	0	0	Neutral
2431.4	Hex5HexNAc4NeuAc1	Complex	0	1	Neutral
2448.4	Hex6HexNAc4Fuc1	Complex	1	0	Neutral
2461.4	Hex5HexNAc4NeuGc1	Complex	0	1	Neutral
2478.4	Hex7HexNAc4	Complex	0	0	Neutral
2489.4	Hex5HexNAc5Fuc1	Bisected	1	0	Neutral
2519.4	Hex6HexNAc5	Complex	0	0	Neutral

TABLE XIII. (continued)

TABLE OF N- LINKED GLYCAN DESCRIPTORS FOR EACH STRUCTURE AS INDICATED BY THE MASS- TO -CHARGE RATIO.

m/z	Composition	Core	# Fucose	# Sialic Acid	Charge
2560.5	Hex5HexNAc6	Complex	0	0	Neutral
2592.5	Hex5HexNAc4Fuc3	Complex	3	0	Charged
2600.5	Hex10HexNAc2	Precursor	0	0	Neutral
2605.5	Hex5HexNAc4Fuc1NeuAc1	Complex	1	1	Neutral
2635.5	Hex5HexNAc4Fuc1NeuGc1	Complex	1	1	Neutral
2652.5	Hex7HexNAc4Fuc1	Complex	1	0	Neutral
2665.5	Hex6HexNAc4NeuGc1	Complex	0	1	Neutral
2676.5	Hex5HexNAc5NeuAc1	Bisected	0	1	Neutral
2693.5	Hex6HexNAc5Fuc1	Complex	1	0	Neutral
2723.5	Hex7HexNAc5	Complex	0	0	Neutral
2734.6	Hex5HexNAc6Fuc1	Bisected	1	0	Neutral
2766.6	Hex5HexNAc4Fuc4	Complex	4	0	Charged
2792.6	Hex5HexNAc4Fuc1NeuAc2	Complex	1	2	Charged
2796.6	Hex6HexNAc4Fuc3	Complex	3	0	Charged
2809.6	Hex5HexNAc4Fuc2NeuGc1	Complex	2	1	Neutral
2820.6	Hex4HexNAc5Fuc2NeuAc1	Bisected	2	1	Neutral
2822.6	Hex5HexNAc4NeuAc1NeuGc1	Complex	0	2	Charged
2839.6	Hex6HexNAc4Fuc1NeuGc1	Complex	1	1	Neutral
2852.6	Hex5HexNAc4NeuGc2	Complex	0	2	Charged
2880.6	Hex6HexNAc5NeuAc1	Complex	0	1	Neutral
2897.7	Hex7HexNAc5Fuc1	Bisected	1	0	Neutral
2910.6	Hex6HexNAc5NeuGc1	Complex	0	1	Neutral
2938.7	Hex6HexNAc6Fuc1	Bisected	1	0	Neutral
2940.7	Hex5HexNAc4Fuc5	Bisected	5	0	Charged
2966.7	Hex5HexNAc4Fuc1NeuAc2	Complex	1	2	Charged
2968.7	Hex7HexNAc6	Complex	0	0	Neutral
2996.7	Hex5HexNAc4Fuc1NeuAc1NeuGc1	Complex	1	2	Charged
3026.7	Hex5HexNAc4Fuc1NeuGc2	Complex	1	2	Charged
3054.7	Hex6HexNAc5Fuc1NeuAc1	Complex	1	1	Neutral
3084.7	Hex6HexNAc5Fuc1NeuGc1	Complex	1	1	Neutral
3101.8	Hex8HexNAc5Fuc1	Complex	1	0	Neutral
3114.8	Hex7HexNAc5NeuGc1	Complex	0	1	Neutral
3142.8	Hex7HexNAc6Fuc1	Complex	1	0	Neutral
3172.8	Hex8HexNAc6	Complex	0	0	Neutral
3183.8	Hex6HexNAc7Fuc1	Bisected	1	0	Neutral
3200.8	Hex7HexNAc4NeuAc2	Hybrid	0	2	Charged
3211.8	Hex5HexNAc5Fuc1NeuAc2	Bisected	1	2	Charged
3213.8	Hex7HexNAc7	Bisected	0	0	Neutral
3215.8	Hex6HexNAc5Fuc4	Complex	4	0	Charged
3241.8	Hex6HexNAc5NeuAc2	Complex	0	2	Charged

TABLE XIII. (continued)

TABLE OF N- LINKED GLYCAN DESCRIPTORS FOR EACH STRUCTURE AS INDICATED BY THE MASS- TO -CHARGE RATIO.

m/z	Composition	Core	# Fucose	# Sialic Acid	Charge
3243.8	Hex5HexNAc4NeuGc3	Complex	0	3	Charged
3254.8	Hex6HexNAc8	Bisected	0	0	Neutral
3258.8	Hex6HexNAc5Fuc2NeuGc1	Complex	2	1	Neutral
3271.8	Hex6HexNAc5NeuAc1NeuGc1	Complex	0	2	Charged
3288.9	Hex7HexNAc5Fuc1NeuGc1	Complex	1	1	Neutral
3301.8	Hex6HexNAc5NeuGc2	Complex	0	2	Charged
3327.8	Hex5HexNAc4Fuc1NeuAc3	Complex	1	3	Charged
3329.8	Hex7HexNAc6NeuAc1	Complex	0	1	Neutral
3346.9	Hex8HexNAc6Fuc1	Complex	1	0	Neutral
3359.9	Hex7HexNAc6NeuGc1	Complex	0	1	Neutral
3387.9	Hex7HexNAc7Fuc1	Bisected	1	0	Neutral
3415.9	Hex6HexNAc5Fuc1NeuAc2	Complex	1	2	Charged
3417.9	Hex8HexNAc7	Complex	0	0	Neutral
3445.9	Hex6HexNAc5Fuc1NeuAc1NeuGc1	Complex	1	2	Charged
3462.9	Hex7HexNAc5Fuc2NeuGc1	Complex	2	1	Neutral
3475.9	Hex6HexNAc5Fuc1NeuGc2	Complex	1	2	Charged
3492.9	Hex8HexNAc5Fuc1NeuGc1	Complex	1	1	Neutral
3504.0	Hex7HexNAc6Fuc1NeuAc1	Complex	1	1	Neutral
3534.0	Hex7HexNAc6Fuc1NeuGc1	Complex	1	1	Neutral
3551.0	Hex9HexNAc6Fuc1	Complex	1	0	Neutral
3564.0	Hex8HexNAc6NeuGc1	Complex	0	1	Neutral
3592.0	Hex8HexNAc7Fuc1	Complex	1	0	Neutral
3620.0	Hex5HexNAc5Fuc3NeuGc2	Bisected	3	2	Charged
3622.0	Hex9HexNAc7	Complex	0	0	Neutral
3635.0	Hex6HexNAc6Fuc5	Bisected	5	0	Charged
3650.0	Hex6HexNAc5Fuc2NeuGc2	Complex	2	2	Charged
3663.0	Hex6HexNAc5NeuAc1NeuGc2	Complex	0	3	Charged
3665.0	Hex7HexNAc6Fuc4	Complex	4	0	Charged
3680.0	Hex7HexNAc5Fuc1NeuGc2	Complex	1	2	Charged
3693.0	Hex6HexNAc5NeuGc3	Complex	0	3	Charged
3738.1	Hex8HexNAc6Fuc1NeuGc1	Complex	1	1	Neutral
3751.1	Hex7HexNAc6NeuGc2	Complex	0	2	Charged
3755.1	Hex10HexNAc6Fuc1	Complex	1	0	Neutral
3777.1	Hex6HexNAc5Fuc1NeuAc3	Complex	1	3	Charged
3796.1	Hex9HexNAc7Fuc1	Complex	1	0	Neutral
3807.1	Hex6HexNAc5Fuc1NeuAc2NeuGc1	Complex	1	3	Charged
3809.1	Hex8HexNAc7NeuGc1	Complex	0	1	Neutral
3837.1	Hex8HexNAc8Fuc1	Bisected	1	0	Neutral
3867.1	Hex6HexNAc5Fuc1NeuGc3	Complex	1	3	Charged
3895.2	Hex7HexNAc6Fuc1NeuAc1NeuGc1	Complex	1	2	Charged

TABLE XIII. (continued)

TABLE OF N- LINKED GLYCAN DESCRIPTORS FOR EACH STRUCTURE AS INDICATED BY THE MASS- TO -CHARGE RATIO.

m/z	Composition	Core	# Fucose	# Sialic Acid	Charge
3925.2	Hex7HexNAc6Fuc1NeuGc2	Complex	1	2	Charged
3949.2	Hex7HexNAc10	Bisected	0	0	Neutral
3983.2	Hex8HexNAc7Fuc1NeuGc1	Complex	1	1	Neutral
4041.2	Hex9HexNAc8Fuc1	Complex	1	0	Neutral
4084.2	Hex6HexNAc5NeuGc4	Complex	0	4	Charged
4099.2	Hex7HexNAc6Fuc2NeuGc2	Complex	2	2	Charged
4129.3	Hex8HexNAc6Fuc1NeuGc2	Complex	1	2	Charged
4142.3	Hex7HexNAc6NeuGc3	Complex	0	3	Charged
4157.3	Hex8HexNAc7Fuc2NeuGc1	Complex	2	1	Neutral
4187.3	Hex9HexNAc7Fuc1NeuGc1	Complex	1	1	Neutral
4200.3	Hex7HexNAc6Fuc5NeuAc1	Complex	5	1	Charged
4204.3	Hex11HexNAc7Fuc1	Complex	1	0	Neutral
4215.3	Hex9HexNAc8Fuc2	Complex	2	0	Neutral
4226.3	Hex7HexNAc6Fuc1NeuAc3	Complex	1	3	Charged
4245.3	Hex10HexNAc8Fuc1	Complex	1	0	Neutral
4258.3	Hex9HexNAc8NeuGc1	Complex	0	1	Neutral
4286.4	Hex9HexNAc9Fuc1	Bisected	1	0	Neutral
4316.4	Hex7HexNAc6Fuc1NeuGc3	Complex	1	3	Charged
4344.4	Hex8HexNAc7Fuc1NeuAc1NeuGc1	Complex	1	2	Charged
4361.4	Hex9HexNAc7Fuc2NeuGc1	Complex	2	1	Neutral
4374.4	Hex8HexNAc7Fuc1NeuGc2	Complex	1	2	Charged
4402.5	Hex9HexNAc8Fuc1NeuAc1	Complex	1	1	Neutral
4432.4	Hex9HexNAc8Fuc1NeuGc1	Complex	1	1	Neutral
4475.5	Hex8HexNAc7Fuc4NeuAc1	Complex	4	1	Charged
4490.5	Hex10HexNAc9Fuc1	Complex	1	0	Neutral
4533.5	Hex7HexNAc6NeuGc4	Complex	0	4	Charged
4548.5	Hex8HexNAc7Fuc2NeuGc2	Complex	2	2	Charged
4578.5	Hex9HexNAc7Fuc1NeuAc1NeuGc1	Complex	1	2	Charged
4606.5	Hex9HexNAc7Fuc1NeuGc2	Complex	2	1	Neutral
4636.6	Hex10HexNAc8Fuc1NeuAc1	Complex	1	1	Neutral
4664.6	Hex10HexNAc9Fuc2	Complex	2	0	Neutral
4677.6	Hex10HexNAc9NeuAc1	Complex	0	1	Neutral
4694.6	Hex11HexNAc9Fuc1	Complex	1	0	Neutral
4707.6	Hex7HexNAc6Fuc1NeuGc4	Complex	1	4	Charged
4765.7	Hex8HexNAc7Fuc1NeuGc3	Complex	1	3	Charged
4793.6	Hex9HexNAc8Fuc1NeuAc1NeuGc1	Complex	1	2	Charged
4823.7	Hex9HexNAc8Fuc1NeuGc2	Complex	1	2	Charged
4851.7	Hex10HexNAc9Fuc1NeuAc1	Complex	1	1	Neutral
4881.7	Hex10HexNAc9Fuc1NeuGc1	Complex	1	1	Neutral
4924.7	Hex9HexNAc8Fuc4NeuAc1	Complex	4	1	Charged

TABLE XIII. (continued)

TABLE OF N- LINKED GLYCAN DESCRIPTORS FOR EACH STRUCTURE AS INDICATED BY THE MASS- TO -CHARGE RATIO.

m/z	Composition	Core	# Fucose	# Sialic Acid	Charge
4939.7	Hex11HexNAc10Fuc1	Complex	1	0	Neutral
5085.8	Hex11HexNAc9Fuc1NeuGc1	Complex	1	1	Neutral
5143.9	Hex12HexNAc10Fuc1	Complex	1	0	Neutral
5156.9	Hex8HexNAc7Fuc1NeuGc4	Complex	1	4	Charged
5214.9	Hex12HexNAc11	Complex	0	0	Neutral
5273.0	Hex10HexNAc9Fuc1NeuGc2	Complex	1	2	Charged
5300.9	Hex11HexNAc10Fuc1NeuAc1	Complex	1	1	Neutral
5331.0	Hex11HexNAc10Fuc1NeuGc1	Complex	1	1	Neutral
5389.1	Hex12HexNAc11Fuc1	Complex	1	0	Neutral
5593.2	Hex13HexNAc11Fuc1	Complex	1	0	Neutral
5606.1	Hex9HexNAc8Fuc1NeuGc4	Complex	1	4	Charged
5664.2	Hex13HexNAc12	Complex	0	0	Neutral
5722.2	Hex11HexNAc10Fuc1NeuGc2	Complex	1	2	Charged
5780.2	Hex12HexNAc11Fuc1NeuGc1	Complex	1	1	Neutral
5838.4	Hex13HexNAc12Fuc1	Complex	1	0	Neutral

When analyzed individually, by mass- to- charge ratio (m/z), no N- linked glycans were differentially regulated between the diabetic and non- diabetic conditions with the FDR cut-off of 0.1. However, prior to the FDR correction, glycans with m/z 2734.6, m/z 2938.7, m/z 3142.8, m/z 3243.8, m/z 3592, m/z 4041.2, m/z 4490.5, m/z 4939.7, and m/z 5389.1 achieved significance ($p \leq 0.05$) for differences between the diabetic and non-diabetic conditions. These glycans corresponded to bisected- core fucosylated (m/z 2734.6, m/z 2938.7), complex- core fucosylated (m/z 3142.8, m/z 3592, m/z 4041.2, m/z 4490.5, m/z 4939.7, m/z 5389.1), and complex- tri- sialylated N- glycan (m/z 3243.8) structures (Table XIII). Furthermore, the glycan demonstrating the most statistical significance between the diabetic and non-diabetic condition had a mass- to- charge ratio of m/z 2734.6 (Figure 44A). Both diabetic and non-diabetic skin significantly downregulated the expression of m/z 2734.6 during the inflammatory phase of wound

healing (Day 3) and remained somewhat downregulated 10 days post- wounding.

However, the diabetic skin demonstrated significantly less abundance of m/z 2734.6 during all timepoints when compared to the non- diabetic skin ($p= 0.016$; FDR= 0.192, $d=0.507$, 95% CI [-1.12, 2.13]; $v=0.69$). $d=0.8477$, CI [0.0124, 1.683], $v=0.1816$).

Additionally, the greatest deficit of ~3- fold occurred 1-day post- wounding (Figure 44A).

Previously observed glycans of this molecular weight are associated with

Hex5HexNAc6Fuc1 and mostly likely represents a core fucosylated, Gal-terminated bisected (tri- antennary) N- glycan ²⁶⁶(Figure 44B). Interestingly, the expression of *FUT8* which encodes the fucosyltransferase responsible for core fucosylation, was also similarly downregulated in the glycotranscriptomics analysis of diabetic and non- diabetic wounds, 3 days post- wounding (Figure 72D, Appendix D).

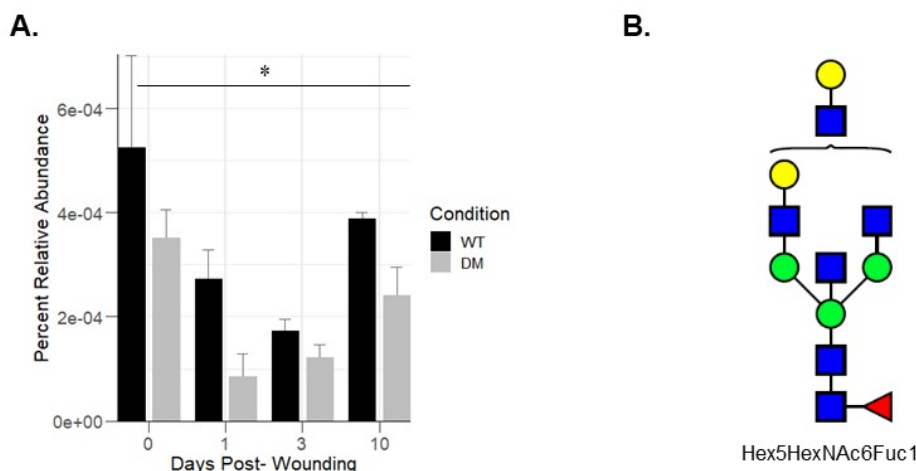


Figure 44. Expression of glycan m/z 2734.6 is downregulated during diabetic more than non-diabetic wound healing. Expression m/z 2734.6 is significantly reduced throughout the course of wound healing in diabetic skin (DM; grey) as compared to non- diabetic skin (WT; black) and is downregulated during wound healing in both (A). Glycan structure most likely representing m/z 2734.6 (B)
 * = statistically significant by between diabetic and non-diabetic conditions.

When examining the expression of all glycans based on their structural classification, structures described as poly-fucosylated, mono-sialylated complex N-glycans (biantennary) were identified. These structures described glycans with mass to charge ratios of m/z 4200.3, m/z 4475.5 and m/z 4924.7 and were composed of the following carbohydrates ($H_{\geq 7}N_{Hex-1}F_{\geq 4}S_1$): 1) Hexose ≥ 7 ; 2) N-acetylhexosamines = # of Hexose-1; 3) Fucose ≥ 4 ; and 4) Sialic acid =1. The cumulative sum of the abundance of these structures is graphed for each timepoint and condition in Figure 45. It was found that non- diabetic wounds downregulated the expression of $H_{\geq 7}N_{Hex-1}F_{\geq 4}S_1$ structures during the inflammatory phase of healing. Additionally, diabetic skin demonstrated increased expression of $H_{\geq 7}N_{Hex-1}F_{\geq 4}S_1$ when compared to uninjured, non- diabetic skin and non- diabetic wounds in the inflammatory phase healing (>2- fold). Furthermore, these structures are likely to represent fucosylated polylactosamines and the presence of a single sialic acid raises suspicion for these structures being sialyl Lewis structures. Interestingly previous analysis of human neutrophils identified m/z 4475.5 and m/z 4924.7 as glycans that occur in human neutrophils²⁶⁷. Additionally, m/z 4200.3 has been previously identified on glycophorin C, a transmembrane erythrocyte protein²⁶⁸ that has been associated with a poor prognosis for acute lymphoblastic leukemia²⁶⁹⁻²⁷⁰.

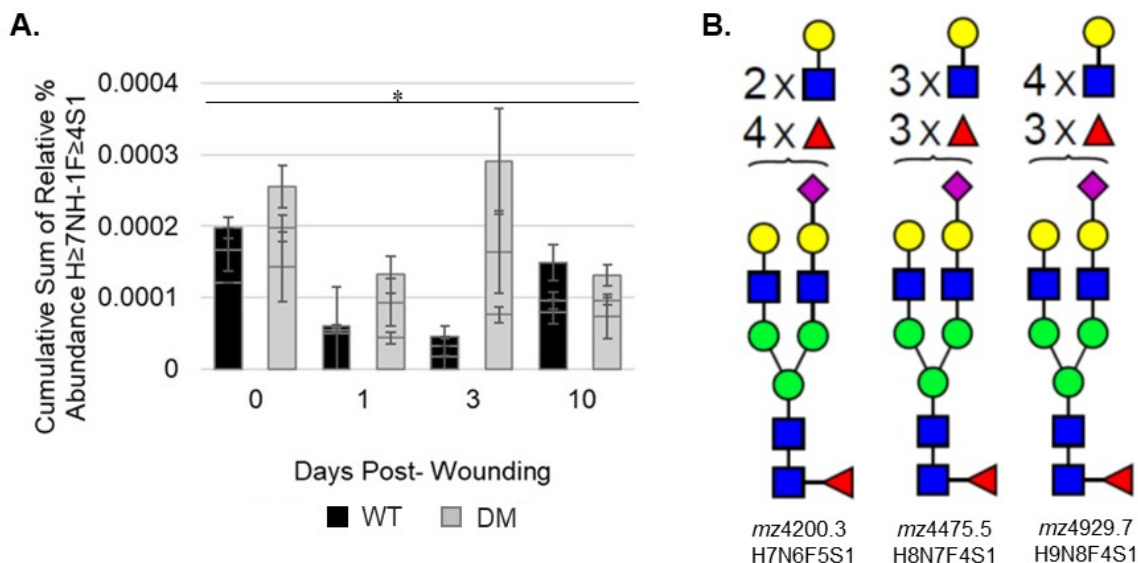


Figure 45. Expression of H₇NHex-1F₄S₁ structures is downregulated in wound healing and upregulated in the diabetic versus non- diabetic condition.

Expression of structures containing H₇NHex-1F₄S₁ are represented in uninjured skin and wounds 1-, 3-, and 10 days post- wounding in diabetic skin (DM; grey) and non-diabetic skin (WT; black) (A). N- glycan structures representing H₇NHex-1F₄S₁ N-glycans had molecular weights of *m/z*4200.3, *m/z* 4475.5, and *m/z* 4929.7 respectively (B, left to right).

* = statistically significant by between diabetic and non-diabetic conditions

Relevant changes in glycosylation and glycan features can be overlooked when assessing individual glycan structures, so profiling the glycans based on broad traits may be more useful when assessing overall glycan differences. When examined broadly by traits using semiquantitative methods, complex N- glycans are the most prevalent structure in both diabetic and non-diabetic skin and wounds, followed by high mannose> bisected>precursor> hybrid N- linked glycans (Figure 46A). In uninjured skin, high mannose and precursor N- linked glycans were 2.4 fold (11.6% versus 4.9%) and 3 fold (2.3% versus 0.76%) higher, respectively, in uninjured diabetic skin as compared to

non-diabetic skin (Figures 46A-B, 46D), however, precursor N-linked glycans were downregulated in diabetic wounds 1 day post-wounding (1.1%) when compared to non-diabetic wounds (2.5%) (Figure 46D). Furthermore, during wound healing, non-diabetic skin (WT) exhibited a trend towards increased expression of high mannose and precursor N glycan structures that remained upregulated through day 10, increasing from 4.9% and 0.76% (~5.6%) respectively at day 0 to 16.2% and 2.4% (18.6%) respectively at day 10 (Figure 46B). Interestingly, during diabetic wound healing (DM), there was a trend for decreased high mannose and precursor N-linked glycan structures 1-3 days post-wounding. The high mannose structures of diabetic wounds decreased from 11.6% on day 0 to 4% on day 1, then increased to ~19.5% by day 10. Similarly, the precursor structures of diabetic wounds decreased from 2.3% on day 0 to 1.1% on day 1, then increased to 2.7% by day 10. Lastly, when compared to the total population of precursor N-linked glycans, precursors with 1 fucose (likely core fucosylated) demonstrated increased relative abundance during wound healing in both diabetic and non-diabetic wounds (Figure 46C).

Overall, this data demonstrates that diabetic and non-diabetic skin exhibit significant differences in the overall production of precursor and high mannose N-linked glycans, however, they demonstrate no changes in the fucosylation of precursor N-linked glycan structures. Interestingly, the downregulation of precursor N-linked glycans during diabetic wound healing that was observed in this data, is consistent with the decreased expression of genes related to lipid linked oligosaccharide N-glycan precursor biosynthesis (ALG8, ALG13) that was observed in human diabetic foot ulcers when compared to uninjured foot skin.

N-glycan profiles of almost all diabetic and non-diabetic skin and wounds were composed of complex N-glycans that occupied over 73% of the total N-glycan abundance across all samples (range 57-95% all samples, 75-91% averaged replicates). The overall abundance of complex N-glycans remained relatively stable throughout wound healing. Non-diabetic wounds (WT) demonstrated no change to a slight decrease in complex N-glycans between 1-3 days post wounding, while diabetic wounds (DM) demonstrated a slight increase in complex N-glycans 1-3 days post wounding (Figure 46F). Furthermore, when examining the sialylation status of complex N-glycans, mono-sialylated, complex N-glycans remained relatively stable between all conditions and timepoints, ranging from 20 to 30% of the total complex N-glycans. The largest change occurred between the number of non-sialylated complex N-glycans and di-/tri-/tetra-sialylated complex N-glycans. Uninjured diabetic and non-diabetic skin demonstrated similar levels of complex, di- to tetra-sialylated glycans with ~29% coverage when examining all complex N-glycans (Figure 46E). During wound healing non-diabetic skin demonstrated increased di- to tetra-sialylation with 45% and 60% relative abundance at days 1 and 3 respectively (WT: Figure 46E). Diabetic skin demonstrated an immediate increase in di- to tetra-sialylation to ~65% at day 1 that did not change on day 3 (DM: Figure 46E). Furthermore, non-diabetic skin (WT) returned to its baseline, while diabetic skin remained 1.5x higher than its baseline 10 days post-wounding (Figure 46E). Overall, this data suggests that diabetic wounds demonstrate early di-, tri-, and tetra-sialylation of complex N-glycans during the early inflammatory phase of healing that is prolonged through the proliferative phase. Though the mass spectrometry methods used were unable to preserve polysialic acids (8+ sialic acids in

length), this data correlates with the increased expression of *ST8SIA2* and *ST8SIA4* that was observed in wounds when compared to unwounded skin and between the diabetic and non-diabetic condition respectively. Furthermore, previous studies have identified neural cell adhesion molecule (NCAM-1), SynCam 1, and Neuropilin 2 as protein targets for polySia addition, integrin $\alpha 5$ as a protein target for oligo-sialic acid addition, and glycoprotein (Gp), glycophorin, fetuin, adiponectin (ADIPOQ), $\alpha 2$ -macroglobulin, vitronectin, plasminogen, immunoglobulins (Ig), chromogranin, sodium channels, CD166 antigen (ALCAM), and IgLON family proteins as protein targets for di-sialic acid ¹⁴. Interestingly this short list of proteins carrying di-sialic, oligo-sialic acid, and polySia play distinct roles in hemostasis and the inflammatory and proliferative phases of wound healing and/ or play an important role in neurite outgrowth as discussed in the introduction ¹⁴.

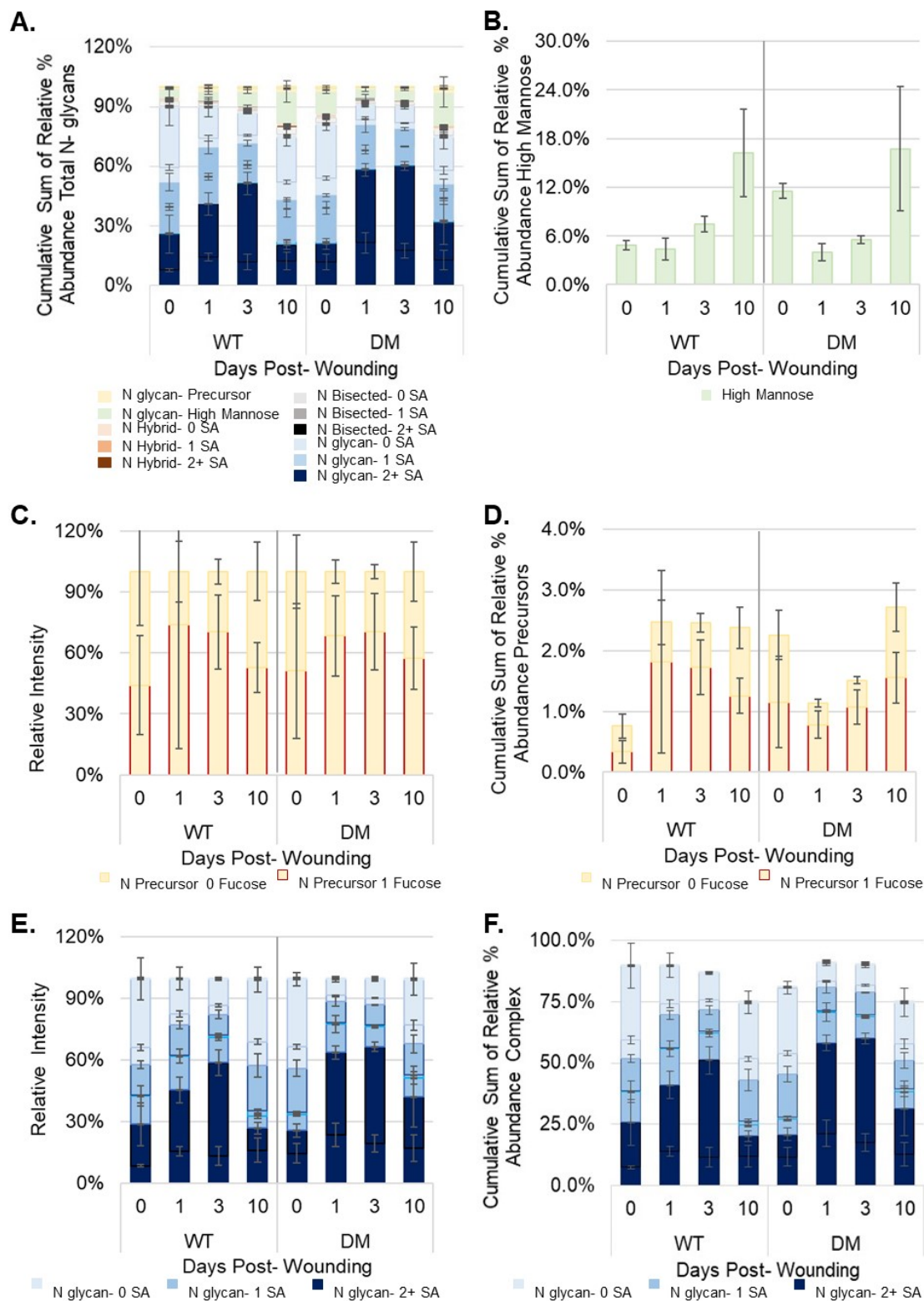


Figure 46. Comparison of N- glycan profiles in uninjured skin and wounds from diabetic and non- diabetic mice.

Figure 46. Comparison of N- glycan profiles in uninjured skin and wounds from diabetic and non- diabetic mice. N- glycan profiles of uninjured skin and wounds days 1-, 3-, and 10- post wounding in non-diabetic (left) and diabetic mice (right). The relative total intensity of each core glycan feature subtype was scaled to 100% of the total % abundance of each core glycan. The cumulative sum of the relative % abundance compared the total abundance of each core glycan feature across all N- glycan features. All N- glycans (A), represented by 100%, compared to high mannose glycans (B; green), precursors (C, D; yellow), and complex N- linked glycans alone (E, F; blue). Glycan feature subtypes: fucosylation (red outline); increasing sialylation represented by darker coloring.

Diabetic and non-diabetic skin and wounds also contained bisected N-glycans that occupied less than 10% of the abundance across all samples (range 1-6.8% all samples, 1.8- 6.8% averaged replicates). Both diabetic and non-diabetic skin downregulated the relative expression of bisecting N-glycans by ~2-fold over the inflammatory phase of wound healing (Day 1- 3) when compared to uninjured skin (Figure 47B). Mono- and di-sialylated bisecting N-glycans represented 10% of the total bisecting glycan coverage in uninjured non-diabetic (WT) skin, which increased to 20-40% between days 1-3 post-wounding. In uninjured, diabetic skin, 5% of the total bisecting glycan coverage consisted of mono- and di-sialylated bisecting N-glycans and this increased to 40-70% between days 1-3 post-wounding. This demonstrates that wounds in the inflammatory phases of healing reduce the expression of overall bisected glycans while preserving and perhaps increasing the expression of sialylated bisected N-glycans. Furthermore, diabetic wounds express more sialylated bisected N-glycans when compared to non-diabetic wounds during the inflammatory phase of healing.

Hybrid N-glycans composed the lowest amount of N-glycans within our sample set and accounted for less than 1.5% of the total glycan coverage. Overall, both diabetic and non-diabetic wounds downregulated the expression of hybrid N-glycans during the inflammatory phase of wound healing when compared to uninjured skin (Figures 47C-D).

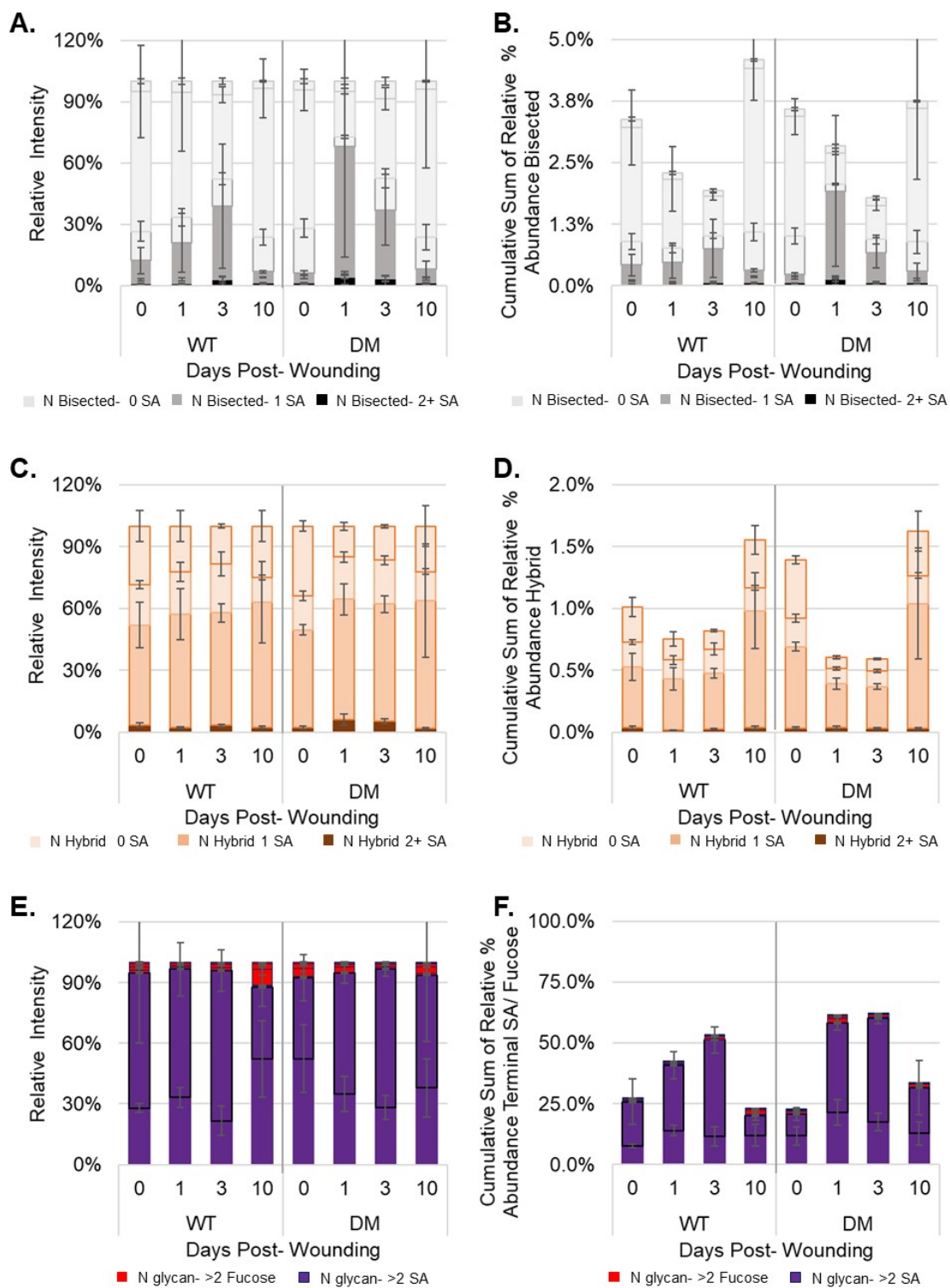


Figure 47. Comparison of N- glycan profiles in uninjured skin and wounds from diabetic and non- diabetic mice (continued).

Figure 47. Comparison of N- glycan profiles in uninjured skin and wounds from diabetic and non- diabetic mice (continued). N- glycan profiles of uninjured skin and wounds days 1-, 3-, and 10- post wounding in non-diabetic (left) and diabetic mice (right). The relative total intensity of each core glycan feature subtype was scaled to 100% of the total % abundance of each core glycan. The cumulative sum of the relative % abundance compared the total abundance of each core glycan feature across all N- glycan features. All N- glycans represented by 100%, compared to bisected glycans (A, B; grey), hybrid (C, D; orange), and any N- linked glycan containing more than 2 fucose (red) and/or more than 2 sialic acid (purple) (E, F).

Glycan feature subtypes: increasing sialylation represented by darker coloring.

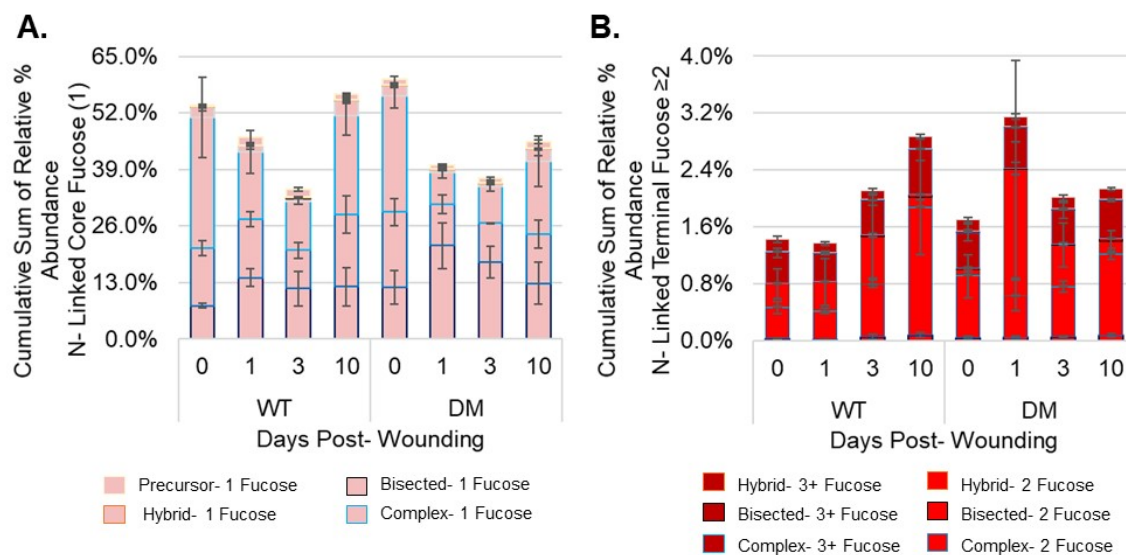


Figure 48. Comparison of N- glycan fucosylation in uninjured skin and wounds from diabetic and non- diabetic mice (continued). N- glycan fucosylation profiles of uninjured skin and wounds days 1-, 3-, and 10- post wounding in non-diabetic (left) and diabetic mice (right). The cumulative sum of the relative % abundance of core fucosylated glycans (1 fucose) (A) and glycans with terminal fucose (B) containing 2 (red) or more (burgundy) fucose residues

Terminal sialylation and fucosylation were also examined among glycans with 2 or more sialic acid residues versus 2 or more fucose residues. When comparing the overall sialic acid and fucose coverage across all sialylated and fucosylated N- linked glycans, both diabetic and non- diabetic skin and wounds demonstrated significantly more sialylation than fucosylation. When examined across all samples, sialic acids occupied over 89% of the glycan coverage when sialylated and fucosylated glycans are scaled to 100% (Figure 47E). Furthermore, the increased sialylation was consistent with the sialylation pattern of complex N- glycans which likely drove the observed differences. When examining fucosylated N- glycans alone, N- glycans carrying 1 fucose (likely core fucosylated) covered ~33-60% of the total N- glycan coverage

(Figure 48A), while those that are likely carrying terminal fucose monosaccharides (≥ 2) only accounted for 1.4-3.2%.

Interestingly, core fucosylated glycans were downregulated while terminally fucosylated glycans were upregulated during the inflammatory phase of healing (days 1-3) in both the diabetic and non-diabetic conditions. The decreased core fucosylation and increased terminal fucosylation occurred gradually in the non-diabetic condition, while the diabetic condition exhibited an immediate 21% decrease in core fucosylation and doubling of terminally fucosylated glycans 1-day post wounding. Furthermore, the upregulation of terminally fucosylated glycans continued through day 10 in the non-diabetic condition, however, diabetic wounds demonstrated downregulation in expression on days 3 and 10 when compared to day 1- post- wounding. Previous studies have identified that terminal fucoses play a role in blood group antigen, mediating host-microbe interactions, neural synapse formation and pathfinding, neurite outgrowth and migration, neurotransmitter release, lymphocyte homing, selectin dependent leukocyte adhesion to vascular endothelium, and hepatic vascular development. Interestingly core fucoses have been found to inhibit antibody mediated cellular toxicity and killing via NK cells and macrophages and are required for the function of TGF β 1 and α 3 β 1, as well as VEGF and EGF signaling. Downregulation of core fucoses during days 1-3 and upregulation by day 10 appears to align with decreased vascular and epidermal growth factor signaling during the acute inflammatory phase of healing, while progressive upregulation of terminal fucoses is consistent with leukocyte dependent adhesion during the inflammatory phase of healing from day 1-3 and neurite outgrowth during the proliferative phase of healing on day 10.

4.3.2 Diabetic and Non- Diabetic Skin and Wounds Demonstrate Differential Expression of High Mannose Structures.

Because the overall abundance of high mannose structures was so dynamically altered over the course of wound healing in diabetic and non- diabetic skin (Figure 46B), a closer examination of the regulation of these glycans was performed. High mannose (HM) structures were differentially regulated with time and condition specific differences as Man9 structures convert to Man5 structures. In non-diabetic skin, the abundance by number of mannose residues increases when structures change from Man9 to Man5. In non-diabetic skin, as wounds progress through hemostasis and inflammation (day 0- 3) structure-specific differences were noted: 1) Man8-9 structures are downregulated (Figures 49B-C); 2) Man6-7 structures are equal (Figures 49D-E); and 3) Man5 structures are upregulated (Figure 49F). In contrast, diabetic skin exhibited a downregulation of all HM structures during the hemostasis and inflammatory phases of wound healing. Interestingly, MANEA which encodes an enzyme involved in the conversion of HM structures from 9Man to 8Man, was modestly increased over the course of wound healing and remained upregulated in the diabetic mice throughout all time points (Figure 49F). While increased MANEA would be expected to increase the abundance of HM structures with fewer mannose residues over the course of wound healing, this relationship doesn't explain why non-diabetic skin (WT) produced a higher abundance of 5Man structures 3 days post wounding (Figures 36B and 49F).

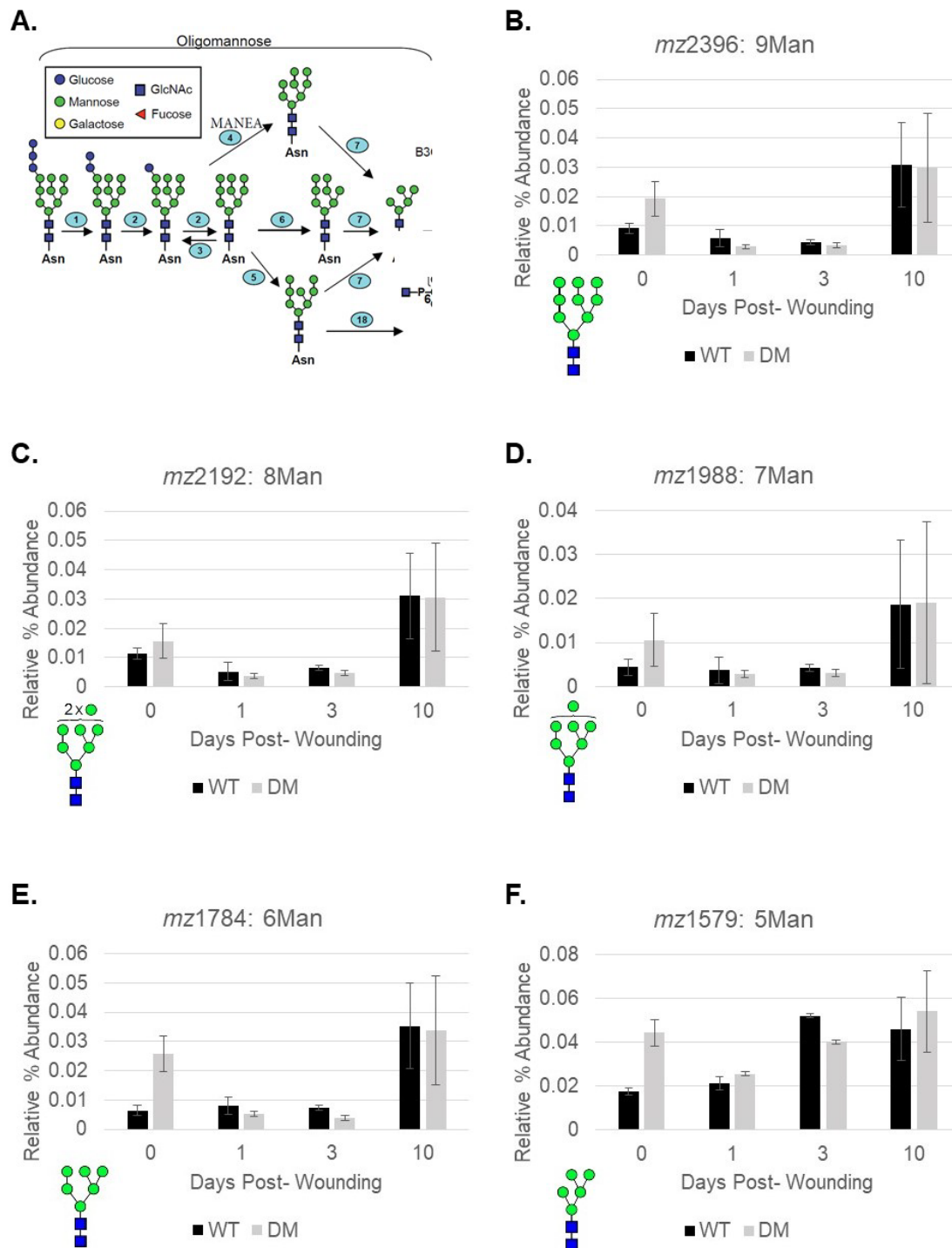


Figure 49. The relative expression of high/ oligo- mannose structures by mannose # is different in diabetic and non- diabetic skin and wounds. Diabetic wounds (DM; grey) 1-3 days- post wounding demonstrate downregulation of all high and oligo- structures in wound healing, while non-diabetic wounds (WT; black) downregulate high branching HM structures 9Man (B), 8Man (C), 7Man (D) progressive upregulation of the smaller structures 6Man (E) and 5Man (F).

4.3.3 Diabetic and Non- Diabetic Skin and Wounds Demonstrate Differential O-linked Glycosylation

When analyzed individually, by mass- to- charge ratio, 6 O-linked glycans were differentially regulated between diabetic and non- diabetic skin ($\text{FDR} < 0.1$). Glycans with a mass- to-charge ratio (m/z) of 779.5 (Figure 50A), achieved statistical significance ($\text{FDR} \leq 0.005$) for differences within the interaction of time post- wounding and the diabetic and non-diabetic conditions. Additionally, glycans m/z 1157.7 (Figure 51B), m/z 895.5, m/z 925.5 (sialyl T Antigen; Figure 51C), m/z 1374.8 (Figure 51D), and m/z 1473.8 (Figure 50B), achieved statistical significance ($\text{FDR} \leq 0.05$) for differences between the diabetic and non-diabetic conditions. Glycans with m/z 708.4 (Figure 51A), m/z 1286.7 (Figure 51E), and m/z 1766 (Figure 51F) are also included as they demonstrated significance by p- value, but not FDR (p- value ≤ 0.05 , $\text{FDR} > 0.1$). Overall these glycans corresponded to core 1 and core 2 fucosylated-, sialylated-, and disialylated- O- linked glycans in addition to 2 neutral core 2 structures with terminal GalNAc/GlcNAc residues. Interestingly, fucosylated core 1 and core 2 glycans demonstrated increased expression in the diabetic condition when compared to the non-diabetic condition (Figures 51A-B). Additionally, sialylated- core 1 and core 2 glycans demonstrate decreased expression in the diabetic condition as compared to the non- diabetic condition across most timepoints. Furthermore, the expression of fucosylated O- glycans is downregulated during the inflammatory phase of healing, while sialylated O- glycans are upregulated. Increased sialylation is consistent with what was observed in the N- linked glycomics profiling and suggests that these changes may not be a protein specific response.

TABLE XIV.

TABLE OF O- LINKED GLYCAN DESCRIPTORS FOR EACH STRUCTURE AS INDICATED BY THE MASS- TO -CHARGE RATIO.

m/z	Composition	Core	# Fucose	# Sialic Acid	# Sulfate	Charge
534.3	Hex1HexNAc1	Core1	0	0	0	Neutral
708.4	Hex1HexNAc1Fuc1	Core1	1	0	0	Neutral
779.5	Hex1HexNAc2	Core2	0	0	0	Neutral
895.5	Hex1HexNAc1NeuAc1	Core1	0	1	0	Charged
925.5	Hex1HexNAc1NeuGc1	Core1	0	1	0	Charged
983.6	Hex2HexNAc2	Core2	0	0	0	Neutral
1140.7	Hex1HexNAc2NeuAc1	Core2	0	1	0	Charged
1157.7	Hex2HexNAc2Fuc1	Core2	1	0	0	Neutral
1187.7	Hex3HexNAc2	Core2	0	0	0	Neutral
1228.7	Hex2HexNAc3	Core2	0	0	0	Neutral
1256.7	Hex1HexNAc1NeuAc2	Core1	0	2	0	Charged
1286.7	Hex1HexNAc1NeuAc1NeuGc1	Core1	0	2	0	Charged
1316.7	Hex1HexNAc1NeuGc2	Core1	0	2	0	Charged
1344.8	Hex2HexNAc2NeuAc1	Core2	0	1	0	Charged
1374.8	Hex2HexNAc2NeuGc1	Core2	0	1	0	Charged
1402.8	Hex2HexNAc3Fuc1	Core2	1	0	0	Neutral
1432.8	Hex3HexNAc3	Core2	0	0	0	Neutral
1473.8	Hex2HexNAc4	Core2	0	0	0	Neutral
1497.8	Hex3HexNAc3 + SO3	Core2	0	0	1	Charged
1548.9	Hex3HexNAc2NeuAc1	Core2	0	1	0	Charged
1578.9	Hex3HexNAcNeuGc1	Core2	0	1	0	Charged
1706.0	Hex2HexNAc2NeuAc2	Core2	0	2	0	Charged
1736.0	Hex2HexNAc2NeuAc1NeuGc1	Core2	0	2	0	Charged
1766.0	Hex2HexNAc2NeuGc2	Core2	0	2	0	Charged
1882.1	Hex4HexNAc4	Core2	0	0	0	Neutral

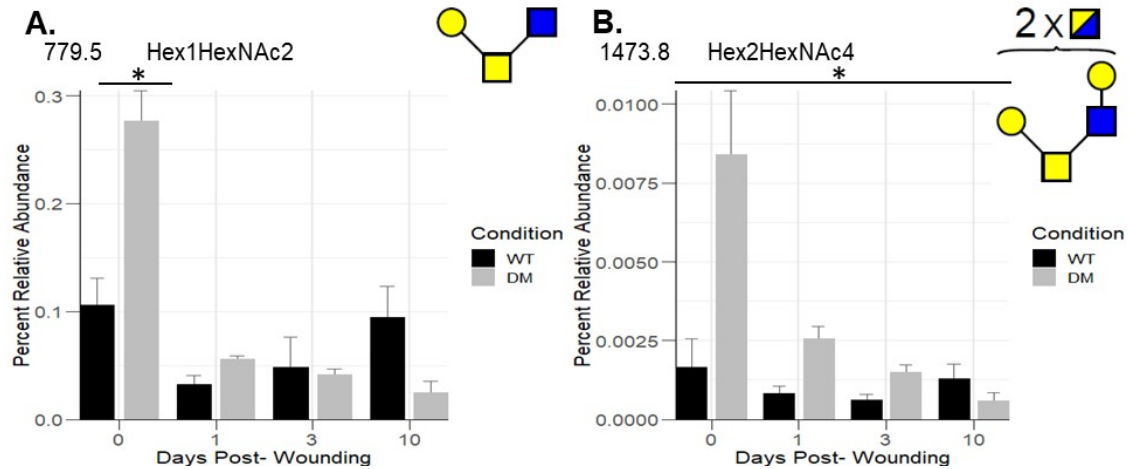


Figure 50. Neutral core 2 O- linked glycans are upregulated in uninjured skin and wounds when compared to non-diabetic samples. *m/z* 779.5 is significantly upregulated in uninjured diabetic skin (DM; grey) when compared to non- diabetic skin (WT; black) (A), while *m/z* 1473.8 is upregulated at baseline and throughout the course of wound healing in diabetic skin (DM; grey) as compared to non- diabetic skin (WT; black).

* = statistically significant by between diabetic and non-diabetic conditions

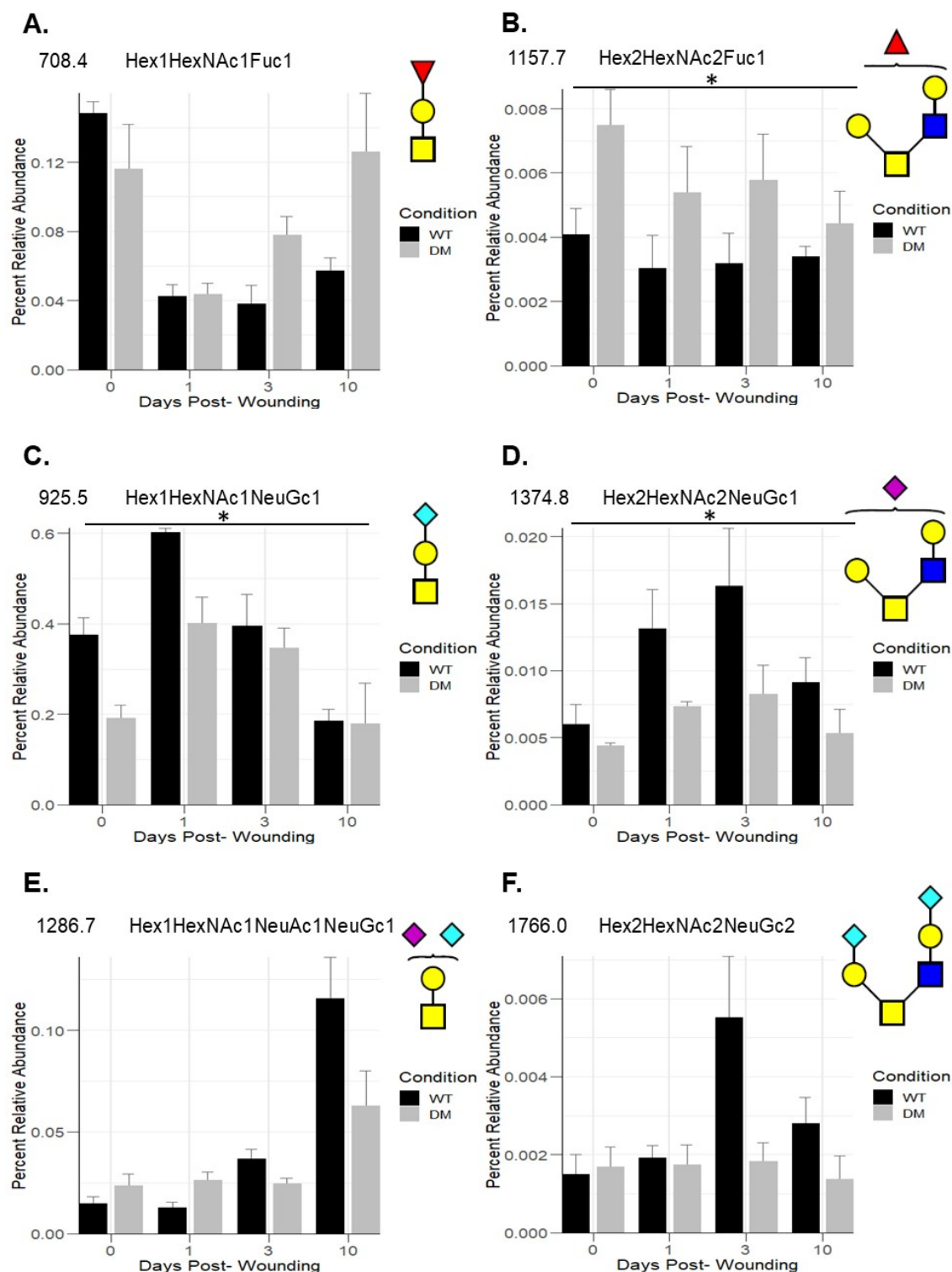


Figure 51. Increased fucosylation and decreased sialylation of core 1 & core 2 O-linked glycans in diabetic skin and wounds.

Figure 51. Increased fucosylation and decreased sialylation of core 1 & core 2 O-linked glycans in diabetic skin and wounds. Core 1 O- glycans (left) and core 2 glycans (right) levels are shown. Fucosylated structures m/z 708.4(A) and m/z 1157.7 (B) are upregulated in diabetic wounds (DM; grey) 3 and 10 days post wounding, while sialylated structures m/z 925.5 (C), m/z 1286.7 (D), m/z 1286.7 (E), and m/z 1766.0 (F) are downregulated in diabetic skin and wounds when compared to non- diabetic skin and wounds (WT; black) between 1- and 10- days post-wounding.

* = statistically significant by between diabetic and non-diabetic conditions

When examined by structural traits, as depicted in Figure 52A, core 1 O- glycans account for the greatest abundance in both diabetic and non-diabetic skin and wounds, accounting for approximately 80% of all O- glycans across all of the sample conditions/times (range 65-91%). There is a more complex interplay of glycans when assessing the O glycan data than the N- glycan data. Overall uninjured diabetic skin demonstrates 65% abundance of O- linked glycans likely represent core 1 structures, while non-diabetic skin exhibits 85% abundance (Figure 52D). While core 1 abundance remains relatively stable in non-diabetic wounds with 90%, 85%, and 80% abundance noted at days 1, 3, and 10 respectively, diabetic wounds demonstrate an initial increase in core 1 structures to 86% 1-day post wounding, that remains consistent through day 10 (Figure 52D). When examining the charge and sialic acid distribution across core 1 glycans, both uninjured diabetic and non-diabetic skin demonstrated the following distribution of structures: 1) ~10% neutral non fucosylated; 2) ~18% neutral and fucosylated; 3) 53-55% charged mono- sialylated; and 4) 15-18% charged di- sialylated core 1 O- glycans (Figure 52C). This distribution was not maintained during the wound healing process. Non-diabetic wounds, 1-day post- wounding, exhibited an increased abundance in charged, monosialylated glycans (76%), decreased neutral (5%) and neutral fucosylated (5%) core 1 glycans, and no change in charged, di- sialylated core 1 glycans (~12%). Diabetic wounds (DM) 1-day post wounding, demonstrated a similar reduction in neutral core 1 structures (5%), however, the abundance of monosialylated core 1 glycans only increased to ~63%, while the di-sialylated glycans increased to ~27%. Additional differences continued to be observed 3 days post- wounding with stable expression of neutral core 1 glycans, decreased monosialylated core 1 glycans

(60%), and increased disialylated core 1 glycans (30%) occurring in non-diabetic skin (Figures 52C-D). Furthermore, when examining core 2 glycans, uninjured diabetic skin demonstrated more than 2 times the amount of total core 2 glycans when compared to uninjured non-diabetic skin. This was primarily driven by increased expression of neutral core 2 glycans in uninjured diabetic skin (32%; Figure 52F) when compared to uninjured, nondiabetic skin (~13.5%, Figure 52F). Both diabetic and non-diabetic wounds downregulated the expression of total core 2 glycans 1-day post-wounding (13.5% and 8.2% respectively), however, diabetic wounds remained at ~13.5% while non-diabetic wounds increased the expression of core 2 glycans between days 3 and 10 post-wounding (~15.5% and ~18.5, respectively, Figure 52F). Reduced coverage by di-sialylated core 2 O-glycans was also observed in diabetic wounds (5%) as compared to non-diabetic wounds (10%) 3-days post-wounding (Figure 52E). Furthermore, disialylation of core 2 O-linked glycans remained upregulated in diabetic skin 10-days post-wounding (5%), while the non-diabetic skin began to return towards baseline (5%). Overall, we observed core 2 O-linked glycans increase progressively during the inflammatory phase between day 1 and day 3, while di-sialylated core 1 O-linked glycans are progressively increased through day 10 in non-diabetic wound healing. However, diabetic wounds exhibit an early, yet blunted response. Overall this suggests that increasing the number of sialic acid residues towards di-sialylation in core 1 and core 2 O-linked glycans during wound healing may be time dependent and that this process is blunted in diabetic wound healing.

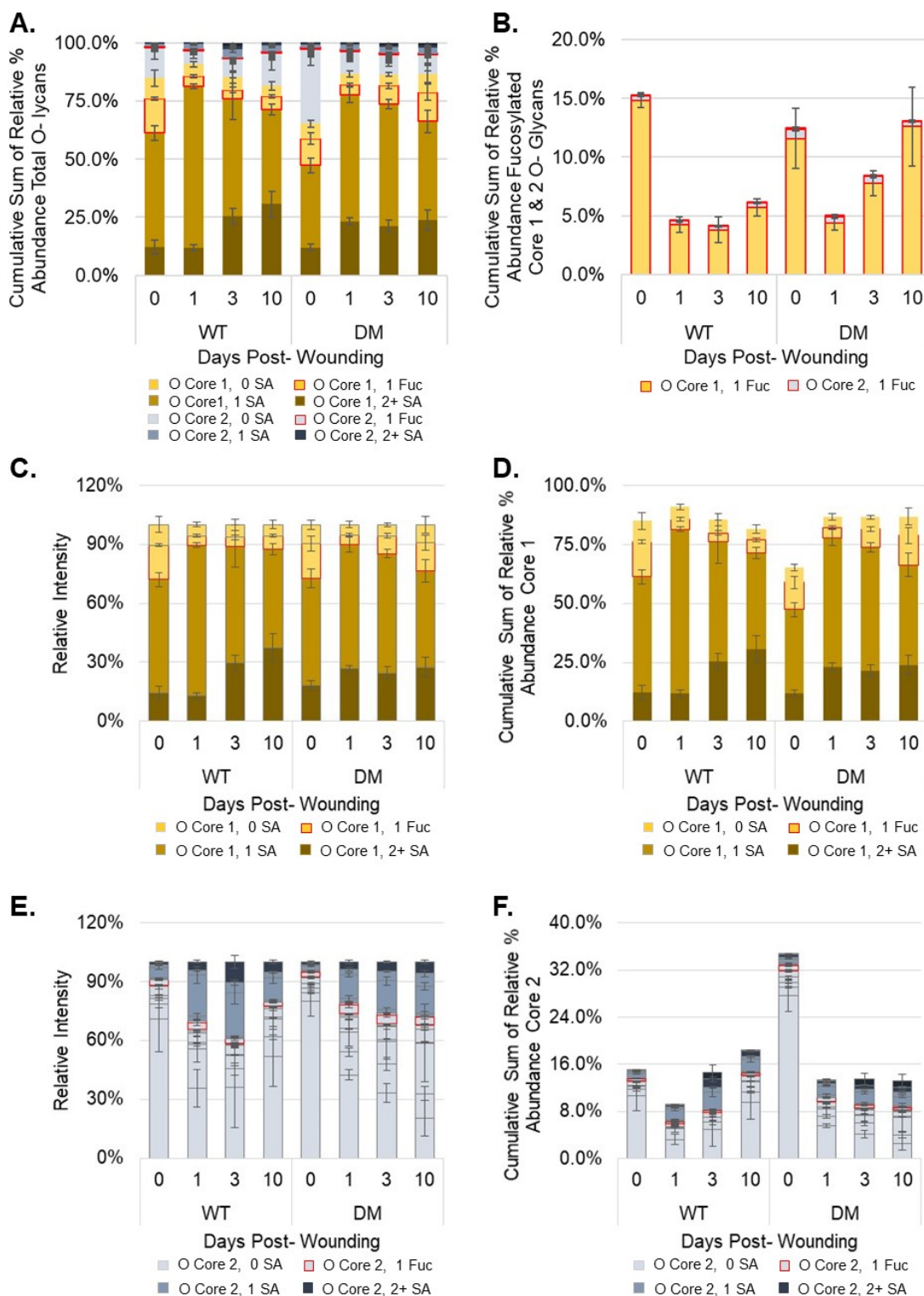


Figure 52. Comparison of O- glycan profiles in uninjured skin and wounds from diabetic and non- diabetic mice.

Figure 52. Comparison of O- glycan profiles in uninjured skin and wounds from diabetic and non- diabetic mice.

O- glycan profiles of uninjured skin and wounds days 1-, 3-, and 10- post wounding in non-diabetic (left) and diabetic mice (right). The relative total intensity of each core O- glycan feature subtype was scaled to 100% of the total % abundance of each O- core glycan. The cumulative sum of the relative % abundance compared the total abundance of each core glycan feature across all O- glycan features. All O- glycans represented by 100%, compared to core 1 O- linked glycans (C, D; gold) and core 2 O- linked glycans (E, F; blue grey).

Glycan feature subtypes: fucosylation (red outline); increasing sialylation represented by darker coloring.

4.4 Discussion

During this study we identified substantial changes in the glycomics profiles of diabetic and non-diabetic skin and wounds. Differential fucosylation and sialylation of N- and O- linked glycans appeared to be a key feature during the inflammatory phase of healing in non- diabetic and diabetic skin. Decreased fucosylation with 1 fucose and increased sialylation with 2 or more sialic acids were identified in the N- and O- glycomic profiles of non- diabetic and diabetic wounds between 1-3 days post wounding when compared to unwounded skin. Decreased fucosylation with 1 fucose on N- and O- linked glycans was consistent with the downregulation of *FUT8*, *FUT1*, and *FUT2*, respectively, observed in wounds 3- days post- wounding when compared to uninjured skin. Furthermore, increased di-, tri-, tetra-sialylation of N- and O- linked glycans throughout the inflammatory phase of wound healing was consistent with the expression of *ST3GAL1*, (not significant Figure 87B, Appendix D), *ST8SIA2* (Figure 89B, Appendix D), and *ST8SIA4* (Figure 37D) as described in Chapter 6. Decreased fucosylation and increased sialylation have also been described in other models of acute inflammation, such as during acute peritonitis⁹⁷. The inverse regulation of fucosylation and sialylation upon activation of the inflammatory response and the importance that proper sialylation, plays in regulating the innate and adaptive immune response (Siglecs, selectins, etc) may provide a means to identify impaired inflammatory responses by examining sialylation and fucosylation.

When examining the regulation of fucosylation and sialylation between non-diabetic and diabetic wound healing, diabetic skin exhibited an acute decrease in fucosylated N- linked glycans and O- linked glycans (core 1 and 2) 1-day post

wounding. This was followed by a decrease in complex N- glycan core fucosylation (Figure 52B) and increased core 2 O- linked glycan fucosylation 10 days post-wounding when compared to non- diabetic wounds. Diabetic wounds also demonstrated early upregulation of di-, tri-, tetra-sialylated N- and O- linked glycans 1-day post-wounding. Interestingly, di-, tri-, tetra-sialylated N- linked glycans remained upregulated through day 10, while, di-, tri-sialylated O- linked glycans were downregulated days 3-10 in diabetic wounds when compared to non- diabetic wounds. This data suggests that gradual fine tuning of N- and O- linked glycan fucosylation and sialylation occurs in response to acute inflammatory signals and that diabetic and non- diabetic wounds exhibit variations in their response 1-10 days post- wounding. This may additionally have importance to the impaired healing phenotype, as noted by the drastic delay in diabetic wound closure observed between days 1-3 post- wounding.

Distinct changes in the expression of individual glycans and glycan subtypes were also identified. Significantly increased neutral and fucosylated core 2 O- linked glycans and decreased sialyl-T antigen (sialyl- core 1) and sialylated core 2 O- linked glycans were identified in uninjured diabetic skin and wounds when compared to the non- diabetic condition. Reduced O- glycan capping by sialic acids in diabetic skin and wounds may suggest a role for impaired O- glycan processing in diabetic skin when compared to non- diabetic skin. Additionally, N- linked glycans with mass-to-charge ratios of *mz*4200.3, *mz*4475.5, and *mz*4929.7 were upregulated in the diabetic condition as compared to the non-diabetic condition and have been associated with structures exhibiting fucosylated, sialosyl-poly-N- acetyllactosamines (poly- LacNAc) containing terminal glycans consistent with Lewis blood group glycans. Glycans with mass-to-

charge ratios of *mz*4475.5 and *mz*4200.3 have been observed in human neutrophils²⁶⁷ and on glycophorin C²⁶⁸ respectively, however, considering the complexity of fucosylated poly- LacNAc these structures could also represent those found on keratan sulfate proteoglycans²⁷¹, galectin- 3 binding sites¹²⁷, or E- selectin ligand (ESL-1)¹⁰⁶. Interestingly, the fucosylated, sialosyl-poly-N- acetyllactosamines found on N- glycans of ESL-1 have been associated with the initial recruitment but not the firm arrest of myeloid cells²⁷². Again, this data demonstrates a potential role for altered myeloid cell glycosylation in mediating the impaired wound healing.

One limitation to this study lies in the glycomics analysis itself. A 20-30% variation in glycan intensity is normally observed between biological replicates making it difficult to detect glycan specific differences across replicate animals and persons of identical samples types. This is especially true when there is a low sample size. In this study, the inability to identify significant differences in many individual N- glycan structures is attributed the high degree of variability in N- glycomes and the limitations of analysis of variance (ANOVA). As the field of glycomics continues to progress, better statistical models will be necessary to validate these finding in preparation for clinical studies. Overall, we have provided new important information regarding baseline changes in the glycosylation of diabetic skin. Further investigations may explore whether these changes will have prognostic potential in predicting impairments in the host inflammatory response to wounding. While more studies are required to validate the importance of these glycans in inflammation and wound healing and to evaluate it's true prognostic ability, previous studies of human neutrophil glycosylation²⁶⁷ and

differential sialylation and fucosylation in peritonitis ⁹⁷ suggests that these findings will have clinical importance.

5 THESIS CONCLUSIONS & FUTURE DIRECTIONS

The major contributions of this thesis are 1) the identification of the regulation of sialylation and polysialylation as potential contributors to the differential wound healing observed in skin and tongue wound healing, 2) the identification of differential regulation of glycosylation associated genes in skin and wounds of diabetic and non-diabetic mice; 3) the identification of differential sialylation and fucosylation in uninjured skin and wounds in diabetes; and 4) the utilization of a more biological relevant means of statistical analysis to make useful for comparisons across wound healing datasets.

Sialyltransferases and sialidases (neuraminidases) are responsible for the addition and removal of sialic acid monosaccharides respectively during glycosylation. Here we demonstrated differential changes among types of wounds and disease states in the pattern, time, type, and degree of gene expression related to sialyltransferase and neuraminidase activity. Lectin blot analysis confirmed that the observed differential gene expression yielded differential sialylation in tongue and skin during wound healing. Furthermore, polysialylation, which is a unique type of protein specific glycosylation, was increased during the proliferative phase of healing. Subsequent protein analysis was unable to identify a singular protein that demonstrated the same magnitude of expression as the polySia. Free polySia doesn't exist and it requires a carrier protein, therefore it is likely that the degree of polySia polymerization and total number of polysialylated proteins, but not the carrier protein itself is important for regulating downstream polySia mediated reactions and interactions. This was previously suggested in studies examining the polysialylation of myeloid cells that contained NRP-

2, ESL-1, NCAM-140, and an unknown protein ¹⁰⁹. Overall, these studies identified linkage specific differences in the regulation of sialic acid in skin and tongue wound healing. Future studies would be designed to elucidate the interplay between α 2,3- and α 2,6 sialic acids and potential their role in modulating β -integrin activity during wound healing. PolySia has been introduced as a therapeutic in spinal cord injury repair ¹³⁹ and drug delivery tool that has completed phase II clinical trials ²⁷³, further underscoring a possible role in the repair of skin, as studied here. Additional studies in wounds would involve the metabolic induction of hyper-sialylation, direct treatment with polySia both acutely and chronically, and/ or time dependent upregulation of polysialyltransferases. These studies would more thoroughly define the role of polySia in regulating the inflammatory response to wounding, epithelial proliferation, and scar formation.

The majority of information in the current studies comes from the assessment of glycosylation- related genes expression. By examining the glycosylation- related gene expression across different tissue models during the diabetic disease process of humans and mouse strains, these studies suggest that differential glycosylation- related gene expression may modulate the repair process in impaired healing phenotypes. One of the most interesting findings is that our glycotranscriptomics study of diabetic and nondiabetic wound healing has parallels to the oral and skin wound microarray data. Our studies show that 29 of the 38 genes that were differentially regulated between diabetic and non-diabetic wound healing were also differentially regulated in skin and tongue wound healing. Among these genes, 21 had the same directionality of expression when comparing the quality of the wounding healing phenotypes (i.e. mucosa>skin and non-diabetic skin> diabetic skin) (Table XV). Interestingly only 4 of

the genes that were differentially expressed between the normal and impaired healing phenotypes were also significantly regulated in non- diabetic wounds when compared to uninjured non- diabetic skin and also shared similar expression patterns when compared to the skin and tongue. These genes included AGL and PYGM which are related to glycogenolysis, GALNT15 which is involved in O- mucin type glycosylation, and CHST11 which is responsible for chondroitin sulfation. These 3 genes, AGL, PYGM, and GALNT15 demonstrated reduced baseline expression or delayed recovery of expression levels during the inflammatory or proliferative phases of healing (days 3 and 10), while CHST11 demonstrated enhanced upregulation. These genes and their potential role in wound healing is discussed further below.

TABLE XV.

TABLE OF GENES DIFFERENTIALLY REGULATED BETWEEN TISSUES WITH AND WITHOUT IMPAIRED HEALING PHENOTYPES AND THEIR ASSOCIATED ENZYME FAMILY

	Gene	Enzyme Family
Upregulated in Impaired Wound Healing	B3GNT2	GT31_M16
	<i>B4GALNT1</i>	GT12_M02
	B3GNT9 (C76566)	GT31_M01
	CHI3L1	GH18_M04
	CHST11	STR_M04
	FUCA 1	GH29_M02
	GALNS	ST_M01
	GLA	GH27_M01
	GNS	ST_M05
	GUSB	GH02_M01
	HS2ST1	STR_M14
	HYAL2	GH56_M04
	<i>NEU1</i>	GH33_M04
	<i>PAPSS2</i>	NSN_M20
	PYGL	GT35_M01
	<i>ST8SIA2/4</i>	GT29_M15
	SULF2	ST_M04
	<i>TPST2</i>	STR_M02
Downregulated in Impaired Wound Healing	AGL	GH13_M06
	GALNT15	GT27_M14
	PYGM	GT35_M02

All genes represent those that demonstrated a similar trend in expression during the glycotranscriptomics analysis of db/db (diabetic) and C57 (non-diabetic) mouse skin and in the microarray analysis of BALB/c skin and tongue wounds. In addition to being differentially expressed between the skin/ tongue and diabetic/ non- diabetic conditions, bolded genes represent those that demonstrated additional time- specific differences during diabetic versus non- diabetic wound healing.

5.1 **AGL, PYGM, and the Importance of Glycogen Accumulation and GSK3 β**

The glycogen debranching enzyme, AGL, along with muscle (PYGM) and liver (PYGL) specific glycogen phosphorylase promote glycogenolysis. Sustained downregulation of AGL and PYGM promotes increased local glycogen storage ²⁷⁴⁻²⁷⁵. Increased glycogen accumulation and enzymes related to glycogen synthesis have been previously observed via histochemical analysis of regenerated epithelium ²⁷⁶ and invading cells throughout the peripheral dermis ²⁷⁷. While AGL and PYGM have not been examined for their roles in wound healing, glycogen accumulation and the expression of glycogen synthase kinase (GSK3 β) have been previously studied for their roles in wound healing. GSK3 β is a constitutively active enzyme that's responsible for downregulating the expression of glycogen synthase (GYS), which in turn decreases local glycogen availability. Furthermore, phosphorylation of GSK3 β inhibits its activity and allows GYS expression and activity which promotes glycogen β synthesis and the accumulation of local glycogen stores. A recent study found that inhibition GSK3 β activity lowers the LPS induced expression of NF- κ β and inflammatory cytokines in macrophages ²⁷⁸. Furthermore inhibition of GSK3 β reduces p65 localization to the promoter regions of the interleukin-6 and monocyte chemoattractant protein 1 genes ²⁷⁹ which reduces their expression and the overall inflammatory response. Inhibition of GSK3 β also increases β -catenin expression ²⁸⁰ which promotes fibroblast proliferation ²⁸¹, delays cutaneous epithelial migration and impairs wound healing. The described role of GSK3 β in these studies and our finding that *AGL* and *PYGM* are downregulated in wound healing may suggest a role for glycogen accumulation in mediating the transition between the inflammatory and proliferative phases of wound healing. This is

further suggested by the downregulation of *AGL* and *PYGM* expression observed between the inflammatory and early proliferative phases of healing (3-10 days post-wounding) in non- diabetic and diabetic skin.

While GSK3 β inhibition has been examined for its contributions to wounding healing processes, the primary reason for its inhibition is to promote glycogen synthesis and accumulation. The role of glycogen accumulation was investigated in the 1960's and 70's via immunohistochemical means, while GSK3B was found to participate in the glycogen accumulation that occurs upon wounding, no clear progression towards isolating GSK3B as the only enzyme related to glycogen metabolism that contributes to wound healing could be found. Furthermore, it is known that *AGL* and *PYGM* downregulation and *GYS* upregulation have the potential to contribute to glycogen accumulation. Interestingly, *AGL* and *PYGL* were also chronically downregulated in uninjured skin and wounds in the diabetic condition when compared to the non-diabetic condition and in the skin when compared to the tongue. Regardless of whether decreased expression of *AGL* and *PYGM* in skin and wounds with impaired healing phenotypes occurs as a consequence of GSK3 β inhibition or as a primary response it appears to be a strong predictor for impaired healing phenotypes. This is further confirmed by a recent publication examining 2mm wounds 1 hour, 12 hours, and 24 hours post- wounding in E17 fetal and adult mice ²⁸². Fetal skin wounds, similar to oral mucosal wounds, are observed to heal faster with less inflammation and with no scar formation when compared to adult skin. The recent microarray of fetal and adult wounds identified that *AGL* was downregulated in adult skin when compared to faster healing fetal skin wounds 1-hour post wounding ²⁸². Furthermore, despite the significant

association between GSK3 β and wound healing, it did not appear as statistically significant in the BALB/c skin and tongue dataset or the fetal wound data set.

5.2 Reduced AGL Expression is Observed in Cancer and may be Correlated with Differential Glycosaminoglycan Expression

Loss of AGL has also been associated with driving cancer growth ²⁴⁷. The mechanisms for this association are complex. For example, AGL loss was shown to lead to increases in proteases (Cas3, Cas9 and PARP) and to support hyaluronan induced proliferation by increasing hyaluronan synthase (HAS2) and HA in bladder cancer ²⁴⁸. AGL loss has been similarly linked to increased proliferation mediated by hyaluronan glycosaminoglycans ²⁴⁷ and poor survival rates in non- small cell lung cancer ²⁸³. Our studies also identified a number of genes related to glycosaminoglycans. In diabetic and non-diabetic skin and wounds, hyaluronidase (*HYAL2*) and β - glucuronidases *GUSB* were upregulated and the only genes related to hyaluronan metabolism, however, these genes are responsible for the degradation of hyaluronan. *HYAL2* and *GUSB* were also upregulated in skin versus tongue wounds in addition to hyaluronan synthases (*HAS1*, *HAS2*, *HAS3*) and hyaluronan and proteoglycan link protein 3 (*HAPLN3*) while hyaluronic acid binding protein (*HABP4*) was downregulated. Furthermore, additional lysosomal glycosaminoglycan degrading enzymes including *FUCA1*, *GNS*, *GALNS*, *SULF2*, *GLA*, were upregulated in in the skin relative to the tongue and in diabetic compared versus non-diabetic wound healing.

5.3 Differential Sulfation may Contribute to Impaired Healing Phenotypes

Increased expression of genes related to sulfate precursors (*PAPSS2*), tyrosine sulfotransferase (*TPST2*), and chondroitin/ dermatan sulfotransferase (*CHST11*) activity was noted diabetic skin and wound compared to the non- diabetic condition. *PAPSS2*, *TPST2* and *CHST11* are responsible for synthesizing and transferring sulfate to proteins and glycosaminoglycans involved in selectin ligand synthesis. *TPST1/2* is known to provide the tyrosine sulfates necessary for P selectin ligand mediated leukocyte rolling²⁸⁴. Furthermore, *CHST11* is required for the synthesis of chondroitin sulfate proteoglycan 4 (CSPG4) which serves as a ligand for P- selectin and requires *CHST11* expression for proper binding to P- selectin²⁸⁵. Increased expression of *PAPSS2*, *TPST2* and *CHST11* and their involvement in P- selectin ligand biosynthesis and binding could be associated with the increased leukocyte counts observed in patients with chronic diabetic wounds²⁸⁶ and the enhanced inflammatory response observed in the skin when compared to the tongue.

The expression of GAG sulfatases (GNS, GALNS) and extracellular sulfatase (SULF2) was also increased. Increased expression of sulfate precursors, tyrosine sulfotransferases, extracellular sulfatases along with increased GAG sulfotransferase and increased GAG sulfatase expression, raises a question of whether sulfation is impaired in GAG's, and other sulfated proteins and glycans in diabetic and non-diabetic wound healing. GAG's were not assessed in our analysis, and only 1 sulfated glycan $\text{H}_3\text{N}_3(\text{SO}_3)$ appeared in the glycomics analysis. The levels of this sulfated glycan demonstrated a trend towards downregulation during wound healing. $\text{H}_3\text{N}_3(\text{SO}_3)$ also demonstrated higher expression in diabetic wounds when compared to non-diabetic

wounds in the hemostasis/ early inflammatory phase of healing (1-day post- wounding). This structure likely corresponds to a core 2 sulfated LacNAc. The lack of sialylation and fucosylation of this sulfated LacNAc makes this structure unlikely to be associated with selectin ligands, and the limited literature available for this structure makes it difficult to identify its function. While future studies are required to determine causation, this data suggests a role for changes in glycosaminoglycan metabolism and sulfation as a potential cause for the differential healing capacity among different organs (skin and tongue) and in disease (diabetic and non-diabetic skin).

5.4 Differential Expression of O- linked Glycans in Impaired Healing phenotypes

ppGALNT15 is responsible for catalyzing the transfer of GalNAc to serine and threonine during the synthesis of O- glycan mucins. The gene encoding ppGALNT15 was downregulated in uninjured skin and wounds when compared to uninjured tongue and wounds, as well as, in uninjured diabetic skin and wounds 10- days post- wounding when compared to the non- diabetic condition. The expression of B4GALNT2 was also downregulated upon wounding when compared to uninjured tissue and when comparing the diabetic to the non-diabetic condition. Glycomics analysis of diabetic and non-diabetic skin revealed: 1) decreased expression of core 2 glycans in wounds when compared to uninjured skin; 2) decreased core 1 glycans in uninjured diabetic skin when compared to non- diabetic skin; 3) and decreased core 2 glycans in diabetic wounds 10- days post wounding when compared to the non-diabetic wounds. Unfortunately, other genes related to O- glycan elongation were not consistent with the

observed glycomics profiling. This is likely attributed to the fact that ppGALNT15 and B4GALNT2 have higher substrate specificity towards glycoproteins while the other glycosyltransferases involved in O- linked glycosylation have higher specificity for glycolipids and glycosaminoglycans, which were not examined during this analysis.

5.5 Differential Expression of Genes related to Terminal Glycan

Monosaccharides and Neutrophil Degranulation in Impaired Healing

Phenotypes

A number of genes related to terminal glycan capping were also examined. While most were related to the sulfation of glycosaminoglycans and glycolipids, 3 genes *ST8SIA2/4*, *NEU1*, and *FUCA1* were upregulated in impaired wound healing phenotypes. Though these genes did not confer global changes in all glycoprotein glycosylation, N- glycan specific correlations with the expression of *NEU1* and *FUCA1* genes were noted. Interestingly the reduced relative abundance of sialylated O- glycans correlated with the enhanced expression of lysosomal neuraminidase (*NEU1*) in the diabetic condition when compared to the non- diabetic condition. Additionally, the increased expression of *FUCA1*, which removes α 1, 6 (core) fucose from N- glycans was upregulated in the diabetic condition and corresponded to a slight reduction in the relative abundance of core fucosylated N- glycans. Lastly increased *ST8SIA2/4* expression correlated with increased polysialylation in response to wounding in all tissues. While the magnitude of polysialyltransferase expression was higher during the proliferative phase of healing (3- days post wounding) in tissues with an impaired healing phenotype when compared to those that heal faster, it appears that the

increased expression is the result of a delay in the downregulation of polysialyltransferase activity as opposed to differences in the magnitude of expression. This was demonstrated by the prolonged and biphasic regulation of polysialyltransferase expression in skin versus tongue wound healing (Figures 13C & 13D and Figure 53, Appendix A) and was preliminarily observed in the diabetic skin. A preliminary screen of polySia expression in skin wounds 1, 3, and 10 days post-wounding demonstrated that non- diabetic skin upregulated the expression of polySia within 1 day post wounding and began to downregulate its expression by day 3, however, diabetic skin upregulated the expression of polySia 3 days post wounding and remained upregulated through day 10 (Figure 63, Appendix C).

Of significant interest is that the Reactome pathway database associates AGL, CHI3L1, FUCA1, GALNS, GLA, GLB1, GNS, GUSB, NEU1, and PYGL with biological processes related to neutrophil degranulation. Previous studies found that CHI3L1, GBA, and HYAL2 are activated in response to IL-1 and/ or TNF α . Additionally, GBA and HYAL2 are associated with the negative regulation of MAPK activity while HYAL2 and CHI3L1 are associated with the positive regulation of protein kinase B signaling. While limited information is available regarding the interaction of all of these involved genes, most are associated or predicted to be associated with lysosomes and exosomes. Future studies examining the regulation and release of this combination of enzymes could hold importance in developing clinical treatments for chronic wounds, however, its current significance is founded in its potential to be used a clinical tool for diagnosing impaired healing phenotypes.

5.6 Novel Statistical Assessment Focuses Our Assessment of Glycosylation-related Gene Expression in Wounds

To discover glycosylation patterns that support ideal repair, our studies used novel methods of statistical analysis. The traditional means of examining differential wound healing between 2 conditions uses multivariate analysis including the Two-way ANOVA with corrections for multiple pairwise comparisons over time. One consequence of this type of analysis is the inclusion of biologically irrelevant comparisons that are made between the conditions at differing timepoints. Another limitation is that pairwise comparisons can't infer information regarding the trajectory of wound healing overtime. While uniform changes in expression between conditions over- time can be perceived as significant in both models, this model allowed us to better delineate whether the significance was observed as an innate variance of the tissue type versus its importance in the process of wound healing. This technique, furthermore, helped to identify a very narrow target of focus and has demonstrated consistency between both studies. Future investigations using this type of analysis will improve our understanding of large-scale data sets that compare wounds over time.

5.7 Limitations

The most obvious limitation of the current study is that the mechanistic importance of the findings has not yet been assessed. Future studies might be designed to selectively alter glycosylation pathways to further understand their importance. The selective manipulation of glycosylation is challenging though, due to the complexity of the enzymatic pathways. Nevertheless, as technology, and perhaps

tissue specific deletions, become more readily available, the importance of the findings may be more directly approached.

Pending the availability of such technologies, suppression of polysialyltransferases ST8SIA2 and ST8SIA4 in myeloid lineage cells upon cutaneous wounding up until the late inflammatory/ proliferative phase of healing might be of interest to examine whether polySia suppression during hemostasis and inflammation blunts the inflammatory response of cutaneous wound healing similar to that which is observed in the tongue. Furthermore, targeted upregulation of these polysialyltransferases in epithelial cells during this time would be useful to assess whether the speed of re-epithelialization is enhanced.

6 APPENDICES

6.1 APPENDIX A

6.1.1 Discussion of Unequal Regulation of Proteins Involved in Polysialylation

To identify proteins that were likely responsible for the presence of polySia expression, the expression of *NCAM1*, *CADM1* (encodes SynCAM 1), *NRP2*, *GSLG1*, and *CCR7* were plotted along with their respective polysialyltransferase. *ST8SIA4* (black) expression was >5 fold higher than the expression of *ST8SIA2* (purple) 3- days post wounding and it's expression over the course of healing was only parallel to *GSLS1* (*GLG1/ESL1*) (yellow, Figure 53E, Appendix A) in the tongue (solid line), but not the skin (dotted line). There were no other strong correlations between the expression of any polysialyltransferase and respective known polysialylated protein throughout the entire course of wound healing, however, parallel regulation at unequal magnitudes were observed among the following comparisons: 1) *ST8SIA2* and *NCAM* in the skin and tongue at 1-5 days post- wounding (Figure 53A, Appendix A); 3) *ST8SIA4* and *NCAM* in the tongue at 1-3 days post- wounding (Figure 53B, Appendix A); *ST8SIA2* and *CADM1* at 1-3 days post- wounding (Figure 53C, Appendix A); and *ST8SIA4* and *CCR7* in the skin at 0.25-3 days post- wounding (Figure 53D, Appendix A).

APPENDIX A (continued)

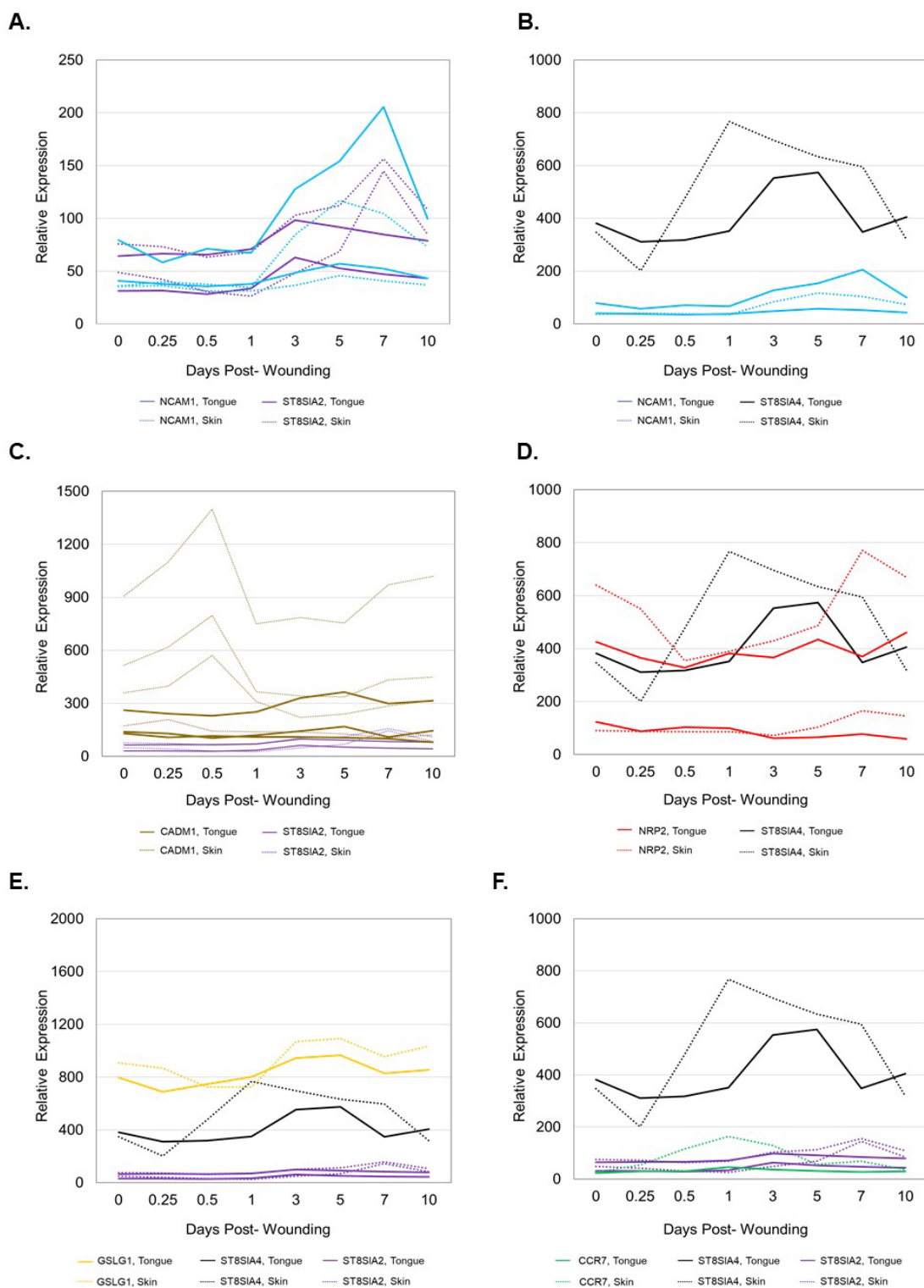


Figure 53. The expression of genes related to polysialyltransferase activity and its correlation with the expression of polysialic acid carrying proteins in skin and tongue wound healing.

APPENDIX A (continued)

Figure 53. The expression of genes related to polysialyltransferase activity and its correlation with the expression of polysialic acid carrying proteins in skin and tongue wound healing. Gene expression in tongue (solid line) and skin (dash) are as follows: A) *ST8SIA2* (purple) and *NCAM* (blue) B) *ST8SIA4* (black) and *NCAM* (blue); C) *ST8SIA2* (purple) and *CADM1* (gold); and D) *ST8SIA4* (black) and *NRP2* (red; E) *ST8SIA2* (purple) and *GSLS1* (*GLG1/ESL1*) (yellow); F) *ST8SIA4* (black), *ST8SIA2* (purple) and *CCR7* (green).

APPENDIX A (continued)

NCAM1 was identified in Figure 53 as a potential candidate for carrying polySia in the skin and tongue. Additionally, the 250kDa molecular weight proteins identified in the 12F8 immunoblot in chapter 5 (Figure 21) is consistent with the molecular weight of polysialylated NCAM1. To determine whether NCAM1 was responsible for carrying the identified polySia, 12F8 immunoblots were stripped and reprobed for NCAM1 (Figure 55B). No significant staining was observed at the molecular weights represented by NCAM-180 or NCAM-140 in any sample or replicate. At the expected molecular weight for NCAM-120, a trend for equal expression was observed in the tongue at all timepoints (Figure 55B, left; replicates in Figure 59, Appendix B) and in the skin at all time points (Figure 55B, right; replicates in Figure 59, Appendix B). Unexpected and/or non-specific bands were observed at ~82kDa, 74kDa, and 25-30kDa as identified by the red arrows. These bands likely occurred due to protein degradation during the EndoNt precipitation and endoN digestion steps as brains samples that did not undergo these processes demonstrated 2-3 NCAM1 positive bands, while those that underwent EndoNt and catalytic endoN incubation had 6-7 bands similar to the skin and tongue samples. Lastly, the NCAM1 Ab was found to non-specifically stain the immunoblots at 45kDa which is associated with the molecular weight of CCR7. When the blots were stripped and reprobed for CCR7, no staining was identified among EndoNt samples, however, staining in brain samples that did not undergo immunoprecipitation demonstrated expression at approximately 45kDa (Figure 55C). Though unclear, it appears that polySia co-occurred with NCAM-120, however, the upregulation of polySia occurred independent of both CCR7 and NCAM-120 abundance

APPENDIX A (continued)

during tongue and skin wound healing. Preliminary attempts to evaluate the expression of NRP2 and CADM1/SynCAM 1 on new blots were unsuccessful as no staining was observed, however, this was only performed in one group of samples. Interestingly, when CCR7 was re-evaluated on new blots among samples that did not undergo EndoNt precipitation, increased expression of CCR7 was detected 3 days post-wounding in the skin, but not the tongue. The presence of CCR7 at this timepoint, may help to explain the ~50kDa 12F8 positive, endoneuraminidase resistant bands observed in the polySia immunoblots (Figure 21). Furthermore, EndoNt precipitation of uninjured skin samples underwent mass spectroscopy analysis following in-gel digestion did not reveal any peptides (Table XVI) associated with known polysialyltransferase protein substrates between 50- 250kDa (Table XVII) indicating that the level of protein expression fell below the detectable range of 5 picomole.

During the bulk of the past year, attempts were made to identify NCAM-180 as the 250kDa polysialylated protein, while this evidence indicates that NCAM-180 was an unlikely candidate, it can't be completely excluded as other factors including proteolytic degradation may be to blame. Previous studies found that 38-40kDa and 46-48kDa NCAM1 fragments are related to MMP-9 mediated degradation of NCAM1²⁸⁷, and that these fragments maybe polysialylated at 110-115kDa^{144, 288-289}.

Staining of polySia using the 735 antibody, which binds polySia specifically, demonstrated increased expression in uninjured skin when compared to skin and tongue wounds 3-days post wounding (n=1, Figure 57A). This was opposite of what was found using the 12F8 antibody which demonstrated increased polySia expression 3-

APPENDIX A (continued)

days post-wounding. Though further analysis would be required for confirmation, these differing results may reflect the specificity of these two antibodies for polySia chains of different lengths. The 735 antibody recognizes polySia chains of 8-11 units and longer, while the specificity of the 12F8 is uncharacterized. Three days post wounding, when leukocytes are likely to still be present, proteins may express oligo and polySia chains of shorter lengths which are cleaved and shed from the cell surface in response to injury^{14, 108-109}. This polySia shedding may have also contributed to the difficulty we had obtaining microscopic images of polySia colocalization with proteins outside of the Golgi and on the cell surface. Furthermore, previous studies have identified polySia expression on proteins including NRP-2, ESL-1, and NCAM with molecular weights between 85-140kDa in myeloid cell lineages¹⁰⁹. Additionally, NRP and ESL-1 previously demonstrated a 10-15kDa difference in molecular weight when compared to their respective non-polysialylated counterparts¹⁰⁸. These previous studies were also performed on single cell lines and less heterogenous populations when compared to the skin, including peripheral blood and bone marrow. The addition of shorter polySia chains and smaller molecular weight shifts together with the heterogenous nature of the skin likely contributed to the difficulty we faced with determining whether there was any change in polySia expression among the lower molecular weight bands. Future studies should employ cell sorting techniques to identify the cells that express and/or uptake polysialylated proteins during wound healing and to reduce the cell/ protein heterogeneity to permit better protein and polySia detection. Furthermore, future studies examining the functional role of epithelial and myeloid lineage cell polysialylation in early

APPENDIX A (continued)

inflammation, late inflammation, and proliferation through the upregulation of polysialyltransferase activity and/or reduced CMP-NeuAc/ CMP-NeuGc or increased free sialic acid expression would be of interest considering the time dependent differential regulation of polysialyltransferases between skin and tongue wound healing and the differential expression of genes regulating the conversion of sialic acid into usable CMP- NeuAc sugar nucleotides.

APPENDIX A (continued)

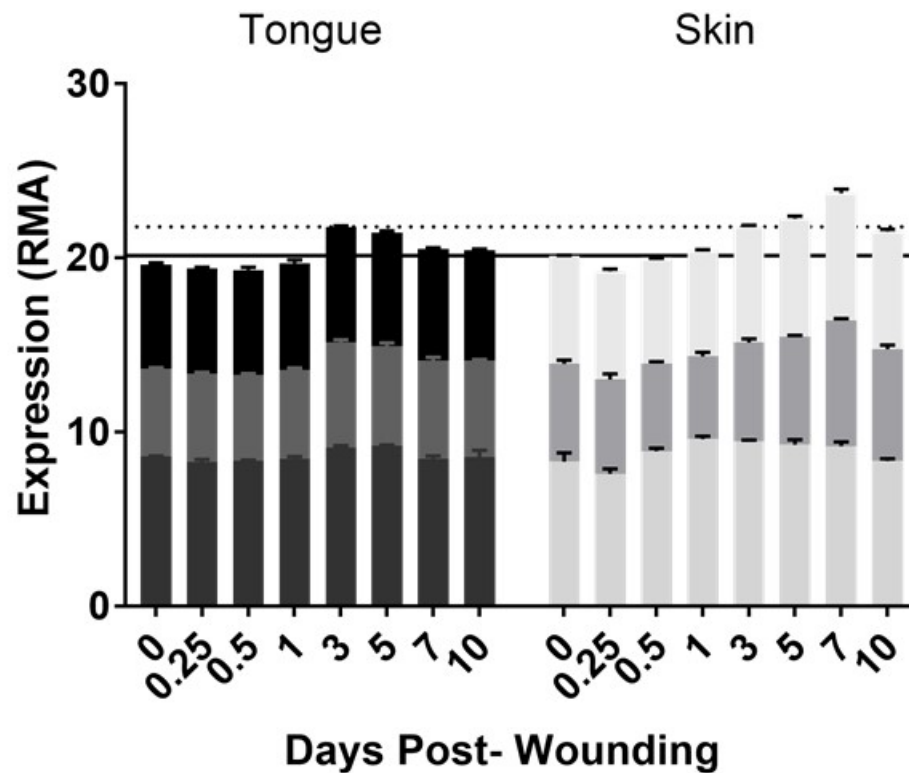


Figure 54. The combinatorial expression of all significantly expressed transcript probes related to polysialyltransferase activity a in skin and tongue wound healing. The combined transcript abundance in uninjured skin (solid line) is higher than in the uninjured tongue. However, the combined transcript abundance in skin 3- days post- wounding (dashed line) is equal to that observed in the tongue 3- days post- wounding.

APPENDIX A (continued)

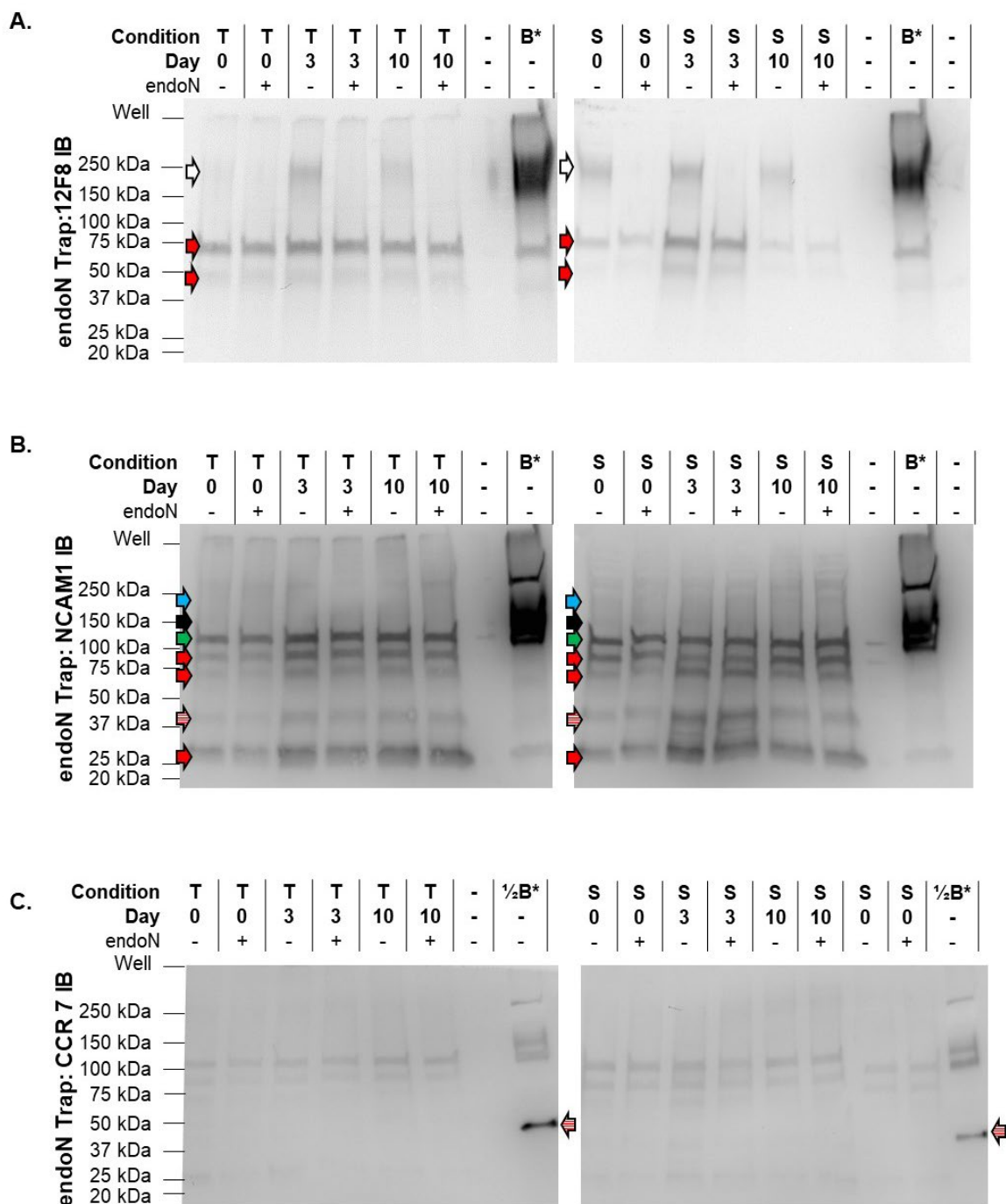


Figure 55. Expression of polysialic acid, NCAM, and CCR7 in EndoNt proteins during skin and tongue wounds healing. Arrows denotes the location/ MW where each expected band would appear for polysialic acid (white). Unexpected and/ or non- specific bands denoted by red arrows.

APPENDIX A (continued)

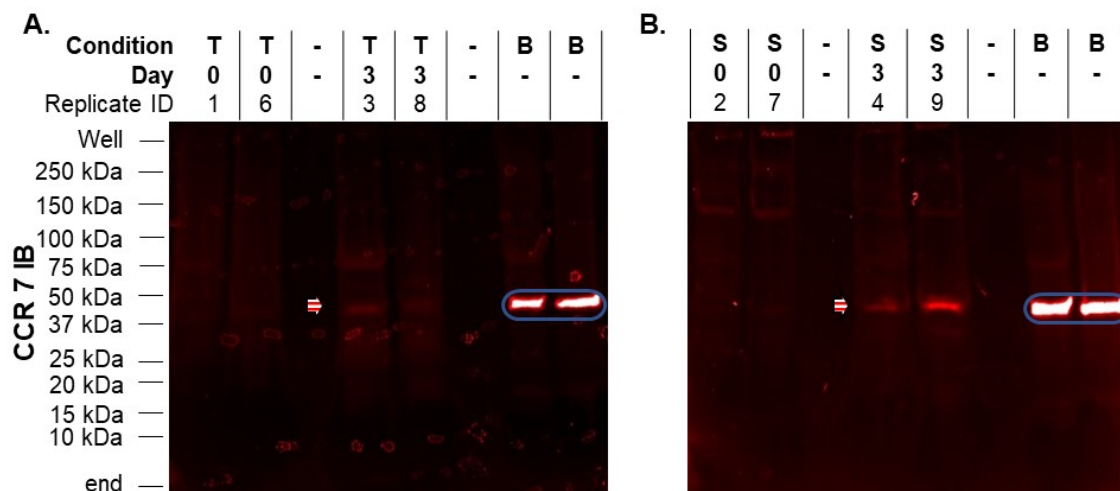


Figure 56. CCR7 is more highly expressed in skin wounds than uninjured skin and tongue wounds. Stripped arrow indicates the location of the CCR7 positive bands (red) in tongue (A) and skin (B) wounds 3- days post- wounding. Blue circle represents overexpression of CCR7 in brain samples (B) which acted as the positive control.

APPENDIX A (continued)

TABLE XVI.TABLE OF PEPTIDES IDENTIFIED FROM UNINJURED SKIN FOLLOWING
ENDONT IP.

Peptide sequence	Previous amino acid	Next amino acid	Best Peptide ID Prob.	Best Mascot Ion Score	Best Mascot Identity Score	Best Mascot Homology Score	Best Mascot Delta Ion Score
TNAENEFVTIK	R	K	99.70%	70.5	34.6	15.5	64.1
GDGGPPGMTGFPGAAGR	R	T	98.70%	34.1	31.8	0	28.7
GEAGAAGPSGPAGPR	R	G	99.70%	65.6	33.5	22	57.1
GENGIVGPTGSVGAAGPSGPNPPGPVGSR	K	G	99.70%	53	35.5	0	5.63
GEPGPAGSVGPVGAAGPR	R	G	99.70%	68	34.9	0	68
GEVGPAGPNGFAGPAGAAGQPGAK	R	G	99.70%	106	35.4	0	40.6
GPAGPSGPVVK	R	D	99.70%	55.4	31.8	13.7	55.4
GVSSGPGPMGLMGPR	K	G	99.70%	57.5	33.5	0	50.7
PGPIGPAGPR	R	G	99.70%	45.7	33.2	15.1	14.8
SGQPGPVGPAGVR	R	G	99.70%	42.7	33.8	14.3	36.1
DGEAGAQQAGPAGPAGER	K	G	99.70%	62.4	33.3	13.1	61.9
GETGPAGPAGPIGPAGAR	R	G	99.70%	75.1	34.9	13.1	60.4
GFPGADGVAGPK	R	G	99.70%	50.2	32.9	15.1	43.5
GQAGVMGFPGPK	R	G	99.70%	68	34.4	16.1	64
GVQGPAGPAGPR	R	G	99.70%	40.9	34.9	23.1	30.2
NGDRGETGPAGPAGPIGPAGAR	K	G	99.70%	62.7	35.4	16.7	53.6
SAGVSVPGPMGPSGPR	K	G	98.80%	33.1	33.9	0	33.1
SLNNQFASFDK	R	V	99.70%	51.2	33.3	13.4	51.2
LAELEDALQK	K	A	99.70%	60.5	34.9	30.1	35.9
EVATNSELVQSGK	R	S	99.70%	64.7	35	14.8	63.5
VTMQNLNDR	K	L	99.70%	64.9	34.1	34.1	0
GPAGPMGLTGR	R	P	99.70%	54.1	32.1	18.3	50.6
EGVLYVGSK	K	T	99.70%	71.4	32.5	27.9	57.9
EQVTNVGGAVVTGVTAVAQK	K	T	99.70%	74.5	32.6	0	72.2
TKEQVTNVGGAVVTGVTAVAQK	K	T	99.70%	140	30.5	14.3	127
DLNMDCVVAEIK	R	A	99.70%	57.6	33.1	16.7	53.2
LTAEIENAK	R	C	97.30%	37.1	35.2	18.7	26.7
ALEESNYELEGK	R	I	99.70%	76.1	32.8	13.3	76.1
LENEIQTYR	R	S	99.70%	50.5	34	23.9	39.3
QSLEASLAETEGR	K	Y	99.70%	64.6	35.2	18.4	58.8
VTMQNLNDR	R	L	99.70%	64.9	34.1	34.1	0
IWHHTFYNELR	K	V	99.70%	29.7	34.3	13.3	28
LCYVALDFEQEMATAASSSSLEK	K	S	99.70%	30.4	34.1	0	30.4
TTGIVMDSGDGVTHTVPIYEGYALPHAILR	R	L	99.70%	55.8	34.2	13.1	55.8
VAPEEHPVLLTEAPLNPK	R	A	99.70%	35	31.8	0	13.8
NSLENTLTSEAR	R	Y	99.60%	43.5	34.4	20.6	41.5
YVNWIQQTIAAN	K	-	99.50%	42.3	34.5	14.9	11.4

APPENDIX A (continued)

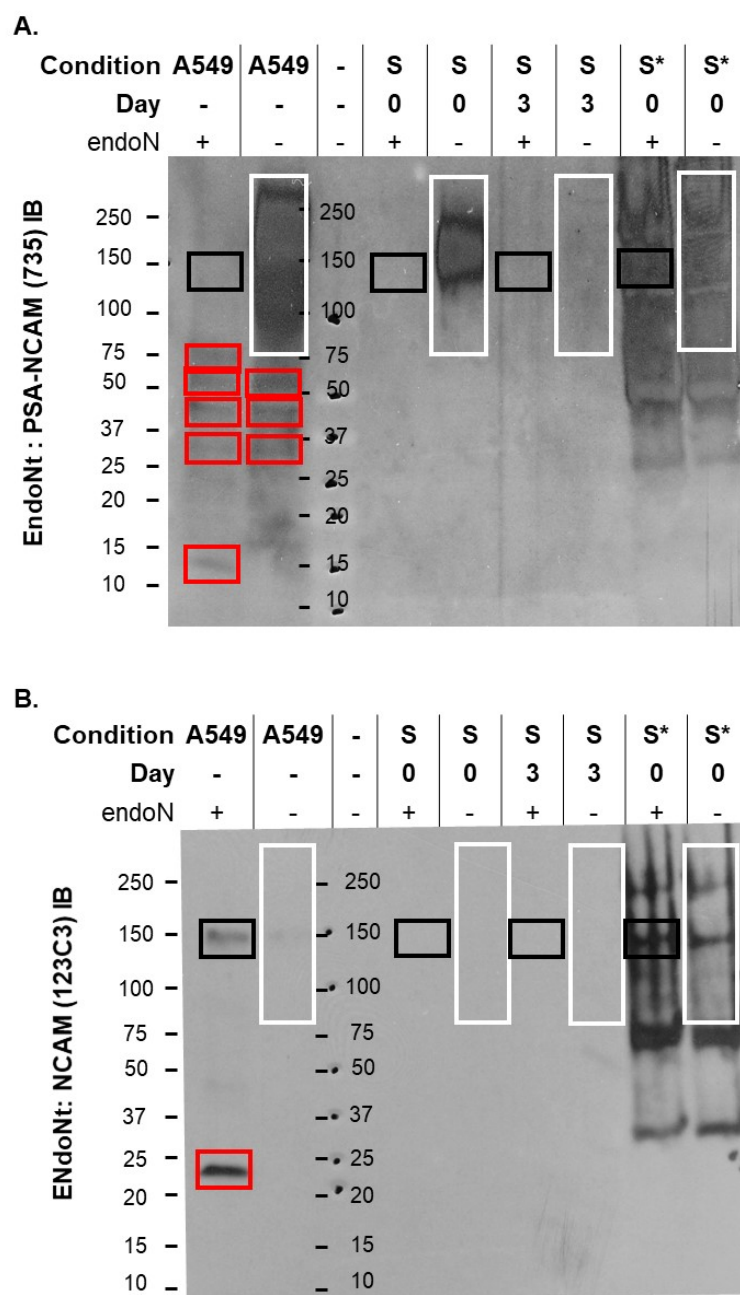


Figure 57. 735 reactivity to polysialyic acid is observed in uninjured skin, but not wounds and neither express NCAM-140.

APPENDIX A (continued)

Figure 57. 735 reactivity to polysialic acid is observed in uninjured skin, but not wounds and neither express NCAM-140.

Proteins underwent EndoNt recovery in positive control (A549, lanes 1-2) NCAM overexpressing cell lysates, uninjured skin (S0, lanes 4-5), and skin 3 days post-wounding (S3, lanes 6-7) or no EndoNt recovery (S*0, lanes 8-9) followed by 735 polysialic acid Ab (A) or 123C3 NCAM Ab (B) immunoblotting. All samples were treated concurrently. SDS- PAGE and immunoblotting were ran concomitantly in individual gels/blots. Results revealed treatment with catalytically active endoN (+) confirmed polysialic acid specificity in EndoNt recovered samples, but not in samples that did not undergo endoNt recovery (S*0, lanes 8-9).

As expected, EndoNt recovered proteins obtained from A549 cells (A, lane 2) and uninjured skin (A, lane 5) express polysialic in the 735 IB (A) when they are not treated with endoN (-), however, skin 3 days post- wounding did not demonstrate any polysialic acid expression. This finding was in contrast to what was observed in the 12F8 immunoblots. Additionally, the 123C3 Ab didn't bind NCAM when A549 cell lysates contained polysialic acid (B, lane 2). However, when treated with endoneuraminidase (+), 123C3 bound EndoNt recovered proteins from A549 cells (B, lane 1)), but not uninjured skin (B, lane 4). 123C3 binding to A549 cell lysates identified a band at the expected molecular weight of NCAM-140 (black box) in addition to multiple unexpected and/ or non- specific bands (red). The absence of NCAM-180 and NCAM-140 staining in the uninjured skin, aligns with the previous NCAM (PT) immunoblots. Presence of 735 reactivity in uninjured skin, no 735 reactivity in wounds, 12F8 reactivity in uninjured skin with higher 12F8 reactivity in wounds may suggest that uninjured skin expresses polysialic acids of with longer chain lengths, while 12F8 expresses higher quantities of polysialic acid with shorter chain lengths. This is suggested by the specificity that 735 Ab has for polysialic acids that are 11 sialic acids in length or more. This occurs as 735 has 4 binding sites which recognize every three sialic acid units in a paired manner⁹. While the specificity of 12F8 is not well understood, it likely binds similar to endoNF (K1F), endoNA (PK1A2), or endoN (PK1E) which bind oligo-/ polysialic acids that are 6 sialic acids in length or more, or endoNE (12E3) which bind oligo-/ polysialic acids that are 5 sialic acids in length or more¹⁴.

Expected band for polysialic acid (white box).

Unexpected and/ or non- specific bands (red box) in A549 cells.

Note blot A was over exposed after 2-5 s of exposure to the film, while blot B required >5 min of exposure to identify the 123C3 band in A549 cell lines.

APPENDIX A (continued)

TABLE XVII.

TABLE OF EXPECTED POLYSIALIC ACID ACCEPTOR PROTEINS, MW, ENZYMES INVOLVED, AND THE LOCATION OF POLYSIALIC ACID

Protein Name	Uniprot Estimated MW by a.a <i>mmu</i> / <i>hsa</i> (kDa)	Observed Glycosylated MW (kDa)	Polysialyl- Transferase Related Enzyme (Gene)	Observed MW + Polysialic Acid (kDa)	Location of Polysialic Acid
Neural cell adhesion molecule (NCAM1)	67-119/ 41- 95	85- 180 by WB	ST8Sia-II (<i>ST8SIA2</i>) / ST8Sia-IV (<i>ST8SIA4</i>)	110-115, 250+	Ig-like C2-type 5 (407-492)
NCAM-180	119/ 95	180			
NCAM1-140	94/ 93	140			
NCAM1-120	80/ 84	120			
NCAM1_v4	67/ 80	unknown			
NCAM1_v5	- / 74	unknown			
NCAM1_v6	- / 41	unknown			
Cell adhesion molecule (CADM1/ SynCam)	50 /49	85-110 (44, 48, 60-65, 107 by WB)	ST8Sia-II (<i>ST8SIA2</i>)	100-150	Ig-like C2-type 1 (147-241)
Neuropilin (NRP2)	105	115	ST8Sia-IV (<i>ST8SIA4</i>)	125, 130	MAM -F5/8 type C2 linker region (592- 642)
C-C chemokine receptor type 7 (CCR7)	43				-
E-selectin ligand also known as Golgi apparatus protein 1 (ESL1/ GLG1/ GSLG1)	134/ 135	135, 150 (130- 160 by WB)	ST8Sia-IV (<i>ST8SIA4</i>)	150- 160	-
Alpha-2,8- sialyltransferase 8B (ST8Sia-II /STX/ SIAT8B)	42		ST8Sia-II (<i>ST8SIA2</i>)	150-250	Polybasic regions (86-120, 261-292) Lys114/118. Can add sialic acid to α 2,3- or α 2,6- sialic acids.
CMP-N- acetylneuraminate- poly-alpha-2,8- sialyltransferase (ST8Sia-IV/ SIAT8D/ PST)	41		ST8Sia-IV (<i>ST8SIA4</i>)	150-250	Polybasic regions (71-105, 246-277) Arg82/Lys99. Adds to α 2, 8 sialic acids only.
Unknown protein from monocyte lysate				80-105	

APPENDIX A (continued)

TABLE XVIII.
GENES UPREGULATED IN SKIN VERSUS TONGUE WOUND HEALING

Entrez ID	Gene Name (Upregulated in Skin)	Gene Symbol	KEGG ID
333424	alpha-1,4-N-acetylglucosaminyltransferase(A4gnt)	<i>A4GNT</i>	mmu:333424
67758	arylacetamide deacetylase (esterase)(Aadac)	<i>AADAC</i>	mmu:67758
11595	aggrecan(Acan)	<i>ACAN</i>	mmu:11595
171168	alkaline ceramidase 1(Acer1)	<i>ACER1</i>	mmu:171168
66190	alkaline ceramidase 3(Acer3)	<i>ACER3</i>	mmu:66190
11461	actin, beta(Actb)	<i>ACTB</i>	mmu:11461
70292	actin filament associated protein 1(Afap1)	<i>AFAP1</i>	mmu:70292
11576	alpha fetoprotein(Afp)	<i>AFP</i>	mmu:11576
11603	agrin(Agrn)	<i>AGRN</i>	mmu:11603
11676	aldolase C, fructose-bisphosphate(Aldoc)	<i>ALDOC</i>	mmu:11676
208211	asparagine-linked glycosylation 1 (beta-1,4-mannosyltransferase)(Alg1)	<i>ALG1</i>	mmu:208211
380959	asparagine-linked glycosylation 10B (alpha-1,2-glucosyltransferase)(Alg10b)	<i>ALG10B</i>	mmu:380959
207958	asparagine-linked glycosylation 11 (alpha-1,2-mannosyltransferase)(Alg11)	<i>ALG11</i>	mmu:207958
66789	asparagine-linked glycosylation 14(Alg14)	<i>ALG14</i>	mmu:66789
56737	asparagine-linked glycosylation 2 (alpha-1,3-mannosyltransferase)(Alg2)	<i>ALG2</i>	mmu:56737
208624	asparagine-linked glycosylation 3 (alpha-1,3-mannosyltransferase)(Alg3)	<i>ALG3</i>	mmu:208624
66248	asparagine-linked glycosylation 5 (dolichyl-phosphate beta-glucosyltransferase)(Alg5)	<i>ALG5</i>	mmu:66248
102580	asparagine-linked glycosylation 9 (alpha 1,2 mannosyltransferase)(Alg9)	<i>ALG9</i>	mmu:102580
245847	amidohydrolase domain containing 2(Amdhd2)	<i>AMDHD2</i>	mmu:245847
11746	annexin A4(Anxa4)	<i>ANXA4</i>	mmu:11746
11747	annexin A5(Anxa5)	<i>ANXA5</i>	mmu:11747
11750	annexin A7(Anxa7)	<i>ANXA7</i>	mmu:11750
27052	acyloxyacyl hydrolase(Aoah)	<i>AOAH</i>	mmu:27052
11828	aquaporin 3(Aqp3)	<i>AQP3</i>	mmu:11828
11883	arylsulfatase A(Arsa)	<i>ARSA</i>	mmu:11883
74008	arylsulfatase G(Arsg)	<i>ARSG</i>	mmu:74008
545260	arylsulfatase i(Arsi)	<i>ARSI</i>	mmu:545260
11886	N-acylsphingosine amidohydrolase 1(Asah1)	<i>ASAH1</i>	mmu:11886
54447	N-acylsphingosine amidohydrolase 2(Asah2)	<i>ASAH2</i>	mmu:54447
12010	beta-2 microglobulin(B2m)	<i>B2M</i>	mmu:12010
97884	UDP-GalNAc:betaGlcNAc beta 1,3-galactosaminyltransferase, polypeptide 2(B3galnt2)	<i>B3GALNT2</i>	mmu:97884
117592	UDP-Gal:betaGal beta 1,3-galactosyltransferase, pp 6(B3galt6)	<i>B3GALT6</i>	mmu:117592
72727	beta-1,3-glucuronyltransferase 3 (glucuronosyltransferase I)(B3gat3)	<i>B3GAT3</i>	mmu:72727
53625	UDP-GlcNAc:betaGal beta-1,3-N-acetylglucosaminyltransferase2(B3gnt2)	<i>B3GNT2</i>	mmu:53625
232984	UDP-GlcNAc:betaGal beta-1,3-N-acetylglucosaminyltransferase8(B3gnt8)	<i>B3GNT8</i>	mmu:232984
97440	UDP-GlcNAc:betaGal beta-1,3-N-acetylglucosaminyltransferase 9(B3gnt9)	<i>B3GNT9</i>	mmu:97440
14421	beta-1,4-N-acetyl-galactosaminyl transferase 1(B4galnt1)	<i>B4GALNT1</i>	mmu:14421
14422	beta-1,4-N-acetyl-galactosaminyl transferase 2(B4galnt2)	<i>B4GALNT2</i>	mmu:14422
330671	beta-1,4-N-acetyl-galactosaminyl transferase 4(B4galnt4)	<i>B4GALNT4</i>	mmu:330671
14595	UDP-Gal:betaGlcNAc beta 1,4- galactosyltransferase, pp 1(B4galt1)	<i>B4GALT1</i>	mmu:14595
53418	UDP-Gal:betaGlcNAc beta 1,4- galactosyltransferase, pp 2(B4galt2)	<i>B4GALT2</i>	mmu:53418

APPENDIX A (continued)

TABLE XVIII. (continued)

GENES UPREGULATED IN SKIN VERSUS TONGUE WOUND HEALING

Entrez ID	Gene Name (Upregulated in Skin)	Gene Symbol	KEGG ID
57370	UDP-Gal:betaGlcNAc beta 1,4-galactosyltransferase, polypeptide 3(B4galt3)	<i>B4GALT3</i>	mmu:57370
56386	UDP-Gal:betaGlcNAc beta 1,4-galactosyltransferase, polypeptide 6(B4galt6)	<i>B4GALT6</i>	mmu:56386
218271	xylosylprotein beta1,4-galactosyltransferase, polypeptide 7 (galactosyltransferase I) (B4galt7)	<i>B4GALT7</i>	mmu:218271
12111	biglycan(Bgn)	<i>BGN</i>	mmu:12111
94192	core 1 synthase, glycoprotein-N-acetylgalactosamine 3-beta-galactosyltransferase, 1(C1galt1)	<i>C1GALT1</i>	mmu:94192
12317	calreticulin(Calr)	<i>CALR</i>	mmu:12317
12330	calnexin(Canx)	<i>CANX</i>	mmu:12330
12479	CD1d1 antigen(Cd1d1)	<i>CD1D1</i>	mmu:12479
246278	CD207 antigen(Cd207)	<i>CD207</i>	mmu:246278
170786	CD209a antigen(Cd209a)	<i>CD209A</i>	mmu:170786
69165	CD209b antigen(Cd209b)	<i>CD209B</i>	mmu:69165
170779	CD209d antigen(Cd209d)	<i>CD209D</i>	mmu:170779
170780	CD209e antigen(Cd209e)	<i>CD209E</i>	mmu:170780
70192	CD209g antigen(Cd209g)	<i>CD209G</i>	mmu:70192
12505	CD44 antigen(Cd44)	<i>CD44</i>	mmu:12505
16149	CD74 antigen (invariant polypeptide of major histocompatibility complex, class II antigen-associated)(Cd74)	<i>CD74</i>	mmu:16149
12522	CD83 antigen(Cd83)	<i>CD83</i>	mmu:12522
17064	CD93 antigen(Cd93)	<i>CD93</i>	mmu:17064
12550	cadherin 1(Cdh1)	<i>CDH1</i>	mmu:12550
12566	cyclin-dependent kinase 2(Cdk2)	<i>CDK2</i>	mmu:12566
99151	cerebral endothelial cell adhesion molecule(Cercam)	<i>CERCAM</i>	mmu:99151
223753	ceramide kinase(Cerk)	<i>CERK</i>	mmu:223753
76893	ceramide synthase 2(Cers2)	<i>CERS2</i>	mmu:76893
67260	ceramide synthase 4(Cers4)	<i>CERS4</i>	mmu:67260
71949	ceramide synthase 5(Cers5)	<i>CERS5</i>	mmu:71949
241447	ceramide synthase 6(Cers6)	<i>CERS6</i>	mmu:241447
104158	carboxylesterase 1D(Ces1d)	<i>CES1D</i>	mmu:104158
234564	carboxylesterase 1F(Ces1f)	<i>CES1F</i>	mmu:234564
12652	chromogranin A(Chga)	<i>CHGA</i>	mmu:12652
68038	chitinase domain containing 1(Chid1)	<i>CHID1</i>	mmu:68038
12654	chitinase-like 1(Chil1)	<i>CHIL1</i>	mmu:12654
74241	chondroitin polymerizing factor(Chpf)	<i>CHPF</i>	mmu:74241
100910	chondroitin polymerizing factor 2(Chpf2)	<i>CHPF2</i>	mmu:100910
76969	carbohydrate (keratan sulfate Gal-6) sulfotransferase 1(Chst1)	<i>CHST1</i>	mmu:76969
58250	carbohydrate sulfotransferase 11(Chst11)	<i>CHST11</i>	mmu:58250
59031	carbohydrate sulfotransferase 12(Chst12)	<i>CHST12</i>	mmu:59031
71797	carbohydrate (chondroitin 4) sulfotransferase 13(Chst13)	<i>CHST13</i>	mmu:71797
72136	carbohydrate (N-acetylgalactosamine 4-O) sulfotransferase 14(Chst14)	<i>CHST14</i>	mmu:72136
269941	chondroitin sulfate synthase 1(Chsy1)	<i>CHSY1</i>	mmu:269941
78923	chondroitin sulfate synthase 3(Chsy3)	<i>CHSY3</i>	mmu:78923
17312	C-type lectin domain family 10, member A(Clec10a)	<i>CLEC10A</i>	mmu:17312

APPENDIX A (continued)

TABLE XVIII. (continued)**GENES UPREGULATED IN SKIN VERSUS TONGUE WOUND HEALING**

Entrez ID	Gene Name (Upregulated in Skin)	Gene Symbol	KEGG ID
69810	C-type lectin domain family 4, member b1(Clec4b1)	<i>CLEC4B1</i>	mmu:69810
17474	C-type lectin domain family 4, member d(Clec4d)	<i>CLEC4D</i>	mmu:17474
56619	C-type lectin domain family 4, member e(Clec4e)	<i>CLEC4E</i>	mmu:56619
56620	C-type lectin domain family 4, member n(Clec4n)	<i>CLEC4N</i>	mmu:56620
56644	C-type lectin domain family 7, member a(Clec7a)	<i>CLEC7A</i>	mmu:56644
12763	cytidine monophospho-N-acetylneuraminic acid hydroxylase(Cmah)	<i>CMAH</i>	mmu:12763
12822	collagen, type XVIII, alpha 1(Col18a1)	<i>COL18A1</i>	mmu:12822
68018	collagen, type IV, alpha 3 (Goodpasture antigen) binding protein (Col4a3bp)	<i>COL4A3BP</i>	mmu:68018
234407	collagen beta(1-O)galactosyltransferase 1(Colgalt1)	<i>COLGALT1</i>	mmu:234407
11630	crystallin beta-gamma domain containing 1 (crybg1)	<i>CRYBG1</i>	mmu:11630
234356	chondroitin sulfate N-acetylgalactosaminyltransferase 1(Csgalnact1)	<i>CSGALNACT1</i>	mmu:234356
83429	cystinosis, nephropathic(Ctns)	<i>CTNS</i>	mmu:83429
19025	cathepsin A(Ctsa)	<i>CTSA</i>	mmu:19025
109754	cytochrome b5 reductase 3(Cyb5r3)	<i>CYB5R3</i>	mmu:109754
13135	defender against cell death 1(Dad1)	<i>DAD1</i>	mmu:13135
13200	dolichyl-di-phosphooligosaccharide-protein glycotransferase (Ddost)	<i>DDOST</i>	mmu:13200
70059	delta(4)-desaturase, sphingolipid 2(Degs2)	<i>DEGS2</i>	mmu:70059
227697	dolichol kinase (Dolk)	<i>DOLK</i>	mmu:227697
13478	dolichyl-phosphate (UDP-N-acetylglucosamine) acetylglucosaminophosphotransferase1(GlcNAc-1-P transferase) (Dpagt1)	<i>DPAGT1</i>	mmu:13478
13481	dolichol-phosphate (beta-D) mannosyltransferase 2(Dpm2)	<i>DPM2</i>	mmu:13481
68563	dolichyl-phosphate mannosyltransferase polypeptide 3(Dpm3)	<i>DPM3</i>	mmu:68563
13482	dipeptidylpeptidase 4(Dpp4)	<i>DPP4</i>	mmu:13482
212898	dermatan sulfate epimerase (Dse)	<i>DSE</i>	mmu:212898
319901	dermatan sulfate epimerase-like (Dsel)	<i>DSEL</i>	mmu:319901
192193	ER degradation enhancer, mannosidase alpha-like 1(Edem1)	<i>EDEM1</i>	mmu:192193
108687	ER degradation enhancer, mannosidase alpha-like 2(Edem2)	<i>EDEM2</i>	mmu:108687
66967	ER degradation enhancer, mannosidase alpha-like 3(Edem3)	<i>EDEM3</i>	mmu:66967
54325	elongation of very long chain fatty acids (FEN1/Elo2, SUR4/Elo3, yeast)-like 1(Elov1)	<i>ELOVL1</i>	mmu:54325
12686	elongation of very long chain fatty acids (FEN1/Elo2, SUR4/Elo3, yeast)-like 3(Elov13)	<i>ELOVL3</i>	mmu:12686
83603	elongation of very long chain fatty acids (FEN1/Elo2, SUR4/Elo3, yeast)-like 4(Elov14)	<i>ELOVL4</i>	mmu:83603
68801	ELOVL family member 5, elongation of long chain fatty acids (yeast)(Elov15)	<i>ELOVL5</i>	mmu:68801
170439	ELOVL family member 6, elongation of long chain fatty acids (yeast)(Elov16)	<i>ELOVL6</i>	mmu:170439
217364	endo-beta-N-acetylglucosaminidase(Engase)	<i>ENGASE</i>	mmu:217364
101351	EGF domain-specific O-linked N-acetylglucosamine (GlcNAc) transferase (Eogt)	<i>EOGT</i>	mmu:101351
14042	exostoses (multiple) 1(Ext1)	<i>EXT1</i>	mmu:14042
54616	exostoses (multiple)-like 3(Extl3)	<i>EXTL3</i>	mmu:54616
215015	family with sequence similarity 20, member B(Fam20b)	<i>FAM20B</i>	mmu:215015
14121	fructose bisphosphatase 1(Fbp1)	<i>FBP1</i>	mmu:14121

APPENDIX A (continued)

TABLE XVIII. (continued)

GENES UPREGULATED IN SKIN VERSUS TONGUE WOUND HEALING

Entrez ID	Gene Name (Upregulated in Skin)	Gene Symbol	KEGG ID
50760	F-box protein 17(Fbxo17)	<i>FBXO17</i>	mmu:50760
14169	fibroblast growth factor 14(Fgf14)	<i>FGF14</i>	mmu:14169
14172	fibroblast growth factor 18(Fgf18)	<i>FGF18</i>	mmu:14172
14176	fibroblast growth factor 5(Fgf5)	<i>FGF5</i>	mmu:14176
14183	fibroblast growth factor receptor 2(Fgfr2)	<i>FGFR2</i>	mmu:14183
14264	fibromodulin(Fmod)	<i>FMOD</i>	mmu:14264
71665	fucosidase, alpha-L- 1, tissue(Fuca1)	<i>FUCA1</i>	mmu:71665
66848	fucosidase, alpha-L- 2, plasma(Fuca2)	<i>FUCA2</i>	mmu:66848
73068	fucosyltransferase 11(Fut11)	<i>FUT11</i>	mmu:73068
14344	fucosyltransferase 2(Fut2)	<i>FUT2</i>	mmu:14344
14345	fucosyltransferase 4(Fut4)	<i>FUT4</i>	mmu:14345
53618	fucosyltransferase 8(Fut8)	<i>FUT8</i>	mmu:53618
57265	frizzled class receptor 2(Fzd2)	<i>FZD2</i>	mmu:57265
74246	galactose-4-epimerase, UDP(Gale)	<i>GALE</i>	mmu:74246
14635	galactokinase 1(Galk1)	<i>GALK1</i>	mmu:14635
69976	galactokinase 2(Galk2)	<i>GALK2</i>	mmu:69976
50917	galactosamine (N-acetyl)-6-sulfate sulfatase(Galns)	<i>GALNS</i>	mmu:50917
108148	UDP-N-acetyl-alpha-D-galactosamine:polypeptide N-acetylgalactosaminyltransferase 2(Galnt2)	<i>GALNT2</i>	mmu:108148
14425	UDP-N-acetyl-alpha-D-galactosamine:polypeptide N-acetylgalactosaminyltransferase 3(Galnt3)	<i>GALNT3</i>	mmu:14425
14426	UDP-N-acetyl-alpha-D-galactosamine:polypeptide N-acetylgalactosaminyltransferase 4(Galnt4)	<i>GALNT4</i>	mmu:14426
207839	UDP-N-acetyl-alpha-D-galactosamine:polypeptide N-acetylgalactosaminyltransferase 6(Galnt6)	<i>GALNT6</i>	mmu:207839
108150	UDP-N-acetyl-alpha-D-galactosamine: polypeptide N-acetylgalactosaminyltransferase 7(Galnt7)	<i>GALNT7</i>	mmu:108150
14376	alpha glucosidase 2 alpha neutral subunit(Ganab)	<i>GANAB</i>	mmu:14376
14465	GATA binding protein 6(Gata6)	<i>GATA6</i>	mmu:14465
14537	glucosaminyl (N-acetyl) transferase 1, core 2(Gcnt1)	<i>GCNT1</i>	mmu:14537
14538	glucosaminyl (N-acetyl) transferase 2, I-branching enzyme(Gcnt2)	<i>GCNT2</i>	mmu:14538
14583	glutamine fructose-6-phosphate transaminase 1(Gfpt1)	<i>GFPT1</i>	mmu:14583
14594	glycoprotein galactosyltransferase alpha 1, 3(Ggta1)	<i>GGTA1</i>	mmu:14594
11605	galactosidase, alpha(Gla)	<i>GLA</i>	mmu:11605
12091	galactosidase, beta 1(Glb1)	<i>GLB1</i>	mmu:12091
76485	glycosyltransferase 8 domain containing 1(Glt8d1)	<i>GLT8D1</i>	mmu:76485
56356	glycolipid transfer protein(Gltp)	<i>GLTP</i>	mmu:56356
218138	GDP-mannose 4, 6-dehydratase(Gmds)	<i>GMDS</i>	mmu:218138
69080	GDP-mannose pyrophosphorylase A(Gmppa)	<i>GMPPA</i>	mmu:69080
331026	GDP-mannose pyrophosphorylase B(Gmppb)	<i>GMPPB</i>	mmu:331026
14688	guanine nucleotide binding protein (G protein), beta 1(Gnb1)	<i>GNB1</i>	mmu:14688
50798	glucosamine (UDP-N-acetyl)-2-epimerase/N-acetylmannosamine kinase(Gne)	<i>GNE</i>	mmu:50798
26384	glucosamine-6-phosphate deaminase 1(Gnpda1)	<i>GNPDA1</i>	mmu:26384
432486	N-acetylglucosamine-1-phosphate transferase, alpha and beta subunits(Gnptab)	<i>GNPTAB</i>	mmu:432486

APPENDIX A (continued)

TABLE XVIII. (continued)

GENES UPREGULATED IN SKIN VERSUS TONGUE WOUND HEALING

Entrez ID	Gene Name (Upregulated in Skin)	Gene Symbol	KEGG ID
75612	glucosamine (N-acetyl)-6-sulfatase(Gns)	<i>GNS</i>	mmu:75612
14731	GPI anchor attachment protein 1(Gpaa1)	<i>GPAA1</i>	mmu:14731
14735	glypican 4(Gpc4)	<i>GPC4</i>	mmu:14735
23888	glypican 6(Gpc6)	<i>GPC6</i>	mmu:23888
93695	glycoprotein (transmembrane) nmb(Gpnmb)	<i>GNPMB</i>	mmu:93695
227835	glycosyltransferase-like domain containing 1(Gtdc1)	<i>GTDC1</i>	mmu:227835
110006	glucuronidase, beta(Gusb)	<i>GUSB</i>	mmu:110006
223827	glucoside xylosyltransferase 1(Gxylt1)	<i>GXYLT1</i>	mmu:223827
100198	hexose-6-phosphate dehydrogenase (glucose 1-dehydrogenase)(H6pd)	<i>H6PD</i>	mmu:100198
67666	hyaluronan and proteoglycan link protein 3(Hapln3)	<i>HAPLN3</i>	mmu:67666
15116	hyaluronan synthase1(Has1)	<i>HAS1</i>	mmu:15116
15117	hyaluronan synthase 2(Has2)	<i>HAS2</i>	mmu:15117
15118	hyaluronan synthase 3(Has3)	<i>HAS3</i>	mmu:15118
15211	hexosaminidase A(Hexa)	<i>HEXA</i>	mmu:15211
15212	hexosaminidase B(Hexb)	<i>HEXB</i>	mmu:15212
52120	heparan-alpha-glucosaminide N-acetyltransferase(Hgsnat)	<i>HGSNAT</i>	mmu:52120
212032	hexokinase 3(Hk3)	<i>HK3</i>	mmu:212032
15288	hydroxymethylbilane synthase(Hmbs)	<i>HMBS</i>	mmu:15288
15366	hyaluronan mediated motility receptor (RHAMM)(Hmnr)	<i>HMMR</i>	mmu:15366
15404	homeobox A7(Hoxa7)	<i>HOXA7</i>	mmu:15404
23908	heparan sulfate 2-O-sulfotransferase 1(Hs2st1)	<i>HS2ST1</i>	mmu:23908
328779	heparan sulfate (glucosamine) 3-O-sulfotransferase 6(Hs3st6)	<i>HS3ST6</i>	mmu:328779
50786	heparan sulfate 6-O-sulfotransferase 2(Hs6st2)	<i>HS6ST2</i>	mmu:50786
15587	hyaluronoglucosaminidase 2(Hyal2)	<i>HYAL2</i>	mmu:15587
15894	intercellular adhesion molecule 1(Icam1)	<i>ICAM1</i>	mmu:15894
16400	integrin alpha 3(Itga3)	<i>ITGA3</i>	mmu:16400
16477	jun B proto-oncogene(Junb)	<i>JUNB</i>	mmu:16477
70750	3-ketodihydrosphingosine reductase(Kdsr)	<i>KDSR</i>	mmu:70750
16545	keratocan(Kera)	<i>KERA</i>	mmu:16545
170733	killer cell lectin-like receptor, subfamily A, member 17(Klra17)	<i>KLRA17</i>	mmu:170733
16633	killer cell lectin-like receptor, subfamily A, member 2(Klra2)	<i>KLRA2</i>	mmu:16633
80782	killer cell lectin-like receptor subfamily B member 1B(Klrb1b)	<i>KLRB1B</i>	mmu:80782
16641	killer cell lectin-like receptor subfamily C, member 1(Klrc1)	<i>KLRC1</i>	mmu:16641
16784	lysosomal-associated membrane protein 2(Lamp2)	<i>LAMP2</i>	mmu:16784
228366	LARGE xylosyl- and glucuronyltransferase 2(Large2)	<i>LARGE2</i>	mmu:228366
244864	layilin(Layn)	<i>LAYN</i>	mmu:244864
16848	LFNG O-fucosylpeptide 3-beta-N-acetylglucosaminyltransferase(Lfng)	<i>LFNG</i>	mmu:16848
16852	lectin, galactose binding, soluble 1(Lgals1)	<i>LGALS1</i>	mmu:16852
56072	lectin, galactose binding, soluble 12(Lgals12)	<i>LGALS12</i>	mmu:56072
16854	lectin, galactose binding, soluble 3(Lgals3)	<i>LGALS3</i>	mmu:16854
16858	lectin, galactose binding, soluble 7(Lgals7)	<i>LGALS7</i>	mmu:16858
16859	lectin, galactose binding, soluble 9(Lgals9)	<i>LGALS9</i>	mmu:16859
16889	lysosomal acid lipase A(Lipa)	<i>LIPA</i>	mmu:16889
70361	lectin, mannose-binding, 1(Lman1)	<i>LMAN1</i>	mmu:70361
235416	lectin, mannose-binding 1 like(Lman1l)	<i>LMAN1L</i>	mmu:235416
66890	lectin, mannose-binding 2(Lman2)	<i>LMAN2</i>	mmu:66890
17076	lymphocyte antigen 75(Ly75)	<i>LY75</i>	mmu:17076

APPENDIX A (continued)

TABLE XVIII. (continued)**GENES UPREGULATED IN SKIN VERSUS TONGUE WOUND HEALING**

Entrez ID	Gene Name (Upregulated in Skin)	Gene Symbol	KEGG ID
332427	lysozyme G-like 2(Lyg2)	LYG2	mmu:332427
17110	lysozyme 1(Lyz1)	LYZ1	mmu:17110
17105	lysozyme 2(Lyz2)	LYZ2	mmu:17105
17113	mannose-6-phosphate receptor, cation dependent(M6pr)	M6PR	mmu:17113
17155	mannosidase 1, alpha(Man1a)	MAN1A	mmu:17155
227619	mannosidase, alpha, class 1B, member 1(Man1b1)	MAN1B1	mmu:227619
17158	mannosidase 2, alpha 1(Man2a1)	MAN2A1	mmu:17158
110173	mannosidase, beta A, lysosomal(Manba)	MANBA	mmu:110173
17242	midkine(Mdk)	MDK	mmu:17242
217664	mannoside acetylglucosaminyltransferase 2(Mgat2)	MGAT2	mmu:217664
269181	mannoside acetylglucosaminyltransferase 4, isoenzyme A(Mgat4a)	MGAT4A	mmu:269181
107895	mannoside acetylglucosaminyltransferase 5(Mgat5)	MGAT5	mmu:107895
268510	mannoside acetylglucosaminyltransferase 5, isoenzyme B(Mgat5b)	MGAT5B	mmu:268510
76055	meningioma expressed antigen 5 (hyaluronidase)(Mgea5)	MGEA5	mmu:76055
216864	macrophage galactose N-acetyl-galactosamine specific lectin 2(Mgl2)	MGL2	mmu:216864
57377	mannosyl-oligosaccharide glucosidase(Mogs)	MOGS	mmu:57377
24070	mannose-P-dolichol utilization defect 1(Mpdu1)	MPDU1	mmu:24070
17533	mannose receptor, C type 1(Mrc1)	MRC1	mmu:17533
17534	mannose receptor, C type 2(Mrc2)	MRC2	mmu:17534
17869	myelocytomatosis oncogene(Myc)	MYC	mmu:17869
67111	N-acylethanolamine acid amidase(Naaa)	NAAA	mmu:67111
17939	N-acetyl galactosaminidase, alpha(Naga)	NAGA	mmu:17939
56174	N-acetylglucosamine kinase(Nagk)	NAGK	mmu:56174
17975	nucleolin(Ncl)	NCL	mmu:17975
15531	N-deacetylase/N-sulfotransferase (heparan glucosaminyl) 1(Ndst1)	NDST1	mmu:15531
17423	N-deacetylase/N-sulfotransferase (heparan glucosaminyl) 2(Ndst2)	NDST2	mmu:17423
18010	neuraminidase 1(Neu1)	NEU1	mmu:18010
23956	neuraminidase 2(Neu2)	NEU2	mmu:23956
50877	neuraminidase 3(Neu3)	NEU3	mmu:50877
216856	neurologin 2(Nlgn2)	NLGN2	mmu:216856
74091	N-acetylneuraminate pyruvate lyase(Npl)	NPL	mmu:74091
18187	neuropilin 2(Nrp2)	NRP2	mmu:18187
216440	amplified in osteosarcoma(Os9)	OS9	mmu:216440
67695	oligosaccharyltransferase complex subunit 4 (non-catalytic)(Ost4)	OST4	mmu:67695
56401	prolyl 3-hydroxylase 1(P3h1)	P3H1	mmu:56401
23971	3'-phosphoadenosine 5'-phosphosulfate synthase 1(Papss1)	PAPSS1	mmu:23971
23972	3'-phosphoadenosine 5'-phosphosulfate synthase 2(Papss2)	PAPSS2	mmu:23972
18563	pyruvate carboxylase(Pcx)	PCX	mmu:18563
14827	protein disulfide isomerase associated 3(Pdia3)	PDIA3	mmu:14827
170768	6-phosphofructo-2-kinase/fructose-2,6-biphosphatase 3(Pfkfb3)	PFKFB3	mmu:170768
18641	phosphofructokinase, liver, B-type(Pfkl)	PFKL	mmu:18641
56421	phosphofructokinase, platelet(Pfkp)	PFKP	mmu:56421
241062	post-GPI attachment to proteins 1(Pgap1)	PGAP1	mmu:241062
66681	phosphoglucomutase 1(Pgm1)	PGM1	mmu:66681
109785	phosphoglucomutase 3(Pgm3)	PGM3	mmu:109785
18700	phosphatidylinositol glycan anchor biosynthesis, class A(Piga)	PIGA	mmu:18700
67292	phosphatidylinositol glycan anchor biosynthesis, class C(Pigc)	PIGC	mmu:67292

APPENDIX A (continued)

TABLE XVIII. (continued)

GENES UPREGULATED IN SKIN VERSUS TONGUE WOUND HEALING

Entrez ID	Gene Name (Upregulated in Skin)	Gene Symbol	KEGG ID
18701	phosphatidylinositol glycan anchor biosynthesis, class F(Pigf)	<i>PIGF</i>	mmu:18701
329777	phosphatidylinositol glycan anchor biosynthesis, class K(Pigk)	<i>PIGK</i>	mmu:329777
327942	phosphatidylinositol glycan anchor biosynthesis, class L(Pigl)	<i>PIGL</i>	mmu:327942
67556	phosphatidylinositol glycan anchor biosynthesis, class M(Pigm)	<i>PIGM</i>	mmu:67556
27392	phosphatidylinositol glycan anchor biosynthesis, class N(Pign)	<i>PIGN</i>	mmu:27392
56703	phosphatidylinositol glycan anchor biosynthesis, class O(Pigo)	<i>PIGO</i>	mmu:56703
14755	phosphatidylinositol glycan anchor biosynthesis, class Q(Pigq)	<i>PIGQ</i>	mmu:14755
276846	phosphatidylinositol glycan anchor biosynthesis, class S(Pigs)	<i>PIGS</i>	mmu:276846
72084	phosphatidylinositol glycan anchor biosynthesis, class X(Pigx)	<i>PIGX</i>	mmu:72084
18793	plasminogen activator, urokinase receptor(Plaur)	<i>PLAUR</i>	mmu:18793
26433	procollagen-lysine, 2-oxoglutarate 5-dioxygenase 3(Plod3)	<i>PLOD3</i>	mmu:26433
50784	phospholipid phosphatase 2(Plpp2)	<i>PLPP2</i>	mmu:50784
54128	phosphomannomutase 2(Pmm2)	<i>PMM2</i>	mmu:54128
80294	protein O-fucosyltransferase 2(Pofut2)	<i>POFUT2</i>	mmu:80294
224143	protein O-glucosyltransferase 1(Poglut1)	<i>POGLUT1</i>	mmu:224143
244416	protein phosphatase 1, regulatory (inhibitor) subunit 3B(Ppp1r3b)	<i>PPP1R3B</i>	mmu:244416
19089	protein kinase C substrate 80K-H(Prkcsh)	<i>PRKCSH</i>	mmu:19089
19242	pleiotrophin(Ptn)	<i>PTN</i>	mmu:19242
110078	brain glycogen phosphorylase(Pygb)	<i>PYGB</i>	mmu:110078
110095	liver glycogen phosphorylase(Pygl)	<i>PYGL</i>	mmu:110095
14694	receptor for activated C kinase 1(Rack1)	<i>RACK1</i>	mmu:14694
19692	regenerating islet-derived 1(Reg1)	<i>REG1</i>	mmu:19692
19703	renin binding protein(Renbp)	<i>RENBP</i>	mmu:19703
19719	RFNG O-fucosylpeptide 3-beta-N-acetylglucosaminyltransferase(Rfng)	<i>RFNG</i>	mmu:19719
22121	ribosomal protein L13A(Rpl13a)	<i>RPL13A</i>	mmu:22121
67891	ribosomal protein L4(Rpl4)	<i>RPL4</i>	mmu:67891
103963	ribophorin I(Rpn1)	<i>RPN1</i>	mmu:103963
20014	ribophorin II(Rpn2)	<i>RPN2</i>	mmu:20014
66404	replication termination factor 2 domain containing 1(Rtfdc1)	<i>RTFDC1</i>	mmu:66404
20201	S100 calcium binding protein A8 (calgranulin A)(S100a8)	<i>S100A8</i>	mmu:20201
20202	S100 calcium binding protein A9 (calgranulin B)(S100a9)	<i>S100A9</i>	mmu:20202
20249	stearoyl-Coenzyme A desaturase 1(Scd1)	<i>SCD1</i>	mmu:20249
20250	stearoyl-Coenzyme A desaturase 2(Scd2)	<i>SCD2</i>	mmu:20250
30049	stearoyl-coenzyme A desaturase 3(Scd3)	<i>SCD3</i>	mmu:30049
20969	syndecan 1(Sdc1)	<i>SDC1</i>	mmu:20969
20971	syndecan 4(Sdc4)	<i>SDC4</i>	mmu:20971
53378	syndecan binding protein(Sdcbp)	<i>SDCBP</i>	mmu:53378
20343	selectin, lymphocyte(Sell)	<i>SELL</i>	mmu:20343
74442	sphingomyelin synthase 2(Sgms2)	<i>SGMS2</i>	mmu:74442
20397	sphingosine phosphate lyase 1(Sgpl1)	<i>SGPL1</i>	mmu:20397
433323	sphingosine-1-phosphate phosphatase 2(Sgpp2)	<i>SGPP2</i>	mmu:433323
27029	N-sulfoglucosamine sulfohydrolase (sulfamidase)(Sgsh)	<i>SGSH</i>	mmu:27029
20423	sonic hedgehog(Shh)	<i>SHH</i>	mmu:20423
83382	sialic acid binding Ig-like lectin E(Siglece)	<i>SIGLECE</i>	mmu:83382
235504	solute carrier family 17 (anion/sugar transporter), member 5(Slc17a5)	<i>SLC17A5</i>	mmu:235504
268512	solute carrier family 26, member 11(Slc26a11)	<i>SLC26A11</i>	mmu:268512
13521	solute carrier family 26 (sulfate transporter), member 2(Slc26a2)	<i>SLC26A2</i>	mmu:13521
23985	solute carrier family 26, member 4(Slc26a4)	<i>SLC26A4</i>	mmu:23985

APPENDIX A (continued)

TABLE XVIII. (continued)

GENES UPREGULATED IN SKIN VERSUS TONGUE WOUND HEALING

Entrez ID	Gene Name (Upregulated in Skin)	Gene Symbol	KEGG ID
208890	solute carrier family 26, member 7(Slc26a7)	SLC26A7	mmu:208890
20525	solute carrier family 2 (facilitated glucose transporter), member 1(Slc2a1)	SLC2A1	mmu:20525
170441	solute carrier family 2 (facilitated glucose transporter), member 10(Slc2a10)	SLC2A10	mmu:170441
239606	solute carrier family 2 (facilitated glucose transporter), member 13(Slc2a13)	SLC2A13	mmu:239606
20527	solute carrier family 2 (facilitated glucose transporter), member 3(Slc2a3)	SLC2A3	mmu:20527
56485	solute carrier family 2 (facilitated glucose transporter), member 5(Slc2a5)	SLC2A5	mmu:56485
227659	solute carrier family 2 (facilitated glucose transporter), member 6(Slc2a6)	SLC2A6	mmu:227659
11416	solute carrier family 33 (acetyl-CoA transporter), member 1(Slc33a1)	SLC33A1	mmu:11416
22232	solute carrier family 35 (UDP-galactose transporter), member A2(Slc35a2)	SLC35A2	mmu:22232
229782	solute carrier family 35 (UDP-N-acetylglucosamine (UDP-GlcNAc) transporter), member 3(Slc35a3)	SLC35A3	mmu:229782
74102	solute carrier family 35, member A5(Slc35a5)	SLC35A5	mmu:74102
110172	solute carrier family 35, member B1(Slc35b1)	SLC35B1	mmu:110172
73836	solute carrier family 35, member B2(Slc35b2)	SLC35B2	mmu:73836
108652	solute carrier family 35, member B3(Slc35b3)	SLC35B3	mmu:108652
58246	solute carrier family 35, member B4(Slc35b4)	SLC35B4	mmu:58246
228368	solute carrier family 35, member C1(Slc35c1)	SLC35C1	mmu:228368
228875	solute carrier family 35, member C2(Slc35c2)	SLC35C2	mmu:228875
17254	solute carrier family 3 (activators of dibasic and neutral amino acid transport), member 2(Slc3a2)	SLC3A2	mmu:17254
20597	sphingomyelin phosphodiesterase 1, acid lysosomal(Smpd1)	SMPD1	mmu:20597
12702	suppressor of cytokine signaling 3(Socs3)	SOCS3	mmu:12702
20692	secreted acidic cysteine rich glycoprotein(Sparc)	SPARC	mmu:20692
20698	sphingosine kinase 1(Sphk1)	SPHK1	mmu:20698
56632	sphingosine kinase 2(Sphk2)	SPHK2	mmu:56632
268656	serine palmitoyltransferase, long chain base subunit 1(Sptlc1)	SPTLC1	mmu:268656
20773	serine palmitoyltransferase, long chain base subunit 2(Sptlc2)	SPTLC2	mmu:20773
228677	serine palmitoyltransferase, long chain base subunit 3(Sptlc3)	SPTLC3	mmu:228677
57357	steroid 5 alpha-reductase 3(Srd5a3)	SRD5A3	mmu:57357
19073	serglycin(Srgn)	SRGN	mmu:19073
20442	ST3 beta-galactoside alpha-2,3-sialyltransferase 1(St3gal1)	ST3GAL1	mmu:20442
20443	ST3 beta-galactoside alpha-2,3-sialyltransferase 4(St3gal4)	ST3GAL4	mmu:20443
240119	beta galactoside alpha 2,6 sialyltransferase 2(St6gal2)	ST6GAL2	mmu:240119
26938	ST6 (alpha-N-acetyl-neuraminyl-2,3-beta-galactosyl-1,3)-N-acetylgalactosaminide alpha-2,6-sialyltransferase 5(St6galnac5)	ST6GALNAC5	mmu:26938
20449	ST8 alpha-N-acetyl-neuraminide alpha-2,8-sialyltransferase 1(St8sia1)	ST8SIA1	mmu:20449
20450	ST8 alpha-N-acetyl-neuraminide alpha-2,8-sialyltransferase 2(St8sia2)	ST8SIA2	mmu:20450
20452	ST8 alpha-N-acetyl-neuraminide alpha-2,8-sialyltransferase 4(St8sia4)	ST8SIA4	mmu:20452
241230	ST8 alpha-N-acetyl-neuraminide alpha-2,8-sialyltransferase 6(St8sia6)	ST8SIA6	mmu:241230
20905	steroid sulfatase(Sts)	STS	mmu:20905

APPENDIX A (continued)

TABLE XVIII. (continued)**GENES UPREGULATED IN SKIN VERSUS TONGUE WOUND HEALING**

Entrez ID	Gene Name (Upregulated in Skin)	Gene Symbol	KEGG ID
16430	STT3, subunit of the oligosaccharyltransferase complex, homolog A (Stt3a)	STT3A	mmu:16430
68292	STT3, subunit of the oligosaccharyltransferase complex, homolog B (Stt3b)	STT3B	mmu:68292
72043	sulfatase 2(Sulf2)	SULF2	mmu:72043
58911	sulfatase modifying factor 1(Sumf1)	SUMF1	mmu:58911
21374	TATA box binding protein(Tbp)	TBP	mmu:21374
106529	trans-2,3-enoyl-CoA reductase(Tecr)	TECR	mmu:106529
21923	tenascin C(Tnc)	TNC	mmu:21923
22021	protein-tyrosine sulfotransferase 1(Tpst1)	TPST1	mmu:22021
22022	protein-tyrosine sulfotransferase 2(Tpst2)	TPST2	mmu:22022
170829	translocating chain-associating membrane protein 2(Tram2)	TRAM2	mmu:170829
80286	tumor suppressor candidate 3(Tusc3)	TUSC3	mmu:80286
22234	UDP-glucose ceramide glucosyltransferase(Ugcg)	UGCG	mmu:22234
22235	UDP-glucose dehydrogenase(Ugdh)	UGDH	mmu:22235
338362	uronyl-2-sulfotransferase(Ust)	UST	mmu:338362
67883	UDP-glucuronate decarboxylase 1(Uxs1)	UXS1	mmu:67883
13003	versican(Vcan)	VCAN	mmu:13003
22415	wingless-type MMTV integration site family, member 3(Wnt3)	WNT3	mmu:22415
268880	xyloside xylosyltransferase 1(Xxylt1)	XXYLT1	mmu:268880
217119	xylosyltransferase II(Xylt2)	XYLT2	mmu:217119
54401	tyrosine 3-monooxygenase/tryptophan 5-monooxygenase activation protein, beta polypeptide(Ywhab)	YWHAB	mmu:54401
22771	zinc finger protein of the cerebellum 1(Zic1)	ZIC1	mmu:22771

APPENDIX A (continued)

TABLE XIX.**GENES DOWNREGULATED IN SKIN VERSUS TONGUE WOUND HEALING**

Entrez ID	Gene Name (Downregulated in Skin)	Gene Symbol	KEGG ID
11350	c-abl oncogene 1, non-receptor tyrosine kinase(Abl1)	<i>ABL1</i>	mmu:11350
11423	acetylcholinesterase(Ache)	<i>ACHE</i>	mmu:11423
11593	aspartylglucosaminidase(Aga)	<i>AGA</i>	mmu:11593
77559	amylase 1, salivary(Amy1)	<i>AGL</i>	mmu:77559
329828	expressed sequence AI464131(AI464131)	<i>AI464131</i>	mmu:329828
11674	aldolase A, fructose-bisphosphate(Aldoa)	<i>ALDOA</i>	mmu:11674
11722	amylase 1, salivary(Amy1)	<i>AMY1</i>	mmu:11722
11750	annexin A7(Anxa7)	<i>ANXA7</i>	mmu:11750
235606	acylpeptide hydrolase(Apeh)	<i>APEH</i>	mmu:235606
68117	apolipoprotein O-like(Apool)	<i>APOOL</i>	mmu:68117
11947	ATP synthase, H ⁺ transporting mitochondrial F1 complex, beta subunit(Atp5b)	<i>ATP5B</i>	mmu:11947
11990	attractin(Atrn)	<i>ATRN</i>	mmu:11990
226255	attractin like 1(Atrnl1)	<i>ATRNL1</i>	mmu:226255
26879	UDP-GalNAc:betaGlcNAc beta 1,3-galactosaminyltransferase, polypeptide 1(B3galnt1)	<i>B3GALNT1</i>	mmu:26879
97884	UDP-GalNAc:betaGlcNAc beta 1,3-galactosaminyltransferase, polypeptide 2(B3galnt2)	<i>B3GALNT2</i>	mmu:97884
26877	UDP-Gal:betaGlcNAc beta 1,3-galactosyltransferase, polypeptide 1(B3galt1)	<i>B3GALT1</i>	mmu:26877
54218	UDP-Gal:betaGlcNAc beta 1,3-galactosyltransferase, polypeptide 4(B3galt4)	<i>B3GALT4</i>	mmu:54218
108902	beta-1,4-glucuronyltransferase 1(B4gat1)	<i>B4GAT1</i>	mmu:108902
12038	butyrylcholinesterase(Bche)	<i>BCHE</i>	mmu:12038
13480	dolichol-phosphate (beta-D) mannosyltransferase 1(Dpm1)	<i>BETA-D</i>	mmu:13480
12159	bone morphogenetic protein 4(Bmp4)	<i>BMP4</i>	mmu:12159
73316	calreticulin 3(Calr3)	<i>CALR3</i>	mmu:73316
12351	carbonic anhydrase 4(Car4)	<i>CAR4</i>	mmu:12351
12623	carboxylesterase 1G(Ces1g)	<i>CES1G</i>	mmu:12623
72361	carboxylesterase 2G(Ces2g)	<i>CES2G</i>	mmu:72361
67935	carboxylesterase 5A(Ces5a)	<i>CES5A</i>	mmu:67935
71884	chitinase 1 (chitotriosidase)(Chit1)	<i>CHIT1</i>	mmu:71884
246048	chondrolectin(Chodl)	<i>CHODL</i>	mmu:246048
77590	carbohydrate (N-acetylgalactosamine 4-sulfate 6-O) sulfotransferase 15(Chst15)	<i>CHST15</i>	mmu:77590
66864	C-type lectin domain family 14, member a(Clec14a)	<i>CLEC14A</i>	mmu:66864
243653	C-type lectin domain family 1, member a(Clec1a)	<i>CLEC1A</i>	mmu:243653
232409	C-type lectin domain family 2, member e(Clec2e)	<i>CLEC2E</i>	mmu:232409
12764	cytidine monophospho-N-acetylneuraminic acid synthetase(Cmas)	<i>CMAS</i>	mmu:12764
12818	collagen, type XIV, alpha 1(Col14a1)	<i>COL14A1</i>	mmu:12818
269132	collagen beta(1-O)galactosyltransferase 2(Colgal2)	<i>COLGALT2</i>	mmu:269132
224273	beta-gamma crystallin domain containing 3(Crybg3)	<i>CRYBG3</i>	mmu:224273
74245	chitobiase, di-N-acetyl-(Ctbs)	<i>CTBS</i>	mmu:74245
72017	cytochrome b5 reductase 1(Cyb5r1)	<i>CYB5R1</i>	mmu:72017
13138	dystroglycan 1(Dag1)	<i>DAG1</i>	mmu:13138
13179	decorin(Dcn)	<i>DCN</i>	mmu:13179
13356	DiGeorge syndrome critical region gene 2(Dgcr2)	<i>DGCR2</i>	mmu:13356
73708	developmental pluripotency-associated 3(Dppa3)	<i>DPPA3</i>	mmu:73708

APPENDIX A (continued)

TABLE XIX. (continued)**GENES DOWNREGULATED IN SKIN VERSUS TONGUE WOUND HEALING**

Entrez ID	Gene Name (Downregulated in Skin)	Gene Symbol	KEGG ID
13853	epilepsy, progressive myoclonic epilepsy, type 2 gene alpha(Epm2a)	<i>EPM2A</i>	mmu:13853
66753	endoplasmic reticulum lectin 1(Erlec1)	<i>ERLEC1</i>	mmu:66753
71690	endothelial cell-specific molecule 1(Esm1)	<i>ESM1</i>	mmu:71690
56219	exostoses (multiple)-like 1(Extl1)	<i>EXTL1</i>	mmu:56219
58193	exostoses (multiple)-like 2(Extl2)	<i>EXTL2</i>	mmu:58193
14120	fructose bisphosphatase 2(Fbp2)	<i>FBP2</i>	mmu:14120
50762	F-box protein 6(Fbxo6)	<i>FBXO6</i>	mmu:50762
14134	ficolin B(Fcnb)	<i>FCNB</i>	mmu:14134
14164	fibroblast growth factor 1(Fgf1)	<i>FGF1</i>	mmu:14164
14167	fibroblast growth factor 12(Fgf12)	<i>FGF12</i>	mmu:14167
14168	fibroblast growth factor 13(Fgf13)	<i>FGF13</i>	mmu:14168
14175	fibroblast growth factor 4(Fgf4)	<i>FGF4</i>	mmu:14175
14177	fibroblast growth factor 6(Fgf6)	<i>FGF6</i>	mmu:14177
14178	fibroblast growth factor 7(Fgf7)	<i>FGF7</i>	mmu:14178
14180	fibroblast growth factor 9(Fgf9)	<i>FGF9</i>	mmu:14180
243853	fukutin related protein(Fkrp)	<i>FKRP</i>	mmu:243853
246179	fukutin(Fktn)	<i>FKTN</i>	mmu:246179
14254	FMS-like tyrosine kinase 1(Flt1)	<i>FLT1</i>	mmu:14254
14257	FMS-like tyrosine kinase 4(Flt4)	<i>FLT4</i>	mmu:14257
234730	fucokinase(Fuk)	<i>FUK</i>	mmu:234730
53618	fucosyltransferase 8(Fut8)	<i>FUT8</i>	mmu:53618
14381	glucose-6-phosphate dehydrogenase X-linked(G6pdx)	<i>G6PDX</i>	mmu:14381
14387	glucosidase, alpha, acid(Gaa)	<i>GAA</i>	mmu:14387
230145	UDP-N-acetyl-alpha-D-galactosamine:polypeptide N-acetylgalactosaminyltransferase 12(Galnt12)	<i>GALNT12</i>	mmu:230145
78754	UDP-N-acetyl-alpha-D-galactosamine:polypeptide N-acetylgalactosaminyltransferase 15(Galnt15)	<i>GALNT15</i>	mmu:78754
108760	UDP-N-acetyl-alpha-D-galactosamine:polypeptide N-acetylgalactosaminyltransferase 16(Galnt16)	<i>GALNT16</i>	mmu:108760
241391	UDP-N-acetyl-alpha-D-galactosamine:polypeptide N-acetylgalactosaminyltransferase 5(Galnt5)	<i>GALNT5</i>	mmu:241391
14430	galactose-1-phosphate uridyl transferase(Galt)	<i>GALT</i>	mmu:14430
76051	glucosidase, alpha; neutral C(Ganc)	<i>GANC</i>	mmu:76051
14466	glucosidase, beta, acid(Gba)	<i>GBA</i>	mmu:14466
74185	glucan (1,4-alpha-), branching enzyme 1(Gbe1)	<i>GBE1</i>	mmu:74185
244757	galactosidase, beta 1-like 2(Glb1l2)	<i>GLB1L2</i>	mmu:244757
93683	glucuronyl C5-epimerase(Glce)	<i>GLCE</i>	mmu:93683
320302	glycosyltransferase 28 domain containing 2(Glt28d2)	<i>GLT28D2</i>	mmu:320302
74782	glycosyltransferase 8 domain containing 2(Glt8d2)	<i>GLT8D2</i>	mmu:74782
14667	GM2 ganglioside activator protein(Gm2a)	<i>GM2A</i>	mmu:14667
14733	glypican 1(Gpc1)	<i>GPC1</i>	mmu:14733
14735	glypican 4(Gpc4)	<i>GPC4</i>	mmu:14735
74182	glycerophosphocholine phosphodiesterase 1(Gpcpd1)	<i>GPCPD1</i>	mmu:74182
14751	glucose phosphate isomerase 1(Gpi1)	<i>GPI1</i>	mmu:14751
14756	glycosylphosphatidylinositol specific phospholipase D1(Gpld1)	<i>GPLD1</i>	mmu:14756
227835	glycosyltransferase-like domain containing 1(Gtdc1)	<i>GTDC1</i>	mmu:227835
27357	glycogenin(Gyg)	<i>GYG</i>	mmu:27357

APPENDIX A (continued)

TABLE XIX. (continued)**GENES DOWNREGULATED IN SKIN VERSUS TONGUE WOUND HEALING**

Entrez ID	Gene Name (Downregulated in Skin)	Gene Symbol	KEGG ID
14936	glycogen synthase 1, muscle(Gys1)	<i>GYS1</i>	mmu:14936
56541	hyaluronic acid binding protein 4(Habp4)	<i>HABP4</i>	mmu:56541
15275	hexokinase 1(Hk1)	<i>HK1</i>	mmu:15275
15277	hexokinase 2(Hk2)	<i>HK2</i>	mmu:15277
15288	hydroxymethylbilane synthase(Hmbs)	<i>HMBS</i>	mmu:15288
15442	heparanase(Hpse)	<i>HPSE</i>	mmu:15442
15476	heparan sulfate (glucosamine) 3-O-sulfotransferase 1(Hs3st1)	<i>HS3ST1</i>	mmu:15476
15478	heparan sulfate (glucosamine) 3-O-sulfotransferase 3A1(Hs3st3a1)	<i>HS3ST3A1</i>	mmu:15478
54710	heparan sulfate (glucosamine) 3-O-sulfotransferase 3B1(Hs3st3b1)	<i>HS3ST3B1</i>	mmu:54710
50785	heparan sulfate 6-O-sulfotransferase 1(Hs6st1)	<i>HS6ST1</i>	mmu:50785
101502	hydroxy-delta-5-steroid dehydrogenase, 3 beta- and steroid delta-isomerase 7(Hsd3b7)	<i>HSD3B7</i>	mmu:101502
15530	perlecan (heparan sulfate proteoglycan 2)(Hspg2)	<i>HSPG2</i>	mmu:15530
15896	intercellular adhesion molecule 2(Icam2)	<i>ICAM2</i>	mmu:15896
15931	iduronate 2-sulfatase(Ids)	<i>IDS</i>	mmu:15931
15932	iduronidase, alpha-L-(Idua)	<i>IDUA</i>	mmu:15932
16004	insulin-like growth factor 2 receptor(Igf2r)	<i>IGF2R</i>	mmu:16004
104360	insulin related protein 2 (islet 2)(Isl2)	<i>ISLET 2</i>	mmu:104360
16542	kinase insert domain protein receptor(Kdr)	<i>KDR</i>	mmu:16542
16795	LARGE xylosyl- and glucuronyltransferase 1(Large1)	<i>LARGE1</i>	mmu:16795
216551	lectin, galactoside binding-like(Lgalsl)	<i>LGALS1</i>	mmu:216551
214895	lectin, mannose-binding 2-like(Lman2l)	<i>LMAN2L</i>	mmu:214895
69541	lysozyme G-like 1(Lyg1)	<i>LYG1</i>	mmu:69541
17123	mucosal vascular addressin cell adhesion molecule 1(Madcam1)	<i>MADCAM1</i>	mmu:17123
17136	myelin-associated glycoprotein(Mag)	<i>MAG</i>	mmu:17136
140481	mannosidase 2, alpha 2(Man2a2)	<i>MAN2A2</i>	mmu:140481
73744	mannosidase, alpha, class 2C, member 1(Man2c1)	<i>MAN2C1</i>	mmu:73744
215090	mannosidase, endo-alpha-like(Maneal)	<i>MANEAL</i>	mmu:215090
17174	mannan-binding lectin serine peptidase 1(Masp1)	<i>MASP1</i>	mmu:17174
17285	mesenchyme homeobox 1(Meox1)	<i>MEOX1</i>	mmu:17285
17309	mannoside acetylglucosaminyltransferase 3(Mgat3)	<i>MGAT3</i>	mmu:17309
110119	mannose phosphate isomerase(Mpi)	<i>MPI</i>	mmu:110119
67111	N-acylethanolamine acid amidase(Naaa)	<i>NAAA</i>	mmu:67111
17967	neural cell adhesion molecule 1(Ncam1)	<i>NCAM1</i>	mmu:17967
320024	neutral cholesterol ester hydrolase 1(Nceh1)	<i>NCEH1</i>	mmu:320024
59007	N-glycanase 1(Ngly1)	<i>NGLY1</i>	mmu:59007
77583	notum pectinacylesterase homolog (Drosophila)(Notum)	<i>NOTUM</i>	mmu:77583
18186	neuropilin 1(Nrp1)	<i>NRP1</i>	mmu:18186
103850	5',3'-nucleotidase, mitochondrial(Nt5m)	<i>NT5M</i>	mmu:103850
108155	O-linked N-acetylglucosamine (GlcNAc) transferase (UDP-N-acetylglucosamine:polypeptide-N-acetylglucosaminyl transferase)(Ogt)	<i>OGT</i>	mmu:108155
18613	platelet/endothelial cell adhesion molecule 1(Pecam1)	<i>PECAM1</i>	mmu:18613
18640	6-phosphofructo-2-kinase/fructose-2,6-biphosphatase 2(Pfkfb2)	<i>PFKFB2</i>	mmu:18640
18642	phosphofructokinase, muscle(Pfkm)	<i>PFKM</i>	mmu:18642
18655	phosphoglycerate kinase 1(Pgk1)	<i>PGK1</i>	mmu:18655
72157	phosphoglucomutase 2(Pgm2)	<i>PGM2</i>	mmu:72157

APPENDIX A (continued)

TABLE XIX. (continued)**GENES DOWNREGULATED IN SKIN VERSUS TONGUE WOUND HEALING**

Entrez ID	Gene Name (Downregulated in Skin)	Gene Symbol	KEGG ID
226041	phosphoglucosyltransferase 5(Pgm5)	<i>PGM5</i>	mmu:226041
329777	phosphatidylinositol glycan anchor biosynthesis, class K(Pigk)	<i>PIGK</i>	mmu:329777
56176	phosphatidylinositol glycan anchor biosynthesis, class P(Pigp)	<i>PIGP</i>	mmu:56176
228812	phosphatidylinositol glycan anchor biosynthesis, class U(Pigu)	<i>PIGU</i>	mmu:228812
72084	phosphatidylinositol glycan anchor biosynthesis, class X(Pigx)	<i>PIGX</i>	mmu:72084
18764	polycystic kidney disease 2(Pkd2)	<i>PKD2</i>	mmu:18764
26432	procollagen lysine, 2-oxoglutarate 5-dioxygenase 2(Plod2)	<i>PLOD2</i>	mmu:26432
19012	phospholipid phosphatase 1(Plpp1)	<i>PLPP1</i>	mmu:19012
67916	phospholipid phosphatase 3(Plpp3)	<i>PLPP3</i>	mmu:67916
29858	phosphomannomutase 1(Pmm1)	<i>PMM1</i>	mmu:29858
68273	protein O-linked mannose beta 1,2-N-acetylglucosaminyltransferase(Pomgnt1)	<i>POMGNT1</i>	mmu:68273
215494	protein O-linked mannose beta 1,4-N-acetylglucosaminyltransferase 2(Pomgnt2)	<i>POMGNT2</i>	mmu:215494
140491	protein phosphatase 1, regulatory (inhibitor) subunit 3A(Ppp1r3a)	<i>PPP1R3A</i>	mmu:140491
53412	protein phosphatase 1, regulatory (inhibitor) subunit 3C(Ppp1r3c)	<i>PPP1R3C</i>	mmu:53412
19309	muscle glycogen phosphorylase(Pygm)	<i>PYGM</i>	mmu:19309
66459	Pigy upstream reading frame(Pyurf)	<i>PYURF</i>	mmu:66459
67709	regenerating islet-derived family, member 4(Reg4)	<i>REG4</i>	mmu:67709
84585	ring finger protein 123(Rnf123)	<i>RNF123</i>	mmu:84585
15529	syndecan 2(Sdc2)	<i>SDC2</i>	mmu:15529
20970	syndecan 3(Sdc3)	<i>SDC3</i>	mmu:20970
66945	succinate dehydrogenase complex, subunit A, flavoprotein (Fp)(Sdha)	<i>SDHA</i>	mmu:66945
56546	secretory blood group 1(Sec1)	<i>SEC1</i>	mmu:56546
208449	sphingomyelin synthase 1(Sgms1)	<i>SGMS1</i>	mmu:208449
171429	solute carrier family 26, member 6(Slc26a6)	<i>SLC26A6</i>	mmu:171429
224661	solute carrier family 26, member 8(Slc26a8)	<i>SLC26A8</i>	mmu:224661
353169	solute carrier family 2 (facilitated glucose transporter), member 12(Slc2a12)	<i>SLC2A12</i>	mmu:353169
20528	solute carrier family 2 (facilitated glucose transporter), member 4(Slc2a4)	<i>SLC2A4</i>	mmu:20528
56017	solute carrier family 2, (facilitated glucose transporter), member 8(Slc2a8)	<i>SLC2A8</i>	mmu:56017
22232	solute carrier family 35 (UDP-galactose transporter), member A2(Slc35a2)	<i>SLC35A2</i>	mmu:22232
74102	solute carrier family 35, member A5(Slc35a5)	<i>SLC35A5</i>	mmu:74102
14385	solute carrier family 37 (glucose-6-phosphate transporter), member 4(Slc37a4)	<i>SLC37A4</i>	mmu:14385
20537	solute carrier family 5 (sodium/glucose cotransporter), member 1(Slc5a1)	<i>SLC5A1</i>	mmu:20537
20598	sphingomyelin phosphodiesterase 2, neutral(Smpd2)	<i>SMPD2</i>	mmu:20598
58994	sphingomyelin phosphodiesterase 3, neutral(Smpd3)	<i>SMPD3</i>	mmu:58994
20322	sorbitol dehydrogenase(Sord)	<i>SORD</i>	mmu:20322
20671	SRY (sex determining region Y)-box 17(Sox17)	<i>SOX17</i>	mmu:20671
20692	secreted acidic cysteine rich glycoprotein(Sparc)	<i>SPARC</i>	mmu:20692
72902	sparc/osteonection, cwcw and kazal-like domains proteoglycan 3(Spock3)	<i>SPOCK3</i>	mmu:72902
20441	ST3 beta-galactoside alpha-2,3-sialyltransferase 3(St3gal3)	<i>ST3GAL3</i>	mmu:20441

APPENDIX A (continued)

TABLE XIX. (continued)**GENES DOWNREGULATED IN SKIN VERSUS TONGUE WOUND HEALING**

Entrez ID	Gene Name (Downregulated in Skin)	Gene Symbol	KEGG ID
54613	ST3 beta-galactoside alpha-2,3-sialyltransferase 6(St3gal6)	ST3GAL6	mmu:54613
20446	ST6 (alpha-N-acetyl-neuraminy-2,3-beta-galactosyl-1,3)-N-acetylgalactosaminide alpha-2,6-sialyltransferase 2(St6galnac2)	ST6GALNAC2	mmu:20446
20447	ST6 (alpha-N-acetyl-neuraminy-2,3-beta-galactosyl-1,3)-N-acetylgalactosaminide alpha-2,6-sialyltransferase 3(St6galnac3)	ST6GALNAC3	mmu:20447
50935	ST6 (alpha-N-acetyl-neuraminy-2,3-beta-galactosyl-1,3)-N-acetylgalactosaminide alpha-2,6-sialyltransferase 6(St6galnac6)	ST6GALNAC6	mmu:50935
225742	ST8 alpha-N-acetyl-neuraminide alpha-2,8-sialyltransferase 5(St8sia5)	ST8SIA5	mmu:225742
52331	starch binding domain 1(Stbd1)	STBD1	mmu:52331
240725	sulfatase 1(Sulf1)	SULF1	mmu:240725
21824	thrombomodulin(Thbd)	THBD	mmu:21824
232078	threonine synthase-like 2 (bacterial)(Thnsl2)	THNSL2	mmu:232078
21991	triosephosphate isomerase 1(Tpi1)	TPI1	mmu:21991
170829	translocating chain-associating membrane protein 2(Tram2)	TRAM2	mmu:170829
22153	tubulin, beta 4A class IVA(Tubb4a)	TUBB4A	mmu:22153
66435	UDP-glucose glycoprotein glucosyltransferase 2(Uggt2)	UGGT2	mmu:66435
216558	UDP-glucose pyrophosphorylase 2(Ugp2)	UGP2	mmu:216558
22239	UDP galactosyltransferase 8A(Ugt8a)	UGT8A	mmu:22239

6.2 APPENDIX B

6.2.1 Replicate Western Blots from Chapter 2

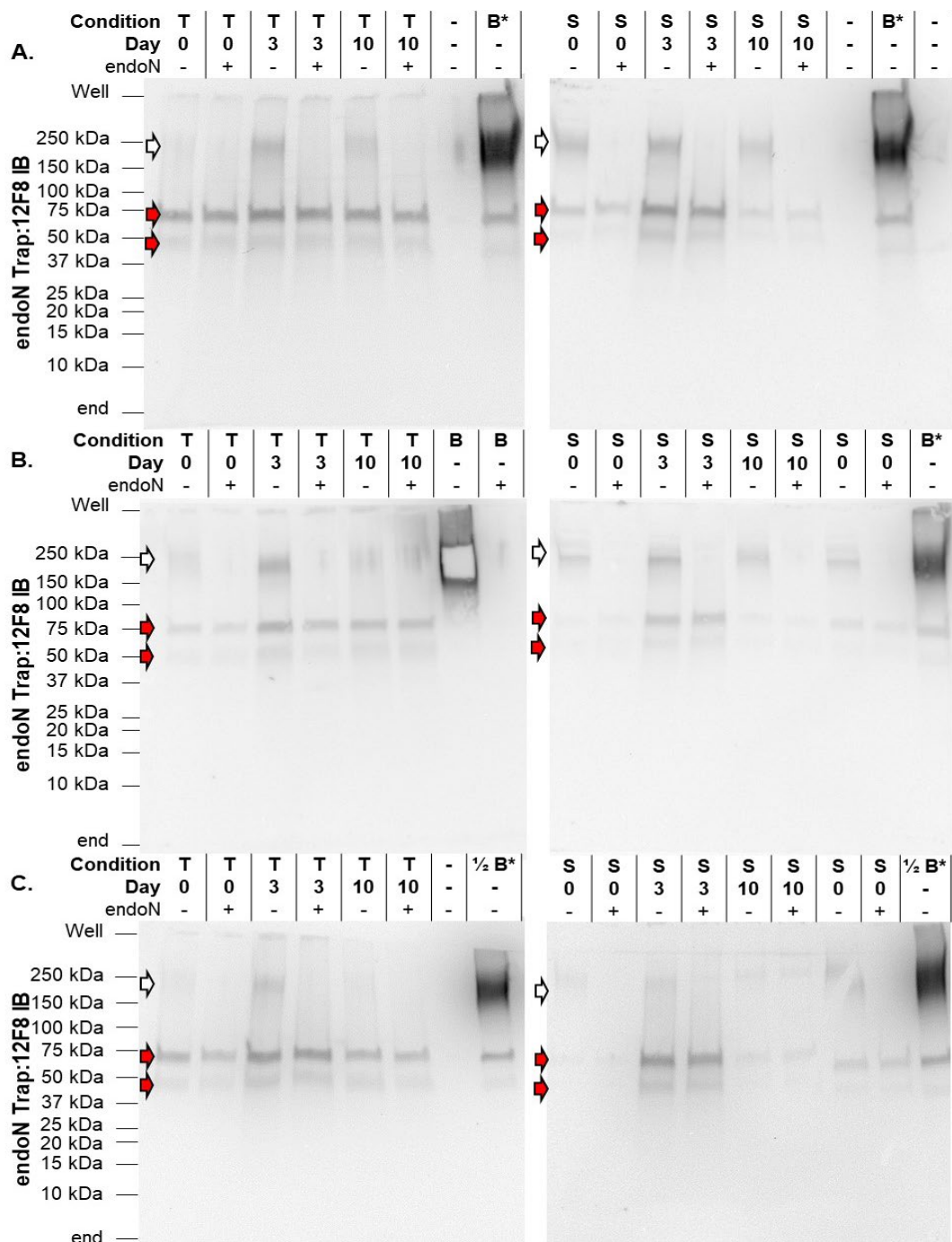


Figure 58. Expression of polysialic acid in EndoNT proteins during skin and tongue wounds healing.

APPENDIX B (continued)

Figure 58. Expression of polysialic acid in EndoNT proteins during skin and tongue wounds healing. Expression in tongue (left) and skin (right) across replicates 1-3 (A-C). Arrows denotes the location/ MW where each expected band appears specifically for polysialyic acid (white) and would appear for NCAM-180 (blue), NCAM-140 (black), NCAM-120 (green), CCR7 (horizontal red stripe). Unexpected and/ or non- specific bands denoted by red arrows. In B, the horizontal red strip denoted NCAM 1 Ab non- specifically staining at the molecular weight of the protein target CCR7. *asterisks represent brain samples that did not undergo EndoNt.

APPENDIX B (continued)

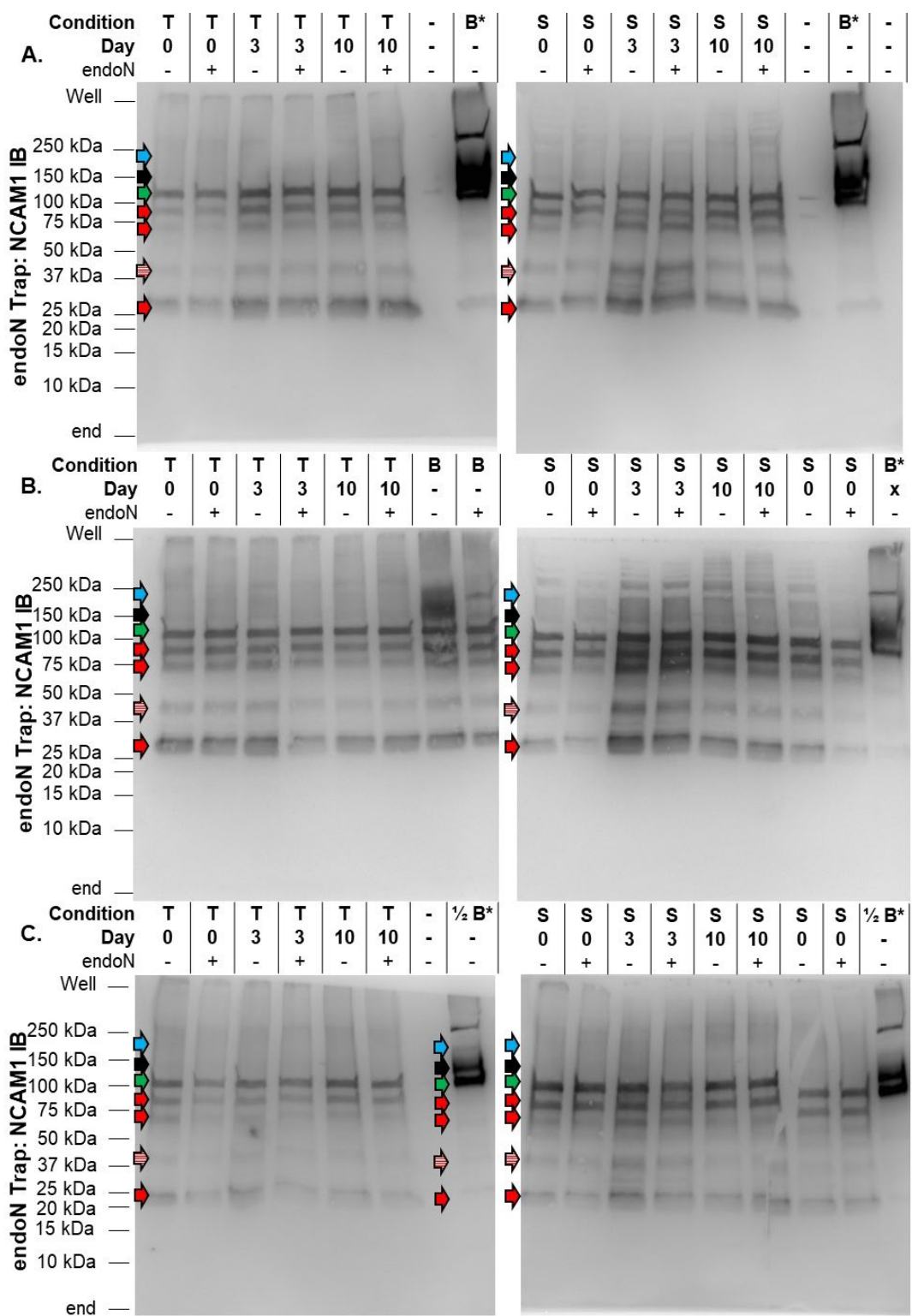


Figure 59. Expression of NCAM1 in EndoNT proteins during skin and tongue wounds healing.

APPENDIX B (continued)

Figure 59. Expression of NCAM1 in EndoNT proteins during skin and tongue wounds healing. Expression in tongue (left) and skin (right) across replicates 1-3 (A-C). Arrows denotes the location/ MW where each expected band would appear for NCAM-180 (blue), NCAM-140 (black), NCAM-120 (green). Unexpected and/ or non-specific bands denoted by red arrows. Horizontal red strip denoted NCAM 1 Ab non-specifically stained a known protein target (CCR7). *asterisks represent brain samples that did not undergo EndoNt.

APPENDIX B (continued)

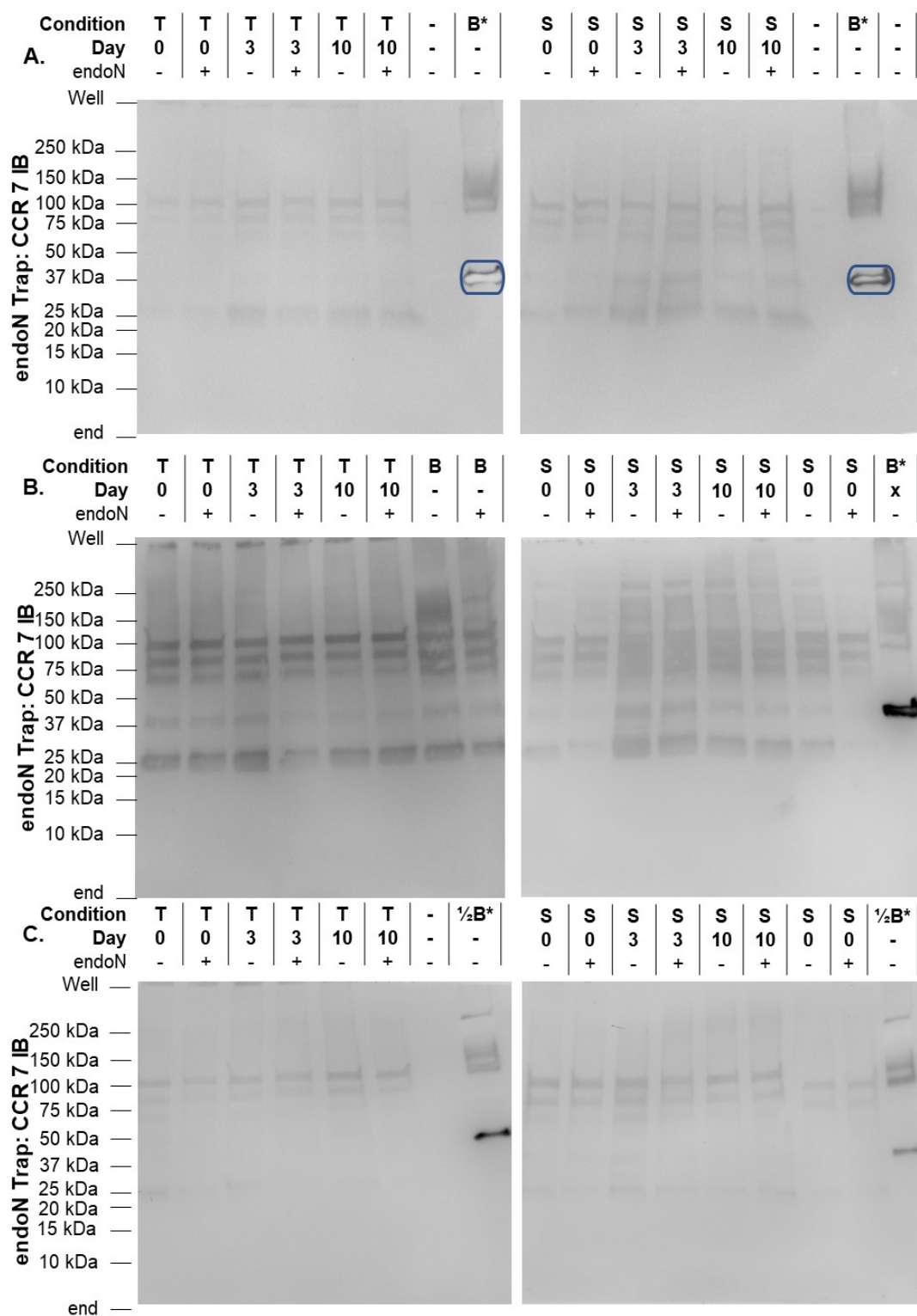


Figure 60. Expression of CCR7 in EndoNT proteins during skin and tongue wounds healing.

APPENDIX B (continued)

Figure 60. Expression of CCR7 in EndoNT proteins during skin and tongue wounds healing. Expression in tongue (left) and skin (right) across replicates 1-3 (A-C). Blue circles represent overexposed CCR7 staining. *asterisks represent brain samples that did not undergo EndoNt.

APPENDIX B (continued)

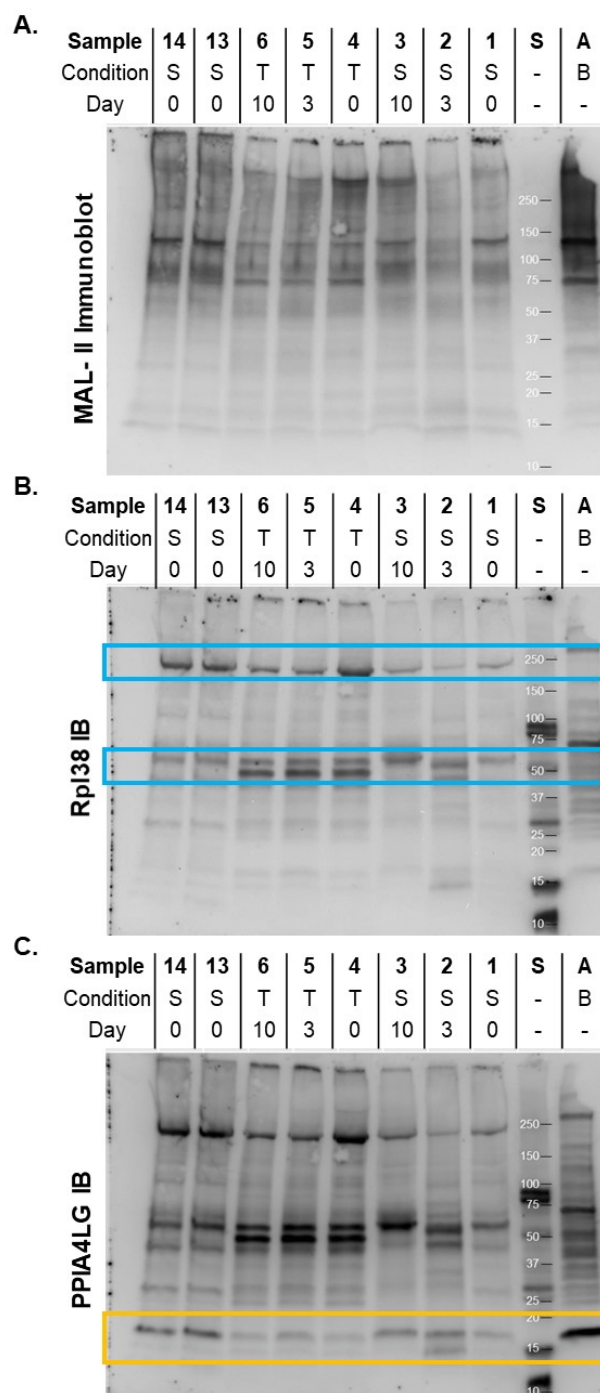


Figure 61. Housekeeping proteins are not consistently expressed in uninjured tongue, skin, and their respective wounds.

APPENDIX B (continued)

Figure 61. Housekeeping proteins are not consistently expressed in uninjured tongue, skin, and their respective wounds. MAL-II and SNA immunoblots were stripped and reprobed to assess housekeeping gene expression of 60S ribosomal protein L38 (Rpl38; B) and Peptidyl-prolyl cis-trans isomerase A 4LG (PPIA4LG; C). Among the genes examined Rpl38 and PPIA4LG demonstrated the most consistent expression among all samples. The expression of Rpl38 was higher in the tongue than skin (~250kDa, ~70kDa and 50kDa). Rpl38 (blue box) demonstrated equal expression of 2 bands (at ~70kDa and 50kDa) throughout all timepoints in the tongue (B, lanes 3-5), however, it was differentially regulated in skin wound healing with 1 band appearing at days 0 (B, lane 8) and 10 (B, lane 6) and 2 bands appearing at day 3. (B, lane 7). Rpl38 demonstrated equal expression of 1 250kDa band throughout all timepoints in the skin (B, lanes 6-8), however, it was differentially regulated in tongue wound healing with uninjured tongue (B, lane 5) demonstrating higher expression than the wounds (B, lane 3-4).

The expression of PPIA4LG (yellow box) was lower in the tongue (C, lane 3-5) than the skin (C, lane 6-8) at ~18kDa. Tongue wounds demonstrated slightly increased expression of PPIA4LG 3- days post- wounding (C, 4) when compared to uninjured tongue (C, lane 5). Uninjured skin demonstrated variable expression between the samples and was therefore averaged for all comparisons. Interesting uninjured skin and wounds 10 days post wounding expressed a single 18kDa band, while wounds 3 days post wounding expressed higher levels of the 15kDa band in addition to a 15kDa band) Overall this data suggests housekeeping genes including Rpl38 and PPIA4LG may be used to compare tongue wound healing (Rpl38)

6.3 APPENDIX C

6.3.1 Additional Experiments and Preliminary Data for Diabetic and Non- Diabetic

Skin and Wounds

Polysialic acid (polySia) is difficult to detect via glycomics analysis as polySia is both temperature (stable up to 65 °C) and pH labile (stable at pH7-8). Maintenance of polySia for glycomics analysis requires the process of lactonization²⁹⁰ which was not performed during these experiments. However, polySia can be probed via western blotting techniques. During the glycomics analysis, the expression of glycans containing 3-4 sialic acids were found to mimic the gene expression pattern of polysialyltransferase *ST8SIA4* (Figure 37D). The subsequent experiments were performed to identify whether polySia was differentially expressed in diabetic and non-diabetic skin and wounds.

6.3.2 Methods and Materials

6.3.2.1 Recovery of Polysialylated Proteins

To determine whether polysialylated proteins were present in tissue samples, inactive PKIE endo-N-neuraminidase was used to trap polysialylated proteins. Each sample (500µL of 0.5-2mg/mL sample resuspended in TBS) was incubated on an end-over-end rocker with 50 microliters of a 50% slurry of GST.PKIE endo-N-acetylneuraminidase Trap (EndoNt) bound to glutathione-Sepharose beads in RIPA lysis buffer (50mM Tris HCl pH7.5, 150mM NaCl, 5mM EDTA, 0.5% Nonidet P-40, 0.1%SDS) for 6h at 4° C. After 3 washes with PBS samples were prepared for gel electrophoresis. The specificity of the EndoNt and the presence of polySia on the

APPENDIX C (continued)

protein was confirmed by treating half of the precipitated proteins for each condition/ time point with 5 μ L of 20mM Tris (pH 7.8) or 5 μ L of catalytically active endo-N-acetylneuraminidase (endoN) in 60 μ L buffer (10:10:50 ratio of NP-40, 1x Glycobuffer 2 (New England BioLabs, Ipswich, MA), and 20mM Tris, pH 8.0) for 4 hours at 37° C.

6.3.2.2 Protein Electrophoresis and Transfer

Equal amounts (50 μ L) of the protein bound EndoNt were resuspended in 2X sample buffer (a 1:1 dilution of 4X protein sample loading buffer (Licor, Lincoln, Nebraska, USA) in Tris/ Glycine/ SDS buffer) with 10% β -mercaptoethanol (BME) and heated to 65°C for 10 minutes. SDS PAGE was performed at 110V for 1.5 hours between 4-25° C (n=3) to minimize over-heating and sample loss. Following SDS PAGE, proteins were transferred onto a PVDF membrane at 100V for 1 hour at 4° C.

6.3.2.3 Dual Immunoblotting of Protein and Carbohydrate Markers During Wound Healing

Following SDS PAGE and membrane transfer as above, membranes were blocked using Odyssey Blocking Buffer TBS or PBS (Licor, Lincoln, Nebraska, USA) at 37°C for 30 minutes or overnight at 4° C. Primary antibodies and biotinylated lectins were diluted in Odyssey Blocking Buffer TBS supplemented with 0.05% Tween 20 and incubated overnight at 4° C. After thorough washing, secondary antibodies were diluted in Odyssey Blocking Buffer TBS supplemented with 0.1% Tween 20 and incubated for 60 min at room temperature. To assess the total protein content, Licor REVERT total protein stain assay was utilized per the manufacture instructions for dual blotting.

APPENDIX C (continued)

6.3.2.4 Microscopy

Following euthanasia, samples were embedded in OCT (Fisher Healthcare, Houston, TX) and stored at -80° C or fixed in 10% formalin for 44 hours, dehydrated with ethanol, and stored in paraffin until further processing. Eight to ten micrometer thick frozen sections were obtained from OCT embedded samples using the Leica Cryostat (Leica Biosystems, Wetzlar, Germany).

To analyze the expression and localization of α 2-8 polysialylated proteins and NCAM1, 8 μ m frozen section were fixed in pre-cooled (-20° C) 4% paraformaldehyde. Following permeabilization, and thorough washing, carbohydrate binding specificity was confirmed by incubating the sections in Glycobuffer 3/2 with or without the catalytically active α 2-3, -6, -8, -9 neuraminidase (New England BioLabs, Ipswich, MA) and/ or endoneuraminidase at 37° C for 2-4 h or 24 h, respectively. Slides were then blocked with blocking buffer (5% BSA, 1% GSA, 0.1% Triton X-100, 0.05% Tween-20) and streptavidin/biotin as indicated by manufacturer instructions (Vector Labs). Additionally, to reduce non-specific binding to the Fc region of the rat IgM (12F8) and rabbit IgG (NCMA1) secondary antibodies, slides stained for 12F8 and NCAM-1, were additionally blocked using 100 μ g/mL of unconjugated AffiniPure monovalent Fab Fragment (H+L) antibodies (Jackson ImmunoResearch) relative to each respective secondary antibody. Following a brief washing, slides were incubated with 12F8 and NCAM antibodies overnight at 4° C diluted in antibody dilution buffer (1% BSA/ 0.1% Triton X-100/ 0.05% Tween-20). After washing, the slides were incubated at room temperature for 45 min in the respective secondary antibodies; 1:500 Alexa Fluor 488 conjugated goat anti-rat

APPENDIX C (continued)

IgM (for 12F8), 1:400 Alexa Fluor 594 conjugated goat anti-rabbit IgG (for NCAM1), Each slide contained a negative control for the 12F8 and NCAM1 targets.

6.3.3 Results

6.3.3.1 Polysialic acid is increased in diabetic skin.

Microscopic analysis of uninjured non-diabetic and diabetic skin revealed increased expression of polysialic acid in the epithelium of diabetic skin which demonstrated coincidence staining with neural cell adhesion molecule (NCAM1). Coincidence staining was identified on the dermal microvasculature of both diabetic and non-diabetic skin (Figures 62A-D, Appendix C), cells along the basement membrane in non-diabetic wounds (Figure 62, Appendix C), and epidermal cell in diabetic wounds 1-day post-wounding (Figure 62, Appendix D). Furthermore, specificity of 12F8 staining for polySia was confirmed when incubation in endoN abrogated the intensity of 12F8 staining (Figures 62B and 62D *right*, Appendix C).

APPENDIX C (continued)

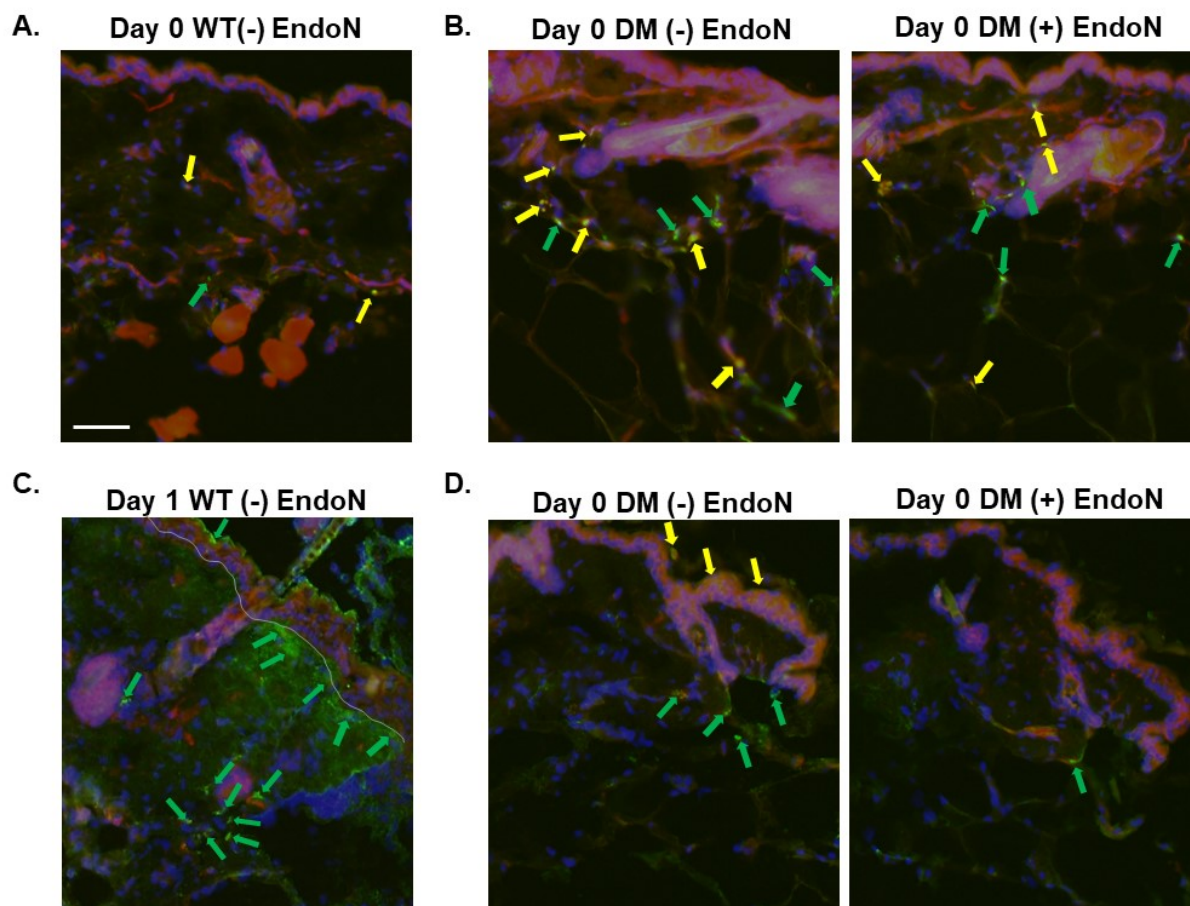


Figure 62. Immunohistochemical staining of polysialic acid and NCAM1 in diabetic (*db/db*) and non- diabetic (*C57*) skin and wounds.

APPENDIX C (continued)

6.3.3.2 Polysialic acid, NCAM, and NRP2 is upregulated in diabetic and nondiabetic wound healing

Low molecular weight oligo- or polysialic acid, NCAM1, and NRP2, exhibited delayed upregulation during the inflammatory phase of diabetic wound healing (days 1-3), enhanced polysialic acid expression on day 3, and delayed downregulation as demonstrated by the sustained signal observed 10 days post wounding when compared to the non- diabetic condition. Each sample was treated with and without endoN to confirm the specificity for polysialic acid, however, the samples were not completely digested as demonstrated by the abundant signal in the endoN treated samples. This is attributed to the short duration that the endoNt samples were incubated in endoN in efforts to avoid protein degradation. Interestingly, there were still at least 2 polysialic acid positive bands observed at approximately 250kDa and 65kDa, however, NRP2 and NCAM1²⁹¹ were only identified in the bands near 65kDa (Figure 63, Appendix C).

APPENDIX C (continued)

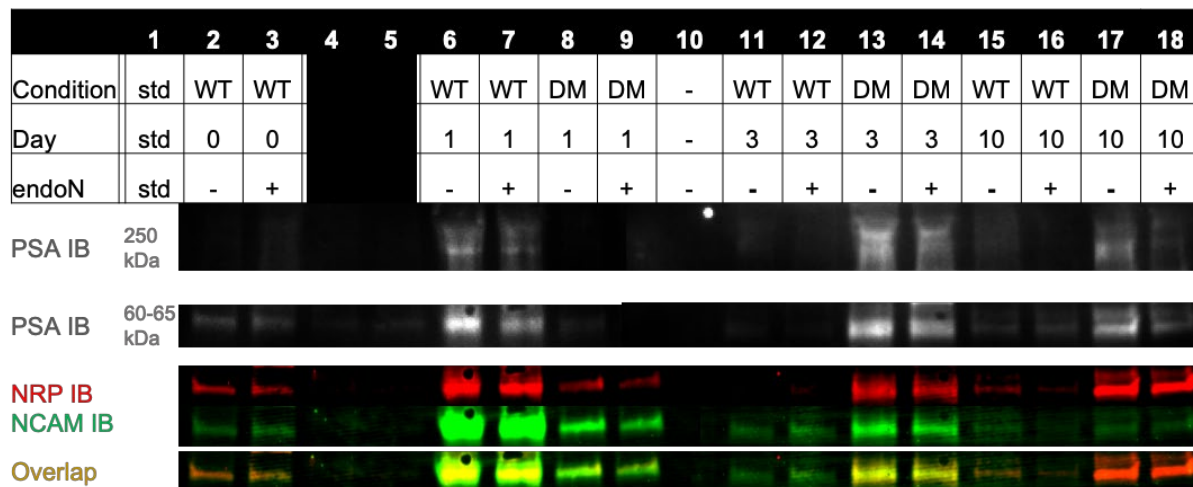


Figure 63. Increased expression of polysialic acid, NCAM1, and NRP2 overlap occurs in the inflammatory phase of non- diabetic wound healing, yet is delayed through the proliferative phase in diabetic wounds. The expression of polysialic acid (PSA; grey), NRP2 (red), and NCAM1 (green) were observed in uninjured skin and wounds 1, 3, and 10 days post wounding in non-diabetic, C57 (WT) and diabetic *db/db* (DM) mice. Each sample was treated with (+) and without (-) endoN to confirm 12F8 specificity for polysialic acid.

6.4 APPENDIX D

6.4.1 Glycosylation-related Gene Expression in Diabetic and Non-Diabetic Skin and Wounds (Alphabetical Order)

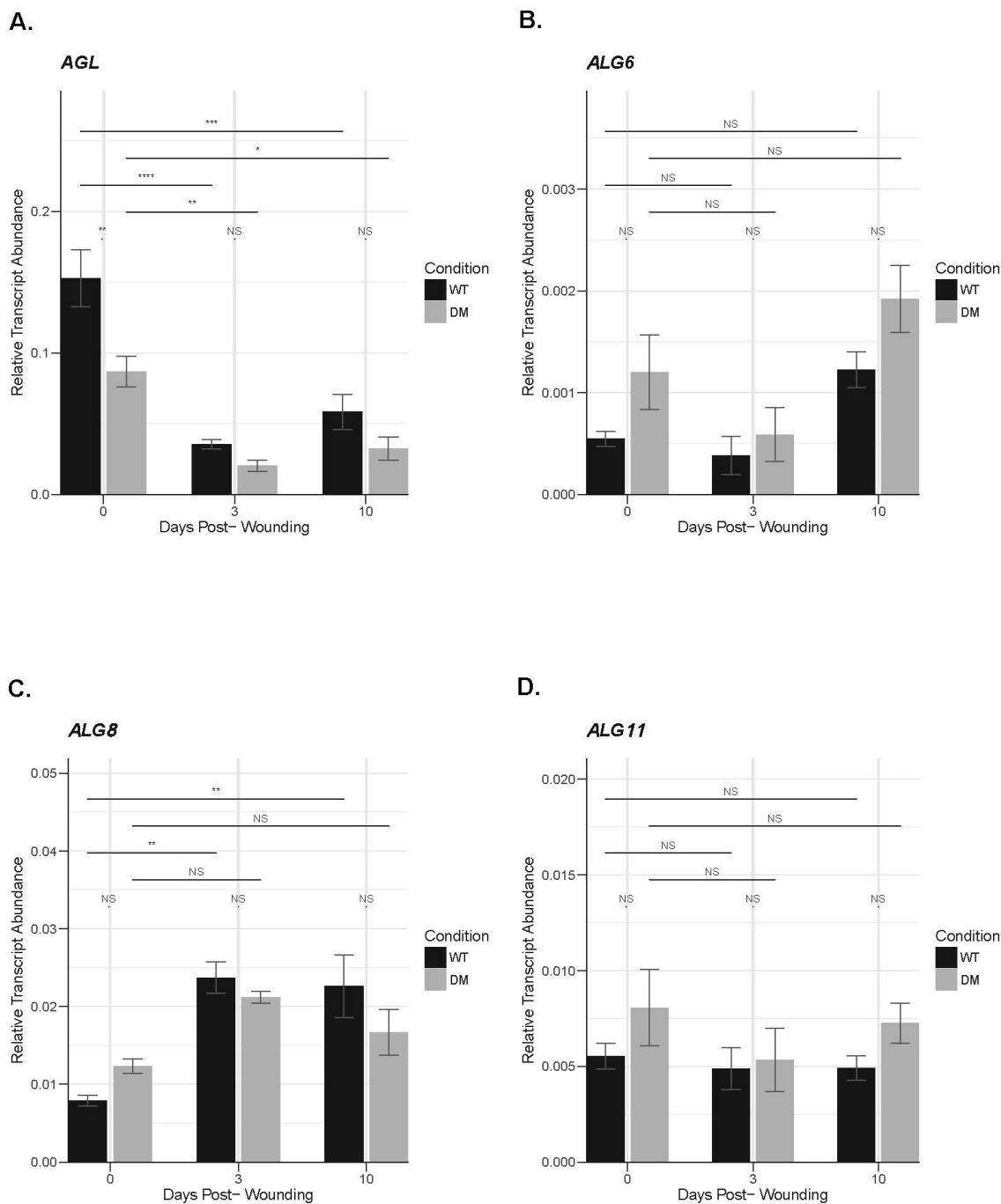


Figure 64. Glycosylation Related Gene Expression in Diabetic and Non-Diabetic Skin and Wounds.

APPENDIX D (continued)

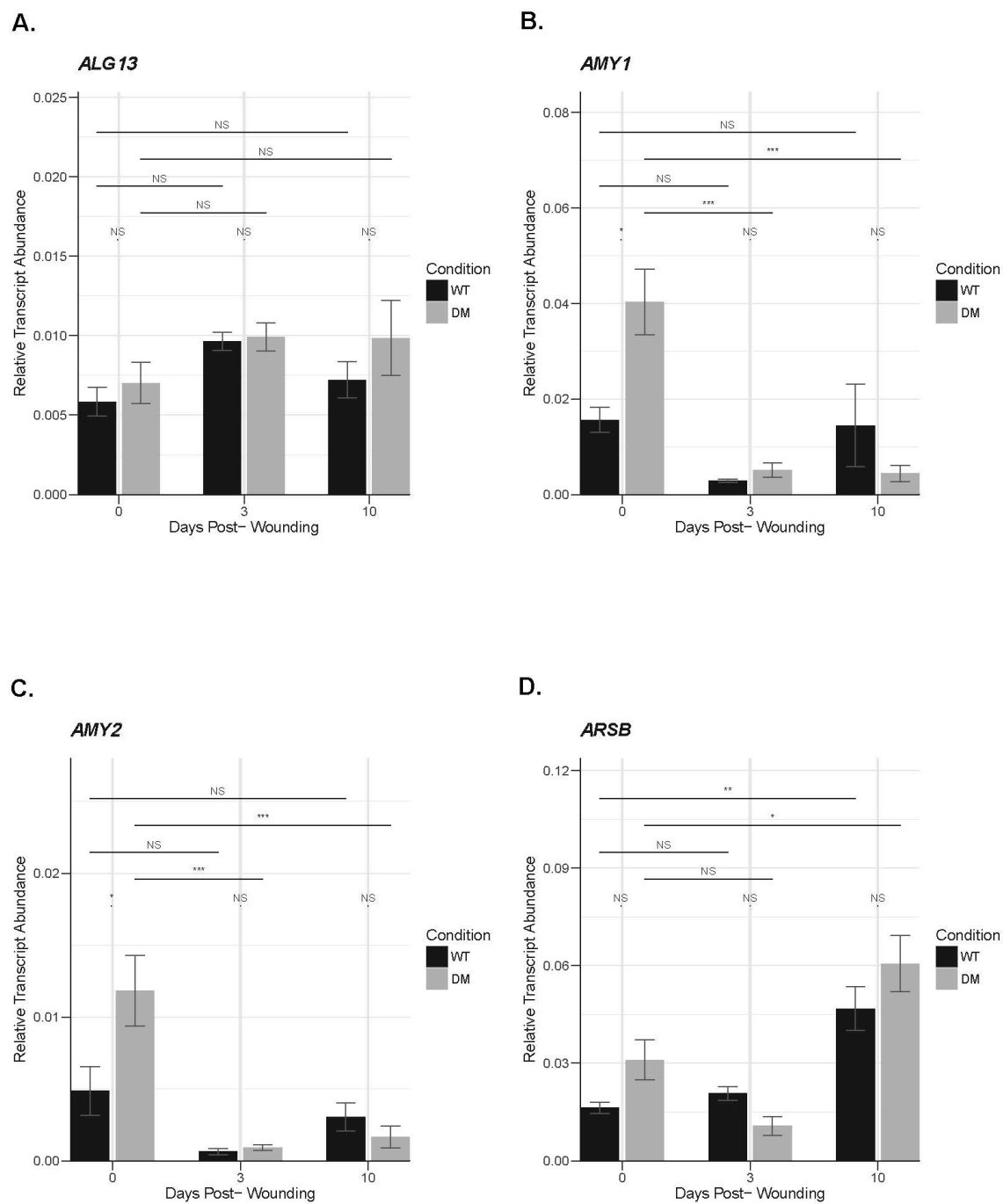


Figure 65. Glycosylation Related Gene Expression in Diabetic and Non-Diabetic Skin and Wounds. (continued)

APPENDIX D (continued)

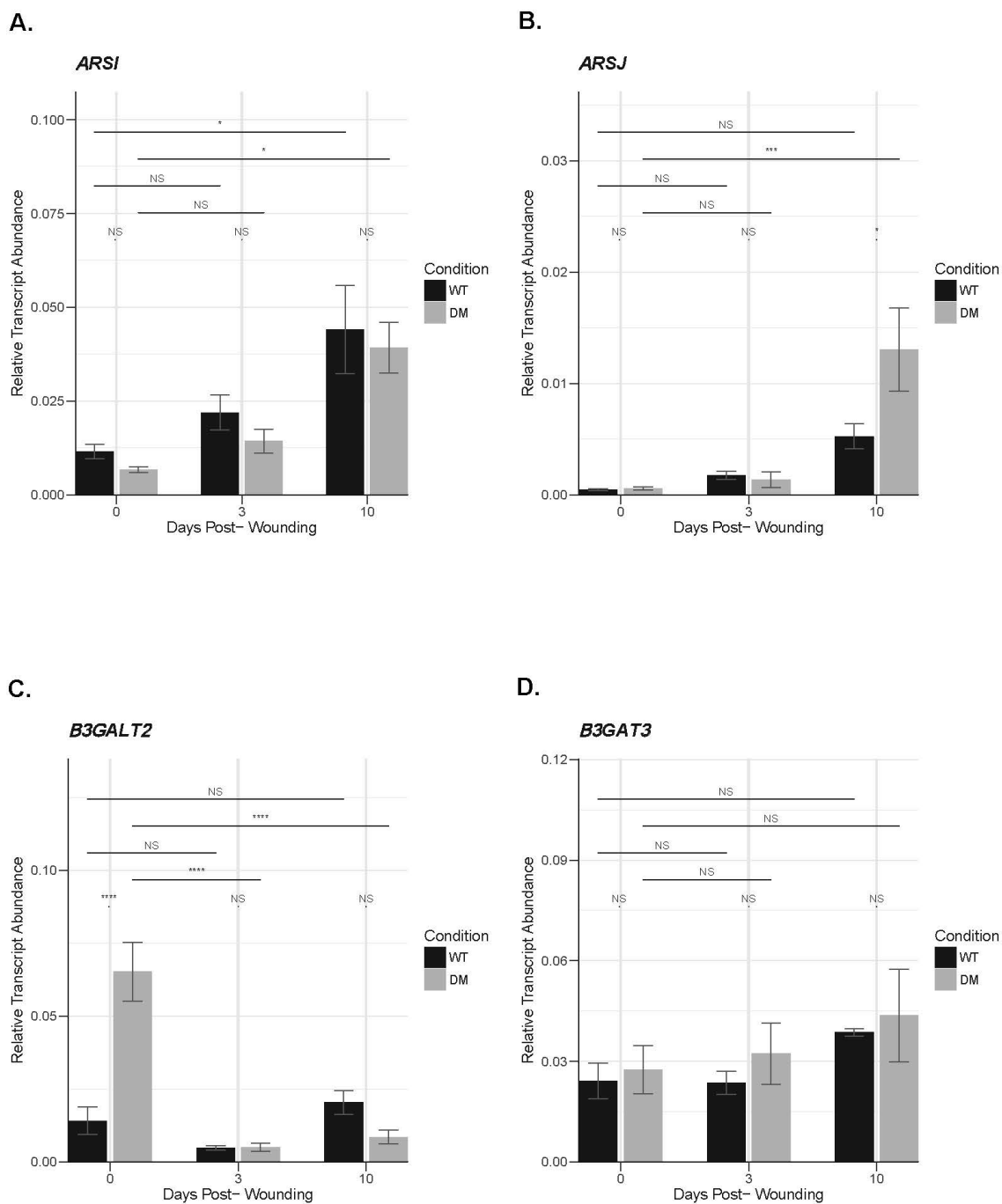


Figure 66. Glycosylation Related Gene Expression in Diabetic and Non-Diabetic Skin and Wounds. (continued)

APPENDIX D (continued)

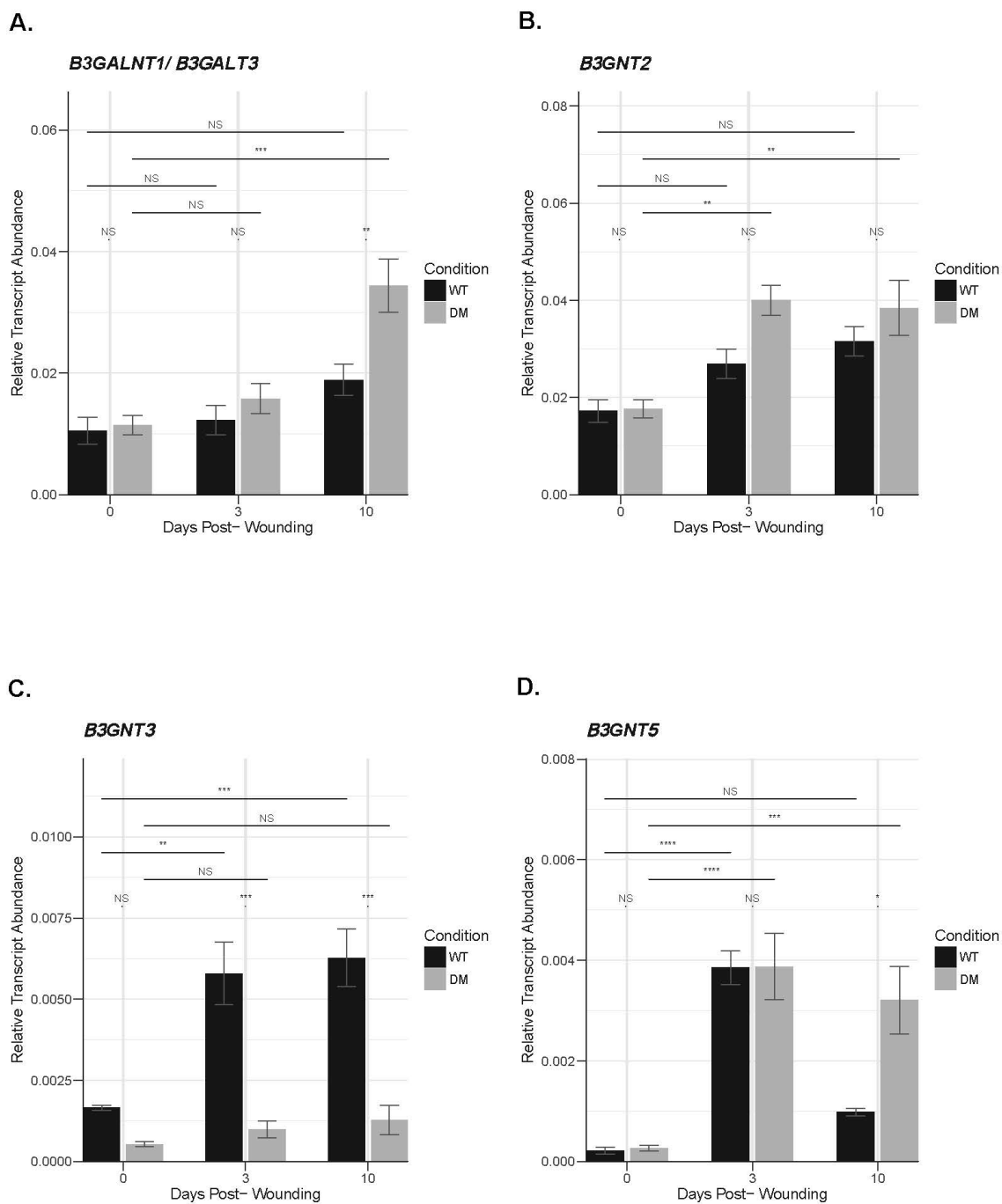


Figure 67. Glycosylation Related Gene Expression in Diabetic and Non-Diabetic Skin and Wounds. (continued)

APPENDIX D (continued)

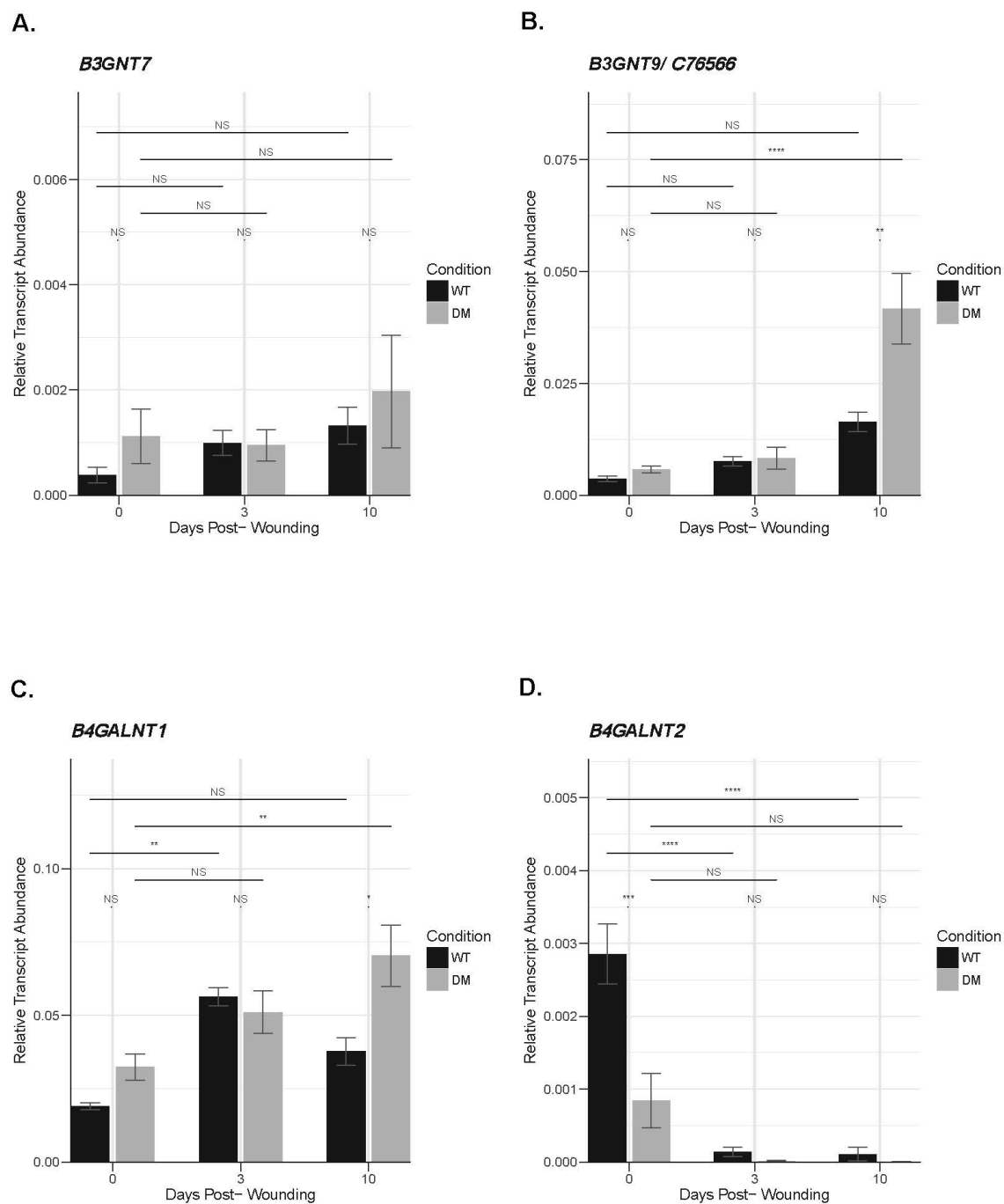


Figure 68. Glycosylation Related Gene Expression in Diabetic and Non-Diabetic Skin and Wounds. (continued)

APPENDIX D (continued)

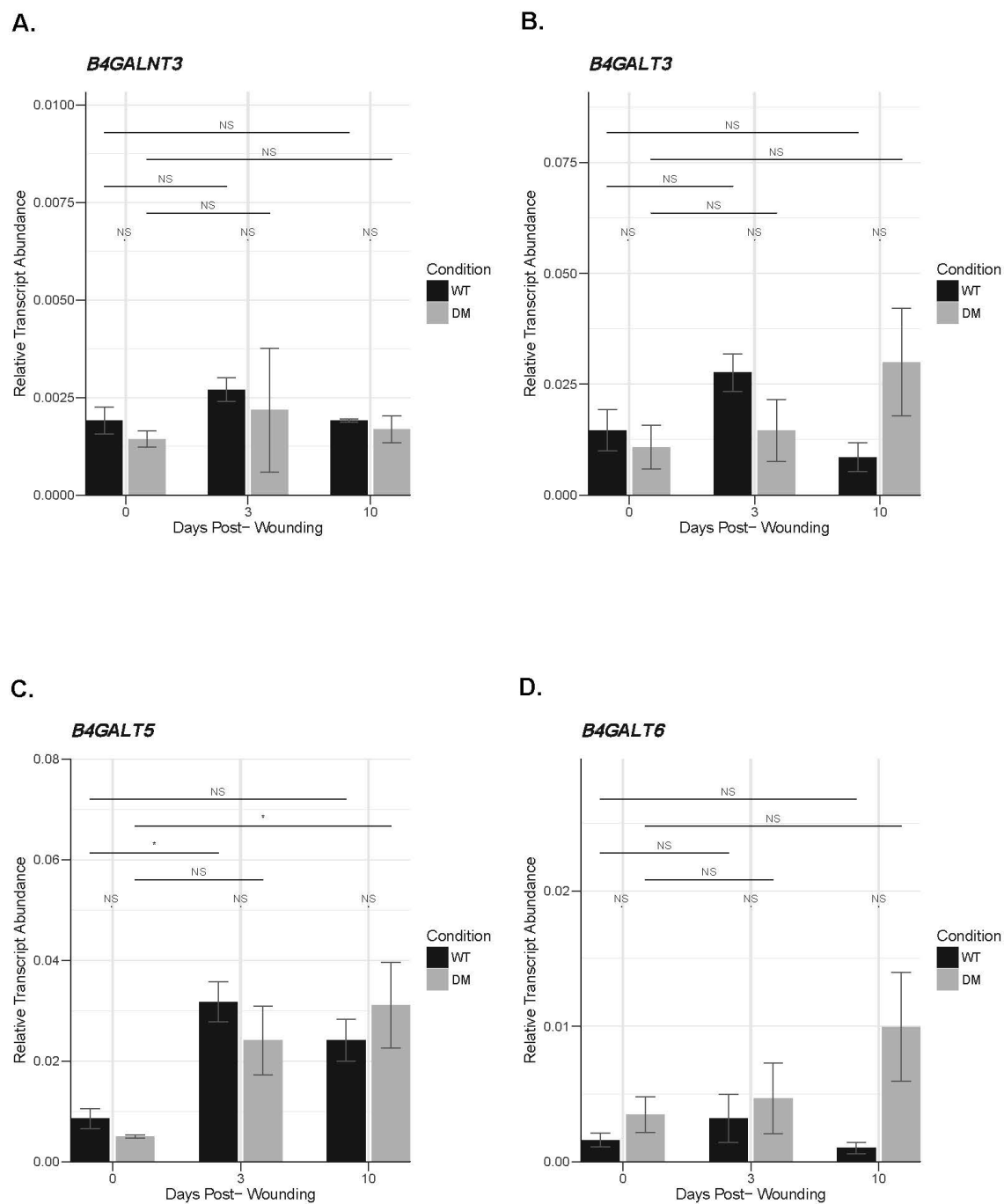
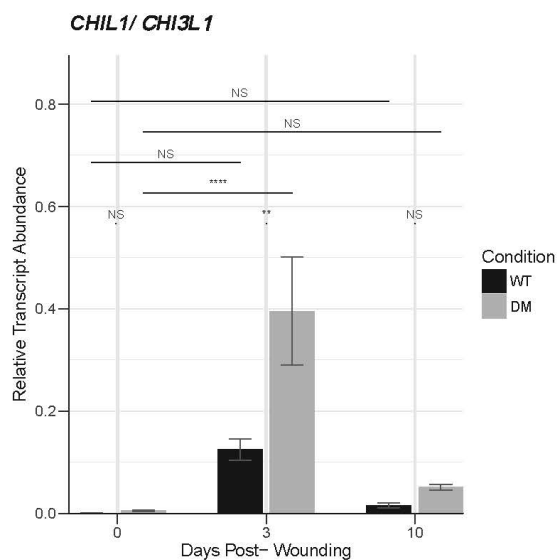


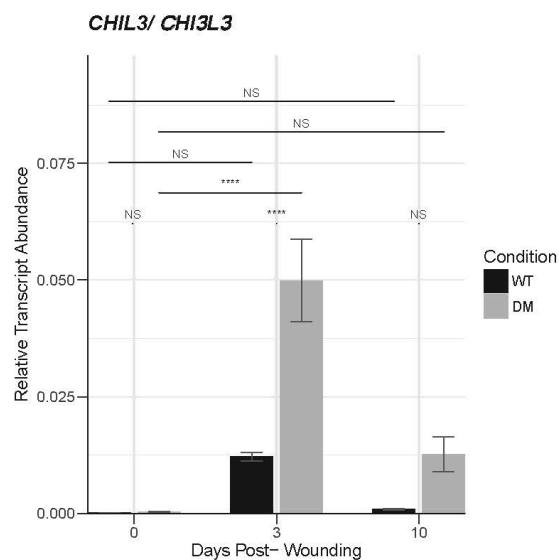
Figure 69. Glycosylation Related Gene Expression in Diabetic and Non-Diabetic Skin and Wounds. (continued)

APPENDIX D (continued)

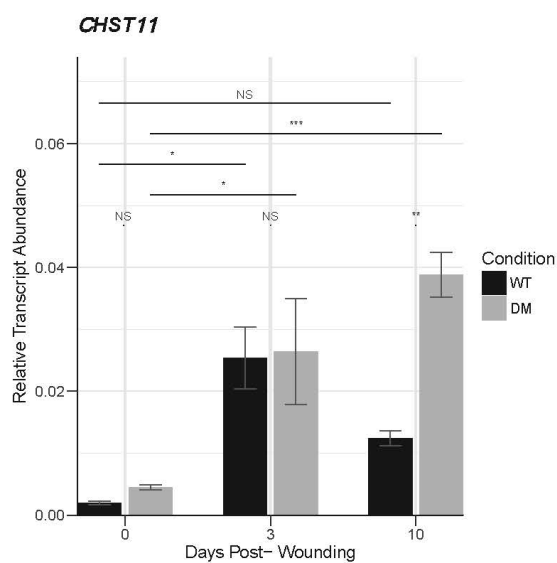
A.



B.



C.



D.

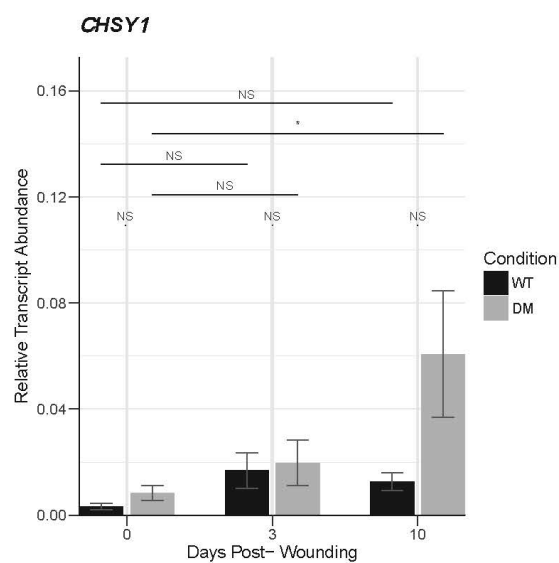
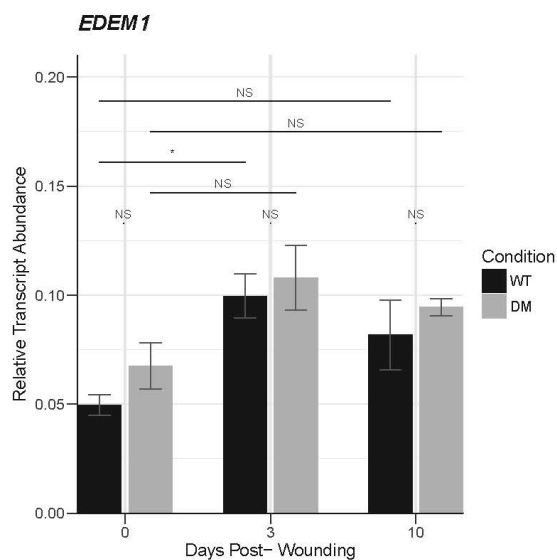


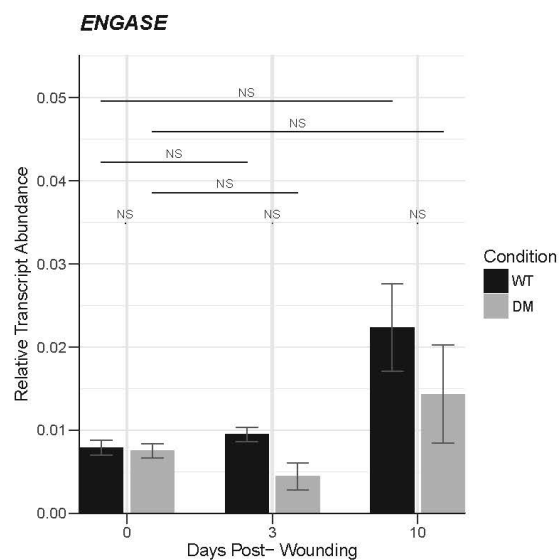
Figure 70. Glycosylation Related Gene Expression in Diabetic and Non-Diabetic Skin and Wounds. (continued)

APPENDIX D (continued)

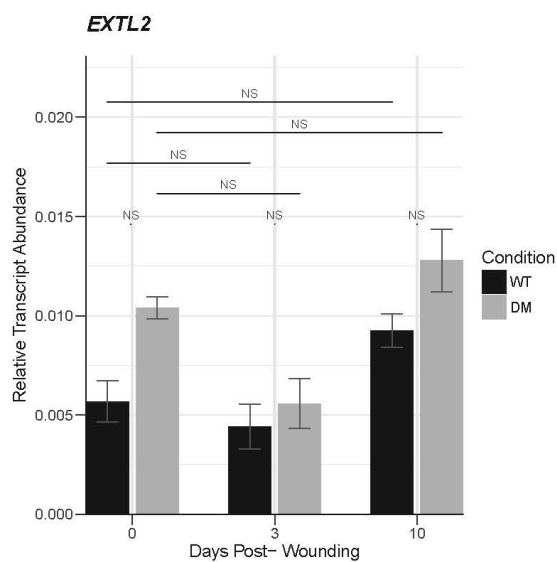
A.



B.



C.



D.

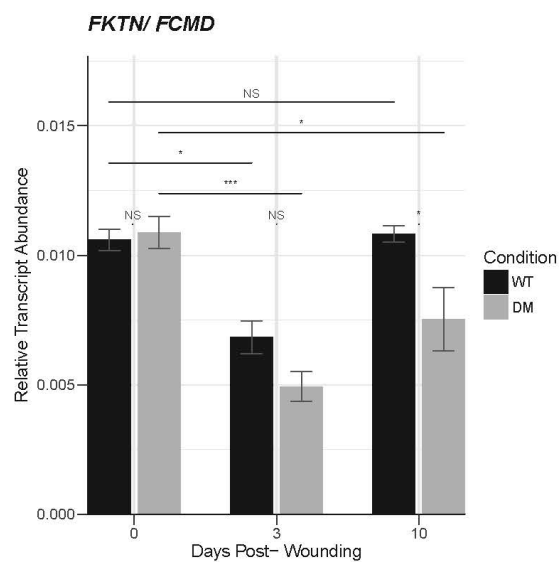


Figure 71. Glycosylation Related Gene Expression in Diabetic and Non-Diabetic Skin and Wounds. (continued)

APPENDIX D (continued)

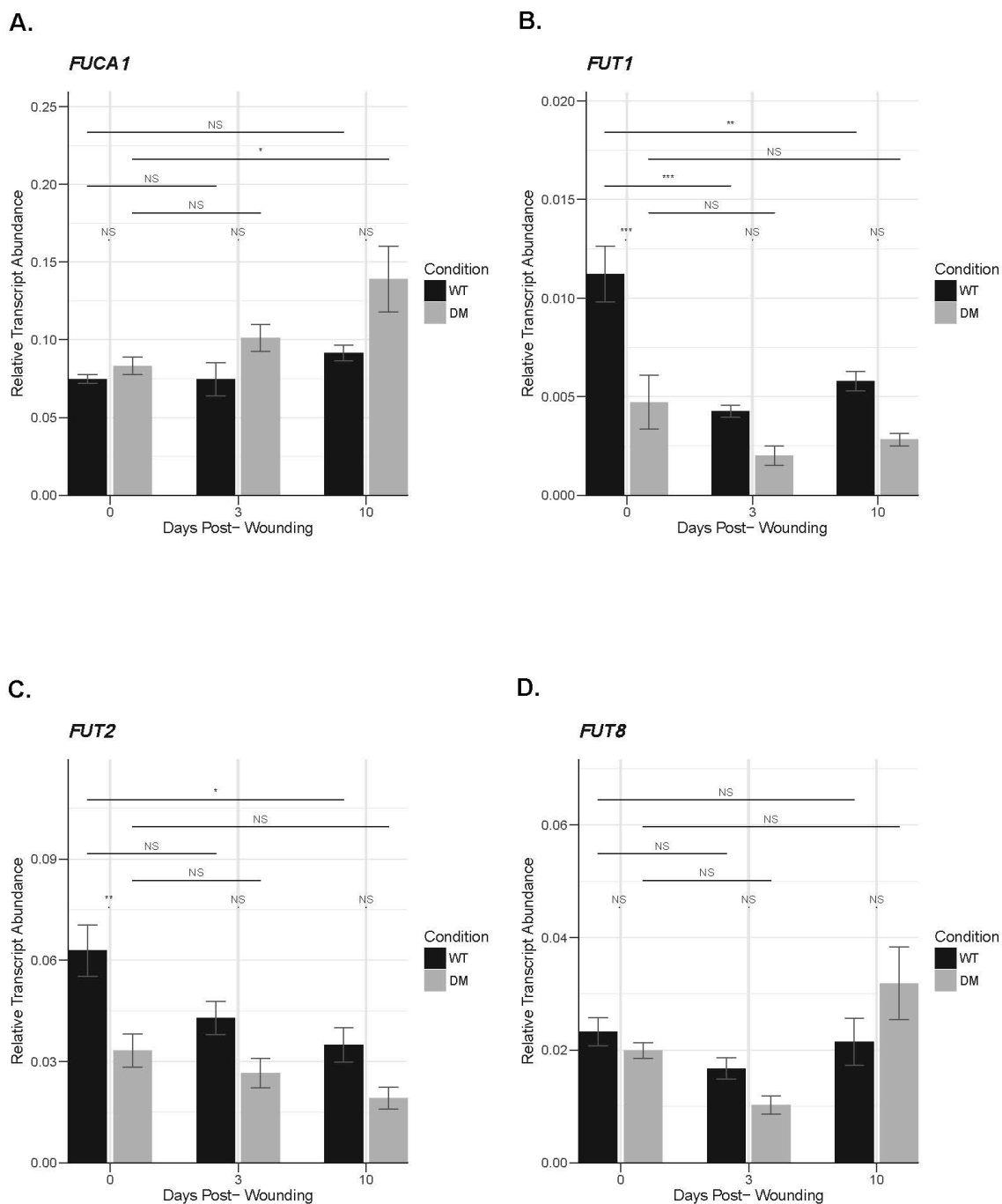


Figure 72. Glycosylation Related Gene Expression in Diabetic and Non-Diabetic Skin and Wounds. (continued)

APPENDIX D (continued)

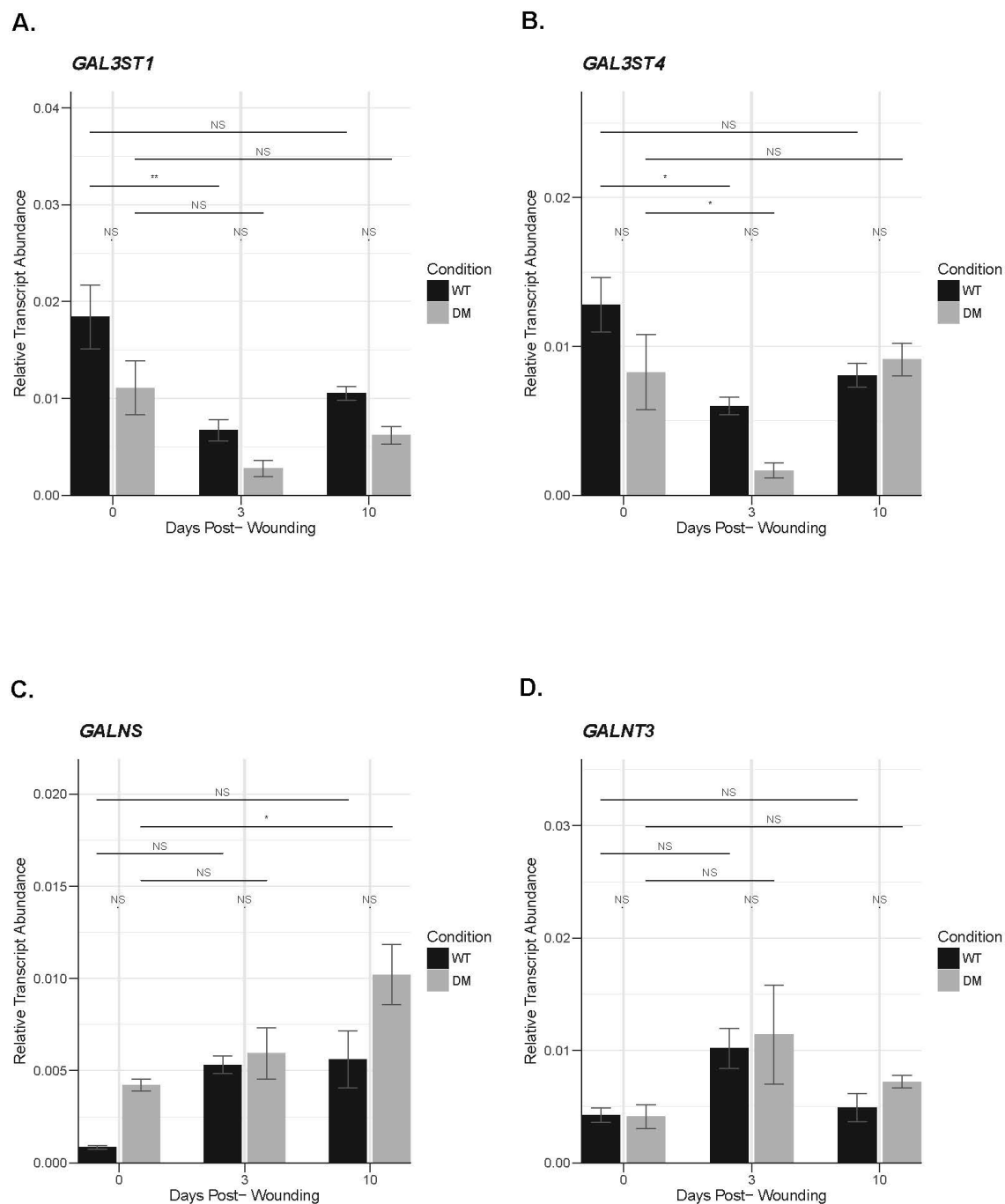


Figure 73. Glycosylation Related Gene Expression in Diabetic and Non-Diabetic Skin and Wounds. (continued)

APPENDIX D (continued)

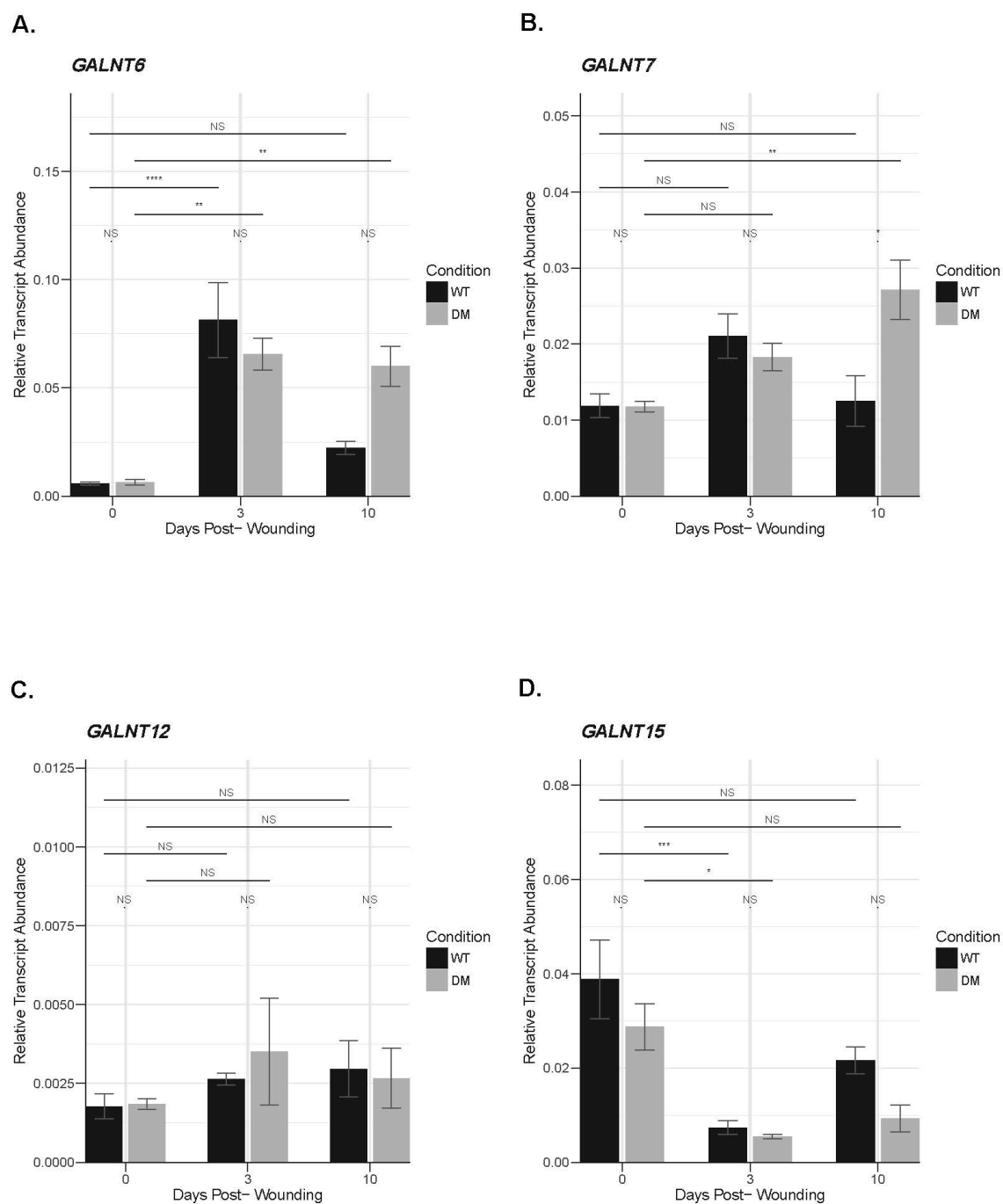


Figure 74. Glycosylation Related Gene Expression in Diabetic and Non-Diabetic Skin and Wounds. (continued)

APPENDIX D (continued)

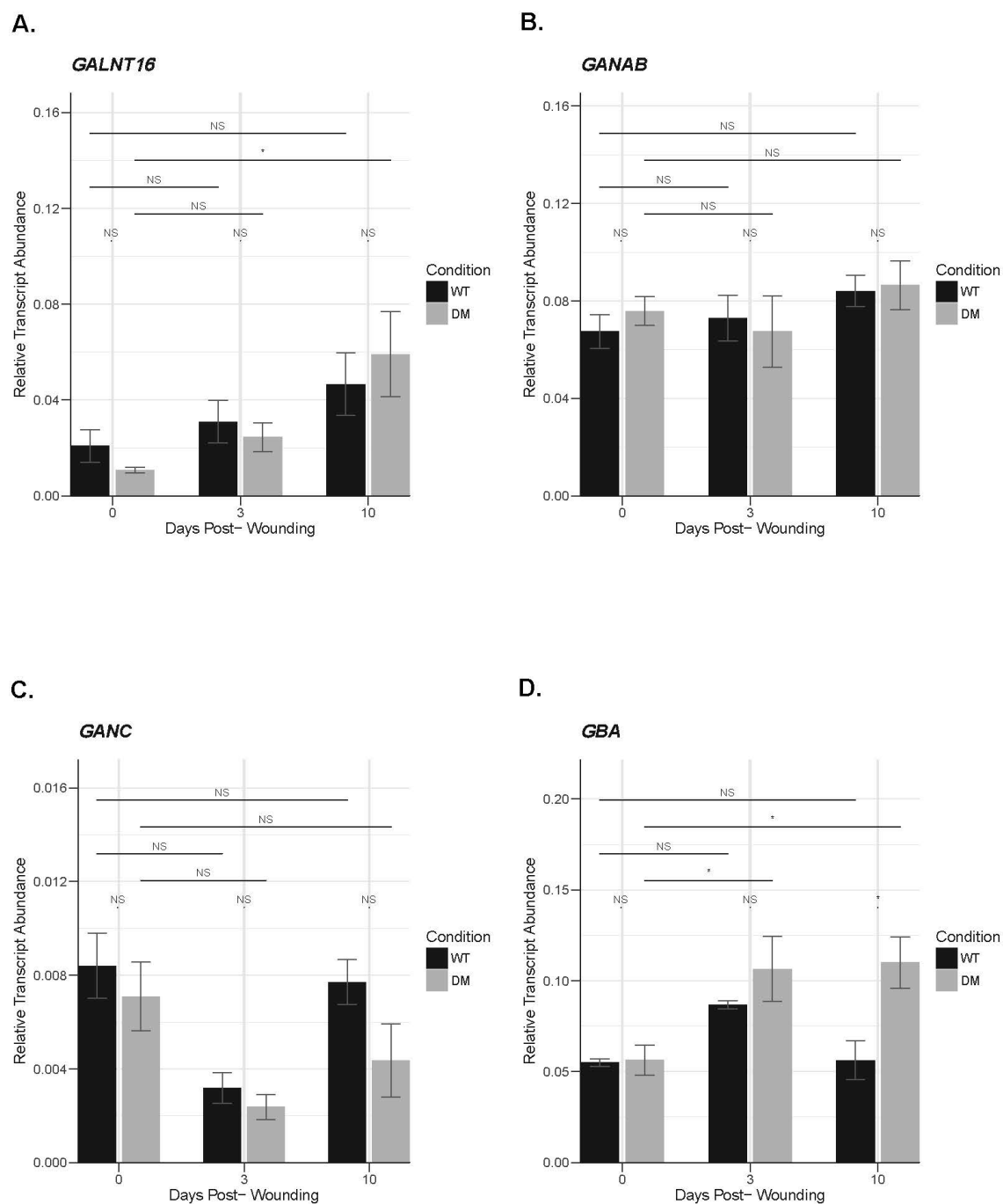


Figure 75. Glycosylation Related Gene Expression in Diabetic and Non-Diabetic Skin and Wounds. (continued)

APPENDIX D (continued)

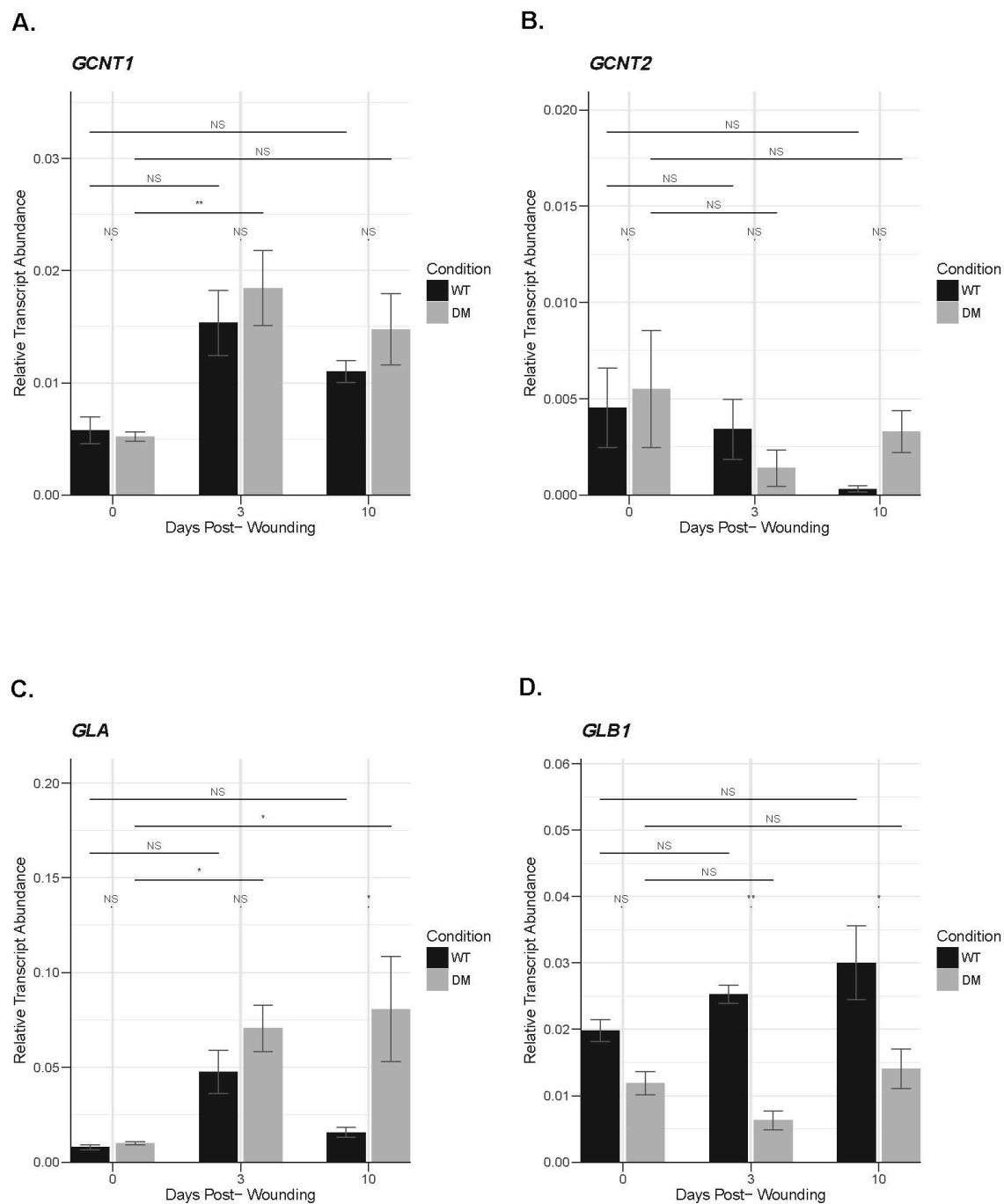


Figure 76. Glycosylation Related Gene Expression in Diabetic and Non-Diabetic Skin and Wounds. (continued)

APPENDIX D (continued)

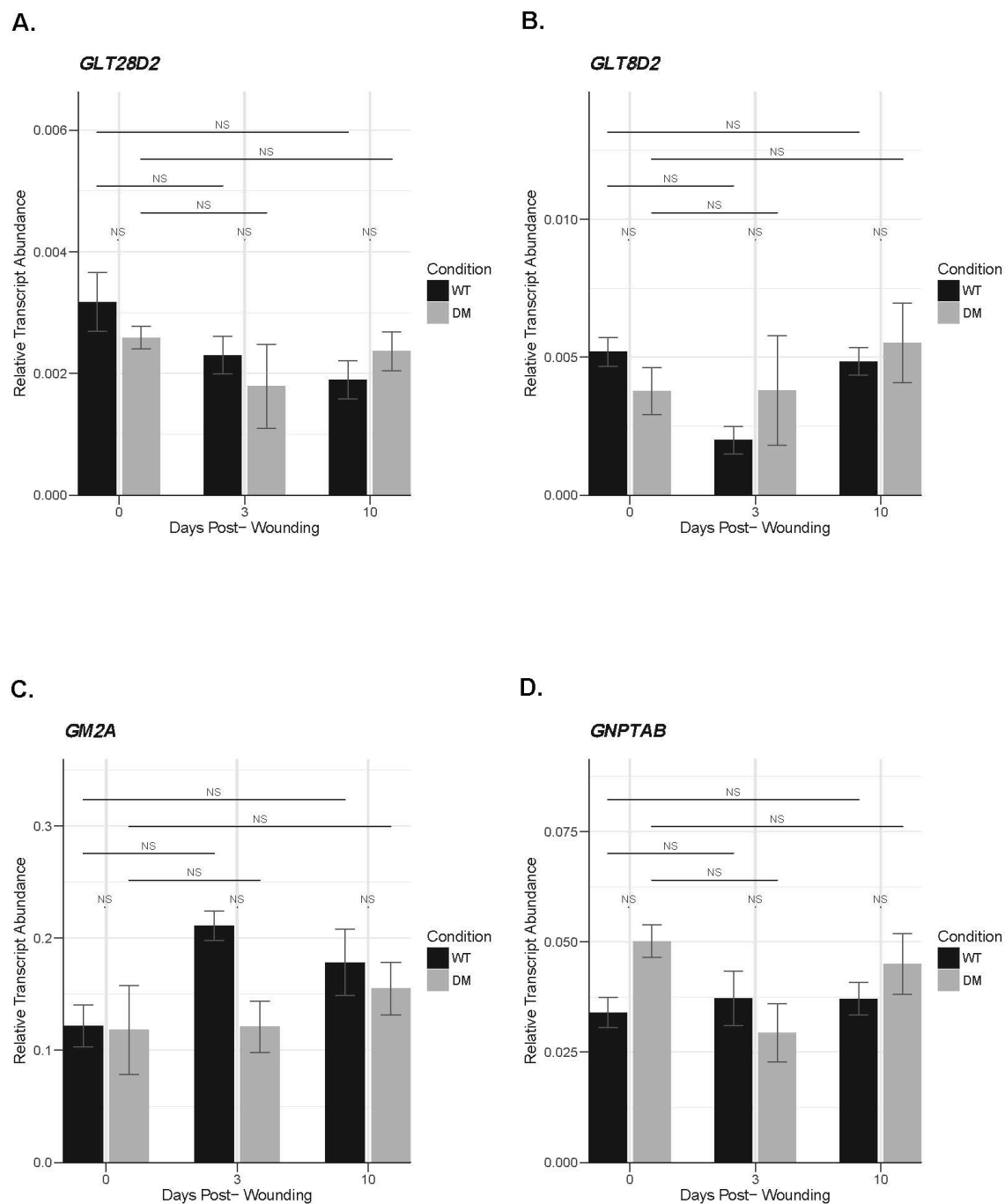


Figure 77. Glycosylation Related Gene Expression in Diabetic and Non-Diabetic Skin and Wounds. (continued)

APPENDIX D (continued)

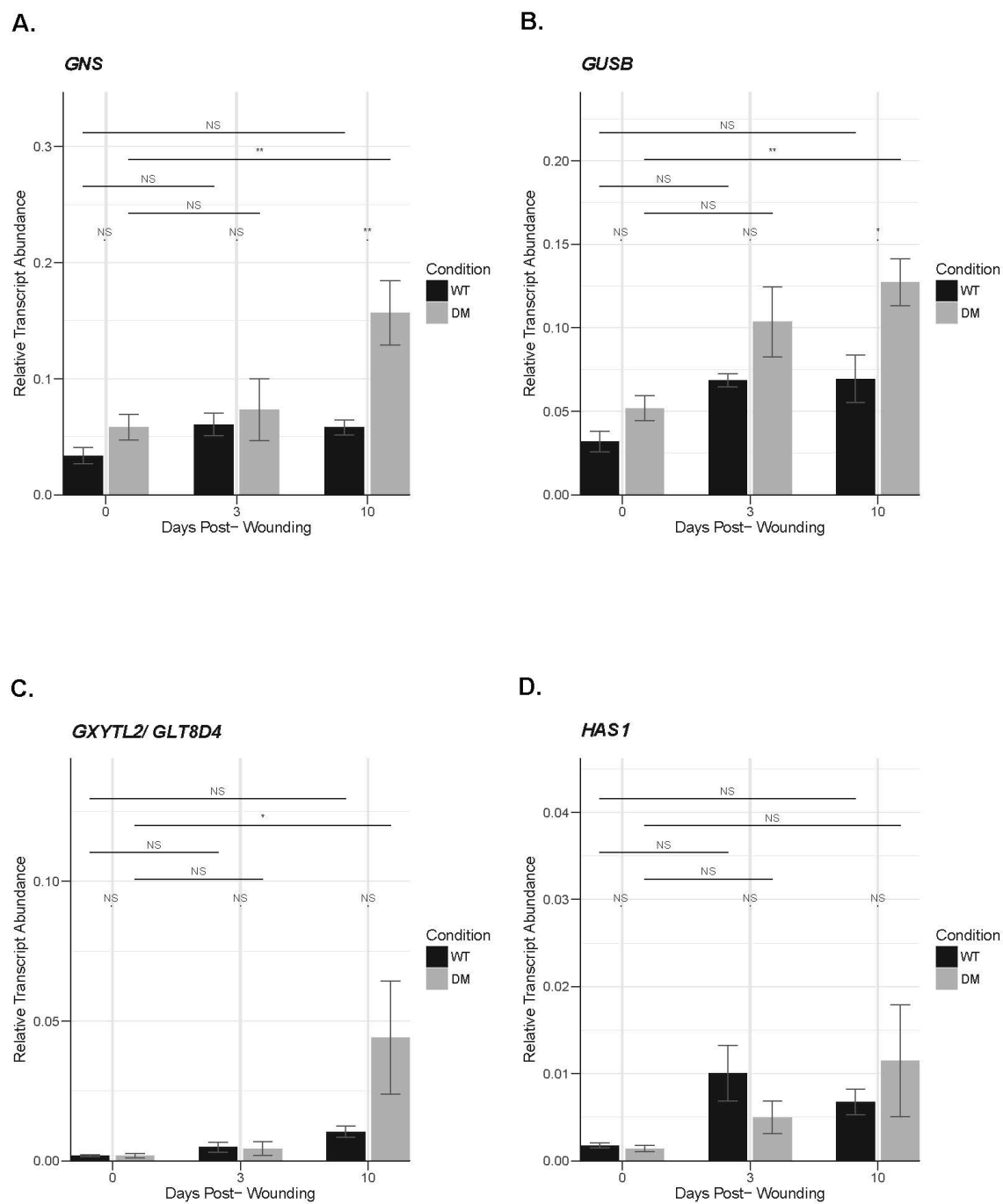


Figure 78. Glycosylation Related Gene Expression in Diabetic and Non-Diabetic Skin and Wounds. (continued)

APPENDIX D (continued)

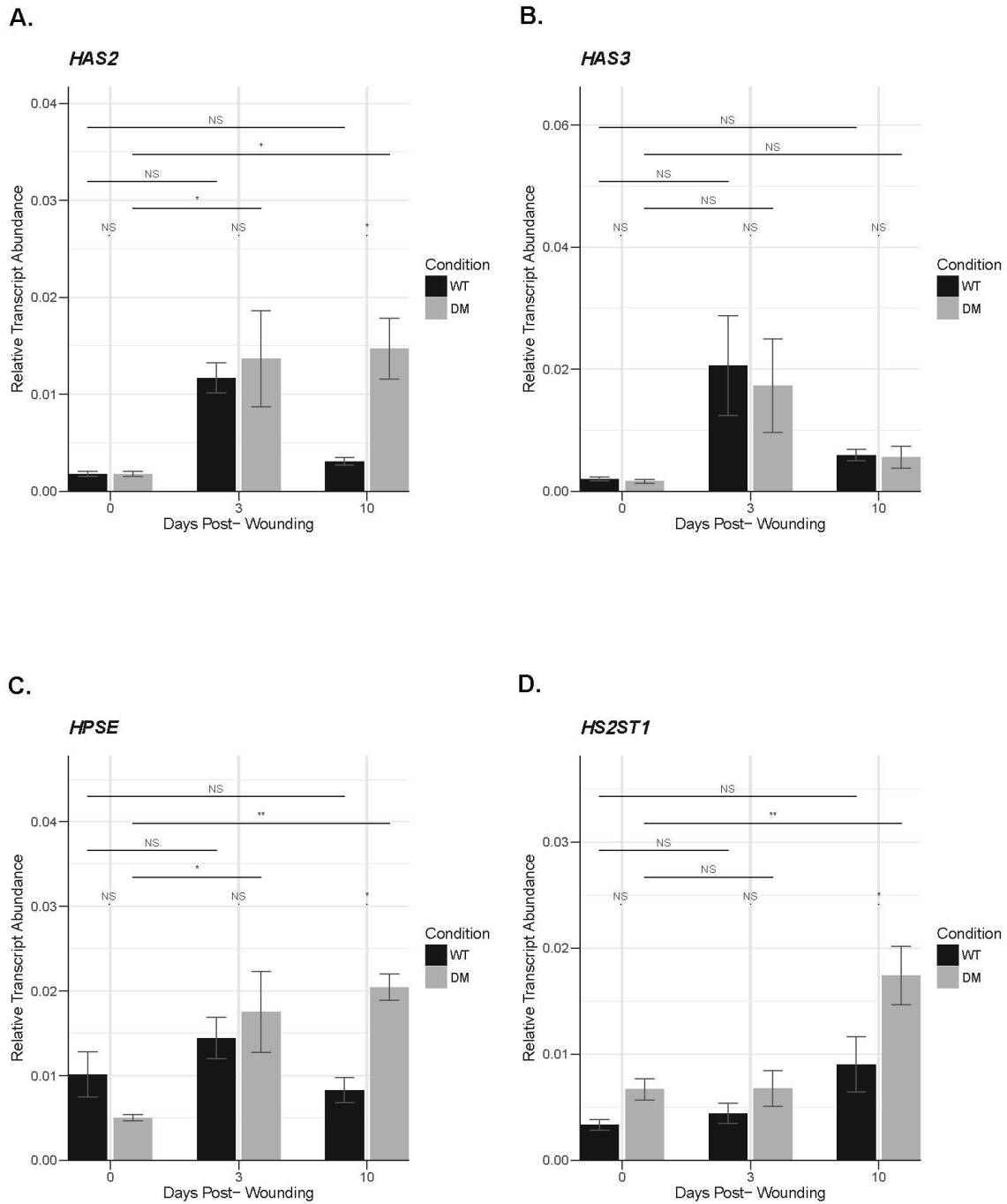


Figure 79. Glycosylation Related Gene Expression in Diabetic and Non-Diabetic Skin and Wounds. (continued)

APPENDIX D (continued)

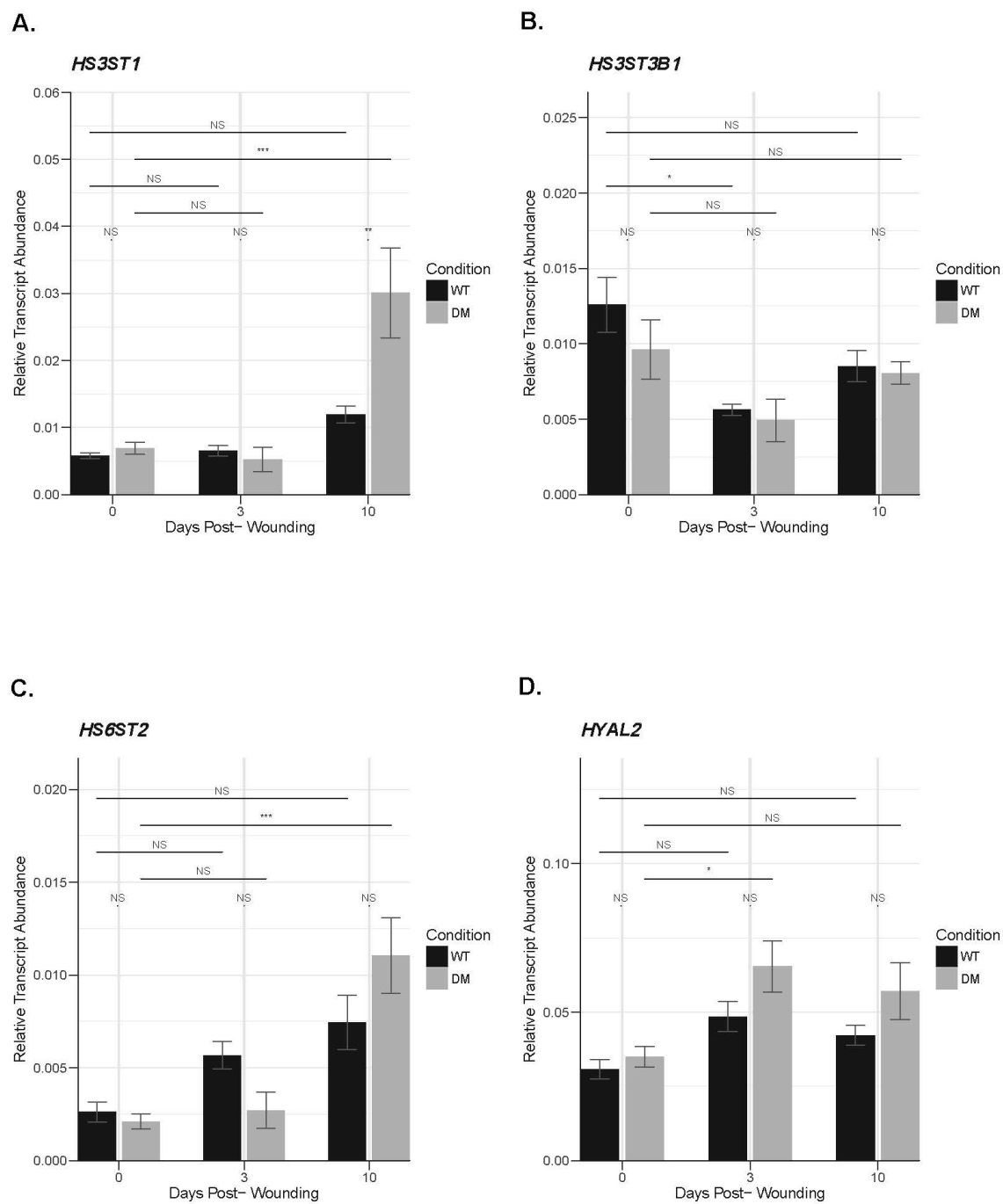


Figure 80. Glycosylation Related Gene Expression in Diabetic and Non-Diabetic Skin and Wounds. (continued)

APPENDIX D (continued)

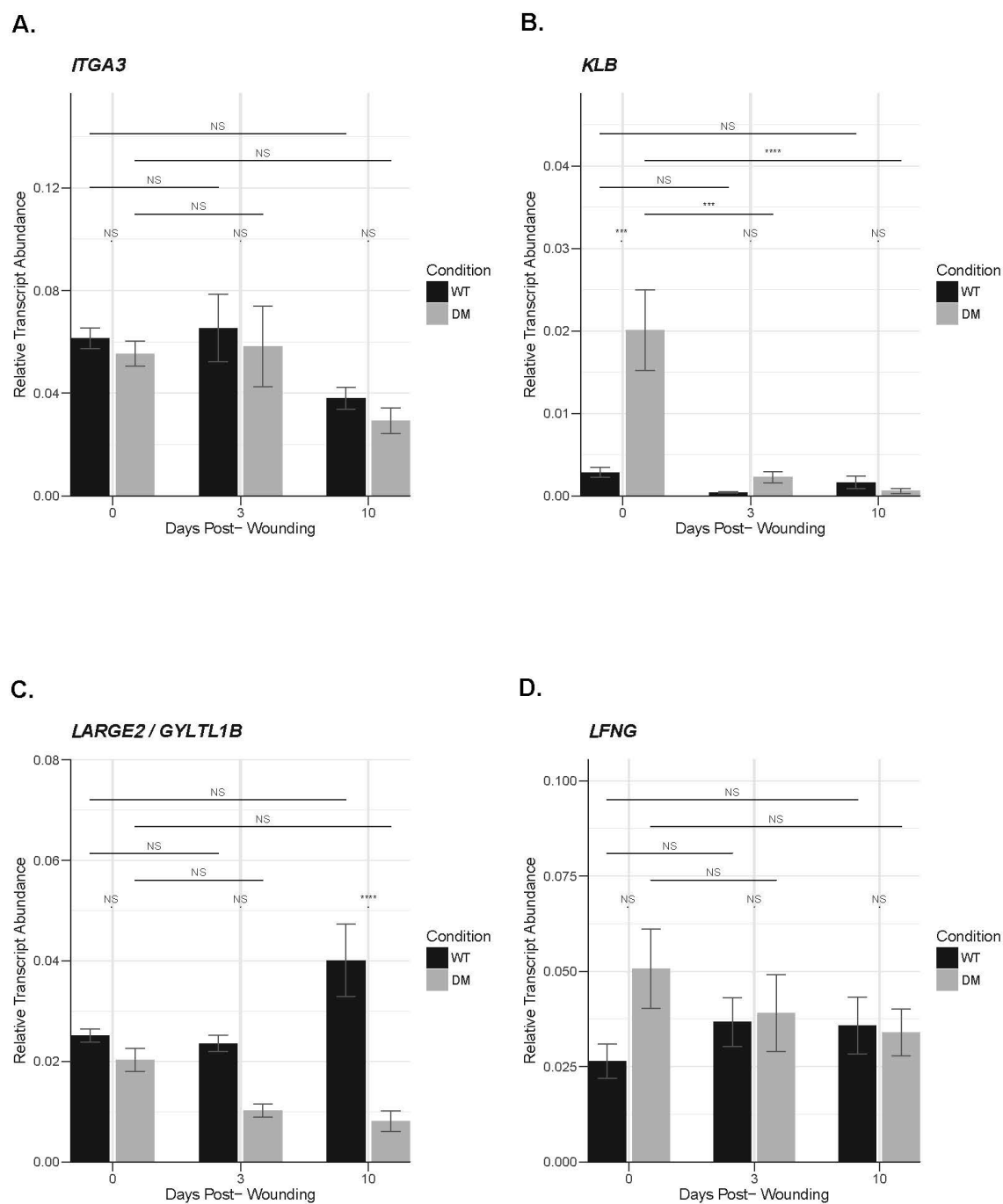


Figure 81. Glycosylation Related Gene Expression in Diabetic and Non-Diabetic Skin and Wounds. (continued)

APPENDIX D (continued)

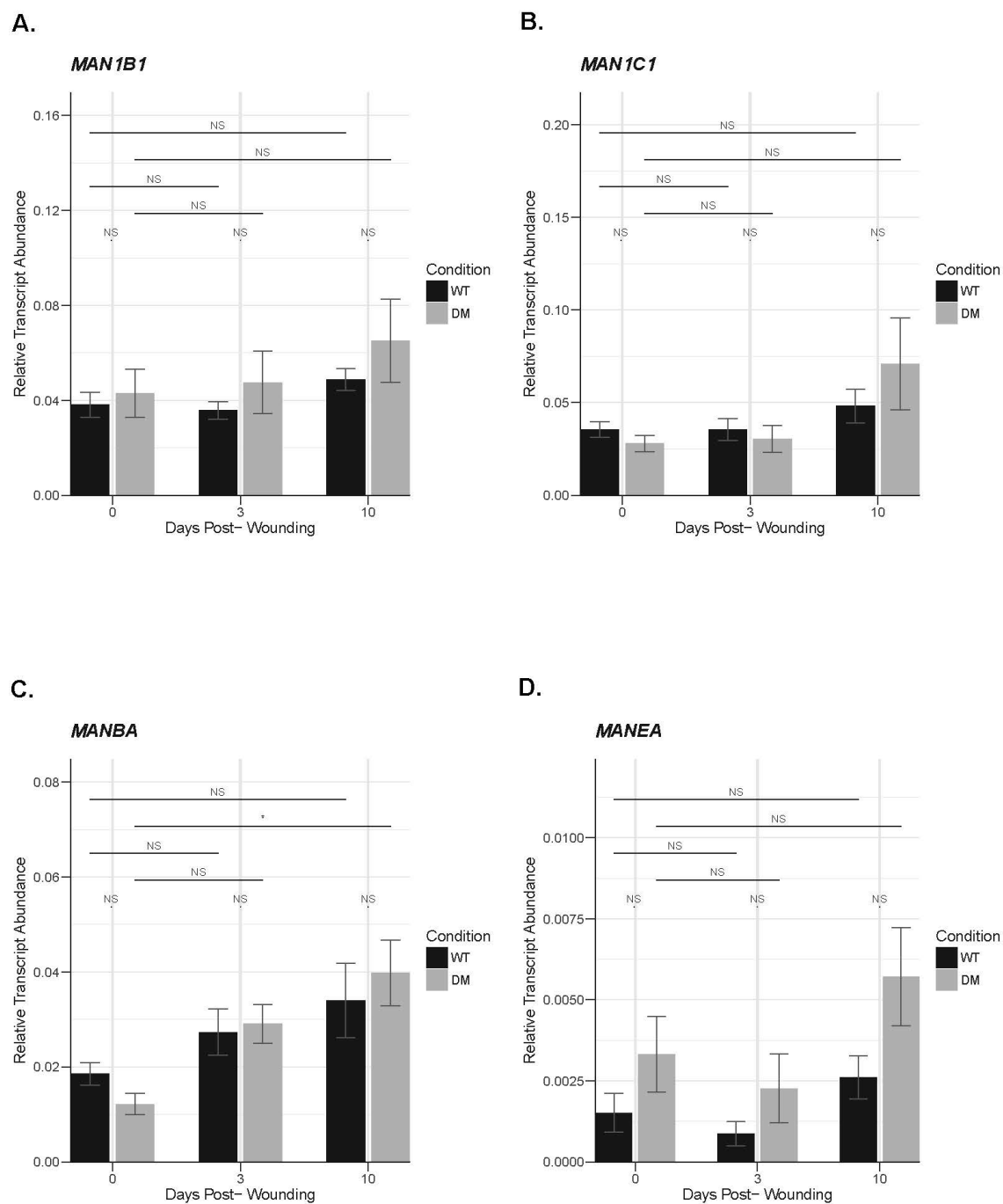


Figure 82. Glycosylation Related Gene Expression in Diabetic and Non-Diabetic Skin and Wounds. (continued)

APPENDIX D (continued)

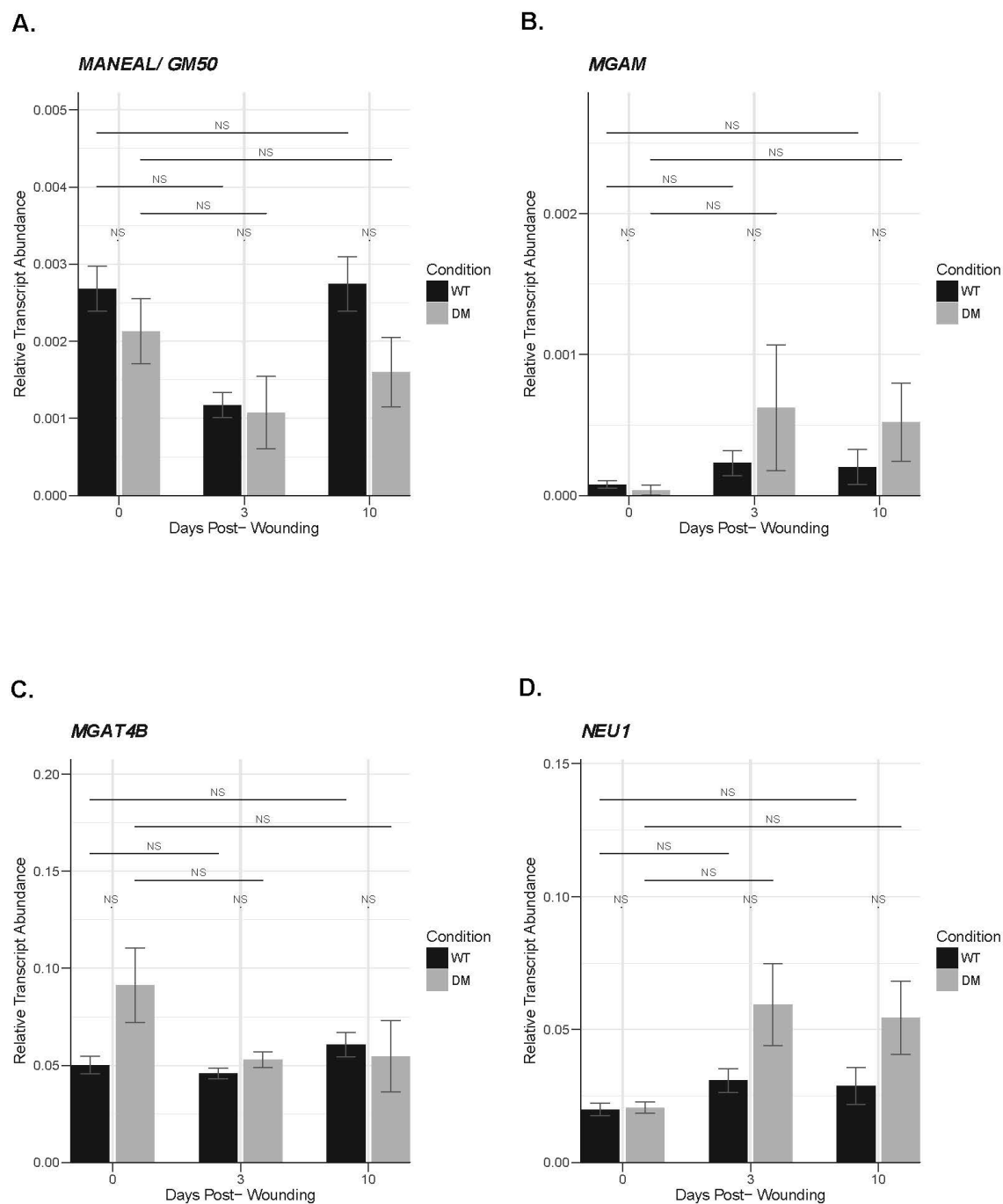


Figure 83. Glycosylation Related Gene Expression in Diabetic and Non-Diabetic Skin and Wounds. (continued)

APPENDIX D (continued)

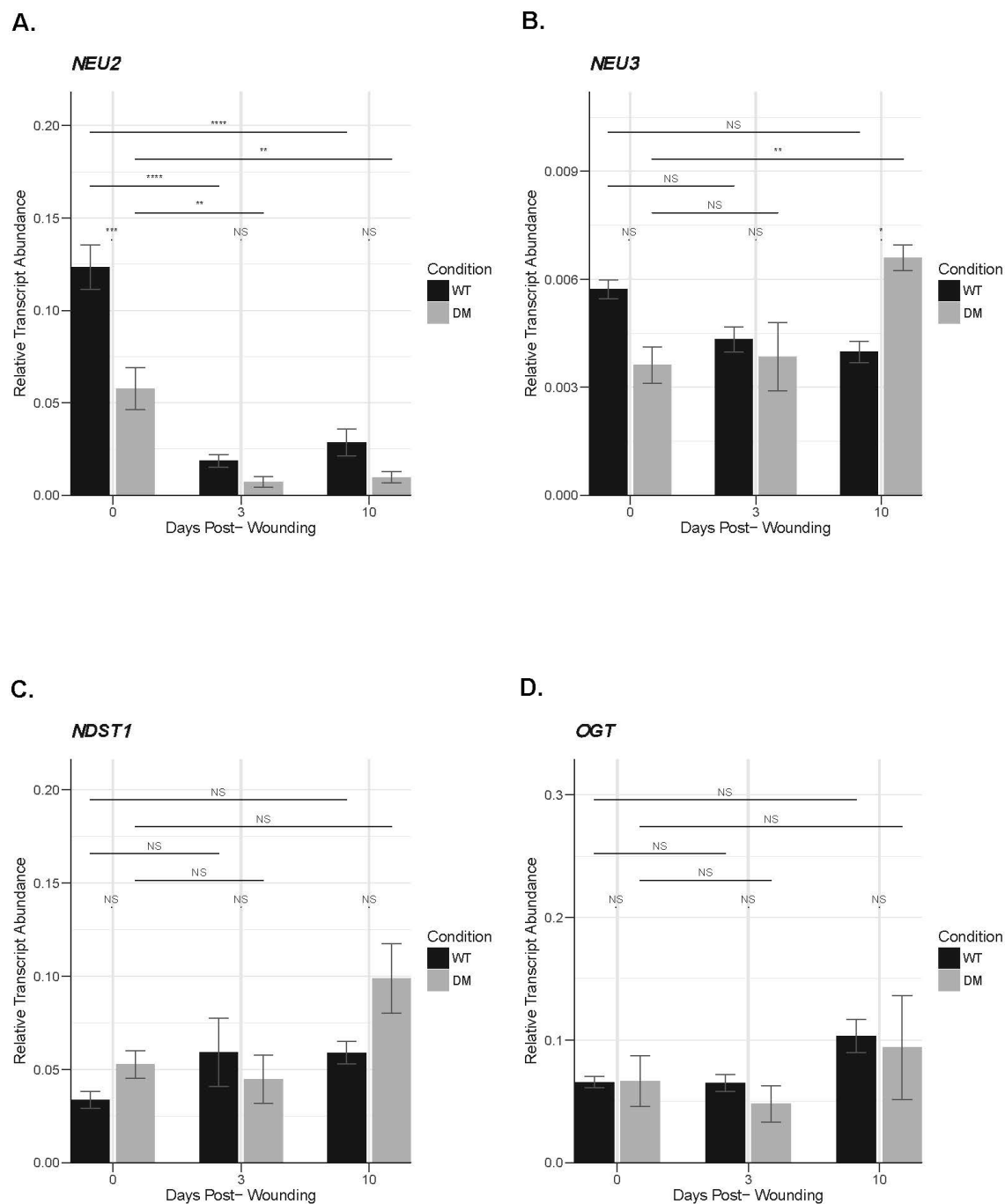


Figure 84. Glycosylation Related Gene Expression in Diabetic and Non-Diabetic Skin and Wounds. (continued)

APPENDIX D (continued)

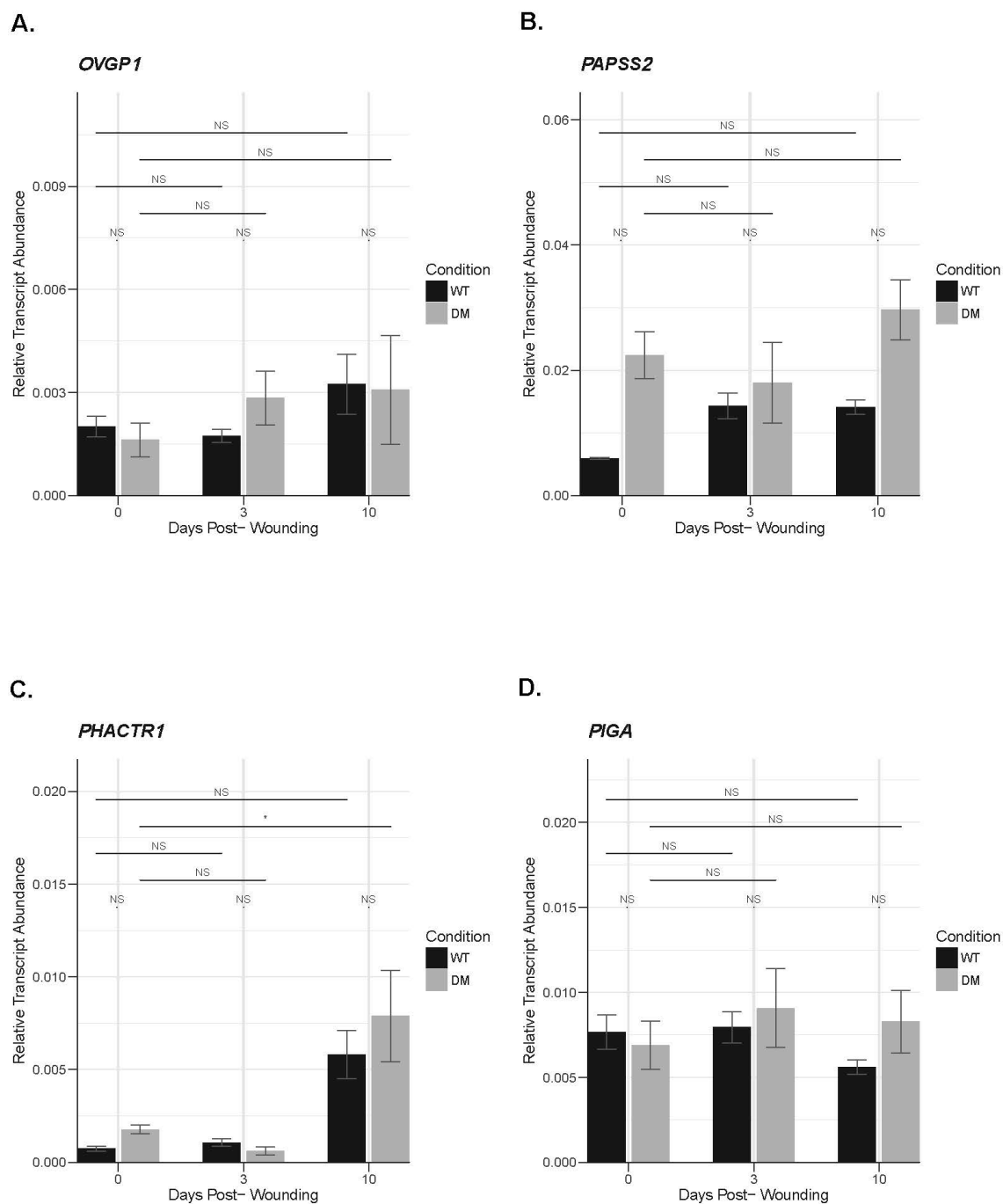


Figure 85. Glycosylation Related Gene Expression in Diabetic and Non-Diabetic Skin and Wounds. (continued)

APPENDIX D (continued)

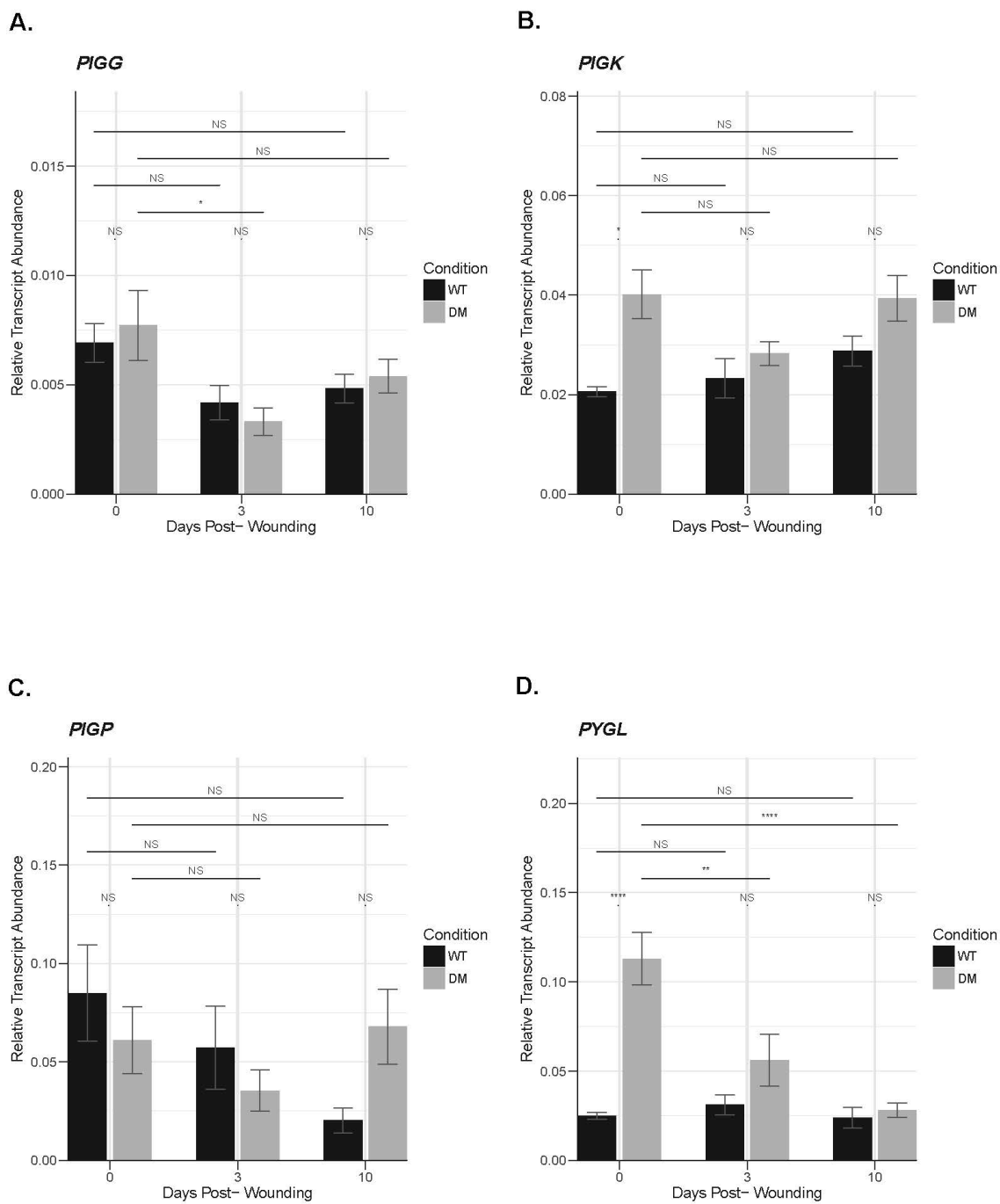


Figure 86. Glycosylation Related Gene Expression in Diabetic and Non-Diabetic Skin and Wounds. (continued)

APPENDIX D (continued)

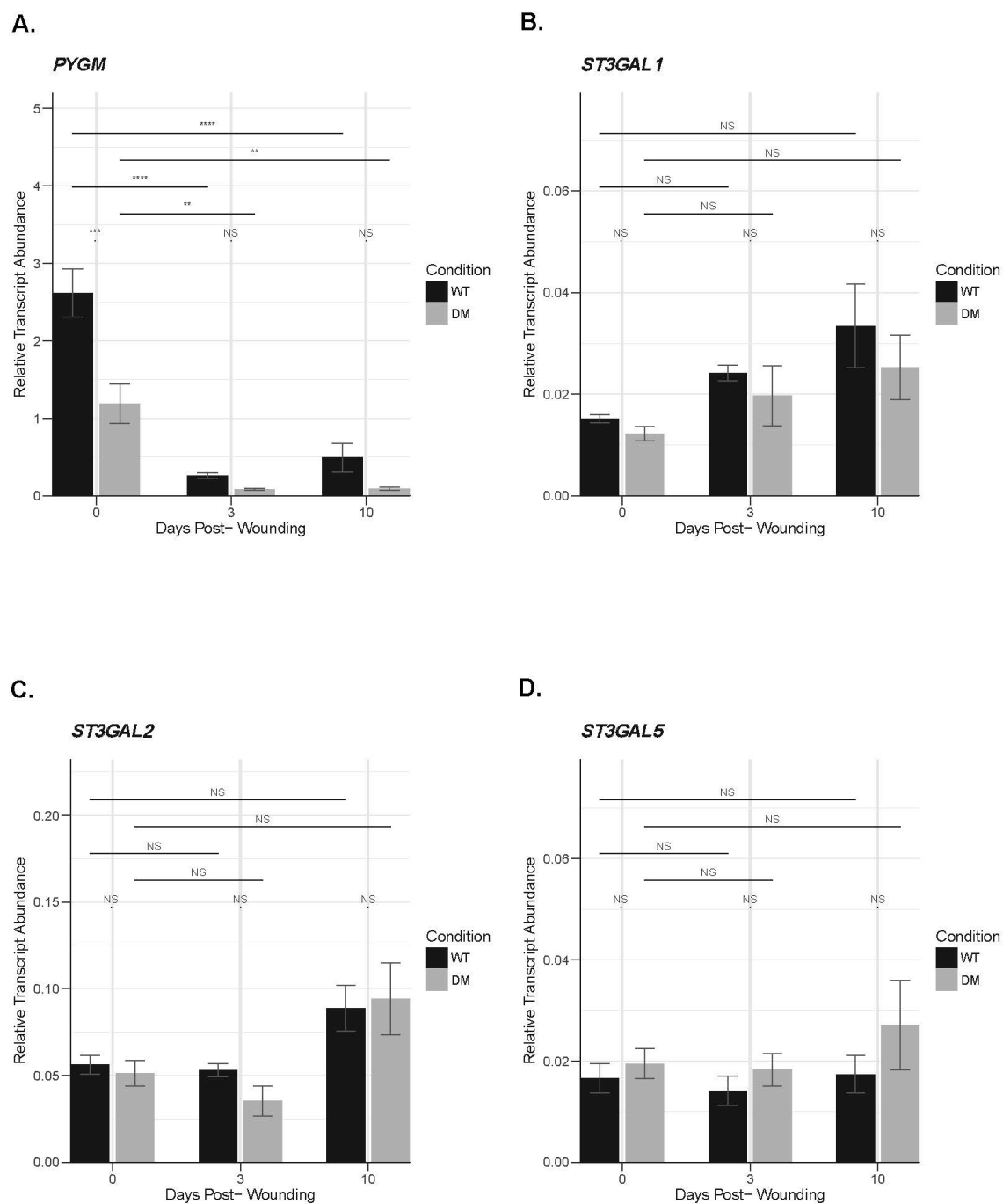


Figure 87. Glycosylation Related Gene Expression in Diabetic and Non-Diabetic Skin and Wounds. (continued)

APPENDIX D (continued)

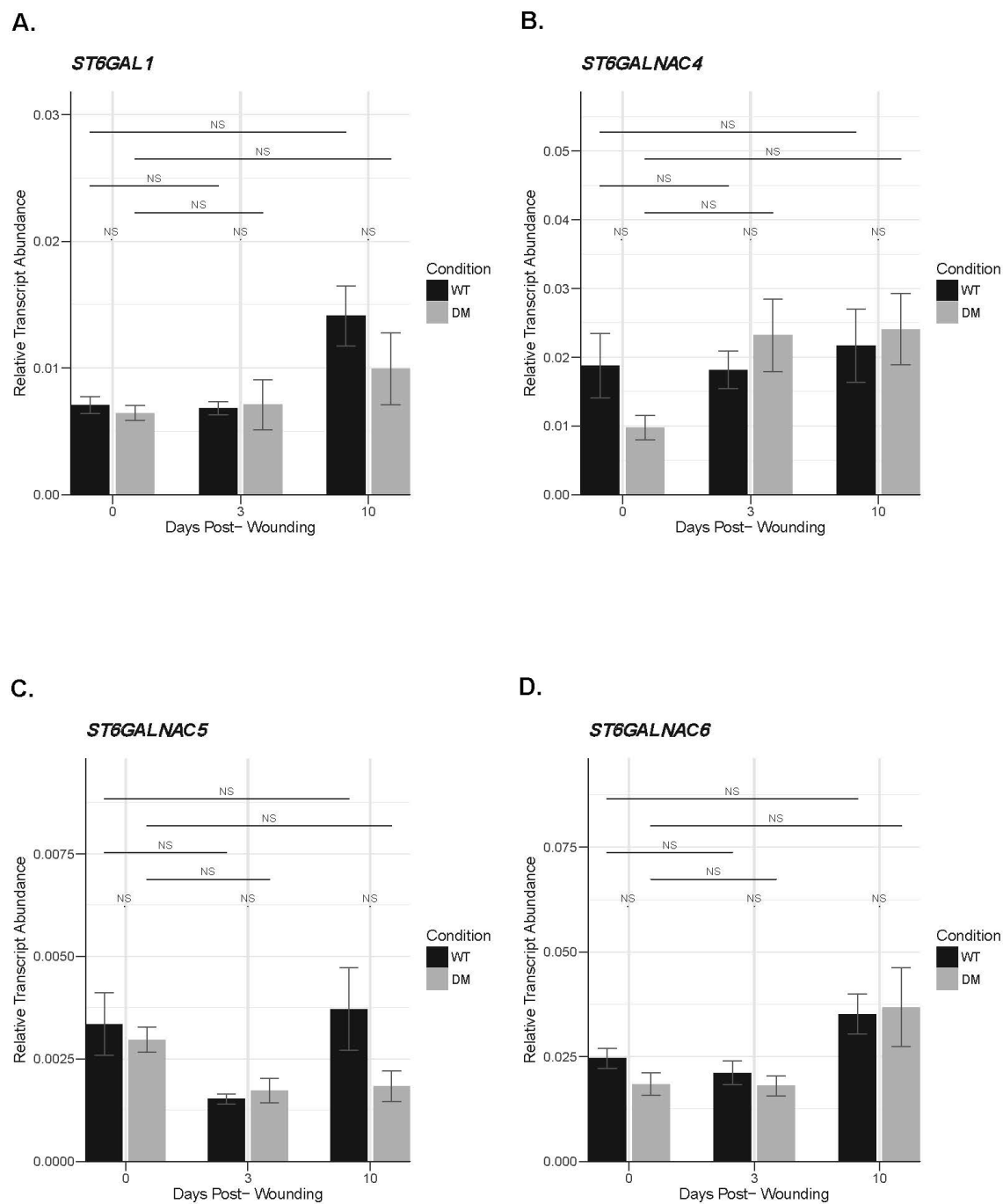


Figure 88. Glycosylation Related Gene Expression in Diabetic and Non-Diabetic Skin and Wounds. (continued)

APPENDIX D (continued)

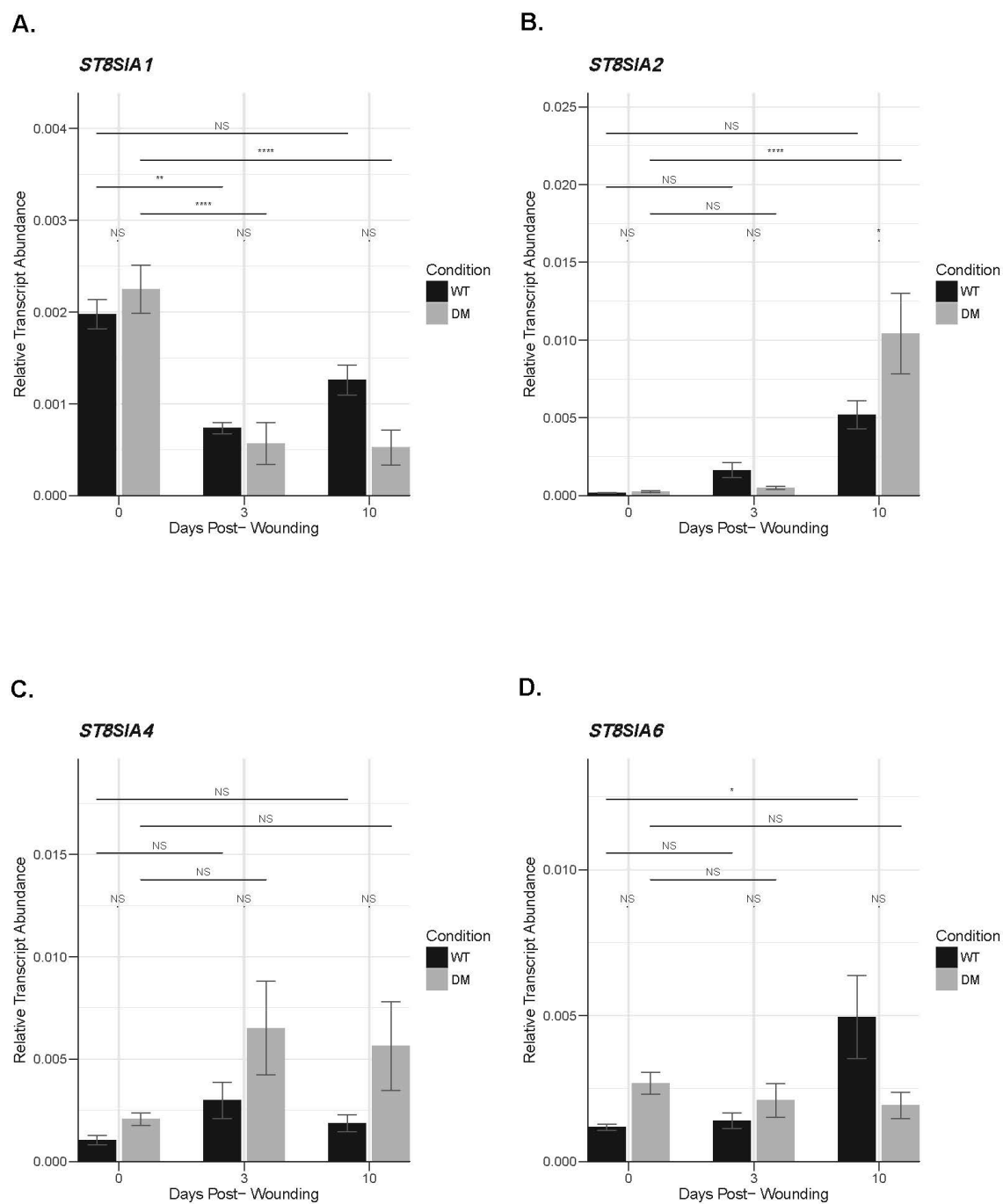


Figure 89. Glycosylation Related Gene Expression in Diabetic and Non-Diabetic Skin and Wounds. (continued)

APPENDIX D (continued)

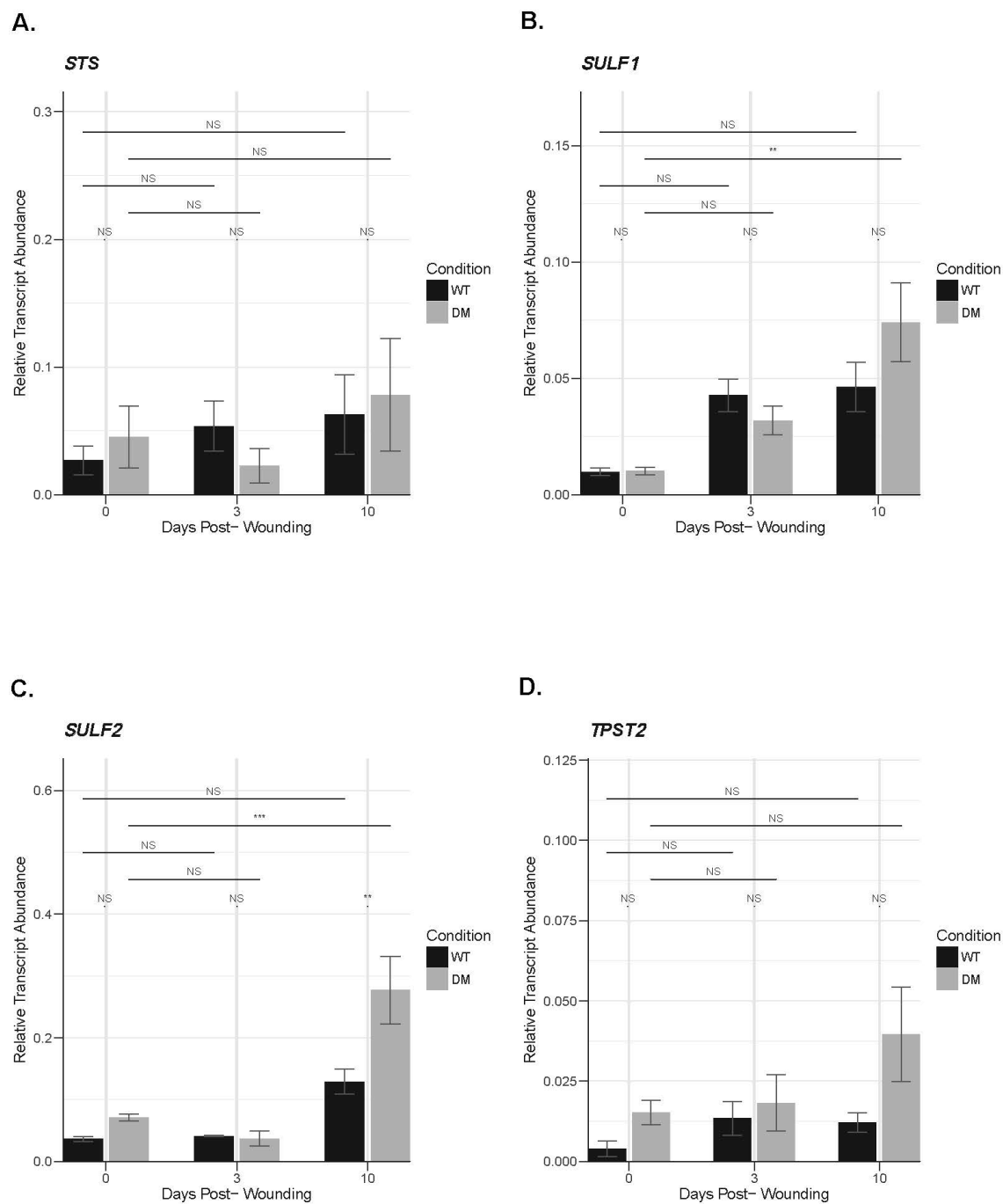


Figure 90. Glycosylation Related Gene Expression in Diabetic and Non-Diabetic Skin and Wounds. (continued)

APPENDIX D (continued)

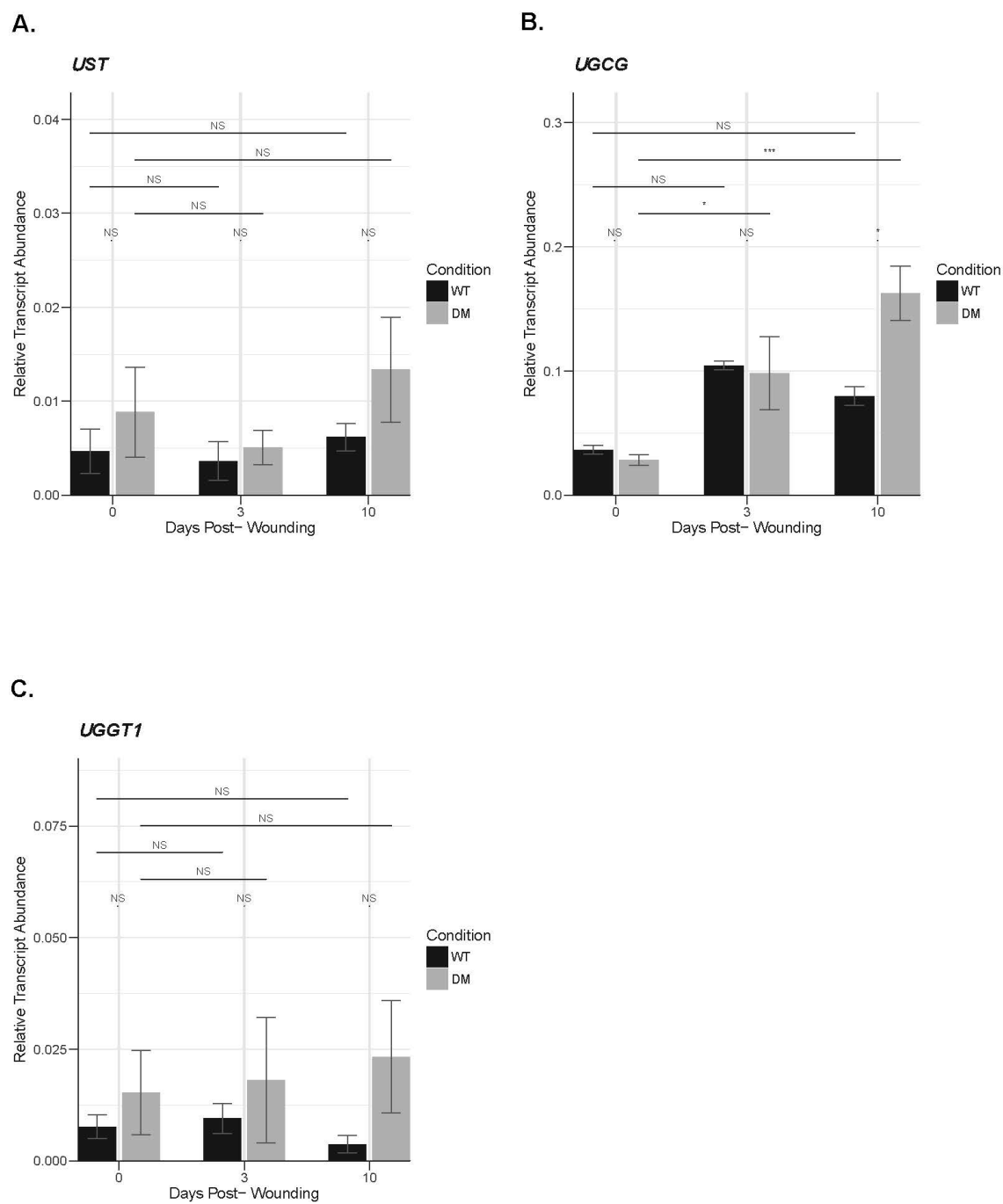


Figure 91. Glycosylation Related Gene Expression in Diabetic and Non-Diabetic Skin and Wounds. (continued)

APPENDIX E

7/22/2019

Reprints and permissions

Reprints and permissions

Reprint service

Reprint services are available for those requiring professional quality reproductions of articles.

Open access articles

The open access articles published in BMC's journals are made available under the Creative Commons Attribution (CC-BY) license, which means they are accessible online without any restrictions and can be re-used in any way, subject only to proper attribution (which, in an academic context, usually means citation).

The re-use rights enshrined in our [license agreement](#) include the right for anyone to produce printed copies themselves, without formal permission or payment of permission fees. As a courtesy, however, anyone wishing to reproduce large quantities of an open access article (250+) should inform the copyright holder and we suggest a contribution in support of open access publication.

Free articles

All articles in BMC journals are available online without charge or other barriers to access. The following journals have published a small number of articles that, while freely accessible, are not open access as outlined in the section above:

[Alzheimer's Research & Therapy](#)

[Arthritis Research & Therapy](#)

[Breast Cancer Research](#)

[Critical Care](#)

[Genome Biology](#)

[Genome Medicine](#)

[Stem Cell Research & Therapy](#)

These articles may be flagged as 'Free' content and their bibliographic information may indicate that copyright rests with the publisher or another organization. With the exception of a few co-published articles (see below), these free articles may be reproduced for non-commercial purposes without formal permission from BMC or payment of fees, provided full attribution is given. If you wish to reproduce such an article, or parts thereof, for commercial purposes (other than original figures and/or tables), please [contact us](#) to check whether formal permission is needed.

Co-publications: Different rules may apply to articles which are co-published (i.e. published in a BMC journal and simultaneously in another publication); in such cases a statement of co-publication is included in the bibliographic information. Please [contact us](#) for permission to reproduce content from these articles.

Figures and tables

Reproduction of figures or tables from any article is permitted free of charge and without formal written permission from the publisher or the copyright holder, provided that the figure/table is original, BMC is duly identified as the original publisher, and that proper attribution of authorship and the correct citation details are given as acknowledgment. If you have any questions about reproduction of figures or tables please [contact us](#).

Reprints

APPENDIX E (continued)

7/22/2019

Reprints and permissions

Reprint services are available for those requiring professional quality reproductions of articles. Reprints are produced from the final PDF of the article; if you are interested in reprints of an article which is at Provisional PDF stage, please [email us](#).

25-500 copies of any article with a final PDF can be ordered using the online ordering system provided by EzReprint. From the full text or abstract of the article, selecting the option to 'Order reprints' takes you directly to the order page, where the article details will be automatically inserted.

This simple to use service offers a variety of production and payment options, and enables users to have reprints delivered to their door.

For orders of 500+ copies, or for commercial reprints, please contact BMC_Reprints@springer.com or use the EzReprint service and select the "Commercial Orders & Higher Quantities" link (see screenshot below).

Publication: BMC Systems Biology	
Select Country of Destination:	Select Country Help

Author Name:	Bettina M Langer		
Article Title:	<p>Modeling of leishmaniasis infection dynamics: novel application to the		
Article Identifier:	10.1186/1752-0509-6-1 Help		
Start Page:	1	End Page:	
Volume:	6	Issue:	1
Total No. of Pages in Reprint:	0 pages Help		

PRINTED ARTICLE REPRINT ORDER PRICING	
Number of Copies:	25 Commercial Orders & Higher Quantities. Click here
Journal Covers:	See Help Link Help
This article is published in open access and copies may be made for Click here to Update Price	

APPENDIX E (continued)

7/22/2019

Creative Commons — Attribution 4.0 International — CC BY 4.0

This page is available in the following languages:



Creative Commons License De

Attribution 4.0 International (CC BY 4.0)



This is a human-readable summary of (and not a substitute for) the [license](#).

You are free to:

Share — copy and redistribute the material in any medium or format

Adapt — remix, transform, and build upon the material

for any purpose, even commercially.

The licensor cannot revoke these freedoms as long as you follow the license terms.

Under the following terms:



Attribution — You must give appropriate credit, provide a link to the license, and indicate if changes were made. You may do so in any reasonable manner, but not in any way that suggests the licensor endorses you or your use.

No additional restrictions — You may not apply legal terms or technological measures that legally restrict others from doing anything the license permits.

Notices:

You do not have to comply with the license for elements of the material in the public domain or where your use is permitted by an applicable exception or limitation.

No warranties are given. The license may not give you all of the permissions necessary for your intended use. For example, other rights such as publicity, privacy, or moral rights may limit how you use the material.

APPENDIX E (continued)

SPRINGER NATURE LICENSE
TERMS AND CONDITIONS

Feb 28, 2019

This Agreement between Veronica Haywood ("You") and Springer Nature ("Springer Nature") consists of your license details and the terms and conditions provided by Springer Nature and Copyright Clearance Center.

License Number	4537750814883
License date	Feb 28, 2019
Licensed Content Publisher	Springer Nature
Licensed Content Publication	Nature Reviews Molecular Cell Biology
Licensed Content Title	Vertebrate protein glycosylation: diversity, synthesis and function
Licensed Content Author	Kelley W. Moremen, Michael Tiemeyer, Alison V. Nairn
Licensed Content Date	Jun 22, 2012
Licensed Content Volume	13
Licensed Content Issue	7
Type of Use	Thesis/Dissertation
Requestor type	academic/university or research institute
Format	print and electronic
Portion	figures/tables/illustrations
Number of figures/tables/illustrations	5
High-res required	no
Will you be translating?	no
Circulation/distribution	<501
Author of this Springer Nature content	no
Title	PhD Candidate
Institution name	University of Illinois at Chicago College of Dentistry
Expected presentation date	Mar 2019
Portions	Table 1 on page 449; Box 1 figure on page 450; Figure 1 on page 452; Box 2 on page 454; and Figure 2 on page 457.
Requestor Location	Veronica Haywood 9301 S. Winchester CHICAGO, IL 60643 United States Attn: Veronica Haywood
Billing Type	Invoice
Billing Address	Veronica Haywood 9301 S. Winchester CHICAGO, IL 60643 United States Attn: Veronica Haywood
Total	0.00 USD
Terms and Conditions	

Springer Nature Terms and Conditions for RightsLink Permissions

Springer Nature Customer Service Centre GmbH (the Licensor) hereby grants you a non-exclusive, world-wide licence to reproduce the material and for the purpose and requirements specified in the attached copy of your order form, and for no other use, subject to the conditions below:

1. The Licensor warrants that it has, to the best of its knowledge, the rights to license reuse of this material. However, you should ensure that the material you are requesting is original to the Licensor and does not carry the copyright of another entity (as credited in the published version).
If the credit line on any part of the material you have requested indicates that it was reprinted or adapted with permission from another source, then you should also seek permission from that source to reuse the material.
2. Where **print only** permission has been granted for a fee, separate permission must be obtained for any additional electronic re-use.
3. Permission granted **free of charge** for material in print is also usually granted for any electronic version of that work, provided that the material is incidental to your work as a whole and that the electronic version is essentially equivalent to, or substitutes for, the print version.
4. A licence for 'post on a website' is valid for 12 months from the licence date. This licence does not cover use of full text articles on websites.
5. Where '**reuse in a dissertation/thesis**' has been selected the following terms apply: Print rights of the final author's accepted manuscript (for clarity, NOT the published version) for up to 100 copies, electronic rights for use only on a personal website or institutional repository as defined by the Sherpa guideline (www.sherpa.ac.uk/romeo/).
6. Permission granted for books and journals is granted for the lifetime of the first edition and does not apply to second and subsequent editions (except where the first edition permission was granted free of charge or for signatories to the STM Permissions Guidelines <http://www.stm-assoc.org/copyright-legal-affairs/permissions/permissions-guidelines/>), and does not apply for editions in other languages unless additional translation rights have been granted separately in the licence.
7. Rights for additional components such as custom editions and derivatives require additional permission and may be subject to an additional fee. Please apply to Journalpermissions@springernature.com/bookpermissions@springernature.com for these rights.
8. The Licensor's permission must be acknowledged next to the licensed material in print. In electronic form, this acknowledgement must be visible at the same time as the figures/tables/illustrations or abstract, and must be hyperlinked to the journal/book's homepage. Our required acknowledgement format is in the Appendix below.
9. Use of the material for incidental promotional use, minor editing privileges (this does not include cropping, adapting, omitting material or any other changes that affect the meaning, intention or moral rights of the author) and copies for the disabled are permitted under this licence.
10. Minor adaptations of single figures (changes of format, colour and style) do not require the Licensor's approval. However, the adaptation should be credited as shown in Appendix below.

APPENDIX E (continued)

Appendix — Acknowledgements:

For Journal Content:

Reprinted by permission from [the Licensor]: [Journal Publisher (e.g. Nature/Springer/Palgrave)] [JOURNAL NAME]
[REFERENCE CITATION (Article name, Author(s) Name), [COPYRIGHT] (year of publication)]

For Advance Online Publication papers:

Reprinted by permission from [the Licensor]: [Journal Publisher (e.g. Nature/Springer/Palgrave)] [JOURNAL NAME]
[REFERENCE CITATION (Article name, Author(s) Name), [COPYRIGHT] (year of publication), advance online publication,
day month year (doi: 10.1038/sj.[JOURNAL ACRONYM]).

For Adaptations/Translations:

Adapted/Translated by permission from [the Licensor]: [Journal Publisher (e.g. Nature/Springer/Palgrave)] [JOURNAL NAME]
[REFERENCE CITATION (Article name, Author(s) Name), [COPYRIGHT] (year of publication)]

Note: For any republication from the British Journal of Cancer, the following credit line style applies:

Reprinted/adapted/translated by permission from [the Licensor]: on behalf of Cancer Research UK: : [Journal Publisher (e.g. Nature/Springer/Palgrave)] [JOURNAL NAME] [REFERENCE CITATION (Article name, Author(s) Name), [COPYRIGHT] (year of publication)]

For Advance Online Publication papers:

Reprinted by permission from The [the Licensor]: on behalf of Cancer Research UK: [Journal Publisher (e.g. Nature/Springer/Palgrave)] [JOURNAL NAME] [REFERENCE CITATION (Article name, Author(s) Name), [COPYRIGHT] (year of publication), advance online publication, day month year (doi: 10.1038/sj.[JOURNAL ACRONYM])]

For Book content:

Reprinted/adapted by permission from [the Licensor]: [Book Publisher (e.g. Palgrave Macmillan, Springer etc)] [Book Title] by [Book author(s)] [COPYRIGHT] (year of publication)

Other Conditions:

Version 1.1

Questions? customer@copyright.com or +1-855-239-3415 (toll free in the US) or +1-978-646-2777.

APPENDIX E (continued)

7/22/2019

Copyright Clearance Center



Note: Copyright.com supplies permissions but not the copyrighted content itself.

1
PAYMENT2
REVIEW3
CONFIRMATION**Step 3: Order Confirmation**

Thank you for your order! A confirmation for your order will be sent to your account email address. If you have questions about your order, you can call us 24 hrs/day, M-F at +1.855.239.3415 Toll Free, or write to us at info@copyright.com. This is not an invoice.

Confirmation Number: 11834164
Order Date: 07/23/2019

If you paid by credit card, your order will be finalized and your card will be charged within 24 hours. If you choose to be invoiced, you can change or cancel your order until the invoice is generated.

Payment Information

Veronica Haywood
 vhaywo2@uic.edu
 +1 (773) 919-7949
 Payment Method: n/a

Order Details**Journal of biological chemistry**

Order detail ID: 71952569
Order License Id: 4634571244740

ISSN: 1083-351X
Publication Type: e-Journal

Volume:**Issue:****Start page:**

Publisher: AMERICAN SOCIETY FOR
 BIOCHEMISTRY AND MOLECULAR BI
Author/Editor: AMERICAN SOCIETY FOR
 BIOCHEMISTRY & MOLECULAR BIOL

Permission Status: **Granted**

Permission type: Republish or display content
Type of use: Thesis/Dissertation

Requestor type Publisher, for-profit

Format Print, Electronic

Portion chart/graph/table/figure

Number of charts/graphs/tables/figures 2

The requesting person/organization Veronica Haywood/
 University of Illinois at Chicago

Title or numeric reference of the portion(s) Figure 2A, Supplemental Figure 5.

Title of the article or chapter the portion is from Regulation of Glycan Structures in Animal Tissues. TRANSCRIPT PROFILING OF GLYCAN-RELATED GENES

APPENDIX E (continued)

7/22/2019

Copyright Clearance Center

Editor of portion(s)	N/A
Author of portion(s)	Alison V. Nairn, William S. York, Kyle Harris, Erica M. Hall, J. Michael Pierce and Kelley W. Moremen
Volume of serial or monograph	283
Issue, if republishing an article from a serial	25
Page range of portion	17304 and supplemental page 6
Publication date of portion	4-14-2008
Rights for	Main Product, any product related to main product, and other compilations/derivative products
Duration of use	Life of current and all future editions
Creation of copies for the disabled	no
With minor editing privileges	no
For distribution to	Worldwide
In the following language(s)	Original language of publication
With incidental promotional use	no
Lifetime unit quantity of new product	Up to 499
Title	PhD Candidate
Institution name	University of Illinois at Chicago College of Dentistry
Expected presentation date	Jul 2019

Note: This item will be invoiced or charged separately through CCC's **RightsLink** service. [More info](#)

\$ 0.00

APPENDIX E (continued)

7/22/2019

Copyright Clearance Center

Total order items: 1**This is not an invoice.****Order Total: 0.00 USD**

APPENDIX E (continued)

7/22/2019

Copyright Clearance Center

Confirmation Number: 11834164**Special Rightsholder Terms & Conditions**

The following terms & conditions apply to the specific publication under which they are listed

Journal of biological chemistry**Permission type:** Republish or display content**Type of use:** Thesis/Dissertation**TERMS AND CONDITIONS****The following terms are individual to this publisher:**

None

Other Terms and Conditions:**STANDARD TERMS AND CONDITIONS**

1. Description of Service; Defined Terms. This Republication License enables the User to obtain licenses for republication of one or more copyrighted works as described in detail on the relevant Order Confirmation (the "Work(s)"). Copyright Clearance Center, Inc. ("CCC") grants licenses through the Service on behalf of the rightsholder identified on the Order Confirmation (the "Rightsholder"). "Republication", as used herein, generally means the inclusion of a Work, in whole or in part, in a new work or works, also as described on the Order Confirmation. "User", as used herein, means the person or entity making such republication.

2. The terms set forth in the relevant Order Confirmation, and any terms set by the Rightsholder with respect to a particular Work, govern the terms of use of Works in connection with the Service. By using the Service, the person transacting for a republication license on behalf of the User represents and warrants that he/she/it (a) has been duly authorized by the User to accept, and hereby does accept, all such terms and conditions on behalf of User, and (b) shall inform User of all such terms and conditions. In the event such person is a "freelancer" or other third party independent of User and CCC, such party shall be deemed jointly a "User" for purposes of these terms and conditions. In any event, User shall be deemed to have accepted and agreed to all such terms and conditions if User republishes the Work in any fashion.

3. Scope of License; Limitations and Obligations.

3.1 All Works and all rights therein, including copyright rights, remain the sole and exclusive property of the Rightsholder. The license created by the exchange of an Order Confirmation (and/or any invoice) and payment by User of the full amount set forth on that document includes only those rights expressly set forth in the Order Confirmation and in these terms and conditions, and conveys no other rights in the Work(s) to User. All rights not expressly granted are hereby reserved.

3.2 General Payment Terms: You may pay by credit card or through an account with us payable at the end of the month. If you and we agree that you may establish a standing account with CCC, then the following terms apply: Remit Payment to: Copyright Clearance Center, 29118 Network Place, Chicago, IL 60673-1291. Payments Due: Invoices are payable upon their delivery to you (or upon our notice to you that they are available to you for downloading). After 30 days, outstanding amounts will be subject to a service charge of 1-1/2% per month or, if less, the maximum rate allowed by applicable law. Unless otherwise specifically set forth in the Order Confirmation or in a separate written agreement signed by CCC, invoices are due and payable on "net 30" terms. While User may exercise the rights licensed immediately upon issuance of the Order Confirmation, the license is automatically revoked and is null and void, as if it had never been issued, if complete payment for the license is not received on a timely basis either from User directly or through a payment agent, such as a credit card company.

3.3 Unless otherwise provided in the Order Confirmation, any grant of rights to User (i) is "one-time" (including the editions and product family specified in the license), (ii) is non-exclusive and non-transferable and (iii) is subject to any and all limitations and restrictions (such as, but not limited to, limitations on duration of use or circulation) included in the Order Confirmation or invoice and/or in these terms and conditions. Upon completion of the licensed use, User shall either secure a new permission for further use of the Work(s) or immediately cease any new use of the Work(s) and shall render inaccessible (such as by deleting or by removing or severing links or other locators) any further copies of the Work (except for copies printed on paper in accordance with this license and still in User's stock at the end of such period).

3.4 In the event that the material for which a republication license is sought includes third party materials (such as photographs, illustrations, graphs, inserts and similar materials) which are identified in such material as having been used by permission, User is responsible for identifying, and seeking separate licenses (under this Service or otherwise) for, any of such third party materials; without a separate license, such third party materials may not be used.

3.5 Use of proper copyright notice for a Work is required as a condition of any license granted under the Service. Unless otherwise provided in the Order Confirmation, a proper copyright notice will read substantially as follows: "Republished with permission of [Rightsholder's name], from [Work's title, author, volume, edition number and year of copyright]; permission conveyed through Copyright Clearance Center, Inc. " Such notice must be provided in a reasonably legible font size and must be placed either immediately adjacent to the Work as used (for example, as part of a by-line or footnote

APPENDIX E (continued)

7/22/2019

Copyright Clearance Center

but not as a separate electronic link) or in the place where substantially all other credits or notices for the new work containing the republished Work are located. Failure to include the required notice results in loss to the Rightsholder and CCC, and the User shall be liable to pay liquidated damages for each such failure equal to twice the use fee specified in the Order Confirmation, in addition to the use fee itself and any other fees and charges specified.

3.6 User may only make alterations to the Work if and as expressly set forth in the Order Confirmation. No Work may be used in any way that is defamatory, violates the rights of third parties (including such third parties' rights of copyright, privacy, publicity, or other tangible or intangible property), or is otherwise illegal, sexually explicit or obscene. In addition, User may not conjoin a Work with any other material that may result in damage to the reputation of the Rightsholder. User agrees to inform CCC if it becomes aware of any infringement of any rights in a Work and to cooperate with any reasonable request of CCC or the Rightsholder in connection therewith.

4. Indemnity. User hereby indemnifies and agrees to defend the Rightsholder and CCC, and their respective employees and directors, against all claims, liability, damages, costs and expenses, including legal fees and expenses, arising out of any use of a Work beyond the scope of the rights granted herein, or any use of a Work which has been altered in any unauthorized way by User, including claims of defamation or infringement of rights of copyright, publicity, privacy or other tangible or intangible property.

5. Limitation of Liability. UNDER NO CIRCUMSTANCES WILL CCC OR THE RIGHTSHOLDER BE LIABLE FOR ANY DIRECT, INDIRECT, CONSEQUENTIAL OR INCIDENTAL DAMAGES (INCLUDING WITHOUT LIMITATION DAMAGES FOR LOSS OF BUSINESS PROFITS OR INFORMATION, OR FOR BUSINESS INTERRUPTION) ARISING OUT OF THE USE OR INABILITY TO USE A WORK, EVEN IF ONE OF THEM HAS BEEN ADVISED OF THE POSSIBILITY OF SUCH DAMAGES. In any event, the total liability of the Rightsholder and CCC (including their respective employees and directors) shall not exceed the total amount actually paid by User for this license. User assumes full liability for the actions and omissions of its principals, employees, agents, affiliates, successors and assigns.

6. Limited Warranties. THE WORK(S) AND RIGHT(S) ARE PROVIDED "AS IS". CCC HAS THE RIGHT TO GRANT TO USER THE RIGHTS GRANTED IN THE ORDER CONFIRMATION DOCUMENT. CCC AND THE RIGHTSHOLDER DISCLAIM ALL OTHER WARRANTIES RELATING TO THE WORK(S) AND RIGHT(S), EITHER EXPRESS OR IMPLIED, INCLUDING WITHOUT LIMITATION IMPLIED WARRANTIES OF MERCHANTABILITY OR FITNESS FOR A PARTICULAR PURPOSE. ADDITIONAL RIGHTS MAY BE REQUIRED TO USE ILLUSTRATIONS, GRAPHS, PHOTOGRAPHS, ABSTRACTS, INSERTS OR OTHER PORTIONS OF THE WORK (AS OPPOSED TO THE ENTIRE WORK) IN A MANNER CONTEMPLATED BY USER; USER UNDERSTANDS AND AGREES THAT NEITHER CCC NOR THE RIGHTSHOLDER MAY HAVE SUCH ADDITIONAL RIGHTS TO GRANT.

7. Effect of Breach. Any failure by User to pay any amount when due, or any use by User of a Work beyond the scope of the license set forth in the Order Confirmation and/or these terms and conditions, shall be a material breach of the license created by the Order Confirmation and these terms and conditions. Any breach not cured within 30 days of written notice thereof shall result in immediate termination of such license without further notice. Any unauthorized (but licensable) use of a Work that is terminated immediately upon notice thereof may be liquidated by payment of the Rightsholder's ordinary license price therefor; any unauthorized (and unlicensable) use that is not terminated immediately for any reason (including, for example, because materials containing the Work cannot reasonably be recalled) will be subject to all remedies available at law or in equity, but in no event to a payment of less than three times the Rightsholder's ordinary license price for the most closely analogous licensable use plus Rightsholder's and/or CCC's costs and expenses incurred in collecting such payment.

8. Miscellaneous.

8.1 User acknowledges that CCC may, from time to time, make changes or additions to the Service or to these terms and conditions, and CCC reserves the right to send notice to the User by electronic mail or otherwise for the purposes of notifying User of such changes or additions; provided that any such changes or additions shall not apply to permissions already secured and paid for.

8.2 Use of User-related information collected through the Service is governed by CCC's privacy policy, available online here: <http://www.copyright.com/content/cc3/en/tools/footer/privacypolicy.html>.

8.3 The licensing transaction described in the Order Confirmation is personal to User. Therefore, User may not assign or transfer to any other person (whether a natural person or an organization of any kind) the license created by the Order Confirmation and these terms and conditions or any rights granted hereunder; provided, however, that User may assign such license in its entirety on written notice to CCC in the event of a transfer of all or substantially all of User's rights in the new material which includes the Work(s) licensed under this Service.

8.4 No amendment or waiver of any terms is binding unless set forth in writing and signed by the parties. The Rightsholder and CCC hereby object to any terms contained in any writing prepared by the User or its principals, employees, agents or affiliates and purporting to govern or otherwise relate to the licensing transaction described in the Order Confirmation, which terms are in any way inconsistent with any terms set forth in the Order Confirmation and/or in these terms and conditions or CCC's standard operating procedures, whether such writing is prepared prior to, simultaneously with or subsequent to the Order Confirmation, and whether such writing appears on a copy of the Order Confirmation or in a separate instrument.

8.5 The licensing transaction described in the Order Confirmation document shall be governed by and construed under the law of the State of New York, USA, without regard to the principles thereof of conflicts of law. Any case, controversy, suit, action, or proceeding arising out of, in connection with, or related to such licensing transaction shall be brought, at CCC's sole discretion, in any federal or state court located in the County of New York, State of New York, USA, or in any federal or state court whose geographical jurisdiction covers the location of the Rightsholder set forth in the Order Confirmation. The parties expressly submit to the personal jurisdiction and venue of each such federal or state court. If you have any comments or questions about the Service or Copyright Clearance Center, please contact us at 978-750-8400 or send an e-mail to info@copyright.com.

APPENDIX E (continued)

7/22/2019

Copyright Clearance Center

v 1.1

APPENDIX E (continued)

7/22/2019

Copyright Clearance Center

Confirmation Number: 11834164**Citation Information****Order Detail ID:** 71952569

Journal of biological chemistry by AMERICAN SOCIETY FOR BIOCHEMISTRY & MOLECULAR BIOL Reproduced with permission of AMERICAN SOCIETY FOR BIOCHEMISTRY AND MOLECULAR BI in the format Thesis/Dissertation via Copyright Clearance Center.

7 CITED LITERATURE

1. Chen, L.; Arbieva, Z. H.; Guo, S.; Marucha, P. T.; Mustoe, T. A.; DiPietro, L. A., Positional differences in the wound transcriptome of skin and oral mucosa. *BMC Genomics* **2010**, *11*, 471.
2. Nairn, A. V.; York, W. S.; Harris, K.; Hall, E. M.; Pierce, J. M.; Moremen, K. W., Regulation of glycan structures in animal tissues: transcript profiling of glycan-related genes. *J Biol Chem* **2008**, *283* (25), 17298-313.
3. Schachter, H., The joys of HexNAc. The synthesis and function of N- and O-glycan branches. *Glycoconjugate journal* **2000**, *17* (7-9), 465-83.
4. Kornfeld, R.; Kornfeld, S., Assembly of asparagine-linked oligosaccharides. *Annu Rev Biochem* **1985**, *54*, 631-64.
5. Magalhaes, A.; Gomes, J.; Ismail, M. N.; Haslam, S. M.; Mendes, N.; Osorio, H.; David, L.; Le Pendu, J.; Haas, R.; Dell, A.; Boren, T.; Reis, C. A., Fut2-null mice display an altered glycosylation profile and impaired BabA-mediated *Helicobacter pylori* adhesion to gastric mucosa. *Glycobiology* **2009**, *19* (12), 1525-36.
6. Magalhaes, A.; Rossez, Y.; Robbe-Masselot, C.; Maes, E.; Gomes, J.; Shevtsova, A.; Bugaytsova, J.; Boren, T.; Reis, C. A., Muc5ac gastric mucin glycosylation is shaped by FUT2 activity and functionally impacts *Helicobacter pylori* binding. *Sci Rep* **2016**, *6*, 25575.
7. Zielinska, D. F.; Gnad, F.; Wisniewski, J. R.; Mann, M., Precision mapping of an in vivo N-glycoproteome reveals rigid topological and sequence constraints. *Cell* **2010**, *141* (5), 897-907.
8. Valliere-Douglass, J. F.; Eakin, C. M.; Wallace, A.; Ketchem, R. R.; Wang, W.; Treuheit, M. J.; Balland, A., Glutamine-linked and non-consensus asparagine-linked oligosaccharides present in human recombinant antibodies define novel protein glycosylation motifs. *J Biol Chem* **2010**, *285* (21), 16012-22.

CITED LITERATURE

9. Nagae, M.; Ikeda, A.; Hane, M.; Hanashima, S.; Kitajima, K.; Sato, C.; Yamaguchi, Y., Crystal structure of anti-polysialic acid antibody single chain Fv fragment complexed with octasialic acid: insight into the binding preference for polysialic acid. *J Biol Chem* **2013**, *288* (47), 33784-96.
10. Esko, J. D.; Selleck, S. B., Order out of chaos: assembly of ligand binding sites in heparan sulfate. *Annu Rev Biochem* **2002**, *71*, 435-71.
11. Schreiner, R.; Schnabel, E.; Wieland, F., Novel N-glycosylation in eukaryotes: laminin contains the linkage unit beta-glucosylasparagine. *J Cell Biol* **1994**, *124* (6), 1071-81.
12. Smith, M. H.; Ploegh, H. L.; Weissman, J. S., Road to ruin: targeting proteins for degradation in the endoplasmic reticulum. *Science (New York, N.Y.)* **2011**, *334* (6059), 1086-90.
13. Gerken, T. A.; Jamison, O.; Perrine, C. L.; Collette, J. C.; Moinova, H.; Ravi, L.; Markowitz, S. D.; Shen, W.; Patel, H.; Tabak, L. A., Emerging paradigms for the initiation of mucin-type protein O-glycosylation by the polypeptide GalNAc transferase family of glycosyltransferases. *J Biol Chem* **2011**, *286* (16), 14493-507.
14. Sato, C.; Kitajima, K., Disialic, oligosialic and polysialic acids: distribution, functions and related disease. *J Biochem* **2013**, *154* (2), 115-36.
15. Wang, A.; de la Motte, C.; Lauer, M.; Hascall, V., Hyaluronan matrices in pathobiological processes. *FEBS J* **2011**, *278* (9), 1412-8.
16. Gupta, R.; Brunak, S., Prediction of glycosylation across the human proteome and the correlation to protein function. *Pac Symp Biocomput* **2002**, 310-22.
17. Roch, C.; Kuhn, J.; Kleesiek, K.; Gotting, C., Differences in gene expression of human xylosyltransferases and determination of acceptor specificities for various proteoglycans. *Biochem Biophys Res Commun* **2010**, *391* (1), 685-91.

CITED LITERATURE

18. Many, H.; Suzuki, T.; Akasaka-Many, K.; Ishida, H. K.; Mizuno, M.; Suzuki, Y.; Inazu, T.; Dohmae, N.; Endo, T., Regulation of mammalian protein O-mannosylation: preferential amino acid sequence for O-mannose modification. *J Biol Chem* **2007**, *282* (28), 20200-6.
19. Stalnaker, S. H.; Hashmi, S.; Lim, J. M.; Aoki, K.; Porterfield, M.; Gutierrez-Sanchez, G.; Wheeler, J.; Ervasti, J. M.; Bergmann, C.; Tiemeyer, M.; Wells, L., Site mapping and characterization of O-glycan structures on alpha-dystroglycan isolated from rabbit skeletal muscle. *J Biol Chem* **2010**, *285* (32), 24882-91.
20. Schegg, B.; Hulsmeier, A. J.; Rutschmann, C.; Maag, C.; Hennet, T., Core glycosylation of collagen is initiated by two beta(1-O)galactosyltransferases. *Molecular and cellular biology* **2009**, *29* (4), 943-52.
21. Moremen, K. W.; Tiemeyer, M.; Nairn, A. V., Vertebrate protein glycosylation: diversity, synthesis and function. *Nature reviews. Molecular cell biology* **2012**, *13* (7), 448-62.
22. Tian, E.; Ten Hagen, K. G., Recent insights into the biological roles of mucin-type O-glycosylation. *Glycoconjugate journal* **2009**, *26* (3), 325-34.
23. Barresi, R.; Campbell, K. P., Dystroglycan: from biosynthesis to pathogenesis of human disease. *Journal of cell science* **2006**, *119* (Pt 2), 199-207.
24. Inamori, K.; Yoshida-Moriguchi, T.; Hara, Y.; Anderson, M. E.; Yu, L.; Campbell, K. P., Dystroglycan function requires xylosyl- and glucuronyltransferase activities of LARGE. *Science (New York, N.Y.)* **2012**, *335* (6064), 93-6.
25. Issoglio, F. M.; Carrizo, M. E.; Romero, J. M.; Curtino, J. A., Mechanisms of monomeric and dimeric glycogenin autoglucosylation. *J Biol Chem* **2012**, *287* (3), 1955-61.
26. Luther, K. B.; Haltiwanger, R. S., Role of unusual O-glycans in intercellular signaling. *The international journal of biochemistry & cell biology* **2009**, *41* (5), 1011-24.
27. Rumbaut, R. E.; Thiagarajan, P., Platelet Adhesion to Vascular Walls. Morgan & Claypool Life Sciences: 2010.

CITED LITERATURE

28. Periyah, M. H.; Halim, A. S.; Mat Saad, A. Z., Mechanism Action of Platelets and Crucial Blood Coagulation Pathways in Hemostasis. *Int J Hematol Oncol Stem Cell Res* **2017**, *11* (4), 319-327.
29. Hofsteenge, J.; Huwiler, K. G.; Macek, B.; Hess, D.; Lawler, J.; Mosher, D. F.; Peter-Katalinic, J., C-mannosylation and O-fucosylation of the thrombospondin type 1 module. *J Biol Chem* **2001**, *276* (9), 6485-98.
30. Rumbaut, R. E.; Thiagarajan, P., Platelet Aggregation. In *Platelet-Vessel Wall Interactions in Hemostasis and Thrombosis*, San Rafael (CA), 2010.
31. Hart, G. W.; Slawson, C.; Ramirez-Correa, G.; Lagerlof, O., Cross talk between O-GlcNAcylation and phosphorylation: roles in signaling, transcription, and chronic disease. *Annu Rev Biochem* **2011**, *80*, 825-58.
32. Pierleoni, A.; Martelli, P. L.; Casadio, R., PredGPI: a GPI-anchor predictor. *BMC Bioinformatics* **2008**, *9*, 392.
33. Pontier, S. M.; Schweisguth, F., Glycosphingolipids in signaling and development: from liposomes to model organisms. *Developmental dynamics : an official publication of the American Association of Anatomists* **2012**, *241* (1), 92-106.
34. Wood, L. C.; Elias Pm Fau - Calhoun, C.; Calhoun C Fau - Tsai, J. C.; Tsai Jc Fau - Grunfeld, C.; Grunfeld C Fau - Feingold, K. R.; Feingold, K. R., Barrier disruption stimulates interleukin-1 alpha expression and release from a pre-formed pool in murine epidermis. (0022-202X (Print)).
35. Zarbock, A.; Ley, K.; McEver, R. P.; Hidalgo, A., Leukocyte ligands for endothelial selectins: specialized glycoconjugates that mediate rolling and signaling under flow. *Blood* **2011**, *118* (26), 6743-6751.
36. Essentials of Glycobiology. 2nd ed.; Varki, A., RDEsko, JD, Ed. Cold Spring Harbor Laboratory Press Cold Spring Harbor, NY, 2009. <http://www.ncbi.nlm.nih.gov/books/NBK1908>.

CITED LITERATURE

37. Sperandio, M.; Gleissner, C. A.; Ley, K., Glycosylation in immune cell trafficking. *Immunological reviews* **2009**, 230 (1), 97-113.
38. Doucey, M. A.; Hess, D.; Cacan, R.; Hofsteenge, J., Protein C-mannosylation is enzyme-catalysed and uses dolichyl-phosphate-mannose as a precursor. *Molecular biology of the cell* **1998**, 9 (2), 291-300.
39. Behm, B.; Babilas, P.; Landthaler, M.; Schreml, S., Cytokines, chemokines and growth factors in wound healing. *Journal of the European Academy of Dermatology and Venereology* **2012**, 26 (7), 812-820.
40. Pierce, G. F.; Tarpley Je Fau - Yanagihara, D.; Yanagihara D Fau - Mustoe, T. A.; Mustoe Ta Fau - Fox, G. M.; Fox Gm Fau - Thomason, A.; Thomason, A., Platelet-derived growth factor (BB homodimer), transforming growth factor-beta 1, and basic fibroblast growth factor in dermal wound healing. Neovessel and matrix formation and cessation of repair. (0002-9440 (Print)).
41. Xue, M.; Jackson, C. J., Extracellular Matrix Reorganization During Wound Healing and Its Impact on Abnormal Scarring. *Advances in wound care* **2015**, 4 (3), 119-136.
42. Ferrara, N., Vascular endothelial growth factor. *Trends in cardiovascular medicine* **1993**, 3 (6), 244-50.
43. Folkman, J.; D'Amore, P., Expression of the angiogenic phenotype during development of murine and human cancer. 1991.
44. Kumar, V.; Abbas, A. K.; Fausto, N.; Mitchel, R., Inflammation and Repair. In *Robbins Basic Pathology*, 9 ed.; Elsevier Saunders: 2013; pp 29-74.
45. Risau, W., Mechanisms of angiogenesis. *Nature* **1997**, 386 (6626), 671-4.
46. Cines, D. B.; Pollak, E. S.; Buck, C. A.; Loscalzo, J.; Zimmerman, G. A.; McEver, R. P.; Pober, J. S.; Wick, T. M.; Konkle, B. A.; Schwartz, B. S.; Barnathan, E. S.; McCrae, K. R.; Hug,

CITED LITERATURE

- B. A.; Schmidt, A. M.; Stern, D. M., Endothelial cells in physiology and in the pathophysiology of vascular disorders. *Blood* **1998**, *91* (10), 3527-61.
47. Sheehan, P.; Jones, P.; Caselli, A.; Giurini, J. M.; Veves, A., Percent Change in Wound Area of Diabetic Foot Ulcers Over a 4-Week Period Is a Robust Predictor of Complete Healing in a 12-Week Prospective Trial. *Diabetes Care* **2003**, *26* (6), 1879.
48. Wong, J. W.; Gallant-Behm C Fau - Wiebe, C.; Wiebe C Fau - Mak, K.; Mak K Fau - Hart, D. A.; Hart Da Fau - Larjava, H.; Larjava H Fau - Hakkinen, L.; Hakkinen, L., Wound healing in oral mucosa results in reduced scar formation as compared with skin: evidence from the red Duroc pig model and humans. (1524-475X (Electronic)).
49. Mak, K.; Manji A Fau - Gallant-Behm, C.; Gallant-Behm C Fau - Wiebe, C.; Wiebe C Fau - Hart, D. A.; Hart Da Fau - Larjava, H.; Larjava H Fau - Hakkinen, L.; Hakkinen, L., Scarless healing of oral mucosa is characterized by faster resolution of inflammation and control of myofibroblast action compared to skin wounds in the red Duroc pig model. (1873-569X (Electronic)).
50. Szpaderska, A. M.; DiPietro, L. A., Inflammation in surgical wound healing: friend or foe? *Surgery* **2005**, *137* (5), 571-3.
51. Turabelidze, A.; Guo, S.; Chung, A. Y.; Chen, L.; Dai, Y.; Marucha, P. T.; DiPietro, L. A., Intrinsic differences between oral and skin keratinocytes. *PLoS One* **2014**, *9* (9), e101480.
52. Li, J.; Farthing Pm Fau - Thornhill, M. H.; Thornhill, M. H., Oral and skin keratinocytes are stimulated to secrete monocyte chemoattractant protein-1 by tumour necrosis factor-alpha and interferon-gamma. (0904-2512 (Print)).
53. Li, J.; Ireland, G. W.; Farthing, P. M.; Thornhill, M. H., Epidermal and Oral Keratinocytes Are Induced to Produce RANTES and IL-8 by Cytokine Stimulation. *Journal of Investigative Dermatology* **1996**, *106* (4), 661-666.

CITED LITERATURE

54. Presland, R. B.; Dale, B. A., Epithelial structural proteins of the skin and oral cavity: function in health and disease. *Crit Rev Oral Biol Med* **2000**, *11* (4), 383-408.
55. Szpaderska, A. M.; Walsh, C. G.; Steinberg, M. J.; DiPietro, L. A., Distinct patterns of angiogenesis in oral and skin wounds. *J Dent Res* **2005**, *84* (4), 309-14.
56. Chen, L.; Gajendrareddy, P. K.; DiPietro, L. A., Differential expression of HIF-1alpha in skin and mucosal wounds. *J Dent Res* **2012**, *91* (9), 871-6.
57. Schrementi, M. E.; Ferreira, A. M.; Zender, C.; DiPietro, L. A., Site-specific production of TGF-beta in oral mucosal and cutaneous wounds. *Wound repair and regeneration : official publication of the Wound Healing Society [and] the European Tissue Repair Society* **2008**, *16* (1), 80-6.
58. Natsuga, K., Epidermal barriers. *Cold Spring Harbor perspectives in medicine* **2014**, *4* (4), a018218.
59. Ott, C.; Jacobs, K.; Haucke, E.; Navarrete Santos, A.; Grune, T.; Simm, A., Role of advanced glycation end products in cellular signaling. *Redox biology* **2014**, *2*, 411-429.
60. Peppas, M.; Brem H Fau - Ehrlich, P.; Ehrlich P Fau - Zhang, J.-G.; Zhang Jg Fau - Cai, W.; Cai W Fau - Li, Z.; Li Z Fau - Croitoru, A.; Croitoru A Fau - Thung, S.; Thung S Fau - Vlassara, H.; Vlassara, H., Adverse effects of dietary glycotoxins on wound healing in genetically diabetic mice. (0012-1797 (Print)).
61. Van Putte, L.; De Schrijver, S.; Moortgat, P., The effects of advanced glycation end products (AGEs) on dermal wound healing and scar formation: a systematic review. *Scars, burns & healing* **2016**, *2*, 2059513116676828-2059513116676828.
62. Svensjo, T.; Pomahac B Fau - Yao, F.; Yao F Fau - Slama, J.; Slama J Fau - Eriksson, E.; Eriksson, E., Accelerated healing of full-thickness skin wounds in a wet environment. (0032-1052 (Print)).

CITED LITERATURE

63. Junker, J. P. E.; Kamel, R. A.; Caterson, E. J.; Eriksson, E., Clinical Impact Upon Wound Healing and Inflammation in Moist, Wet, and Dry Environments. *Advances in wound care* **2013**, 2 (7), 348-356.
64. Hinman Cd Fau - Maibach, H.; Maibach, H., EFFECT OF AIR EXPOSURE AND OCCLUSION ON EXPERIMENTAL HUMAN SKIN WOUNDS. (0028-0836 (Print)).
65. Duff, M.; Demidova, O.; Blackburn, S.; Shubrook, J., Cutaneous Manifestations of Diabetes Mellitus. *Clinical Diabetes* **2015**, 33 (1), 40-48.
66. Kim, J.-H.; Yoon, N. Y.; Kim, D. H.; Jung, M.; Jun, M.; Park, H.-Y.; Chung, C. H.; Lee, K.; Kim, S.; Park, C. S.; Liu, K.-H.; Choi, E. H., Impaired permeability and antimicrobial barriers in type 2 diabetes skin are linked to increased serum levels of advanced glycation end-product. *Experimental Dermatology* **2018**, 27 (8), 815-823.
67. Trivedi, U.; Parameswaran, S.; Armstrong, A.; Burgueno-Vega, D.; Griswold, J.; Dissanaik, S.; Rumbaugh, K. P., Prevalence of Multiple Antibiotic Resistant Infections in Diabetic versus Nondiabetic Wounds. *Journal of Pathogens* **2014**, 2014, 6.
68. Seitz, O.; Schurmann, C.; Hermes, N.; Muller, E.; Pfeilschifter, J.; Frank, S.; Goren, I., Wound healing in mice with high-fat diet- or ob gene-induced diabetes-obesity syndromes: a comparative study. *Experimental diabetes research* **2010**, 2010, 476969.
69. Negre-Salvayre, A.; Salvayre, R.; Auge, N.; Pamplona, R.; Portero-Otin, M., Hyperglycemia and glycation in diabetic complications. *Antioxidants & redox signaling* **2009**, 11 (12), 3071-109.
70. Yan, L. J., Pathogenesis of Chronic Hyperglycemia: From Reductive Stress to Oxidative Stress. *J Diabetes Res* **2014**, 2014.
71. Goyal, A.; Raina, S.; Kaushal, S. S.; Mahajan, V.; Sharma, N. L., Pattern of cutaneous manifestations in diabetes mellitus. *Indian journal of dermatology* **2010**, 55 (1), 39-41.

CITED LITERATURE

72. de Macedo, G. M. C.; Nunes, S.; Barreto, T., Skin disorders in diabetes mellitus: an epidemiology and physiopathology review. *Diabetology & metabolic syndrome* **2016**, 8 (1), 63-63.
73. Ban, C. R.; Twigg, S. M., Fibrosis in diabetes complications: pathogenic mechanisms and circulating and urinary markers. (1176-6344 (Print)).
74. Litwak, L.; Goh, S. Y.; Hussein, Z.; Malek, R.; Prusty, V.; Khamseh, M. E., Prevalence of diabetes complications in people with type 2 diabetes mellitus and its association with baseline characteristics in the multinational A1chieve study. In *Diabetol Metab Syndr*, England, 2013; Vol. 5, p 57.
75. Loe, H., Periodontal disease. The sixth complication of diabetes mellitus. *Diabetes Care* **1993**, 16 (1), 329-34.
76. Zhong, G. C.; Ye, M. X.; Cheng, J. H.; Zhao, Y.; Gong, J. P., HbA1c and Risks of All-Cause and Cause-Specific Death in Subjects without Known Diabetes: A Dose-Response Meta-Analysis of Prospective Cohort Studies. In *Sci Rep*, 2016; Vol. 6.
77. Bansal, N., Prediabetes diagnosis and treatment: A review. *World Journal of Diabetes* **2015**, 6 (2), 296-303.
78. Robinson, C. C.; Balbinot, L. F.; Silva, M. F.; Achaval, M.; Zaro, M. A., Plantar pressure distribution patterns of individuals with prediabetes in comparison with healthy individuals and individuals with diabetes. *J Diabetes Sci Technol* **2013**, 7 (5), 1113-21.
79. Lopez, P. R.; Leicht, S.; Sigmon, J. R.; Stigall, L., Bullosis diabeticorum associated with a prediabetic state. *Southern medical journal* **2009**, 102 (6), 643-4.
80. Arora, N.; Papapanou, P. N.; Rosenbaum, M.; Jacobs, D. R., Jr.; Desvarieux, M.; Demmer, R. T., Periodontal infection, impaired fasting glucose and impaired glucose tolerance: results from the Continuous National Health and Nutrition Examination Survey 2009-2010. *J Clin Periodontol* **2014**, 41 (7), 643-52.

CITED LITERATURE

81. Zheng, H.; Wu, J.; Jin, Z.; Yan, L. J., Protein Modifications as Manifestations of Hyperglycemic Glucotoxicity in Diabetes and Its Complications. *Biochemistry insights* **2016**, *9*, 1-9.
82. Gautieri, A.; Redaelli, A.; Buehler, M. J.; Vesentini, S., Age- and diabetes-related nonenzymatic crosslinks in collagen fibrils: candidate amino acids involved in Advanced Glycation End-products. *Matrix Biol* **2014**, *34*, 89-95.
83. Goldin, A.; Beckman, J. A.; Schmidt, A. M.; Creager, M. A., Advanced Glycation End Products: Sparking the Development of Diabetic Vascular Injury. *Circulation* **2006**, *114* (6), 597-605.
84. Haitoglou, C. S.; Tsilibary, E. C.; Brownlee, M.; Charonis, A. S., Altered cellular interactions between endothelial cells and nonenzymatically glucosylated laminin/type IV collagen. *J Biol Chem* **1992**, *267* (18), 12404-7.
85. Miyata, M.; Mifude, C.; Matsui, T.; Kitamura, H.; Yoshioka, H.; Yamagishi, S.; Kaseda, K., Advanced glycation end-products inhibit mesenchymal-epidermal interaction by up-regulating proinflammatory cytokines in hair follicles. In *Eur J Dermatol*, France, 2015; Vol. 25, pp 359-61.
86. Hu, H.; Jiang, H.; Ren, H.; Hu, X.; Wang, X.; Han, C., AGEs and chronic subclinical inflammation in diabetes: disorders of immune system. *Diabetes/metabolism research and reviews* **2015**, *31* (2), 127-37.
87. Song, Z. Q.; Wang, R. X.; Yu, D. M.; Wang, P. H.; Lu, S. L.; Tian, M.; Xie, T.; Huang, F.; Yang, G. Z., [Impact of advanced glycosylation end products-modified human serum albumin on migration of epidermal keratinocytes: an in vitro experiment]. *Zhonghua Yi Xue Za Zhi* **2008**, *88* (38), 2690-4.

CITED LITERATURE

88. Xie, T.; Niu, Y. W.; Ge, K.; Lu, S. L., [Effect of advanced glycosylation end products on cell cycle of epidermal keratinocyte and the role of signal pathway]. *Zhonghua shao shang za zhi = Zhonghua shaoshang zazhi = Chinese journal of burns* **2008**, *24* (1), 22-5.
89. Varki, A.; Sharon, N., Historical Background and Overview. In *Essentials of Glycobiology*, 2nd ed.; Varki, A.; Cummings, R.; Esko, J., Eds. Cold Spring Harbor Laboratory Press: Cold Spring Harbor, NY, 2009.
90. Brockhausen, I.; Stanley, P., O-GalNAc Glycans. In *Essentials of Glycobiology*, rd; Varki, A.; Cummings, R. D.; Esko, J. D.; Stanley, P.; Hart, G. W.; Aebi, M.; Darvill, A. G.; Kinoshita, T.; Packer, N. H.; Prestegard, J. H.; Schnaar, R. L.; Seeberger, P. H., Eds. Cold Spring Harbor (NY), 2015; pp 113-123.
91. Bhide, G. P.; Colley, K. J., Sialylation of N-glycans: mechanism, cellular compartmentalization and function. *Histochem Cell Biol* **2017**, *147* (2), 149-174.
92. Colley, K. J.; Kitajima, K.; Sato, C., Polysialic acid: biosynthesis, novel functions and applications. *Critical reviews in biochemistry and molecular biology* **2014**, *49* (6), 498-532.
93. Martersteck, C. M.; Kedersha, N. L.; Drapp, D. A.; Tsui, T. G.; Colley, K. J., Unique alpha 2, 8-polysialylated glycoproteins in breast cancer and leukemia cells. *Glycobiology* **1996**, *6* (3), 289-301.
94. Wang, X.; Li, X.; Zeng, Y. N.; He, F.; Yang, X. M.; Guan, F., Enhanced expression of polysialic acid correlates with malignant phenotype in breast cancer cell lines and clinical tissue samples. *Int J Mol Med* **2016**, *37* (1), 197-206.
95. Hart, G. W.; Housley, M. P.; Slawson, C., Cycling of O-linked beta-N-acetylglucosamine on nucleocytoplasmic proteins. *Nature* **2007**, *446* (7139), 1017-22.
96. Leney, A. C.; El Atmioui, D.; Wu, W.; Ovaa, H.; Heck, A. J. R., Elucidating crosstalk mechanisms between phosphorylation and O-GlcNAcylation. *Proceedings of the National Academy of Sciences* **2017**, *114* (35), E7255.

CITED LITERATURE

97. Rombouts, Y.; Jónasdóttir, H. S.; Hipgrave Ederveen, A. L.; Reiding, K. R.; Jansen, B. C.; Freysdóttir, J.; Hardardóttir, I.; Ioan-Facsinay, A.; Giera, M.; Wuhrer, M., Acute phase inflammation is characterized by rapid changes in plasma/peritoneal fluid N-glycosylation in mice. *Glycoconjugate journal* **2016**, 33 (3), 457-470.
98. Holland, M.; Yagi, H.; Takahashi, N.; Kato, K.; Savage, C. O.; Goodall, D. M.; Jefferis, R., Differential glycosylation of polyclonal IgG, IgG-Fc and IgG-Fab isolated from the sera of patients with ANCA-associated systemic vasculitis. *Biochimica et biophysica acta* **2006**, 1760 (4), 669-77.
99. Jefferis, R., Glycosylation of recombinant antibody therapeutics. *Biotechnology progress* **2005**, 21 (1), 11-6.
100. Abel, C. A.; Spiegelberg, H. L.; Grey, H. M., The carbohydrate contents of fragments and polypeptide chains of human gamma-G-myeloma proteins of different heavy-chain subclasses. *Biochemistry* **1968**, 7 (4), 1271-8.
101. Jefferis, R., Antibody therapeutics: isotype and glycoform selection. *Expert opinion on biological therapy* **2007**, 7 (9), 1401-13.
102. Stadlmann, J.; Weber, A.; Pabst, M.; Anderle, H.; Kunert, R.; Ehrlich, H. J.; Peter Schwarz, H.; Altmann, F., A close look at human IgG sialylation and subclass distribution after lectin fractionation. *Proteomics* **2009**, 9 (17), 4143-53.
103. Cebo, C.; Dambrouck, T.; Maes, E.; Laden, C.; Strecker, G.; Michalski, J.-C.; Zanetta, J.-P., Recombinant Human Interleukins IL-1 α , IL-1 β , IL-4, IL-6, and IL-7 Show Different and Specific Calcium-independent Carbohydrate-binding Properties. *Journal of Biological Chemistry* **2001**, 276 (8), 5685-5691.
104. Pahlsson, P.; Strindhall J Fau - Srinivas, U.; Srinivas U Fau - Lundblad, A.; Lundblad, A., Role of N-linked glycosylation in expression of E-selectin on human endothelial cells. (0014-2980 (Print)).

CITED LITERATURE

105. Cebo, C.; Durier, V.; Lagant, P.; Maes, E.; Florea, D.; Lefebvre, T.; Strecker, G.; Vergoten, G.; Zanetta, J.-P., Function and Molecular Modeling of the Interaction between Human Interleukin 6 and Its HNK-1 Oligosaccharide Ligands. *Journal of Biological Chemistry* **2002**, 277 (14), 12246-12252.
106. Silva, M.; Videira, P. A.; Sackstein, R., E-Selectin Ligands in the Human Mononuclear Phagocyte System: Implications for Infection, Inflammation, and Immunotherapy. *Frontiers in immunology* **2017**, 8, 1878.
107. Subramanian, H.; Grailer, J. J.; Ohlrich, K. C.; Rymaszewski, A. L.; Loppnow, J. J.; Koder, M.; Conway, R. M.; Steeber, D. A., Signaling through L-selectin mediates enhanced chemotaxis of lymphocyte subsets to secondary lymphoid tissue chemokine. *J Immunol* **2012**, 188 (7), 3223-36.
108. Werneburg, S.; Buettner, F. F.; Erben, L.; Mathews, M.; Neumann, H.; Muhlenhoff, M.; Hildebrandt, H., Polysialylation and lipopolysaccharide-induced shedding of E-selectin ligand-1 and neuropilin-2 by microglia and THP-1 macrophages. *Glia* **2016**, 64 (8), 1314-30.
109. Stamatou, N. M.; Zhang, L.; Jokilampi, A.; Finne, J.; Chen, W. H.; El-Maarouf, A.; Cross, A. S.; Hankey, K. G., Changes in polysialic acid expression on myeloid cells during differentiation and recruitment to sites of inflammation: role in phagocytosis. *Glycobiology* **2014**, 24 (9), 864-79.
110. Inoue, M.; Fujii, Y.; Furukawa, K.; Okada, M.; Okumura, K.; Hayakawa, T.; Sugiura, Y., Refractory skin injury in complex knock-out mice expressing only the GM3 ganglioside. *J Biol Chem* **2002**, 277 (33), 29881-8.
111. Hara-Chikuma, M.; Takeda, J.; Tarutani, M.; Uchida, Y.; Holleran, W. M.; Endo, Y.; Elias, P. M.; Inoue, S., Epidermal-Specific Defect of GPI Anchor in Pig-a Null Mice Results in Harlequin Ichthyosis-Like Features. *Journal of Investigative Dermatology* **2004**, 123 (3), 464-469.

CITED LITERATURE

112. Uchida, Y., Ceramide signaling in mammalian epidermis. *Biochimica et biophysica acta* **2014**, *1841* (3), 453-62.
113. Allende, M. L.; Proia, R. L., Simplifying complexity: genetically resculpting glycosphingolipid synthesis pathways in mice to reveal function. In *Glycoconjugate journal*, 2014; Vol. 31, pp 613-22.
114. Amen, N.; Mathow, D.; Rabionet, M.; Sandhoff, R.; Langbein, L.; Gretz, N.; Jackel, C.; Grone, H. J.; Jennemann, R., Differentiation of epidermal keratinocytes is dependent on glucosylceramide:ceramide processing. *Hum Mol Genet* **2013**, *22* (20), 4164-79.
115. Borodzicz, S.; Rudnicka, L.; Mirowska-Guzel, D.; Cudnoch-Jedrzejewska, A., The role of epidermal sphingolipids in dermatologic diseases. *Lipids in health and disease* **2016**, *15*, 13.
116. Saravanan, C. Molecular basis of Galectin 3 mediated wound closure. Doctoral, Tufts University, Proquest LLC, 2009.
117. Saravanan, C.; Cao, Z.; Head, S. R.; Panjwani, N., Detection of differentially expressed wound-healing-related glycogenes in galectin-3-deficient mice. *Invest Ophthalmol Vis Sci* **2009**, *50* (12), 5690-6.
118. Saravanan, C.; Cao, Z.; Head, S. R.; Panjwani, N., Analysis of differential expression of glycosyltransferases in healing corneas by glycogene microarrays. *Glycobiology* **2010**, *20* (1), 13-23.
119. Kariya, Y.; Kawamura, C.; Tabei, T.; Gu, J., Bisecting GlcNAc residues on laminin-332 down-regulate galectin-3-dependent keratinocyte motility. *J Biol Chem* **2010**, *285* (5), 3330-40.
120. Cao, Z.; Said, N.; Amin, S.; Wu, H. K.; Bruce, A.; Garate, M.; Hsu, D. K.; Kuwabara, I.; Liu, F. T.; Panjwani, N., Galectins-3 and -7, but not galectin-1, play a role in re-epithelialization of wounds. *J Biol Chem* **2002**, *277* (44), 42299-305.
121. Gal, P.; Vasilenko, T.; Kostelnikova, M.; Jakubco, J.; Kovac, I.; Sabol, F.; Andre, S.; Kaltner, H.; Gabius, H. J.; Smetana, K., Jr., Open Wound Healing In Vivo: Monitoring Binding

CITED LITERATURE

and Presence of Adhesion/Growth-Regulatory Galectins in Rat Skin during the Course of Complete Re-Epithelialization. *Acta Histochem Cytochem* **2011**, 44 (5), 191-9.

122. Panjwani, N., Role of galectins in re-epithelialization of wounds. *Ann Transl Med* **2014**, 2 (9), 89.

123. Compagno, D.; Gentilini, L. D.; Jaworski, F. M.; Gonzalez Perez, I.; Contrufo, G.; Laderach, D. J., Glycans and galectins in prostate cancer biology, angiogenesis and metastasis. *Glycobiology* **2014**, 24 (10), 899-906.

124. Bax, M.; Garcia-Vallejo, J. J.; Jang-Lee, J.; North, S. J.; Gilmartin, T. J.; Hernandez, G.; Crocker, P. R.; Leffler, H.; Head, S. R.; Haslam, S. M.; Dell, A.; van Kooyk, Y., Dendritic cell maturation results in pronounced changes in glycan expression affecting recognition by siglecs and galectins. *J Immunol* **2007**, 179 (12), 8216-24.

125. Thornalley, P. J., Cell activation by glycated proteins. AGE receptors, receptor recognition factors and functional classification of AGEs. *Cellular and Molecular Biology* **1998**, 44 (7), 1013-1023.

126. Compagno, D.; Gentilini, L. D.; Jaworski, F. M.; Perez, I. G.; Contrufo, G.; Laderach, D. J., Glycans and galectins in prostate cancer biology, angiogenesis and metastasis. *Glycobiology* **2014**, 24 (10), 899-906.

127. Stowell, S. R.; Arthur, C. M.; Mehta, P.; Slanina, K. A.; Blixt, O.; Leffler, H.; Smith, D. F.; Cummings, R. D., Galectin-1, -2, and -3 exhibit differential recognition of sialylated glycans and blood group antigens. *J Biol Chem* **2008**, 283 (15), 10109-23.

128. Xue, H.; Liu, L.; Zhao, Z.; Zhang, Z.; Guan, Y.; Cheng, H.; Zhou, Y.; Tai, G., The N-terminal tail coordinates with carbohydrate recognition domain to mediate galectin-3 induced apoptosis in T cells. *Oncotarget* **2017**, 8 (30), 49824-49838.

CITED LITERATURE

129. Saegusa, J.; Hsu, D. K.; Liu, W.; Kuwabara, I.; Kuwabara, Y.; Yu, L.; Liu, F. T., Galectin-3 protects keratinocytes from UVB-induced apoptosis by enhancing AKT activation and suppressing ERK activation. *J Invest Dermatol* **2008**, *128* (10), 2403-11.
130. Tang, W.; Chang, S. B.; Hemler, M. E., Links between CD147 function, glycosylation, and caveolin-1. *Molecular biology of the cell* **2004**, *15* (9), 4043-50.
131. Mauris, J.; Woodward, A. M.; Cao, Z.; Panjwani, N.; Argueso, P., Molecular basis for MMP9 induction and disruption of epithelial cell-cell contacts by galectin-3. *Journal of cell science* **2014**, *127* (Pt 14), 3141-8.
132. Gendronneau, G.; Sanii, S.; Dang, T.; Deshayes, F.; Delacour, D.; Pichard, E.; Advedissian, T.; Sidhu, S. S.; Viguier, M.; Magnaldo, T.; Poirier, F., Overexpression of galectin-7 in mouse epidermis leads to loss of cell junctions and defective skin repair. *PLoS One* **2015**, *10* (3), e0119031.
133. Gendronneau, G.; Sidhu, S. S.; Delacour, D.; Dang, T.; Calonne, C.; Houzelstein, D.; Magnaldo, T.; Poirier, F., Galectin-7 in the control of epidermal homeostasis after injury. *Molecular biology of the cell* **2008**, *19* (12), 5541-9.
134. Kuwabara, I.; Kuwabara, Y.; Yang, R. Y.; Schuler, M.; Green, D. R.; Zuraw, B. L.; Hsu, D. K.; Liu, F. T., Galectin-7 (PIG1) exhibits pro-apoptotic function through JNK activation and mitochondrial cytochrome c release. *J Biol Chem* **2002**, *277* (5), 3487-97.
135. Ferreira, I. G.; Pucci, M.; Venturi, G.; Malagolini, N.; Chiricolo, M.; Dall'Olio, F., Glycosylation as a Main Regulator of Growth and Death Factor Receptors Signaling. *Int J Mol Sci* **2018**, *19* (2).
136. Al-Saraireh, Y. M.; Sutherland M Fau - Springett, B. R.; Springett Br Fau - Freiburger, F.; Freiburger F Fau - Ribeiro Morais, G.; Ribeiro Morais G Fau - Loadman, P. M.; Loadman Pm Fau - Errington, R. J.; Errington Rj Fau - Smith, P. J.; Smith Pj Fau - Fukuda, M.; Fukuda M Fau - Gerardy-Schahn, R.; Gerardy-Schahn R Fau - Patterson, L. H.; Patterson Lh Fau - Shnyder,

CITED LITERATURE

- S. D.; Shnyder Sd Fau - Falconer, R. A.; Falconer, R. A., Pharmacological inhibition of polysialyltransferase ST8Siall modulates tumour cell migration. (1932-6203 (Electronic)).
137. Drake, P. M.; Nathan, J. K.; Stock, C. M.; Chang, P. V.; Muench, M. O.; Nakata, D.; Reader, J. R.; Gip, P.; Golden, K. P.; Weinhold, B.; Gerardy-Schahn, R.; Troy, F. A.; Bertozzi, C. R., Polysialic acid, a glycan with highly restricted expression, is found on human and murine leukocytes and modulates immune responses. *J Immunol* **2008**, *181* (10), 6850-8.
138. Drake, P. M.; Stock, C. M.; Nathan, J. K.; Gip, P.; Golden, K. P.; Weinhold, B.; Gerardy-Schahn, R.; Bertozzi, C. R., Polysialic acid governs T-cell development by regulating progenitor access to the thymus. *Proc Natl Acad Sci U S A* **2009**, *106* (29), 11995-2000.
139. Ghosh, M.; Tuesta, L. M.; Puentes, R.; Patel, S.; Melendez, K.; El Maarouf, A.; Rutishauser, U.; Pearse, D. D., Extensive cell migration, axon regeneration, and improved function with polysialic acid-modified Schwann cells after spinal cord injury. *Glia* **2012**, *60* (6), 979-92.
140. Hsu, H. J.; Palka-Hamblin, H.; Bhide, G. P.; Myung, J. H.; Cheong, M.; Colley, K. J.; Hong, S., Noncatalytic Endosialidase Enables Surface Capture of Small-Cell Lung Cancer Cells Utilizing Strong Dendrimer-Mediated Enzyme-Glycoprotein Interactions. *Anal Chem* **2018**, *90* (6), 3670-3675.
141. Komminoth, P.; Roth J Fau - Saremaslani, P.; Saremaslani P Fau - Matias-Guiu, X.; Matias-Guiu X Fau - Wolfe, H. J.; Wolfe HJ Fau - Heitz, P. U.; Heitz, P. U., Polysialic acid of the neural cell adhesion molecule in the human thyroid: a marker for medullary thyroid carcinoma and primary C-cell hyperplasia. An immunohistochemical study on 79 thyroid lesions. (0147-5185 (Print)).
142. Ono, S.; Hane, M.; Kitajima, K.; Sato, C., Novel regulation of fibroblast growth factor 2 (FGF2)-mediated cell growth by polysialic acid. *The Journal of biological chemistry* **2012**, *287* (6), 3710-3722.

CITED LITERATURE

143. Schnaar, R. L.; Gerardy-Schahn, R.; Hildebrandt, H., Sialic acids in the brain: gangliosides and polysialic acid in nervous system development, stability, disease, and regeneration. *Physiological reviews* **2014**, *94* (2), 461-518.
144. Ulm, C.; Saffarzadeh, M.; Mahavadi, P.; Muller, S.; Prem, G.; Saboor, F.; Simon, P.; Middendorff, R.; Geyer, H.; Henneke, I.; Bayer, N.; Rinne, S.; Lutteke, T.; Bottcher-Friebertshauser, E.; Gerardy-Schahn, R.; Schwarzer, D.; Muhlenhoff, M.; Preissner, K. T.; Gunther, A.; Geyer, R.; Galuska, S. P., Soluble polysialylated NCAM: a novel player of the innate immune system in the lung. *Cell Mol Life Sci* **2013**, *70* (19), 3695-708.
145. Madsen, D. H.; Leonard, D.; Masedunskas, A.; Moyer, A.; Jurgensen, H. J.; Peters, D. E.; Amornphimoltham, P.; Selvaraj, A.; Yamada, S. S.; Brenner, D. A.; Burgdorf, S.; Engelholm, L. H.; Behrendt, N.; Holmbeck, K.; Weigert, R.; Bugge, T. H., M2-like macrophages are responsible for collagen degradation through a mannose receptor-mediated pathway. *J Cell Biol* **2013**, *202* (6), 951-66.
146. Jürgensen, H. J.; Madsen, D. H.; Ingvarsen, S.; Melander, M. C.; Gårdsvoll, H.; Patthy, L.; Engelholm, L. H.; Behrendt, N., A Novel Functional Role of Collagen Glycosylation: INTERACTION WITH THE ENDOCYTIC COLLAGEN RECEPTOR α PARAP/ENDO180*. In *J Biol Chem*, 2011; Vol. 286, pp 32736-48.
147. Tang, S.; Lucius, R.; Wenck, H.; Gallinat, S.; Weise, J. M., UV-mediated downregulation of the endocytic collagen receptor, Endo180, contributes to accumulation of extracellular collagen fragments in photoaged skin. *J Dermatol Sci* **2013**, *70* (1), 42-8.
148. Engelholm, L. H.; List, K.; Netzel-Arnett, S.; Cukierman, E.; Mitola, D. J.; Aaronson, H.; Kjølner, L.; Larsen, J. K.; Yamada, K. M.; Strickland, D. K.; Holmbeck, K.; Danø, K.; Birkedal-Hansen, H.; Behrendt, N.; Bugge, T. H., α PARAP/Endo180 is essential for cellular uptake of collagen and promotes fibroblast collagen adhesion. *J Cell Biol* **2003**, *160* (7), 1009-15.

CITED LITERATURE

149. Tanaka, F.; Otake Y Fau - Nakagawa, T.; Nakagawa T Fau - Kawano, Y.; Kawano Y Fau - Miyahara, R.; Miyahara R Fau - Li, M.; Li M Fau - Yanagihara, K.; Yanagihara K Fau - Inui, K.; Inui K Fau - Oyanagi, H.; Oyanagi H Fau - Yamada, T.; Yamada T Fau - Nakayama, J.; Nakayama J Fau - Fujimoto, I.; Fujimoto I Fau - Ikenaka, K.; Ikenaka K Fau - Wada, H.; Wada, H., Prognostic significance of polysialic acid expression in resected non-small cell lung cancer. (0008-5472 (Print)).
150. Trouillas, J.; Daniel L Fau - Guigard, M.-P.; Guigard Mp Fau - Tong, S.; Tong S Fau - Gouvernet, J.; Gouvernet J Fau - Jouanneau, E.; Jouanneau E Fau - Jan, M.; Jan M Fau - Perrin, G.; Perrin G Fau - Fischer, G.; Fischer G Fau - Tabarin, A.; Tabarin A Fau - Rougon, G.; Rougon G Fau - Figarella-Branger, D.; Figarella-Branger, D., Polysialylated neural cell adhesion molecules expressed in human pituitary tumors and related to extrasellar invasion. (0022-3085 (Print)).
151. Pinho, S. S.; Reis, C. A., Glycosylation in cancer: mechanisms and clinical implications. *Nature Reviews Cancer* **2015**, *15*, 540.
152. Elkashef, S. M.; Allison, S. J.; Sadiq, M.; Basheer, H. A.; Ribeiro Morais, G.; Loadman, P. M.; Pors, K.; Falconer, R. A., Polysialic acid sustains cancer cell survival and migratory capacity in a hypoxic environment. *Scientific Reports* **2016**, *6*, 33026.
153. Rellier, N.; Ruggiero, D.; Lecomte, M.; Lagarde, M.; Wiernsperger, N., Advanced glycation end products induce specific glycoprotein alterations in retinal microvascular cells. *Biochemical and Biophysical Research Communications* **1997**, *235* (2), 281-285.
154. Rellier, N.; Ruggiero-Lopez, D.; Lecomte, M.; Lagarde, M.; Wiernsperger, N., In vitro and in vivo alterations of enzymatic glycosylation in diabetes. *Life Sci* **1999**, *64* (17), 1571-83.
155. Varki, A.; Esko, J. D.; Colley, K. J., Cellular Organization of Glycosylation. In *Essentials of Glycobiology*, Varki, A.; Cummings, R. D.; Esko, J. D.; Freeze, H. H.; Stanley, P.; Bertozzi, C.

CITED LITERATURE

R.; Hart, G. W.; Etzler, M. E., Eds. The Consortium of Glycobiology Editors, La Jolla, California: Cold Spring Harbor NY, 2009.

156. Varki, A.; Sharon, N., Historical Background and Overview. In *Essentials of Glycobiology*, 2nd ed.; Varki, A.; Cummings, R.; Esko, J., Eds. Cold Spring Harbor Laboratory Press: Cold Spring Harbor, NY, 2009.

157. Ma, J.; Hart, G. W., Protein O-GlcNAcylation in diabetes and diabetic complications. *Expert review of proteomics* **2013**, *10* (4), 365-80.

158. Runager, K.; Bektas, M.; Berkowitz, P.; Rubenstein, D. S., Targeting O-glycosyltransferase (OGT) to promote healing of diabetic skin wounds. *J Biol Chem* **2014**, *289* (9), 5462-6.

159. Lee, C. L.; Chiu, P. C.; Pang, P. C.; Chu, I. K.; Lee, K. F.; Koistinen, R.; Koistinen, H.; Seppala, M.; Morris, H. R.; Tissot, B.; Panico, M.; Dell, A.; Yeung, W. S., Glycosylation failure extends to glycoproteins in gestational diabetes mellitus: evidence from reduced alpha2-6 sialylation and impaired immunomodulatory activities of pregnancy-related glycodefin-A. *Diabetes* **2011**, *60* (3), 909-17.

160. Wang, X. Q.; Lee, S.; Wilson, H.; Seeger, M.; Iordanov, H.; Gatla, N.; Whittington, A.; Bach, D.; Lu, J. Y.; Paller, A. S., Ganglioside GM3 depletion reverses impaired wound healing in diabetic mice by activating IGF-1 and insulin receptors. *J Invest Dermatol* **2014**, *134* (5), 1446-55.

161. Randeria, P. S.; Seeger, M. A.; Wang, X. Q.; Wilson, H.; Shipp, D.; Mirkin, C. A.; Paller, A. S., siRNA-based spherical nucleic acids reverse impaired wound healing in diabetic mice by ganglioside GM3 synthase knockdown. *Proc Natl Acad Sci U S A* **2015**, *112* (18), 5573-8.

162. Randeria, P. S.; Seeger, M. A.; Wang, X. Q.; Wilson, H.; Shipp, D.; Mirkin, C. A.; Paller, A. S., siRNA-based spherical nucleic acids reverse impaired wound healing in diabetic mice by

CITED LITERATURE

ganglioside GM3 synthase knockdown. In *Proc Natl Acad Sci U S A*, United States, 2015; Vol. 112, pp 5573-8.

163. Daleme, A.; Ruggiero, D.; Lecomte, M.; Lagarde, M.; Wiernsperger, N., *Effects of advanced glycation end products on glycosphingolipids of retinal pericytes*. 2000; Vol. 50, p 357-357.

164. Denis, U.; Lecomte, M.; Paget, C.; Ruggiero, D.; Wiernsperger, N.; Lagarde, M., *Advanced glycation end-products induce apoptosis of bovine retinal pericytes in culture: Involvement of diacylglycerol/ceramide production and oxidative stress induction*. 2002; Vol. 33, p 236-47.

165. Geoffroy, K.; Troncy, L.; Wiernsperger, N.; Lagarde, M.; Bawab, S., *Glomerular proliferation during early stages of diabetic nephropathy is associated with local increase of sphingosine-1-phosphate levels*. 2005; Vol. 579, p 1249-54.

166. Geoffroy, K.; Wiernsperger, N.; Lagarde, M.; Bawab, S., *Bimodal Effect of Advanced Glycation End Products on Mesangial Cell Proliferation Is Mediated by Neutral Ceramidase Regulation and Endogenous Sphingolipids*. 2004; Vol. 279, p 34343-52.

167. Masson, E.; Troncy, L.; Ruggiero, D.; Wiernsperger, N.; Lagarde, M.; Bawab, S., *a-Series Gangliosides Mediate the Effects of Advanced Glycation End Products on Pericyte and Mesangial Cell Proliferation: A Common Mediator for Retinal and Renal Microangiopathy?* 2005; Vol. 54, p 220-7.

168. Masson, E.; Wiernsperger, N.; Lagarde, M.; Bawab, S., *Involvement of gangliosides in glucosamine-induced proliferation decrease of retinal pericytes*. 2005; Vol. 15, p 585-91.

169. Zhuo, Y.; Chammas, R.; Bellis, S. L., *Sialylation of beta1 integrins blocks cell adhesion to galectin-3 and protects cells against galectin-3-induced apoptosis*. *J Biol Chem* **2008**, 283 (32), 22177-85.

CITED LITERATURE

170. Janik, M. E.; Litynska, A.; Vereecken, P., Cell migration-the role of integrin glycosylation. *Biochimica et biophysica acta* **2010**, *1800* (6), 545-55.
171. Zhao, Y.; Sato, Y.; Isaji, T.; Fukuda, T.; Matsumoto, A.; Miyoshi, E.; Gu, J.; Taniguchi, N., Branched N-glycans regulate the biological functions of integrins and cadherins. *FEBS J* **2008**, *275* (9), 1939-48.
172. Weis, M. A.; Hudson, D. M.; Kim, L.; Scott, M.; Wu, J. J.; Eyre, D. R., Location of 3-hydroxyproline residues in collagen types I, II, III, and V/XI implies a role in fibril supramolecular assembly. *J Biol Chem* **2010**, *285* (4), 2580-90.
173. Watt, F. M.; Fujiwara, H., Cell-extracellular matrix interactions in normal and diseased skin. *Cold Spring Harb Perspect Biol* **2011**, *3* (4).
174. Wu, A. M., *The molecular immunology of complex carbohydrates-3*. Springer Science+Business Media: New York, 2011; p xxxv, 809 p.
175. Schauer, R., Sialic acids as regulators of molecular and cellular interactions. *Curr Opin Struct Biol* **2009**, *19* (5), 507-14.
176. Team, R. C. R Foundation for Statistical Computing. <https://www.r-project.org/>.
177. Gautier, L.; Cope, L.; Bolstad, B. M.; Irizarry, R. A., affy--analysis of Affymetrix GeneChip data at the probe level. *Bioinformatics (Oxford, England)* **2004**, *20* (3), 307-15.
178. Dumur, C. I.; Nasim, S.; Best, A. M.; Archer, K. J.; Ladd, A. C.; Mas, V. R.; Wilkinson, D. S.; Garrett, C. T.; Ferreira-Gonzalez, A., Evaluation of quality-control criteria for microarray gene expression analysis. *Clin Chem* **2004**, *50* (11), 1994-2002.
179. Mas, V. R.; Archer, K. J.; Dumur, C. I.; Scian, M. J.; Suh, J. L.; King, A. L.; Wardius, M. E.; Straub, J. A.; Posner, M. P.; Brayman, K.; Maluf, D. G., Reduced Expression of Inflammatory Genes in Deceased Donor Kidneys Undergoing Pulsatile Pump Preservation. *PLOS ONE* **2012**, *7* (4), e35526.

CITED LITERATURE

180. Irizarry, R. A.; Hobbs, B.; Collin, F.; Beazer-Barclay, Y. D.; Antonellis, K. J.; Scherf, U.; Speed, T. P., Exploration, normalization, and summaries of high density oligonucleotide array probe level data. *Biostatistics* **2003**, *4* (2), 249-64.
181. Kessner, D.; Chambers, M.; Burke, R.; Agus, D.; Mallick, P., ProteoWizard: open source software for rapid proteomics tools development. *Bioinformatics (Oxford, England)* **2008**, *24* (21), 2534-6.
182. Keller, A.; Nesvizhskii Ai Fau - Kolker, E.; Kolker E Fau - Aebersold, R.; Aebersold, R., Empirical statistical model to estimate the accuracy of peptide identifications made by MS/MS and database search. (0003-2700 (Print)).
183. Nesvizhskii, A. I.; Keller A Fau - Kolker, E.; Kolker E Fau - Aebersold, R.; Aebersold, R., A statistical model for identifying proteins by tandem mass spectrometry. (0003-2700 (Print)).
184. Ritchie, M. E.; Phipson, B.; Wu, D.; Hu, Y.; Law, C. W.; Shi, W.; Smyth, G. K., limma powers differential expression analyses for RNA-sequencing and microarray studies. *Nucleic Acids Res* **2015**, *43* (7), e47.
185. Benjamini, Y.; Hochberg, Y., Controlling the False Discovery Rate: A Practical and Powerful Approach to Multiple Testing. *Journal of the Royal Statistical Society. Series B (Methodological)* **1995**, *57* (1), 289-300.
186. Metsalu, T.; Vilo, J., ClustVis: a web tool for visualizing clustering of multivariate data using Principal Component Analysis and heatmap. *Nucleic Acids Res* **2015**, *43* (W1), W566-70.
187. Charrad, M.; Ghazzali, N.; Boiteau, V.; Niknafs, A., NbClust: An R Package for Determining the Relevant Number of Clusters in a Data Set. *Journal of Statistical Software; Vol 1, Issue 6 (2014)* **2014**.
188. Rousseeuw, P. J., Silhouettes: A graphical aid to the interpretation and validation of cluster analysis. *Journal of Computational and Applied Mathematics* **1987**, *20*, 53-65.

CITED LITERATURE

189. Mi, H.; Huang, X.; Muruganujan, A.; Tang, H.; Mills, C.; Kang, D.; Thomas, P. D., PANTHER version 11: expanded annotation data from Gene Ontology and Reactome pathways, and data analysis tool enhancements. *Nucleic Acids Research* **2017**, *45* (D1), D183-D189.
190. Mi, H.; Muruganujan, A.; Casagrande, J. T.; Thomas, P. D., Large-scale gene function analysis with the PANTHER classification system. *Nature protocols* **2013**, *8*, 1551.
191. Mi, H.; Thomas, P., PANTHER Pathway: An Ontology-Based Pathway Database Coupled with Data Analysis Tools. In *Protein Networks and Pathway Analysis*, Nikolsky, Y.; Bryant, J., Eds. Humana Press: Totowa, NJ, 2009; pp 123-140.
192. Tang, H.; Thomas, P. D., PANTHER-PSEP: predicting disease-causing genetic variants using position-specific evolutionary preservation. *Bioinformatics (Oxford, England)* **2016**, *32* (14), 2230-2.
193. Thomas, P. D.; Kejariwal, A.; Guo, N.; Mi, H.; Campbell, M. J.; Muruganujan, A.; Lazareva-Ulitsky, B., Applications for protein sequence–function evolution data: mRNA/protein expression analysis and coding SNP scoring tools. *Nucleic Acids Research* **2006**, *34* (suppl_2), W645-W650.
194. Thomas, P. D., GIGA: a simple, efficient algorithm for gene tree inference in the genomic age. *BMC Bioinformatics* **2010**, *11* (1), 312.
195. Wuhrer, M.; Stam, J. C.; van de Geijn, F. E.; Koeleman, C. A.; Verrips, C. T.; Dolhain, R. J.; Hokke, C. H.; Deelder, A. M., Glycosylation profiling of immunoglobulin G (IgG) subclasses from human serum. *Proteomics* **2007**, *7* (22), 4070-81.
196. Hinderlich, S.; Weidemann, W.; Yardeni, T.; Horstkorte, R.; Huizing, M., UDP-GlcNAc 2-Epimerase/ManNAc Kinase (GNE): A Master Regulator of Sialic Acid Synthesis. *Topics in current chemistry* **2015**, *366*, 97-137.

CITED LITERATURE

197. Seppala, R.; Lehto, V. P.; Gahl, W. A., Mutations in the human UDP-N-acetylglucosamine 2-epimerase gene define the disease sialuria and the allosteric site of the enzyme. *Am J Hum Genet* **1999**, *64* (6), 1563-9.
198. Leroy, J. G.; Seppala, R.; Huizing, M.; Dacremont, G.; De Simpel, H.; Van Coster, R. N.; Orvisky, E.; Krasnewich, D. M.; Gahl, W. A., Dominant inheritance of sialuria, an inborn error of feedback inhibition. *Am J Hum Genet* **2001**, *68* (6), 1419-1427.
199. Bork, K.; Reutter, W.; Gerardy-Schahn, R.; Horstkorte, R., The intracellular concentration of sialic acid regulates the polysialylation of the neural cell adhesion molecule. *FEBS Letters* **2005**, *579* (22), 5079-5083.
200. Bork, K.; Weidemann, W.; Berneck, B.; Kuchta, M.; Bennmann, D.; Thate, A.; Huber, O.; Gnanapragassam, V. S.; Horstkorte, R., The expression of sialyltransferases is regulated by the bioavailability and biosynthesis of sialic acids. *Gene Expr Patterns* **2017**, *23-24*, 52-58.
201. Avril, T.; North, S. J.; Haslam, S. M.; Willison, H. J.; Crocker, P. R., Probing the cis interactions of the inhibitory receptor Siglec-7 with alpha2,8-disialylated ligands on natural killer cells and other leukocytes using glycan-specific antibodies and by analysis of alpha2,8-sialyltransferase gene expression. *Journal of leukocyte biology* **2006**, *80* (4), 787-96.
202. Pillai, S.; Netravali, I. A.; Cariappa, A.; Mattoo, H., Siglecs and immune regulation. *Annual review of immunology* **2012**, *30*, 357-392.
203. Varchetta, S.; Brunetta, E.; Roberto, A.; Mikulak, J.; Hudspeth, K. L.; Mondelli, M. U.; Mavilio, D., Engagement of Siglec-7 receptor induces a pro-inflammatory response selectively in monocytes. *PloS one* **2012**, *7* (9), e45821-e45821.
204. Beare, A.; Stockinger, H.; Zola, H.; Nicholson, I., Monoclonal antibodies to human cell surface antigens. *Current protocols in immunology* **2008**, *Appendix 4*, 4a.

CITED LITERATURE

205. Togarrati, P. P.; Dinglasan, N.; Desai, S.; Ryan, W. R.; Muench, M. O., CD29 is highly expressed on epithelial, myoepithelial, and mesenchymal stromal cells of human salivary glands. *Oral Dis* **2018**, 24 (4), 561-572.
206. Hinderlich, S.; Stasche, R.; Zeitler, R.; Reutter, W., A bifunctional enzyme catalyzes the first two steps in N-acetylneuraminic acid biosynthesis of rat liver. Purification and characterization of UDP-N-acetylglucosamine 2-epimerase/N-acetylmannosamine kinase. *J Biol Chem* **1997**, 272 (39), 24313-8.
207. Thomas, G. H.; Scocca, J.; Miller, C. S.; Reynolds, L. W., Accumulation of N-acetylneuraminic acid (sialic acid) in human fibroblasts cultured in the presence of N-acetylmannosamine. *Biochimica et biophysica acta* **1985**, 846 (1), 37-43.
208. Severi, E.; Hood, D. W.; Thomas, G. H., Sialic acid utilization by bacterial pathogens. *Microbiology* **2007**, 153 (Pt 9), 2817-22.
209. Fabris, L.; Brivio, S.; Cadamuro, M.; Strazzabosco, M., Revisiting Epithelial-to-Mesenchymal Transition in Liver Fibrosis: Clues for a Better Understanding of the "Reactive" Biliary Epithelial Phenotype. *Stem cells international* **2016**, 2016, 2953727-2953727.
210. Strazzabosco, M.; Fabris, L., Neural cell adhesion molecule and polysialic acid in ductular reaction: the puzzle is far from completed, but the picture is becoming more clear. *Hepatology (Baltimore, Md.)* **2014**, 60 (5), 1469-1472.
211. Tsuchiya, A.; Lu, W. Y.; Weinhold, B.; Boulter, L.; Stutchfield, B. M.; Williams, M. J.; Guest, R. V.; Minnis-Lyons, S. E.; MacKinnon, A. C.; Schwarzer, D.; Ichida, T.; Nomoto, M.; Aoyagi, Y.; Gerardy-Schahn, R.; Forbes, S. J., Polysialic acid/neural cell adhesion molecule modulates the formation of ductular reactions in liver injury. *Hepatology* **2014**, 60 (5), 1727-40.
212. CDC - 2011 National Estimates - 2011 National Diabetes Fact Sheet - Publications - Diabetes DDT. **2014**.

CITED LITERATURE

213. Dall, T. M.; Yang, W.; Halder, P.; Pang, B.; Massoudi, M.; Wintfeld, N.; Semilla, A. P.; Franz, J.; Hogan, P. F., The economic burden of elevated blood glucose levels in 2012: diagnosed and undiagnosed diabetes, gestational diabetes mellitus, and prediabetes. *Diabetes Care* **2014**, 37 (12), 3172-9.
214. Driver, V. R.; Fabbi, M.; Lavery, L. A.; Gibbons, G., The costs of diabetic foot: the economic case for the limb salvage team. *Journal of vascular surgery* **2010**, 52 (3 Suppl), 17S-22S.
215. Moremen, K.; Nairn, A. Glycan Biosynthetic Pathways and Glycotranscriptome analysis.
216. Ramakers, C.; Ruijter Jm Fau - Deprez, R. H. L.; Deprez Rh Fau - Moorman, A. F. M.; Moorman, A. F., Assumption-free analysis of quantitative real-time polymerase chain reaction (PCR) data. (0304-3940 (Print)).
217. Livak, K. J.; Schmittgen, T. D., Analysis of relative gene expression data using real-time quantitative PCR and the 2(-Delta Delta C(T)) Method. *Methods* **2001**, 25 (4), 402-8.
218. Schmittgen, T. D.; Zakrajsek, B. A.; Mills, A. G.; Gorn, V.; Singer, M. J.; Reed, M. W., Quantitative reverse transcription-polymerase chain reaction to study mRNA decay: comparison of endpoint and real-time methods. *Anal Biochem* **2000**, 285 (2), 194-204.
219. Winer, J.; Jung, C. K.; Shackel, I.; Williams, P. M., Development and validation of real-time quantitative reverse transcriptase-polymerase chain reaction for monitoring gene expression in cardiac myocytes in vitro. *Anal Biochem* **1999**, 270 (1), 41-9.
220. Miller, R. G., *Simultaneous statistical inference*. 2d ed.; Springer-Verlag: New York, 1981; p xvi, 299 p.
221. Yandell, B. S., *Practical data analysis for designed experiments*. Chapman & Hall: London ; New York, 1997; p xiv, 437 p.

CITED LITERATURE

222. Taylor, K. R.; Mills, R. E.; Costanzo, A. E.; Jameson, J. M., Gammadelta T cells are reduced and rendered unresponsive by hyperglycemia and chronic TNFalpha in mouse models of obesity and metabolic disease. *PLoS One* **2010**, *5* (7), e11422.
223. Barrett, T.; Wilhite, S. E.; Ledoux, P.; Evangelista, C.; Kim, I. F.; Tomashevsky, M.; Marshall, K. A.; Phillippy, K. H.; Sherman, P. M.; Holko, M.; Yefanov, A.; Lee, H.; Zhang, N.; Robertson, C. L.; Serova, N.; Davis, S.; Soboleva, A., NCBI GEO: archive for functional genomics data sets—update. *Nucleic Acids Research* **2013**, *41* (D1), D991-D995.
224. Groux-Degroote, S.; Wavelet, C.; Krzewinski-Recchi, M. A.; Portier, L.; Mortuaire, M.; Mihalache, A.; Trinchera, M.; Delannoy, P.; Malagolini, N.; Chiricolo, M.; Dall'Olio, F.; Harduin-Lepers, A., B4GALNT2 gene expression controls the biosynthesis of Sda and sialyl Lewis X antigens in healthy and cancer human gastrointestinal tract. *The international journal of biochemistry & cell biology* **2014**, *53*, 442-9.
225. Sadiku, P.; Willson, J. A.; Dickinson, R. S.; Murphy, F.; Harris, A. J.; Lewis, A.; Sammut, D.; Mirchandani, A. S.; Ryan, E.; Watts, E. R.; Thompson, A. A. R.; Marriott, H. M.; Dockrell, D. H.; Taylor, C. T.; Schneider, M.; Maxwell, P. H.; Chilvers, E. R.; Mazzone, M.; Moral, V.; Pugh, C. W.; Ratcliffe, P. J.; Schofield, C. J.; Ghesquiere, B.; Carmeliet, P.; Whyte, M. K.; Walmsley, S. R., Prolyl hydroxylase 2 inactivation enhances glycogen storage and promotes excessive neutrophilic responses. *The Journal of clinical investigation* **2017**, *127* (9), 3407-3420.
226. Hiebert, L. M.; Han, J.; Mandal, A. K., Glycosaminoglycans, Hyperglycemia, and Disease. *Antioxidants & redox signaling* **2013**, *21* (7), 1032-1043.
227. Lennon, F. E.; Singleton, P. A., Hyaluronan regulation of vascular integrity. *Am J Cardiovasc Dis* **2011**, *1* (3), 200-13.
228. Tkachenko, E.; Rhodes, J. M.; Simons, M., Syndecans: new kids on the signaling block. *Circ Res* **2005**, *96* (5), 488-500.

CITED LITERATURE

229. Ramirez, H. A.; Liang, L.; Pastar, I.; Rosa, A. M.; Stojadinovic, O.; Zwick, T. G.; Kirsner, R. S.; Maione, A. G.; Garlick, J. A.; Tomic-Canic, M., Comparative Genomic, MicroRNA, and Tissue Analyses Reveal Subtle Differences between Non-Diabetic and Diabetic Foot Skin. *PLoS One* **2015**, *10* (8), e0137133.
230. Ramirez, H.; Liang, L.; Pastar, I.; Rosa, A.; Stojadinovic, O.; Zwick, T.; Kirsner, R.; Maione, A.; Garlick, J.; Kirsner, R.; Tomic-Canic, M., Comparative genomic, microRNA, and tissue analyses reveal subtle differences between non-diabetic and diabetic foot skin [gene expression]. NCBI GEO database (Edgar *et al.*, 2002), 2015.
231. Tomic-Canic, M.; al, e., Diabetic Foot Ulcers. NCBI GEO database (Edgar *et al.*, 2002), 2016.
232. Lombard, V.; Golaconda Ramulu, H.; Drula, E.; Coutinho, P. M.; Henrissat, B., The carbohydrate-active enzymes database (CAZy) in 2013. *Nucleic Acids Res* **2014**, *42* (Database issue), D490-5.
233. Konishi, Y.; Aoki-Kinoshita, K. F., The GlycomeAtlas tool for visualizing and querying glycome data. *Bioinformatics (Oxford, England)* **2012**, *28* (21), 2849-50.
234. Akune, Y.; Hosoda, M.; Kaiya, S.; Shinmachi, D.; Aoki-Kinoshita, K. F., The RINGS resource for glycome informatics analysis and data mining on the Web. *Omics : a journal of integrative biology* **2010**, *14* (4), 475-86.
235. Fabregat, A.; Sidiropoulos, K.; Garapati, P.; Gillespie, M.; Hausmann, K.; Haw, R.; Jassal, B.; Jupe, S.; Korninger, F.; McKay, S.; Matthews, L.; May, B.; Milacic, M.; Rothfels, K.; Shamovsky, V.; Webber, M.; Weiser, J.; Williams, M.; Wu, G.; Stein, L.; Hermjakob, H.; D'Eustachio, P., The Reactome pathway Knowledgebase. In *Nucleic Acids Res*, The Author(s) 2015. Published by Oxford University Press on behalf of Nucleic Acids Research.: England, 2016; Vol. 44, pp D481-7.

CITED LITERATURE

236. Functional Glycomics Gateway. <http://www.functionalglycomics.org/static/index.shtml> (accessed January 15).
237. Ekins, S.; Nikolsky, Y.; Bugrim, A.; Kirillov, E.; Nikolskaya, T., Pathway mapping tools for analysis of high content data. *Methods in molecular biology (Clifton, N.J.)* **2007**, 356, 319-50.
238. von Mering, C.; Huynen, M.; Jaeggi, D.; Schmidt, S.; Bork, P.; Snel, B., STRING: a database of predicted functional associations between proteins. In *Nucleic Acids Res*, 2003; Vol. 31, pp 258-61.
239. Tagami, S.; Inokuchi Ji, J.; Kabayama, K.; Yoshimura, H.; Kitamura, F.; Uemura, S.; Ogawa, C.; Ishii, A.; Saito, M.; Ohtsuka, Y.; Sakaue, S.; Igarashi, Y., Ganglioside GM3 participates in the pathological conditions of insulin resistance. *J Biol Chem* **2002**, 277 (5), 3085-92.
240. Hamed, E. A.; Zakary, M. M.; Abdelal, R. M.; Abdel Moneim, E. M., Vasculopathy in type 2 diabetes mellitus: role of specific angiogenic modulators. *J Physiol Biochem* **2011**, 67 (3), 339-49.
241. Dam, D. H. M.; Paller, A. S., Gangliosides in Diabetic Wound Healing. *Progress in molecular biology and translational science* **2018**, 156, 229-239.
242. Pescador, N.; Villar, D.; Cifuentes, D.; Garcia-Rocha, M.; Ortiz-Barahona, A.; Vazquez, S.; Ordonez, A.; Cuevas, Y.; Saez-Morales, D.; Garcia-Bermejo, M. L.; Landazuri, M. O.; Guinovart, J.; del Peso, L., Hypoxia promotes glycogen accumulation through hypoxia inducible factor (HIF)-mediated induction of glycogen synthase 1. *PLoS One* **2010**, 5 (3), e9644.
243. Kleczkowski, L. A.; Decker, D.; Wilczynska, M., UDP-sugar pyrophosphorylase: a new old mechanism for sugar activation. *Plant Physiol* **2011**, 156 (1), 3-10.
244. Aiello, D. P.; Fu L Fau - Miseta, A.; Miseta A Fau - Bedwell, D. M.; Bedwell, D. M., Intracellular glucose 1-phosphate and glucose 6-phosphate levels modulate Ca²⁺ homeostasis in *Saccharomyces cerevisiae*. (0021-9258 (Print)).

CITED LITERATURE

245. Fujinaka, H.; Nakamura J Fau - Kobayashi, H.; Kobayashi H Fau - Takizawa, M.; Takizawa M Fau - Murase, D.; Murase D Fau - Tokimitsu, I.; Tokimitsu I Fau - Suda, T.; Suda, T., Glucose 1-phosphate increases active transport of calcium in intestine. (0003-9861 (Print)).
246. Tu, C.-L.; Celli, A.; Mauro, T.; Chang, W., Calcium-Sensing Receptor Regulates Epidermal Intracellular Ca²⁺ Signaling and Re-Epithelialization after Wounding. *Journal of Investigative Dermatology* **2019**, *139* (4), 919-929.
247. Guin, S.; Ru, Y.; Agarwal, N.; Lew, C. R.; Owens, C.; Comi, G. P.; Theodorescu, D., Loss of Glycogen Debranching Enzyme AGL Drives Bladder Tumor Growth via Induction of Hyaluronic Acid Synthesis. *Clinical cancer research : an official journal of the American Association for Cancer Research* **2016**, *22* (5), 1274-83.
248. Oldenburg, D.; Ru, Y.; Weinhaus, B.; Cash, S.; Theodorescu, D.; Guin, S., CD44 and RHAMM are essential for rapid growth of bladder cancer driven by loss of Glycogen Debranching Enzyme (AGL). *BMC cancer* **2016**, *16* (1), 713-713.
249. Libreros, S.; Garcia-Areas, R.; Iragavarapu-Charyulu, V., CHI3L1 plays a role in cancer through enhanced production of pro-inflammatory/pro-tumorigenic and angiogenic factors. *Immunologic research* **2013**, *57* (1-3), 99-105.
250. Hong, Y. B.; Kim, E. Y.; Jung, S.-C., Upregulation of proinflammatory cytokines in the fetal brain of the Gaucher mouse. *J Korean Med Sci* **2006**, *21* (4), 733-738.
251. Menzel, E. J.; Farr, C., Hyaluronidase and its substrate hyaluronan: biochemistry, biological activities and therapeutic uses. *Cancer Letters* **1998**, *131* (1), 3-11.
252. Herzog, C.; Has, C.; Franzke, C.-W.; Echtermeyer, F. G.; Schlötzer-Schrehardt, U.; Kröger, S.; Gustafsson, E.; Fässler, R.; Bruckner-Tuderman, L., Dystroglycan in Skin and Cutaneous Cells: β -Subunit Is Shed from the Cell Surface. *Journal of Investigative Dermatology* **2004**, *122* (6), 1372-1380.

CITED LITERATURE

253. Durbeej, M.; Henry, M. D.; Campbell, K. P., Dystroglycan in development and disease. *Current opinion in cell biology* **1998**, *10* (5), 594-601.
254. Inamori, K.; Willer, T.; Hara, Y.; Venzke, D.; Anderson, M. E.; Clarke, N. F.; Guicheney, P.; Bonnemann, C. G.; Moore, S. A.; Campbell, K. P., Endogenous glucuronyltransferase activity of LARGE or LARGE2 required for functional modification of alpha-dystroglycan in cells and tissues. *J Biol Chem* **2014**, *289* (41), 28138-48.
255. Praissman, J. L.; Willer, T.; Sheikh, M. O.; Toi, A.; Chitayat, D.; Lin, Y.-Y.; Lee, H.; Stalnaker, S. H.; Wang, S.; Prabhakar, P. K.; Nelson, S. F.; Stemple, D. L.; Moore, S. A.; Moremen, K. W.; Campbell, K. P.; Wells, L., The functional O-mannose glycan on α -dystroglycan contains a phospho-ribitol primed for matriglycan addition. *eLife* **2016**, *5*, e14473.
256. Nakagawa, N.; Manya, H.; Toda, T.; Endo, T.; Oka, S., Human natural killer-1 sulfotransferase (HNK-1ST)-induced sulfate transfer regulates laminin-binding glycans on α -dystroglycan. *The Journal of biological chemistry* **2012**, *287* (36), 30823-30832.
257. Kovacs, K.; Decatur, C.; Toro, M.; Pham, D. G.; Liu, H.; Jing, Y.; Murray, T. G.; Lampidis, T. J.; Merchan, J. R., 2-Deoxy-Glucose Downregulates Endothelial AKT and ERK via Interference with N-Linked Glycosylation, Induction of Endoplasmic Reticulum Stress, and GSK3beta Activation. *Mol Cancer Ther* **2016**, *15* (2), 264-75.
258. Alonso, J.; Schimpl, M.; van Aalten, D. M., O-GlcNAcase: promiscuous hexosaminidase or key regulator of O-GlcNAc signaling? *J Biol Chem* **2014**, *289* (50), 34433-9.
259. Landen, N. X.; Li, D.; Stahle, M., Transition from inflammation to proliferation: a critical step during wound healing. *Cell Mol Life Sci* **2016**, *73* (20), 3861-85.
260. Guillard, M.; Gloerich, J.; Wessels, H. J. C. T.; Morava, E.; Wevers, R. A.; Lefeber, D. J., Automated measurement of permethylated serum N-glycans by MALDI-linear ion trap mass spectrometry. *Carbohydrate Research* **2009**, *344* (12), 1550-1557.

CITED LITERATURE

261. Weiskopf, A. S.; Vouros, P.; Harvey, D. J., Characterization of oligosaccharide composition and structure by quadrupole ion trap mass spectrometry. *Rapid Commun Mass Spectrom* **1997**, *11* (14), 1493-504.
262. Behrens, A.-J.; Duke, R. M.; Petralia, L. M.; Harvey, D. J.; Lehoux, S.; Magnelli, P. E.; Taron, C. H.; Foster, J. M., Glycosylation profiling of dog serum reveals differences compared to human serum. *Glycobiology* **2018**, *28* (11), 825-831.
263. Strohm, M.; Kavan, D.; Novak, P.; Volny, M.; Havlicek, V., mMass 3: a cross-platform software environment for precise analysis of mass spectrometric data. *Anal Chem* **2010**, *82* (11), 4648-51.
264. Campbell, M. P.; Ranzinger, R.; Lutteke, T.; Mariethoz, J.; Hayes, C. A.; Zhang, J.; Akune, Y.; Aoki-Kinoshita, K. F.; Damerell, D.; Carta, G.; York, W. S.; Haslam, S. M.; Narimatsu, H.; Rudd, P. M.; Karlsson, N. G.; Packer, N. H.; Lisacek, F., Toolboxes for a standardised and systematic study of glycans. *BMC Bioinformatics* **2014**, *15 Suppl 1*, S9.
265. Damerell, D.; Ceroni, A.; Maass, K.; Ranzinger, R.; Dell, A.; Haslam, S. M., Annotation of glycomics MS and MS/MS spectra using the GlycoWorkbench software tool. *Methods in molecular biology (Clifton, N.J.)* **2015**, *1273*, 3-15.
266. Treuheit, M.; E Costello, C.; Kirley, T., *Structures of the complex glycans found on the β -subunit of (Na,K)-ATPase*. 1993; Vol. 268, p 13914-9.
267. Babu, P.; North, S. J.; Jang-Lee, J.; Chalabi, S.; Mackerness, K.; Stowell, S. R.; Cummings, R. D.; Rankin, S.; Dell, A.; Haslam, S. M., Structural characterisation of neutrophil glycans by ultra sensitive mass spectrometric glycomics methodology. *Glycoconjugate journal* **2009**, *26* (8), 975-986.
268. Kiang, K. M.; Leung, G. K., A Review on Adducin from Functional to Pathological Mechanisms: Future Direction in Cancer. *Biomed Res Int* **2018**, *2018*, 3465929.

CITED LITERATURE

269. Pitre, A.; Ge, Y.; Lin, W.; Wang, Y.; Fukuda, Y.; Temirov, J.; Phillips, A. H.; Peters, J. L.; Fan, Y.; Ma, J.; Nourse, A.; Sinha, C.; Lin, H.; Kriwacki, R.; Downing, J. R.; Gruber, T. A.; Centonze, V. E.; Naren, A. P.; Chen, T.; Schuetz, J. D., An unexpected protein interaction promotes drug resistance in leukemia. *Nat Commun* **2017**, *8* (1), 1547.
270. Zhang, J. B.; Li, X. H.; Ning, F.; Guo, X. S., [Relationship between expression of GYPC and TRIP3 genes and prognosis of acute lymphoblastic leukemia in children]. *Zhongguo Dang Dai Er Ke Za Zhi* **2009**, *11* (1), 29-32.
271. Caterson, B.; Melrose, J., Keratan sulfate, a complex glycosaminoglycan with unique functional capability. *Glycobiology* **2018**, *28* (4), 182-206.
272. Stolfi, G.; Mondal, N.; Zhu, Y.; Yu, X.; Buffone, A., Jr.; Neelamegham, S., Using CRISPR-Cas9 to quantify the contributions of O-glycans, N-glycans and Glycosphingolipids to human leukocyte-endothelium adhesion. *Sci Rep* **2016**, *6*, 30392.
273. Meng, H.; Jain, S.; Lockshin, C.; Shaligram, U.; Martinez, J.; Genkin, D.; Hill, D. B.; Ehre, C.; Clark, D.; Hoppe IV, H., Clinical Application of Polysialylated Deoxyribonuclease and Erythropoietin. *Recent Pat Drug Deliv Formul* **2018**, *12* (3), 212-222.
274. Pagliarini, S.; Lucchiari, S.; Ulzi, G.; Violano, R.; Ripolone, M.; Bordoni, A.; Nizzardo, M.; Gatti, S.; Corti, S.; Moggio, M.; Bresolin, N.; Comi, G. P., Glycogen storage disease type III: A novel Agl knockout mouse model. *Biochimica et Biophysica Acta (BBA) - Molecular Basis of Disease* **2014**, *1842* (11), 2318-2328.
275. Nogales-Gadea, G.; Pinos, T.; Lucia, A.; Arenas, J.; Camara, Y.; Brull, A.; de Luna, N.; Martin, M. A.; Garcia-Arumi, E.; Marti, R.; Andreu, A. L., Knock-in mice for the R50X mutation in the PYGM gene present with McArdle disease. *Brain* **2012**, *135* (Pt 7), 2048-57.
276. E. Hoopes, J.; J. C. Im, M., *Glycogen metabolism in epidermal wound healing*. 1974; Vol. 6, p 409-412.

CITED LITERATURE

277. Raekallio, J.; Levonen, E., Histochemical demonstration of transglucosylases and glycogen in the “lag” phase of wound healing. *Experimental and Molecular Pathology* **1963**, 2 (1), 69-73.
278. Das, A.; Ganesh, K.; Khanna, S.; Sen, C. K.; Roy, S., Engulfment of apoptotic cells by macrophages: a role of microRNA-21 in the resolution of wound inflammation. *Journal of immunology (Baltimore, Md. : 1950)* **2014**, 192 (3), 1120-1129.
279. Steinbrecher, K. A.; Wilson, W., 3rd; Cogswell, P. C.; Baldwin, A. S., Glycogen synthase kinase 3 β functions to specify gene-specific, NF-kappaB-dependent transcription. *Molecular and cellular biology* **2005**, 25 (19), 8444-8455.
280. Peng, J.; Ramesh, G.; Sun, L.; Dong, Z., Impaired wound healing in hypoxic renal tubular cells: roles of hypoxia-inducible factor-1 and glycogen synthase kinase 3 β / β -catenin signaling. *The Journal of pharmacology and experimental therapeutics* **2012**, 340 (1), 176-184.
281. Cheon, S.; Poon, R.; Yu, C.; Khoury, M.; Shenker, R.; Fish, J.; Alman, B. A., Prolonged β -catenin stabilization and tcf-dependent transcriptional activation in hyperplastic cutaneous wounds. *Laboratory Investigation* **2005**, 85, 416.
282. Hu, M. S.; Hong, W. X.; Januszyk, M.; Walmsley, G. G.; Luan, A.; Maan, Z. N.; Moshrefi, S.; Tevlin, R.; Wan, D. C.; Gurtner, G. C.; Longaker, M. T.; Lorenz, H. P., Pathway Analysis of Gene Expression in Murine Fetal and Adult Wounds. *Advances in wound care* **2018**, 7 (8), 262-275.
283. Richmond, C. S.; Oldenburg, D.; Dancik, G.; Meier, D. R.; Weinhaus, B.; Theodorescu, D.; Guin, S., Glycogen debranching enzyme (AGL) is a novel regulator of non-small cell lung cancer growth. *Oncotarget* **2018**, 9 (24), 16718-16730.
284. Westmuckett, A. D.; Thacker, K. M.; Moore, K. L., Tyrosine sulfation of native mouse Psgl-1 is required for optimal leukocyte rolling on P-selectin in vivo. *PLoS One* **2011**, 6 (5), e20406.

CITED LITERATURE

285. Cooney, C. A.; Jousheghany, F.; Yao-Borengasser, A.; Phanavanh, B.; Gomes, T.; Kieber-Emmons, A. M.; Siegel, E. R.; Suva, L. J.; Ferrone, S.; Kieber-Emmons, T.; Monzavi-Karbassi, B., Chondroitin sulfates play a major role in breast cancer metastasis: a role for CSPG4 and CHST11 gene expression in forming surface P-selectin ligands in aggressive breast cancer cells. *Breast cancer research : BCR* **2011**, *13* (3), R58-R58.
286. Hobizal, K. B.; Wukich, D. K., Diabetic foot infections: current concept review. *Diabetic foot & ankle* **2012**, *3*.
287. Jaako, K.; Waniek, A.; Parik, K.; Klimaviciusa, L.; Aonurm-Helm, A.; Noortoots, A.; Anier, K.; Van Elzen, R.; Gérard, M.; Lambeir, A.-M.; Roßner, S.; Morawski, M.; Zharkovsky, A., Prolyl endopeptidase is involved in the degradation of neural cell adhesion molecules &em>in vitro. *Journal of cell science* **2016**, *129* (20), 3792.
288. Hinkle, C. L.; Diestel, S.; Lieberman, J.; Maness, P. F., Metalloprotease-induced ectodomain shedding of neural cell adhesion molecule (NCAM). *J Neurobiol* **2006**, *66* (12), 1378-95.
289. Diestel, S.; Hinkle, C. L.; Schmitz, B.; Maness, P. F., NCAM140 stimulates integrin-dependent cell migration by ectodomain shedding. *J Neurochem* **2005**, *95* (6), 1777-84.
290. Galuska, C. E.; Maass, K.; Galuska, S. P., Mass Spectrometric Analysis of Oligo- and Polysialic Acids. *Methods in molecular biology (Clifton, N.J.)* **2015**, *1321*, 417-26.
291. Conant, K.; Allen, M.; Lim, S. T., Activity dependent CAM cleavage and neurotransmission. *Front Cell Neurosci* **2015**, *9*, 305.

VITA

Veronica Haywood

A. Education and Training

INSTITUTION AND LOCATION	DEGREE	Completion	FIELD OF STUDY
Marquette University, Milwaukee, WI	BS	12/2008	Athletic Training/Exercise Physiology
Marquette University, Milwaukee, WI	DPT, Doctor of Physical Therapy	05/2010	Physical Therapy, concentration in wound healing
Louisiana State University, Shreveport, LA	Other training	05/2010	Pre-doctoral training in Physical Therapy based clinical wound care management.
Advocate Christ Medical Center/ UIC Physician Affiliates, Oak Lawn, IL	Other training	01/2012	Postdoctoral clinical wound care training.
Marquette University, Milwaukee, WI	PhD, Graduate Student	05/2015	Program in Clinical and Translational Rehabilitation Health Science
University of Illinois-Chicago, Chicago, IL	PhD, PhD Candidate	present	PhD in Oral Sciences- Wound Healing and Tissue Regeneration. Current pursuance
University of Illinois-Chicago, Chicago, IL	Postdoctoral Fellow	present	Emphasis on tissue regeneration and wound healing in the Diabetic population. PI: Dr. Luisa DiPietro

B. Positions and Honors

Positions and Employment

- 2013 - Physical Therapist, ADVOCATE HEALTH AND HOSPITALS CORP, Oak Lawn, IL
- 2015 - PhD Candidate, UNIVERSITY OF ILLINOIS AT CHICAGO, Chicago, IL

Professional Licensure and Board Certifications

2009- 2013 Certified Athletic Trainer

2010 - Licensed Physical Therapist, State of Illinois

Laboratory Skills and Training

Protocol development, cell culture, tissue culture, animal handling, *in vivo* and *in vitro* models of wound healing, molecular biological techniques, microscopy techniques, biochemical and immunoassay development, bioinformatics and statistical analysis of genomic and glycomic data using the R programming environment, Western blot and lectin probing, immunohistochemistry, immunoprecipitation, bacterial culture, protein overexpression and purification.

Grant Support

1. T32 Postdoctoral Fellowship (02/16/16-02/15/18)
NIH-NIDCR 5T32DE018381-08 (Bedran-Russo, PI)
“The Role of Enzymatic Glycosylation in Wound Healing and Tissue Regeneration”
Role: Trainee, Post- Doctoral Fellowship

2. WHF-3M Fellowship (07/01/17-06/30/18)
Wound Healing Foundation
“Enzymatic Protein Glycosylation During Normal and Diabetic Wound Healing”
\$15,000
Role: Principal Investigator

Honors/ Awards

- | | |
|-----------|--|
| 2007-2008 | Ronald E. McNair Scholar (Marquette University), US Department of Education TRIO Program |
| 2013-2015 | Diversity Fellowship, Marquette University |
| 2016- | T32 Fellowship Awardee, University of Illinois- Chicago |
| 2017- | Wound Healing Foundation- 3M Fellowship |
| 2017 | FASEB MARC/DREAM Mentored Travel Award- Society for Glycobiology |
| 2018 | NIH Data Science RoAD Trip Award Recipient |

Teaching Experience

- 2015- 2018 Lecturer, “Lymphedema Wounds and Skin Care” (2015-2018), “Skin Pathologies Arterial/ Venous/ Neuropathic Wounds/ Wound Measurement, Evaluation, and Documentation” (2018), for the course “Applied Pathophysiology” (PT636), Physical Therapy Department- University of Illinois Chicago
- 2017- 2018 Laboratory Instructor, “Wound Care Etiology, Evaluation, Dressings, and Debridement”, for the course “Applied Pathophysiology” (PT636), Physical Therapy Department- University of Illinois Chicago; coordinated clinical laboratory skills training and assessment for doctoral physical therapy students.

Student Advising/ Mentoring

- Raghavan, Summer Research Mentor, 2017, Summer Laboratory Rotation, University of Illinois at Chicago
- Vidhath
- Shah, Maitri Laboratory Training Mentor, 2017, GPPA Dentistry Program, University of Illinois at Chicago

Professional Service Activities

- 2012 Community presentation, Smith Village Assisted Living Facility, “Diabetic Foot Ulcers” on the behalf of Advocate Christ Medical Center Rehabilitation Department, Oak Lawn, IL
- 2016 Judge, Student Research Forum, University of Illinois at Chicago, Chicago, IL
- 2018 Judge, Young Investigators Award WHS Symposium, 31st SAWC Spring/ Wound Healing Society Annual Meeting, Charlotte, NC.

C. Publications and Contributions to Science

Published Abstracts

Haywood V, Hoeger Bement M (2008). The management of pain using isometric contractions. 22nd National Conference on Undergraduate Research (National), Salisbury, MD.

Haywood V, Colley K, DiPietro LA (2016). Differential Expression of Sialic Acid Related Genes in Skin and Oral Mucosal Wound Healing. 9th annual Translational to Clinical (T2C) Regenerative Medicine Wound Care Conference, Ohio State University, Columbus, OH.

Haywood V, Nairn A, Colley K, DiPietro LA (2017). Differential Expression of Glycosylation Related Genes in Diabetic and Non-Diabetic Wound Healing. 30th Annual Meeting of the Wound Healing Society with the Symposium on Advanced Wound Care (SAWC), San Diego, CA.

Haywood V, Chen L, Colley K, DiPietro LA (2017). Differential Sialylation and Polysialylation in Skin and Oral Mucosal Wound Healing. Society for Glycobiology Meeting, Portland, OR.

Haywood V, Chen L, Colley K, DiPietro LA (2018). Differential Expression of Glycosylation Related Genes during Wound Healing. American Association for Dental Research Annual Meeting, Fort Lauderdale, FL.

Non-Peer Reviewed Abstracts

Haywood V, Hoeger Bement M (2007). The management of pain using isometric contractions. McNair Summer Research Program (local), Marquette University, Milwaukee, WI.

Haywood V, Hoeger Bement M (2007). The management of pain using isometric contractions. Annual National McNair Research Conference and Graduate Fair (regional), Delavan, WI.

Weyer A, **Haywood V**, Hunter S, Hoeger Bement M (2007). The effect of mental stress on healthy men and women. College of Health Sciences Summer Research Program, Marquette University, Milwaukee, WI.

Haywood V, Colley K, DiPietro LA (2017). Differential Expression of Sialic Acid Related Genes in Skin and Oral Mucosal Wound Healing-Update. Clinic and Research Day, UIC College of Dentistry, University of Illinois at Chicago, Chicago, IL.

Haywood V, Nairn A, Colley K, DiPietro LA (2017). Differential Expression of Glycosylation Related Genes in Diabetic and Non-Diabetic Wound Healing. 2nd GEMSSA Graduate Medical Education Research Symposium, University of Illinois at Chicago, Chicago, IL.

D. Memberships, Conferences, and Other Experiences

Memberships

2005 - 2011 Member, National Athletic Training Association (NATA)

2008 - 2011 Member, American Physical Therapy Association (APTA)
2015

- 2012, 2015- Member, American College of Wound Healing and Tissue Repair (ACWHTR)
- 2012 - 2018 Member, American Association for the Advancement of Science (AAAS)
- 2015- Member, Wound Healing Society (WHS)
- 2016 - 2017 Secretary and Treasurer, UIC Advanced Degree Consulting Club
- 2016 - Member, Society for Glycobiology
- 2017 - 2018 Member, Graduate Women in Science
- 2017 - 2018 Member, American Association for Dental Research
- 2018 Award Committee Member, Wound Healing Society (WHS)

Conferences/ Workshops

- 2009 *Practical Wound Care: A Multidisciplinary Approach*. Lutheran General Hospital.
- 2011 Diabetic Foot Conference 2011, Valley Presbyterian Hospital, Los Angeles, CA.
- 2012 APTA Clinical Instructor Education and Credentialing Program, Marquette University.
- 2012, 2015- Annual Meeting of the American College of Tissue Repair and Wound Healing, Chicago, IL.
- 2014 CBC Tech Day. *Cutting-Edge Technologies-Driving Science Forward*. **Northwestern University**.
- 2015 CCTS Summer Program. *Clinical and Translational Research Methods*. University of Illinois at Chicago.
- 2015 CBC Workshop. *Summer Workshop in Proteomics and Informatics*. University of Illinois at Chicago.
- 2015 **Annual CBC Symposium. The Unseen Majority: Microbes in Health and Disease**. *Northwestern University*.
- 2016 Translational to Clinical (T2C) Regenerative Medicine Wound Care Conference, Ohio State University.
- 2016 MATTER Legal Clinic. *Negotiating Sponsored Research Agreements – What Startups Need to Know*.
- 2016 Center for Research Informatics and Core Genomics Facility at the Research Resources Center. *MetaCore™ Seminar & Hands-on Training*. University of Illinois at Chicago.
- 2017 Annual Clinic and Research Day, UIC College of Dentistry- University of Illinois at Chicago.
- 2017 30th SAWC Spring/ Wound Healing Society Annual Meeting, San Diego, CA.

- 2017 Annual Experimental Biology 2017 Meeting, Chicago, IL.
- 2017 2nd GEMSSA Graduate Medical Education Research Symposium, University of Illinois at Chicago.
- 2017 Annual Society for Glycobiology 2017 Meeting, Portland, OR.
- 2017 **Annual CBC Symposium. *Small Molecule Discovery*.** University of Illinois at Chicago.
- 2018 Annual Clinic and Research Day, UIC College of Dentistry- University of Illinois at Chicago.
- 2018 American Association for Dental Research, Fort Lauderdale, FL.
- 2018 31st SAWC Spring/ Wound Healing Society Annual Meeting, Charlotte , NC.
- 2019 Office of Postdoctoral Affairs. *Mentoring Up Workshop Series for Postdocs: Chicago Introductory Session*, Northwestern University, Chicago, IL.
- 2019 32nd SAWC Spring/ Wound Healing Society Annual Meeting, San Antonio, TX.

Presentations

- 2007 Poster presentation. *The Management of Pain Using Isometric Contractions: Call to Action for Patients with Fibromyalgia*. National Ronald E. McNair Research Conference, Delavan, WI.
- 2008 Oral presentation. *The Management of Pain Using Isometric Contractions: Call to Action for Patients with Fibromyalgia*. National Conference for Undergraduate Research, Salisbury University.
- 2016 Poster Presentation, "*Differential Expression of Sialic Acid Related Genes in Skin and Oral Mucosal Wound Healing*", 9th annual Translational to Clinical (T2C) Regenerative Medicine Wound Care Conference, Ohio State University.
- 2017 Poster Presentation. *Differential Expression of Sialic Acid Related Genes in Skin and Oral Mucosal Wound Healing-Update*. Clinic and Research Day, UIC College of Dentistry, University of Illinois at Chicago.
- 2017 Poster Presentation. *Differential Expression of Glycosylation Related Genes in Diabetic and Non-Diabetic Wound Healing*. 30th SAWC Spring/ Wound Healing Society Annual Meeting, San Diego, CA.
- 2017 Poster Presentation. *Differential Expression of Glycosylation Related Genes in Diabetic and Non-Diabetic Wound Healing*. 2nd GEMSSA Graduate Medical Education Research Symposium, University of Illinois at Chicago.
- 2017 Poster Presentation. *Differential Sialylation and Polysialylation in Skin and Oral Mucosal Wound Healing*. Society for Glycobiology Meeting, Portland, OR.

- 2018 Poster Presentation. *Differential Expression of Glycosylation Related Genes in Wound Healing: Skin and Oral Mucosa*. Clinic and Research Day, UIC College of Dentistry, University of Illinois at Chicago.
- 2018 Poster Presentation. *Differential Expression of Glycosylation Related Genes in Wound Healing: Skin and Oral Mucosa*. American Association for Dental Research, Fort Lauderdale, FL.
- 2018 Invited Lecture. *Enzymatic Protein Glycosylation During Normal and Diabetic Wound Healing*. 31st SAWC Spring/ Wound Healing Society Annual Meeting, Charlotte, NC.
- 2019 Oral Presentation. *Comparative Glycomics of Diabetic and Non-Diabetic Skin Reveal Significant Differences During Wound Healing*. 32nd SAWC Spring/ Wound Healing Society Annual Meeting, San Antonio, TX.